IDENTIFICATION AND CHARACTERIZATION OF CHROMOSOME INSTABILITY MUTANTS IN THE YEAST *SACCHAROMYCES CEREVISIAE* AND IMPLICATIONS TO HUMAN CANCER

by

WING YEE KAREN YUEN

B.Sc. (Hon), Simon Fraser University, 2001

A Thesis Submitted in Partial Fulfillment of
the Requirements for the Degree of
DOCTOR OF PHILOSOPHY
in
The Faculty of Graduate Studies
(Medical Genetics)

The University of British Columbia
January 2007

ABSTRACT

Chromosome instability (CIN) is a hallmark of cancers and may contribute to tumorigenesis. Many genes involved in maintaining chromosome stability are conserved in eukaryotes, and some are mutated in cancers. The goal of this thesis is to use *Saccharomyces cerevisiae* as a model to identify and characterize genes important for chromosome maintenance, investigate the relevance of CIN to cancer, and develop a strategy to identify candidate therapeutic target genes for selective killing of cancer cells.

To systematically identify genes important for chromosome stability, non-essential gene deletion yeast mutants were examined using 3 complementary CIN assays. The chromosome transmission fidelity assay monitors loss of an artificial chromosome. The bimater assay monitors loss of heterozygosity at the mating type locus in homozygous diploid deletion mutants. The a-like faker assay detects loss of the *MATα* mating type locus in haploid deletion mutants. 293 CIN mutants were identified, including genes functioning in the chromosome or cell cycle, and genes not clearly implicated in chromosome maintenance, such as *MMS22*, *MMS1*, *RTT101* and *RTT107*. Phenotypic, genetic and biochemical analyses of these 4 gene products indicate that they function in double strand break repair. They may form a ubiquitin ligase complex that regulates the level of some proteins, including Mms22p itself, during DNA damage response.

Human homologues of 10 yeast CIN genes identified were previously shown to be mutated in cancers, suggesting that other human homologues are candidate cancer genes. 101 human homologues of yeast CIN genes were sequenced in a panel of colorectal cancers, identifying 20 somatic mutations in 8 genes. In particular, 17 mutations were found in 5 genes involved in sister chromatid cohesion. Further functional studies should reveal whether mutations in cohesion genes contribute to CIN in cancers.

While CIN mutations may contribute to cancer, CIN cancer cells may become inviable when combined with another non-essential mutation, providing the basis for

cancer cell-specific therapy. Mutations in *CTF4*, *CTF18*, and *DCC1* in yeast cause synthetic lethality when combined with mutations in various CIN genes whose human homologues are mutated in cancers. Such analyses in yeast can propose potential drug targets in human for cancer therapy.

TABLE OF CONTENTS

LIST OF TABLES

LIST OF FIGURES

CHAPTER 1:

CHAPTER 2:

CHAPTER 3:

CHAPTER 4:

ACKNOWLEDGMENTS

The completion of this thesis would not be possible without the help and support of many people, who I would like to take this opportunity to thank and acknowledge.

First, I would like to thank my supervisor Phil Hieter for his guidance and advices throughout the course of my PhD study. Phil has provided a very supportive lab environment with many great scientists and resourceful colleagues. Phil also has extensive networking with scientists in the yeast community and worldwide. Phil has introduced me to many experienced scientists, and he has been instrumental in setting up productive collaborations. I am also thankful for Phil's openness, positivity and generosity.

Second, I would like to thank members of the Hieter lab for a constructive and fun working and learning atmosphere. I want to thank the many helpful post-doctoral fellows/visiting professors in the lab, including Vivien Measday, Kristin Batez, Melanie Mayer, Daniel Kornitzer, Shay Ben-Aroya, Kirk McManus, Amir Aharoni, and Giora Simchen, who all never hesitated to offer guidance and assistance. I am grateful to grow scientifically with fellow students in the lab. Thanks Andy Page for introducing me to the basics of yeast biology and genetics. Thanks Isabelle Pot for teaching me many molecular and biochemical techniques. I would not survive these years without Isabelle's consistent encouragement and our daily energizing 'cookie club'. Thanks Ben Cheng, Elaine Law, Ben Montpetit, and Jan Stopel for insightful discussion and interactions (and a little bit of pressure). I am appreciative of the technical assistance by Teresa Kwok. And thanks Irene Barrett and Dave Thomson for keeping the lab in place.

Next, I like to thank collaborators who have contributed to this work. I am indebted to Forrest Spencer at Johns Hopkins University for enormous guidance and support. Her enthusiasm, compassion and understanding always brighten my days. Thanks also go to Cheryl Warren (from Forrest Spencer's lab) who performed the a-like faker screen and subsequent analysis (Chapter 2); Mark Flory (from Rudi Aebersold's lab at the Institute of Systems Biology) who performed the mass spectrometry analysis

(Chapter 4); Tony Hazbun (from Stan Fields' lab at the Yeast Resource Centre) who performed the yeast-two-hybrid analysis (Chapter 4); Shira Goldstein (from Martin Kupiec's lab at Tel Aviv University) who performed the Southern blot and PCR analysis for monitoring the repair kinetics of double-strand DNA breaks (Chapter 4). Tom Barber, Marcelo Reis (in Victor Velculescu and Bert Vogelstein group at Johns Hopkins University) and Christoph Lengauer have been instrumental to the cancer mutation testing project (Chapter 3).

In addition, I need to thank members of my advisory committee, Carolyn Brown, Ann Rose, and Liz Conibear, for guidance, directions and support throughout the years, and invaluable feedbacks on my thesis. I also want to thank Michel Roberge and Mike Kobor for stimulating discussion and Joanne Fox (in UBC Bioinformatics Centre) for bioinformatic assistance (Chapter 2).

Besides, I would like to thank teachers and mentors who have inspired me to pursue a scientific endeavor. My high school physics teacher in Hong Kong, Mr. Y.S. Au, has exposed me to the excitements in doing experiments. Dennis Jewell demonstrated his passion in teaching and supported me tremendously during my first year in Canada. Working with Jean St. Pierre at Ballard Power Systems in my first co-op experience has exposed me to a new perspective in applied research. My honor thesis supervisor Lynne Quarmby at Simon Fraser University has demonstrated to me her creativity and enthusiasm in studying cellular biology.

Finally, I am thankful to my parents, Mandy and John Yuen, for their unconditional love, continuous trust, support and an unlimited supply of heart-warming soups! I could not imagine how my years of graduate life would be like without the love, back-up, encouragement and understanding of my soul mate Simon Chiu. I need to thank my brother Ken, aunt Pamela Cheng, very good friends Rosa Tchao, Helen Leung, Vernice Yu, Ivy Ng, Daphne Chow and WaiTak Tsun for their long-distance support as well. I also want to say thanks to the brothers and sisters at Pacific Grace MB Church, especially Oliver Chan and Rev. Issac Chang, for their prayers and support. And thank God for all the blessings and challenges.

Throughout this thesis work, I was financially supported by the National Science and Engineering Research Council (NSERC) postgraduate scholarships and the University of British Columbia graduate fellowship, who I would like to thank here.

CO-AUTHORSHIP STATEMENT

Chapter 2 of this thesis was co-written by Cheryl D. Warren. I designed and performed all the work described in this chapter except for the following:

- a-like faker screen and retest
- sequencing of unique tags of mutants
- electrophoretic karyotyping of a-like fakers

These experiments were performed by Cheryl Warren and Ou Chen in Forrest Spencer's laboratory.

CHAPTER 1

Introduction:
Maintenance of Chromosome Stability in Eukaryotes and the Relationship with Cancer

Part of this chapter has been published. Karen WY Yuen*, Ben Montpetit* and Phil Hieter (*These authors contributed equally to this work). (2005) The Kinetochore and Cancer: What's the Connection? Current Opinion in Cell Biology. 17:1-7.

1.1 Maintenance of chromosome stability in eukaryotes

1.1.1 The cell and chromosome cycles in eukaryotes

Over 100 years ago, Walter Flemming first described mitosis (1874), and Theodor Boveri showed the dramatic synchronous separation of chromosomes during the first mitotic division of fertilized sea urchin eggs (1902) (reviewed in (Manchester, 1995; Paweletz, 2001)). The maintenance of an individual organism requires that each daughter cell receives a full and exact complement of genetic information from its mother cell. To ensure the conservation of euploidy (normal number of chromosomes) in eukaryotic cells, genetic information must be accurately copied and transmitted to each daughter cell during every mitotic division cycle. Errors in chromosome segregation (including chromosome non-disjunction and chromosome loss) result in aneuploidy (abnormal number of chromosomes). Phenotypic consequences of these imbalances in chromosome number could be profound and dire. Boveri later postulated that unequal segregation of chromosomes might be a cause for tumor development and birth defects (1914) (reviewed in (Manchester, 1995)). Indeed, aneuploidy is a hallmark of cancer, and the relationship between chromosome missegregation and cancer will be discussed in section 1.2. First, the progression of a normal mitotic cell cycle is reviewed.

The mitotic/somatic cell cycle is divided into 4 phases: G1 (growth/gap), S (DNA synthesis), G2 and M (mitosis). The M phase is subdivided into: prophase, prometaphase, metaphase, anaphase, and telophase. In prophase of metazoans, sister chromatids condense, and the nuclear envelope breaks downs. During prometaphase, sister kinetochores undergo the process of establishing bi-polar orientation with opposite spindle poles. Once bi-polar orientation has been achieved by all kinetochores, the cell enters metaphase when all chromosomes congress to a central position called the metaphase plate. Anaphase then begins and is composed of 2 steps: anaphase A during which sister chromatids separate, and move away from each other toward spindle poles; and anaphase B when the spindle poles separate by moving in opposite directions. In telophase, chromosomes decondense and a new nuclear envelope forms. Finally, cytokinesis occurs when cytoplasm divides and 2 daughter cells are formed. Each step in

the cell cycle has to be executed with high fidelity and coordinated temporally and spatially in order to maintain genetic integrity.

Cell cycle progression is regulated mainly through stage-specific phosphorylation of proteins by cyclin-dependent kinases (CDKs). CDK activity is controlled by both positive and negative regulatory subunits called cyclins, and CDK inhibitors (CKI) (e.g. *SIC1*), respectively. Cyclins are targeted for ubiquitin-mediated degradation at specific stages of the cell cycle. In addition, key proteins are degraded in a cell cycle-specific manner to prevent events such as DNA re-replication and centrosome re-duplication. Otherwise, polyploidy (multiple sets of the normal number of chromosomes) or aneuploidy could result at an unacceptably high level. Proteins targeted for degradation are first ubiquitylated. Ubiquitin (Ub) is an essential 76-amino acid protein that is conserved in all eukaryotes. The polyubiquitylation reaction requires enzymes E1-3. The ubiquitin-activating enzyme (E1) activates Ub by forming unstable thioester bonds with Ub. The ubiquitin-conjugating enzyme (E2) then transfers Ub covalently to the substrate. The ubiquitin-ligase (E3) determines the specificity of the reaction by binding with the substrate and E2. One large class of E3 is cullin-dependent ubiquitin ligase (CDL), which contains a catalytic core that is composed of a cullin and a RING finger protein, and substrate recognition modules. The cullin 'culls' or sorts different substrates for ubiquitylation, and the RING finger protein stabilizes the E2-cullin interaction. Two CDLs crucial for the cell cycle progression are the Skp1p-cullin-F-box protein (SCF) complex or the anaphase promoting-complex/cyclosome (APC/C). Covalent attachment of a polyubiquitin chain on lysine residues of the substrate mediates its recognition and subsequent degradation by the 26S proteasome.

At various points of the cell cycle (e.g. S phase, metaphase), checkpoints exist and serve as surveillance mechanisms to ensure sequential execution of events within the cell cycle, such that the execution of a later event is dependent upon the completion of a prior event (Hartwell and Weinert, 1989). In the event of a spontaneous error or a failure to complete a step, activation of a checkpoint causes transient arrest of cell cycle

progression until the earlier event has been successfully completed, giving the cell more time to correct the error.

Similar to the mitotic cell cycle, the fidelity of DNA transfer in the germ-line during meiosis has to be precise for the maintenance of a species. Meiosis I involves recombination (exchange of DNA) between homologous chromosomes and their segregation, whereas meiosis II, like mitosis, involves segregation of sister chromatids. Defects in meiosis have devastating effects like miscarriage or birth defects, but a detailed discussion of this topic is beyond the scope of this thesis and will not be elaborated upon further.

1.1.2 Budding yeast as a model organism to study the cell and chromosome cycle

Since the cell cycle and chromosome cycle are basic and fundamental cellular processes, the mechanisms and genes involved are highly conserved among eukaryotes (reviewed in (Chan et al., 2005; Kitagawa and Hieter, 2001)). Therefore, studies in model organisms greatly facilitate the understanding of normal human biology and mechanisms of human diseases. For instance, the baker's yeast *Saccharomyces cerevisiae* has multiple experimental advantages, including its short life cycle and ease of genetic manipulation as either haploids or diploids, and the availability of a battery of powerful molecular and biochemical techniques. In addition, the cell cycle of *S. cerevisiae* can be followed by cellular morphology because it divides by budding. Therefore, the size of the daughter bud and the location of nuclear DNA allow assessment of the cell cycle stage within a population of cells. For example, cells in G1 are unbudded; cells in S phase are small budded; and those in G2/M are large budded (Figure 1.1). Indeed, Leland Hartwell, the 2001 Nobel prize laureate in Physiology and Medicine, identified key regulators of the cell cycle in the cell division cycle (*cdc*) mutant collection by isolating mutants that arrest at particular stages of the cell cycle (Hartwell et al., 1974; Hartwell et al., 1970). His studies laid the foundation for our understanding of the eukaryotic cell cycle. However, due to the small size of budding yeast chromosomes, microscopic examination of chromosome behaviors has traditionally been hindered by poor resolution. Cytological

studies in larger eukaryotic cells have provided descriptions of spindle dynamics and chromosome movements (Rieder and Salmon, 1994). More recently, elegant molecular genetic methods such as tagging chromosomes with green fluorescent protein (GFP) fused to a repressor, which binds to operator arrays integrated at a specific location in the genome, have allowed direct observation of chromosome dynamics in wild-type and mutant yeast strains (Straight et al., 1996). Studies in different organisms thus complement each other and often reveal common, conserved cellular mechanisms.

Phenotype screening based on marker stability in budding yeast has provided a powerful approach for detecting and analyzing mutants in genes that act to preserve genome structure. Several collections of yeast mutants were isolated in the last 2 decades by forward genetics (proceedings from phenotype to genotype) with the primary criterion of chromosome or plasmid loss, including the *smc*, *mcm*, *chl*, *cin* and *ctf* collections (Hegemann et al., 1999; Hoyt et al., 1990; Kouprina et al., 1988; Larionov et al., 1985; Larionov et al., 1987; Maine et al., 1984; Spencer et al., 1990). *MIF* and *CST* genes are wild-type loci that induce chromosome instability when overexpressed (Meeks-Wagner et al., 1986; Ouspenski et al., 1999; Sarafan-Vasseur et al., 2002). Assays for gross chromosomal rearrangements (GCRs) have also been developed (Huang et al., 2003; Myung et al., 2001a; Myung et al., 2001b). Many of the *cdc* mutants also exhibit increased chromosome loss and/or mitotic recombination (Hartwell and Smith, 1985). Not surprisingly, different genetic screens have led to the identification of different yet overlapping gene sets important for various steps in the chromosome cycle, including proteins that function at the kinetochores, telomeres, origins of replication, and in microtubule dynamics, sister chromatid cohesion, DNA replication, DNA repair, DNA condensation and cell cycle checkpoints. Genes identified by this strategy have often supported successful identification of functional homologues in other eukaryotes.

In 1996, *S. cerevisiae* became the first eukaryote to have its genome completely sequenced (Bassett et al., 1996; Goffeau et al., 1996), and has subsequently served as a test-bed for the development of genomic, proteomic, bioinformatic and systems biology tools. These advances have greatly facilitated and accelerated the identification and

characterization of genes important for chromosome maintenance. In the following sections, key cellular components and mechanisms pertinent to chromosome segregation in the budding yeast will be discussed, and major differences with other eukaryotes will be highlighted.

1.1.3 Biological processes that affect chromosome stability

1.1.3.1 Kinetochores mediate the attachment with mitotic spindles

Centromere is the region of DNA on a chromosome where the multiprotein kinetochore complex binds, and mediates chromosome-microtubule attachment. Interestingly, the CEN DNA size and composition vary greatly in eukaryotes. The budding yeast CEN DNA consists of only 125bp, with 3 conserved elements – the 8bp non-essential CDEI, the 78-86bp AT-rich CDEII and the 25bp essential CDEIII (Fitzgerald-Hayes et al., 1982) (Figure 1.2B). The CDE elements are flanked by highly phased nucleosome arrays for >2 kb (Bloom and Carbon, 1982). In contrast, the fission yeast *S. pombe* CEN DNA is more similar to higher eukaryotes CEN DNA in terms of size and organization. Fission yeast CEN DNA is 35-100kb, consisting of a 4-7kb central core of non-repetitive sequence (*cnt*) flanked by innermost repeats (*imr*) and outer repeats (*otr*) (Figure 1.2B). Interestingly, some plants, insects and the nematode *Caenorhabditis elegans* contain holocentric chromosomes, where the kinetochores assemble all along the entire length of the chromosome. Mammalian CEN DNA spans 2-4Mb, and is composed of highly repeated α-satellite (171bp) DNA arrays (reviewed in (Chan et al., 2005; Kitagawa and Hieter, 2001; Pidoux and Allshire, 2005; Sharp and Kaufman, 2003; Yanagida, 2005)) (Figure 1.2B). The difference in CEN DNA sizes may be related to the difference in chromosome size: budding yeast chromosomes are ~1Mb, whereas human chromosomes are ~150Mb. The increase in chromosome size in mammals may require larger forces for chromosome movements. Indeed, one kinetochore of budding yeast binds only one microtubule, whereas one kinetochore of fission yeast binds 2-4 microtubules, and one kinetochore of higher eukaryotes binds 10-45 microtubules. Despite the differences in CEN DNA size and the number of microtubules binding to a kinetochore in eukaryotes,

many kinetochore proteins and spindle checkpoint components are conserved (see below). This raises the possibility that metazoan kinetochores are assembled from repeated subunits, where each repeat might resemble the unit module of the yeast kinetochore.

With advances in experimental techniques, the list of kinetochore-associated proteins in model organisms and human exploded in recent years (reviewed in (Chan et al., 2005; Fukagawa, 2004; Houben and Schubert, 2003; McAinsh et al., 2003; Pidoux and Allshire, 2004; Yanagida, 2005)). To date, over 65 *S. cerevisiae* kinetochore proteins have been identified (McAinsh et al., 2003), while the number of the mammalian kinetochore proteins is predicted to be over 100 (Fukagawa, 2004). Kinetochore proteins are classified as structural or regulatory. Structural components physically bridge CEN DNA to spindle MTs (McAinsh et al., 2003). Structural kinetochore components are further classified as inner, central, and outer kinetochore proteins based on their proximity to the CEN DNA (reviewed in (Cheeseman et al., 2002b; McAinsh et al., 2003)). Inner kinetochore proteins interact with centromeric chromatin (e.g. Cse4p (yeast)/CENP-A (human) (see below)), while outer kinetochore mediates interaction with microtubules (e.g. the Dam1p/DASH complex in yeast). Central kinetochore complexes (including the conserved, essential Ndc80p complex in yeast and mammalian cells (Janke et al., 2001; Wigge and Kilmartin, 2001)) link the inner and outer layers. Regulatory proteins, including motor proteins, MT-associated proteins, regulatory proteins such as Ipl1 (yeast)/Aurora B (human) kinase, and spindle checkpoint components, function to regulate kinetochore-MT attachment and to co-ordinate events within the cell cycle (Biggins and Walczak, 2003; McAinsh et al., 2003). Centromeres of higher eukaryotes are visualized as primary constrictions in metaphase (Figure 1.2A). Of particular note is the continued discovery of the conservation of individual kinetochore proteins and the overall organization of protein complexes between higher eukaryotes and yeast. These findings support the concept that the basic building blocks of kinetochores in these organisms may not be as different as first suspected based on the differences in underlying DNA sequence and size.

Despite that CEN DNA sequences vary among eukaryotes, CEN chromatin organization is conserved. DNA of eukaryotic chromosomes is packaged into chromatin. The most basic level of packaging involves 146bp of DNA wrapping in 1.75 turns around a nucleosome, which is composed of an octamer of core histones (2 of each of H2A, H2B, H3 and H4). All eukaryotes contain a centromere-specific nucleosomal structure, and the inner kinetochores contain a specialized histone H3, Cse4p (yeast)/CENP-A (mammals) (Stoler et al., 1995). Centromeres of fission yeast and higher eukaryotes contain transcriptionally inactive heterochromatin and involve epigenetic control. Centromeric silencing in fission yeast and higher eukaryotes depends on the RNA interference machinery (Hall et al., 2002; Volpe et al., 2002), requires the histone methyltransferase CLR4/SU(VAR)3-9, which methlyates lysine 9 of H3 (Lehnertz et al., 2003), and the heterochromatin-binding protein SWI6/HP1, which binds to the trimethylated lysine 9 of H3 (Bannister et al., 2001; Lachner et al., 2001). Mutation of either gene leads to chromosome instability (CIN) (Wang et al., 2000a). Mutation of histone deacetylase (David et al., 2003) or of its target H3 also results in improper establishment of pericentric heterochromatin and leads to aneuploidy (Wei, 1999).

Outer kinetochore proteins include microtubule-associated proteins (MAP) (e.g. Dam1p (yeast), Bik1p (yeast)/CLIP-170 (human), Bim1p (yeast)/EB1 (human)) and motor proteins (e.g. CENP-E (human), Kip3 (yeast)/MCAK (human), Cin8p (yeast)/BIMC (human), dynein), all of which interact with microtubules (Heald, 2000; Hoyt and Geiser, 1996). Microtubules are hollow cylindrical tubes consisting of a heterodimer of α and β tubulins. Microtubules are polar molecules, with a dynamic 'plus' end and a 'minus' end at the microtubule organizing centre (MTOC). The plus end, which will capture kinetochores, undergoes rapid growth and shrinkage by polymerization and depolymerization, respectively, switching between these two states in events called "catastrophes" and "rescues" (Maddox et al., 2000). The minus side of microtubules nucleates at the MTOC, which is called spindle pole body (SPB) in yeast and centrosome in higher eukaryotes. The centrosome is made up of 2 barrel-shaped centrioles surrounded by a matrix of pericentriolar material. The SPB is a disk-shaped

structure made up of three plaques. Besides kinetochore microtubules, there are 2 other types of microtubules: (1) interpolar microtubules which project towards the spindle midzone and interact with chromosome arms or overlap with microtubules emanating from the other pole, through the interaction of microtubule-associated factors and motors; and (2) astral (cytoplasmic) microtubules which project towards the cortex and are instrumental in spindle orientation and positioning (Wittmann et al., 2001). Spindle disassembly is necessary for cytokinesis, and it is thought to occur by depolymerization of the interpolar microtubules from their plus ends.

Unlike other eukaryotes, the yeast nuclear membrane does not break down during mitosis, so the SPBs remain embedded within the nuclear membrane (Hoyt and Geiser, 1996). The nuclear and cytoplasmic faces of the SPB are linked by a central plaque embedded in the nuclear envelope. During S phase, the SPB duplicates, while in prometaphase and metaphase, the SPBs separate (Winey and O'Toole, 2001). Initially, yeast sister kinetochores are both attached to one SPB, the "old" SPB, and this type of kinetochore-microtubule attachment is called 'syntelic attachment' (Tanaka, 2002). The yeast kinetochores are positioned near the SPBs throughout the cell cycle (Jin et al., 2000). On the other hand, kinetochore-microtubule interactions in mammalian cells only take place during mitosis after the nuclear envelope breaks down. At the onset of mitosis, rapidly growing and shrinking microtubules probe the cytoplasm for kinetochores, in a 'search and capture' mechanism that is stochastic and error-prone in nature (Figure 1.3). During the early stage of chromosome orientation, usually only one sister is attached to a pole, and this kind of attachment is called 'monotelic attachment' (Figure 1.4C). Recently, mono-oriented chromosomes in mammalian cells were shown to laterally interact with kinetochore microtubules of bi-oriented chromosomes, which serve as tracks to help the mono-oriented chromosomes to 'hitch a hike' to the spindle equator (Kapoor et al., 2006). This interaction and chromosome movement is dependent on the mammalian kinesin-7 family member CENP-E. This cooperative process increases the likelihood that mono-oriented chromosomes will achieve bi-orientation because the middle of the spindle is rich in microtubules extending from the opposite spindle poles. If

both sister kinetochores attach to the same spindle pole (syntelic attachment, Figure 1.4B), the Ipl1p/Aurora B kinase facilitates re-orientation by phosphorylating kinetochore targets (see below). The spindle checkpoint signal is maintained until sister kinetochores of all chromosomes bi-orient to opposite spindle poles, and this manner of attachment is called 'amphitelic attachment' (Figure 1.4A). When bipolar attachment is achieved, tension generated at the kinetochore by forces from opposite spindle poles and cohesin (see below) has a stabilizing effect on kinetochore microtubules (Ault and Nicklas, 1989; King and Nicklas, 2000). Another type of attachment error occurs when a single kinetochore becomes attached to microtubules from both spindle poles, which is called 'merotelic attachment' (Figure 1.4D). However, this defect is not detected by the spindle checkpoint (Cimini et al., 2001). Nevertheless, merotelic attachment rarely cause chromosome missegregation in mammals because the kinetochores usually make enough bipolar attachments to pull the sister chromatids to opposite poles. Interestingly, budding yeast chromosomes do not undergo congression to the metaphase plate (O'Toole et al., 1999), but form two lobes that lie on either side of the spindle midzone (Goshima and Yanagida, 2000; He et al., 2000). Both yeast and mammalian centromeric chromatin undergo transient separation before cohesion degradation at anaphase (Goshima and Yanagida, 2000; He et al., 2000; Shelby et al., 1996; Tanaka et al., 2000).

1.1.3.2 Mitotic spindle checkpoint

Spindle checkpoint components present at the kinetochore in turn monitor MT attachment and/or tension and sense the completion of metaphase, when bi-polar attachment of all chromosomes has been achieved (Lew and Burke, 2003; Tanaka, 2002). *BUB1* and *3* (budding uninhibited by benzimidazole) and *MAD1*, *2*, and *3* (mitotic arrest deficient) are checkpoint genes first identified in yeast in genetic screens that looked for mutants that fail to detect kinetochore-microtubule attachment errors caused by microtubule-depolymerizing drugs. As a result, these mutants do not arrest before anaphase despite the presence of chromosomes not properly attached to the spindle, which leads to increased chromosome missegregation and increased sensitivity to

microtubule-depolymerizing drugs (Hoyt et al., 1991; Li and Murray, 1991; Weiss and Winey, 1996). These findings lead to the description of a spindle checkpoint pathway that detects kinetochores that are not attached to microtubules or are not under tension (Yu, 2002). Even a single unattached kinetochore can delay segregation of already aligned chromosomes (Rieder et al., 1995). Mammalian and yeast checkpoint proteins were shown to localize to kinetochores that have not yet attached to the mitotic spindle (reviewed in (Cleveland et al., 2003)).

The exact sequence of spindle checkpoint sensing and signaling is not completely understood, but probably involves amplification of diffusible signals. BUB1 is a kinase that is known to phosphorylate MAD1 and BUB3, and BUB3 in turn binds to and activates BUB1. BUBR1 is the mammalian homolog of yeast Mad3p, but it has evolved to contain a kinase domain that is not present in Mad3p. Localization of BUBR1 to the kinetochore is dependent on its interaction with BUB3, and BUBR1 is postulated to act as a mechanosensor. Interaction of BUBR1 with the kinesin-like protein CENP-E stimulates BUBR1 kinase activity is stimulated (Chan et al., 1999; Mao et al., 2003). CENP-E is thought to act as a tension sensor and increases the efficiency of microtubule capture; it is able to activate the spindle checkpoint in the presence of mono-oriented chromosomes (reviewed in (Compton, 2006)). Yeast Mps1p (monopolar spindle) was originally identified to be involved in SPB duplication, but was later found to have a role in the spindle checkpoint by phosphorylating Mad1p and recruiting other checkpoint components to unattached kinetochores (Weiss and Winey, 1996 (Winey and Huneycutt, 2002). MAD1 binds to and recruits MAD2 to the kinetochore (Chen et al., 1999). MAD2 binds to CDC20/SLP1/FIZZY/P55, the substrate specificity factor of the APC/C, inhibiting its ubiquitin ligase activity (Yu, 2002). Interestingly, MAD1 and CDC20 contain a similar domain to interact with MAD2, so their interaction with MAD2 is mutually exclusive (Luo et al., 2002). MAD1-MAD2 binding may catalyze a conformational change in MAD2 so that it is compatible for CDC20 binding. MAD1 hyperphosphorylation may be required to dissociate MAD2 from MAD1 for CDC20 binding. BUBR1 also directly binds CDC20 and APC/C components (Chan et al., 1999).

In addition, BUBR1 forms a stoichiometric mitotic checkpoint complex (MCC) with BUB3, MAD2 and CDC20 (Sudakin et al., 2001).

Vertebrate MAD1 and MAD2 are displaced from kinetochores with proper MT attachments. MAD2 phosphorylation may be involved in silencing of the checkpoint (Wassmann et al., 2003). The microtubule motor dynein has been implicated in the highly dynamic turnover of checkpoint components and in checkpoint silencing. Checkpoint proteins like MAD2 and BUBR1are thought to be released from the kinetochore through dynein-dependent transport via spindle MTs, and also via direct release of proteins ((Howell et al., 2001); reviewed in (Chan et al., 2005)). Zw10, Zwilch and Rod which were first identified in *Drosophila* are also found in higher eukaryotes but not in yeast. They form the RZZ complex that is required for dynein localization ((Wojcik et al., 2001); reviewed in (Karess, 2005)).

Even when kinetochore-microtubule connections are intact, a lack of tension at the kinetochore can activate the checkpoint (Stern and Murray, 2001). The Aurora B/IPL1 kinase works with INCENP/SLI15 as a tension sensor to promote turnover of syntelic attachments; it works by destabilizing kinetochore-microtubule attachments through phosphorylation of the microtubule-destabilizing mitotic centromere-associated kinesin (MCAK) in vertebrate, analogous to Dam1p in yeast (Andrews et al., 2004; Cheeseman et al., 2002a; He et al., 2001; Kang et al., 2001; Lan et al., 2004; Stern and Murray, 2001; Tanaka, 2002). Aurora B may also phosphorylate BUBR1 and MPS1 for checkpoint signaling (Biggins and Murray, 2001). Aurora B/IPL1, INCENP/SLI15 and SURVIVIN/BIR1 are chromosomal passenger proteins that dynamically appear first in the inner centromere region between sister kinetochores, then move onto the elongating spindle in anaphase, and finally concentrate at the spindle midzone. Some structural kinetochore proteins (e.g. the NDC80 complex) are also required for a functional checkpoint, which may first require the assembly of a functional kinetochore (Gardner et al., 2001; He et al., 2001; Janke et al., 2001).

1.1.3.3 Sister chromatid cohesion

At the end of M phase in fission yeast and metazoan cells, or during late G1 in budding yeast, the cohesin complex, the "molecular glue" that holds sister chromatids together is loaded onto unreplicated DNA by the loading complex (SCC2, SCC4) (Ciosk et al., 2000). Cohesin is composed of 4 subunits: SCC1/MCD1/RAD21, SCC3/IRR1 (SA1 and SA2 variants in human), SMC1 and SMC3 (structural maintenance of chromosomes). SMC1 and SMC3 contain globular ends with a hinge dimerization domain and a head ABC-type ATPase domain, and a coiled-coil domain (Losada et al., 1998; Michaelis et al., 1997) (Figure 1.5A). They form intra-molecular coiled coils by folding back on themselves, forming rod shaped proteins with the globular ATPase head at one end and the heterodimerization domain at the other (Haering et al., 2002). SMC1 and SMC3 dimerize through the hinge domain. The C-terminal and N-terminal ends of SCC1 bind to the head region of SMC1 and SMC3, respectively, and SCC3 binds to the complex through SCC1 (Haering et al., 2002; Haering et al., 2004). ATP hydrolysis is needed for cohesin loading onto DNA. Cohesion is first established while sister chromatids are replicated in S phase and is maintained until anaphase. A working model for cohesin is that it forms a ring structure that wraps around the sister chromatids in a topological association (Figure 1.5B). Cohesion is established along the whole length of chromosomes, but is concentrated at the pericentromeric regions, spanning 50-60 kb, and at convergent transcription sites (intergenic AT-rich region) (Glynn et al., 2004). Kinetochores stimulate the recruitment of cohesin, but this ability is not necessarily dependent on the centromere sequence *per se* (Megee et al., 1999; Weber et al., 2004). Cohesin recruited by the kinetochore may move to flanking regions, or kinetochores may influence surrounding chromatin to recruit cohesin. In *S. pombe*, the enrichment of cohesin at peri-centromeric regions depends on the binding of the HP1-like protein SWI6 to histone H3 that is trimethylated on lysine 9 by CLR4 (Bernard et al., 2001; Nonaka et al., 2002). In contrast, the nucleosome-remodeling complex RSC has been implicated in the establishment of chromatid arm cohesion only (Huang et al., 2004; Huang and Laurent, 2004). Cohesin may also be redistributed to different places during transcription.

The establishment of cohesion is not completely understood, but is thought to require the acetyltransferase ESCO1/CTF7 (Skibbens et al., 1999; Toth et al., 1999), a variant replication factor C (RFC-CTF18, CTF8, DCC1) (Mayer et al., 2001; Mayer et al., 2004), a polymerase α–interacting protein CTF4 (Hanna et al., 2001; Petronczki et al., 2004), MRE11 (Warren et al., 2004a), and the helicase CHL1 (S, 2000; Skibbens, 2004). Additionally, PDS5 is required to maintain cohesion at centromere proximal and distal sequences (Hartman et al., 2000).

Cohesion sterically forces a back-to-back orientation to sister centromeres and promotes bi-orientation (Tanaka et al., 2000). Cohesion resists the force exerted by spindle microtubules emanating from opposite spindle poles on sister kinetochores, thereby generating tension (He et al., 2000). Cohesin is also recruited to double strand break (DSB) sites in S/G2/M, and this recruitment requires SCC2 (Strom et al., 2004; Unal et al., 2004). Damage-induced cohesion may be important for DSB repair by holding broken ends close to homologous sequences, thereby facilitating homologous recombination.

In budding yeast, cohesin remains associated with whole chromosomes until anaphase, whereas in mammalian cells, cohesins dissociate from chromosome arms in prophase in a Polo-like kinase 1 (PLK1)-dependent manner (Hauf et al., 2005). PLK1 is activated as CDK levels rise at the onset of M phase, and PLK1 promotes arm cohesin dissociation through phosphorylation of the SCC3-like subunits, SA1 and SA2. However, cohesin at centromeres persists until anaphase. This retention is dependent on shugosin (SGO1/MEI-S332 in *Drosophila*) (Hauf et al., 2005). Protein phosphatase 2A (PP2A) associates with SGO1 and is required for protection of centromeric cohesion by dephosphorylation of cohesin (Kitajima et al., 2006; Riedel et al., 2006). Before the onset of anaphase, an inhibitory chaperone, securin/PDS1, binds to the separase/ESP1, thereby inhibiting it but also priming its activity, possibly by promoting its nuclear localization or protecting it from degradation (Ciosk et al., 1998). When all chromosomes align at the metaphase plate, APC/C^{CDC20} targets securin for degradation (Cohen-Fix et al., 1996). Separase is then released, and it cleaves the cohesin subunit SCC1, leading to the

breakdown of cohesion and the beginning of anaphase where sister chromatids move to opposite spindle poles (Michaelis et al., 1997; Uhlmann et al., 1999; Uhlmann et al., 2000) (Figure 1.6). PLK1 phosphorylation of SCC1 enhances its cleavage by separase. APC/C also degrades cyclins, lowering CDK activity and promoting exit from M phase.

In meiosis, sister chromatids segregate to the same pole during meiosis I and bi-orientation of sister chromatids is suppressed by monopolin (MAM1, CSM1, and LRS4) (Toth et al., 2000). The *SCC1* subunit of the meiotic cohesin complex is replaced by REC8. The paired homologous chromosomes are held together at chiasmata that are formed during recombination. In meiosis I, REC8 present on chromosomal arms is cleaved, thereby resolving chiasmata, while centromeric REC8 is protected during meiosis I by SGO1. In anaphase I, homologous chromosomes segregate to opposite poles (Buonomo et al., 2000; Klein et al., 1999). Meiosis II resembles mitosis with sister chromatids segregating to opposite poles.

1.2 Chromosome instability (CIN) and cancer

1.2.1 Aneuploidy is a hallmark of cancer

Two types of genetic instability are observed in cancers: (1) instability at the nucleotide level, especially at microsatellite repeats (MIN, microsatellite instability) and (2) instability involving whole chromosomes or large portions of chromosomes (CIN, chromosomal instability). The majority of solid tumors exhibit genomic instability at the chromosomal level (Rajagopalan et al., 2003) (e.g. 85% colon cancers exhibit CIN and 15% exhibit MIN), and the occurrence of MIN and CIN usually does not overlap. MIN tumors exhibit a 1000-fold increase in point mutation rate, in particular accumulation of length alterations in simple repeated sequences (units of 1-3bp), whereas CIN tumors exhibit increased rates of chromosome missegregation, leading to the generation of aneuploid cells.

Changes in whole chromosome number or structural rearrangement of chromosomes are commonly observed in tumors (Cahill et al., 1998; Rajagopalan et al., 2003). Large-scale chromosomal gains or losses can be detected by flow cytometry in a

cell population, and chromosomal rearrangements (≥1 Mb) in an individual cell can be revealed by comparative genomic hybridization (CGH), multiplex fluorescence in situ hybridization (M-FISH) or spectral karyotyping (SKY). Aneuploidy and chromosomal rearrangements may play a role in tumor progression by causing an imbalance in the dosage of many genes at once. For instance, chromosome loss or partial chromosomal deletion results in loss of heterozygosity (LOH), which can lead to reduced expression of tumor suppressor genes located in the region, or uncover recessive mutations in the remaining allele. Chromosome gain or partial amplification can amplify oncogenes within the region. Overexpression of oncogenes and/or reduced expression of tumor suppressor genes would create a growth advantage through increased proliferation or reduced cell death, and result in clonal expansion. This scenario would repeat for each new growth-promoting mutation, and constitutes the basis of the theory of multi-step carcinogenesis (Boland and Ricciardiello, 1999). Identifying recurrent chromosomal aberrations at specific loci in cancer cells may provide clues for the identification of oncogenes and tumor suppressor genes. An average cancer of the colon, breast, pancreas or prostate loses 25% of its alleles on a chromosome (Lengauer et al., 1998). Some primary breast cancers exhibit >20 regions with LOH when analyzed with microsatellite markers (reviewed in (Loeb, 2001)). Interestingly, analysis of polymorphic markers in 5 chromosomes in colorectal cancer cell lines indicated that mechanisms underlying LOH were chromosome-specific. Partial losses were predominant for some chromosomes, while whole chromosome losses were responsible for others. For partial loss, gross chromosomal rearrangement (GCR), not mitotic recombination, was the predominant mechanism. For whole chromosome loss, mitotic nondisjunction was responsible, and reduplication of the remaining chromosome was followed in some cases. LOH occurs at different frequency at different regions of each chromosome, implying that LOH is coupled with clonal selection for loss of tumor suppressor genes (Thiagalingam et al., 2001).

1.2.2 Relationship between a *state* of aneuploidy and an increased *rate* of chromosome instability (CIN)

Observation of a *state* of aneuploidy in cancer cells does not directly imply an increased *rate* of CIN, because aneuploidy may be caused by factors other than CIN. For instance, aneuploidy can be caused by chromosome missegregation in a single cell division (at a normal rate), followed by clonal expansion of the aneuploid cell due to some selective advantage; or, the survival of an aneuploid cell can result from a defect in the apoptotic pathway. However, an analysis of 98 aneuploid gastric tumors by FISH and flow cytometry showed intratumoral variations in chromosome copy number; this population heterogeneity suggests that aneuploidy is associated with CIN (Furuya et al., 2000). In another study, 16 out of 25 pancreatic carcinomas showed karyotypically related clones, signifying monoclonal origin and evolutionary variation (Gorunova et al., 1998). Similarly, FISH analysis of aneuploid colorectal cancer cell lines for 6-7 generations showed that losses or gains of chromosomes occurred at $>10^{-2}$ per chromosome per generation, which is 10-100 times more often than in diploid cancers of the same histological subtype (Lengauer et al., 1997). These observations are consistent with the hypothesis that aneuploidy in cancers is caused by CIN. To further delineate the relationship between CIN and aneuploidy, Lengauer et al. introduced an extra chromosome into a diploid cell line and fused two diploid lines to artificially create aneuploid cell lines. These lines, unlike natural CIN tumor lines, did not display CIN, suggesting aneuploidy *per se* does not cause CIN (Lengauer et al., 1997).

1.2.3 CIN occurs at early stage of cancer, and can be a driving force in tumorigenesis

The timing of CIN occurrence during tumorigenesis, and the role of CIN in tumorigenesis have been highly debated. One hypothesis postulates that for a cancer cell to accumulate the 6-10 genetic alterations required for its proliferation and survival, it must be genetically unstable, thereby suggesting that genetic instability occurs at the early stage of cancer, and represents an important step in the initiation and/or progression

of tumorigenesis (Davies et al., 2002; Hartwell et al., 1997; Parsons et al., 2005). In support of this hypothesis, aneuploidy has been observed in small benign colorectal tumors and uterine leiomyomas (El-Rifai et al., 1998), and >90% of early colorectal adenomas studied (1-3 mm in size) have allelic imbalance (Bardi et al., 1997; Bomme et al., 1998; Lengauer et al., 1998; Shih et al., 2001). The prevalence of aneuploidy in benign colorectal tumors is less than that in cancers, but the deviations from a normal karyotype increase as the tumors enlarge in size (Bardi et al., 1997; Shih et al., 2001). Aneuploidy is associated with poor prognosis and correlates with the severity of the disease (Rajagopalan and Lengauer, 2004a). CIN may serve as an engine of both tumor progression and heterogeneity (Jallepalli and Lengauer, 2001; Vogelstein and Kinzler, 2004).

1.2.4 Genetic basis of CIN in cancer

1.2.4.1 Cancer-prone syndromes

Germline mutations causing genomic instability, particularly in genes involved in DNA damage recognition and repair, are now recognized as being important predisposing conditions for cancer (reviewed in (Hoeijmakers, 2001; Levitt and Hickson, 2002; Vogelstein and Kinzler, 2004)). For instance, the less common MIN phenotype in colorectal cancer was first described in 1992. The similarity of phenotype in MIN tumor cells and DNA mismatch repair (MMR) mutants in yeast and *E. coli* rapidly led to the identification of mutations in MMR genes (based on a candidate gene approach) in hereditary nonpolyposis colon cancer (HNPCC), which account for 3% of colon cancer (Fishel et al., 1993; Leach et al., 1993; Papadopoulos et al., 1994; Strand et al., 1993). Another example is provided by xeroderma pigmentosum (XP) patients whose cells have defects in the nucleotide excision repair (NER) pathway and high mutation rates due to pyrimidine dimers; these patients develop skin cancers at high rates. Table 1.1 summarizes germline mutations in genes involved in maintaining genomic integrity that are known to underlie cancer-prone syndromes, and lists the function/pathway of the encoded protein, evolutionary conservation between yeast and human genes, and the

mode of inheritance of the diseases. These "caretaker" genes, unlike conventional oncogenes and tumor suppressor genes which directly control cell birth and death, affect the integrity of the genome and control the mutation rate.

Interestingly, despite the ubiquitous expression of these genome maintenance proteins, mutations in these genes lead to tissue-specific tumor predispositions. In addition, somatic mutations in these same genes may not occur in sporadic tumors of the same type (Sieber et al., 2003). In fact, although tumor types from one specific organ have a tendency to share mutations in certain genes or in different genes within a single pathway, they rarely have uniform genetic alterations, demonstrating the heterogeneous nature of cancer (Boland and Ricciardiello, 1999).

In contrast to MIN, the genetic basis of the commonly observed CIN in sporadic cancers is not well understood. Cytologically, many cancer cells exhibit aberrant cell architecture, including abnormal centrosomes, multipolar spindles, and breakage-fusion-bridge cycles (Gisselsson, 2003; Saunders et al., 2000). Intuitively, CIN, and therefore aneuploidy, can be caused by errors in chromosome segregation. Many cellular mechanisms are responsible for proper chromosome transmission, such as DNA replication, sister chromatid cohesion, centrosome duplication and segregation, kinetochore-microtubule attachment, mitotic spindle checkpoint, DNA condensation, DNA repair and cytokinesis (Figure 1.7). One approach to determine the genetic basis of CIN in tumors is to identify mutations in genes known to be important for chromosome segregation in human cells, or in human homologues of CIN genes discovered in model organisms, which serve as cross-species candidate CIN genes.

1.2.4.2 Mutations in mitotic spindle checkpoint

Many CIN genes were originally identified and studied in model organisms such as yeast, and later found to have conserved functions and cancer relevance, including the genes listed in Table 1.1 and mitotic spindle checkpoint components. One important class of cancer relevant genes first discovered in yeast are the spindle checkpoint proteins, which monitor kinetochore-MT attachment and alert the cell to potential chromosome

segregation errors by specifically binding to kinetochores that have not attached to MTs. *BUB1* and *BUB1B* (encoding BUBR1) are mutated in colorectal tumors and several other cancer types at a low frequency (Cahill et al., 1998; Gemma et al., 2000; Ohshima et al., 2000; Ru et al., 2002; Shichiri et al., 2002) (Table 1.2). Epigenetic silencing through promoter hypermethylation of *BUB1* and *BUB1B* has also been found in aneuploid colon carcinoma (Shichiri et al., 2002). The recent report that germline biallelic mutations in the spindle checkpoint gene, *BUB1B*, is associated with mosaic variegated aneuploidy (MVA) and inherited cancer predispositions strongly supports a causal link between CIN and cancer development (Hanks et al., 2004). Human homologues of other yeast mitotic checkpoint proteins (*MAD1, 2, 3* and *BUB1, 3*) then became candidate CIN genes and were subsequently tested for mutations in tumors. *MAD2* is mutated in gastric cancers (Kim et al., 2005), and downregulated in cancer cell lines (Li and Benezra, 1996; Michel et al., 2001; Wang et al., 2002b). However, no mutation in other spindle checkpoint genes was found (Cahill et al., 1999), suggesting they could be altered by misregulation or that other CIN genes could be affected. For example, *MAD1* binds to the Tax oncoprotein from the human T-cell leukaemia virus type 1 (HTLV-1) and prevents *MAD2* activation (Jin et al., 1998). LATS1/WARTS (large tumor suppressor homologue 1), a paralog of BUB1, is a mitosis-specific serine/threonine kinase that interacts with MOB1 (Mps1-One binder) and may play a role in the mitotic exit network, cytokinesis, and coordination between cell proliferation and apoptosis. Downregulation of LATS1 has been found to contribute to tumor formation (Bothos et al., 2005; Hergovich et al., 2006; Lai et al., 2005; Yang et al., 2004). The recent survey of CIN colorectal tumors for mutations in 100 human homologues of CIN genes identified in yeast and flies, including 6 kinetochore/spindle checkpoint proteins, represents a stunning proof of principle: Wang et al. identified 5 new CIN cancer genes, including the kinetochore/spindle checkpoint genes *Rod*, *Zw10*, and *Zwilch* (Table 1.2), which together account for ~2% of the mutational spectrum in colorectal cancers (Wang et al., 2004b). These proteins function together as the RZZ complex to recruit the dynein-dynactin complex and MAD1-MAD2 to the kinetochore. The RZZ complex is thought to have a role in spindle checkpoint

activation and inactivation (reviewed in (Karess, 2005)). The infrequent mutation rate in spindle checkpoint genes raises the possibility that CIN in cancer cells could be caused by mutation of any one of many genes involved in chromosome segregation, including other kinetochore proteins. Because of the large number of candidate genes that could be mutated to give a CIN phenotype, the frequency of a particular mutation may be low, as is observed for the spindle checkpoint genes.

Interestingly, analysis of the mitotic index of cancer cell lines in response to microtubule-disrupting reagents showed that the mitotic spindle checkpoint is often impaired, but not completely absent (Gascoyne et al., 2003; Saeki et al., 2002; Takahashi et al., 1999). Absence of the checkpoint proteins MAD2, BUB3, or BUBR1 in mice and *C. elegans* yields early embryonic lethality (Babu et al., 2003; Baker et al., 2004; Dai et al., 2004; Kalitsis et al., 2000; Kitagawa and Rose, 1999; Kops et al., 2004; Michel et al., 2001). Mouse models of defective checkpoints, where a checkpoint component is reduced in concentration, result in a small increase in cancer susceptibility. For example, mice heterozygous for *BUB1B* or *BUB3* are more prone to colorectal or lung tumors after challenge with carcinogen (Babu et al., 2003; Dai et al., 2004). RAE1, which has homology to BUB3, mediates nuclear export of mRNA through nuclear pores during interphase and binds to BUB1 at kinetochores during mitosis. Heterozygous *RAE1* mice have increased aneuploidy and develop lung tumors at an increased rate (Babu et al., 2003). 28% of heterozygous *MAD2* mice develop lung tumors at high rates after long latencies (Babu et al., 2003; Baker et al., 2004; Dai et al., 2004; Kitagawa and Rose, 1999; Kops et al., 2004; Michel et al., 2001). Additionally, some tumor suppressor genes affect the levels of checkpoint components at the transcript level. For example, BRCA1 regulates *MAD2* transcript levels directly by binding to its promoter, and mouse cells that express mutant *BRCA1* have decreased expression of MAD2, BUB1, BUBR1 and Zw10 (Wang et al., 2004a). A single nucleotide polymorphism in *MAD1* that affects MAD2 binding and recruitment of MAD2 to kinetochores has recently been found in a breast cancer cells (Iwanaga et al., 2002). These results suggest that biallelic expression of

checkpoint components is important for their function, and a weakened checkpoint might facilitate tumorigenesis.

1.2.4.3 Misregulation of kinetochore proteins

Mutations in genes encoding structural kinetochore proteins have not yet been identified in cancer cells, possibly because most have not been examined. Since 5 out of 8 (*BUB1*, *BUBR1*, *Rod*, *Zw10*, *Zwilch*, *CDC4*, *MRE11A*, and *Ding*) CIN genes known to be mutated in CIN colon cancers encode kinetochore or spindle checkpoint proteins (Cahill et al., 1998; Rajagopalan et al., 2004; Wang et al., 2004b), the kinetochore offers a logical choice for mutational testing. Furthermore, the ~100 predicted human genes that encode kinetochore components comprise a large mutational target that could be mutable to a CIN phenotype (Fukagawa, 2004). For example, kinetochore proteins constitute a significant portion of the collection of chromosome transmission fidelity (*ctf*) mutants identified in a classical genetic screen in yeast (9 out of the 24 CTF genes cloned and characterized to date; see Table 2.1) (Spencer et al., 1990). Systematic mutational analysis of kinetochore genes in various cancers would shed light on the frequency of specific mutations in kinetochore genes and their potential role in tumorigenesis.

On the other hand, expression studies have suggested a correlation between overexpression of several kinetochore proteins and cancer (Table 1.2). CENP-A is overexpressed and mistargeted in colorectal cancer tissues (Tomonaga et al., 2003). Overexpressed CENP-A localizes to the entire chromosome and dissociates from native centromeres. This causes a subset of kinetochore proteins to be recruited to non-centromeric chromatin, leading to ectopic formation of pre-kinetochore complexes, potentially depleting some kinetochore components, thereby disrupting the native centromere-kinetochore complex and causing CIN (Van Hooser et al., 2001). Another inner kinetochore protein, CENP-H, which is important for kinetochore organization, is also upregulated in colorectal cancer tissues (Tomonaga et al., 2005). Transfection of a CENP-H expression plasmid into diploid cell lines induces aneuploidy and increases the incidence of aberrant micronuclei, suggesting that upregulation of CENP-H can lead to a

CIN phenotype. In addition, Aurora B (AIM-1) and INCENP, two chromosome passenger proteins that localize to the kinetochore from prophase to metaphase and to the mitotic spindle in cytokinesis, are upregulated in tumor cell lines (Adams et al., 2001; Sorrentino et al., 2005; Tatsuka et al., 1998). Aurora B phosphorylation is required for chromosome condensation, controlling MT dynamics including destabilizing syntelic MT attachments to kinetochores, and regulation of cytokinesis (reviewed in (Giet et al., 2005)). Aurora B-overexpressing cells exhibit CIN and contain multinuclei, and injection of these cells into nude mice induces tumor growth (Ota et al., 2002; Sorrentino et al., 2005). Conversely, a block of Aurora B expression increases the latency period and reduces the growth of thyroid anaplastic carcinoma cells (Sorrentino et al., 2005), supporting a causative link between Aurora B expression and cancer initiation or progression. Similarly, overexpression of CENP-F (mitosin) correlates with tumor proliferation and metastasis; hence, CENP-F is suggested to be a potentially valuable proliferation marker for diagnosis and prognosis (Clark et al., 1997; de la Guardia et al., 2001; Erlanson et al., 1999; Esguerra et al., 2004; Liu et al., 1998; Shigeishi et al., 2005). CENP-F is a cell cycle-regulated protein that associates with the outer kinetochore in M phase and is rapidly degraded upon completion of mitosis. It associates preferentially with kinetochores of unaligned chromosomes, and may play a role in the spindle checkpoint (Chan et al., 1998; Yang et al., 2005; Yang et al., 2003).

The evidence above suggests that overexpression of kinetochore components may contribute to tumor progression by driving CIN. Stoichiometric expression of kinetochore components may be important for functional kinetochore assembly and the dosage may be crucial for spindle checkpoint signalling. However, it is possible that overexpression is a consequence rather than a cause of dysfunctional cell cycle regulation in carcinogenesis. To delineate the causal relationship between kinetochore protein mutation/misregulation and cancer development, further functional studies must be performed in diploid cell lines or mouse models to investigate whether kinetochore mutation/misregulation leads to CIN or cellular transformation.

1.2.4.4 Additional examples of mutations in genes involved in chromosome segregation

Systematic mutation testing of candidate CIN genes in colorectal cancer also identified somatic mutations in *CDC4*, *MRE11A*, and *Ding* (Rajagopalan and Lengauer, 2004b; Wang et al., 2004b). Known mutations together account for only ~20% of the CIN mutational spectrum of colon cancer. CDC4 is a conserved F-box protein that functions in the SCF E3 ubiquitin ligase, involved in regulating the G1-S cell cycle checkpoint. Cyclin E, an oncoprotein and a known target of CDC4 in mammalian cells, is overexpressed when CDC4 is defective (Rajagopalan et al., 2004; Strohmaier et al., 2001). MRE11A is involved in sister chromatid cohesion and DSB repair. Germline mutations in MRE11A are responsible for ataxia telangiectasia-like syndrome (see Table 1.1). Ding is uncharacterised, but its C-terminus is homologous with the yeast securin, PDS1 (Wang et al., 2004b). The human securin, also known as pituitary tumor transforming gene 1 (PTTG1), is overexpressed in some cancers and its expression level is correlated with the invasiveness (Pei and Melmed, 1997; Zhang et al., 1999; Zou et al., 1999). Aurora A kinase (STK15/BTAK) at the centrosome is amplified and overexpressed in cancers (Zhou et al., 1998), and is associated with centrosome amplification, tetraploidization and aneuploidy. Indeed, approximately 80% of invasive tumors show centrosome abnormalities in size and number, and a significant proportion of solid tumors are tetraploid, such as in Barrett's oesophagus and ulcerative colitis (Rajagopalan and Lengauer, 2004a).

Familial polyposis coli (FAP) patients and over 85% of colorectal tumors have somatic mutations of adenopolyposis coli (*APC*) (see Table 1.1), and this is the earliest event in sporadic colorectal tumor. Most *APC* mutations lead to loss of the C-terminal domain that interacts with microtubules (and binds components of checkpoint), failure to degrade beta-catenin, and have been postulated to contribute to CIN (Fodde et al., 2001a; Fodde et al., 2001b; Green and Kaplan, 2003; Kaplan et al., 2001). However, some cells with *APC* mutations undergo polyploidization in whole-genome increments instead of

aneuploidy, and some MIN cell lines with *APC* mutations remain diploid, so the exact significance of *APC* mutation in CIN is still unclear (Fodde et al., 2001b).

The genetic basis for CIN is just beginning to be understood (Figure 1.8). The daunting task of screening the remaining hundreds of candidate CIN genes lies ahead. Systematic mutation screening in candidate genes in signalling pathways have yielded success (Davies et al., 2002; Parsons et al., 2005). However, mutations in CIN genes could be functional (leading to CIN) or merely "passenger" mutations that accompany tumorigenesis. The prevalence of point mutations in sporadic CIN colorectal cancers was determined to be approximately one nonsynonymous somatic change per Mb of tumor DNA, which is consistent with a rate of mutation in normal cells (Wang et al., 2002a). These data suggested that most sporadic CIN colorectal cancers do not display MIN or instability at the nucleotide level (Wang et al., 2002a). These results have significant implications for the interpretation of somatic mutation observations in candidate tumor-suppressor genes, suggesting these are likely to be of functional relevance.

1.2.4.5 Therapeutic implications

Designing effective therapeutics for cancer will rely first on understanding the genetic basis of cancer, including the cause of CIN and its contribution to human cancers. This will involve identifying the mutational spectrum and analyzing expression profiling of candidate CIN genes, and determining their functional consequence. Such knowledge could have several important practical applications. First, it would allow sub-classification of tumors based on the specific CIN gene mutation or misregulation, which could have implications for improved diagnostics, prognosis, or predictions of response to therapy. For example, overexpression of either Aurora A or B kinases causes CIN. Inhibition of aurora kinases results in a 98% reduction in tumor volume in nude mice injected with human leukemia cells (Harrington et al., 2004). One complication in studying cancer is that cancer is a heterogeneous disease, with many different genes mutated at low frequencies in different tumors and in sub-population of cells within individual tumors. Genetic instability is expected to contribute to heterogeneity.

However, if a defined subset of CIN genes represents the major CIN mutational targets in cancer, they may provide a rationale for therapeutic design to selectively kill tumor cells carrying CIN mutations (Hartwell et al., 1997; Hartwell and Weinert, 1989). While CIN may be important in the development of a tumor, understanding the genetic and phenotypic differences between CIN tumor cells and normal cells may define an "Achilles heel" in CIN tumors (relative to adjacent normal tissue), allowing selective killing of tumor cells (Hartwell et al., 1997; Hartwell and Weinert, 1989).

One approach is to identify drug targets that are specifically present and essential for the viability of cancer cells, but are not present in normal cells. For instance, fusion oncoproteins are generated by cancer-associated chromosomal translocations, such as the fusion of the breakpoint cluster region (BCR) with Ableson murine leukemia viral oncogene homologue (ABL) in chronic myelogenous leukaemia (CML). However, it is difficult to identify drugs that can discriminate a protein between its normal and pathogenic state. Imatinib mesylate (produced by Glivec) inhibits both BCR-ABL and ABL, and several other kinases. On the other hand, a drug screening strategy aimed at restoring the function of tumor suppressor genes and defective apoptotic pathways, though genetically different in tumor and cancer cells, might turn out to be a suboptimal approach, because it will be unlikely to identify drugs that can reactivate genes/proteins to restore normal protein function (Sager and Lengauer, 2003).

Context-driven therapeutics depend on the identification of conditions in which the requirement for a particular target is enhanced in the context of cancer cells compared with normal cells, which can be due to intrinsic (e.g. genetic or epigenetic) or extrinsic (microenvironmental) changes, or both. Most anticancer drugs in use today affect targets present in both normal and cancer cells (Kaelin, 2005). One scenario of differential requirements that can be exploited is the phenomenon of synthetic lethality (SL). Synthetic lethality occurs when mutations in two different genes, while non-lethal as mutations, become lethal when combined in a cell as a double mutant. By targeting a specific gene in a cancer cell containing another known mutation could lead to synthetic lethality and selective killing. In this regard, an on-going effort in model organisms such

as yeast has been to construct a comprehensive synthetic lethal genetic interaction map. By definition, these second-site loss-of-function mutations (which are otherwise non-lethal in the CIN-gene wild-type cells) define proteins that, when reduced in activity, cause lethality in the reference CIN mutant. If the synthetic lethal interactions are conserved in humans, these second-site genes may suggest cross-species candidate proteins in humans that when inhibited (e.g., by a drug) would specifically kill tumor cells relative to normal cells. Synthetic lethal interactors that are common to multiple CIN mutants may suggest candidate drug targets that are effective for selective killing CIN cancers with different CIN gene mutations. If kinetochore proteins, for example, turn out to represent a significant fraction of the CIN mutational spectrum in cancer, it is conceivable that second-site genes will exist that are synthetically lethal in combination with an entire set of the kinetochore gene mutations, and therefore provide common drug targets for killing a broad spectrum of CIN cancers. While the relevance of kinetochore dysfunction to cancer still needs to be verified, defects in human mismatch-repair genes, *MLH1*, *MSH2*, and *PMS2*, are known to confer predisposition to colon cancer. Synthetic lethality data in yeast show that they are lethal in combination with mutations in DNA polymerase δ and ε that are otherwise viable. These latter enzymes catalyze DNA replication, and in the process they proofread the growing strand of DNA for errors. The results in yeast reveal the possibility of selectively killing MIN cancer cells by interfering with DNA polymerases (reviewed in (Friend and Oliff, 1998)). Recently, RNA interference screens have been applied in mammalian cells to decipher synthetic lethality relationships and identify novel targets (Ngo et al., 2006; Willingham et al., 2004) (reviewed in (Brummelkamp and Bernards, 2003)).

The selective killing concept can be expanded to synthetic dosage lethality where one loss-of-function mutation causes lethality when combined with overexpression of another protein. In therapeutics, loss of function of the second gene can be caused by drug inhibition. One example is that inactivation of retinoblastoma protein (RB) in cancer leads to an increase in E2F activation, which in turn activates various genes involved in S-phase entry, including topoisomerase 2. Topoisomearse II inhibitors such as etoposide

bind to topoisomerase II, causing DNA strand breaks and apoptosis. Therefore, *RB*-pathway mutations sensitize cells to topoisomerase II inhibitors. In a similar way, phosphatase and tensin homologue (PTEN) tumor-suppressor protein negatively regulates the phosphatidylinositol 3-kinase (PI3K) pathway, and a mammalian target of the rapamycin (mTOR) pathway. *PTEN*$^{-/-}$ cells are reported be more sensitive to the antiproliferative effects of mTOR inhibitors than wild-type cells (Neshat et al., 2001).

Defective mechanisms to maintain genomic stability render most cancers more vulnerable to genotoxic challenges. For example, *XP* mutations cause sensitivity to UV radiation, and mutations in *ATM* and *BRCA2* cause sensitivity to ionizing radiation (IR). In addition, caffeine inhibits ATR, and can induce S-phase cells to undergo premature chromosomal condensation. Cells lacking P53 in G1 control are found to be more susceptible to caffeine treatment. To identify the target pathway of anticancer drugs, the differential sensitivity of isogenic yeast mutants, each defective in a particular DNA repair or cell cycle checkpoint function, to Food and Drug Administration (FDA)-approved cytotoxic anticancer agents, such as cisplatin, camptothecin, and hydroxyurea, were tested (Dunstan et al., 2002; Hartwell et al., 1997; Lum et al., 2004; Simon et al., 2000). Similar drug sensitivity assays can be set up in matched pairs of cell lines (which differ in one genetic alteration) and in tumor cell lines (Dolma et al., 2003; Hartwell et al., 1997; Torrance et al., 2001).

Another avenue of cancer therapeutics is to activate the cell cycle checkpoint, arrest cells and induce apoptosis. Taxanes (stabilizing microtubules) and vinca alkaloids (inhibiting microtubule assembly) are used to treat breast and ovarian cancer patients, and they reduce tension or produce unattached kinetochores in mitosis by altering microtubule dynamics and cause long-term mitotic arrest. It is suggested that cells exit long-term mitotic arrest (through adaptation), but then apoptosis is induced in G1 (Tao, 2005). An inhibitor of KSP/EG5, a kinesin MT-dependent motor, is under phase I and II clinical trials and has the advantage that it only affects dividing cells because KSP only functions in mitosis. However, cells with a weakened checkpoint are less sensitive to microtubule-targeted drugs.

Paradoxically, complete inhibition of the mitotic checkpoint can also be effective in cancer therapeutics. Reducing MAD2 or BUBR1 to <10% level in various tumor cell lines causes complete inactivation of the mitotic checkpoint and results in massive chromosome misdistributions, and lethality results in 2-6 cell division (Kops et al., 2004; Michel et al., 2004). This is probably because the rate of chromosome missegregation is elevated to such high level that is incompatible with cell viability. As mentioned above, *MAD* and *BUB* genes were indeed first identified as mutants defective in triggering cell cycle arrest in response to microtubule inhibitors. If drugs could be used as tools to identify genes involved in a related process, we should be able to use CIN genes to identify new anticancer drugs and better understand their modes of action.

Whether genomic instability reflects cause or effect of altered cell physiology during tumorigenesis, a comprehensive identification of genes whose mutation leads to chromosome instability is an important, but daunting, goal yet to be achieved. Understanding the etiology and tolerance of genome instability in viable cells is fundamental to understanding the development and survival of cancers, and may be instrumental in the design of therapeutic approaches that take advantage of specific vulnerabilities exhibited by cancer cells.

1.3 Overview of thesis

The goal of my thesis was to systemically identify functional determinants required for mitotic chromosome transmission in yeast, and extend the investigation to human cells based on cross-species protein sequence comparison. This analysis provided candidate CIN genes for cancer mutation testing in cancer patients. The results will be directly relevant to understanding of cancer development, and may be useful in developing strategies for cancer therapy and for sub-classification of tumors based on their CIN mutational spectrum (Figure 1.9).

Chapter 2 describes the systematic identification of non-essential yeast genes important for the maintenance of chromosome stability using multiple assays. The comprehensive CIN gene set includes expected and unexpected genes, providing not only

a rich resource for the study of mechanisms required for accurate chromosome transmission, but also a list of candidate human CIN genes based on protein sequence similarities. Examples of known CIN gene mutations in cancers are shown, suggesting others are also candidate cancer genes needing to be tested. A CIN cancer cell-selective killing concept, utilizing synthetic lethality interactions between a CIN gene mutation and a second-site mutation, is discussed.

Chapter 3 describes mutation testing of the list of candidate human CIN genes generated from Chapter 2 in a panel of colorectal cancer patients. The significance of novel mutations, including genes involved in sister chromatid cohesion is discussed with regards to the mutation frequency and prevalence of mutations in CIN tumors. Functional analysis of several of the mutations found in colon cancers was performed in yeast by introduction of the mutations at the corresponding sites in the yeast *SMC1* gene and scoring the CIN phenotype.

Chapter 4 describes the characterization of 4 CIN genes identified in the genome-wide screens in Chapter 2. These 4 genes were only preliminarily characterized at the time the screens were completed. They potentially form an ubiquitin ligase complex. Phenotypic, genetic, and protein interaction data pertaining to this complex are analyzed and discussed.

Chapter 5 draws conclusions from the above chapters, discusses the future directions of research in CIN, and show how yeast research can benefit cancer research.

Table 1.1 Germline mutations of CIN and MIN genes causing cancer-prone syndromes

Human gene	Yeast gene	Protein Function	Associated disease/syndrome	Major tumor types	Mode of Inheritance	Reference
MSH2, MLH1, MSH6, PMS2	*MSH2, MLH1*	Mismatch repair (MMR)	Hereditary nonpolyposis colon cancer (HNPCC) (accounting for 3-5% of colorectal cancer)	Colon, uterus, endometrium, ovary	Autosomal dominant	(Fishel et al., 1993)
MYH /MUTYH	*mutY (E.coli)*	Base excision repair (BER)	MYH-associated polyposis (MAP)	Colon	Autosomal recessive	(Al-Tassan et al., 2002)
XPA-G	*RAD1-4, RAD14*	Nucleotide excision repair (NER)	Xeroderma pigmentosum (XP)	Skin	Autosomal recessive	OMIM
BRCA1, BRCA2		Double strand break (DSB) repair	Hereditary breast cancer	Breast, ovary	Autosomal dominant	(Tutt et al., 1999; Weaver et al., 2002)
NBS1	*XRS2*	Double strand break (DSB) repair	Nijmegen breakage syndrome (NBS)	Lymphoma, brain	Autosomal recessive	(Varon et al., 1998)
MRE11A	*MRE11*	Double strand break (DSB) repair	Ataxia Telangiectasia-like (ATL)	Myelodysplasia, acute myeloid leukemia	Autosomal recessive	(Stewart et al., 1999)
BLM /RECQL3	*SGS1*	DNA helicase	Bloom Syndrome	Leukemia, lymphoma, skin	Autosomal recessive	(Mohaghegh and Hickson, 2001)
WRN /RECQL2	*SGS1*	DNA helicase	Werner syndrome	Bone, skin	Autosomal recessive	(Mohaghegh and Hickson, 2001)
RECQL4	*SGS1*	DNA helicase	Rothmund-Thomson syndrome (RTS)	Bone, skin	Autosomal recessive	(Mohaghegh and Hickson, 2001)
ATM	*MEC1, TEL1*	DNA damage checkpoint	Ataxia Telangiectasia (AT) Seckel syndrome	Leukemia, lymphoma, medulloblastomas and gliomas	Autosomal recessive	(Savitsky et al., 1995)

Human gene	Yeast gene	Protein Function	Associated disease/syndrome	Major tumor types	Mode of Inheritance	Reference
P53, CHK2	*RAD53*	DNA damage checkpoint	Li-Fraumeni syndrome (LFS)	Soft tissue sarcomas and osteosarcomas, breast cancer, brain tumors, leukemia, and adrenocortical carcinoma	Autosomal dominant	(Varley et al., 1997) (Bell et al., 1999)
BUB1B	*MAD3*	Mitotic spindle checkpoint	Mosaic variegated aneuploidy (MVA)	Rhabdomyosarcoma, Wilms tumor, and leukemia	Autosomal recessive	(Hanks et al., 2004)
APC		Wnt signaling inhibition; chromosome segregation?	Familial adenomatous polyposis (FAP)	Colon, thyroid, stomach, intestine	Autosomal dominant	(Green and Kaplan, 2003)
FANCA,B,C,D 1,D2,E,F,G,I,J ,L,M		repair of DNA interstrand cross-links	Fanconi anemia (FA)	Leukemia	Autosomal recessive & X-linked	(Niedernhofer et al., 2005)

Table 1.2 Kinetochore and spindle checkpoint gene mutation or misregulation associated with cancer. (* shown as No. of positive patients or cell lines over the total No. tested)

Gene	Mutation/misregulation	Frequency*	Tumor type	Reference
BUB1	Dominant negative heterozygous deletion and missense mutation	2/19	Colorectal cancer	(Cahill et al., 1998)
	Heterozygous missense mutation	1/30	Lung tumor	(Gemma et al., 2000)
	Heterozygous missense mutation	1/10	Acute T-cell lymphoblastic leukemia	(Ohshima et al., 2000)
	Dominant negative heterozygous deletion in kinetochore localization domain	1/2	Acute lymphoblastic leukemia	(Ru et al., 2002)
	Deletion in kinetochore localization domain	2/2	Hodgkin's lymphoma	(Ru et al., 2002)
	Overexpressed	30/36	Gastric cancer	(Grabsch et al., 2003)
BUB1B	One heterozygous deletion, and one missense mutation	2/19	Colorectal cancer	(Cahill et al., 1998)
	One heterozygous and one homozygous missense mutation, one homozygous deletion	3/10	Acute T-cell lymphoblastic leukemia	(Ohshima et al., 2000)
	Downregulated (10 fold)	3/109	Colorectal cancer and others	(Shichiri et al., 2002)
	Overexpressed	19/28	Gastric cancer	(Grabsch et al., 2003)
BUB3	Overexpressed	26/34	Gastric cancer	(Grabsch et al., 2003)
MAD2	Missense mutation	22/49	Gastric cancer	(Kim et al., 2005)
	Downregulated	1/1	Breast cancer cell line	(Li and Benezra, 1996)
	Downregulated	2/5	Nasopharyngeal cancer cell lines	(Wang et al., 2000b)
	Downregulated	3/7	Ovarian cancer cell lines	(Wang et al., 2002b)
Rod	Homozygous missense mutation	1/192	Colorectal cancer	(Wang et al., 2004b)
Zw10	Heterozygous missense mutation	2/192	Colorectal cancer	(Wang et al., 2004b)
Zwilch	Heterozygous premature truncation	1/192	Colorectal cancer	(Wang et al., 2004b)
CENP-A	Overexpressed (1.5–32.5 fold)	11/11	Colorectal cancer	(Tomonaga et al., 2003)
CENP-H	Overexpressed (1.7–9.6 fold)	15/15	Colorectal cancer	(Tomonaga et al., 2005)
CENP-F (mitosin)	Amplified (1.6–2.5 fold) Overexpressed (2.1–4.2 fold)	7/72 25/72	Head and neck squamous cell carcinomas	(de la Guardia et al., 2001)
	Overexpressed	25/26	Salivary gland tumor	(Ota et al., 2002)
HEC1 (highly expressed in cancer; NDC80)	Overexpressed	9/9	Cervical, acute lymphocytic leukemia, breast and colorectal cancer lines	(Chen et al., 1997)
Aurora-B (AIM1)	Overexpressed	12/12	Thyroid cancer lines	(Sorrentino et al., 2005)
	Overexpressed	7/7	Colorectal cancer	(Tatsuka et al., 1998)
INCENP	Overexpressed (2.4–4.7 fold)	4/4	Colorectal cancer cell lines	(Adams et al., 2001)

Figure 1.1 The budding yeast cell cycle and chromosome cycle (adapted from Pot, 2004)

A. Yeast cells reproduce by budding. The cell cycle is divided into four stages [G1, S (DNA replication), G2 and M (mitosis)]. The size of the bud gives an approximate indication of cell cycle stage. The nucleus is shown in red; in yeast, the nuclear membrane does not break down during mitosis. During cell division, chromosomes undergo a replication and segregation cycle that is synchronized with the cell cycle

B. To follow the chromosome cycle in yeast, DNA content can be analyzed by flow cytometry of cells in which DNA has been stained with a fluorescent dye such as propidium iodide. A typical histogram showing the fluorescence distribution of a population of cycling cells is shown. Haploid cells in G1 phase have a 1N DNA content, while cells that have replicated their DNA and are undergoing mitosis (G2/M) have a 2N DNA content.

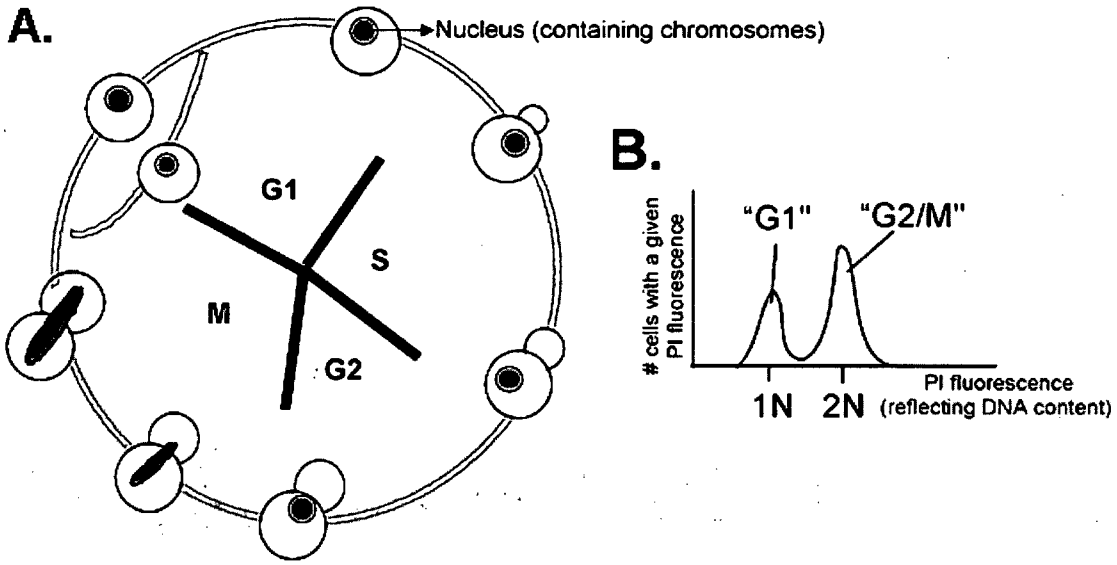

Figure 1.2 Organization of centromere (reprinted from (Cleveland et al., 2003) Centromeres and kinetochores: from epigenetics to mitotic checkpoint signaling, *Cell*, **112**, 407-421, Copyright 2003, with permission from Elsevier)

A. Overall organization of the centromere. A mitotic chromosome has been sectioned along the plane of the spindle axis, revealing the symmetric bipolar organization of a chromosome fully engaged on the spindle. (Right) Key elements have been pseudo colored. (Violet) The inner centromere, a heterochromatin domain that is a focus for cohesins and regulatory proteins such as Aurora B. (Red) The inner kinetochore, a region of distinctive chromatin composition attached to the primary constriction. (Yellow) The outer kinetochore, the site of microtubule binding, is comprised of a diverse group of microtubule motor proteins, regulatory kinases, microtubule binding proteins, and mitotic checkpoint proteins.

B. Schematic illustration of centromere loci. Organization of centromeric DNA sequences from the four example organisms. (Top) Budding yeast with a 125 bp centromere comprised of three sequence domains (pink, red, yellow). Fission yeast centromeres show an organized structure, with a nonconserved central core (red), flanking inner repeats (pink arrows) at which the CENP-A-containing nucleosomes assemble, and conserved outer repeats (stippled purple). The *Drosophila* centromere spans ~400 kb (red) embedded in constitutive heterochromatin (purple). (Bottom) Human centromeres have sizes approaching 10 Mb and are comprised of α-I satellite DNA (red) and a more divergent, less regular α-II satellite (pink), flanked by heterochromatin (purple).

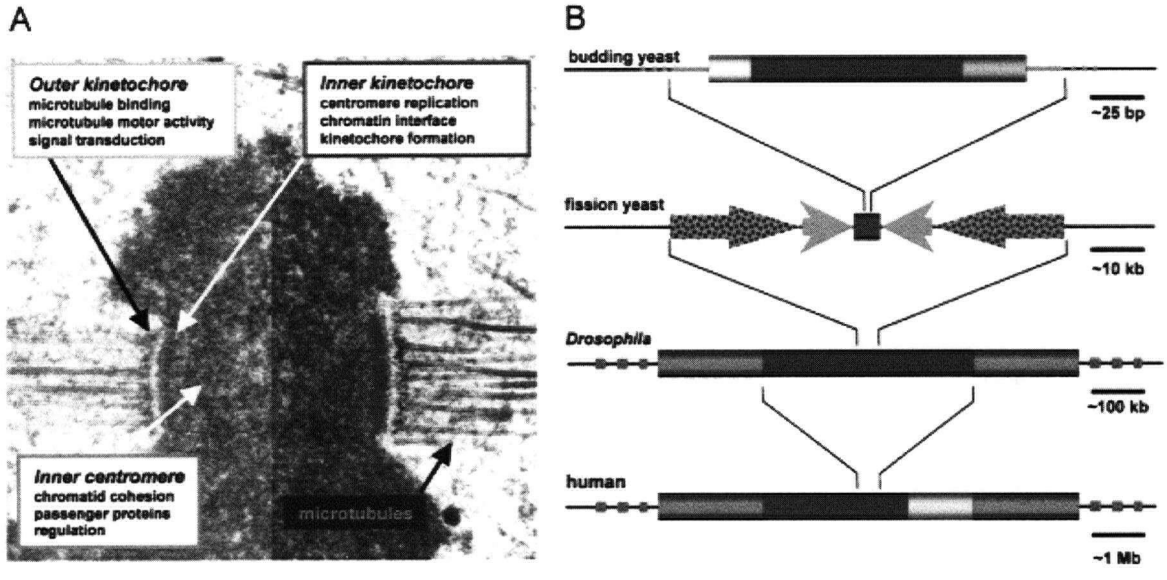

Figure 1.3 The process of achieving bipolar attachment (reprinted from (Pinsky and Biggins, 2005) The spindle checkpoint: tension versus attachment, *Trends Cell Biol*, **15**, 486-493, Copyright 2005, with permission from Elsevier)

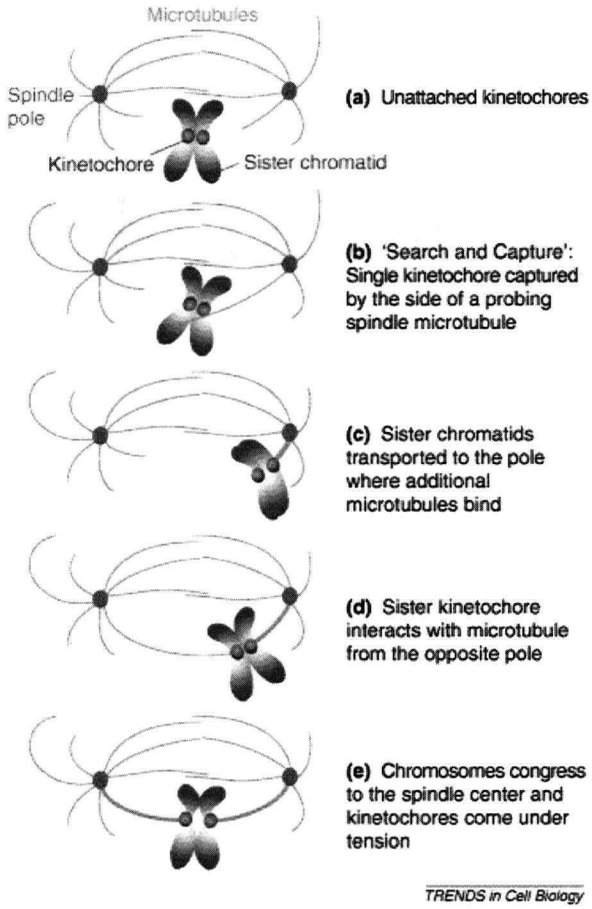

Figure 1.4 Types of kinetochore–microtubule attachments (reprinted from (Pinsky and Biggins, 2005) The spindle checkpoint: tension versus attachment, *Trends Cell Biol*, **15**, 486-493, Copyright 2005, with permission from Elsevier)

(a) Amphitelic: either bipolar or bioriented attachment. Sister kinetochores face opposite poles and bind only microtubules arising from the adjacent pole.

(b) Syntelic: sister kinetochores face the same pole and attach to microtubules emanating from that pole.

(c) Monotelic: sister kinetochores face opposite poles but only one kinetochore binds microtubules, leaving an unattached kinetochore.

(d) Merotelic: sister kinetochores face opposite poles but one (or both) kinetochore(s) interact with microtubules from both poles.

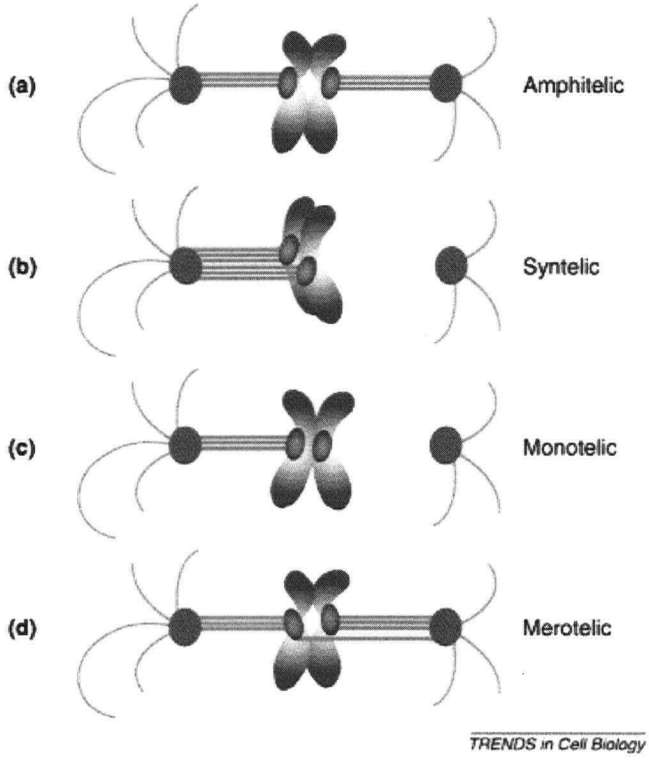

Figure 1.5 Structure of cohesin and a possible mechanism by which it might hold sister chromatids together (reprinted from (Nasmyth, 2002) Segregating sister genomes: the molecular biology of chromosome separation, *Science*, **297**, 559-565, Copyright 2002, with permission from AAAS)

(**A**) Smc1 (red) and Smc3 (blue) form intramolecular antiparallel coiled coils, which are organized by hinge or junction domains (triangles). Smc1/3 heterodimers are formed through heterotypic interactions between the Smc1 and Smc3 junction domains. The COOH terminus of Scc1 (green) binds to Smc1's ABC-like ATPase head, whereas its NH_2 terminus binds to Smc3's head, creating a closed ring. Scc3 (yellow) binds to Scc1's COOH-terminal half and does not make any direct stable contact with the Smc1/3 heterodimer. Scc1's separase cleavage sites are marked by arrows. Cleavage at either site is sufficient to destroy cohesion. By analogy with bacterial SMC proteins, it is expected that ATP binds both the Smc1 and Smc3 heads, alters their conformation, and possibly brings them into close proximity. By altering Scc1's association with Smc heads, ATP binding and/or hydrolysis could have a role in opening and/or closing cohesin's ring.

(**B**) Cohesin could hold sister DNA molecules together by trapping them both within the same ring. Cleavage of Scc1 by separase would open the ring, destroy coentrapment of sister DNAs, and cause dissociation of cohesin from chromatin.

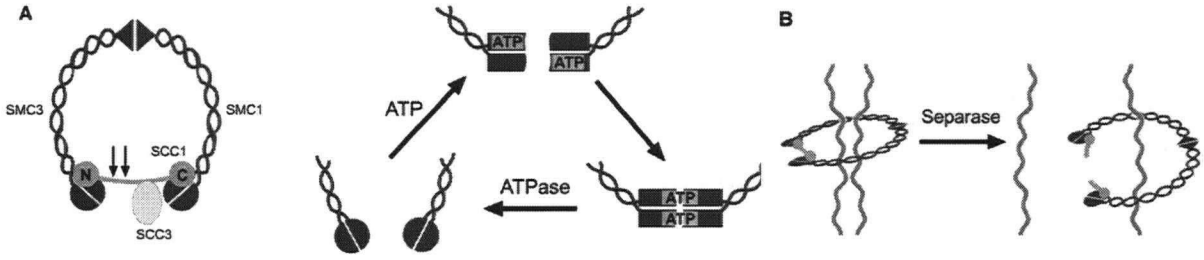

Figure 1.6 The stages of mitosis (reprinted from (Weaver and Cleveland, 2005) Decoding the links between mitosis, cancer, and chemotherapy: The mitotic checkpoint, adaptation, and cell death, *Cancer Cell*, **8**, 7-12, Copyright 2005, with permission from Elsevier)

Chromosomes enter mitosis as pairs of replicated sister chromatids that are linked by proteins known as cohesins.

A: The chromatids condense during prophase and are released into the cytoplasm by nuclear envelope breakdown, which marks the transition into prometaphase and also represents the first irreversible transition into mitosis.

B: During prometaphase, the initially unattached chromatids make connections to the microtubules of the mitotic spindle and the mitotic checkpoint is active, which means that the kinetochores assembled at the centromeres of unattached chromosomes generate a diffusible "wait anaphase" inhibitor. Antimitotic drugs delay cells in prometaphase by producing unattached kinetochores.

C: At metaphase, every chromosome has made proper attachments to the mitotic spindle and has congressed to a central position. Production of the diffusible "wait anaphase" inhibitor has been silenced by stable kinetochore-microtubule interactions. As the checkpoint inhibitors decay, the anaphase promoting complex (APC), an E3 ubiquitin ligase, becomes active and recognizes securin and cyclin B, provoking their degradation.

D: Loss of securin activates the protease, separase, that cleaves the cohesins, triggering sister chromatid separation and chromosome segregation during anaphase A.

E: At anaphase B, the spindle elongates.

F: At telophase, the now segregated chromosomes begin decondensing and the nuclear envelopes reform.

G: Cytokinesis separates the nuclei into two daughter cells that re-enter interphase.

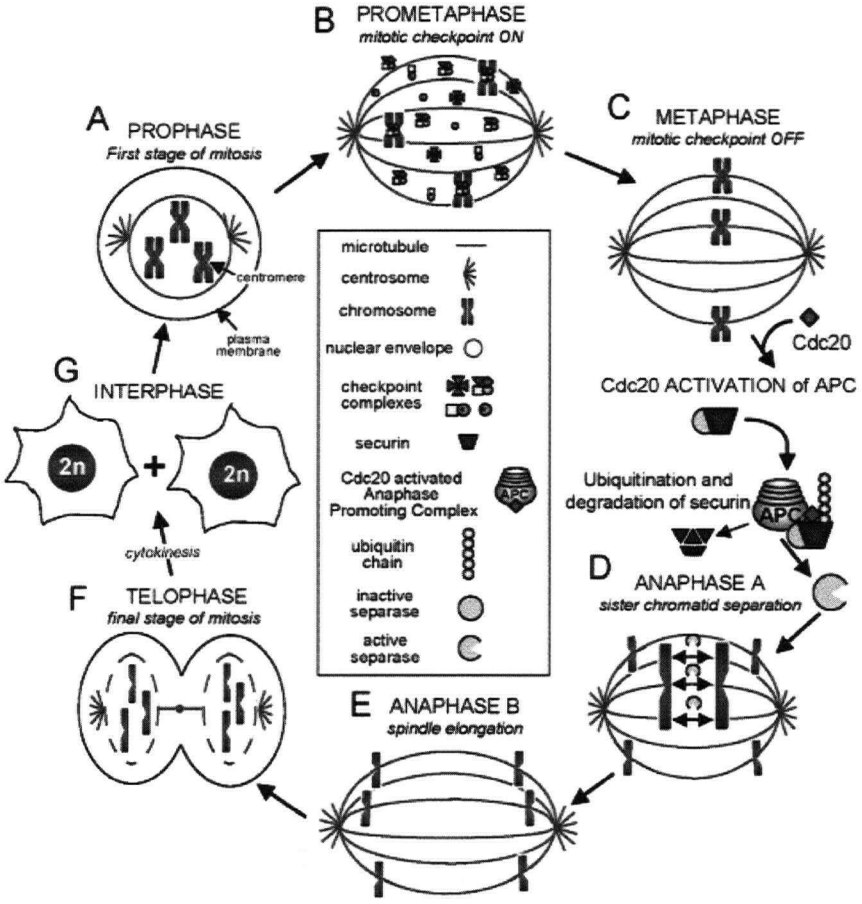

Figure 1.7 Cellular processes involved in replication and segregation of chromosomes during mitosis (reprinted from (Lengauer et al., 1998) Genetic instabilities in human cancers, *Nature*, **396**, 643-649, Copyright 1998, with permission from Macmillan Publishers Ltd)

Processes involved include chromosome condensation, cohesion of sister chromatids, and centrosome/microtubule formation and dynamics. Checkpoints that are required in chromosome replication and segregation include the mitotic spindle checkpoint, which ensures that chromosomes are aligned correctly before anaphase, and the DNA-damage checkpoint, which prevents cells with DNA damage from entering prophase. Aberrations in these processes and checkpoints could give rise to the CIN phenotype.

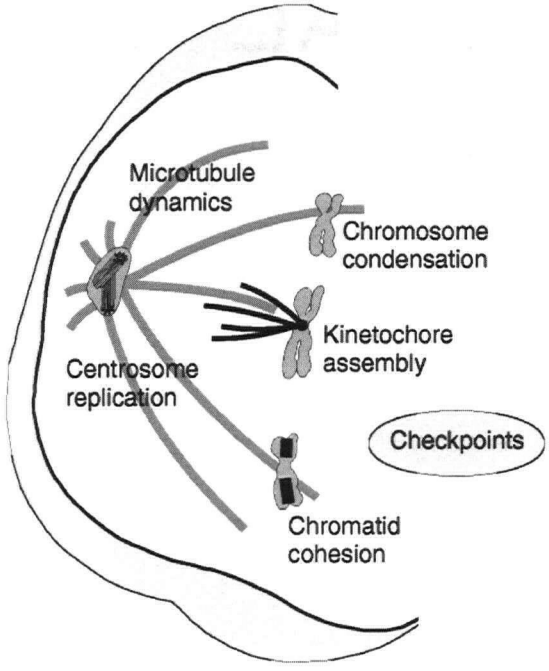

Figure 1.8 Multiple roads to aneuploidy (reprinted from (Rajagopalan and Lengauer, 2004a) Aneuploidy and cancer, *Nature*, **432**, 338-341, Copyright 2004, with permission from Macmillan Publishers Ltd)

The schematic illustrates a simplified cell cycle, highlighting processes that have been implicated in the advent of aneuploidy. Several pathways within the cell cycle (indicated in red) can be disrupted. Genes (indicated in green) associated with these processes and structures have been found to be mutated or functionally altered in aneuploid cancers.

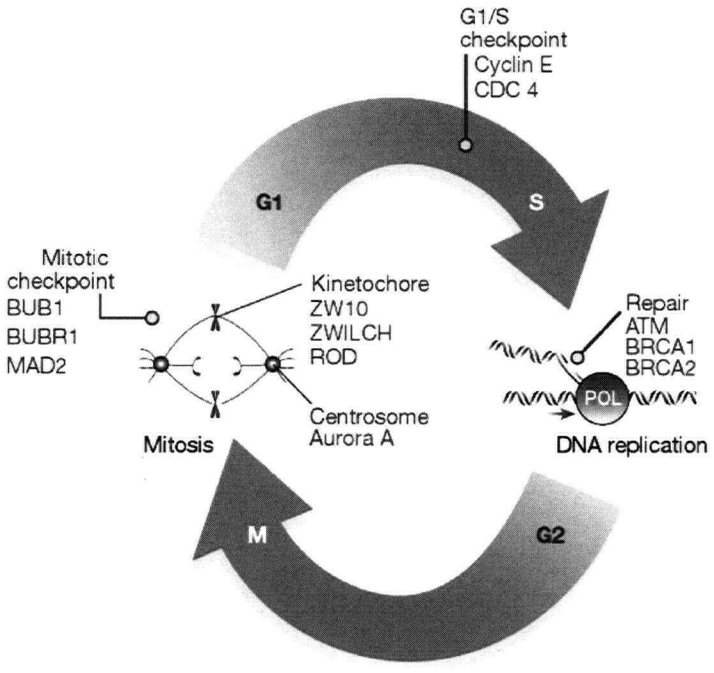

Figure 1.9 Flowchart of developing therapeutic strategy based on candidate CIN gene identification.

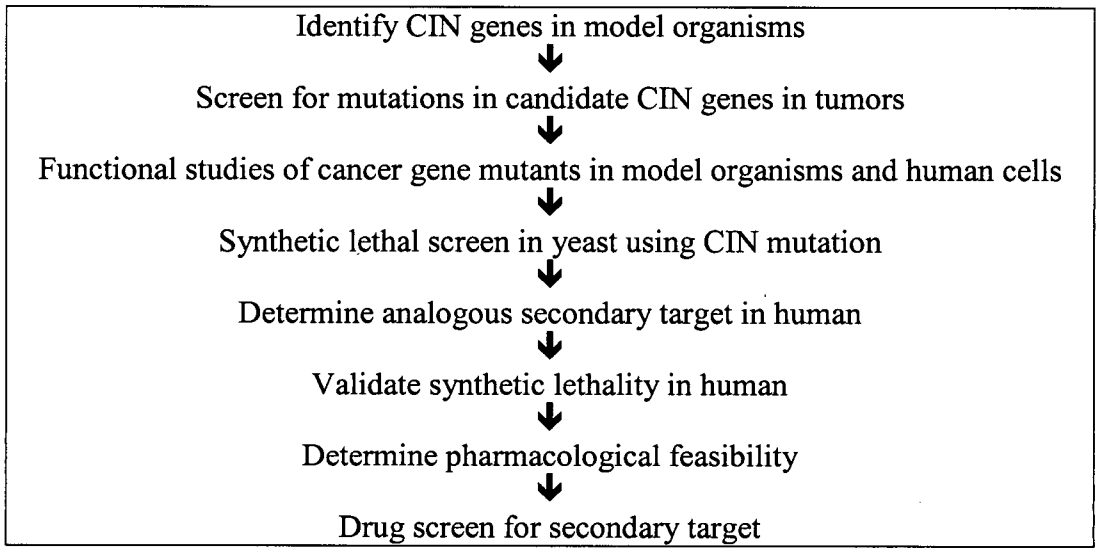

CHAPTER 2

Identification of Chromosome Instability Mutants in the Budding Yeast *Saccharomyces cerevisiae* and the Implication to Human Cancer

A modified version of this chapter has been accepted for publication. Karen W.Y. Yuen*, Cheryl D. Warren*, Ou Chen, Teresa Kwok, Phil Hieter, and Forrest A. Spencer (*These authors contributed equally to this work). Systematic Genome Instability Screens in Yeast and Their Potential Relevance to Cancer. Proceedings of the National Academy of Sciences of the United States of America.

2.1 Introduction

Genome instability is a hallmark of cancer and falls into 2 classes: MIN (microsatellite instability, reflecting an increased mutation rate) or CIN (chromosome instability, reflecting an increased chromosome missegregation rate). While much is known about the spectrum of germline and somatic mutations causing MIN in cancer cells, little is known about the spectrum of somatic gene mutations causing CIN in cancer cells (as described in Chapter 1). Recently, a cross-species candidate gene approach has been used to define ~20% of the CIN mutational spectrum in colon cancer (Cahill et al., 1998; Rajagopalan and Lengauer, 2004b);(Wang et al., 2004b). To comprehensively identify additional CIN gene mutations in cancers, one approach would be to identify all genes mutable to a CIN phenotype in a model organism, and to systematically test human homologues of the model organism CIN gene set for somatic mutations in tumors. Such a cross-species candidate gene approach, previously termed 'homologue probing' (Bassett et al., 1997), should in theory significantly expand our understanding of the CIN mutational spectrum in cancer.

Comprehensive identification of genes whose mutation leads to CIN is an important, but daunting, goal yet to be achieved. Phenotype screening based on marker stability in budding yeast by random mutagenesis has provided several gene collections (e.g. chromosome transmission fidelity (*ctf*), chromosome loss (*chl*), minichromosomes maintenance (*mcm*), and chromosome instability (*cin*)), and these genes are often functionally conserved in other eukaryotes (Hoyt et al., 1990; Kouprina et al., 1988; Maine et al., 1984; Meeks-Wagner et al., 1986; Ouspenski et al., 1999; Spencer et al., 1990). Not surprisingly, different genetic screens have led to identification of gene sets important for various steps in the chromosome cycle, including those functioning at kinetochores, telomeres, and origins of replication, or in microtubule dynamics, sister chromatid cohesion, DNA replication, DNA repair, DNA condensation and cell cycle checkpoints. All these processes must be executed at high fidelity and coordinated temporally and spatially within the cell cycle to maintain genetic integrity.

For instance, the chromosome transmission fidelity (*ctf*) mutant collection was generated by Spencer *et al.* (Spencer et al., 1990) in the Hieter laboratory through mild EMS mutagenesis (0% killing, 10-fold increase in canavanine resistant colonies), followed by screening of ~600,000 yeast colonies for an elevated colony sectoring phenotype, which reflects loss of an artificial chromosome fragment. In total, 136 mutant strains were isolated. Based on complementation tests, this collection represents ~50 genes that could encode any of the many components necessary for the chromosome cycle to proceed with high fidelity. Specific secondary screens have been applied to the *ctf* collection with the aim of identifying mutants defective in a particular structure or process (Doheny et al., 1993). To date, about half (24) of the genes represented in the *ctf* collection have been cloned and characterized (Table 2.1). Among these, 9 genes encode kinetochore proteins, 10 encode proteins important for sister chromatid cohesion, and 5 encode other functions in DNA/RNA metabolism. Both essential and non-essential genes were identified from the screen. Interestingly, the top 7 complementation groups altogether contain 75 alleles, representing over half of the total number of isolates. These 7 yeast genes are the most highly mutable to CIN in this particular assay.

Despite the ease of random mutagenesis and the possible recovery of hypomorphs of essential genes, random mutagenesis approaches rarely achieve screen saturation, because mutability varies among genes due to differences in size, base composition, and the frequency of mutable sites that can lead to viable cells with a detectable phenotype. However, the use of the *S. cerevisiae* gene knockout collection supports new and powerful strategies based on direct phenotyping of the null mutants. The ~4,700 non-essential gene-deletion mutants represent >70% of yeast genes, but over 30% of mutants remain functionally unclassified (Giaever et al., 2002; Winzeler et al., 1999) (Saccharomyces Genome Database, www.yeastgenome.org).

In this study, I have used the gene knockout set to carry out 3 systematic screens that follow marker inheritance in different chromosomal contexts to identify genes important for maintaining genome stability in yeast (i.e. non-essential yeast CIN genes). In addition to extending the catalog of genes known to affect genome stability, several

themes emerge from the analysis of the screen results. Because all mutants characterized are null, phenotype strength reflects the magnitude of the role played by each gene in genome stability. Thus direct comparisons are meaningful, between different mutants in a given assay system or between different assay systems for a given mutant. Some mutants exhibit phenotypes that are screen-specific, suggesting that chromosomal contexts determine what pathways predominate in protecting against genomic change. Protein similarity was used to identify candidate CIN homologues in other species, in particular human genes with relevance to cancer. For yeast CIN genes whose human homologues are mutated in cancers, yeast genetic interaction data were analyzed to identify common synthetic lethal interactors. Human homologues of these common synthetic lethal interactors may be useful as drug targets with broad spectrum applicability for selective elimination of CIN cancer cells.

2.2 Materials and methods

2.2.1 Genome-wide screens

2.2.1.1 CTF screen

The synthetic genetic array (SGA) selection scheme (Tong et al., 2001a) was used to introduce the *ade2-101* ochre mutation and an artificial chromosome fragment (CF) into *MATa* deletion mutants obtained from Research Genetics (www.resgen.com). To construct donor strains used to mate with the *MATa* deletion mutant array, Y2454 (see Table 2.2 for strain list) was first co-transformed with 2 PCR products. One PCR product contained an *ade2-101* allele and terminated with an adjoining 20-bp of *TEF* promoter. The other PCR product contained the *TEF* promoter, the *natMX* cassette, the *TEF* terminator, and 40-bp overlap with genomic *ADE2* downstream sequence. Transformants were selected on medium containing 100mg/L clonNAT (Werner BioAgents, Germany). Cointegration of *ade2-101* and *natMX* at the *ADE2* gene locus was confirmed by PCR. The resulting strain (YPH1724) was crossed with either YPH255 or YPH1124, which contained CFVII(RAD2.d) or CFIII(CEN3.L), respectively (Spencer et al., 1990). The 2 CFs were derived from different yeast chromosome arms and will cover recessive mutations in that chromosomal region. The resulting diploids were sporulated, and spore progeny with the appropriate markers were recovered as the donor strains YPH1725 and YPH1726.

Two SGA analyses, each using one of the donor strains, were performed as described previously (Tong et al., 2004) with the following modifications. The *MATa* yeast deletion mutant set (*MATa ura3 his3 ykoΔ::kanMX*) was arrayed at a density of 768 colonies/omni tray for robotic pinning. Each deletion mutant strain was represented in duplicate in each SGA analysis. The donor strain (*MATα ade2-101::natMX ura3 his3 can1Δ mfa1Δ::MFA1pr-HIS3*), containing a *URA3*-marked CF, was mated with yeast deletion mutants on rich medium for 1 day. All plates were incubated at 25°C. Then diploids were selected twice (2 days and 1 day) on synthetic complete medium (SC) containing 200mg/L G418 (Invitrogen) and lacking uracil. Diploids were then pinned onto sporulation medium for 9 days, and *MATa* spore progeny with a CF were selected

on haploid selection medium (SC medium lacking histidine, uracil, and arginine but containing 50mg/L-canavanine (Sigma)) for 2 days. Finally, *MATa* deletion mutants with a CF and the *ade2-101* mutation were selected in 2 successive rounds (2 days each time) on the haploid selection medium with G418 and clonNAT. All strains from the final selection plate were streaked to single colonies on SC medium with 20% of the standard adenine concentration. Plates were incubated at 25°C for 6-7 days, then at 4°C for 5-7 days to enhance the development of red pigment. An instability of the CF was indicated by a colony color-sectoring phenotype as in (Spencer et al., 1990). Briefly, red color in yeast cells is caused by accumulation of pigment due to a block in adenine production caused by the *ade2-101* (ochre) mutation. This block is relieved in the presence of the *SUP11* gene located on the telocentric arm of the CF, encoding an ochre-suppressing $tRNA^{Tyr}$. Cells that contain the CF are therefore unpigmented, whereas cells that do not develop red color (Gerring et al., 1990; Hegemann et al., 1988; Warren et al., 2002). Colonies exhibiting unstable inheritance of this CF develop red sectors, whereas wild-type strains form mostly white colonies. The severity of the phenotype was scored qualitatively by eye as mild, intermediate and severe (indicated as 1, 2, and 3, respectively in Appendix 1 and Appendix 2). Figure 2.1.a shows the scheme of the CTF screen, and examples of severe and mild sectoring colonies.

All deletion mutants that displayed a sectoring phenotype, or were identified in at least 1 of the other screens (BiM or ALF) were retested for sectoring phenotype. A miniarray was constructed and SGA analyses were undertaken as described above. Deletion mutants showing a sectoring phenotype in at least 2 out of 8 isolates (either in the original genomic screen or in the retest) were scored as having a CTF phenotype.

2.2.1.2 Bimater screen

The homozygous diploid deletion set obtained from Open Biosystems (www.openbiosystems.com) in 96-array format was grown on YPD agar medium containing 200mg/L G418 for 3 days at 25°C. *MATa* and *MATα* mating tester lawns (YPH315 and YPH316 respectively) were generated by spreading 2 ml of saturated

culture on solid medium and grown at 25°C for 2 days. Each plate containing 96 deletion mutants was replica plated onto 4 test plates: an YPD plate with 200mg/L G418 (a positive control), a synthetic complete medium plate lacking histidine, uracil, adenine, lysine, tryptophan and leucine (SC-6, a negative control), and 2 YPD pre-mating plates. *MATa* and *MATα* mating tester lawns were each replica plated to the YPD plate containing freshly replica plated deletion mutants. These were incubated at 25°C for 2 days for mating. The 2 YPD plates were each replica plated to synthetic complete medium lacking histidine, uracil, lysine, adenine, tryptophan, and leucine (SC-6) and incubated at 25°C for 3 days to select mated products. These SC-6 plates were visually inspected, and densitometry measurements were obtained for each deletion mutant using the QuantityOne program (BioRad). Deletion mutants that exhibited elevated mating rates with both *MATa* and *MATα* mating testers were identified as candidate bimaters for further study (Figure 2.1.b).

For confirmation, all bimater candidates were retested for bimater phenotype along with all positive mutants from the other two screens (ALF and CTF). For the retest, 4 independent isolates per mutant were patched in $1cm^2$ squares. Each plate also contained negative and positive control patches: wild-type diploid (YPH1738) and *chl1Δ/chl1Δ*, respectively. After selection, the number of colonies in each patch was estimated. To minimize the effect of early or late events during population growth, the median number of colonies was used to calculate fold-change (mutant/wild-type ratio). Homozygous deletion mutants with an average of ≥1.5-fold increase in mating tests with both *MATa* and *MATα* testers were identified as bimaters. The severity of each mutant phenotype was recorded as an estimate of 2- to ≥5-fold increase over wild-type frequency after rounding (see Appendix 1 and 4).

2.2.1.3 a-like faker screen

The *MATα* haploid deletion collection (*MATα ykoΔ::kanMX*) obtained from Research Genetics were manually arrayed in $1cm^2$ squares on YPD plates. Each plate contained 3 controls: wild-type *MATα* (BY4742), wild-type *MATa* (BY4741), and the

MATα bim1Δ::kanMX from the *MATα* deletion collection. A lawn of 5 x 10^7 *MATα his1* mating tester cells (YPH316) freshly spread and dried onto solid rich medium. The presence of a-type mating cells in *MATα* mutant populations was detected as previously described (Warren et al., 2004a). *ykoΔ* patches were transferred onto the mating tester lawn by replica plating, followed by incubation at 30°C for 20-24 hr. Mated patches were then replica plated to SC-6, incubated for 2 days at 30°C to select mated products. Results from the primary screen were scored by comparing the number of colonies per patch to the wild-type *MATα* control patch for that plate (Figure 2.1.c).

All positive mutants were retested as described above (along with all positive mutants from bimater and ctf screens), but using 4 independent isolates for each mutant. After selection, mated products were counted and a fold-change calculation was generated (mutant median colonies per patch/wild-type median colonies per patch). Mutants were scored as positive if they exhibited $\geq$ 2-fold increase over wild-type frequency.

2.2.2 Strain verification

To evaluate the mutant identity of the 96-well content from each collection, cells from frozen stocks were patched on YPD plates containing G418. A barely visible clump of cells (~10^5) was added directly to 20 µl lysis buffer (25mM Tris-HCl pH8.0, 0.005% sodium dodecyl sulfate, 14 mM β-mercaptoethanol, 0.5 mM EDTA), and incubated at 85°C for 10 min. PCR was performed in 96 well format using primers D1 and KanC for downtags (Shoemaker et al., 1996). PCR products were purified using Qiagen Qiaquick PCR purification kit or Macherey Nagel NucleoFast 96 PCR kit. DNA yield was determined using PicoGreen (Molecular Probes), and the concentration of each well was adjusted to 10-50 ng/ml. The downtag sequence was determined using oligonucleotide 5'-catctgcccagatgcgaagttaag-3' as primer. For mutants lacking a downtag, or when the downtag sequence analysis was ambiguous, the uptag sequence was obtained from PCR products generated using primers U1 and KanB, followed by sequencing obtained using a KanB1 (Shoemaker et al., 1996) sequencing primer.

The sequence of the tag PCR products was determined by dideoxy termination at the JHMI Sequencing Core Facility or SeqWright Incorporated (www.seqwright.com). The results were analyzed using BLASTN against a tag database, and alignments with expected tags having e-values $<10^{-10}$ were considered evidence of well validation. Sequence traces for BLASTn outcomes $>10^{-10}$ were read manually. Among these were clean traces indicating tag mutations present in yeast that prevented alignment with the correct tag sequences with significant e-value (Eason et al., 2004), or traces with two or more peaks at many positions. Often when two tags were present, the identity of a contaminating mutant in a given well could be determined. In homozygous diploids, different but 'correct' tag alleles were often noted (e.g. where one tag was a frameshifted version of the expected sequence) (Eason et al., 2004). Failure in mutant verification by tag sequencing is classified as "wrong" (incorrect strain(s) present), "contamination" (correct strain present but a contaminating strain was evident), or "nd" (not determined because the sequence obtained was unreadable, or that deletion collection contained no yeast to validate).

Subsets of CIN mutants were freshly generated by transformation and phenotyped. The *ykoΔ::kanMX* cassette was PCR from the deletion set mutant with gene flanking primers located ~300bp upstream and downstream of the gene, and the PCR product was transformed in the respective parental wild-type. Transformants were confirmed by primers flanking the PCR product to confirm integration of the deletion allele and ensure removal of the wild-type locus.

2.2.3 Bioinformatic analysis

2.2.3.1 Functional analysis

Over-representation of GO biological process and cellular component annotation in the yeast CIN gene list, compared to all yeast genes, was determined using GO TermFinder as of May 3, 2006 (db.yeastgenome.org/cgi-bin/GO/goTermFinder.pl).

2.2.3.2 BLAST analysis

Protein sequences of yeast CIN genes were used as queries in a BLASTp alignment search against protein sequence downloads for *Homo sapiens* (RefSeq protein database, as of June 2004), *Mus musculus* (RefSeq protein database June 2004), C. elegans (Wormbase June 2004), *D. melanogaster* (FlyBase release 3.2.0), and *S. pombe* (Sanger Institute, pompep June 2004). Human proteins from RefSeq with BLASTp alignments to yeast CIN protein queries (e-value $<10^{-10}$, July 2004) were searched against OMIM (www.ncbi.nlm.nih.gov/omim) and cancer census (Futreal et al., 2004) protein datasets for disease, especially cancer, association.

2.2.3.3 Protein and synthetic lethal interaction network

Protein-protein interactions and genetic interactions with yeast CIN genes were obtained from the GRID database, and the interaction networks were visualized through the OSPREY program (v1.2.0) (Breitkreutz et al., 2003a; Breitkreutz et al., 2003b).

2.2.4 Electrophoretic karyotype of a-like fakers

For the electrophoretic karyotype analysis, a *MATα his5Δ::kanMX* tester strain was used. This strain contains a chromosome III length polymorphism that distinguishes it from chromosome III of the deletion collection background. Mating between *MATα* strains will occur when the *MATα* locus from either parental genotype is lost. During the ALF screen, the basal rate of loss for the *MATα his1* mating tester (YPH315) was observed to be much lower than that of BY4742 (parental strain to the *MATα* deletion collection). Thus, nearly all events detected were due to genome instability in the deletion mutant being characterized. Sample preparation, pulsed field gel analysis, and in-gel hybridizations were performed as described in (Warren et al., 2004a).

2.3 Results

2.3.1 Genome-wide marker loss screens identify 130 yeast deletion mutants

Three complementary marker loss assays were performed using the non-essential gene-deletion mutant set. In the first screen (CTF, for chromosome transmission fidelity, Figure 2.2a), inheritance of an artificial chromosome fragment (CF) was monitored using a colony color marker. I modified the Synthetic Genetic Array (SGA) methodology (Tong et al., 2001a) to construct haploid deletion strains carrying a CF, and performed a colony color-sectoring assay as an indicator of chromosome instability (Hieter et al., 1985; Spencer et al., 1990). Linear artificial CFs serve as sensitive indicators because their presence or absence does not affect viability, and they resemble natural chromosomes in their structure and stability (with 1.7–7 loss events per 10^4 divisions) (Gerring et al., 1990; Hegemann et al., 1988; Koshland and Hieter, 1987; Shero et al., 1991; Warren et al., 2002). Since the markers on the CF are surrounded by sequences that have no similarity to the yeast genome, loss of markers primarily represent loss of the whole CF.

In the second and third screens, an endogenous locus (the mating type locus *MAT* on chromosome III) was exploited as a marker. A bimater screen (designated BiM, Figure 2.2.b) followed inheritance of the *MATa* and *MATα* loci in homozygous diploid deletion mutants. Diploid cells heterozygous at *MAT* do not mate due to codominant suppression of haploid-specific cell differentiation pathways. Loss of either the *MATa* or the *MATα* allele results in mating competence, where the mating type is determined by the remaining allele. Reciprocal mating tests with *MATa* or *MATα* mating testers were performed on the homozygous diploid deletion set to identify cell populations which form mated products with both *MATa* and *MATα* at high rates. The endogenous rate of loss of either *MAT* allele in wild-type cells is 2-4 events in 10^5 divisions (Liras et al., 1978; Spencer et al., 1990), where the predominant mechanism is mitotic recombination between homologues. This loss of heterozygosity can also be due to chromosome loss, chromosomal rearrangement (deletions or translocations with loss), or gene conversion (allele replacement).

In the third screen (designated ALF, for a-like faker, Figure 2.2.c), the *MATα* locus inheritance was similarly followed in the *MATα* haploid deletion set by a mating test. The *MATα* locus encodes transcription factors that suppress a-specific and promote α-specific gene expression (Strathern et al., 1981). Loss of the *MATα* locus leads to the default mating type in yeast, which is the a-type differentiation state. Thus, *MATα* cells that lose the *MAT* locus will mate as a-type cells, and are called 'a-like fakers' (Strathern et al., 1981). The frequency of a-like faker cells in a population is detected by prototrophic selection of mated products. In wild-type yeast, ALF mitotic segregants are generated at a rate of $\sim 10^{-6}$ ((Herskowitz, 1988b); CDW and FAS unpublished). Mechanisms leading to *MATα* locus loss in *MATα* cells are similar to LOH in diploid cells, except that in haploids there is no homolog for mitotic recombination. However, the silent mating type locus *HMRa* can mitotically recombine with the *MATα* locus (see below).

The mutants identified in the 3 assays were subjected to additional validations. First, mutants from each primary screen were retested by all 3 assays to ensure phenotype reproducibility. 310 knockout strains were identified after secondary screening (84 CTF, 130 BiM, and 247 ALF). Next, the effect of cross-well contamination was evaluated by determining the identity of the deletion mutations present in each of the 310 well locations in each of the 3 deletion arrays (see Appendix 1 and 2 for details). This was accomplished by sequencing the oligonucleotide 'tag' unique to each deletion allele (Giaever et al., 2002). The presence of >1 tag sequence or an incorrect tag sequence was evidence of contaminating or wrong deletion strains, and the phenotypes of these locations were discarded. The 310 well positions exhibited 22%, 9%, and 14% error in the *MATa*, *MATα*, and homozygous diploid sets, respectively. After adjustment, 293 knockout strains were verified as exhibiting CIN in at least 1 of the 3 assays. Of these, 210 (72%) were uncontaminated in all 3 sets. To investigate the overall error rate in each deletion set, we sequenced strains from 60 randomly chosen well addresses and found 12%, 3%, and 3% contaminated wells in *MATa*, *MATα*, and homozygous diploid sets, respectively. The higher error rate among yeast CIN mutants, relative to a randomly

chosen set, may reflect a higher representation of slow-growing yeast strains among the CIN gene set that are readily replaced by faster growing contaminants. These tag sequence analyses suggest that the false negative frequency was between 3 and 22% (i.e. phenotype detection cannot be performed due to the absence or contamination of mutant from the appropriate position in a collection). Several different error origins were observed in each collection. These included neighboring-well spillover (20-50% of cases), plate-to-plate carryover (mutants from a conserved well position but from a different plate, 5-15% of cases), common substitution by a single recurrent strain (that could occur from media contamination, ~10%), and individual events with no apparent physical pattern (30-50% of cases).

Finally, an additional source of artifact in deletion collection phenotyping is the occasional presence of undesired 'secondary' mutations that cause the phenotype being screened (i.e. positive phenotypes caused by mutations that are not at the site of the knockout allele). Gaiever *et al.* estimated the presence of lethal or slow-growth phenotypes caused by mutations in genes that do not segregate with a knockout allele to occur at a frequency of 6.5% (Giaever et al., 2002). Such "collateral damage" would be expected to occur at an even higher frequency in non-essential genes. To verify that the CIN phenotype is actually due to the knockout allele, subsets of mutants were regenerated by independent transformation and phenotyped. Mutants with phenotypes in at least 2 screens were reconfirmed as CIN mutants in new transformants at a high rate (13/13 CTF, 9/10 BiM, 9/11 ALF). On the other hand, mutants identified with phenotypes in only a single assay were reconfirmed in new transformants at lower rates, ~43% for the haploid collections (2/6 of mutants exhibiting CTF only, 4/8 of mutants with ALF phenotype only, and ~75% for the diploid collection (3/4 of mutants exhibiting BiM phenotype only). These data indicate a significant frequency of secondary mutation effects in the assay-specific subsets of CIN mutants identified in the primary screens, and emphasize the validation inherent in performing screens in multiple collections. The higher reconfirmation rate of BiM from the homozygous deletion mutants is consistent with the presence of secondary mutations, which would often be covered by the wild-type

allele during the construction of diploids when independent haploid segregants were mated.

In total, 130 mutants are of high confidence (the 115 deletion strains identified in more than 1 assay, together with 15 mutants reconfirmed independently to have a positive phenotype in only 1 assay). These 130 genes are listed in Figure 2.3 and Appendix 1, which reflect the current data status including all confirmations performed to date. The remaining 163 mutants identified in only 1 screen are listed in Appendix 2, and are regarded with lower confidence (with ~43% and ~75% true positive frequencies among the assay-specific subsets identified in the haploid and diploid mutant screens, respectively). Appendix 1 and 2 include measures of phenotype severity, as well as annotations for well contamination in any of the 3 deletion sets and changes due to independent knockout evaluation.

2.3.2 Functional distribution of yeast CIN genes

Comparing the gene ontology (GO) annotations of the 293 CIN genes to that of the entire yeast genome (Harris et al., 2004) indicated that the CIN gene set has an over-representation in numerous expected cellular components: nucleus, chromosome, kinetochore, microtubule, cytoskeleton, spindle, nuclear pore, spindle pole body, replication fork, and chromatin (Appendix 3). For GO biological processes, the CIN gene list is enriched in genes involved in cell cycle, cell proliferation, response to DNA damage response, and nuclear division (Appendix 4). Using GO biological process annotation, the 293 CIN genes fall in broad functional groups, including ~40% functioning in DNA metabolism, chromosome, or cell cycle, ~40% functioning in processes not obviously implicated in marker loss, and ~20% with unknown function (Figure 2.4). These GO annotations reflect the current knowledge of studied genes, indicating that these screens identified genes known to be functioning in genome maintenance. Interestingly, genes not previously known to contribute to stability were also identified. For example, 7 yeast mutants in the adenine biosynthetic pathway (*ade1, ade2, ade4, ade5/7, ade6, ade8, ade17*) gave rise to elevated a-like fakers at frequencies

ranging from 2- to 31-fold above wild-type (Appendix 1 and 4). Three of these (*ade1*, *ade6* and *ade17*, shown in Figure 2.3) were tested in fresh transformants, and all 3 were validated. This indicates that adenine, adenine pathway intermediates or derivative metabolites are important for genome stability, and that compensatory mechanisms used by cells when de novo adenine synthesis is blocked are not fully sufficient.

Using the GRID database and OSPREY network visualization program, 92 physical interactions were found among 103 of 293 CIN proteins, including protein complexes, networks and pathways that are known to be important for maintaining chromosome stability (Breitkreutz et al., 2003a; Breitkreutz et al., 2003b) (Fig. 2.7). Inspection of network interactions should reveal novel hypotheses regarding functions of uncharacterized genes. For example, *msb2Δ* was identified as a bimater, and Msb2p physically interacts with Mad2p and Mad3p in the spindle checkpoint pathway and Ndc80p at the kinetochore. While Msb2p is known to be an osmosensor protein and is required to establish cell polarity, its role in maintaining chromosome stability has not been explored. *YBP2*, identified in the bimater test, is implicated in oxidative stress response and the gene product interacts with Nup145p, which is essential. Nup145p interacts with Nup120p and Nup84p, which were found in our screens along with another nucleoporin Nup133p, suggesting that nucleoporins play important roles in maintaining chromosome stability. A subcomplex of nucleoporins containing Nup53p, Nup170p, and Nup157p are associated with the spindle checkpoint proteins Mad1p and Mad2p. Interestingly, *ybp2Δ* is synthetic lethal with *mad2Δ*, suggesting Ybp2p may play a role in genome stability in association with nucleoporins and the spindle checkpoint. Indeed, Ybp2p was recently found to interact with multiple kinetochore proteins, and was found to specifically interact with centromere DNA sequences by chromatin immunoprecipitation (Kentaro Ohkuni and Katsumi Kitagawa, personal communication). In addition, several CIN genes identified in the screens were recently characterized to play a role in genomic stability. For example, Dia2p, a F-box protein in the SCF (Skp1p-Cdc53p/Cullin-F-box) E3 ubiquitin ligase complex, was recently shown to be involved in regulating DNA replication and important for stable passage of replication forks through

regions of damaged DNA and natural fragile regions (Blake et al., 2006; Koepp et al., 2006). Nce4p is involved in mediating Sgs1p-Top3p helicase-topoisomerase complex (Chang et al., 2005; Mullen et al., 2005), and Mms22p and Mms1p are in a novel DNA damage repair pathway (Baldwin et al., 2005) (see Chapter 4). Integrating the CIN gene catalog with other phenotypic, genetic and physical interaction data proves to be a fruitful avenue to further our understanding of mechanisms that maintain genomic stability.

2.3.3 Integration of genome-wide phenotypic screen with genetic screens reveals functions of uncharacterized genes in chromosome stability maintenance

Using 14 hypomorphic and 3 hypermorphic kinetochore alleles as queries, genome-wide synthetic lethal (SL) and synthetic dosage lethality (SDL) screens were performed on the non-essential yeast deletion mutant set (Measday et al., 2005). SL interactions occur between genes involved in the same, parallel or redundant biological pathway. SDL interaction occurs when overexpression of a protein in wild-type cells remains viable, but causes lethality in a mutant. SDL can occur between genes within the same complex where their stoichiometry is important. Overexpression of the query protein may titrate out another protein that is required for cell viability in the knockout strain. If the function of the query protein is to regulate the mutant protein, then overexpression of the regulatory factor could be detrimental to the knockout mutant. Conversely, if the normal function of the mutant protein is to regulate the query protein, then overexpressing the query protein in a strain defective for its regulatory factor could be lethal (Measday and Hieter, 2002). The kinetochore SL and SDL screens identified 211 non-essential deletion mutants in total, but surprisingly, only 14 gene mutants were identified in both SL and SDL screens. However, these overlapping mutants were enriched for chromosome transmission fidelity (*ctf*) defects (8/14 mutants from both SL and SDL screens vs. 20/197 mutants from either SL or SDL screens displayed a *ctf* phenotype) (reviewed in (Baetz et al., 2006; Eisenstein, 2005)). One gene identified in this overlapping set and the *ctf* screen was *RCS1/AFT1*, an iron-regulated transcription factor (Rutherford and Bird, 2004). Indeed, Rcs1p co-localizes with a kinetochore protein

by indirect immunofluorescence analysis on chromosome spreads, and has both genetic and physical interactions with the inner kinetochore protein Cbf1p (Measday et al., 2005). Such an example illustrates the power of complementing genome-wide SL, SDL and phenotypic screens to uncover hidden relationships and predict functions of genes.

2.3.4 Chromosome loss is the major mechanism of *MATα* loss in a-like fakers

The CTF and BiM phenotypes have been widely used to study genome instability. However, the ALF phenotype has been only rarely used (Lemoine et al., 2005; Liras et al., 1978; Warren et al., 2004a), and has not been as well characterized. The electrophoretic karyotype of mated colonies obtained after selection was analyzed to infer the mechanism of *MATα* locus loss. Possible events include loss of the entire chromosome III, deletion or translocation removing the *MAT* locus, or gene conversion from *MATα* to *MATa* by recombination with *HMRa*. The chromosome III in the mating tester strain was larger than that in the knockout strains, and could be visually differentiated by pulsed-field gel electrophoresis (Figure 2.6a). In-gel hybridizations with a probe that hybridizes to 3 distant sites on chromosome III (the *MAT* locus, and the silent mating type loci located distally on each arm) allowed detection of the 2 parental chromosome III bands as well as aberrant chromosome III derivatives. Aberrant chromosomes III were observed in a variety of sizes, including a 200 kb product likely to represent homologous recombination between *MATα* and the silent locus *HMRa*, known to generate an active *MATa* locus concomitant with a large deletion on the right arm of chromosome III (reviewed in (Herskowitz, 1988a)).

Electrophoretic karyotyping of mated products from wild-type indicated that 68% of events were due to whole chromosome loss, 20% to chromosomal rearrangement, and 12% to gene conversion (Figure 2.6b). Karyotype analysis of 13 high frequency ALF mutants showed that in 11 ALF mutants, loss of whole chromosome III was the predominant mechanism, similar to wild-type cells. In 2 ALF mutants, different predominant mechanisms were observed in a statistically significant manner. *rad27Δ* showed predominantly chromosome rearrangement, whereas most *sov1Δ* had an intact

chromosome III. *RAD27* encodes an endonuclease that promotes Okazaki fragment maturation during DNA replication. The ALF associated rearrangements are consistent with previous characterization of *RAD27* as a gene that protects against gross chromosomal rearrangements (Chen and Kolodner, 1999). *SOV1* has been implicated in respiration based on its localization to the mitochondria (SGD). To further define the events giving rise to a-like fakers in the *sov1Δ* mutant, PCR was used to detect the presence of *MATa* and *MATα* loci in the mated products (Huxley et al., 1990). Interestingly, all mated products from the *sov1Δ* mutant contained both *MATa* and *MATα* loci, indicating introduction of the *MATa* allele into *MAT* by gene conversion. This was not the general pattern observed in wild-type or in other mutants, where only 3% (1/39) or 6% (24/386) of isolates tested were of this type, respectively.

Interestingly, some high frequency a-like fakers that showed whole chromosome III loss failed to exhibit a sectoring phenotype in the CTF screen. Of 13 frequent ALF mutants analyzed in Figure 2.6, only 5 were identified by CTF phenotype in the high-throughput screen: 3 with strong (*kar3Δ, sic1Δ,* and *dia2Δ*) and 2 with weak (*rad27Δ* and *nce4Δ*) phenotypes. To confirm the presence of assay difference, 5 frequent ALF mutants were directly retested for the CTF phenotype in fresh transformants. Two of these (*kar3Δ, sic1Δ*) exhibited a strong CTF phenotype as expected, and 3 showed mild sectoring (*esc2Δ, rad50Δ, xrs2Δ*, Figure 2.6c). Thus, frequent ALF production does not strictly correlate with frequent CF loss. This could indicate that different factors influence the inheritance of endogenous chromosome III and the CF. One explanation is that the telocentric structure of the CF may enhance instability in some mutants. Another is that the presence of a partial homologous chromosome provided by the CF may suppress instability. Further work will be required to determine the underlying biological mechanisms that explain these uncorrelated phenotypes.

2.3.5 Many yeast CIN genes are conserved

Current understanding of mechanisms that contribute to genome stability has been largely fueled by work from model systems. This approach has been informative for

human biology because of the remarkable functional conservation within the chromosome cycle. To evaluate conservation of yeast CIN genes identified in the screens, BLASTp searches using yeast amino acid sequences against proteomes from *S. pombe*, *C. elegans*, *D. melanogaster*, *M. musculus*, and *H. sapiens* were performed. Among the 293 yeast CIN genes, 103 (35%) have homologues with e-values $<10^{-10}$ in all 5 organism proteomes searched (see Appendix 5, which contains alignment results and functional summaries). Previous work showed that ~40% of yeast proteins are conserved through eukaryotic evolution (Rubin et al., 2000), and 30% of known genes involved in human diseases have yeast homologues (Bassett et al., 1997). In agreement, 124 (42%) of the yeast CIN genes identified in this study have homologues in human, with e-values $<10^{-10}$. Human homologues of yeast CIN genes represent candidates that may cause a CIN phenotype in human cells when mutated. Genetic perturbation causing a CIN phenotype can be a predisposing condition for cancer initiation or progression. Among the 130 high confidence CIN gene list, 10 'top hit' human homologues (with e-values $<10^{-10}$) (Table 2.3 and Appendix 6) have been previously shown to exhibit somatic mutations in cancer.

2.3.6 A strategy for cancer therapy: synthetic lethality and selective cancer cell killing

While CIN mutations can contribute to tumorigenesis, the altered genotype of a cancer cell may define a genetic "Achilles heel" that supports the selective killing of tumor cells relative to adjacent normal cells. Genetic interactions resulting in cell lethality hold promise for the design of therapeutic approaches in cancer. One kind of genetic interaction with properties useful for this strategy is synthetic lethality, observed when two mutations individually capable of supporting viability cause cell death when present together. Synthetic lethal mutant pairs identify genes that function in parallel or related pathways that cannot be simultaneously lost (Ooi et al., 2006). Following this logic, cancer cells with a specific CIN mutation can be killed through loss of function of a synthetic lethal partner, while sparing normal cells (Hartwell et al., 1997; Kaelin, 2005). Systematic, large scale synthetic lethality analysis in yeast provides a means for identifying such second-site loss-of-function mutations (Eason et al., 2004; Harris et al.,

2004; Pan et al., 2006; Tong et al., 2004). These budding yeast studies provide candidate human proteins whose inhibition (e.g., by a drug) may specifically kill tumor cells relative to normal cells. In this regard, gene deletions that exhibit synthetic lethality with multiple different CIN gene mutants are particularly attractive, as they might define broad-spectrum therapeutic targets.

To address this concept, an analysis all known synthetic lethal interactions available for the yeast CIN genes that have cancer gene homologues (shown in Table 2.3) was performed (8 of the 10 have published synthetic lethal data). These 8 mutants are connected to 250 partners by 371 synthetic lethal interactions based on BioGrid (Stark et al., 2006) (data not shown). Among the 250 partners, 61 bridge at least 2 yeast cancer homologues (Figure 2.7). Notably, 3 mutants (*ctf4Δ*, *ctf18Δ*, *dcc1Δ*) exhibit synthetic lethality with at least 6 cancer gene homologues. Interestingly, these 3 yeast genes share a role in sister chromatid cohesion (Mayer et al., 2004; Warren et al., 2004a). The 'hub' position of these 3 mutants in the interaction network implies that different CIN gene mutants share a common genetic vulnerability, and these common synthetic lethal interactors can serve as broad spectrum targets. The existant synthetic lethal dataset in budding yeast, although incomplete, is continuously expanding (Tong et al., 2004). Therefore, more 'hubs/common nodes' may be identified. A comprehensive synthetic lethal network, together with an increased understanding of the mutation spectrum in cancers, could provide insights pertinent to the design of therapeutic approaches in which human cancer cells are efficiently targeted for death by clinical intervention. Integration of knowledge among emerging high throughput datasets in model organisms will stimulate new research directions and applications in combating human diseases.

2.4 Discussion

This work identified an extensive catalog of genome instability mutants, based on phenotypic testing of haploid and diploid yeast knockout collections for chromosome transmission fidelity (CTF), bimater behavior (BiM), and a-like faker formation (ALF). This study characterized all non-essential yeast genes due to their accessibility for

phenotyping. Because many essential genes are known to contribute to genome stability from traditional approaches, a similar systematic screening effort for essential genes would be of great interest, but will first require the development of a comprehensive hypomorphic mutation resource.

An extensive catalog is useful for the understanding of mechanisms that maintain genome stability, for the identification of new pathways important for genome maintenance, and for the organization of functional networks. Systematic screening of arrayed non-essential mutants avoids the sampling problem in traditional mutagenesis methods, and supports the direct comparison of phenotypes observed because all alleles are null. Differences in both phenotype severity and assay specificity were observed. The relative contributions of specific gene products to genome maintenance are revealed directly by phenotype strength. For example, *rad27Δ*, *dia2Δ*, *nce4Δ*, and *xrs2Δ* exhibited the strongest ALF phenotypes (> 56-fold above wild type) among the high confidence yeast CIN genes, whereas well-studied damage response genes such as *mec3Δ*, *mrc1Δ*, *ddc1Δ*, and *rad9Δ* showed milder phenotypes (~11-fold). Apparently, under the growth conditions used in the screen, damage caused by the absence of Rad27p, Dia2p, Nce4p, or Xrs2p proteins exceeds that resulting from checkpoint loss. In addition to phenotype comparisons within a given assay, results from different assays can be compared. For example, *xrs2Δ* exhibited one of the highest ALF frequencies but a mild or absent CTF phenotype, indicating that the damage associated with *xrs2Δ* is more relevant to the maintenance of a haploid chromosome III than to the artificial CF. In general terms, different chromosome marker stability assays (CTF, ALF, and BiM) defined both distinct and overlapping gene sets. The screen specificities could be due to sensitivity differences, but likely reflect mechanistic differences revealed by the assay systems. For instance, screening in both haploids and diploids may give insight into how ploidy affects the maintenance of chromosomes. The results demonstrate the importance of using complementary assays to comprehensively identify genome maintenance determinants.

The error observed in the deletion arrays for non-essential genes underscore the importance of mutant validation. It is widely known that mutant arrays are "evolving

resources" that accumulate changes due to manipulation and selective pressure (i.e. cross well contamination, aneuploidy, second site mutation, etc.). For example, 8% of deletion mutants exhibit chromosome-wide expression biases indicative of aneuploidy for whole chromosomes or chromosomal segments (Hughes et al., 2000). Lethal or slow-growth phenotypes caused by mutations in genes that do not segregate with a knockout allele occur at a frequency of 6.5% (Giaever et al., 2002). However, parameters indicative of array quality are usually not reported in studies using deletion sets. This issue becomes increasingly important as phenotypic data derived from distantly related replicates of the deletion resource are compared and integrated. In this study, tag sequence analysis of CIN mutant strains suggests false negative observations from well contamination were between 3 and 22% in different screens (see Appendix 1 and 4 for details). This phenomenon is likely to be observed in other copies of the deletion sets. Because the data were derived from 3 different array sets obtained from commercial distribution sources, and involved 2 laboratories both with experience in handling large strain collections, it is unlikely that well address errors were due to laboratory specific manipulation of the sets. An empirical measure agrees: the CTF screen of the knockout collection identified 12 of 15 non-essential *ctf* mutants found previously in a traditional mutagenesis (Spencer et al., 1990). Two out of the 3 missed mutants were due to incorrect strains at the well positions of the array plates obtained from the commercial distribution source when checked by PCR. The false positive frequency due to secondary mutations or aneuploidy in the deletion collection strains can also be estimated. For the haploid collections, the false positive rates were relatively high:

1-{26X33%+(10+19)X91%+32}/86=18% for the *MATa* collection;

1-{126X50%+(54+19)X91%+32}/231=31% for the *MATα* collection; and for the diploid collection, the false positive rate was lower:

1-{26X75%+(10+54)X91%+32}/122=5%. These frequencies are consistent with the frequency of unlinked recessive lethal mutations segregating independently of the deletion mutations that was observed during construction of the mutant resource (Giaever et al., 2002). In this study, false positive observations were rare among genes identified

in >1 chromosome marker loss assay (i.e. in >1 deletion resource). The results were therefore partitioned into 130 high confidence genes (115 genes identified by >1 screen, plus 15 genes confirmed in new transformants), and 163 lower confidence genes identified by single screens only.

A full catalog of yeast CIN genes will provide a rich resource for ongoing studies of genomic instability in many organisms, including human. Additional screens of non-essential yeast mutants (such as GCR screens in (Huang and Koshland, 2003; Smith et al., 2004)) and systematic incorporation of essential mutants will enhance the utility of the yeast model system. Yeast CIN genes define cross-species candidate genes in humans that could contribute to CIN during tumorigenesis. A recent survey of CIN colorectal tumors (Wang et al., 2004b) provides a proof of principle. One hundred human candidate genes (chosen for similarity to model organism CIN genes) were screened for mutations in tumor samples, yielding 5 new CIN human genes mutated in colorectal cancer (*MRE11*, *Zw10*, *Zwilch*, *Rod*, and *Ding*, in addition to the 2 previously known (*CDC4*, and *BUB1*) (reviewed in (Yuen et al., 2005)). These 7 CIN cancer genes account for <20% of the CIN mutational spectrum in colon cancer, and many other candidate CIN genes remain untested. Systematic analysis of the mutational spectrum leading to a CIN phenotype in a model eukaryotic organism such as yeast will therefore help to define the mutational spectrum leading to a CIN phenotype in human cancer, and may accelerate the identification of protein targets for selective killing of cancer cells.

Table 2.1 24 *ctf* mutants cloned to date
An additional 27 single member ctf isolates have not been cloned.

ctf	# alleles	Gene name	Essential?	Function	Cohesion	Kinetochore	DNA/RNA metabolism
1	30	CTF1/CHL1/LPA9		Cohesion	X		
2	11	(not cloned)					
3	11	CTF3/CHL3		Central kinetochore		X	
4	8	CTF4/POB1/CHL15		Cohesion	X		
5	5	CTF5/MCM21		Central kinetochore		X	
6	5	CTF6/RAD61		Cohesion	X		
7	5	CTF7/ECO1	X	Cohesion (establishment)	X		
8	3	CTF8		Cohesion (alternative RFC)	X		
9	3	(not cloned)					
10	3	CTF10/CDC6	X	DNA replication			X
11	3	PDS5/SPO27		Cohesion/condensation	X		
12	3	CTF12/SCC2/AMC3	X	Chromosome condensation	X		
13	1	CTF13/CBF3C	X	Inner kinetochore (CBF3)		X	
14	1	CTF14/NDC10	X	Inner kinetochore (CBF3)		X	
15	1	CTF15/RPB4/ SEX3		Subunit of RNA polymerase II			X
16	1	(not cloned)					
17	2	CTF17/CHL4/MCM1		Central kinetochore		X	
18	3	CTF18/CHL12		Cohesion (alternative RFC)	X		
19	2	CTF19/MCM18/LPB		Central kinetochore		X	
s3	1	BIM1/HSN9/YEB1		Microtubule-binding at SPB/kinetochore		X	
s127	1	SIC1		Cell cycle regulator			X
s138	1	SPT4		Chromatin structure/ transcription			X
S141	1	NUP170/NLE3		Nucleoporin			X
S143	1	MAD1		Kinetochore protein /spindle checkpoint		X	
s155	1	MCM16		Central kinetochore		X	
s165	1	SCC3/IRR1	X	Cohesion	X		
s166	1	SMC1/CHL10	X	Cohesion/condensation	X		
27	**109**	**Total**	**7**		**10**	**9**	**5**

Table 2.2 List of yeast strains used in Chapter 2

The genotypes and origins of strains used in this study are shown.

Strain	Genotype	Reference
BY4741	*MATa*	(Brachmann et al., 1998)
BY4742	*MATα*	(Brachmann et al., 1998)
Y2454	*MATα mfa1Δ::MFA1pr-HIS3 can1Δ ura3Δ0 leu2Δ0 his3Δ1 lys2Δ0*	(Tong et al., 2001b)
YPH1724	*MATα ade2-101::natMX mfa1Δ::MFA1pr-HIS3 can1Δ ura3Δ0 leu2Δ0 his3Δ1 lys2Δ0*	This study
YPH255	*MATa ade2-101 his3-Δ200 ura3-52 lys2-801 trp1-Δ63 leu2-Δ1 CFVII(RAD2.d)::URA3 SUP11*	Hieter lab
YPH1124	*MATa ade2-101 his3-Δ200 ura3-52 lys2-801 trp1-Δ63 leu2-Δ1 CFIII(CEN3.L)::URA3 SUP11*	(Pot et al., 2003)
YPH1725	*MATα ade2-101:: natMX his3 ura3 lys2 can1Δ mfa1Δ::MFA1pr-HIS3 CFVII(RAD2.d)::URA3 SUP11*	This study
YPH1726	*MATα ade2-101:: natMX his3 ura3 lys2 can1Δ mfa1Δ::MFA1pr-HIS3 CFIII(CEN3.L)::URA3 SUP11*	This study
YPH315	*MATa his1*	(Spencer et al., 1990)
YPH 316	*MATα his1*	(Spencer et al., 1990)
YPH1738	*MATa/MATα ura3Δ0/ura3Δ0 leu2Δ0/leu2Δ0 his3Δ1/ his3Δ1 LYS2/ lys2Δ::kanMX6 MET15/met15Δ::kanMX6*	This study

Table 2.3 Human proteins homologous to yeast CIN genes are mutated in cancer
The protein sequences corresponding to 130 high confidence yeast CIN genes were used as queries in a BLASTP search against the human RefSeq protein database. Online Mendelian Inheritance in Man (OMIM, www.ncbi.nlm.nih.gov/omim) and cancer census (Futreal et al., 2004) databases were used to identify cancer associated mutations in 'top hit' human genes.

Yeast Gene	Top Human Hit	E-value	Disease Description, MIM#(disease)	MIM# (gene)	Reference
ADE17	*ATIC*	0	Anaplastic large cell lymphoma		Cancer census
RAD54	*RAD54L*	1E-164	Non-Hodgkin lymphoma; Breast cancer, invasive intraductal; Colon adenocarcinoma	603615	OMIM
RAD51	*RAD51*	1E-122	susceptibility to Breast cancer, 114480	179617	OMIM
RDH54	*RAD54B*	1E-121	Non-Hodgkin lymphoma; Colon adenocarcinoma	604289	OMIM
SGS1	*BLM*	1E-115	Bloom syndrome, 210900	604610	OMIM, Cancer census
MRE11	*MRE11A*	1E-108	Ataxia-telangiectasia-like disorder, 604391; Colorectal cancer	600814	OMIM, (Wang et al., 2004b)
DUN1	*CHEK2*	6E-55	Li-Fraumeni syndrome, 151623; Osteosarcoma, somatic, 259500; susceptibility to Breast cancer, 114480; Prostate cancer, familial, 176807; susceptibility to colorectal cancer	604373	OMIM
BUB1	*BUB1*	1E-41	Colorectal cancer with chromosomal instability	602452	OMIM
MAD1	*MAD1*	5E-12	Lymphoma, somatic; Prostate cancer, somatic, 176807	602686	OMIM
CDC73	*HRPT2*	9E-12	Hyperparathyroidism-jaw tumor syndrome, 145001; Hyperparathyroidism, familial primary, 145000; Parathyroid adenoma with cystic changes, 145001	607393	OMIM

Figure 2.1 Three screen methods

a) CTF screen method

The genotypes of the donor strain and the *MATa* deletion mutants are shown within the schematic yeast cell respectively. The gray line with a gray circle depicts the CF. Each filled circle represents a selectable marker used in the SGA scheme, whereas an open circle in the corresponding color represents the unmarked allele. The 'X' indicates mating between the 2 strains. The arrows indicates the selection procedures. Yeast cells enclosed by the dashed rectangles represent cells that were selected. The dashed arrow indicates the loss of a CF. Examples of severe and mild sectoring colonies, as well as wild-type colonies are shown.

b) BiM screen method

An example of an agar plate containing homozygous deletion mutants grown in 96-array format is shown. The yellow rectangles represents agar plates containing the specified media, and the indicated yeast strains were grown on them. The arrows indicates replica plating, pointing from the source plates to fresh destination plates. The blue blocked arrows indicate scanning, visual inspection and densitormetry reading of the Sc-6 plates, which selected for mated products. An example of a set of plates mated with *MATa* and *MATα* mating testers, respectively, is shown. Yeast cells enclosed by yellow squares had high mating with both *MATa* and *MATα* mating testers; whereas yeast cells enclosed by red and green squares had high mating with *MATa* and *MATα* mating testers, respectively, and these were not included in further analysis. The bottom shows an example of a retested plate containing 3 homozygous deletion mutants, each represented by 4 independent colonies, together with the wild-type diploid (YPH1738) and *chl1Δ/chl1Δ*. On the left is the SC-6 plate replica plated from the YPD plate with *MATa* mating tester (X MATa), and on the right is the SC-6 plate replica plated from the YPD plate with *MATα* mating tester (X *MATα*).

c) ALF screen method

The scheme of a-like faker selection is shown in the box, with the genotypes of the starting and selected strains indicated. The actual patching and replica plating procedures are shown below. An example of SC-6 plate with mated products derived from mating of the *MATα* mating tester with 12 deletion mutants, positive and negative controls on the same plate, is shown. *bub3Δ*, *hst3Δ* and *yor024wΔ* showed elevated mating frequencies with the *MATα* mating tester. The retest plate of these 3 mutants, each represented by 4 independent patches, is shown.

Figure 2.1a CTF screen method

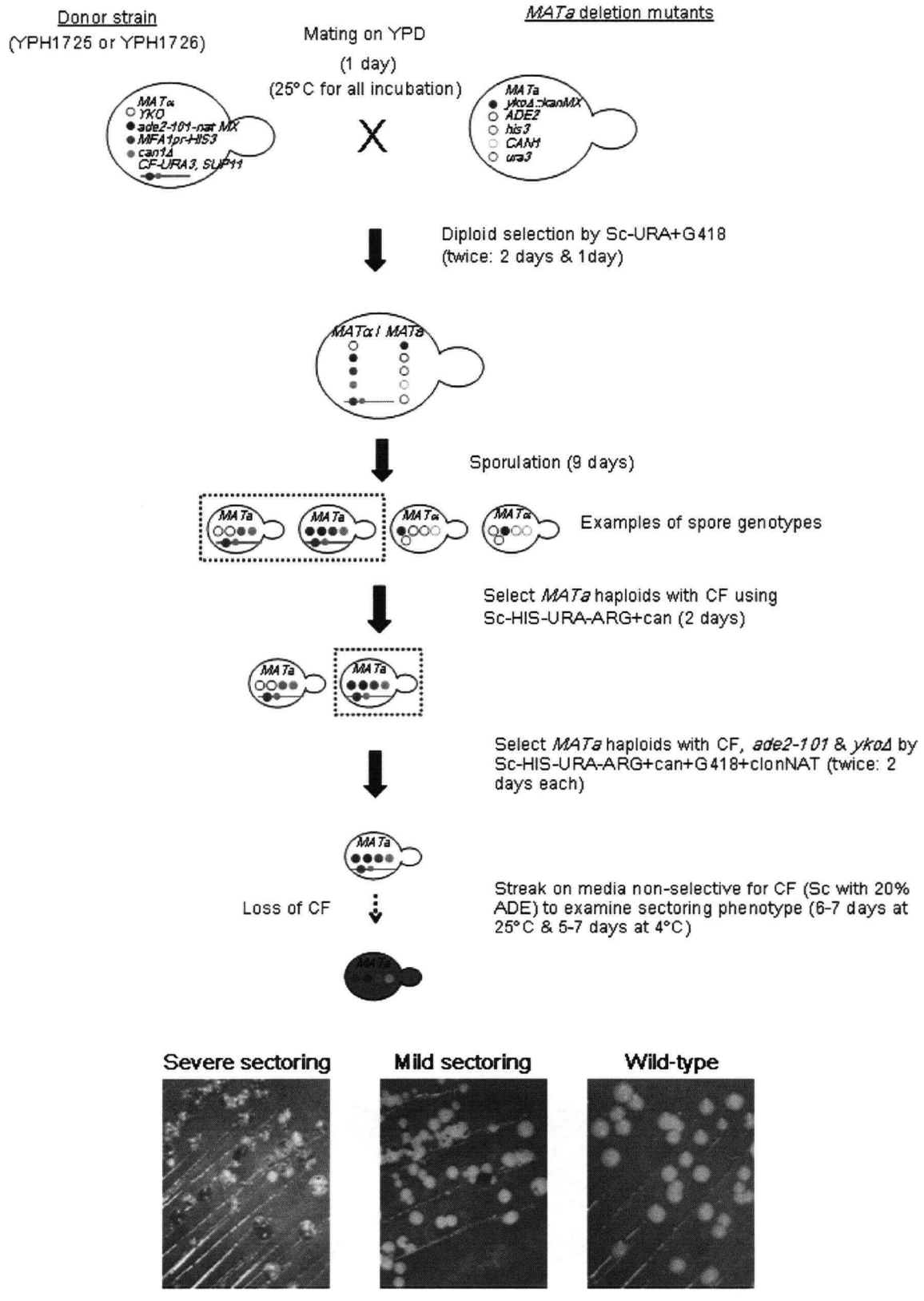

Figure 2.1b BiM screen method

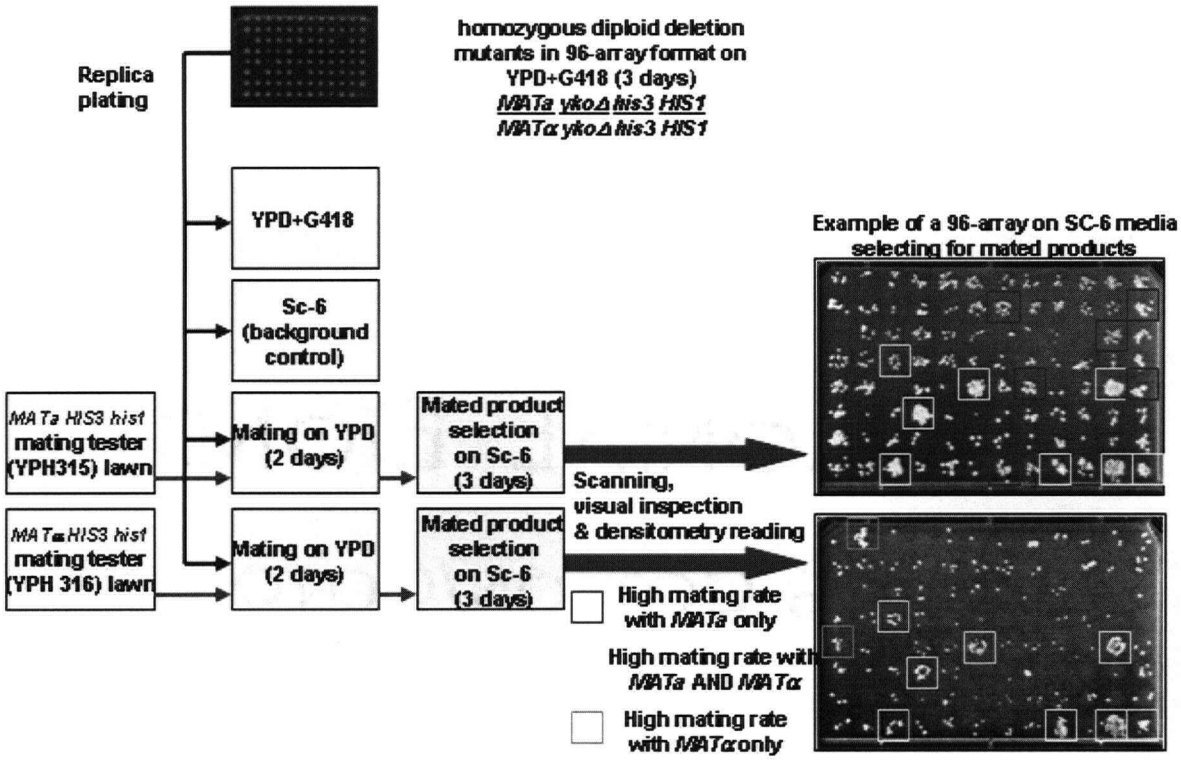

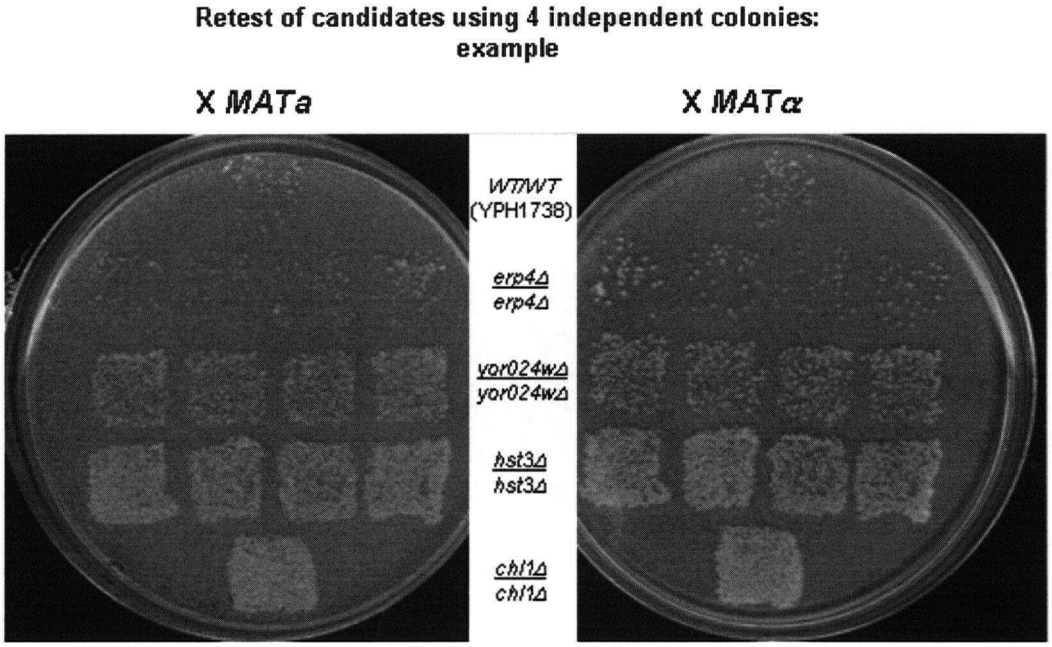

Figure 2.1c ALF screen method

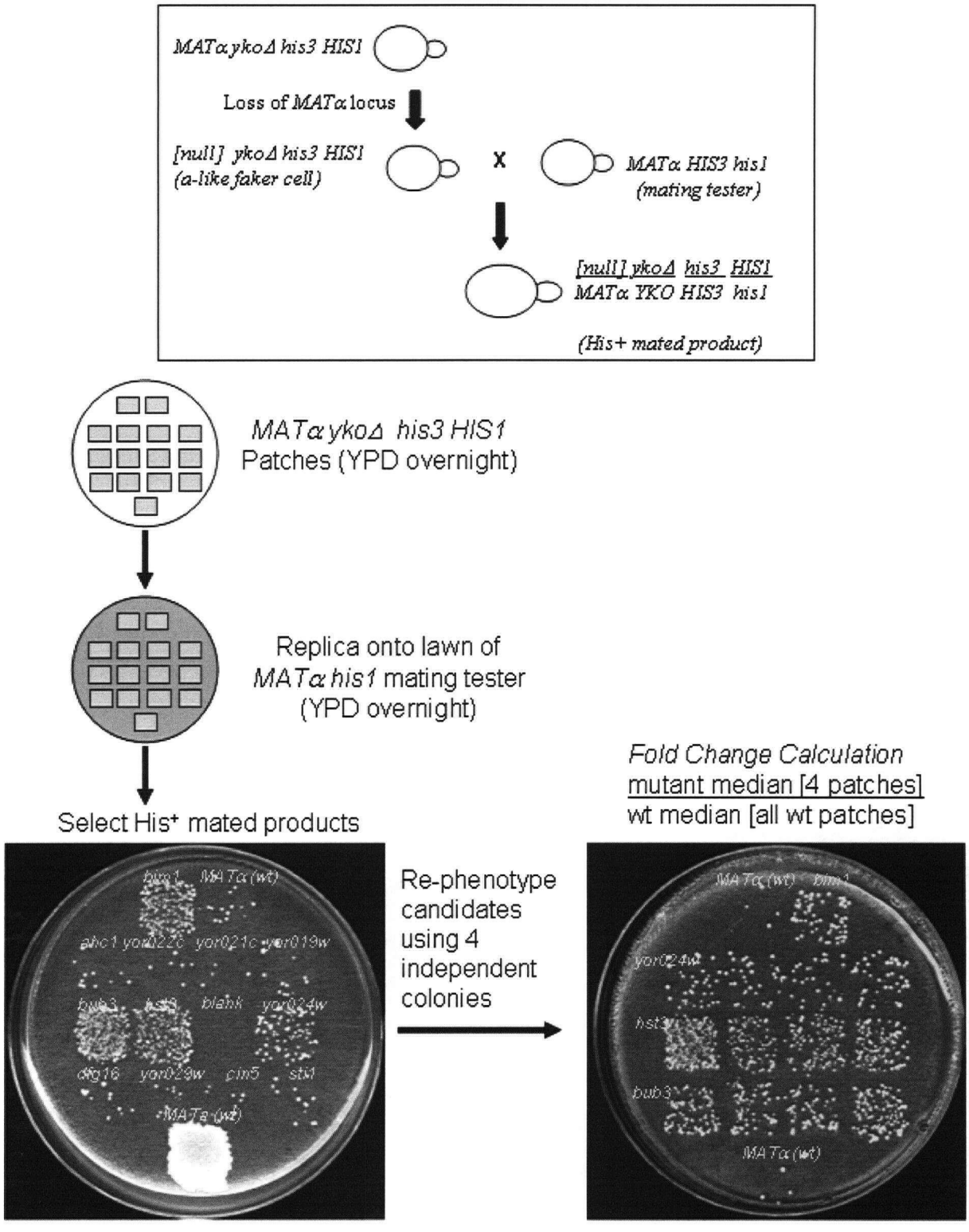

Figure 2.2 Three marker loss screens

A. Haploid yeast knockout mutants (*ykoΔ*) containing *ade2-101* and a chromosome fragment (CF, blue line whose centromere is depicted as a circle) were generated. The CF contains the *SUP11* gene (blue rectangle) on the telocentric arm. *ade2-101* cells develop red color, but the *SUP11* gene on the CF suppress the pigment formation (Gerring et al., 1990; Hegemann et al., 1988; Warren et al., 2002). Cells that contain the CF are therefore unpigmented, whereas cells without the CF are red. Mutants that inherit the CF unstabliy form colonies with red sectors. An example was shown. The chromosomal context of the tested strains was shown at the bottom. Loss of *SUP11* is caused by loss of the whole CF.

B. Homozygous diploid yeast knockout mutants were tested for 'bimater' phenotype. For example, loss of the *MATa* allele (depicted in gray) causes the development of an α-type mating cell, which is detected by its ability to mate (depicted by 'X') with a *MATa* tester strain containing complementing auxotrophy to support selection of mated diploids. Mutant strains exhibiting unstable inheritance of the *MAT* locus will lose either allele in individual cell and exhibit a 'bimater' phenotype in a population. The mutants in the squares show elevated formation of mated cells after exposure to either *MATα* or *MATa* testers (Spencer et al., 1990). The heterozygous MAT locus in the homozygous diploid knockout strains was shown. Loss of heterozygosity of the MAT locus can be caused by various mechanisms indicated

C. *MATα* haploid yeast knockout mutants were tested for elevated frequency of a-like faker cells. Loss of the *MATα* locus (depicted in gray) in haploids results in dedifferentiation to a-mating type. The presence of these cells is detected by selection for mated products after exposure to a *MATα* tester strain. Examples of mated products formed from a wild-type and an *alf* mutant were shown

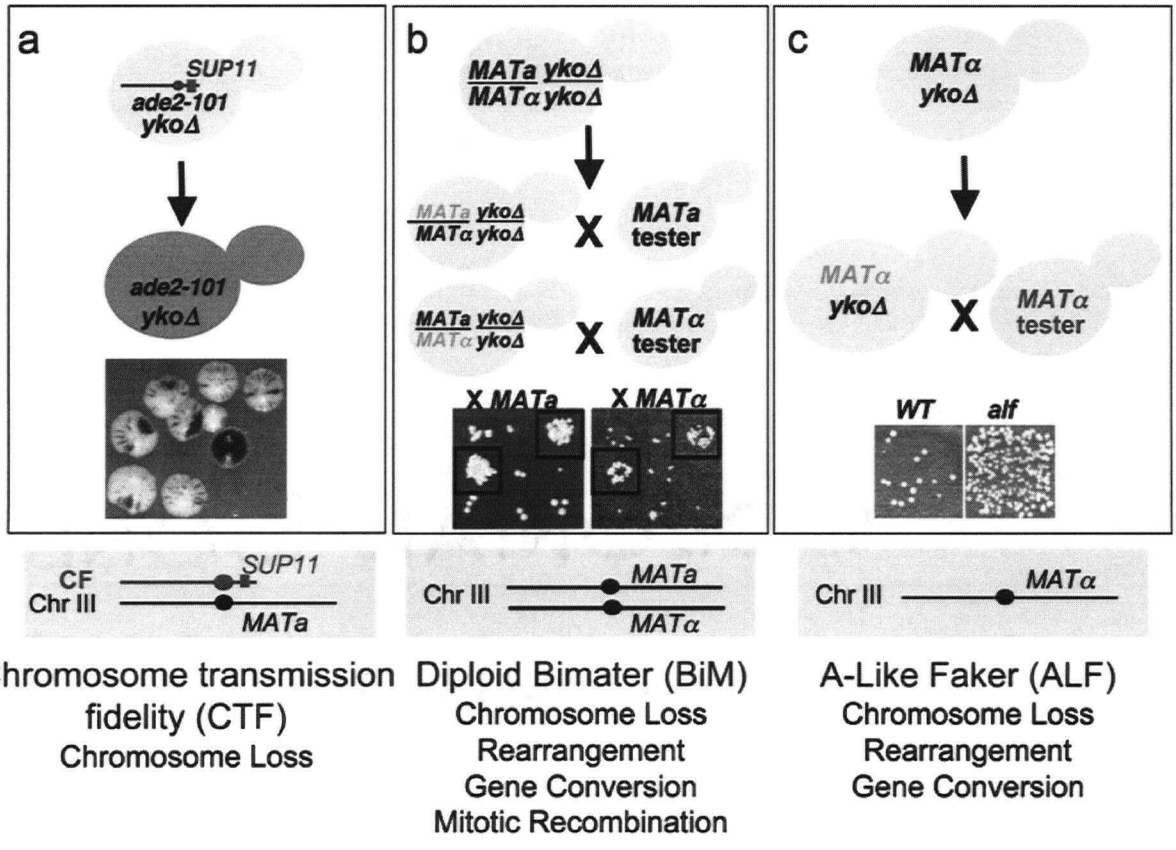

Figure 2.3 130 high confidence non-essential yeast CIN genes

The Venn diagram shows the distribution of 293 mutants identified initially across the 3 screens. The numbers in parenthesis denote single-assay knockouts confirmed in independent transformants, which are included in the detailed diagram to the right. The detailed diagram to the right summarizes the 130 high confidence genes described in Appendix 1 (For the other 163 genes, see Appendix 2). All gene names are connected to 1 or more of the 3 screen nodes (CTF, BiM, or ALF), indicating the screen phenotypes the knockout mutants exhibit. Gene names in black typeface are those fully validated in all 3 deletion arrays: i.e. tag sequencing indicated the presence of only the correct mutation. For these mutant, a present or absent CIN phenotype observed in any screen is meaningful. Gene names in blue italic typeface failed tag validation in at least 1 of the deletion collections, and therefore phenotype information is missing from at least 1 screen. These partially characterized genes are placed to indicate positive phenotypes known from validated deletion sets (Appendix 1 and Appendix 2 contain details of the validation status). The node colors indicate biological process. Genes associated with more than one functional group is represented by the one highest in the color key for simplicity.

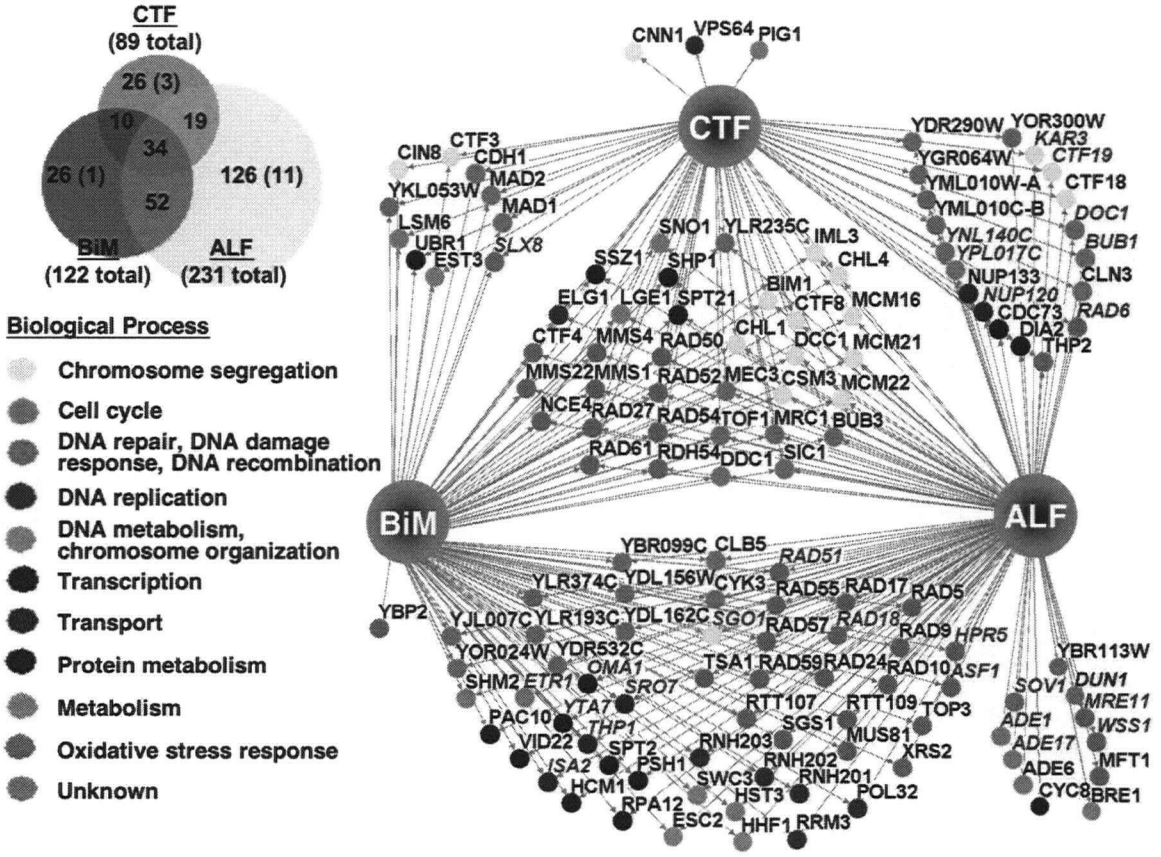

Figure 2.4 Functional groups of 293 CIN genes

GO biological process terms for the 293 marker loss genes were obtained using Osprey (v1.2.0) functional groupings (Breitkreutz et al., 2003b). For genes associated with more than one GO biological process, a single GO process was assigned according to the priority shown in the Figure 2.3 color key for simplicity.

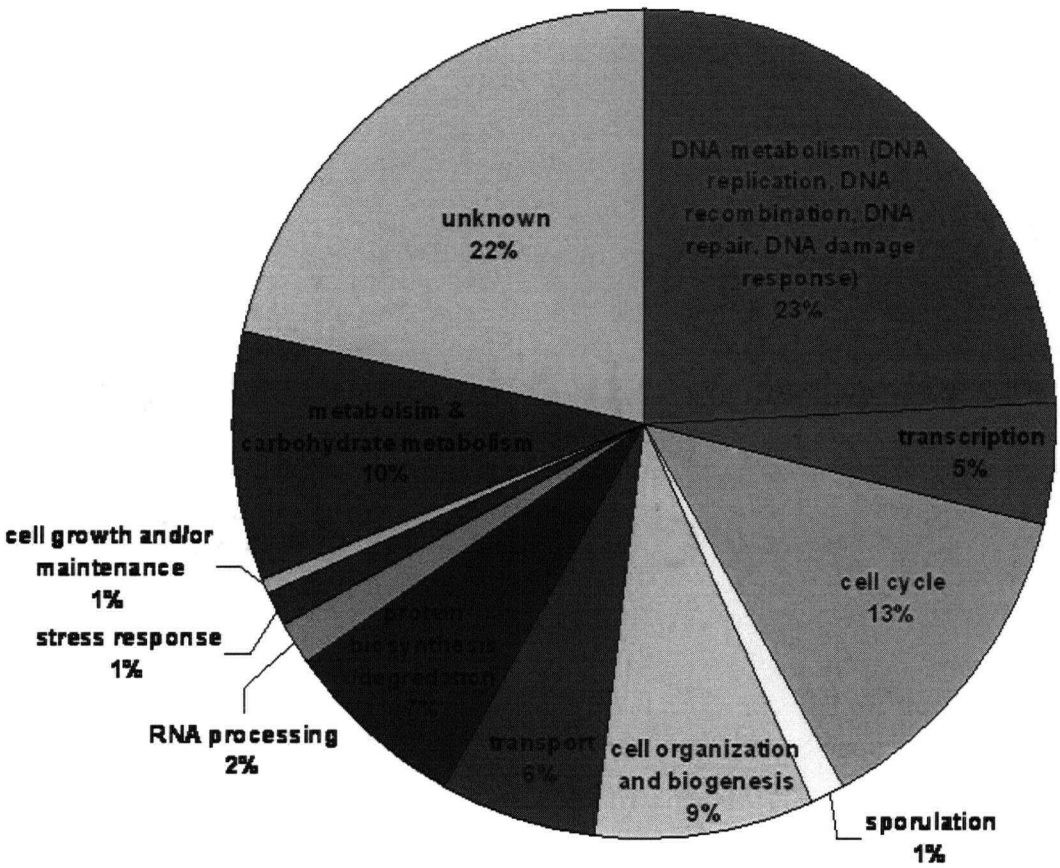

Figure 2.5 92 protein interactions among 102 CIN proteins

Different types of protein interactions were shown among CIN proteins using GRID database and OSPREY program, indicated by arrows pointing from a bait/query. Color of the proteins represents the GO biological process. Known complexes or pathways were circled and annotated in red. Abbreviations: chkpt. (checkpoint); rec. (recombination); ctrl. (control); mod. (modification).

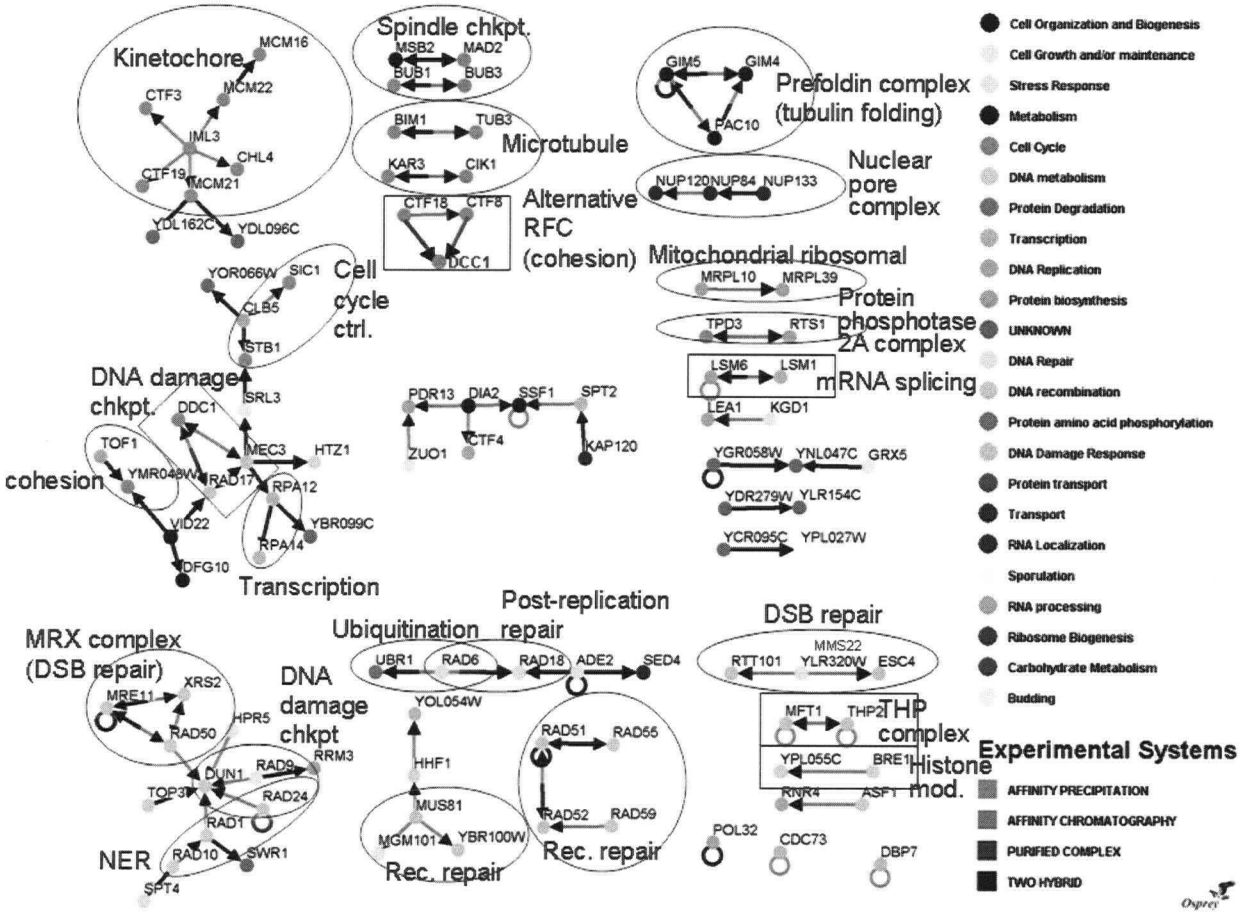

Figure 2.6 A-like fakers result from whole chromosome loss, gross chromosomal rearrangement, and gene conversion

A. Individual colonies selected after mating were characterized using pulsed-field gel electrophoresis (top, ethidium bromide stained gel) and in-gel hybridization with a radiolabeled probe (bottom, autoradiogram) that hybridizes chromosomal bands containing the mating type locus and/or silent mating type loci located distally on each arm. Chromosomes III from the mating tester and deletion mutant were of distinct size (top and bottom chr III bands, respectively). In some strains, a less intense signal for rearrangement chromosomes reflects poor mitotic transmission or hybridization only to *HMRa* which has imperfect homology to the radiolabeled probe.

B. Summary of electrophoretic karyotypes from 13 ALF mutants. ALF frequency is shown as fold over wild type. Event percentages (chr III loss, gross chromosome rearrangement (GCR), or retention of normal structure) are calculated from independent wild-type or mutant mated products (n=40 and n>10, respectively). The outcome distributions for *sov1Δ* and *rad27Δ* are significantly different from wild type (chi square, $p < 0.01$).

C. Discordant CTF sectoring phenotypes are observed in knockout mutations with similar ALF frequencies.

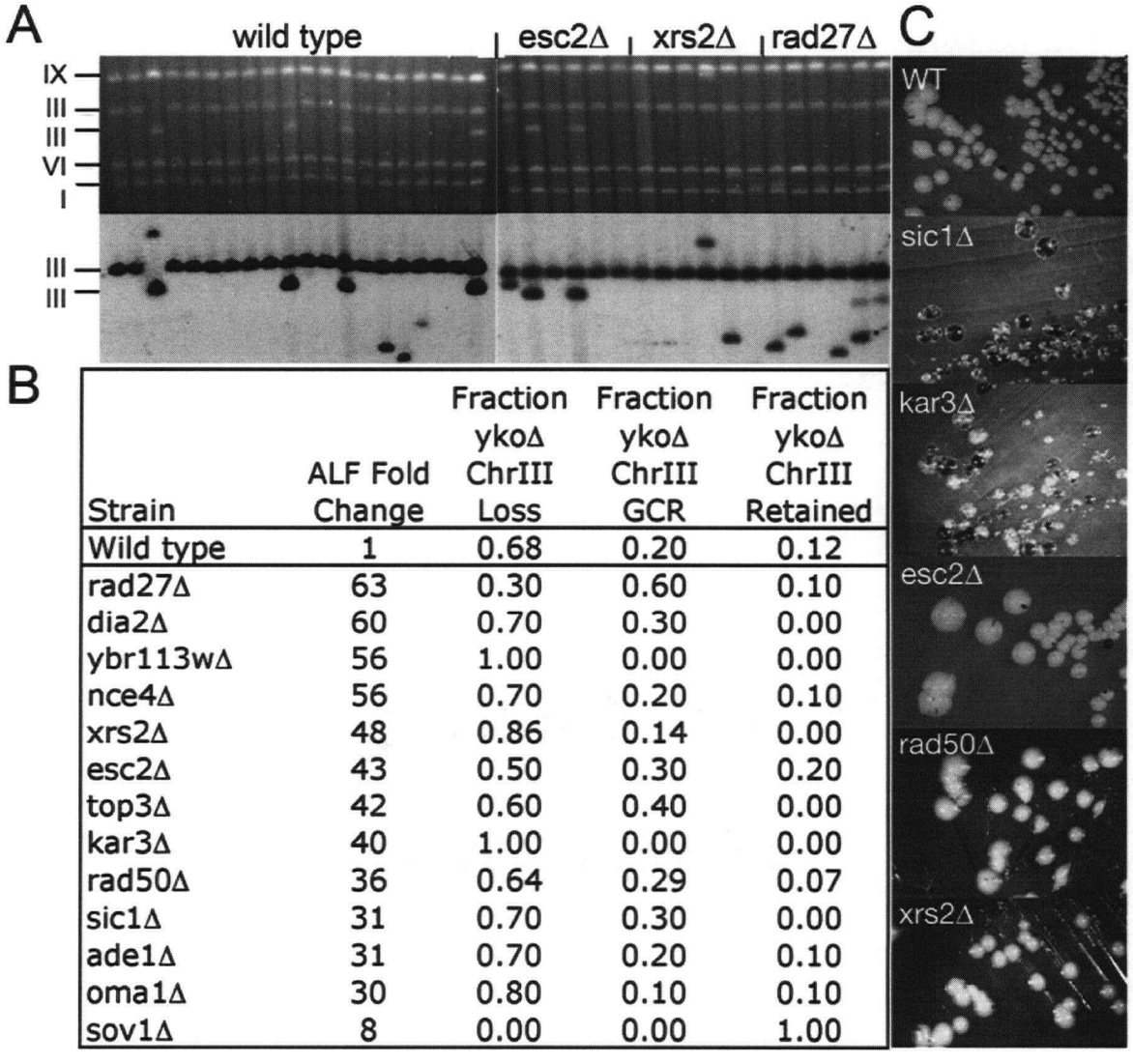

B

Strain	ALF Fold Change	Fraction ykoΔ ChrIII Loss	Fraction ykoΔ ChrIII GCR	Fraction ykoΔ ChrIII Retained
Wild type	1	0.68	0.20	0.12
rad27Δ	63	0.30	0.60	0.10
dia2Δ	60	0.70	0.30	0.00
ybr113wΔ	56	1.00	0.00	0.00
nce4Δ	56	0.70	0.20	0.10
xrs2Δ	48	0.86	0.14	0.00
esc2Δ	43	0.50	0.30	0.20
top3Δ	42	0.60	0.40	0.00
kar3Δ	40	1.00	0.00	0.00
rad50Δ	36	0.64	0.29	0.07
sic1Δ	31	0.70	0.30	0.00
ade1Δ	31	0.70	0.20	0.10
oma1Δ	30	0.80	0.10	0.10
sov1Δ	8	0.00	0.00	1.00

Figure 2.7. Common synthetic lethal interactions among yeast CIN genes that have human homologues mutated in cancer

Eight yeast CIN genes with top hit human homologues mutated in cancer (e-value $<10^{-10}$) are also found in the public interaction database BioGrid (Stark et al., 2006). They are placed peripherally, and shown in black. 61 interactors that have at least 2 synthetic lethal connections with the yeast cancer homologues are shown. The arrows point from a query to a target gene hit in the synthetic lethal screens. The 27 genes in blue fonts are themselves high confidence CIN genes identified by the screens, and 12 genes in purple fonts are in the lower confidence CIN gene list. The 3 genes that have 6 common synthetic lethal interactions

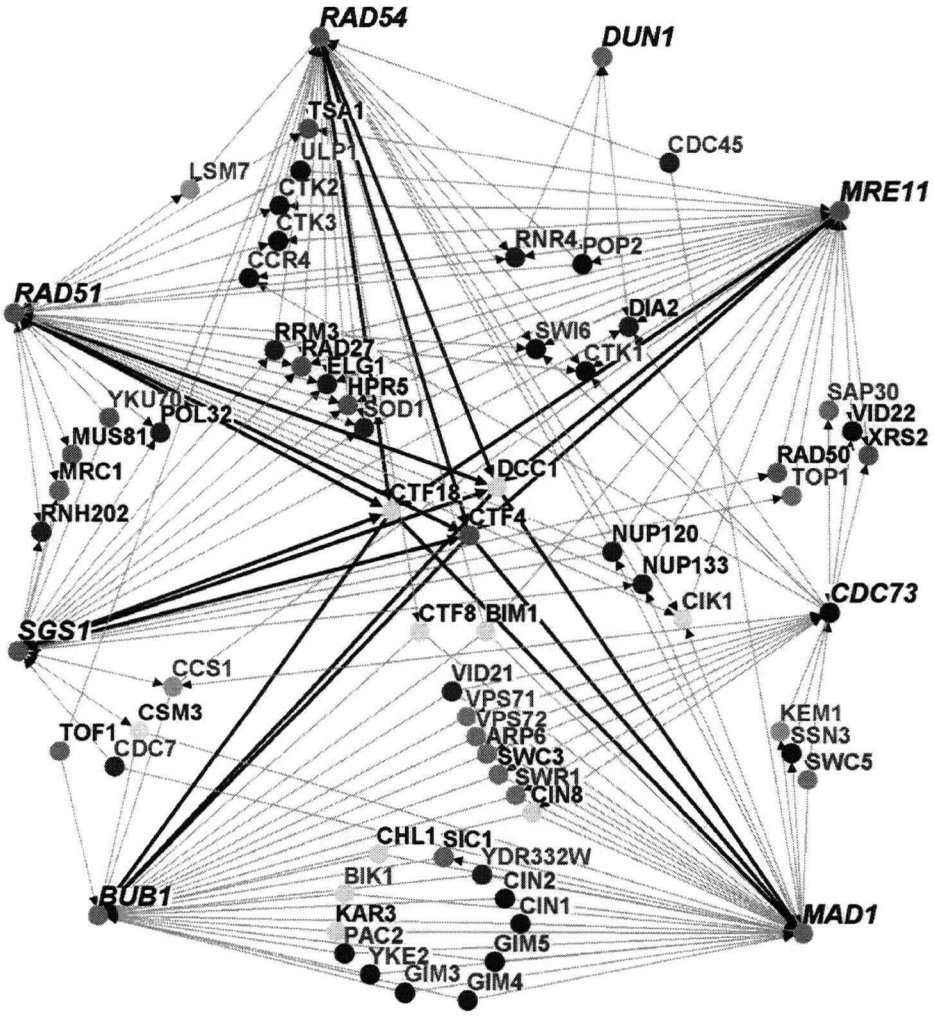

CHAPTER 3

Identification of Somatic Mutations in Cohesion Genes in Colorectal Cancers with Chromosome Instability

A modified version of this chapter has been prepared for publication. Karen W.Y. Yuen*, Tom Barber*, Marcelo Reis*, Kirk McManus, Forrest Spencer, Bert Vogelstein, Victor Velculescu, Phil Hieter, and Christoph Lengauer (*These authors contributed equally to this work). Identification of Somatic Mutations in Cohesion Genes in Colorectal Cancers with Chromosome Instability.

3.1 Introduction

While the majority of colorectal cancers exhibit CIN, the molecular and genetic basis for this phenotype is not well characterized. Over the last decade, only a handful of genes known to be important for maintaining chromosome stability (CIN genes) have been systemically tested and identified to have mutations in colorectal cancers, including *BUB1*, *BUB1B* (Cahill et al., 1998), *CDC4* (Rajagopalan and Lengauer, 2004b), *MRE11A*, *Zw10*, *Zwilch*, *Rod* and *Ding* (Wang et al., 2004b). All these genes were first identified based on chromosome segregation or cell cycle phenotypes in model organisms such as yeast and fly. These cross-species connections are examples of the high degree of evolutionary conservation in basic cellular mechanisms, and how basic biology studies in model organisms can be applied efficiently to gain an understanding of human disease. Recently, germline biallelic mutations in *BUB1B* have been associated with mosaic variegated aneuploidy and inherited predispositions to cancer, strongly supporting a causal link between CIN and cancer development (Hanks et al., 2004). However, each of the 8 genes mentioned above accounted for only a small fraction of the somatic mutation spectrum in colon cancer (1-10%), suggesting that more CIN genes could each be mutated to cause CIN in cancer. Systematic mutational analysis of CIN genes in colorectal cancers would therefore be useful to determine the complete mutational spectrum and mutation frequency leading to CIN. Indeed, the Lengauer/Vogelstein groups sequenced 100 candidate CIN genes (based on their similarity to yeast and fly genes) and identified 5 of the 8 genes mentioned above, suggesting that expansion of this kind of study would lead to the identification of additional relevant CIN genes (Wang et al., 2004b). Among the 100 candidate human CIN genes pursued in the study, the best yeast homologue of 30 human CIN genes yields the same human genes by reciprocally searching the best human homologue by BLASTp (Table 3.1), outlining the number of yeast genes that have been used previously to identify human CIN gene mutation in cancer.

In this study, the potential role of CIN genes in a panel of colorectal cancers was systematically analyzed by sequencing 101 candidate human CIN genes based on their

similarity to yeast homologues. 20 somatic mutations were identified genes that function in 4 functional groups. Seventeen of the mutations were found in 5 genes that are directly involved in sister chromatid cohesion (*SMC1L1*, *CSPG6*, *NIPBL*, *STAG2*, and *STAG3*). Furthermore, single somatic mutations were identified in each of these 3 genes: *BLM*, the Bloom syndrome gene; *RPN20*, a E3 ubiquitin ligase; and *UTX*, a transcription factor. This study broadens the mutational spectrum of CIN genes in colorectal cancer. The results are consistent with a genetic basis for CIN, and with CIN having a role in tumorigenesis. Phenotypic analysis of a conserved missense mutation in yeast *SMC1* revealed a modest recessive CIN phenotype in yeast cells. Further functional studies of the somatic mutations found will enhance our understanding on whether these mutations cause CIN in cancer cells.

3.2 Materials and Methods

3.2.1 Gene identification

293 non-essential yeast CIN genes identified from recent comprehensive genome-wide screens (Yuen et al., submitted; see Chapter 2) were searched for human homologues by BLASTp using Refseq database, and 88 human genes were selected based on the extent of sequence similarity (63 had a e-value <1E-10) and strength of the CIN phenotype in yeast. 64 were derived from the high confidence list (including 2 homologues of *CHL1*) and 24 were from the low confidence list. 2 non-essential *CTF* genes identified by traditional random mutagenesis (Spencer et al., 1990) but missed in the high-throughput screens (*NUP170*, *RPB4*) were also included; as well as 11 human genes homologous to essential yeast genes involved in chromosome transmission fidelity (Spencer et al., 1990) and cohesion. A total of 101 candidate CIN genes were analyzed.

3.2.2 Sequencing

PCR primer design, amplification, sequencing, and sequence analysis were performed as previously described in (Sjoblom et al., 2006; Wang et al., 2004b).

3.2.3 Yeast *smc1* mutants construction and characterization

Mutations were introduced into the yeast *SMC1* gene by performing two rounds of PCR. One set of primary PCR product was amplified from wild-type (*WT*) genomic DNA using a sense primer ~500b upstream of the mutation, and an antisense primer containing the mutation in the middle; and a second primary PCR product was amplified with a sense primer containing the mutation in the middle and an antisense primer ~200b downstream of *SMC1* that included a 20b homology to the TEF promoter. The primary PCR products were gel purified and used as template for a secondary round of PCR using the sense primer ~500b upstream of the mutation and the antisense primer ~200b downstream of *SMC1* that included the 20b homology to the TEF promoter. The secondary PCR product was gel purified, cloned in Topo2.1 vector and sequenced. The insert was cut with flanking restriction enzymes and co-transformed with a PCR product

containing kanMX, with flanking TEF promoter and terminator sequences, into a *WT* diploid strain (YPH986) containing CFIII(CEN3.L). Transformants were selected on G418 and checked by colony PCR. The mutation was sequenced in the heterozygotes by PCR amplification with a primer upstream of the mutation and a kanMX-specific antisense primer. The heterozygotes were sporulated, and dissected to isolate haploid spore clones. The chromosome transmission fidelity (*ctf*) phenotype of both the heterozygous diploids and the haploids were checked at 25°C, 30°C, and 37°C (Spencer et al., 1990). Quantitative *ctf* assays were performed by counting the frequency of half-sectored colonies in haploids at 37°C on SC media with 20% adenine concentration as in (Shero et al., 1991). Yeast strains used in this study are listed in Table 3.2. At least 3000 cells were plated, and the experiment was done in duplicate.

3.3 Results

3.3.1 20 somatic mutations were found in 8 CIN genes

Based on recent comprehensive genome-wide screens of the yeast non-essential gene deletion set for CIN mutants (Yuen et al.; see Chapter 2), and previously identified essential yeast CIN genes identified by traditional random mutagenesis (Spencer et al., 1990), a list of yeast CIN genes was complied and used to identify their human homologues based on protein sequence similarity. The list was prioritized based on the extent of yeast/human similarity and phenotype strength in yeast, and 101 human candidate CIN genes were selected for somatic mutation detection in a panel of 36 colorectal cancers (Table 3.3). In total, 1066 exons encode these 101 candidate genes, and corresponding primer pairs were used to PCR amplify these exons. After excluding known polymorphisms present in the human genomic database, all novel variants were resequenced using matched normal DNA from the patient to distinguish true somatic mutations from pre-existing variants. Somatic mutations in 8 genes (*SMC1L1*, *CSPG6*, *NIPBL*, *STAG2*, *STAG3*, *BLM*, *UTX*, and *RNF20*) were identified, 5 of which are involved in sister chromatid cohesion. To assess the frequency at which the genes are mutated in colon cancer, mutational analysis was expanded to an additional 96 colorectal cancer samples for 4 of the 8 genes (Table 3.4). This revealed that three of the cohesion genes, *SMC1L1*, *CSPG6* and *NIPBL*, have a mutation frequency of ~3.8% in colon cancers.

3.3.2 Mutation frequency in comparison to prevalence of mutations

The identified somatic mutations could represent either 'passenger' mutations that occur as a consequence of tumorigenesis, or 'functional' mutations that underlie tumorigenesis. Mutations in genes with functional relevance are expected to occur at a frequency higher than random chance. Assuming that there is ~1.5kb of coding sequence per gene, ~5.4Mb was sequenced in the initial screening of 101 genes in ~36 cancers (1.5kb X 101 genes X 36 tumors). A study by Wang et al. indicated that ~1 nonsynonymous somatic change accumulates per Mb of CIN tumor DNA, suggesting that

the mutation rate in CIN tumor cells is similar to that in normal cells and that most sporadic colorectal cancers do not display a mutator phenotype at the nucleotide level (Wang et al., 2002a). Another study found 151 mutations in 250Mb of DNA for a mutation rate of 0.6 changes per Mb (Bert Vogelstein, unpublished). These data have significant implications for the interpretation of somatic mutations in candidate tumor-suppressor genes. Based on this estimation, ~3-5 mutations are expected from the first pass sequencing. Indeed, 8 somatic mutations were identified, suggesting that at least some (or all) of the mutations identified could be passenger mutations.

In order to accurately determine the mutation frequency, the sequencing of 4 genes identified in the initial round was scaled up to an additional 96 tumors. Among the 4 genes, *SMC1L1*, *CSPG6*, and *NIPBL* are involved in cohesion, and one (*BLM*) functions in DNA repair. For each of these 4 genes, ~200kb genomic DNA was sequenced (1.5kb X 132 tumors). Based on the 1 mutation/Mb estimation, 0.2 mutations are anticipated for each gene. 5 mutations were identified in each of the 3 cohesion genes, which is 19 times higher than expected. Such non-randomness in mutation pattern suggests that the mutations in cohesion genes are of functional relevance rather than "passenger" changes. However, no additional mutation was identified for *BLM*.

3.3.3 A conserved missense mutation in yeast *SMC1* causes mild CIN

In order to elucidate whether the mutations found can lead to CIN, human *SMC1L1* was aligned with yeast *SMC1* (Fig. 3.1a), and the analogous mutations found in human *SMC1L1* were constructed in yeast *SMC1* (Fig. 3.1a,b). The *smc1* mutants were then assayed for chromosome transmission fidelity (CTF) by monitoring the loss of an artificial chromosome fragment in heterozygous diploid and haploid strains. The I877 nonsense mutation, which results in truncation of the C-terminal region, led to lethality in a haploid background. V1187I, one of the 3 missense mutations is in the conserved ATPase domain at the C-terminal region. In haploids, this conserved mutation caused a 2-fold increase in chromosome loss at 37°C (Fig. 3.1c). Antisense inhibition of *SMC1L1* in human fibroblast cells has been shown to lead to aneuploidy and chromosome

aberrations, as well as an increased frequency of micronuclei formation and apoptotic cells in long-term cultures (Musio et al., 2003).

3.4 Discussion

3.4.1 *SMC1L1*, *CSPG6*, *NIPBL*, *STAG2* and *STAG3*

SMC1L1, *CSPG6* and *NIPBL* (*Delangin/SCC2*) were each found to be mutated in 5 of the 132 tumor samples analyzed (i.e. a frequency of ~3.8% for these genes), and *STAG2* and *STAG3* each had a single mutation in 36 tumors sequenced. *SMC1L1* and *CSPG6* (*SMC3*), together with *SCC1* (*MCD1/RAD21*) and *SCC3* (*STAG1*, *STAG2* and *STAG3* isoforms in vertebrates), form the essential cohesin complex, which is required for cohesion of sister chromatids and for accurate chromosome segregation (Tanaka et al., 2000). *NIPBL*, together with *SCC4*, forms an essential complex that loads cohesin to replicated sister chromatids during DNA replication (Ciosk et al., 2000). Recently, *NIPBL* and *SMC1L1* were found to be mutated in Cornelia de Lange (CdL) syndrome, characterized by facial dysmorphisms, upper limb abnormalities, growth delay and cognitive retardation (Krantz et al., 2004; Musio et al., 2006; Tonkin et al., 2004). *NIPBL* is expressed ubiquitously, but with variable tissue-specific expression. *NIPBL* not only has a role in cohesion, but also functions in developmental regulation by affecting gene expression (Rollins et al., 2004); whether these functions are independent from each other, and how much *NIPBL* expression is required for each function remains unknown. Recently, *CTF7/ESCO2*, an acetyltransferase required for cohesion establishment in S phase, was found to be mutated in Roberts syndrome and SC phocomelia, which has several phenotypes overlapping with Roberts syndrome (Schule et al., 2005; Vega et al., 2005). Precocious sister chromatid separation has been described in CdL syndrome, Roberts syndrome, and mosaic variegated aneuploidy, and various cancers (Kaur et al., 2005). However, patients of CdL and Roberts syndromes do not have cancer predisposition. The present study is the first report identifying mutations in genes functioning in cohesion in human cancers.

3.4.2 *BLM*

BLM was found to be mutated in one out of 132 tumor samples analyzed. *BLM*, together with *WRN* and *RECQL4*, are homologous to yeast *SGS1* in the RecQ helicase

family, and all 3 genes are mutated in cancer prone syndromes (see Table 1.1). *BLM* is a DNA structure-specific helicase, which plays a role in the resolution of DNA structures that arise during the process of homologous recombination repair, by catalyzing Holliday-junction branch migration and annealing of complementary single-stranded DNA molecules (reviewed in (Cheok et al., 2005)). In the absence of *BLM*, cells show genomic instability and a high incidence of sister-chromatid exchanges. Gruber et al. (Gruber et al., 2002) determined that carriers of the *BLM(Ash)* founder mutation (causing frameshift and truncation) have an increased risk of colorectal cancer, and they also observed a low frequency of the *BLM(Ash)* mutation in lymphoma, breast, ovarian, and uterine cancers. Mice heterozygous for a null mutation of *BLM* develop lymphoma earlier than wild-type littermates in response to challenge with murine leukemia virus, suggesting that *BLM* haploinsufficiency is associated with tumor predisposition (Goss et al., 2002). However, further functional analysis is required to determine whether the heterozygous missense mutation found in this study causes a CIN phenotype.

3.4.3 *RNF20*

One heterozygous missense mutation was found in *RNF20*, which encodes a E3 ubiquitin ligase. *RNF20* forms a complex with *RNF40*, interacts with an ubiquitin E2-conjugating enzyme *UBCH6*, and establishes *H2B* lysine 120 monoubiquitylation, which is associated with transcriptional activity (Pavri et al., 2006; Zhu et al., 2005). This modification subsequently regulates *H2B* methylation and expression of homeobox (HOX) genes, which are required for proper development. In yeast, *H2B* ubiquitylation by *RAD6*(E2)-*BRE1*(E3) has been shown to be required for the DNA damage checkpoint response (Giannattasio et al., 2005). Interestingly, yeast-two-hybrid analysis of the yeast homologue of *RNF20*, *BRE1*, indicated that it interacts with the coiled-coil region of 3 proteins in the structural maintenance of chromosomes family (*SMC1*, *SMC2*, *SMC3*) and some kinetochore components (*SLK19*, *NUF2*) (Newman et al., 2000), and may play a direct role in chromosome maintenance.

3.4.4 *UTX*

One heterozygous missense mutation was found in *UTX*. *UTX* is a transcription factor that contains the tetratricopeptide repeat (TPR) motif. The yeast homologue *SSN6/CYC8*, together with *TUP1*, is involved in histone deacetylation, which is associated with transcriptional repression. *SSN6* functions as a negative regulator of the expression of a broad spectrum of genes (reviewed in (Smith and Johnson, 2000)), which explains why the phenotype of *ssn6* mutant is pleiotropic. *ssn6* mutants exhibits a modest effect on the maintenance of minichromosomes (Schultz et al., 1990).

While it is evident that the role of cohesion genes and *BLM* in chromosome maintenance is well conserved, it is still unclear whether *RNP20* and *UTX* play a direct role in chromosome maintenance in yeast or in human. Further functional studies in model organisms and in mammalian cells will delineate the roles of these candidate CIN genes, reveal whether the mutations cause CIN, and elucidate the degree of functional conservation.

This study initiated the characterization of the cancer somatic mutations in *SMC1L1* by introducing the corresponding mutations in yeast *SMC1*. The conserved mutation caused a mild CIN phenotype in haploids. Although the heterozygous diploids of this conserved mutation or the truncation do not exhibit a detectable CIN phenotype in yeast, it is possible that human cells may be more sensitive to perturbations in CIN genes, due to larger chromosome and genome size. A precedent for this hypothesis is that mitotic checkpoint components are dispensable in yeast, but are essential in higher eukaryotes (Babu et al., 2003; Baker et al., 2004; Dai et al., 2004; Kitagawa and Rose, 1999; Kops et al., 2004; Michel et al., 2001).

The results presented here broaden the mutational spectrum of colorectal cancers, and are consistent with previous observations that each CIN gene is mutated at a low frequency (~3.8% for each of the 3 cohesin related genes). Therefore, a variety of CIN genes could each be responsible for a small proportion of cancers. CIN is a hallmark of most solid tumors, so it will be of interest to compare the mutational spectrum for

colorectal cancers to that of other types of solid cancers. The technical information gained in colorectal cancer will be useful for similar analysis in other tumor types. Mutational spectra may also allow classification of tumors, which could have implications for improved diagnosis, prognosis, or predictions of response to therapy. For example, the Vogelstein group recently pursued another large-scale mutational analysis of 13,023 genes in 11 breast and 11 colorectal cancers (Sjoblom et al., 2006). This unbiased study provided an estimate of the total number of nonsynonymous mutations that arise in a typical cancer, thereby allowing statistical differentiation between passenger mutations and mutations with functional implications. Their study revealed 189 genes that were mutated at significant frequency. These cancer genes encode a wide range of cellular functions, including genes that have been shown to be somatically mutated or implicated in tumorigenesis in expression studies, but also many genes that were not previously suspected to contribute to the pathogenesis of cancer. Interestingly, that study also identified substantial differences in the mutational spectra in different tumor types.

Knowing the mutational spectra in cancers would be useful for therapeutic design. As described in Chapters I and II, a second-site loss-of-function mutation that causes synthetic lethality with a CIN mutation can lead to selective killing of tumor cells. Combining synthetic lethal data available in yeast (Pan et al., 2006; Tong et al., 2004) with mutational spectrum of colorectal cancers found in studies like the one presented here may help to highlight potential targets for this therapeutic strategy. Indeed, mutations of 4 non-essential cohesion genes (*ctf4Δ*, *ctf8Δ*, *ctf18Δ*, and *dcc1Δ*) are synthetically lethal with mutations of 5 different CIN gene homologues which are mutated in colorectal cancer (Fig. 3.2). 3 of the 4 same cohesion gene mutations (*ctf4Δ*, *ctf18Δ*, and *dcc1Δ*) are also synthetically lethal with mutations of CIN gene homologues which are mutated in other cancer types (Fig 2.9). Such analyses suggested that these common synthetic lethal interactors may be attractive drug targets that are effective to a broad spectrum of CIN tumors with CIN gene mutations.

Table 3.1 Relationship of 100 human candidate CIN genes used in (Wang et al., 2004b) with yeast genes

The 100 human candidate CIN genes were searched for the best yeast homologue by BLASTp according to the proteome database (www.proteome.com), and the e-value is indicated. The list is sorted by the human gene name in ascending order. 19 genes contain only hCT# but not Genbank accession #, so the gene identities of these human genes are not known (highlighted in gray). 3 genes (ATR, POLE, and RAD51C) have 2 different hCT#, representing different isoforms (highlighted in orange). 13 human genes have no BLASTp hit in yeast (highlighted in purple, or blue, which have putative homologs with an e-value >1E-3). 66 human genes yield a yeast hit by BLASTp with an e-value <1E-3. The best yeast hits for these 66 genes were reciprocally searched for their best human homologue by BLASTp. Among these, 30 of them were reciprocal best hits (highlighted in yellow). 15 of the yeast best hits were found in the CIN screens described in Chapter 2 (highlighted in red), and 10 of the 15 are reciprocal best hits; 3 of them correspond to family members of yeast DUN1.

Table 3.1 Page 1 of 2

No.	Celera accession	Genbank accession	Human Gene	Other gene name	Top yeast hit	E-value	Reciprocal top human hit	E-value	Yeast hit found in CIN screens?
5	hCT12678	NM_005883	APCL	APC2	VAC8	5E-04	ARMC3	1E-23	VAC8
90	hCT7133	NM_014840	ARK5		SNF1	2E-60	PRKAA2	1E-113	
42	hCT1826039	NM_001184	ATR		MEC1	1E-108	ATR	1E-108	
43	hCT1826040	NM_001184	ATR		MEC1	1E-108	ATR	1E-108	
1	hCT10388	NM_016374	BCAA	ARID4B; BRCAA1	N/A				
80	hCT31470	NM_006768	BRAP		YHL010C	7E-54	BRAP	7E-54	
9	hCT14094	NM_020439	CAMK1G	VWS1	CMK2	1E-59	CMK1D	1E-60	
99	hCT9356	NM_172080	CAMK2B		CMK2	1E-52	CMK1D	1E-60	
19	hCT1643963	NM_001254	CDC6		CDC6	8E-33	CDC6	8E-33	CDC6
37	hCT1816212	NM_001813	CENPE		KIP3	2E-54	KIF18A	1E-81	
46	hCT18305	NM_022909	CENPH		N/A				
72	hCT30161	NM_001274	CHK1		CHK1	9E-45	CHEK1	9E-45	
82	hCT32245	NM_007194	CHK2		DUN1	3E-50	DCAMKL1	2E-53	DUN1
21	hCT1646711	NM_001340	CYLC2		YFR016C	4E-09	NEF2	1E-10	
11	hCT14628	NM_001348	DAPK3		CMK1	1E-48	CMK1D	9E-63	
61	hCT23387	NM_004734	DCAMKL1		DUN1	2E-53	DCAMKL1	2E-53	DUN1
54	hCT20446	NM_015070	DING		N/A PDS1	?			
85	hCT32971	NM_007068	DMC1		DMC1	1E-99	DMC1	1E-99	
55	hCT20952	NM_000123	ERCC5		RAD2	7E-47	ERCC5	7E-47	
81	hCT32115	NM_004111	FEN1	RAD27	RAD27	1E-104	FEN1	1E-104	RAD27
51	hCT1961597	NM_017975	FLJ10036		N/A				
3	hCT11790	NM_012415	FSBP	RAD54B	RDH54	1E-122	RAD54B	1E-122	RDH54
31	hCT17786	NM_014635	GCC185		NUM1/PAC12	9E-08	RSN	3E-09	
96	hCT8974		HCA127		N/A				
86	hCT401149	NM_014586	HUNK		SNF1	1E-51	PRKAA2	1E-113	
16	hCT16364	NM_014915	KIAA1074		AKR2	9E-09	ZDHHC17	1E-48	
70	hCT29475	NM_032430	KIAA1811	BRSK1	SNF1	2E-76	PRKAA2	1E-113	
58	hCT2308143	NM_014708	KNTC1	ROD	N/A				
35	hCT1788172		LATS1		CBK1	1E-100	STK38I	1E-131	
32	hCT1783089	NM_003550	MAD1L1		N/A MAD1	?			MAD1
57	hCT22552	NM_014791	MELK		SNF1	2E-65	PRKAA2	1E-113	
98	hCT9098	NM_152619	MGC45428		DUN1	4E-52	DCAMKL1	2E-53	DUN1
13	hCT14856	NM_016195	MPHOSPH1		CIN8	6E-37	KIF11	1E-48	CIN8
59	hCT2334792	NM_005591	MRE11A	MRE11	MRE11	1E-104	MRE11	1E-104	MRE11
65	hCT24254	NM_002485	NBS1		N/A XRS2	?			
84	hCT32914	NM_021076	NEFH		CHS5	6E-13	NEFH	6E-13	
64	hCT23665	NM_004153	ORC1L		ORC1	2E-39	ORCL1	2E-39	
77	hCT30866	NM_177990	PAK7		STE20	5E-80	PAK1	1E-111	
74	hCT30362	NM_002592	PCNA		POL30	1E-52	PCNA	1E-52	
88	hCT6664		PIK3C2A		VPS34	3E-48	PIK3C3	1E-139	
91	hCT7448	NM_002646	PIK3C2B		VPS34	3E-48	PIK3C3	1E-139	
7	hCT13660	NM_002647	PIK3C3	VPS34	VPS34	1E-139	PIK3C3	1E-139	
89	hCT7084	NM_006219	PIK3CB		VPS34	2E-47	PIK3C3	1E-139	
34	hCT1787138	NM_005026	PIK3CD		VPS34	2E-57	PIK3C3	1E-139	
92	hCT7976	NM_002649	PIK3CG		VPS34	7E-51	PIK3C3	1E-139	
8	hCT14027	NM_002691	POLD1		CDC2	0E+00	POLD1	0E+00	
63	hCT23655	NM_006231	POLE		POL2	0E+00	POLE	0E+00	
95	hCT87415	NM_006231	POLE		POL2	0E+00	POLE	0E+00	
100	hCT9836	NM_006904	PRKDC		TOR1	1E-34	FRAP1	0E+00	
68	hCT28965	NM_133377	RAD1		N/A				
66	hCT28290	NM_133338	RAD17		RAD24	4E-17	RAD17	4E-17	RAD24
14	hCT15239	NM_005732	RAD50		RAD50	2E-59	RAD50	2E-59	RAD50
73	hCT30207	NM_133487	RAD51		RAD51	1E-112	RAD51	1E-112	RAD51
25	hCT1686635	NM_058216	RAD51C		DMC1	3E-18	DMC1	1E-99	
28	hCT1767458	NM_058216	RAD51C		DMC1	3E-18	DMC1	1E-99	
49	hCT18816	NM_133627	RAD51L3		DMC1	1E-13	DMC1	1E-99	
24	hCT1686440	NM_134422	RAD52		RAD52	5E-41	RAD52	5E-41	RAD52
6	hCT13183	NM_003579	RAD54L		RAD54	1E-160	RAD54L	1E-160	RAD54
71	hCT29790	NM_002913	RFC1		RFC1	1E-115	RFC1	1E-115	
97	hCT9089	NM_002914	RFC2		RFC4	1E-109	RFC2	1E-109	
60	hCT23382	NM_002915	RFC3		RFC5	2E-67	RFC3	2E-67	
40	hCT1823014	NM_002916	RFC4		RFC3	5E-42	RFC5	5E-80	
78	hCT30904	NM_007370	RFC5		RFC3	5E-80	RFC5	5E-80	
52	hCT19876	NM_002945	RPA1		RFA1	1E-92	RPA1	1E-92	
62	hCT23494	NM_012238	SIRT1		SIR2	1E-56	SIRT1	1E-56	
2	hCT11285		SIRT2		HST2	2E-59	SIRT3	4E-60	
69	hCT29050	NM_012239	SIRT3		HST2	4E-60	SIRT3	4E-60	
50	hCT18916	NM_176827	SIRT4		HST2	7E-14	SIRT3	4E-60	

Table 3.1 Page 2 of 2

67	hCT28652	NM_012241	SIRT5		SIR2	9E-16	SIRT1	1E-56	
12	hCT14647	NM_016539	SIRT6		HST2	3E-12	SIRT3	4E-60	
33	hCT1786284	NM_016538	SIRT7		HST1	3E-10	SIRT1	5E-48	
56	hCT21449	NM_018225	SMU-1		PFS2	7E-17	WRD33	9E-70	
36	hCT17934	AA447812	SNRK		SNF1	3E-53	PRKAA2	1E-113	
87	hCT6634	NM_007027	TOPBP1		N/A				
83	hCT32452	NM_003292	TPR		AGA1	2E-04	MUC17	3E-25	
48	hCT18373	NM_004628	XPC		RAD4	3E-26	XPC	3E-26	
75	hCT30596	NM_006297	XRCC1		N/A				
23	hCT16627	NM_005432	XRCC3		DMC1	2E-19	DMC1	1E-99	
76	hCT30844	NM_004724	ZW10		N/A				
79	hCT31391	NM_007057	ZWINT		N/A				
39	hCT1817729	NM_012291		ESPL1/SEPARASE	ESP1	1E-36	ESPL1	1E-36	
4	hCT12352								
10	hCT14327								
15	hCT15320								
17	hCT1642589								
18	hCT1643619								
20	hCT1644019								
22	hCT1657158								
26	hCT173001								
27	hCT1766645								
29	hCT1770914								
30	hCT1775724								
38	hCT1817706								
41	hCT1824077								
44	hCT1829493								
45	hCT1829782								
47	hCT1834200								
53	hCT201497								
93	hCT87379								
94	hCT87385								

Table 3.2 List of yeast strains used in Chapter 3

Strain	Genotype
YPH986	*MATa/MATα ura3-52/ura3-52 trp1Δ-63/trp1Δ-63 his3Δ-200/his3Δ-200 leu2Δ-1/leu2Δ-1 ade2-101/ade2-101 lys2-801/ lys2-801 CFIII(CEN3.L)-HIS3 SUP11*
YKY1038	*MATa ura3-52 trp1Δ-63 his3Δ-200 leu2Δ-1 ade2-101 lys2-801 smc1-Q449W::kanMX CFIII(CEN3.L)-HIS3 SUP11*
YKY1042	*MATα ura3-52 trp1Δ-63 his3Δ-200 leu2Δ-1 ade2-101 lys2-801 smc1-Q449W::kanMX CFIII(CEN3.L)-HIS3 SUP11*
YKY1053	*MATa ura3-52 trp1Δ-63 his3Δ-200 leu2Δ-1 ade2-101 lys2-801 smc1-L574M::kanMX CFIII(CEN3.L)-HIS3 SUP11*
YKY1051	*MATα ura3-52 trp1Δ-63 his3Δ-200 leu2Δ-1 ade2-101 lys2-801 smc1-L574M::kanMX CFIII(CEN3.L)-HIS3 SUP11*
YKY1034	*MATα ura3-52 trp1Δ-63 his3Δ-200 leu2Δ-1 ade2-101 lys2-801 smc1- V1187I::kanMX CFIII(CEN3.L)-HIS3 SUP11*
YKY1031	*MATa ura3-52 trp1Δ-63 his3Δ-200 leu2Δ-1 ade2-101 lys2-801 smc1- V1187I::kanMX CFIII(CEN3.L)-HIS3 SUP11*
YKY1011	*MATa ura3-52 trp1Δ-63 his3Δ-200 leu2Δ-1 ade2-101 lys2-801 SMC1::kanMX CFIII(CEN3.L)-HIS3 SUP11*
YKY1023	*MATα ura3-52 trp1Δ-63 his3Δ-200 leu2Δ-1 ade2-101 lys2-801 SMC1::kanMX CFIII(CEN3.L)-HIS3 SUP11*

Table 3.3 101 candidate CIN genes analyzed in this study

88 human genes were selected from the non-essential yeast CIN genes based on the extent of yeast/human similarity (63 had a e-value <1E-10) and CIN phenotype strength in yeast. 2 human genes were selected based on their similarity to 2 non-essential *CTF* genes identified by traditional random mutagenesis (Spencer et al., 1990) but missed in the high-throughput screens. Another 11 human genes were selected because they have sequence similarity to essential yeast *CTF* genes identified by traditional random mutagenesis (Spencer et al., 1990). Most of these human genes correspond to the top hits of yeast CIN genes, except for 5 human genes which are second or third hits (families are indicated in orange). In total, 101 candidates were analyzed, 74 of which had a e-value <1E-10. The list is sorted in ascending order by the yeast gene name. 15 candidate genes are involved in cohesion (indicated in yellow).

Table 3.3 Page 1 of 2

No.	Yeast ORF	Yeast gene	Essential?	ctf	bim	alf	Top human hit	E-value	Protein Accession	mRNA Accession
1	YAR015W	ADE1		wrong	0	31	phosphoribosylaminoimidazole c	6E-08	NP_006443	NM_006452.2
2	YGL234W	ADE5,7		0	0	12	phosphoribosylglycinamide form	0E+00	NP_000810	NM_000819.3
3	YGR061C	ADE6		0	0	16	phosphoribosylformylglycinamidi	1E-176	NP_036525	NM_012393.1
4	YBR231C	AOR1		0	4	0	craniofacial development protein	5E-10	NP_006315	NM_006324.1
5	YLR085C	ARP6		0	3	0	ARP6 actin-related protein 6 hor	2E-44	NP_071941	NM_022496.2
6	YJL115W	ASF1		wrong	3	22	ASF1 anti-silencing function 1 h	8E-51	NP_054753	NM_014034.1
7	YER016W	BIM1/CTFs3		3	5	16	microtubule-associated protein,	2E-28	NP_036457	NM_012325.1
8	YDL074C	BRE1		0	0	11	RPN20, ring finger protein 20; h	5E-26	NP_062538	NM_019592.5
9	YOR026W	BUB3		2	5	24	BUB3 budding uninhibited by be	2E-24	NP_004716	NM_004725.1
10	YJL194W	CDC6/CTF10	Ess	3	#N/A	#N/A	CDC6 homolog; CDC18 (cell div	2E-32	NP_001245	NM_001254.2
11	YLR418C	CDC73		1	0	2	parafibromin; chromosome 1 ope	9E-12	NP_078805	NM_024529.3
12	YGL003C	CDH1		3	3	0	Fzr1 protein; fizzy-related protei	1E-92	NP_057347	NM_016263.2
13	YPL008W	CHL1/CTF1		3	5	7	DEAD/H (Asp-Glu-Ala-Asp/His)	1E-112	NP_085911	NM_030653.2
14	YPL008W	CHL1/CTF1		3	5	7	CHLR2/DDX12, DEAD box prote	4E-94	AAB06963.1	U33834
15	YMR198W	CIK1		3	wrong	0	golgi autoantigen, golgin subfam	4E-07	NP_002069	NM_002078.3
16	YEL061C	CIN8		3	4	0	kinesin family member 11; Eg5;	2E-67	NP_004514	NM_004523.2
17	YPR120C	CLB5		0	3	4	cyclin B1; G2/mitotic-specific cyc	6E-39	NP_114172	NM_031966.2
18	YMR048W	CSM3		3	5	12	timeless-interacting protein; tipin	8E-08	NP_060328	NM_017858.1
19	YMR078C	CTF18		3	0	29	CTF18, chromosome transmissi	3E-36	NP_071375	NM_022092.1
20	YLR381W	CTF3		3	4	0	LRPR1 (CENPI), follicle-stimulat	see Measday V, 200	NP_006724	NM_006733.2
21	YPR135W	CTF4		3	5	27	WD repeat and HMG-box DNA b	1E-18	NP_009017	NM_007086.1
22	YHR191C	CTF8		3	6	18	hCTF8, hypothetical protein MG	see Mayer M, 2001	NP_00103523	NM_001039690
23	YJL006C	CTK2		3	wrong	contam	cyclin K [Homo sapiens]	2E-11	NP_003849	NM_003858.2
24	YCL016C	DCC1		0	5	18	hypothetical protein MGC5528 [H	8E-11	NP_076999	NM_024094.1
25	YIR004W	DJP1		0	0	13	DnaJ (Hsp40) homolog, subfami	4E-18	NP_061854	NM_018981.1
26	YGL240W	DOC1		3	nd	3	anaphase-promoting complex su	5E-22	NP_055700	NM_014885.1
27	YFR027W	ECO1/CTF7	Ess	3	#N/A	#N/A	establishment factor-like protein	5E-11	NP_443143	NM_052911.1
28	YFR027W	ECO1/CTF7	Ess	3	#N/A	#N/A	ESCO2, Establishment of cohes	3E-07	NP_001017420.1	NM_001017420
29	YOR144C	ELG1		1	4	12	hypothetical protein FLJ12735 [H	2E-05	NP_079133	NM_024857.3
30	YBR026C	ETR1		wrong	5	5	nuclear receptor-binding factor 1	5E-47	NP_057095	NM_016011.1
31	YEL003W	GIM4		0	contam	19	prefoldin 2 [Homo sapiens]	1E-15	NP_036526	NM_012394.2
32	YCR065W	HCM1		0	4	2	forkhead box L2; Blepharophimo	1E-20	NP_075555	NM_023067.2
33	YBR009C	HHF1		0	4	6	histone 2, H4; H4 histone, family	2E-37	NP_003539	NM_003548.2
34	YPR067W	ISA2		contam	3	3	HESB like domain containing 1 [	2E-05	NP_919255	NM_194279.1
35	YPR141C	KAR3		3	nd	40	kinesin family member C1 [Homo	2E-69	XP_371813	XM_371813.1
36	YDR532C	KRE28		0	4	30	retinoblastoma-binding protein 1	3E-06	NP_002883	NM_002892.2
37	YDR378C	LSM6		1	2	0	Sm protein F [Homo sapiens]	5E-09	NP_009011	NM_007080.1
38	YJL030W	MAD2		2	3	0	MAD2-like 1; MAD2 (mitotic arre	5E-38	NP_002349	NM_002358.2
39	YPR046W	MCM16/CTFs155		3	4	4	high density lipoprotein binding p	2E-03	NP_976221	NM_203346.1
40	YDR318W	MCM21/CTF5		3	5	3	SCC1/MCD1, RAD21 homolog;	3E-02	NP_006256	NM_006265.1
41	YFL016C	MDJ1		0	0	19	DnaJ (Hsp40) homolog, subfami	2E-31	NP_005138	NM_005147.3
42	YOL064C	MET22		0	3	wrong	inositol(myo)-1(or 4)-monophosp	4E-05	NP_005527	NM_005536.2
43	YOR241W	MET7		0	wrong	13	folylpolyglutamate synthase; foly	1E-11	NP_004948	NM_004957.2
44	YDR386W	MUS81		0	4	9	MUS81 endonuclease homolog	1E-18	NP_079404	NM_025128.3
45	YBL079W	NUP170/CTFs141		3	#N/A	#N/A	nucleoporin 155kDa isoform 1; n	2E-30	NP_705618	NM_153485.1
46	YDL116W	NUP84		0	4	contam	nuclear pore complex protein [H	5E-16	NP_065134	NM_020401.1
47	YKL055C	OAR1		wrong	wrong	6	DKFZP566O084 protein [Homo	2E-13	NP_056325	NM_015510.3
48	YKR087C	OMA1		wrong	2	30	metalloprotease related protein 1	6E-29	NP_660286	NM_145243.2
49	YGR078C	PAC10		0	2	3	von Hippel-Lindau binding protei	4E-30	NP_003363	NM_003372.3
50	YHR064C	PDR13		1	2	3	heat shock 70kDa protein 8 isofo	2E-56	NP_006588	NM_006597.3
51	YMR076C	PDS5/CTF11	Ess	3	#N/A	#N/A	androgen-induced prostate proli	1E-29	NP_055847	NM_015032.1
52	YLR273C	PIG1		3	0	0	protein phosphatase 1, regulator	2E-06	NP_005389	NM_005398.3
53	YOL054W	PSH1		0	4	11	tripartite motif-containing 25; Zin	1E-07	NP_005073	NM_005082.3
54	YPL022W	RAD1		0	contam	5	excision repair cross-complemer	1E-109	NP_005227	NM_005236.1
55	YML095C	RAD10		0	3	2	excision repair cross-complemer	1E-12	NP_001974	NM_001983.2
56	YCR066W	RAD18		wrong	5	19	postreplication repair protein hR	9E-20	NP_064550	NM_020165.2
57	YER173W	RAD24		0	4	6	RAD17 homolog isoform 2; Rad1	8E-17	NP_579917	NM_133339.1
58	YLR032W	RAD5		0	2	5	SWI/SNF-related matrix-associa	5E-70	NP_620636	NM_139048.1
59	YER095W	RAD51		wrong	4	7	RAD51 homolog protein isoform	1E-122	NP_002866	NM_002875.2
60	YML032C	RAD52		2	5	22	RAD52 homolog isoform alpha;	2E-40	NP_002870	NM_002879.2
61	YDR076W	RAD55		0	4	18	RAD51-like 3 isoform 1; recombi	1E-05	NP_002869	NM_002878.2
62	YDR004W	RAD57		0	5	15	RAD51-like 1 isoform 3; RecA-lik	4E-19	NP_598193	NM_133509.2
63	YDL059C	RAD59		0	4	2	RAD52 homolog isoform alpha;	8E-09	NP_002870	NM_002879.2
64	YGL058W	RAD6		1	nd	25	ubiquitin-conjugating enzyme E2	7E-61	NP_003327	NM_003336.2
65	YDR014W	RAD61/CTF6		3	4	5	hypothetical protein LOC57821 [	4E-03	NP_067002	NM_021179.1
66	YDR217C	RAD9		0	3	10	dentin sialophosphoprotein prep	1E-07	NP_055023	NM_014208.1
67	YNL072W	RNH35		0	3	6	ribonuclease HI, large subunit [H	7E-46	NP_006388	NM_006397.2
68	YJR063W	RPA12		0	2	5	zinc ribbon domain containing, 1	1E-14	NP_740753	NM_170783.1

Table 3.3 Page 2 of 2

69	YJL140W	RPB4/CTF15		3	#N/A	#N/A	DNA directed RNA polymerase I	3E-12	NP_004796	NM_004805.2
70	YIL018W	RPL2B		wrong	0	17	ribosomal protein L8; 60S ribosc	1E-102	NP_150644	NM_033301.1
71	YDL204W	RTN2		0	0	16	reticulon 2 isoform A; NSP-like p	5E-08	NP_005610	NM_005619.3
72	YOR014W	RTS1		wrong	0	19	delta isoform of regulatory subur	1E-148	NP_006236	NM_006245.2
73	YJL047C	RTT101		wrong	wrong	15	cullin 2 [Homo sapiens]	9E-06	NP_003582	NM_003591.2
74	YDR289C	RTT103		2	0	0	chromosome 20 open reading fr	3E-14	NP_067038	NM_021215.2
75	YDR159W	SAC3		contam	wrong	5	minichromosome maintenance p	4E-26	NP_003897	NM_003906.3
76	YDR180W	SCC2/CTF12/CHL8	Ess	3	#N/A	#N/A	NIPBL, IDN3 protein isoform A [I	3E-19	NP_597677	NM_015384.3
77	YIL026C	SCC3/IRR1/CTFs165	Ess	3	#N/A	#N/A	STAG1, stromal antigen 1; nucle	2E-21	NP_005853	NM_005862.1
78	YIL026C	SCC3/IRR1/CTFs165	Ess	3	#N/A	#N/A	STAG3, Stromal antigen 3 (stror	3E-13	NP 036579.2	NM_012447
79	YIL026C	SCC3/IRR1/CTFs165	Ess	3	#N/A	#N/A	STAG2, Stromal antigen 2, a me	2E-11	NP 006594.3	NM_006603
80	YMR190C	SGS1		0	4	14	Bloom syndrome protein [Homo	1E-115	NP_000048	NM_000057.1
81	YLR058C	SHM2		0	4	2	serine hydroxymethyltransferase	1E-148	NP_004160	NM_004169.3
82	YBL058W	SHP1		2	4	2	p47 protein isoform a [Homo sap	6E-34	NP_057227	NM_016143.3
83	YLR079W	SIC1/CTFs127		3	6	31	hypothetical gene supported by	7E-02	NP_963859	NM_201565.1
84	YER116C	SLX8		1	5	wrong	ring finger protein 10 [Homo sap	7E-08	NP_055683	NM_014868.3
85	YFL008W	SMC1/CTFs166	Ess	3	#N/A	#N/A	SMC1 structural maintenance of	1E-149	NP_006297	NM_006306.2
86	YFL008W	SMC1/CTFs166	Ess	3	#N/A	#N/A	SMC1L2, Protein with strong sim	6E-41	NP 683515.3	NM_148674
87	YJL074C	SMC3	Ess	#N/A	#N/A	#N/A	CSPG6, Chondroitin sulfate prot	1E-45	NP 005436.1	NM_005445.3
88	YOR308C	SNU66		2	0	0	squamous cell carcinoma antige	2E-07	NP_005137	NM_005146.3
89	YGR063C	SPT4/CTFs138		1	0	0	suppressor of Ty 4 homolog 1 [H	1E-18	NP_003159	NM_003168.1
90	YPR032W	SRO7		wrong	2	3	tomosyn-like [Homo sapiens]	4E-14	XP_045911	XM_045911.8
91	YBR112C	SSN6/CYC8		0	nd	80	UTX, ubiquitously transcribed te	9E-44	NP_066963	NM_021140.1
92	YOL072W	THP1		wrong	4	19	hypothetical protein FLJ11305 [H	6E-07	NP_060856	NM_018386.1
93	YNL273W	TOF1		3	5	10	timeless homolog [Homo sapien	5E-07	NP_003911	NM_003920.1
94	YLR234W	TOP3		0	5	42	topoisomerase (DNA) III alpha; t	1E-124	NP_004609	NM_004618.2
95	YAL016W	TPD3		nd	nd	75	beta isoform of regulatory subun	1E-133	NP_859050	NM_181699.1
96	YML028W	TSA1		0	4	8	peroxiredoxin 2 isoform a; thiore	7E-71	NP_005800	NM_005809.4
97	YGR184C	UBR1		3	3	0	ubiquitin ligase E3 alpha-II; likely	9E-28	NP_056070	NM_015255.1
98	YDL156W	YDL156W		0	2	2	hypothetical protein FLJ12973 [H	3E-19	NP_079184	NM_024908.1
99	YLR193C	YLR193C		0	2	2	similar to Px19-like protein (25 k	2E-22	XP_371496	XM_371496.2
100	YGR270W	YTA7		wrong	4	6	two AAA domain containing prot	1E-131	NP_054828	NM_014109.2
101	YGR285C	ZUO1		0	4	wrong	similar to M-phase phosphoprote	1E-48	XP_379909	XM_379909.1

Table 3.4 Somatic mutations identified in candidate CIN genes in CIN colorectal cancer cells

20 mutations were identified in 8 genes. The number of mutations found and the number of tumors sequenced are indicated. The nucleotide mutation and corresponding amino acid mutation are indicated by the position based on the coding sequence (CDS), followed by the wild-type sequence>tumor sequence. Thus, 2 different nucleotides in the tumor sequence represent a heterozygous mutation, and a single nucleotide in the tumor sequence represents a homozygous or hemizygous mutation. The corresponding amino acid change is indicated in the same manner. The corresponding tumor, exon number and primer used are indicated. The yeast gene used as query and the e-value are also indicated.

Gene No.	Human Gene Name	Yeast Gene Name	e-value	Human RNA ID	Human Protein ID	No. mutations	No. tumors sequenced	PRIMER	Exon	Somatic Mutation	Tumor
1	SMC1L1	SMC1	1E-149	NM_006306.2	NP_006297.2	5	132	hCT9553-7	7	1186T>CT: 396F>L/F	CO94
								hCT9553-8	8	1300C>T: 434R>W	HX8
								hCT9553-10	10	1680C>CG: 560I>I/M	CX3
								hCT9553-16	16	2562_2563het_insA	HX171
								hCT9553-24	24	3556G>AG: 1186V>I/V	HX129
2	CSPG6	SMC3	1E-45	NM_005445.3	NP 005436.1	5	130	CSPG6_23	23	2635C>CT:879R>R/X	MX13
								CSPG6_7	7	415G>AG:139V>I/V	HX155
								CSPG6_8	8	512G>AG,171R>Q/R	HX171
								CSPG6_12	12	100C>CT:334L>L/F	HX152
								CSPG6_21	21	2321G>A:774R>K	HX133
3	NIPBL	SCC2	3E-19	NM_015384.3	NP 597677.2	5	132	hCT2293447_9_3	8	1435C>CT:479R>R/X	HX7
								hCT2293447_9_4	9	2967_2968het_insT	CO71
								hCT2293447_10_1	9	1660C>CT:554Q>Q/X	HX168
								YC03C04F	28	5378T>TA: 1793M>M/K	MX24
								hCT2293447_40	39	6893G>AG: 2298R>H/R	HX171
4	STAG2	SCC3	2E-11	NM_006603	NP_006594.3	1	34	STAG2_24	24	2456C>CT:819S>S/F	HX147
5	STAG3	SCC3	3E-13	NM_012447.2	NP_036579.2	1	34	STAG3_32	31	33963G>AG	HX110
6	BLM	SGS1	1E-115	NM_000057.1	NP_000048.1	1	132	YC08C06B	15	3128C>AC: 1043A>D/A	HX63
7	UTX	SSN6/CYC8	9E-44	NM_021140	NP_066963.1	1	36	YC14C06D	17	2380A>AC:794Y>Y/S	HX68
8	RNF20	BRE1	5E-26	NM_019592	NP_062538.5	1	36	YC16C06G	3	370C>CT:124R>R/X	HX88

Figure 3.1 Mutations in human *SMC1L1* in colorectal cancers and analogous mutations in yeast *SMC1*

A. Protein sequence alignment of human *SMC1L1* with yeast *SMC1* reveals 27.8% identity and 42.1% similarity. Known domains are highlighted: the P-loop containing ATPase domain at N- and C-terminus are in blue; the SMC hinge domain is in orange. Somatic mutations found in human cancers and the analogous yeast amino acids are shown in red boxes. A nucleotide insertion leading to frameshift and truncation is indicated by a red arrow and stop sign.

B. The table indicates the corresponding mutations constructed.

C. Frequency of chromosome fragment loss per division is indicated for *WT* and missense mutant haploids. The lower panel shows the sectoring phenotypes of the V1187I mutant and control *WT* cells.

Figure 3.1
A.

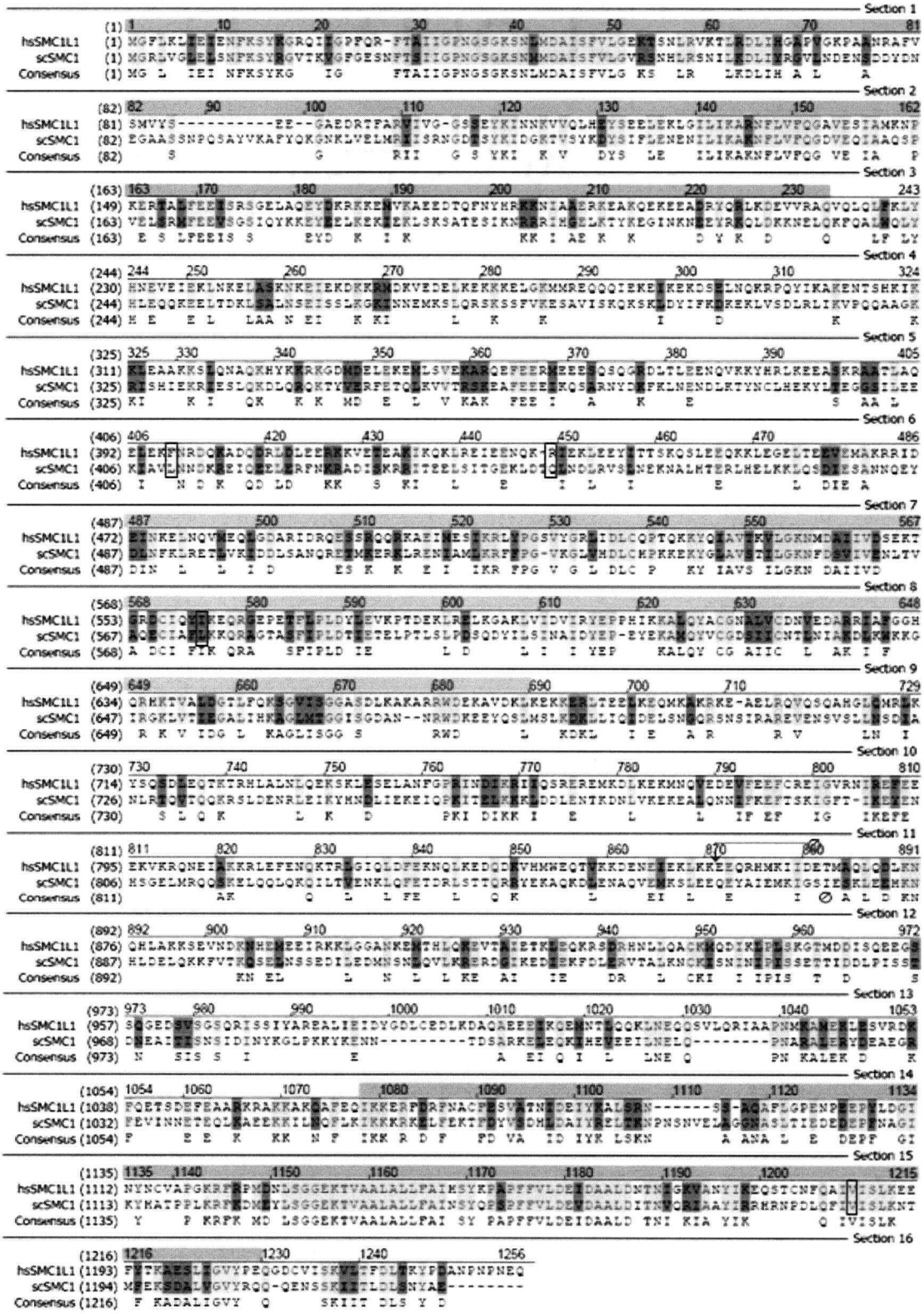

B

Human SMC1L1 amino acid substitution	Type of *SMC1L1* mutation	Yeast *SMC1* amino acid substitution
F396L	Homo/Hemi	L380 (no mutation made)
R434W	Hetero	Q449W
I560M	Hetero	L574M
Insertion of A between coding sequence 2562 & 2563, leading to amino acid change starting from 855 and termination at amino acid 864	Hetero	I877Z
V1186I	Hetero	V11871

C

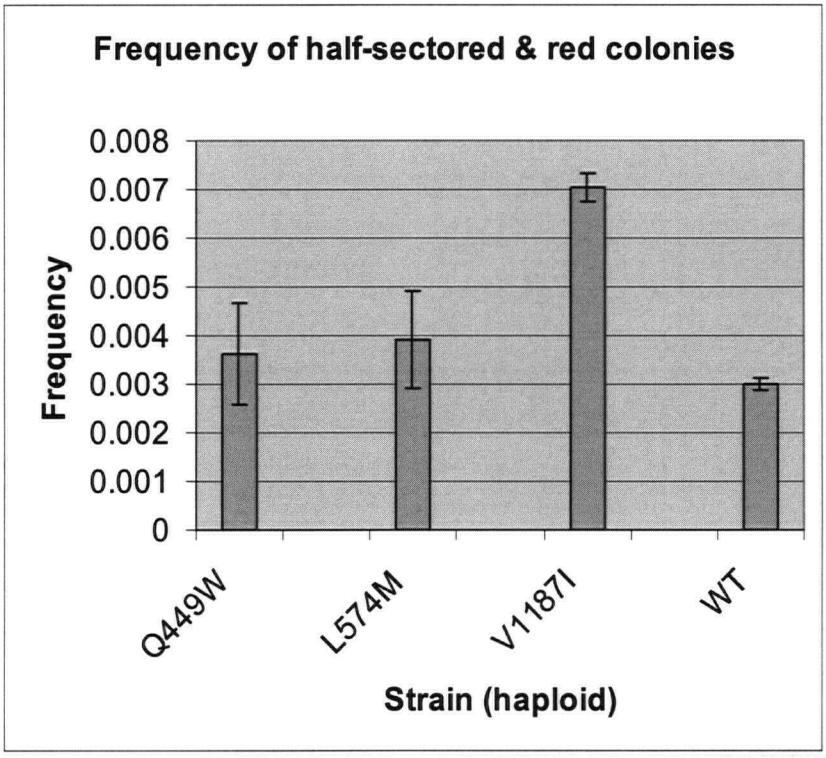

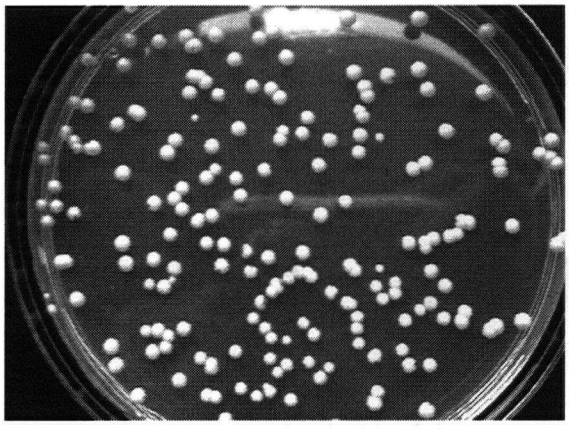

V1187I

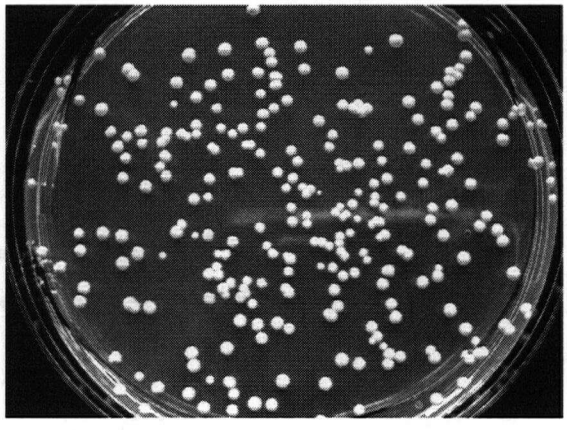

WT

Figure 3.2 Synthetic lethal interactions of yeast CIN genes whose human homologues were found to be mutated in colorectal cancers (which are placed on the rim and depicted in blue fonts).

A. Only genes synthetic lethal with more than 1 of these CIN genes are shown.

B. Only genes synthetic lethal with at least 5 CIN genes are shown.

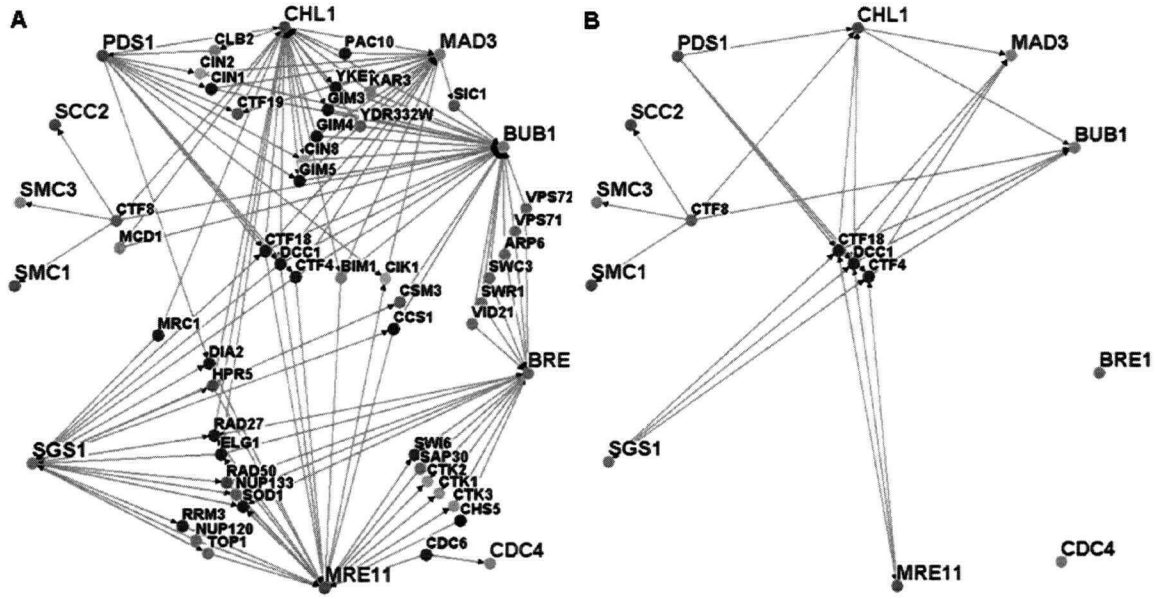

CHAPTER 4

Characterization of *MMS22*, *MMS1*, *RTT101* and *RTT107* in the Maintenance of Genome Integrity

4.1 Introduction

One of the goals of performing genome-wide chromosome instability screens is to identify novel genes and characterize their functions. Among the 293 genes identified in the CIN screens described in Chapter 2, 46 (16%) were uncharacterized (see Appendix 1 and 2; by GO Slim Mapper on SGD, http://db.yeastgenome.org/cgi-bin/GO/goTermMapper). To prioritize genes for further study, I first examined the 34 genes that were identified in all 3 CIN screens. Many of the genes within this subset are known to be important for maintaining genome integrity, such as those that function at the kinetochore, in cell cycle checkpoints and in DNA repair pathways. At the time the screens were completed, only a few of the 34 genes were largely uncharacterized, including *NCE4*, *MMS1* and *MMS22*. However, I was able to gain insights into the functions of these genes by integrating data derived from large scale phenotypic screening (such as the CIN, GCR and drug sensitivity screens (see below)), as well as genetic and physical interaction analyses (Figure 2.5).

Mass spectrometry (MS) analysis of immunoprecipitates of overexpressed tagged Mms22p identified Rtt101p/Cul8p, a cullin, and Rtt107p/Esc4p as interacting proteins (Ho et al., 2002), all of which were also identified in the CIN screens. In addition, Rtt101p and Mms1p/Rtt108p/Kim3p were identified as protein-protein interactors with Roc1p/Hrt1p, a RING finger protein known to bind to cullins in E3 ubiquitin ligases (Ho et al., 2002). These physical interactions suggested that these proteins may function together to maintain genome integrity.

Indeed, *RTT* (retrotransposition) genes were originally identified in a screen for mutants that increase the transposition rate of Ty1, a long terminal repeat (LTR) retrotransposon (Scholes et al., 2001). Many of the *rtt* mutants, including *rtt101Δ*, *rtt107Δ* and *mms1Δ/rtt108Δ*, were found to have elevated rates of gross chromosomal rearrangement (GCR) (Kanellis et al., 2003; Luke et al., 2006; Rouse, 2004). On the other hand, *MMS22* was identified in another screen set up to look for mutants leading to reduced levels of Ty1 retrotransposition, and it was shown that the level of Ty1 cDNA was not affected in *mms22Δ* mutants, suggesting that Mms22p affects steps that occur

after DNA replication, possibly in the repair of chromosomal DNA damage at integration sites (Griffith et al., 2003).

Many CIN mutants are sensitive to DNA damaging agents. Different DNA damaging agents cause different types of DNA lesions and sometimes one agent generates pleiotropic lesions (Table 4.1 and Figure 4.1). Genes whose proteins function in the same or parallel pathway are expected to display similar genetic interaction profiles and phenotypes such as CIN and drug sensitivity (Parsons et al., 2004; Tong et al., 2004). For example, base excision repair (BER) mutants are sensitive to base damaging agents, but not to UV or IR. Nucleotide excision repair (NER) mutants are sensitive to UV and 4NQO, but only moderately sensitive to MMS and IR. Post-replication repair mutants are sensitive to MMS, UV and IR. Homologous recombination (HR) mutants are extremely sensitive to IR, but are only moderately sensitive to UV (Figure 4.1). Indeed, *MMS* genes, including *MMS22* and *MMS1*, were originally identified in a screen for mutants that are sensitive to the MMS (Prakash and Prakash, 1977). In addition, both *mms22Δ* and *mms1Δ* mutants are sensitive to many other DNA damaging agents including HU, CPT, and moderately sensitive to UV (Baldwin et al., 2005; Bennett et al., 2001; Chang et al., 2002; Hanway et al., 2002; Parsons et al., 2004; Prakash and Prakash, 1977);(Hryciw et al., 2002). Similarly, *rtt101Δ* and *rtt107Δ* mutants are also sensitive to MMS, HU, and CPT (Bennett et al., 2001; Chang et al., 2002; Hanway et al., 2002). The drug sensitivity profiles of these 4 mutants were most similar to that of post-replication repair gene mutants, but not identical (see below), suggesting they may constitute a novel pathway involved in DNA repair.

During the last few years, the role of Rtt107p, Rtt101p, Mms1p and Mms22p in DNA damage response has been characterized in more detail as summarized below.

4.1.1 *RTT107*

Rtt107p contains 6 BRCT domains, which are usually found in proteins involved in signaling, repairing of DNA damage or cell cycle regulation (e.g. BRCA1, XRCC1, and 53BP1). *rtt107Δ* causes delays in S phase, accumulation in G2/M, and an increased

fraction of cells with checkpoint protein Ddc2p foci, which suggest a higher level of spontaneous DNA damage (Roberts et al., 2006). However, double mutant analysis for MMS sensitivity showed that Rtt107p is not involved in NER, HR or cell cycle control (Hanway et al., 2002). Indeed, Rtt107p is not required at the time of damage, and *rtt107Δ* mutants are competent for activation of the intra-S-phase checkpoint, which is indicated by Rad53p phosphorylation. In response to DNA damage occurring in S phase, Rtt107p is phosphorylated by the checkpoint protein Mec1p, and Rtt107p is important for recovery from DNA damage by promoting restart of stalled replication forks (Rouse, 2004).

Slx4p and Slx1p, which form a structure-specific DNA endonuclease required for resolving replication intermediates specifically in the rDNA (Fricke and Brill, 2003), physically interact with Rtt107p. The Slx4p-Rtt107p interaction is independent of DNA damage, and requires the BRCT domains of Rtt107p. The interaction is required for Mec1p-mediated phosphorylation of Rtt107p (Roberts et al., 2006). In another study, yeast-two-hybrid (Y2H) analysis of the N-terminal region of Rtt107p (containing 4 BRCT domains) identified Rad55p, Mms22p, Tof1p and Sgs1p (Chin et al., 2006). Like the interaction with Slx4p, the physical interaction between Rtt107p and Rad55p does not depend on DNA damage (Chin et al., 2006). Like Rtt107p, Rad55p is also phosphorylated by Mec1p in response to DNA damage, and it forms a heterodimer with Rad57p, which together orchestrates the assembly of the Rad51p filament on replication protein A (RPA)-coated ssDNA. Taken together, these physical interactions suggest that Rtt107p may associate with ssDNA of stalled replication forks to modulate repair and reinitiation of DNA synthesis.

Subcellular localization of Rtt107p is in agreement with its putative function at stalled replication forks. Rtt107p displays diffuse nuclear localization in G1 and G2/M, which is unaffected by MMS treatment (Chin et al., 2006). However, half of S phase cells have Rtt107p foci at the edge of the nucleus, and treatment with MMS increases the fraction of cells containing such foci (Chin et al., 2006). Pax2 transactivation domain interacting protein (PTIP), the mammalian protein with highest sequence similarity to

Rtt107p, was recently shown to form foci after DNA damage (Manke et al., 2003). The number of cells with Rtt107p foci also increase in *mrc1Δ* or *tof1Δ* mutants, which contain ssDNA accumulated at stalled replication forks (Chin et al., 2006). Interestingly, Rtt107p foci partially overlap with rDNA repeats. These results support that Rtt107p may bind stalled replication forks that accumulate ssDNA, and may be involved in the repair of replication forks that collapse within the rDNA repeats.

4.1.2 *RTT101*

Rtt101p is one of the 3 cullins in *S. cerevisiae*, with demonstrable ubiquitin ligase activity *in vitro*, but as yet no known substrate *in vivo* (Michel et al., 2003). *rtt101Δ* mutants accumulate with a short spindle and nucleus positioned at the bud neck (Luke et al., 2006; Michel et al., 2003). The anaphase onset in *rtt101Δ* mutants is delayed, and this is dependent on the intra-S-phase checkpoint (Mec1p and Rad9p) (Luke et al., 2006; Michel et al., 2003).

rtt101Δ mutants display several phenotypes resembling *rtt107Δ* mutants. For example, *rtt101Δ* mutants have increased numbers of Ddc1p and Rad52p foci, indicating an increase in spontaneous DNA damage (Luke et al., 2006). *rtt101Δ* mutants are also competent in Rad53p checkpoint activation in response to HU treatment (Luke et al., 2006). Based on double mutant analysis for MMS sensitivity, Rtt101p is not involved in non-homologous end joining (NHEJ) or HR (Luke et al., 2006; Michel et al., 2003).

Like Rtt107p, Rtt101p may play a role in replication fork reinitiation or progression. In *rtt101Δ* mutants, replication forks arrested at natural pause sites (e.g. rDNA barriers, centromeres) are more unstable, as indicated by the increased formation of extrachromosomal rDNA circles (Luke et al., 2006). *rtt101Δ* mutants cannot complete DNA replication during recovery from MMS, which induces fork arrest. On the other hand, *rtt101Δ* mutants can recover from HU, which causes fork pausing. These results suggest that Rtt101p promotes fork progression through alkylated DNA (Luke et al., 2006).

4.1.3 *MMS22* and *MMS1*

Phenotypically, both *mms22Δ* and *mms1Δ* mutants exhibit slow growth and abnormal cell morphology including large, round and elongated cells (Araki et al., 2003; Hryciw et al., 2002). To determine whether *MMS22* and *MMS1* function in known repair pathway, double mutant analysis for MMS sensitivity was performed and suggested that both *MMS22* and *MMS1* are not involved in NHEJ, and NER (Araki et al., 2003; Hryciw et al., 2002). However, *mms22Δ* is synthetically lethal with *rad6Δ* (post-replication repair) and *rad52Δ* (homologous recombination repair) (Araki et al., 2003; Hryciw et al., 2002), and *mms1Δ* is also synthetically lethal with *rad52Δ* in some strain backgrounds (Araki et al., 2003; Hryciw et al., 2002), suggesting that *MMS22* and *MMS1* may function in a pathway redundant to *RAD52* and *RAD6*. An *mms22Δ mms1Δ* double mutant exhibits MMS, HU, UV sensitivity that is similar to the *mms22Δ* mutant, indicating that *mms22Δ* is epistatic to *mms1Δ* (Araki et al., 2003). *mms22Δ* is also epistatic to *rtt101Δ* and *rtt107Δ* (Baldwin et al., 2005). Indeed, sensitivity of *mms1Δ* to DNA damaging agents is suppressed by overexpression of *MMS22*, but not vice versa, suggesting that *MMS1* acts upstream of *MMS22* in a novel repair pathway.

Besides genetically interacting with DNA repair genes, *MMS22* and *MMS1* also genetically and physically interacts with some essential genes involved in replication initiation. First, high-throughput Y2H studies showed that Mms22p (as prey) interacts with Psf1p and Psf2p, 2 of the 4 essential subunits of the GINS complex (Hazbun et al., 2003). The GINS complex binds to DNA replication origins and facilitates assembly of the DNA replication machinery (Hazbun et al., 2003; Takayama et al., 2003). Second, mutations in *MMS22* and *MMS1* were both identified in a screen for mutations synthetically lethal with *mcm10-1* (Araki et al., 2003). Mcm10p/Dna43p is essential for replication initiation and the disassembly of pre-replication complex (pre-RC) after initiation (Araki et al., 2003). Therefore, Mcm10p is required for the smooth passage of replication forks through obstacles such as those created by pre-RCs assembled at active or inactive replication origins. *mcm10-1* causes replication fork pausing at active and silent origins (Araki et al., 2003). Interestingly, *mcm10-1*, *mms2Δ* and *mms1Δ* are all

synthetically lethal with *dna2-2* (Budd et al., 2005). *DNA2* encodes an essential DNA replication protein that contains helicase and single-stranded nuclease activities, and is involved in the processing of Okazaki fragments and in DNA repair. Collectively, *MMS22* and *MMS1* may constitute a novel DNA repair pathway that is specific for replication-dependent DNA damage (Araki et al., 2003), in agreement with Rtt107p and Rtt101p having roles in the restart of replication upon DSBs.

To further elucidate the role of *MMS22* in DSB repair, a series of phenotypic, genetic and physical analyses were performed. The survival rate after exposure to a DSB and the kinetics of DSB repair were determined in *mms22Δ* mutants and compared to wild-type and known DSB repair mutants. Global identification of Mms22p, Rtt101p and Rtt107p physical interactors was performed by mass spectrometry (MS) and yeast-two-hybrid (Y2H) analyses. Since physical interactors of Rtt101p are potential substrates of this putative ubiquitin ligase, the protein expression levels of some interactors were tested.

4.2 Materials and Methods

4.2.1 Yeast strains and media

Yeast strains used in this study are listed in Table 4.1. Media for growth and sporulation were described previously in Rose et al., 1990. Epitope tagging and gene deletions were made directly at the endogenous loci (Longtine et al., 1998). Yeast transformations were performed as in (Gietz et al., 1995).

4.2.2 Quantification of chromosome transmission fidelity (*ctf*)

Quantification of the *ctf* phenotype was performed in homozygous diploid strains containing a chromosome fragment (CF) as in (Shero et al., 1991). Briefly, diploid cells with one CF form pink colonies. Diploid cells that lose the CF form red colonies, whereas those that contain 2 CFs generate white colonies. Chromosome missegregation in the first cell division after plating generates a half-sectored colony, and the frequencies of half-sectored colonies reflect the rates of chromosome loss and non-disjunction (Shero et al., 1991).

4.2.3 Genome-wide yeast-two-hybrid screens

MMS22, *RTT101* and *RTT107* were cloned into pOBD2 as described in (Cagney et al., 2000). The Mms22p-Gal4p-DNA binding domain fusion protein was functional as determined by rescuing sensitivity of *mms22Δ* to 0.2M HU, 10μg/ml camptothecin and 0.01% MMS (data not shown). Genome-wide two-hybrid screens were performed as described in (Uetz et al., 2000). Briefly, each screen was performed in duplicate, and positives that were identified twice were put into a mini-array for retest. Some reproducible positives were observed in many different screens with baits of unrelated function. These were considered common false positives and were excluded from further analyses.

4.2.4 Co-immunoprecipitation

Co-immunoprecipitations were performed as described in (Measday et al., 2002). In brief, yeast extracts were generated using glass beads lysis. The protein concentration

of extracts was measured by Bradford assay, and equal amounts (2-5 mg) of extracts were incubated with anti-MYC- or anti-HA- conjugated beads (Covance) for ~24 hrs at 4°C. Beads were washed in extract buffer for a minimum of 3 times, and immunoprecipitates were eluted with SDS-PAGE loading buffer.

4.2.5 Mass spectrometry

Protein eluates from immunoprecipitation were diluted in 20 mM Tris pH 8.3, 5 mM EDTA so that the final SDS concentration was no greater than 0.05%. 20 ng/µl of sequencing-grade trypsin (Fisher) was added, and digestion was allowed to proceed at 37°C overnight. Samples were then purified using C18 ZipTips (Millipore) according to the manufacturer's instructions. One-dimensional reversed-phase liquid chromatography with on-line mass spectrometry on an ion trap mass spectrometer (Model LCQ, ThermoElectron, San Jose, CA) was performed as described in (Lee et al., 2004), employing a 90 min. binary gradient from 5%-80% solvent B during which each mass spectrum (MS) scan was followed by three MS/MS scans. Experimental mass spectra were compared with theoretical spectra generated from sequences from the *Saccharomyces cerevisiae* genome by using the SEQUEST algorithm (Yates et al., 1995). Data were displayed and filtered by using the INTERACT software (Han et al., 2001).

4.2.6 Survival assay in HO-induced double strand breaks

pJH132 (pGAL-HO-TRP1) (Lisby et al., 2001) was transformed into wild-type, *mms22Δ* and *rad52Δ* strains. pRS414-TRP1 was used as an empty vector control. Equal amounts of cells were plated on SC-TRP (Galactose) and SC-TRP (Glucose). Survival rate was calculated by the number of colonies formed on SC-TRP (Galactose) over that formed on SC-TRP (Glucose) after 8 days.

4.2.7 Microscopy

Strains used for microscopy were grown in FPM (Synthetic complete medium supplemented with adenine and 6.5 g/L sodium citrate) in order to reduce auto-

fluorescence. DAPI (300 ng/ml) was added to live cells for visualization of DNA as described previously (Connelly and Hieter, 1996). Stacks of microscopy images were taken with a Zeiss Axioplan II operated with Metamorph software (Universal Imaging). The presence of Rad52p foci was examined in *WT* (YKY807) and *mms22Δ* (YTK1364) strains as described in (Lisby et al., 2003).

4.3 Results

4.3.1 *mms22Δ*, *mms1Δ*, *rtt101Δ* and *rtt107Δ* exhibit sensitivity to DNA damaging agents and chromosome instability

I analyzed the genome-wide drug sensitivity screen results by 2-dimensional hierarchical clustering, and overlaid them with the CIN screen results (Bennett et al., 2001; Birrell et al., 2001; Chang et al., 2002; Giaever et al., 1999; Hanway et al., 2002; Parsons et al., 2004) (Figure 4.2). Two clusters are enriched for CIN mutants; the cluster showing sensitivity to benomyl is enriched for genes functioning at the kinetochore and spindle, whereas the cluster exhibiting sensitivity to DNA damaging agents is enriched for genes involved in DNA repair and DNA damage checkpoints, including *MMS22*, *MMS1*, *RTT101* and *RTT107*. Interestingly, these 4 genes cluster with the MRX (*MRE11*, *RAD50*, and *XRS2*) complex, which is involved in DSB repair, sister chromatid cohesion and telomere maintenance.

Both *mms22Δ* and *mms1Δ* were identified in all 3 CIN screens, whereas *rtt101Δ* and *rtt107Δ* were identified in at least 1 CIN screen (see Chapter 2). In addition, the GCR rates of the *rtt* mutants are elevated (Kanellis et al., 2003; Luke et al., 2006; Rouse, 2004). When the frequency of chromosome transmission fidelity (*ctf*) was quantified by half-sectoring assay (Shero et al., 1991), all these mutants exhibited CIN at various levels (Table 4.3).

4.3.2 *mms22Δ* exhibits defects in cell cycle progression

Based on the CIN phenotype of *mms22Δ*, Mms22p may function in a cell cycle step that is crucial for chromosome integrity, or it may be important for repairing certain DNA lesions. Indeed, *mms22Δ* cells accumulate at G2/M phase (Bennett et al., 2001) and display increased cell size (Jorgensen et al., 2002). The absence of Mms22p could result in a delay in certain steps of the cell cycle, or it could induce spontaneous DNA damage, which would activate the cell cycle checkpoint and lead to cell cycle arrest. Fluorescence activated cell sorting (FACS) analysis of logarithmically growing *mms22Δ* cells, compared to wild type cells, revealed a larger 2N peak, which is consistent with

abnormalities in cell cycle regulation and aneuploidy (Figure 4.3A). Budding index analysis also revealed that an increased proportion of *mms22Δ* cells exhibit large buds and DNA in the bud necks. To investigate whether the G2/M accumulation is caused by checkpoint activation, *mms22Δ* was combined with several checkpoint mutations. FACS analysis of these double mutants showed that this G2/M delay is not dependent on the spindle checkpoint (*mad2Δ*), the DNA damage checkpoint (*rad9Δ*, *mec3Δ*), or the replication checkpoint (*mrc1Δ*) (Figure 4.3A). These results suggest that *mms22Δ* cells might be slow to enter or exit mitosis, leading to the G2/M accumulation. Indeed, *mms22Δ* is characterized by slow growth (Araki et al., 2003). *WT* and *mms22Δ* cells were synchronized by arresting them in G1 with α-factor and their cell cycle were followed after release from the block (Figure 4.3C). *mms22Δ* cells appear to enter S phase and finish DNA replication at similar times compared to *WT*; however, *mms22Δ* cells enter the next G1 at a much later time than *WT* cells.

4.3.3 *mms22Δ* has reduced survival rate with the introduction of DSBs

mms22Δ cells are sensitive to several DNA damaging agents that cause DSBs. To directly test whether *mms22Δ* is impaired in DSB repair, the survival rate of *mms22Δ* cells was monitored following the introduction of an HO endonuclease-induced DSB (Lisby et al., 2001) (Figure 4.4A). *mms22Δ* mutants have a lower survival rate (30-50%) than *WT* (80-90%), but are not completely inviable as observed in *rad52Δ* mutants. Consistent with the reduced survival rate, when the size of the colonies in the presence of a DSB was examined, *mms22Δ* cells formed much smaller colonies compared to *WT* (Figure 4.4B). This result is consistent with a lower sensitivity of *mms22Δ* mutants to MMS compared to *rad52Δ* mutants, suggesting a less important role for Mms22p in DSB repair, compared to Rad52p. It is possible that Mms22p is only responsible for a subset of DSBs, such as DSBs that occur during replication, or that the Mms22p pathway is not the major repair route chosen by the cells.

Another way to monitor DSB repair is to examine the formation of DNA repair centres in cells, in which Rad52p aggregates multiple DSB sites together and recruits other homologous recombination proteins for repair in S and G2 phases (Lisby et al., 2003). The number of Rad52p foci is not directly proportional to the number of DSBs, suggesting that each focus likely represents the repair centre of multiple DNA lesions (Lisby et al., 2001). Interestingly, *mms22Δ* is synthetically lethal with *rad52Δ* (Araki et al., 2003), suggesting that Mms22p and Rad52p may act in parallel pathways with overlapping functions. To assess the level of spontaneous DNA damage and monitor the dynamics of Rad52p-dependent DSB repair in *mms22Δ* mutants, the percentage of *mms22Δ* and *WT* cells with Rad52p foci in the absence and presence of a single DSB induced by HO or I-SceI, or in 0.1% MMS was recorded (Figure 4.4D). To make sure that Rad52p foci were observed with high confidence, another marker was observed in parallel. Lisby observed that 94% of Rad52p foci colocalize with the DSB site (Lisby et al., 2003). An example of Rad52p foci and DSB site colocalization is shown in Figure 4.4C. 25-50% of budded *WT* cells, but only 5-10% of budded *mms22Δ* cells, exhibited Rad52p foci in the presence of DNA damage. In general, the frequencies obtained were lower than those reported by Lisby et al., who observed that 22% budded *WT* cells form spontaneous Rad52p foci, and 62% budded *WT* cells form foci after 1hr exposure to 0.1% MMS (Lisby et al., 2003). This could be attributed to technical variation (e.g. subjective definition of a Rad52p focus). In *WT*, the proportion of cells with Rad52p foci increases in the presence of DNA damage. In *mms22Δ*, the proportion of cells containing Rad52p foci does not differ in the absence and presence of DNA damage. This result is different from many CIN mutants, in which the percentage of cells with spontaneous Rad52p foci increases, as in *pol2-100*, *mec1Δ* (Lisby et al., 2001), *top3Δ* (71%), *sgs1Δ* (41%) (Shor et al., 2005), *nup133Δ* (30%) and *rad27Δ* (32%) (Loeillet et al., 2005). On the other hand, in *rfa1Δ*, Rad52p foci do not form efficiently, revealing the hierarchy in the repair process (Lisby et al., 2004). This result suggests that Mms22p may act early in the repair process, and may be required for the formation of Rad52p foci.

In order to determine whether the lower survival rate of *mms22Δ* in DSB is related to slower repair kinetics, the presence of a DSB and the completion of repair in *mms22Δ* were monitored by southern blot and PCR analyses as in (Aylon et al., 2003) (personal communication with Martin Kupiec; Figure 4.5). While the DSB is resolved by 4 hours in *WT* cells, the DSB persisted up to 7 hours in *mms22Δ* cells. The level of gene conversion was also lower in *mms22Δ* cells (60%) compared to *WT* cells (90%). Interestingly, the survival level as observed by colony formation was lower than the repair rate based on PCR. This discrepancy implies that some cells repair the DSB, but are still unable to survive. A similar phenomenon has been seen in mutants compromised for checkpoint functions (e.g. *rad24Δ*, *mec1Δ*) (Aylon et al., 2003). Although *mms22Δ* mutants have been shown to be competent for Rad53p activation (Araki et al., 2003), it will be of interest to elucidate whether *mms22Δ* mutants are defective in some aspect of checkpoint function.

4.3.4 Mms22p interacts with replication initiation and DNA repair proteins that may constitute a novel repair pathway

Mass spectrometry (MS) analysis of overexpressed tagged Mms22p immunoprecipitates provided preliminary evidence that Mms22p physically interacts with Rtt101p/Cul8p and Rtt107p/Esc4p (Ho et al., 2002). To confirm these interactions, I performed reciprocal co-immunoprecipitation (co-IP) of endogenously expressed tagged proteins (Figure 4.6A&B).

4.3.4.1 Mass spectrometry analysis

To systematically identify additional protein interactors of this potential novel complex, immunoprecipitation followed by MS was performed using endogenously expressed Mms22p, Rtt101p and Rtt107p. MS analysis for Mms22p immunoprecipitates did not yield any putative interaction partners, including Mms22p itself, possibly because Mms22p is expressed at a low level (data not shown). MS of Rtt107p immunoprecipitates identified only Rtt107p itself but no other protein. Interestingly, MS analysis of Rtt101p

immunoprecipitates identified Mms1p, a protein proposed to function upstream of Mms22p (Figure 4.7A). To verify this interaction, reciprocal co-IP was performed using lysates extracted from logarithmically growing cells that contain no tag, Mms1p-MYC only, Rtt101p-HA only, and both Mms1p-MYC and Rtt101p-HA (Figure 4.7B). In the anti-HA IP, Mms1p-MYC is only detected when both Mms1p-MYC and Rtt101p-HA are expressed. Reciprocally, in the anti-MYC IP, Rtt101p-HA is only detected in strains with Mms1p-MYC and Rtt101p-HA.

4.3.4.2 Yeast-two-hybrid analysis

Given the common occurrence of false-positives and false-negatives in genome-wide assays and screens, combining results using various methods often yield more informative results. Therefore, yeast-two-hybrid (Y2H) screening was performed using Mms22p, Rtt101p and Rtt107p as baits. The Y2H study using Mms22p as bait identified Rtt101p, Mms1p, Mcm10p, Ctf4p and several other proteins as interacting proteins (Figure 4.8A&D). To confirm the physical interactions between Mms22p and Mms1p, reciprocal co-IP experiments were performed (Figure 4.9). Endogenously expressed Mms22p-MYC co-immunoprecipitated with endogenously expressed Mms1-HA in the HA-IP only when both tagged proteins were expressed. Reciprocally, endogenously expressed Mms1-HA co-immunoprecipitated with endogenously expressed Mms22p-MYC in the MYC-IP (Figure 4.9B). However, there was some background immunoprecipitation of Mms1p-HA in the HA-IP in the absence of Mms22p-MYC. Therefore, reciprocal tagging was tried to avoid the background. HA-Mms22p expressed from the GAL1 promoter was used instead. Endogenously expressed Mms1p-MYC co-immunoprecipitated with overexpressed HA-Mms22p in the HA-IP (Figure 4.9A). However, in the reciprocal MYC-IP, HA-Mms22p did not co-immunoprecipitate with Mms1p-MYC. It is possible that the overexpression of Mms22p disrupts the localization of proteins required for its interaction with Mms1p, or it may change the stoichiometry of its physiological protein-protein interactions. Taken together, these results strongly suggest that these two proteins not only interact genetically as reported by Araki et al.

(2003), but also physically, and likely together with Rtt101p. It will be of interest to investigate whether the pairwise interactions among these 3 proteins are dependent on the third protein.

The Y2H interaction of Mcm10p, a replication initiation protein, with Mms22p is also intriguing, since *mcm10-1* and *mms22Δ* are synthetically lethal (Araki et al., 2003). Ctf4p, a Y2H interactor of Mms22p, also functions in replication and cohesion, and is important for chromosome transmission fidelity (Mayer et al., 2004; Petronczki et al., 2004; Warren et al., 2004b). In addition, high-throughput Y2H studies showed that Mms22p (as prey) interacts with Psf1p and Psf2p, 2 of the 4 subunits of the GINS complex, which is required for DNA replication initiation and progression of DNA replication forks (Gambus et al., 2006; Hazbun et al., 2003; Takayama et al., 2003). I have been unable to confirm the physical interactions of Mms22p with these replication proteins by co-immunoprecipitation of endogenously tagged proteins in logarithmic growth condition (data not shown). It is possible that these interactions represent false-positives identified in Y2H screens and do not occur in physiological conditions, but it is also possible that the interactions are transient, occurring only at specific cell cycle stages, or only in a very small fraction of the total protein pool. However, because the Y2H interactors of Mms22p are enriched for replication proteins (p-value = 1.84E-5, by GO Term Finder on SGD, http://db.yeastgenome.org/cgi-bin/GO/goTermFinder), and these replication proteins are not seen as common interactors with many other proteins (false-positives), these interactions may be real and functional. The Y2H results are also in agreement with the observation that *mms22Δ* mutants are sensitive to DNA damaging agents that cause replication-dependent DSBs, such as CPT.

4.3.4.3 Genetic interaction analysis

Genetically, *mms22Δ* interacts with mutations in replication initiation, HR and post-replication repair genes (Pan et al., 2006; Tong et al., 2004), suggesting it may have overlapping functions in these pathways. Unexpectedly, genome-wide SL screens using kinetochore mutants as queries revealed that *mms22Δ* also genetically interacts with

spc24-9 and *spc24-10*, temperature sensitive alleles of a gene encoding a central kinetochore protein, by lowering their permissive temperatures (Figure 4.10A). At semi-permissive temperatures, both *spc24-9* and *spc24-10* mutants have elongated spindles and unequal distribution of chromosomal DNA. *spc24-9* is also sensitive to HU (personal communication with Vivien Measday). It is unlikely that Mms22p functions at the kinetochore, but the combined defects in *mms22Δ* and kinetochore mutants may sensitize cells to chromosome missegregation.

Pan et al. reported that *MMS22*, *MMS1*, *RTT101* and *RTT107* forms a functional module or minipathway based on high congruence in genome-wide synthetic fitness/lethal (SFL) interaction profiles together with the HR and *RAD6*-dependent repair pathways (Pan et al., 2006). Mutations in any of the 4 genes cause similar sensitivity to DNA-damaging treatments, and do not exhibit SFL interaction with one another, except that Pan et al. observed a synthetic fitness defect in the *rtt101Δ rtt107Δ* mutants (Pan et al., 2006). I did not observe a synthetic fitness defect in the *rtt101Δ rtt107Δ* mutants in unperturbed condition, but did observe synergistic sensitivity to MMS and HU (Figure 4.10B).

This study and others large scale physical and genetic interaction studies (Ho et al., 2002; Pan et al., 2006; Tong et al., 2004) have generated enomorous amount of interaction data for *MMS22*, *MMS1*, *RTT101* and *RTT107*, which are invaluable to understanding the biological pathways of these genes. These interactions are summarized in a network diagram (Figure 4.11).

4.3.5 Rtt101p regulates Mms22p

Michel et al. (Michel et al., 2003) showed that Rtt101p has sequence homology with cullins and contains *in vitro* ubiquitin ligase activity, but there is as yet no known *in vivo* substrate. Based on the physical interactions between Mms22p and Mms1p with Rtt101p (Figure 4.6 and 4.7), I hypothesized that Mms22p and Mms1p could be substrates of the Rtt101p E3 ubiquitin ligase complex. Therefore, I analyzed the steady state protein level of Mms1p and Mms22p in *rtt101Δ* mutants. Expression of Mms1p is

not affected by *rtt101Δ* (data not shown). On the contrary, Mms22p is expressed at a much higher level in *rtt101Δ* mutants when compared to *WT* (Figure 4.12A). This is consistent with the hypothesis that Mms22p is a substrate of Rtt101p, whereas Mms1p could regulate Rtt101p activity. Indeed, the Mms22p expression level is similar in *rtt101Δ* and *rtt101Δ mms1Δ* (Figure 4.12A). It will be of interest to also examine whether Mms22p expression level is affected in *mms1Δ*.

To further investigate whether Rtt101p regulates the expression level of Mms22p through its ubiquitin ligase activity, I attempted to analyze Mms22p expression level in an *rtt101* mutant that affects its ubiquitin ligase activity. Rtt101p, like other cullins, is modified by Rub1p at a conserved lysine K791. However, K791 is also the site of Rub1-independent modifications (Michel et al., 2003). The K791A mutation of Rtt101p was observed to reduce its *in vitro* ubiquitin ligase activity by 50% (Michel et al., 2003); however, another study reported that the K791R mutation can still complement for Rtt101p function in a transposition assay, showing that the modification at K791 does not completely disrupt Rtt101p function (Laplaza et al., 2004). I compared the expression level of Mms22p in an *rtt101Δ* mutant containing a 2μ plasmid expressing either wild-type *RTT101* or *rtt101-K791R* under control of the Gal promoter. In both cases, the expression level of Mms22p was intermediate, between that observed in *WT* and *rtt101Δ*, suggesting that both constructs partially complement the lack of Rtt101p (Figure 4.12A). Due to the ambiguity regarding the function of the K791 modification, it is still difficult to conclude with certainty that Mms22p's expression level is affected by Rtt101's ubiquitin ligase activity. To address this ambiguity, it will be useful to asses the effect of a different mutant of Rtt101p. The interaction between Rtt101p and Roc1p is essential for its ubiquitin ligase activity, since deleting the conserved Roc1p-interacting domain in Rtt101p results in complete loss of *in vitro* ubiquitin ligase activity (Michel et al., 2003). Therefore, comparing the expression level of Mms22p in an *rtt101Δ* mutant containing a plasmid expressing either wild-type *RTT101* or an *rtt101* mutant lacking the Roc1p-interacting domain (*rtt101-ΔRoc1*) would delineate whether the ubiquitin ligase activity of *RTT101* is required for regulating Mms22p.

While the above experiments looked at the steady state expression level of Mms22p in logarithmic growth, it was of interest to examine the kinetics of Mms22p degradation in the presence or absence of Rtt101p. Mms22p was expressed from the galactose promoter in medium containing galactose, and the expression was then shut off by growth in glucose medium. The level of Mms22p was monitored at 20 min intervals for 100 min (Figure 4.12B). Interestingly, Mms22p levels increased to a higher level during the induction period in *rtt101Δ* mutants. However, the degradation rate of Mms22p was not reduced in *rtt101Δ*. It is possible that Mms22p is also degraded by an Rtt101p-independent pathway. In this experimental condition, however, the Mms22p could still be translated from residual mRNA transcripts after promoter shut off. Therefore, in future experiments, cycloheximide, a drug that inhibits protein translation, should be added when the culture is released into glucose.

Rtt101p could regulate the degradation of Mms22p in a cell-cycle dependent manner or in response to DNA damage. I therefore analyzed whether Mms22p and Rtt101p are induced or modified under various conditions. Microarray analysis revealed that *MMS22* mRNA expression is induced 5 minutes after 0.02% MMS addition and 20 minutes after heat shock (Gasch et al., 2001). Western blot analysis of Mms22p in different cell cycle stages or 0.01% MMS for 15 min at different cell cycle stages showed similar Mms22p expression level (data not shown). However, Rtt101p showed a slower-migrating band in the presence of HU and nocodazole (Figure 4.13), suggesting it may be modified in a cell cycle-specific manner. Further experiments are required to distinguish whether these modifications are cell cycle specific, or whether they are side effects related to drug treatment.

4.4 Discussion

By integrating phenotypic, genetic and physical interaction data from the literature and from this study, I confirmed that *mms22Δ* is defective in cell cycle progression and DNA DSB repair. Co-immunoprecipitation experiments indicate that Mms22p, Rtt101p and Mms1p physically interact with each other. These data support that Mms22p functions with Mms1p and Rtt101p in an E3 ubiquitin ligase. Indeed, the expression of Mms22p is regulated by Rtt101p, and it is possible that Mms22p is a substrate of the Rtt101 E3 ligase. Since Mms1p expression level is not affected by Rtt101p, Mms1p may serve as a specificity factor the E3 ubiquitin ligase (see below). This work leads to the proposal of a model in which Rtt101p may regulate Mms22p and other protein levels in response to DNA damage.

4.4.1 Conservation of the Rtt101p complex?

While there is as yet no confirmed substrate for the Rtt101p ubiquitin ligase, clues regarding its function may be gained from knowledge about other cullins. Cullin serves a scaffolding function: it interacts through its N-terminal domain with a substrate specificity factor, and through its conserved globular C-terminal domain (called cullin homology domain) with the RING finger protein to form the catalytic core. In addition to Cul1p/Cdc53p/CulAp in SCF, budding yeast has 2 additional cullins: Cul3p/CulBp and Rtt101p/Cul8p/CulCp, whereas humans have 4 additional cullins: CUL2, CUL3, CUL4A, CUL4B, and CUL5. Rtt101p displays protein sequence similarity to all of the human cullins. However, it is unknown whether Rtt101p is the functional ortholog to any of the known human cullins.

Araki et al. (Araki et al., 2003) claimed that Mms1p has weak similarity to Rad17p and Ddc1p. Recently, Mms1p was found to have homology to human DDB1, the adaptor of CUL4A (Mathias Peter, personal communication). The damaged-DNA binding proteins, DDB1 and DDB2, recognize damaged DNA and are important for global genome repair (GGR), one pathway in NER that repairs the DNA damage across the entire genome. XP patients (in the XPE complementation group) have mutations in

DDB2. DDB2, through its binding to DDB1, interacts with CUL4A and ROC1. In response to UV, CUL4A is post-translationally modified, which stimulates the ubiquitin ligase activity of the DDB complex to ubiquitylates XPC (Matsuda et al., 2005). Such ubiquitin modification has non-proteolytic function, but instead signals the cell to a specific DNA repair pathway. Genetic analysis suggests that the Rtt101p complex functions downstream of PCNA and controls the function of the translesion DNA synthesis (TLS)-polymerase zeta, allowing the replication bypass of damaged templates during DNA replication.

Mms22p exhibits weak homology to *S. pombe* Taz1, a telomere-binding protein that is required for efficient replication fork progression through the telomere (Miller et al., 2006). *taz1Δ* mutants have stalled replication forks at telomeres and telomere sequences placed internally on a chromosome. Taz1 may recruit helicases to facilitate unwinding of the G-rich telomere repeats. Taz1 is required to protect telomeres from NHEJ-mediated telomere fusions, and to prevent chromosomal entanglements and missegregation at cold temperatures (Miller et al., 2005). Human TRF1 and TRF2 are putative orthologues of Taz1, and may also orchestrate fork passage through human telomeres. However, no orthologue of Taz1 has been identified in *S. cerevisiae*.
It would be of interest to investigate if Mms22p has a role to facilitate replication fork progression through G-rich regions or other barriers. Interestingly, Rtt101p and Rtt107p also have a role in facilitating replication fork restart through alkylated and rDNA regions, respectively (Chin et al., 2006; Luke et al., 2006). On the other hand, Araki et al. (Araki et al., 2003) found that Mms22p has weak similarity to Rad50p, a component of the MRX complex. Mutants of the MRX complex and MMS22 display similar drug sensitivity profiles, but further studies are required to determine whether Mms22p functions in a similar way as Rad50p.

4.4.2 Dia2p may play a redundant role with the Rtt101p complex in replication regulation

Like *rtt101Δ*, *dia2Δ* mutants accumulate in S/G2/M, exhibit constitutive activation of Rad53p, increased foci of DNA repair proteins, elevated GCR and CIN as found in our screens (Chapter 2), and are unable to overcome MMS-induced replicative stress. Dia2p, a F-box protein in the SCF, is required for stable passage of replication forks through regions of damaged DNA and natural fragile regions, particularly the replication fork barrier (RFB) of rDNA repeat loci (Blake et al., 2006). The synthetic lethal interaction profile of *dia2Δ* mutants clusters with mutants in DNA replication and repair (*rad51Δ*, *rad52Δ*, *rad54Δ*, *rad57Δ*, *hpr5Δ/srs2Δ*), the replication checkpoint (*csm3Δ*, *tof1Δ*, *mrc1Δ*), the alternative RFC (*dcc1Δ*, *ctf8Δ*, *ctf18Δ*), the MRX complex, post-replicative repair (*rad5Δ*, *rad18Δ*), and *rtt101Δ*, *rtt107Δ* and *mms1Δ* (Blake et al., 2006). SCF^{Dia2} may modify or degrade protein substrates that would otherwise impede the replication fork in problematic regions of the genome. Interestingly, Dia2p binds to replication origins after origin firing, possibly to reset them for use in the next S-phase (Koepp et al., 2006). It is possible that Dia2p acts in a redundant fashion with Rtt101p ubiquitin ligase to modify or eliminate substrates at the replication fork.

4.4.3 Identifying targets for Rtt101p ubiquitin ligase

Although Rtt101p has *in vitro* ubiquitin ligase activity, and interacts with the RING finger protein Roc1p and the E2, Cdc34p, no *in vivo* substrate has been confirmed. The next important goal in characterizing the function of the Rtt101p complex is to identify its target substrates. Ubiquitin modification of targets by the Rtt101p complex may lead to cell-cycle or DNA damage specific proteolysis, or may determine the DNA repair pathway used by the cell (reviewed in (Huang and D'Andrea, 2006)). This study suggests that Mms22p is a component of the E3 complex, but it could also be a substrate. Autocatalytic degradation has been described for other ubiquitin ligases. For instance, the BRCA1-BARD1 complex can autopolyubiquitylate in response to DNA damage, and this autoubiquitylation stimulates its E3 ligase activity to ubiquitylate histone proteins (Huang

and D'Andrea, 2006). In addition, DDB2 is also ubiquitylated by the DDB-CUL4A complex in response to UV (Matsuda et al., 2005).

Physical interactors with Mms22p identified from genome-wide methods, in particular the replication proteins such as Mcm10p, Ctf4p, Psf1p and Psf2p, are candidate substrates of the Rtt101p ubiquitin ligase. The GINS complex, including Psf1p and Psf2p, is required for DNA replication initiation and progression of DNA replication forks (Gambus et al., 2006; Hazbun et al., 2003; Takayama et al., 2003). The GINS complex allows the MCM complex to interact with the replisome progression complexes (RPCs), which include Ctf4p, among other replication proteins. Interestingly, RPCs also interact with Mcm10p (Gambus et al., 2006). Since *mms22Δ* mutants exhibit aneuploidy and some cells accumulate >2N DNA contents, it is possible that Mms22p is involved in the proteolysis of some replication proteins help to ensure that DNA is not re-replicated. It is known that budding yeast employ multiple regulatory mechanisms, including proteolysis of important factors, to serve this function. The replication licensing factor Cdc6p is known to be degraded through SCF^{Cdc4} in S phase. In addition, Orc2p and Orc6p, components of the origin recognition complex, are phosphorylated by S phase cyclin/CDK to inhibit pre-RC reassembly. Furthermore, another replication licensing factor Cdt1 and the MCM complex are exported from the nucleus (Guardavaccaro and Pagano, 2004; Pintard et al., 2004). Similarly, human Mcm10p is phosphorylated and degraded in a cell cycle-dependent manner (Izumi et al., 2001). In human cells, overexpression of Cdt1 leads to re-replication and polyploidy, and have been described in many cancers (Feng and Kipreos, 2003). It will be of interest to investigate whether the Rtt101p complex and their targets are involved in such function.

Recently, both Mms22p and Rtt101p were found to physically interact with H3 (Hht1p) and H4 (Hhf1p) (Krogan et al., 2006) (Figure 4.11). In addition, Mms22p interacts with H2B (Htb2p), while Rtt101p interacts with H2A (Hta2p) (Krogan et al., 2006), suggesting the core histones may be potential substrates. Dephosphorylation of H2A is necessary for efficient removal of the cell cycle checkpoint (Keogh et al., 2006), but H2A may also be regulated by degradation upon completion of DNA repair.

In addition to the candidate approach, unbiased target screening methods that have been described for substrate specificity factors should also be applicable for cullins, though the number of substrates for cullins may be greater than that for specificity factors. A preliminary screen was performed using a system described by Deanna Koepp (personal communication), in which an *ADE3*-gene fusion plasmid library was transformed in a strain lacking the gene of interest in the ubiquitin machinery (e.g. *RTT101*). The color of the yeast cells depends on the stability of the fusion protein. At the same time, a plasmid containing *RTT101* was transformed, but with no selection. This leads to loss of the *RTT101* plasmid in some cells during colony formation. The generation of sectored colonies indicates that the stability of the fusion protein is affected by the presence or absence of Rtt101p. Similarly, in a microscopic screening system described by David Toczyski (personal communication), a GFP-fusion protein signal was compared between *WT* and strains lacking the gene of interest. This method has successfully identified and confirmed substrates for the F-box protein Grr1p (David Toczyski, unpublished). Since the cullins in yeast do not seem to be functionally redundant based on their differences in phenotypes, substrate screening for Rtt101p will shed insight to its biological functions.

Table 4.1 Types DNA lesions generated by various DNA damaging agents

DNA damaging agent	**DNA lesion(s)**
Methyl methanesulfonate (MMS)	produces predominately 7-mehtylguanine and 3-methyladenine, which block DNA replication; as well as a small percentage of O6-methylguanine and O4-methylthymine, both of which cause base mispairing
Hydroxyurea (HU)	a ribonucleotide reductase inhibitor, inhibits DNA replication by depleting dNTPs
Camptothecin (CPT)	traps topoisomerase I (Top1) in the cleavage complex, causing single-stranded DNA (ssDNA) nicks that inhibit DNA replication and can be converted into double strand breaks (DSBs) by the advancing replication fork
Ultra-violet (UV) radiation	induces primarily cyclobutane pyrimidine dimers and photoproducts, which are efficiently targeted by the nucleotide excision repair (NER) pathway
4-nitroquinoline-1-oxide (4NQO)	a UV mimetic agent, introduces bulky DNA adducts that are also mainly removed by NER
Ionizing radiation (IR)	induces DSBs that are replication-independent

Table 4.2 List of yeast strains used in Chapter 4

Strain	Genotype	Reference
YKY90	*MATa/MATα ura3-52/ura3-52 trp1Δ-63/ trp1Δ-63 his3Δ-200/his3Δ-200 leu2Δ-1/ leu2Δ-1 ade2-101/ ade2-101 lys2-801/ lys2-801 CFIII(CEN3.L)-URA3 SUP11 mms22Δ::HIS3/ mms22Δ::HIS3*	This study
YKY570	*MATa/MATα ura3-52/ura3-52 trp1Δ-63/ trp1Δ-63 his3Δ-200/his3Δ-200 leu2Δ-1/ leu2Δ-1 ade2-101/ ade2-101 lys2-801/ lys2-801 CFIII(CEN3.L)-URA3 SUP11 rtt101Δ::TRP1/ rtt101Δ::TRP1*	This study
YKY332	*MATa/MATα ura3-52/ura3-52 trp1Δ-63/ trp1Δ-63 his3Δ-200/his3Δ-200 leu2Δ-1/ leu2Δ-1 ade2-101/ ade2-101 lys2-801/ lys2-801 CFIII(CEN3.L)-URA3 SUP11 rtt107Δ::TRP1/ rtt107Δ::TRP1*	This study
YPH499	*MATa ura3-52 trp1Δ-63 his3Δ-200 leu2Δ-1 ade2-101 lys2-801*	Hieter lab
YKY62	*MATα ura3-52 trp1Δ-63 his3Δ-200 leu2Δ-1 ade2-101 lys2-801 CFIII(CEN3.L)-URA3 SUP11 mms22Δ::HIS3*	This study
YKY64	*MATa ura3-52 trp1Δ-63 his3Δ-200 leu2Δ-1 ade2-101 lys2-801 mms22Δ::HIS3*	This study
YKY104	*MATα ura3-52 trp1Δ-63 his3Δ-200 leu2Δ-1 ade2-101 lys2-801 CFIII(CEN3.L)-URA3 SUP11 mms22Δ::HIS3 mad2Δ::HIS3*	This study
YKY108	*MATa ura3-52 trp1Δ-63 his3Δ-200 leu2Δ-1 ade2-101 lys2-801 CFIII(CEN3.L)-URA3 SUP11 mms22Δ::HIS3 rad9Δ::LEU2*	This study
YKY210	*MATa ura3 trp1Δ-63 his3 leu2Δ-1 mms22Δ::HIS3 mec3Δ::kanMX*	This study
YKY248	*MATa ura3 trp1Δ-63 his3 leu2Δ-1 mms22Δ::HIS3 mrc1Δ::kanMX*	This study
YKY249	*MATa ura3-52 trp1Δ-63 his3Δ-200 leu2Δ-1 ade2-101 lys2-801 pRS414-TRP1*	This study
YKY253	*MATa ura3-52 trp1Δ-63 his3Δ-200 leu2Δ-1 ade2-101 lys2-801 rad52Δ::LEU2 pRS414-TRP1*	This study
YKY256	*MATa ura3-52 trp1Δ-63 his3Δ-200 leu2Δ-1 ade2-101 lys2-801 mms22Δ::HIS3 pRS414-TRP1*	This study
YKY260	*MATa ura3-52 trp1Δ-63 his3Δ-200 leu2Δ-1 ade2-101 lys2-801 pJH132(pGAL-HO)-TRP1*	This study
YKY264	*MATa ura3-52 trp1Δ-63 his3Δ-200 leu2Δ-1 ade2-101 lys2-801 rad52Δ::LEU2 pJH132(pGAL-HO)-TRP1*	This study
YKY269	*MATa ura3-52 trp1Δ-63 his3Δ-200 leu2Δ-1 ade2-101 lys2-801 mms22Δ::HIS3 pJH132(pGAL-HO)-TRP1*	This study
YKY807	*MATa ade2-1 bar1::LEU2 trp1-1 LYS2 RAD5 RAD52-CFP ura3::3xURA3-tetOx112 I-Sce(ura3-1) his3-11,15::YFP-LacI-his3-x leu2-3,112::LacO-LEU2HO-iYCL018W(leu2-3,112) TetR-RFP(iYGL119W) pJH1320(pGAL-1SceI)-ADE2 URA3*	(Lisby et al., 2003)
YTK1364	*MATa ade2-1 bar1::LEU2 trp1-1 LYS2 RAD5 RAD52-CFP ura3::3xURA3-tetOx112 I-Sce(ura3-1) his3-11,15::YFP-LacI-his3-x leu2-3,112::LacO-LEU2HO-iYCL018W(leu2-3,112) TetR-RFP(iYGL119W) mms22Δ::kanMX pJH1320(pGAL-1SceI)-ADE2 URA3*	This study
YKY754 /MK203	*MATα-inc ade2 ade3::GALHO ura3::HOcs leu2-3,112 his3-11,13 trp1-1 lys2::ura3::HOcs-inc(RB)*	(Aylon et al., 2003)
YKY755	*MATα-inc ade2 ade3::GALHO ura3::HOcs leu2-3,112 his3-11,13 trp1-1 lys2::ura3::HOcs-inc(RB) rad52Δ::LEU2*	(Aylon et al., 2003)
YKY848	*MATα-inc ade2 ade3::GALHO ura3::HOcs leu2-3,112 his3-11,13 trp1-1 lys2::ura3::HOcs-inc(RB) mms22Δ::kanMX*	This study
YKY713	*MATa ura3-52 trp1Δ-63 his3Δ-200 leu2Δ-1 ade2-101 lys2-801 MMS22-13MYC::HIS3 RTT101-3HA::TRP1*	This study

YKY435	*MATa ura3-52 trp1Δ-63 his3Δ-200 leu2Δ-1 ade2-101 lys2-801 RTT101-3HA::TRP1*	This study
YKY721	*MATa ura3-52 trp1Δ-63 his3Δ-200 leu2Δ-1 ade2-101 lys2-801 MMS22-13MYC::HIS3 RTT107-3HA::TRP1*	This study
YKY461	*MATa ura3-52 trp1Δ-63 his3Δ-200 leu2Δ-1 ade2-101 lys2-801 RTT107-3HA::TRP1*	This study
YKY413	*MATa ura3-52 trp1Δ-63 his3Δ-200 leu2Δ-1 ade2-101 lys2-801 RTT101-13MYC:: TRP1*	This study
YKY447	*MATa ura3-52 trp1Δ-63 his3Δ-200 leu2Δ-1 ade2-101 lys2-801 RTT107-13MYC:: TRP1*	This study
YKY690	*MATa ura3-52 trp1Δ-63 his3Δ-200 leu2Δ-1 ade2-101 lys2-801 MMS22-13MYC:: HIS3*	This study
YTK1168	*MATa ura3-52 trp1Δ-63 his3Δ-200 leu2Δ-1 ade2-101 lys2-801 MMS1-3HA::kanMX RTT101-13MYC:: TRP1*	This study
YTK1132	*MATα ura3-52 trp1Δ-63 his3Δ-200 leu2Δ-1 ade2-101 lys2-801 MMS1-3HA::kanMX*	This study
YKY527	*MATa ura3-52 trp1Δ-63 his3Δ-200 leu2Δ-1 ade2-101 lys2-801 HIS3-pGAL-3HA-MMS22*	This study
YTK1140	*MATα ura3-52 trp1Δ-63 his3Δ-200 leu2Δ-1 ade2-101 lys2-801 MMS1-13MYC::kanMX*	This study
YTK1345	*MATa ura3-52 trp1Δ-63 his3Δ-200 leu2Δ-1 ade2-101 lys2-801 MMS1-13MYC::kanMX HIS3-pGAL-3HA-MMS22*	This study
YTK1375	*MATa ura3-52 trp1Δ-63 his3Δ-200 leu2Δ-1 ade2-101 lys2-801 MMS1-3HA::kanMX MMS22-13MYC::HIS3*	This study
YKY820	*MATa ura3-52 trp1Δ-63 his3Δ-200 leu2Δ-1 ade2-101 lys2-801 spc24-8::kanMX*	V. Measday
YKY821	*MATa ura3-52 trp1Δ-63 his3Δ-200 leu2Δ-1 ade2-101 lys2-801 spc24-9::kanMX*	V. Measday
YKY822	*MATa ura3-52 trp1Δ-63 his3Δ-200 leu2Δ-1 ade2-101 lys2-801 spc24-10::kanMX*	V. Measday
YKY824	*MATa ura3-52 trp1Δ-63 his3Δ-200 leu2Δ-1 ade2-101 lys2-801 spc24-8::kanMX mms22Δ::HIS3*	This study
YKY831	*MATa ura3-52 trp1Δ-63 his3Δ-200 leu2Δ-1 ade2-101 lys2-801 spc24-9::kanMX mms22Δ::HIS3*	This study
YKY836	*MATa ura3-52 trp1Δ-63 his3Δ-200 leu2Δ-1 ade2-101 lys2-801 spc24-10::kanMX mms22Δ::HIS3*	This study
YKY297	*MATa ura3-52 trp1Δ-63 his3Δ-200 leu2Δ-1 ade2-101 lys2-801 rtt101Δ::TRP1*	This study
YKY325	*MATa ura3-52 trp1Δ-63 his3Δ-200 leu2Δ-1 ade2-101 lys2-801 rtt107Δ::TRP1*	This study
YKY657	*MATa ura3-52 trp1Δ-63 his3Δ-200 leu2Δ-1 ade2-101 lys2-801 rtt101Δ::TRP1 mms22Δ::HIS3*	This study
YKY642	*MATa ura3-52 trp1Δ-63 his3Δ-200 leu2Δ-1 ade2-101 lys2-801 rtt107Δ::TRP1 mms22Δ::HIS3*	This study
YKY648	*MATa ura3-52 trp1Δ-63 his3Δ-200 leu2Δ-1 ade2-101 lys2-801 rtt107Δ::TRP1 rtt101Δ::kanMX*	This study
YKY767	*MATa ura3-52 trp1Δ-63 his3Δ-200 leu2Δ-1 ade2-101 lys2-801 MMS22-13MYC::HIS3 rtt101Δ::TRP1*	This study
YKY956	*MATa ura3-52 trp1Δ-63 his3Δ-200 leu2Δ-1 ade2-101 lys2-801 MMS22-*	This study

	13MYC::HIS3 rtt101Δ::TRP1 pYES-RTT101-URA3	
YKY956	*MATa ura3-52 trp1Δ-63 his3Δ-200 leu2Δ-1 ade2-101 lys2-801 MMS22-13MYC::HIS3 rtt101Δ::TRP1 pYES-rtt101-K791R-URA3*	This study
YKY782	*MATa ura3-52 trp1Δ-63 his3Δ-200 leu2Δ-1 ade2-101 lys2-801 HIS3-pGAL-3HA-MMS22 rtt101Δ::TRP1*	This study

Table 4.3 Quantification of chromosome loss (CL), non-disjunction (NDJ) and chromosome gain (CG) by half-sectored assay

Strain	Total no. colonies counted	No. pink-red colonies	CL freq. (fold over *WT*)	No. white-red colonies	NDJ freq. (fold over *WT*)	No. pink-white colonies	CG freq.
WT diploid	N/A	N/A	8.7E-5 (Shero et al., 1991)	N/A	8.7E-5 (Shero et al., 1991)	N/A	N/A
mms22Δ / *mms22Δ*	11890	36	3.0E-3 (35X)	4	3.4E-4 (4X)	3	2.5E-4
rtt101Δ / *rtt101Δ*	14600	40	2.7E-3 (31X)	32	2.2E-3 (25X)	93	6.4E-3
rtt107Δ / *rtt107Δ*	17730	40	2.7E-3 (26X)	16	9.0E-4 (10X)	52	2.9E-3

Figure 4.1 DNA damage and repair mechanisms (reprinted from (Hoeijmakers, 2001) Genome maintenance mechanisms for preventing cancer, *Nature*, **411**, 366-374, Copyright 2001, with permission from Macmillan Publishers Ltd)

Common DNA damaging agents (top); examples of DNA lesions induced by these agents (middle); and most relevant DNA repair mechanism responsible for the removal of the lesions (bottom). (6-4)PP and CPT, 6-4 photoproduct and cyclobutane pyrimidine dimer, respectively (both induced by UV light); EJ, end joining.

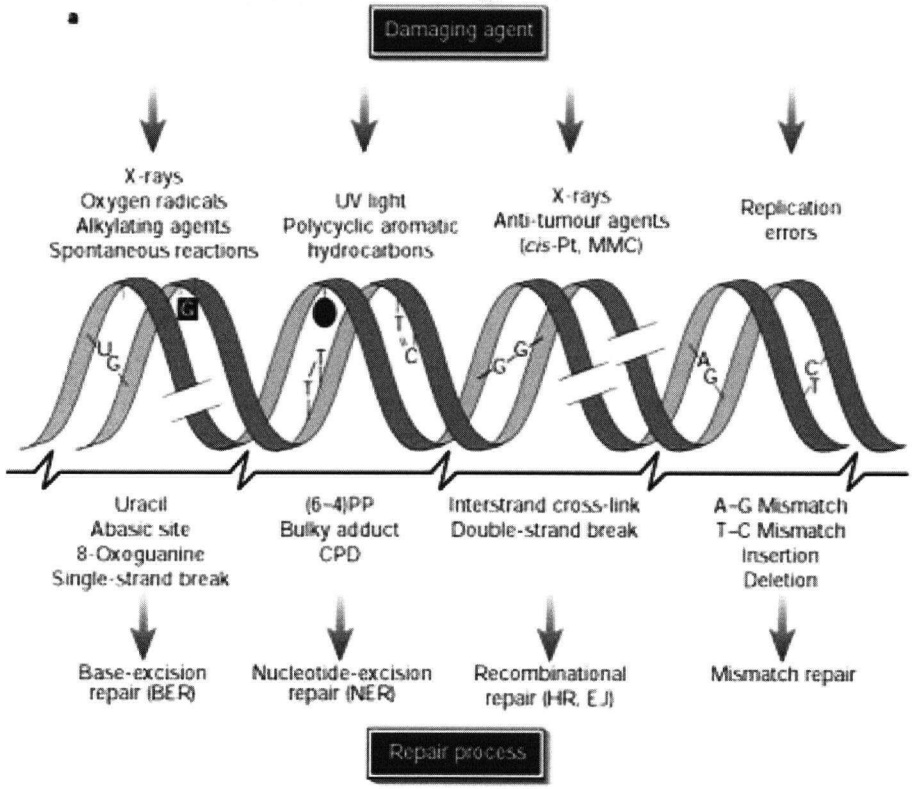

Figure 4.2 Two-dimensional hierarchical clustering of drugs (horizontal) and yeast deletion mutants (vertical) that show sensitivity to at least 1 drug based on genome-wide drug sensitivity screens, and overlaid with the CIN screen results. The clustering was performed using the program Cluster 3.0 and displayed in Java TreeView (version 1.0.8) (Eisen et al., 1998).

A. An overview of all deletion mutants and drugs. The severity of drug sensitivity is indicated by color, with bright red indicating high sensitivity, darker red showing milder sensitivity, and black representing the same sensitivity as wild-type. A positive phenotype in the CTF, BiM and ALF screen is indicated by orange, yellow and green, respectively. The benomyl sensitive cluster is highlighted in lime color, and the DNA damaging sensitive cluster is highlighted in light orange.
B. Magnification of the benomyl sensitive cluster.
C. Magnification of the DNA damaging sensitive cluster. *MMS22*, *MMS1*, *RTT101* and *RTT107* are highlighted in purple, and the MRX complex components are highlighted in green.

Figure 4.2
A.

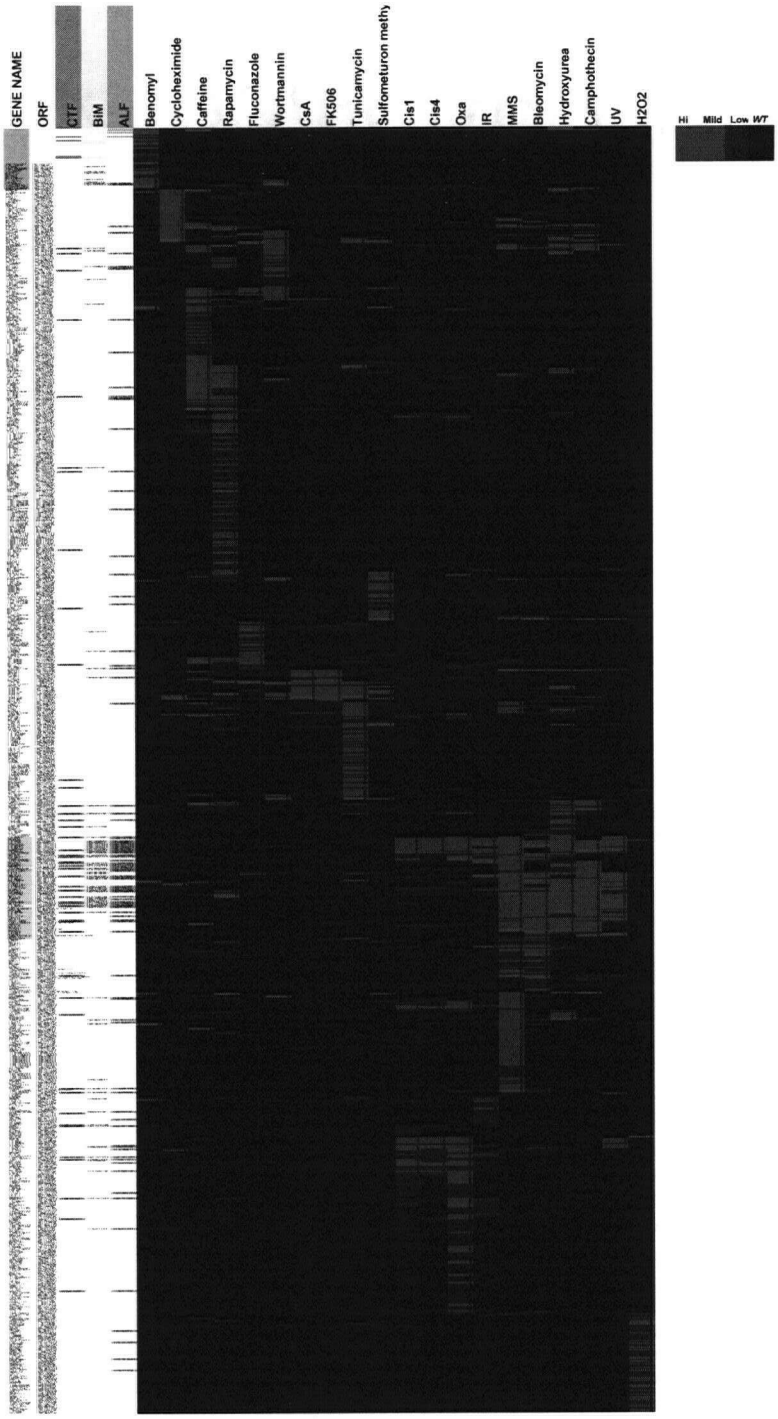
GENE NAME
ORF
CTF
BIM
ALF
Benomyl
Cycloheximide
Caffeine
Rapamycin
Fluconazole
Wortmannin
CsA
FK506
Tunicamycin
Sulfometuron methy
Cis1
Cis4
Oxa
IR
MMS
Bleomycin
Hydroxyurea
Camphothecin
UV
H2O2
Hi
Mild
Low
WT

B.

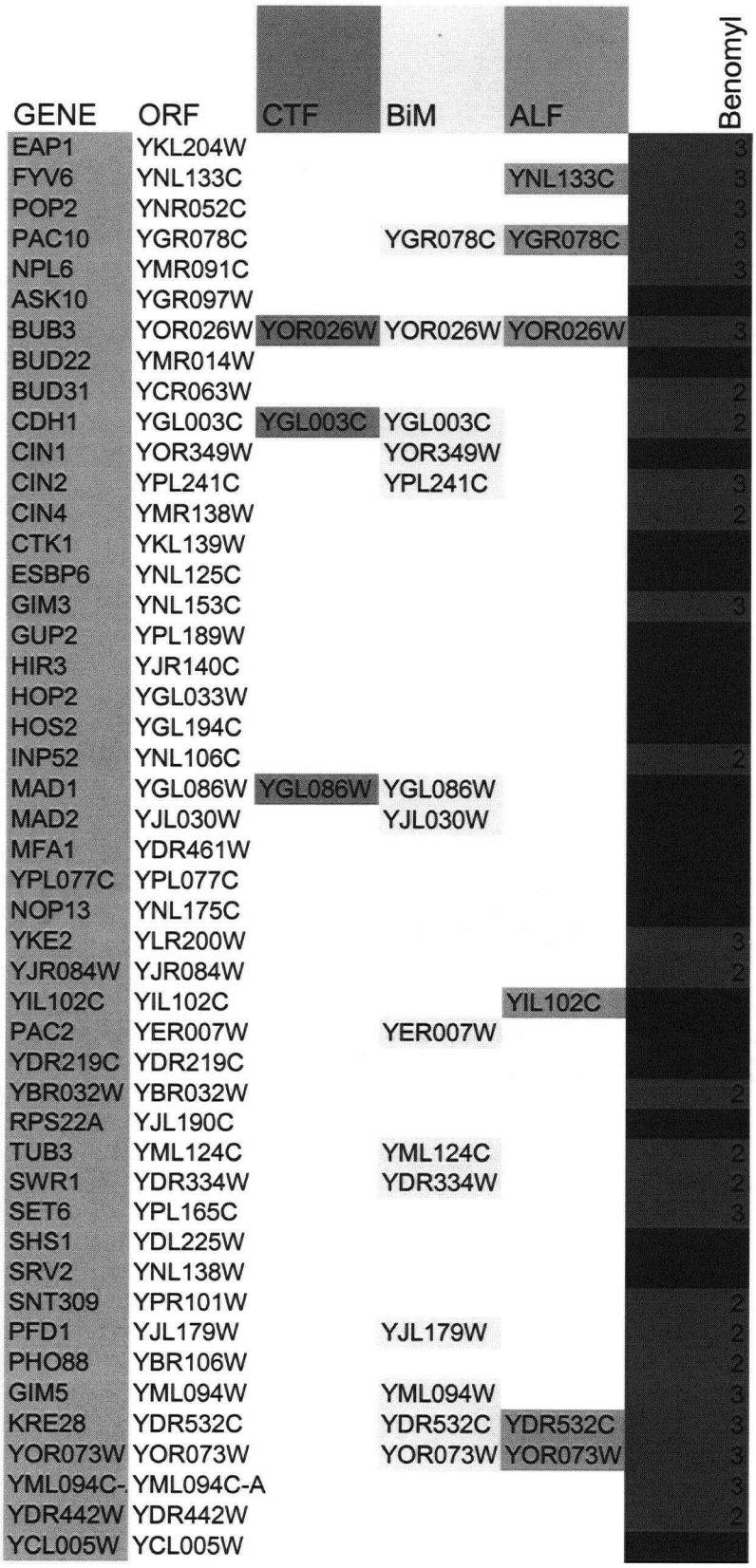
GENE
ORF
CTF
BiM
ALF
Benomyl
EAP1 YKL204W 3
FYV6 YNL133C YNL133C 3
POP2 YNR052C 3
PAC10 YGR078C YGR078C YGR078C 3
NPL6 YMR091C 3
ASK10 YGR097W
BUB3 YOR026W YOR026W YOR026W YOR026W 3
BUD22 YMR014W
BUD31 YCR063W 2
CDH1 YGL003C YGL003C YGL003C 2
CIN1 YOR349W YOR349W
CIN2 YPL241C YPL241C 3
CIN4 YMR138W 2
CTK1 YKL139W
ESBP6 YNL125C
GIM3 YNL153C 3
GUP2 YPL189W
HIR3 YJR140C
HOP2 YGL033W
HOS2 YGL194C
INP52 YNL106C 2
MAD1 YGL086W YGL086W YGL086W
MAD2 YJL030W YJL030W
MFA1 YDR461W
YPL077C YPL077C
NOP13 YNL175C
YKE2 YLR200W 3
YJR084W YJR084W 2
YIL102C YIL102C YIL102C
PAC2 YER007W YER007W
YDR219C YDR219C
YBR032W YBR032W 2
RPS22A YJL190C
TUB3 YML124C YML124C 2
SWR1 YDR334W YDR334W 2
SET6 YPL165C 3
SHS1 YDL225W
SRV2 YNL138W
SNT309 YPR101W 2
PFD1 YJL179W YJL179W 2
PHO88 YBR106W 2
GIM5 YML094W YML094W 3
KRE28 YDR532C YDR532C YDR532C 3
YOR073W YOR073W YOR073W YOR073W 3
YML094C-. YML094C-A 3
YDR442W YDR442W 2
YCL005W YCL005W

C.

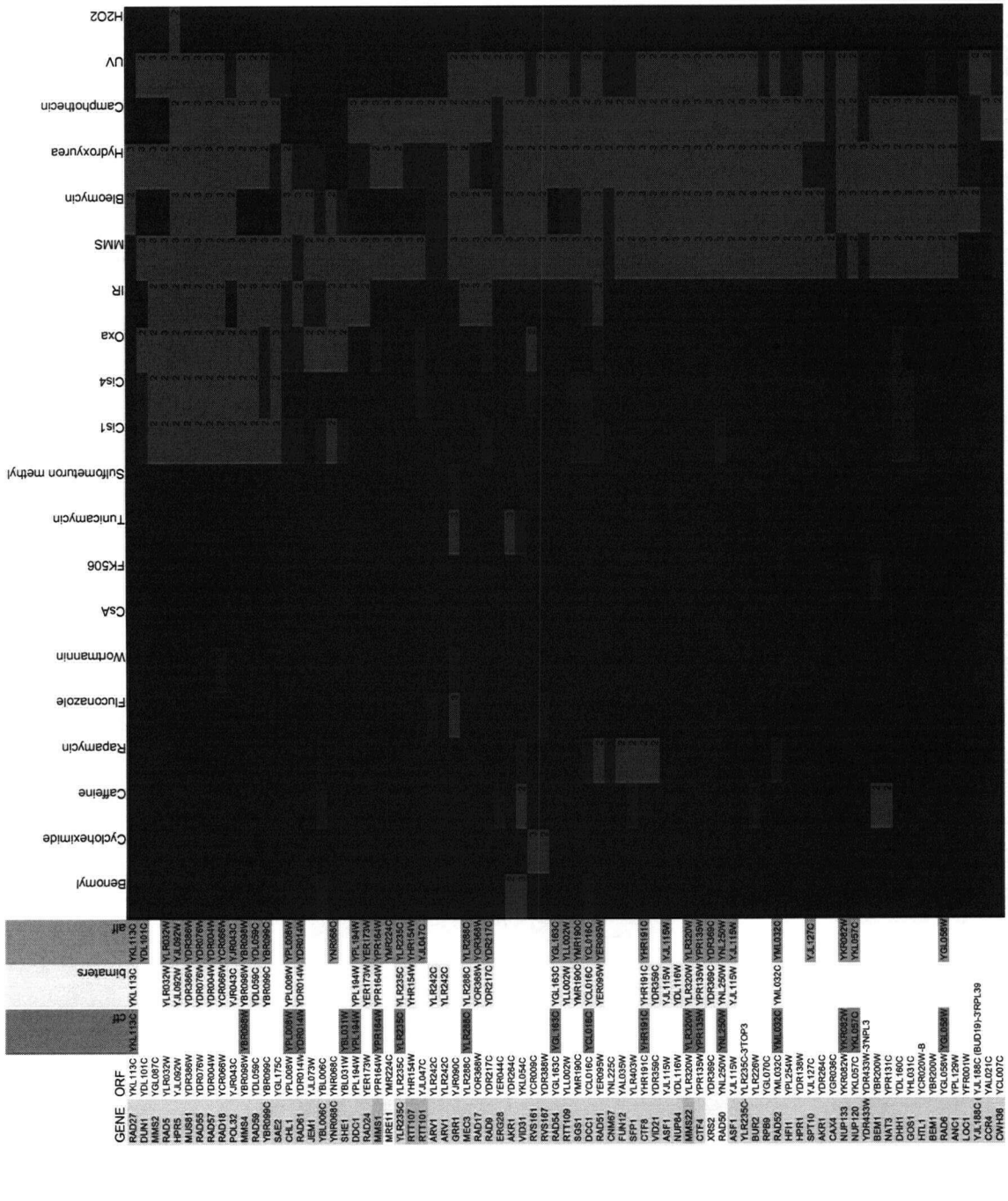
GENE
ORF
tf
bimaters
alf
Benomyl
Cycloheximide
Caffeine
Rapamycin
Fluconazole
Wortmannin
CsA
FK506
Tunicamycin
Sulfometuron methyl
Cis1
Cis4
Oxa
IR
MMS
Bleomycin
Hydroxyurea
Camphothecin
UV
H2O2

Figure 4.3 Cell cycle and morphology defects of *mms22Δ*

A. FACS analysis of *WT* haploid, *mms22Δ*, *mms22Δ mad2Δ*, *mms22Δ rad9Δ*, *mms22Δ mec3Δ*, and *mms22Δ mrc1Δ* cells in logarithmic growth. 1N and 2N DNA contents, corresponding to unreplicated and replicated DNA amount in haploid cells, respectively, are indicated.

B. Budding index of logarithmic growing *WT* haploid and *mms22Δ* cells. n equals the number of cells counted.

C. FACS analysis of *WT* and *mms22Δ* cells in logarithmic growth, synchronized by α-factor block (G1 arrest) and release. After 80 min release from alpha-factor (as indicated by the arrow), a majority of both *WT* and *mms22Δ* cells have undergone replication. After 120 min release from alpha-factor (as indicated by the dashed arrow), a portion of WT cells have gone through mitosis and return to G1, whereas most of *mms22Δ* cells still accumulate at G2M with 2N DNA content.

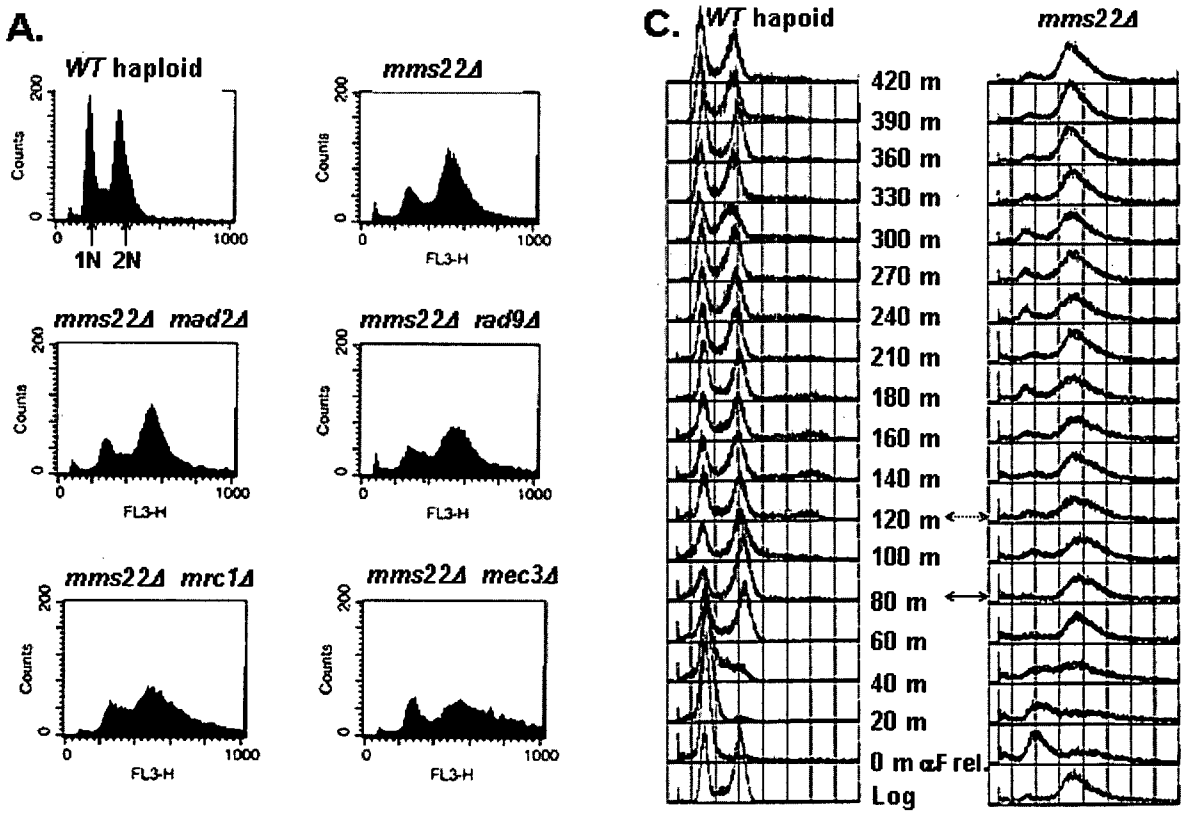

B.

									n
WT haploid	38%	23%	5%	3%	5%	27%	1%	0%	220
mms22Δ	15%	18%	8%	18%	11%	22%	4%	5%	473

Figure 4.4 Defects of *mms22Δ* in double-strand breaks

A. Survival rate of *WT*, *mms22Δ*, and *rad52Δ* in HO-induced DSB.

B. Colony size and number of *WT*, *mms22Δ* in HO-induced DSB, compared to empty vector control (pRS414) on galactose (after 6 days at 30°C).

C. A schematics of chromosome IV (the black line with the centromere represented by a circle) in the tested strains was shown. Adjacent to the I-SceI cut site (I-SceIcs, the black triangle), an array of 336 tetO (336xtetO, the red rectangles) was inserted. The tested strains also contain a plasmid encoding a galactose inducible I-SceI endonuclease, a Rad52-CFP fusion protein, and tet-repressor fused to RFP (tetR-RFP) which binds to the tetO array, indicating the cut site. An example image of Rad52p-CFP foci (top left panel) and tetR-RFP (top right panel) colocalizing (bottom left panel, arrows) was shown. The corresponding differential interference contrast (DIC) image was shown as well.

D. Percentage of cells with Rad52p foci in *WT*, *mms22Δ* in unperturbed condition, I-SceI-induced DSB, and 0.1% MMS.

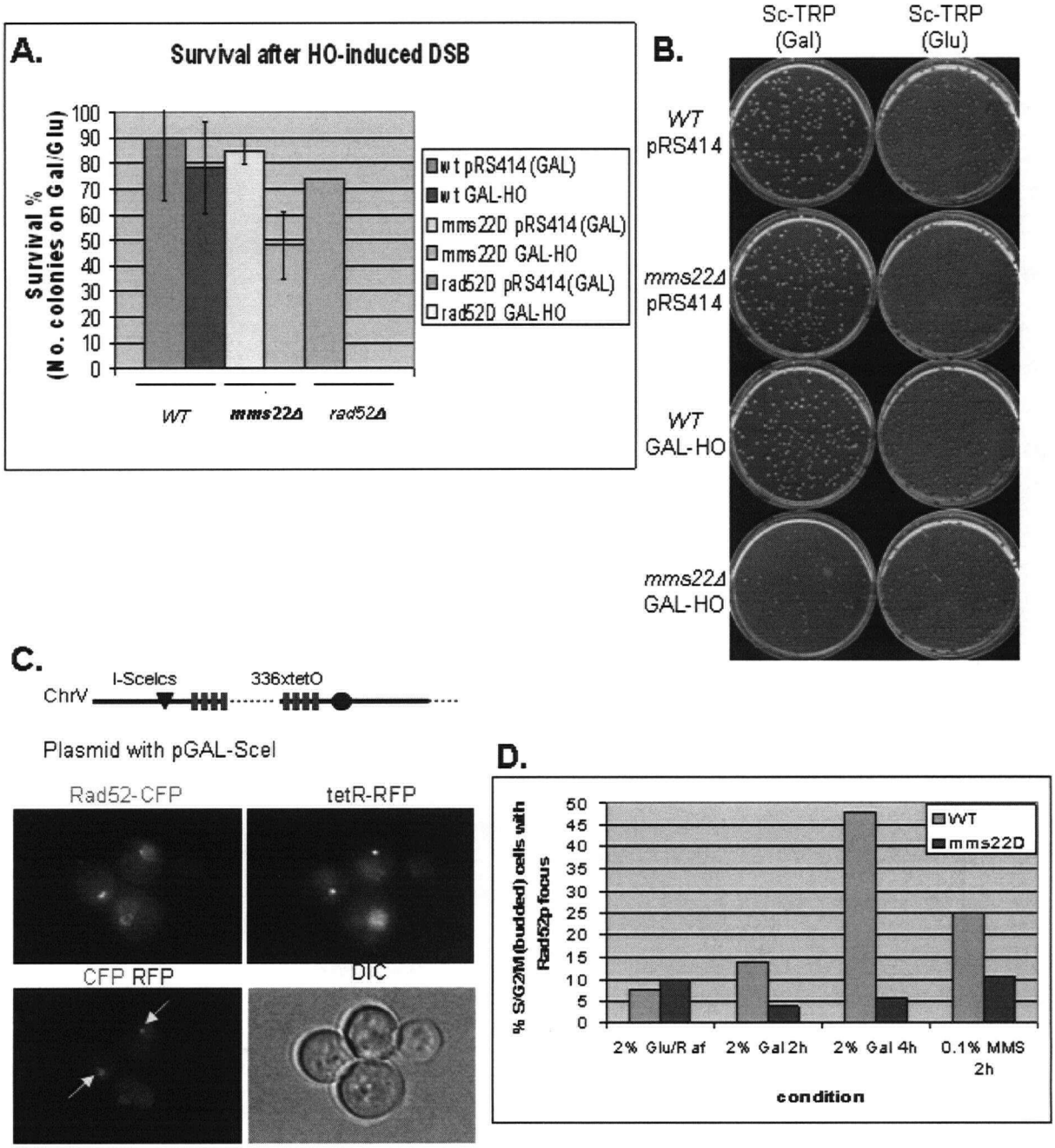

Figure 4.5 Kinetics of DSB repair

A. Schematic diagram of experimental set up reproduced from (Aylon et al., 2003). Open rectangles represent the *ura3* alleles on chromosome II and V. A black box represents the *HOcs*; a gray box depicts the inactive *HOcs-inc* flanked by the *Bam*HI (B) and *Eco*RI (R) restriction sites. These polymorphisms are used to monitor the transfer of information between the chromosomes. The HO gene is under transcriptional control of the GAL1 promoter, and induction results in gene conversion.

B. Southern blot analysis of DNA extracted at different times after transfer to galactose-containing medium. The DNA was digested with *Cla*I and probed with a fragment of chromosome V carrying the *URA3* gene. The % of DSB is quantified and normalized with the standard.

C. Equal amounts of PCR product of the chromosome V region was digested with *Bam*HI and subjected to gel electrophoresis. The extent of gene conversion (GC) is measured by the relative amounts of intact chromosome V containing the *Bam*HI restriction site.

Figure 4.5

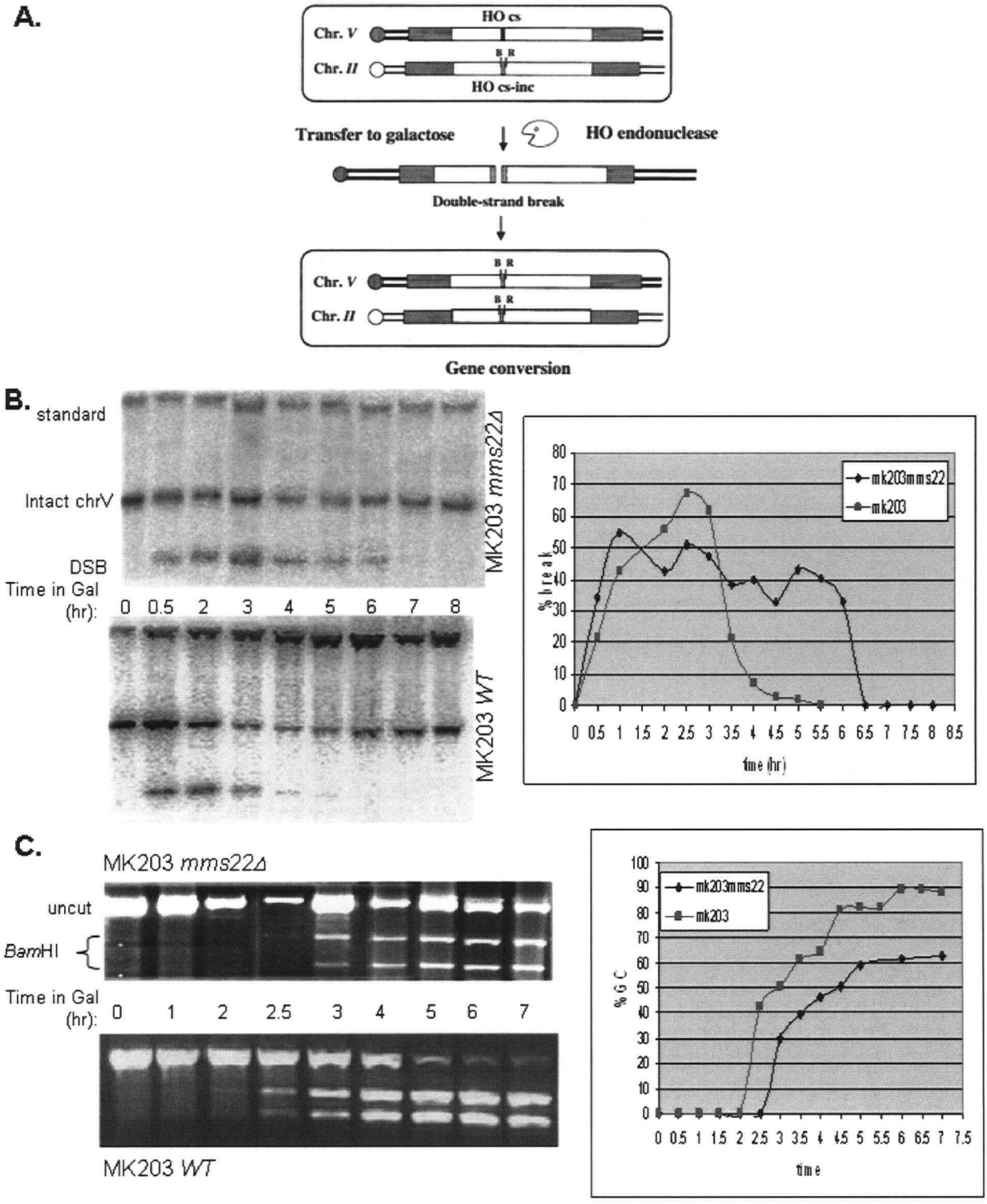
A.
HO cs
Chr. V
B R
Chr. II
HO cs-inc
Transfer to galactose
HO endonuclease
Double-strand break
Chr. V
Chr. II
Gene conversion
B.
standard
Intact chrV
DSB
Time in Gal (hr):
0 0.5 2 3 4 5 6 7 8
MK203 mms22Δ
MK203 WT
mk203mms22
mk203
% break
time (hr)
C.
MK203 mms22Δ
uncut
BamHI
Time in Gal (hr):
0 1 2 2.5 3 4 5 6 7
MK203 WT
mk203mms22
mk203
% G C
time

Figure 4.6 Mms22p co-immunoprecipitates with Rtt101p and Rtt107p

A. Anti-MYC immunoprecipitation using 9E10 affinity matrix (Covance) and anti-HA immunoprecipitation using HA.11 affinity matrix (Covance) were performed in untagged strain and strains containing Mms22p-MYC only, Rtt101p-HA only, and both tagged proteins. The tags were fused to the C-terminus of the proteins and expressed from endogenous promoters. The strains were grown to log phase and lysed. Whole-cell lysates (total) and equal amounts of immunoprecipitates from the 4 strains were loaded on SDS-PAGE gels. Anti-MYC antibodies (9E10, Convance) and anti-HA antibodies (12CA5, Boehringer Mannheim) were used for Western blot analysis.

B. Anti-MYC and anti-HA immunoprecipitations were performed as in A in untagged strain and strains containing Mms22p-MYC only, Rtt107p-HA only, and both tagged proteins.

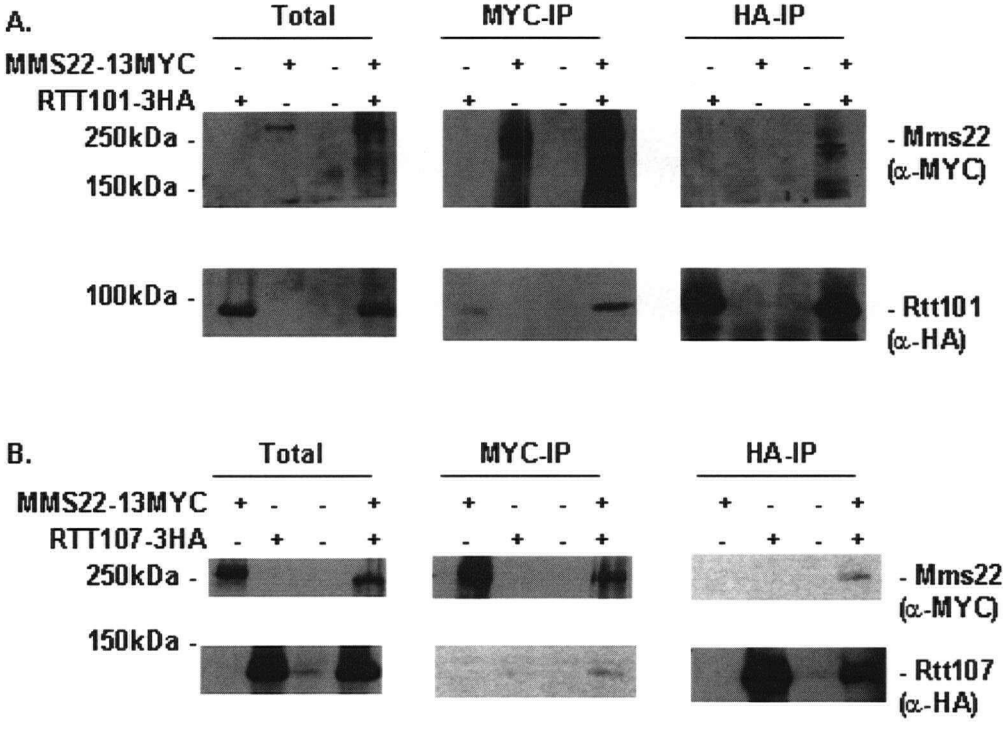

Figure 4.7 Physical interaction of Rtt101p with Mms1p

A. MS analysis of Rtt101p immunoprecipitates. The experiment was performed in duplicates, and only proteins identified reproducibly in both analyses are shown. However, the peptide sequence, the number of peptides, and the peptide score of identified protein may vary in the two independent experiments. The peptides and score shown are obtained from one of the two experiments. Common false positives are not shown.

B. Anti-MYC and anti-HA immunoprecipitations were performed as in figure 4.6, in untagged strain and strains containing Mms1p-MYC only, Rtt101p-HA only, and both tagged proteins.

A.

Prey ORF	Prey Name	Different Peptides Identified	Peptide Prophet Score	Description
YPR164W	MMS1	K.IELQALEEIQQK.H	1	Protein likely involved in protection against replication-dependent DNA damage
		K.IELQALEEIQQK.H	0.96	
		R.LGINQSNTESSLIFATDAVSNNR.I	1	
		Y.NAVALDKPIQDISYDPAVQTLY.V	0.4736	
		K.SISPLPSNPINLDSR.S	0.9972	
		R.LSPYNAVALDKPIQDISYDPAVQTLY.V	0.2537	
YJL047C	RTT101	R.DIDNTYSINESFKPDMK.K	0.9917	Cullin subunit of a Roc1p-dependent E3 ubiquitin ligase complex
		K.DLALVLK.S	0.922	
		K.YLNENLPILR.L	0.9214	
		R.LFDEVVQLANVDHLK.I	0.9998	
YDR028C	REG1	R.IVNNTPSPAEVGASDVAIEGYFSPR.N	0.9999	Regulatory subunit of type 1 protein phosphatase Glc7p

B.

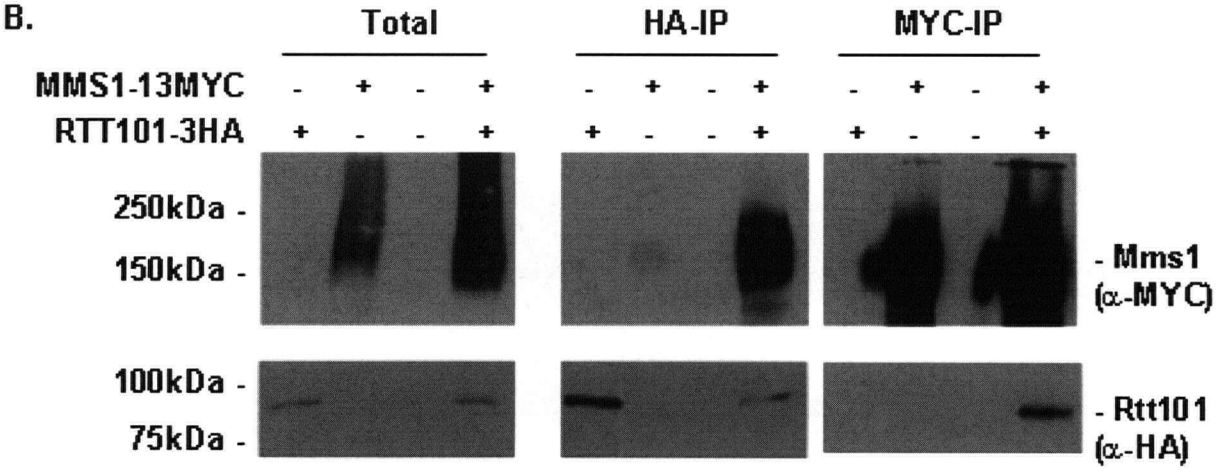

Figure 4.8 Yeast-two-hybrid interactions using bait protein: (A) Mms22p, (B) Rtt101p, and (C) Rtt107p. Out of the 2 genome-wide screens and the retest, only genes identified at least 2 times are shown. (D) Examples of miniarrays in retest. Each strain contains a different pOAD-fusion protein. The interactors are indicated in yellow. A strain with just the pOAD is used as a negative control. MIG1 is a common false positive.

A. pOBD2-MMS22

No. times id.	ORF	Name	GO Biological Process
3	YER180C	ISC10	sporulation
3	YER127W	LCP5	rRNA modification
3	YCL032W	STE50	signal transduction during conjugation with cellular fusion
3	YKL075C		unknown
3	YIL150C	MCM10	DNA replication initiation
3	YJL047C	RTT101	ubiquitin-dependent protein catabolism
3	YDR026C		unknown
3	YPR164W	MMS1	DNA repair
3	YLR320W	MMS22	double-strand break repair
2	YER029C	SMB1	nuclear mRNA splicing, via spliceosome
2	YOL091W	SPO21	meiosis
2	YPR135W	CTF4	DNA repair

B. pOBD2-RTT101

No. times id.	ORF	Name	GO Biological Process
2	YIL105C	LIT2	actin cytoskeleton organization and biogenesis
1 (at retest)	YLR320W	MMS22	double-strand break repair

C. pOBD2-RTT107

No. times id.	ORF	Name	GO Biological Process
3	YLR320W	MMS22	double-strand break repair
2	YLR135W	SLX4	DNA replication

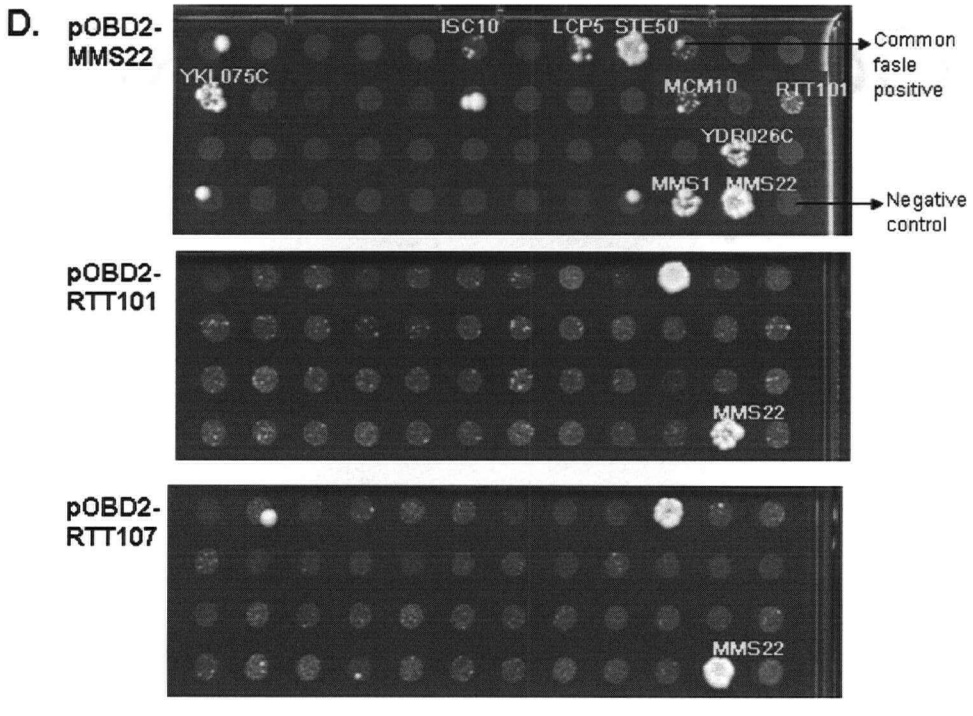

Figure 4.9 Physical interactions of Mms22p with Mms1p

A. Anti-MYC and anti-HA immunoprecipitations were performed as in figure 4.6, in untagged strain and strains containing endogenously expressed Mms1p-MYC only, HA-Mms22p expressed from the GAL1 promoter only, and both tagged proteins. Lysates were prepared from cultures in log phase grown in galactose-containing media.

B. Anti-MYC and anti-HA immunoprecipitations were performed as in figure 4.6, in untagged strain and strains containing endogenously expressed Mms22p-MYC only, endogenously expressed Mms1p-HA only, and both tagged proteins.

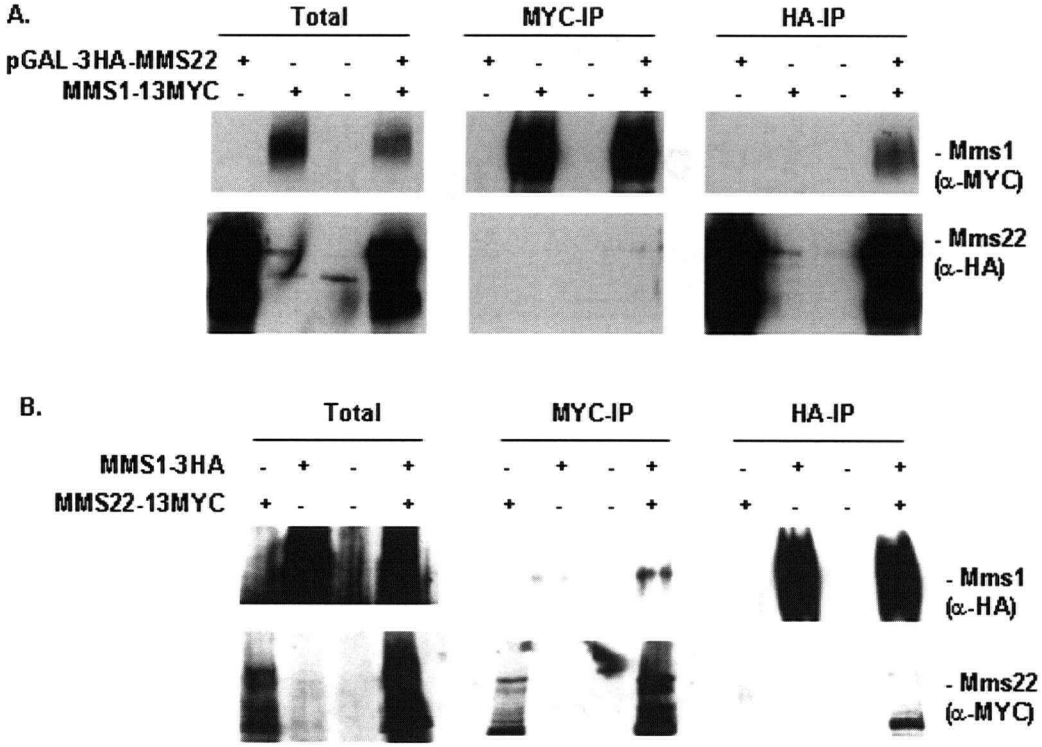

Figure 4.10 Genetic interactions of *mms22Δ* mutants

A. Synthetic lethal interactions of *mms22Δ* with *spc24-9* and *spc24-10* at 33°C. Three temperature-sensitive alleles of *SPC24* (non-permissive temperature is 37°C), *mms22Δ*, and 2 isolates of each double mutants were streaked on YPD plates and inoculated at 33°C.

B. MMS and HU sensitivity of single, double and triple mutants of *MMS22*, *RTT101* and *RTT107* were analyzed by serial dilutions on YPD, 0.01% MMS and 0.05M HU plates. *mec1Δ* is a positive control.

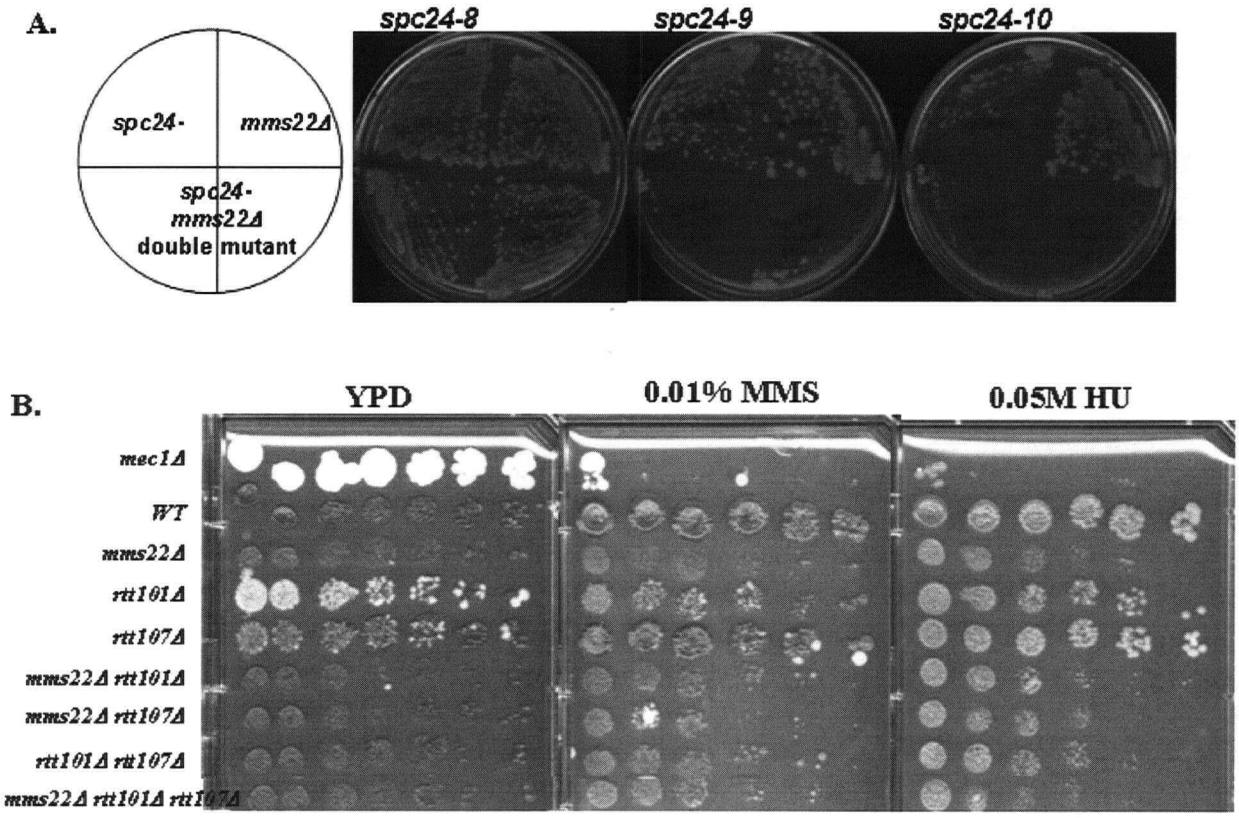

Figure 4.11 Interaction network of *MMS22*, *MMS1*, *RTT101* and *RTT107*

A. Physical interactions obtained from the literature and this study are displayed using OSPREY. Only interactions with the 4 genes (shown in blue fonts) are shown. The color of the nodes indicates the GO biological process, and the color of the edges represents the type of interaction with the arrow pointing from the bait to the prey.

B. Genetic interactions shown as in A.

Figure 4.11

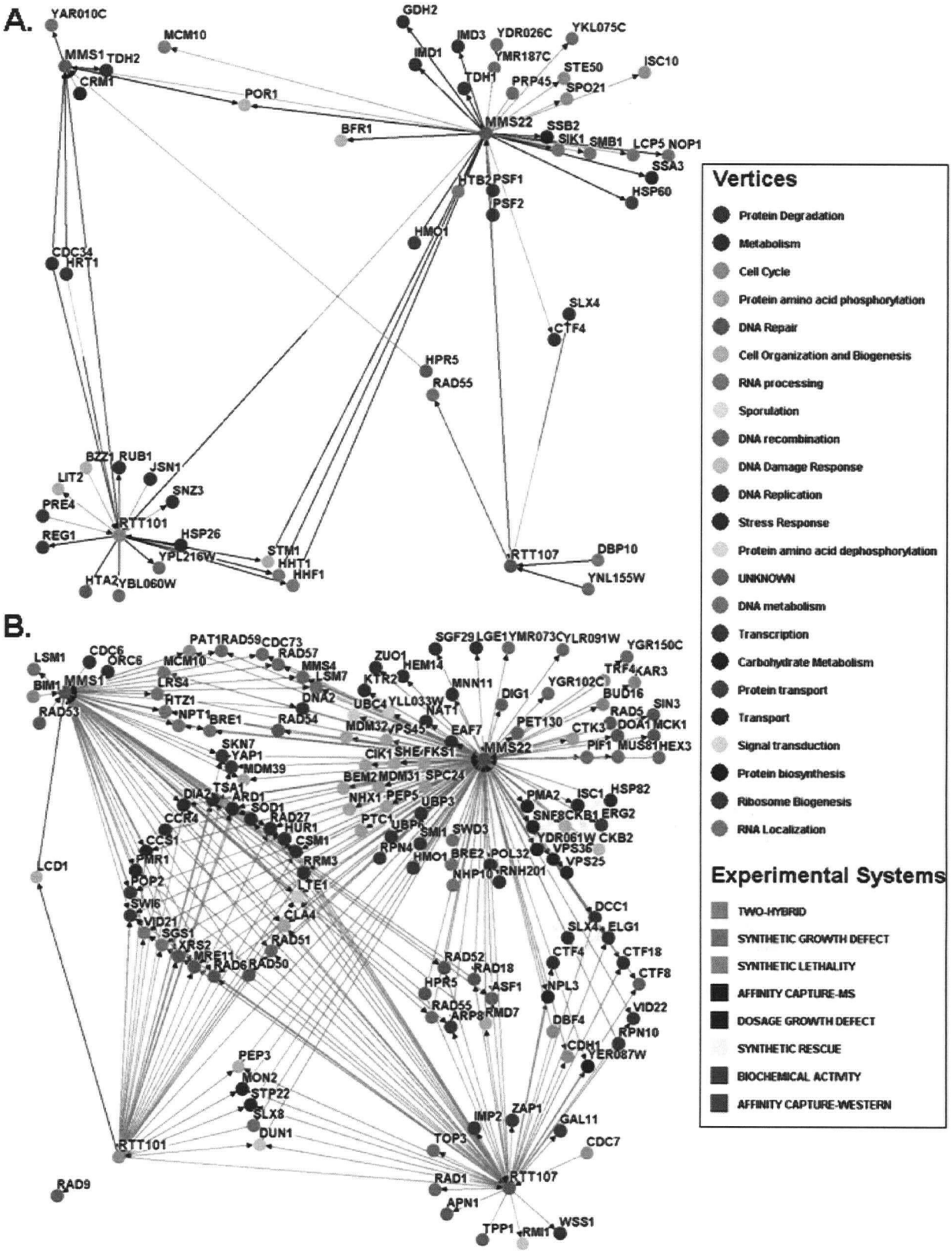
A.
YAR010C
MCM10
GDH2
IMD3
YDR026C
YKL075C
MMS1
TDH2
IMD1
YMR187C
ISC10
CRM1
TDH1
STE50
PRP45
SPO21
POR1
MMS22
SSB2
BFR1
SIK1
SMB1
LCP5
NOP1
SSA3
HTB2
PSF1
HSP60
PSF2
HMO1
CDC34
HRT1
SLX4
CTF4
HPR5
RAD55
BZZ1
RUB1
JSN1
LIT2
SNZ3
PRE4
RTT101
REG1
HSP26
YPL216W
STM1
HHT1
HHF1
HTA2
YBL060W
RTT107
DBP10
YNL155W
B.
PAT1
RAD59
CDC73
SGF29
LGE1
YMR073C
YLR091W
YGR150C
LSM1
CDC6
ORC6
MCM10
RAD57
ZUO1
HEM14
MMS4
LSM7
KTR2
MNN11
TRF4
KAR3
BIM1
MMS1
LRS4
DNA2
UBC4
YLL033W
NAT1
DIG1
YGR102C
BUD16
RAD5
SIN3
RAD53
RTZ1
NPT1
BRE1
RAD54
MDM32
PS45
EAF7
PET130
CTK3
DOA1
MCK1
SKN7
YAP1
CIK1
SHE4
FKS1
MMS22
PIF1
MUS81
HEX3
MDM39
BEM2
MDM31
SPC24
TSA1
DIA2
ARD1
NHX1
PEP5
UBP3
PMA2
ISC1
HSP82
SOD1
SNF8
CKB1
ERG2
CCR4
RAD27
PTC1
UBP6
SMI1
SWD3
YDR061W
CKB2
HUR1
CSM1
RPN4
BRE2
POL32
VPS36
CCS1
HMO1
VPS25
PMR1
RRM3
NHP10
RNH201
LCD1
POP2
LTE1
SWI6
CLA4
DCC1
VID21
SLX4
ELG1
SGS1
RAD51
CTF4
CTF18
XRS2
RAD52
RAD18
MRE11
RAD6
RAD50
CTF8
HPR5
ASF1
NPL3
RAD55
ARP8
RMD7
VID22
DBF4
RPN10
CDH1
YER087W
PEP3
MON2
STP22
SLX8
IMP2
ZAP1
GAL11
DUN1
TOP3
CDC7
RTT101
RAD1
RTT107
RAD9
APN1
WSS1
TPP1
RMI1
Vertices
Protein Degradation
Metabolism
Cell Cycle
Protein amino acid phosphorylation
DNA Repair
Cell Organization and Biogenesis
RNA processing
Sporulation
DNA recombination
DNA Damage Response
DNA Replication
Stress Response
Protein amino acid dephosphorylation
UNKNOWN
DNA metabolism
Transcription
Carbohydrate Metabolism
Protein transport
Transport
Signal transduction
Protein biosynthesis
Ribosome Biogenesis
RNA Localization
Experimental Systems
TWO-HYBRID
SYNTHETIC GROWTH DEFECT
SYNTHETIC LETHALITY
AFFINITY CAPTURE-MS
DOSAGE GROWTH DEFECT
SYNTHETIC RESCUE
BIOCHEMICAL ACTIVITY
AFFINITY CAPTURE-WESTERN

Figure 4.12 Mms22p expression is regulated by Rtt101p

A. The level of endogenously expressed Mms22p-MYC was analyzed in *WT*, *rtt101Δ* and *rtt101Δ mms1Δ* in logarithmic growth. Equal amounts of lysates were loaded on SDS-PAGE gel, and anti-MYC antibodies (9E10) were used in Western blot to detect Mms22p-MYC. Two different exposure times are shown. Polyclonal anti-NDC10 antibodies (from Benjamin Cheng and Phil Hieter, unpublished data) were used to detect Ndc10p, a loading control.

B. Gal shut-off chase experiment of pGal1-HA-Mms22p in *WT* and *rtt101Δ*. Cultures were grown to log phase in media containing 2% raffinose. 2% galactose was then added to the cultures. After 3 hours in galactose, the cultures were washed and release into media with 2% glucose. Western blot was performed as in A using anti-HA (12CA5) and anti-NDC10. Ndc10p expression level was used as a loading control to normalize Mms22p level. The normalized Mms22p level (Mms22p/Ndc10p) in the 2 strains is plotted against time and a logarithmic trendline representing the degradation rate is shown.

Figure 4.12

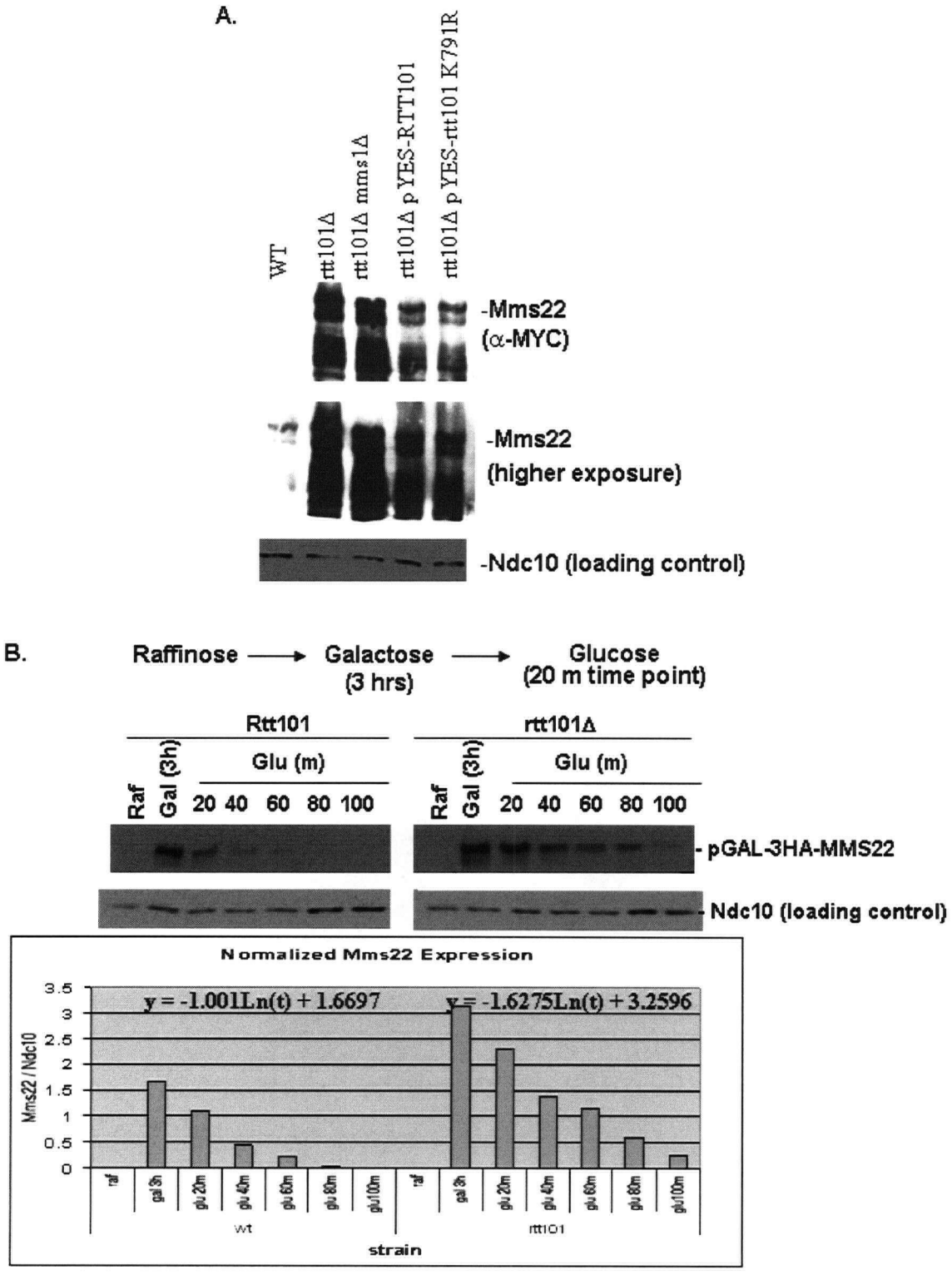
A.
WT
rtt101Δ
rtt101Δ mms1Δ
rtt101Δ pYES-RTT101
rtt101Δ pYES-rtt101 K791R
-Mms22
(α-MYC)
-Mms22
(higher exposure)
-Ndc10 (loading control)
B.
Raffinose
Galactose
(3 hrs)
Glucose
(20 m time point)
Rtt101
rtt101Δ
Raf
Gal (3h)
Glu (m)
20 40 60 80 100
- pGAL-3HA-MMS22
- Ndc10 (loading control)
Normalized Mms22 Expression
y = -1.001Ln(t) + 1.6697
y = -1.6275Ln(t) + 3.2596
Mms22 / Ndc10
3.5
3
2.5
2
1.5
1
0.5
0
raf
gal3h
glu20m
glu40m
glu60m
glu80m
glu100m
wt
rtt101
strain

Figure 4.13 Cell cycle expression of Rtt101p

Cells are arrested in G1 phase by α-factor, S phase by HU, and M phase by nocodazole, and the corresponding FACS analyses are shown. Protein expression of Rtt101p-HA is analyzed, using Ndc10p as a loading control. A slower migrating form of Rtt101p-HA was shown in HU and nocodazole arrested cells (indicated by *).

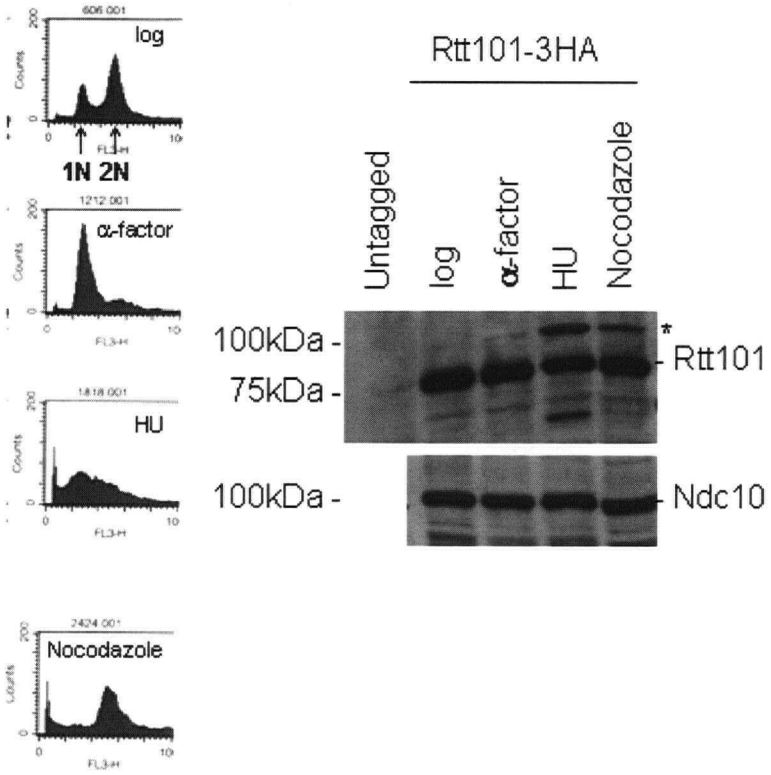

CHAPTER 5

Conclusions
and
Future Directions

5.1 Conclusions

During each cell cycle, accurate transmission of chromosomes to daughter cells is crucial to the maintenance of genetic information in an organism. Failure to do so can be detrimental. Chromosome instability is commonly observed in cancers, and has been proposed to underlie tumorigenesis.

To better understand the cellular mechanisms used to maintain chromosome stability, it is necessary to identify genes required for the various processes involved. Since genes involved in basic cellular mechanisms are often conserved throughout eukaryotes, model organisms have been effectively utilized to study these processes. In Chapter 2, I presented a systematic examination of all non-essential gene deletion mutants in the budding yeast *Saccharomyces cerevisiae* to screen for mutants with a CIN phenotype using 3 complementary chromosome marker loss assays. The chromosome transmission fidelity (CTF) assay monitors loss of an artificial chromosome fragment by a colony color-sectoring readout. The bimater (BiM) assay monitors loss of heterozygosity at the mating type locus in homozygous diploid deletion mutants using a mating test. The a-like faker (ALF) assay detects loss of the *MATα* mating type locus in haploid deletion mutants by a mating test. The 3 screens identified an overlapping and unique set of genes. In total, 293 CIN mutants were identified, including genes already known to function in the maintenance of chromosome integrity, and genes not previously known to be important for chromosome maintenance.

A further application of this study was the ability to provide a list of candidate human CIN genes based on their sequence similarity to the yeast CIN genes identified. Review of the literature indicated that some human CIN genes, including 10 homologous to the yeast CIN genes identified in our screens, were mutated in cancers. By definition, the remaining human CIN genes represent candidate genes that may be somatically mutated in cancers. In Chapter 3, I described the somatic mutation analysis of 101 candidate human CIN genes in a panel of colorectal cancer patients. Novel mutations were identified, including mutations in genes functioning in sister chromatid cohesion with statistically significant frequencies. Knowing the mutational spectrum in different

types of cancers is useful for classification of cancers based on their differential genetic and cellular characteristics. In Chapter 2 and 3, I discussed the strategy of targeting the genetic vulnerability of CIN cancers containing a CIN gene mutation by synthetic lethality. Selective killing of several CIN cancer cells may be possible by inactivating a common protein that is required for the viability in cells with various CIN mutations. The common protein can be identified first using genome-wide synthetic lethal interaction analysis in yeast, and then the synthetic lethal interactions can be tested and verified in human cells.

The genome-wide CIN gene screening in yeast also provided a rich source of genes for the study of cellular processes important for chromosome maintenance. *MMS22*, *MMS1*, *RTT101* and *RTT107*, identified in my CIN screens, were not well characterized at the time of identification. As described in Chapter 4, I performed a battery of molecular, genetic, and biochemical analyses to gain insight into the functions of these 4 genes. Additionally, ongoing more detailed studies of these genes by other groups were published during the course of my study. Taken together, these results demonstrate that these genes are required for the recovery from DSBs and may form a ubiquitin ligase complex that regulates protein stability, possibly including Mms22p, during the response to DNA damage.

As highlighted by this study, research in yeast has significant implications to the development of a cancer therapeutic strategy based on candidate CIN gene identification (as described in Figure 1.9). First, the genome-wide identification of CIN genes in yeast has provided a systematic source of candidate human CIN gene that may be relevant to tumorigenesis. Second, synthetic lethal interactions identified in yeast serve as prototypes for testing analogous interactions in human. Third, detailed characterization of yeast CIN genes may shed insights on the functions of orthologous human genes. Elucidating the conservation in gene function and genetic interactions between human and model organisms is the key for success in such translational studies.

5.2 Future Directions

The construction of the non-essential gene deletion mutant set in yeast, containing ~85% of all the genes, has allowed systematic assessment and comparison of the many phenotypes among mutants, such as CIN, cohesion defects (Marston et al., 2004), morphological defects (Ohya et al., 2005), telomere maintenance (Gatbonton et al., 2006), and sensitivity to a range of agents (Bennett et al., 2001; Birrell et al., 2001; Chang et al., 2002; Giaever et al., 1999; Hanway et al., 2002; Parsons et al., 2004). In order to gain a complete understanding of basic cellular mechanisms such as the maintenance of chromosomes, essential gene mutants will also need to be assessed. In this aspect, several resources have been or are being developed, including a tetracycline-inducible gene collection (Yu et al., 2006), a set of genes that are fused to a heat-inducible-degron cassette which targets the fused protein for proteolysis at 37°C (Dohmen et al., 1994), and a collection of temperature-sensitive or hypomorphic alleles for essential genes (Shay Ben-Aroya and Phil Hieter, personal communication). Phenotypes in hypermorphs have also been explored systematically by overexpressing each protein in yeast (Sopko et al., 2006). With advances in resources developed for reverse genetics approaches, such as RNA interference, screens for genome instability phenotypes have been pursued in other organisms such as C. *elegans*, which serves as an excellent multi-cellular model (Shima et al., 2003; van Haaften et al., 2004). With the rapid and on-going generation of high-throughput data sets, advances in bioinformatics should allow the integration of data in an organized, interpretable way that will be useful to biologists (Kelley and Ideker, 2005).

To delineate the relationship between CIN and cancers, systematic mutation, expression, and DNA modification (e.g. methylation) analyses should be applied to a comprehensive set of candidate human CIN genes derived. The recent large-scale mutational testing project of over 13,000 genes in 2 cancer types by the Vogelstein group has set a baseline for mutation prevalence in a typical CIN cancer, which is important for the interpretation of the significance in any mutation study. Importantly, examining the CIN phenotypes in cells with a mutated or misregulated gene, and understanding how the

underlying mutations cause these phenotypes, will be a critical next step to distinguish between passenger mutations and mutations that perturb function.

As mentioned in Chapter 1, the genetic vulnerability of CIN cancer cells can be explored beyond synthetic lethal interactions to synthetic dosage lethality. In addition, since many cancers are polyploid, identifying genes that are essential only in polyploid cells but not in diploid cells may lead to the discovery of novel drug targets that are specific to cancer cells (Storchova et al., 2006). For example, Pellman found that wild-type tetraploid yeast cells have a high incidence of defective kinetochore-microtubule attachments, which may be related to scaling defects in SPBs, spindles and kinetochores (reviewed in (Storchova and Pellman, 2004)).

Often, the understanding of human cellular biology can benefit from studies in model organisms; but the opposite is also true. Although the Rtt101p-Mms22p-Mms1p complex, a putative ubiquitin ligase complex, has no substrate identified yet, the homology of individual yeast proteins to proteins involved in DNA damage response and chromosome maintenance in other organisms (e.g. CUL4A (*H.s*), Taz1 (*S.p*), *and* DDB1 (*H.s*), respectively) has shed light on the function of the complex in regulating protein levels during DNA damage response. To further characterize the role of this complex, two approaches will be necessary. First, it will be essential to directly test candidate substrates hypothesized based on physical and genetic interactions. In addition, unbiased genome-wide screening for the substrates will also be informative in characterizing the function of the complex.

Complementing basic research in model organisms such as yeast with clinical findings of cancer patients will advance our understanding in the genetic basis of cancer. Such knowledge will allow better diagnosis, classification of tumors, and prognosis. More importantly, this understanding will facilitate the development of therapeutics that is selective to cancer cells.

REFERENCES

Adams, R.R., Eckley, D.M., Vagnarelli, P., Wheatley, S.P., Gerloff, D.L., Mackay, A.M., Svingen, P.A., Kaufmann, S.H. and Earnshaw, W.C. (2001) Human INCENP colocalizes with the Aurora-B/AIRK2 kinase on chromosomes and is overexpressed in tumour cells. *Chromosoma*, **110**, 65-74.

Al-Tassan, N., Chmiel, N.H., Maynard, J., Fleming, N., Livingston, A.L., Williams, G.T., Hodges, A.K., Davies, D.R., David, S.S., Sampson, J.R. and Cheadle, J.P. (2002) Inherited variants of MYH associated with somatic G:C-->T:A mutations in colorectal tumors. *Nat Genet*, **30**, 227-232.

Andrews, P.D., Ovechkina, Y., Morrice, N., Wagenbach, M., Duncan, K., Wordeman, L. and Swedlow, J.R. (2004) Aurora B regulates MCAK at the mitotic centromere. *Dev Cell*, **6**, 253-268.

Araki, Y., Kawasaki, Y., Sasanuma, H., Tye, B.K. and Sugino, A. (2003) Budding yeast mcm10/dna43 mutant requires a novel repair pathway for viability. *Genes Cells*, **8**, 465-480.

Ault, J.G. and Nicklas, R.B. (1989) Tension, microtubule rearrangements, and the proper distribution of chromosomes in mitosis. *Chromosoma*, **98**, 33-39.

Aylon, Y., Liefshitz, B., Bitan-Banin, G. and Kupiec, M. (2003) Molecular dissection of mitotic recombination in the yeast Saccharomyces cerevisiae. *Mol Cell Biol*, **23**, 1403-1417.

Babu, J.R., Jeganathan, K.B., Baker, D.J., Wu, X., Kang-Decker, N. and van Deursen, J.M. (2003) Rae1 is an essential mitotic checkpoint regulator that cooperates with Bub3 to prevent chromosome missegregation. *J Cell Biol*, **160**, 341-353.

Baetz, K., Measday, V. and Andrews, B. (2006) Revealing hidden relationships among yeast genes involved in chromosome segregation using systematic synthetic lethal and synthetic dosage lethal screens. *Cell Cycle*, **5**, 592-595.

Baker, D.J., Jeganathan, K.B., Cameron, J.D., Thompson, M., Juneja, S., Kopecka, A., Kumar, R., Jenkins, R.B., de Groen, P.C., Roche, P. and van Deursen, J.M. (2004) BubR1 insufficiency causes early onset of aging-associated phenotypes and infertility in mice. *Nat Genet*, **36**, 744-749.

Baldwin, E.L., Berger, A.C., Corbett, A.H. and Osheroff, N. (2005) Mms22p protects Saccharomyces cerevisiae from DNA damage induced by topoisomerase II. *Nucleic Acids Res*, **33**, 1021-1030.

Bannister, A.J., Zegerman, P., Partridge, J.F., Miska, E.A., Thomas, J.O., Allshire, R.C. and Kouzarides, T. (2001) Selective recognition of methylated lysine 9 on histone H3 by the HP1 chromo domain. *Nature*, **410**, 120-124.

Bardi, G., Parada, L.A., Bomme, L., Pandis, N., Willen, R., Johansson, B., Jeppsson, B., Beroukas, K., Heim, S. and Mitelman, F. (1997) Cytogenetic comparisons of synchronous carcinomas and polyps in patients with colorectal cancer. *Br J Cancer*, **76**, 765-769.

Bassett, D.E., Jr., Basrai, M.A., Connelly, C., Hyland, K.M., Kitagawa, K., Mayer, M.L., Morrow, D.M., Page, A.M., Resto, V.A., Skibbens, R.V. and Hieter, P. (1996)

Exploiting the complete yeast genome sequence. *Curr Opin Genet Dev*, **6**, 763-766.

Bassett, D.E., Jr., Boguski, M.S., Spencer, F., Reeves, R., Kim, S., Weaver, T. and Hieter, P. (1997) Genome cross-referencing and XREFdb: implications for the identification and analysis of genes mutated in human disease. *Nat Genet*, **15**, 339-344.

Bell, D.W., Varley, J.M., Szydlo, T.E., Kang, D.H., Wahrer, D.C., Shannon, K.E., Lubratovich, M., Verselis, S.J., Isselbacher, K.J., Fraumeni, J.F., Birch, J.M., Li, F.P., Garber, J.E. and Haber, D.A. (1999) Heterozygous germ line hCHK2 mutations in Li-Fraumeni syndrome. *Science*, **286**, 2528-2531.

Bennett, C.B., Lewis, L.K., Karthikeyan, G., Lobachev, K.S., Jin, Y.H., Sterling, J.F., Snipe, J.R. and Resnick, M.A. (2001) Genes required for ionizing radiation resistance in yeast. *Nat Genet*, **29**, 426-434.

Bernard, P., Maure, J.F., Partridge, J.F., Genier, S., Javerzat, J.P. and Allshire, R.C. (2001) Requirement of heterochromatin for cohesion at centromeres. *Science*, **294**, 2539-2542.

Biggins, S. and Murray, A.W. (2001) The budding yeast protein kinase Ipl1/Aurora allows the absence of tension to activate the spindle checkpoint. *Genes Dev*, **15**, 3118-3129.

Biggins, S. and Walczak, C.E. (2003) Captivating capture: how microtubules attach to kinetochores. *Curr Biol*, **13**, R449-460.

Birrell, G.W., Giaever, G., Chu, A.M., Davis, R.W. and Brown, J.M. (2001) A genome-wide screen in Saccharomyces cerevisiae for genes affecting UV radiation sensitivity. *Proc Natl Acad Sci U S A*, **98**, 12608-12613.

Blake, D., Luke, B., Kanellis, P., Jorgensen, P., Goh, T., Penfold, S., Breitkreutz, B.J., Durocher, D., Peter, M. and Tyers, M. (2006) The F-box protein Dia2 overcomes replication impedance to promote genome stability in Saccharomyces cerevisiae. *Genetics*.

Bloom, K.S. and Carbon, J. (1982) Yeast centromere DNA is in a unique and highly ordered structure in chromosomes and small circular minichromosomes. *Cell*, **29**, 305-317.

Boland, C.R. and Ricciardiello, L. (1999) How many mutations does it take to make a tumor? *Proc Natl Acad Sci U S A*, **96**, 14675-14677.

Bomme, L., Bardi, G., Pandis, N., Fenger, C., Kronborg, O. and Heim, S. (1998) Cytogenetic analysis of colorectal adenomas: karyotypic comparisons of synchronous tumors. *Cancer Genet Cytogenet*, **106**, 66-71.

Bothos, J., Tuttle, R.L., Ottey, M., Luca, F.C. and Halazonetis, T.D. (2005) Human LATS1 is a mitotic exit network kinase. *Cancer Res*, **65**, 6568-6575.

Brachmann, C.B., Davies, A., Cost, G.J., Caputo, E., Li, J., Hieter, P. and Boeke, J.D. (1998) Designer deletion strains derived from Saccharomyces cerevisiae S288C: a useful set of strains and plasmids for PCR-mediated gene disruption and other applications. *Yeast*, **14**, 115-132.

Breitkreutz, B.J., Stark, C. and Tyers, M. (2003a) The GRID: the General Repository for Interaction Datasets. *Genome Biol*, **4**, R23.

Breitkreutz, B.J., Stark, C. and Tyers, M. (2003b) Osprey: a network visualization system. *Genome Biol*, **4**, R22.

Brummelkamp, T.R. and Bernards, R. (2003) New tools for functional mammalian cancer genetics. *Nat Rev Cancer*, **3**, 781-789.

Budd, M.E., Tong, A.H., Polaczek, P., Peng, X., Boone, C. and Campbell, J.L. (2005) A Network of Multi-Tasking Proteins at the DNA Replication Fork Preserves Genome Stability. *PLoS Genet*, **1**, e61.

Buonomo, S.B., Clyne, R.K., Fuchs, J., Loidl, J., Uhlmann, F. and Nasmyth, K. (2000) Disjunction of homologous chromosomes in meiosis I depends on proteolytic cleavage of the meiotic cohesin Rec8 by separin. *Cell*, **103**, 387-398.

Cagney, G., Uetz, P. and Fields, S. (2000) High-throughput screening for protein-protein interactions using two-hybrid assay. *Methods Enzymol*, **328**, 3-14.

Cahill, D.P., da Costa, L.T., Carson-Walter, E.B., Kinzler, K.W., Vogelstein, B. and Lengauer, C. (1999) Characterization of MAD2B and other mitotic spindle checkpoint genes. *Genomics*, **58**, 181-187.

Cahill, D.P., Lengauer, C., Yu, J., Riggins, G.J., Willson, J.K., Markowitz, S.D., Kinzler, K.W. and Vogelstein, B. (1998) Mutations of mitotic checkpoint genes in human cancers. *Nature*, **392**, 300-303.

Chan, G.K., Jablonski, S.A., Sudakin, V., Hittle, J.C. and Yen, T.J. (1999) Human BUBR1 is a mitotic checkpoint kinase that monitors CENP-E functions at kinetochores and binds the cyclosome/APC. *J Cell Biol*, **146**, 941-954.

Chan, G.K., Liu, S.T. and Yen, T.J. (2005) Kinetochore structure and function. *Trends Cell Biol*, **15**, 589-598.

Chan, G.K., Schaar, B.T. and Yen, T.J. (1998) Characterization of the kinetochore binding domain of CENP-E reveals interactions with the kinetochore proteins CENP-F and hBUBR1. *J Cell Biol*, **143**, 49-63.

Chang, M., Bellaoui, M., Boone, C. and Brown, G.W. (2002) A genome-wide screen for methyl methanesulfonate-sensitive mutants reveals genes required for S phase progression in the presence of DNA damage. *Proc Natl Acad Sci U S A*, **99**, 16934-16939.

Chang, M., Bellaoui, M., Zhang, C., Desai, R., Morozov, P., Delgado-Cruzata, L., Rothstein, R., Freyer, G.A., Boone, C. and Brown, G.W. (2005) RMI1/NCE4, a suppressor of genome instability, encodes a member of the RecQ helicase/Topo III complex. *Embo J*, **24**, 2024-2033.

Cheeseman, I.M., Anderson, S., Jwa, M., Green, E.M., Kang, J., Yates, J.R., 3rd, Chan, C.S., Drubin, D.G. and Barnes, G. (2002a) Phospho-regulation of kinetochore-microtubule attachments by the Aurora kinase Ipl1p. *Cell*, **111**, 163-172.

Cheeseman, I.M., Drubin, D.G. and Barnes, G. (2002b) Simple centromere, complex kinetochore: linking spindle microtubules and centromeric DNA in budding yeast. *J Cell Biol*, **157**, 199-203.

Chen, C. and Kolodner, R.D. (1999) Gross chromosomal rearrangements in Saccharomyces cerevisiae replication and recombination defective mutants. *Nat Genet*, **23**, 81-85.

Chen, R.H., Brady, D.M., Smith, D., Murray, A.W. and Hardwick, K.G. (1999) The spindle checkpoint of budding yeast depends on a tight complex between the Mad1 and Mad2 proteins. *Mol Biol Cell*, **10**, 2607-2618.

Chen, Y., Riley, D.J., Chen, P.L. and Lee, W.H. (1997) HEC, a novel nuclear protein rich in leucine heptad repeats specifically involved in mitosis. *Mol Cell Biol*, **17**, 6049-6056.

Cheok, C.F., Bachrati, C.Z., Chan, K.L., Ralf, C., Wu, L. and Hickson, I.D. (2005) Roles of the Bloom's syndrome helicase in the maintenance of genome stability. *Biochem Soc Trans*, **33**, 1456-1459.

Chin, J.K., Bashkirov, V.I., Heyer, W.D. and Romesberg, F.E. (2006) Esc4/Rtt107 and the control of recombination during replication. *DNA Repair (Amst)*, **5**, 618-628.

Cimini, D., Howell, B., Maddox, P., Khodjakov, A., Degrassi, F. and Salmon, E.D. (2001) Merotelic kinetochore orientation is a major mechanism of aneuploidy in mitotic mammalian tissue cells. *J Cell Biol*, **153**, 517-527.

Ciosk, R., Shirayama, M., Shevchenko, A., Tanaka, T., Toth, A. and Nasmyth, K. (2000) Cohesin's binding to chromosomes depends on a separate complex consisting of Scc2 and Scc4 proteins. *Mol Cell*, **5**, 243-254.

Ciosk, R., Zachariae, W., Michaelis, C., Shevchenko, A., Mann, M. and Nasmyth, K. (1998) An ESP1/PDS1 complex regulates loss of sister chromatid cohesion at the metaphase to anaphase transition in yeast. *Cell*, **93**, 1067-1076.

Clark, G.M., Allred, D.C., Hilsenbeck, S.G., Chamness, G.C., Osborne, C.K., Jones, D. and Lee, W.H. (1997) Mitosin (a new proliferation marker) correlates with clinical outcome in node-negative breast cancer. *Cancer Res*, **57**, 5505-5508.

Cleveland, D.W., Mao, Y. and Sullivan, K.F. (2003) Centromeres and kinetochores: from epigenetics to mitotic checkpoint signaling. *Cell*, **112**, 407-421.

Cohen-Fix, O., Peters, J.M., Kirschner, M.W. and Koshland, D. (1996) Anaphase initiation in Saccharomyces cerevisiae is controlled by the APC-dependent degradation of the anaphase inhibitor Pds1p. *Genes Dev*, **10**, 3081-3093.

Compton, D.A. (2006) Chromosomes walk the line. *Nat Cell Biol*, **8**, 308-310.

Connelly, C. and Hieter, P. (1996) Budding yeast SKP1 encodes an evolutionarily conserved kinetochore protein required for cell cycle progression. *Cell*, **86**, 275-285.

Dai, W., Wang, Q., Liu, T., Swamy, M., Fang, Y., Xie, S., Mahmood, R., Yang, Y.M., Xu, M. and Rao, C.V. (2004) Slippage of mitotic arrest and enhanced tumor development in mice with BubR1 haploinsufficiency. *Cancer Res*, **64**, 440-445.

David, G., Turner, G.M., Yao, Y., Protopopov, A. and DePinho, R.A. (2003) mSin3-associated protein, mSds3, is essential for pericentric heterochromatin formation and chromosome segregation in mammalian cells. *Genes Dev*, **17**, 2396-2405.

Davies, H., Bignell, G.R., Cox, C., Stephens, P., Edkins, S., Clegg, S., Teague, J., Woffendin, H., Garnett, M.J., Bottomley, W., Davis, N., Dicks, E., Ewing, R., Floyd, Y., Gray, K., Hall, S., Hawes, R., Hughes, J., Kosmidou, V., Menzies, A., Mould, C., Parker, A., Stevens, C., Watt, S., Hooper, S., Wilson, R., Jayatilake, H., Gusterson, B.A., Cooper, C., Shipley, J., Hargrave, D., Pritchard-Jones, K., Maitland, N., Chenevix-Trench, G., Riggins, G.J., Bigner, D.D., Palmieri, G.,

Cossu, A., Flanagan, A., Nicholson, A., Ho, J.W., Leung, S.Y., Yuen, S.T., Weber, B.L., Seigler, H.F., Darrow, T.L., Paterson, H., Marais, R., Marshall, C.J., Wooster, R., Stratton, M.R. and Futreal, P.A. (2002) Mutations of the BRAF gene in human cancer. *Nature*, **417**, 949-954.

de la Guardia, C., Casiano, C.A., Trinidad-Pinedo, J. and Baez, A. (2001) CENP-F gene amplification and overexpression in head and neck squamous cell carcinomas. *Head Neck*, **23**, 104-112.

Doheny, K.F., Sorger, P.K., Hyman, A.A., Tugendreich, S., Spencer, F. and Hieter, P. (1993) Identification of essential components of the S. cerevisiae kinetochore. *Cell*, **73**, 761-774.

Dohmen, R.J., Wu, P. and Varshavsky, A. (1994) Heat-inducible degron: a method for constructing temperature-sensitive mutants. *Science*, **263**, 1273-1276.

Dolma, S., Lessnick, S.L., Hahn, W.C. and Stockwell, B.R. (2003) Identification of genotype-selective antitumor agents using synthetic lethal chemical screening in engineered human tumor cells. *Cancer Cell*, **3**, 285-296.

Dunstan, H.M., Ludlow, C., Goehle, S., Cronk, M., Szankasi, P., Evans, D.R., Simon, J.A. and Lamb, J.R. (2002) Cell-based assays for identification of novel double-strand break-inducing agents. *J Natl Cancer Inst*, **94**, 88-94.

Eason, R.G., Pourmand, N., Tongprasit, W., Herman, Z.S., Anthony, K., Jejelowo, O., Davis, R.W. and Stolc, V. (2004) Characterization of synthetic DNA bar codes in Saccharomyces cerevisiae gene-deletion strains. *Proc Natl Acad Sci U S A*, **101**, 11046-11051.

Eisen, M.B., Spellman, P.T., Brown, P.O. and Botstein, D. (1998) Cluster analysis and display of genome-wide expression patterns. *Proc Natl Acad Sci U S A*, **95**, 14863-14868.

Eisenstein, M. (2005) Uncovering hidden relationships. *Nat Methods*, **2**, 806.

El-Rifai, W., Sarlomo-Rikala, M., Knuutila, S. and Miettinen, M. (1998) DNA copy number changes in development and progression in leiomyosarcomas of soft tissues. *Am J Pathol*, **153**, 985-990.

Erlanson, M., Casiano, C.A., Tan, E.M., Lindh, J., Roos, G. and Landberg, G. (1999) Immunohistochemical analysis of the proliferation associated nuclear antigen CENP-F in non-Hodgkin's lymphoma. *Mod Pathol*, **12**, 69-74.

Esguerra, R.L., Jia, L., Kaneko, T., Sakamoto, K., Okada, N. and Takagi, M. (2004) Immunohistochemical analysis of centromere protein F expression in buccal and gingival squamous cell carcinoma. *Pathol Int*, **54**, 82-89.

Feng, H. and Kipreos, E.T. (2003) Preventing DNA re-replication--divergent safeguards in yeast and metazoa. *Cell Cycle*, **2**, 431-434.

Fishel, R., Lescoe, M.K., Rao, M.R., Copeland, N.G., Jenkins, N.A., Garber, J., Kane, M. and Kolodner, R. (1993) The human mutator gene homolog MSH2 and its association with hereditary nonpolyposis colon cancer. *Cell*, **75**, 1027-1038.

Fitzgerald-Hayes, M., Clarke, L. and Carbon, J. (1982) Nucleotide sequence comparisons and functional analysis of yeast centromere DNAs. *Cell*, **29**, 235-244.

Fodde, R., Kuipers, J., Rosenberg, C., Smits, R., Kielman, M., Gaspar, C., van Es, J.H., Breukel, C., Wiegant, J., Giles, R.H. and Clevers, H. (2001a) Mutations in the

APC tumour suppressor gene cause chromosomal instability. *Nat Cell Biol*, **3**, 433-438.

Fodde, R., Smits, R. and Clevers, H. (2001b) APC, signal transduction and genetic instability in colorectal cancer. *Nat Rev Cancer*, **1**, 55-67.

Fricke, W.M. and Brill, S.J. (2003) Slx1-Slx4 is a second structure-specific endonuclease functionally redundant with Sgs1-Top3. *Genes Dev*, **17**, 1768-1778.

Friend, S.H. and Oliff, A. (1998) Emerging uses for genomic information in drug discovery. *N Engl J Med*, **338**, 125-126.

Fukagawa, T. (2004) Assembly of kinetochores in vertebrate cells. *Exp Cell Res*, **296**, 21-27.

Furuya, T., Uchiyama, T., Murakami, T., Adachi, A., Kawauchi, S., Oga, A., Hirano, T. and Sasaki, K. (2000) Relationship between chromosomal instability and intratumoral regional DNA ploidy heterogeneity in primary gastric cancers. *Clin Cancer Res*, **6**, 2815-2820.

Futreal, P.A., Coin, L., Marshall, M., Down, T., Hubbard, T., Wooster, R., Rahman, N. and Stratton, M.R. (2004) A census of human cancer genes. *Nat Rev Cancer*, **4**, 177-183.

Gambus, A., Jones, R.C., Sanchez-Diaz, A., Kanemaki, M., van Deursen, F., Edmondson, R.D. and Labib, K. (2006) GINS maintains association of Cdc45 with MCM in replisome progression complexes at eukaryotic DNA replication forks. *Nat Cell Biol*, **8**, 358-366.

Gardner, R.D., Poddar, A., Yellman, C., Tavormina, P.A., Monteagudo, M.C. and Burke, D.J. (2001) The spindle checkpoint of the yeast Saccharomyces cerevisiae requires kinetochore function and maps to the CBF3 domain. *Genetics*, **157**, 1493-1502.

Gasch, A.P., Huang, M., Metzner, S., Botstein, D., Elledge, S.J. and Brown, P.O. (2001) Genomic expression responses to DNA-damaging agents and the regulatory role of the yeast ATR homolog Mec1p. *Mol Biol Cell*, **12**, 2987-3003.

Gascoyne, D.M., Hixon, M.L., Gualberto, A. and Vivanco, M.D. (2003) Loss of mitotic spindle checkpoint activity predisposes to chromosomal instability at early stages of fibrosarcoma development. *Cell Cycle*, **2**, 238-245.

Gatbonton, T., Imbesi, M., Nelson, M., Akey, J.M., Ruderfer, D.M., Kruglyak, L., Simon, J.A. and Bedalov, A. (2006) Telomere length as a quantitative trait: genome-wide survey and genetic mapping of telomere length-control genes in yeast. *PLoS Genet*, **2**, e35.

Gemma, A., Seike, M., Seike, Y., Uematsu, K., Hibino, S., Kurimoto, F., Yoshimura, A., Shibuya, M., Harris, C.C. and Kudoh, S. (2000) Somatic mutation of the hBUB1 mitotic checkpoint gene in primary lung cancer. *Genes Chromosomes Cancer*, **29**, 213-218.

Gerring, S.L., Spencer, F. and Hieter, P. (1990) The CHL 1 (CTF 1) gene product of Saccharomyces cerevisiae is important for chromosome transmission and normal cell cycle progression in G2/M. *Embo J*, **9**, 4347-4358.

Giaever, G., Chu, A.M., Ni, L., Connelly, C., Riles, L., Veronneau, S., Dow, S., Lucau-Danila, A., Anderson, K., Andre, B., Arkin, A.P., Astromoff, A., El-Bakkoury,

M., Bangham, R., Benito, R., Brachat, S., Campanaro, S., Curtiss, M., Davis, K., Deutschbauer, A., Entian, K.D., Flaherty, P., Foury, F., Garfinkel, D.J., Gerstein, M., Gotte, D., Guldener, U., Hegemann, J.H., Hempel, S., Herman, Z., Jaramillo, D.F., Kelly, D.E., Kelly, S.L., Kotter, P., LaBonte, D., Lamb, D.C., Lan, N., Liang, H., Liao, H., Liu, L., Luo, C., Lussier, M., Mao, R., Menard, P., Ooi, S.L., Revuelta, J.L., Roberts, C.J., Rose, M., Ross-Macdonald, P., Scherens, B., Schimmack, G., Shafer, B., Shoemaker, D.D., Sookhai-Mahadeo, S., Storms, R.K., Strathern, J.N., Valle, G., Voet, M., Volckaert, G., Wang, C.Y., Ward, T.R., Wilhelmy, J., Winzeler, E.A., Yang, Y., Yen, G., Youngman, E., Yu, K., Bussey, H., Boeke, J.D., Snyder, M., Philippsen, P., Davis, R.W. and Johnston, M. (2002) Functional profiling of the Saccharomyces cerevisiae genome. *Nature*, **418**, 387-391.

Giaever, G., Shoemaker, D.D., Jones, T.W., Liang, H., Winzeler, E.A., Astromoff, A. and Davis, R.W. (1999) Genomic profiling of drug sensitivities via induced haploinsufficiency. *Nat Genet*, **21**, 278-283.

Giannattasio, M., Lazzaro, F., Plevani, P. and Muzi-Falconi, M. (2005) The DNA damage checkpoint response requires histone H2B ubiquitination by Rad6-Bre1 and H3 methylation by Dot1. *J Biol Chem*, **280**, 9879-9886.

Giet, R., Petretti, C. and Prigent, C. (2005) Aurora kinases, aneuploidy and cancer, a coincidence or a real link? *Trends Cell Biol*, **15**, 241-250.

Gietz, R.D., Schiestl, R.H., Willems, A.R. and Woods, R.A. (1995) Studies on the transformation of intact yeast cells by the LiAc/SS-DNA/PEG procedure. *Yeast*, **11**, 355-360.

Gisselsson, D. (2003) Chromosome instability in cancer: how, when, and why? *Adv Cancer Res*, **87**, 1-29.

Glynn, E.F., Megee, P.C., Yu, H.G., Mistrot, C., Unal, E., Koshland, D.E., DeRisi, J.L. and Gerton, J.L. (2004) Genome-wide mapping of the cohesin complex in the yeast Saccharomyces cerevisiae. *PLoS Biol*, **2**, E259.

Goffeau, A., Barrell, B.G., Bussey, H., Davis, R.W., Dujon, B., Feldmann, H., Galibert, F., Hoheisel, J.D., Jacq, C., Johnston, M., Louis, E.J., Mewes, H.W., Murakami, Y., Philippsen, P., Tettelin, H. and Oliver, S.G. (1996) Life with 6000 genes. *Science*, **274**, 546, 563-547.

Gorunova, L., Hoglund, M., Andren-Sandberg, A., Dawiskiba, S., Jin, Y., Mitelman, F. and Johansson, B. (1998) Cytogenetic analysis of pancreatic carcinomas: intratumor heterogeneity and nonrandom pattern of chromosome aberrations. *Genes Chromosomes Cancer*, **23**, 81-99.

Goshima, G. and Yanagida, M. (2000) Establishing biorientation occurs with precocious separation of the sister kinetochores, but not the arms, in the early spindle of budding yeast. *Cell*, **100**, 619-633.

Goss, K.H., Risinger, M.A., Kordich, J.J., Sanz, M.M., Straughen, J.E., Slovek, L.E., Capobianco, A.J., German, J., Boivin, G.P. and Groden, J. (2002) Enhanced tumor formation in mice heterozygous for Blm mutation. *Science*, **297**, 2051-2053.

Grabsch, H., Takeno, S., Parsons, W.J., Pomjanski, N., Boecking, A., Gabbert, H.E. and Mueller, W. (2003) Overexpression of the mitotic checkpoint genes BUB1, BUBR1, and BUB3 in gastric cancer--association with tumour cell proliferation. *J Pathol*, **200**, 16-22.

Green, R.A. and Kaplan, K.B. (2003) Chromosome instability in colorectal tumor cells is associated with defects in microtubule plus-end attachments caused by a dominant mutation in APC. *J Cell Biol*, **163**, 949-961.

Griffith, J.L., Coleman, L.E., Raymond, A.S., Goodson, S.G., Pittard, W.S., Tsui, C. and Devine, S.E. (2003) Functional genomics reveals relationships between the retrovirus-like Ty1 element and its host Saccharomyces cerevisiae. *Genetics*, **164**, 867-879.

Gruber, S.B., Ellis, N.A., Scott, K.K., Almog, R., Kolachana, P., Bonner, J.D., Kirchhoff, T., Tomsho, L.P., Nafa, K., Pierce, H., Low, M., Satagopan, J., Rennert, H., Huang, H., Greenson, J.K., Groden, J., Rapaport, B., Shia, J., Johnson, S., Gregersen, P.K., Harris, C.C., Boyd, J., Rennert, G. and Offit, K. (2002) BLM heterozygosity and the risk of colorectal cancer. *Science*, **297**, 2013.

Guardavaccaro, D. and Pagano, M. (2004) Oncogenic aberrations of cullin-dependent ubiquitin ligases. *Oncogene*, **23**, 2037-2049.

Haering, C.H., Lowe, J., Hochwagen, A. and Nasmyth, K. (2002) Molecular architecture of SMC proteins and the yeast cohesin complex. *Mol Cell*, **9**, 773-788.

Haering, C.H., Schoffnegger, D., Nishino, T., Helmhart, W., Nasmyth, K. and Lowe, J. (2004) Structure and stability of cohesin's Smc1-kleisin interaction. *Mol Cell*, **15**, 951-964.

Hall, I.M., Shankaranarayana, G.D., Noma, K., Ayoub, N., Cohen, A. and Grewal, S.I. (2002) Establishment and maintenance of a heterochromatin domain. *Science*, **297**, 2232-2237.

Han, D.K., Eng, J., Zhou, H. and Aebersold, R. (2001) Quantitative profiling of differentiation-induced microsomal proteins using isotope-coded affinity tags and mass spectrometry. *Nat Biotechnol*, **19**, 946-951.

Hanks, S., Coleman, K., Reid, S., Plaja, A., Firth, H., Fitzpatrick, D., Kidd, A., Mehes, K., Nash, R., Robin, N., Shannon, N., Tolmie, J., Swansbury, J., Irrthum, A., Douglas, J. and Rahman, N. (2004) Constitutional aneuploidy and cancer predisposition caused by biallelic mutations in BUB1B. *Nat Genet*, **36**, 1159-1161.

Hanna, J.S., Kroll, E.S., Lundblad, V. and Spencer, F.A. (2001) Saccharomyces cerevisiae CTF18 and CTF4 are required for sister chromatid cohesion. *Mol Cell Biol*, **21**, 3144-3158.

Hanway, D., Chin, J.K., Xia, G., Oshiro, G., Winzeler, E.A. and Romesberg, F.E. (2002) Previously uncharacterized genes in the UV- and MMS-induced DNA damage response in yeast. *Proc Natl Acad Sci U S A*, **99**, 10605-10610.

Harrington, E.A., Bebbington, D., Moore, J., Rasmussen, R.K., Ajose-Adeogun, A.O., Nakayama, T., Graham, J.A., Demur, C., Hercend, T., Diu-Hercend, A., Su, M., Golec, J.M. and Miller, K.M. (2004) VX-680, a potent and selective small-

molecule inhibitor of the Aurora kinases, suppresses tumor growth in vivo. *Nat Med*, **10**, 262-267.

Harris, M.A., Clark, J., Ireland, A., Lomax, J., Ashburner, M., Foulger, R., Eilbeck, K., Lewis, S., Marshall, B., Mungall, C., Richter, J., Rubin, G.M., Blake, J.A., Bult, C., Dolan, M., Drabkin, H., Eppig, J.T., Hill, D.P., Ni, L., Ringwald, M., Balakrishnan, R., Cherry, J.M., Christie, K.R., Costanzo, M.C., Dwight, S.S., Engel, S., Fisk, D.G., Hirschman, J.E., Hong, E.L., Nash, R.S., Sethuraman, A., Theesfeld, C.L., Botstein, D., Dolinski, K., Feierbach, B., Berardini, T., Mundodi, S., Rhee, S.Y., Apweiler, R., Barrell, D., Camon, E., Dimmer, E., Lee, V., Chisholm, R., Gaudet, P., Kibbe, W., Kishore, R., Schwarz, E.M., Sternberg, P., Gwinn, M., Hannick, L., Wortman, J., Berriman, M., Wood, V., de la Cruz, N., Tonellato, P., Jaiswal, P., Seigfried, T. and White, R. (2004) The Gene Ontology (GO) database and informatics resource. *Nucleic Acids Res*, **32 Database issue**, D258-261.

Hartman, T., Stead, K., Koshland, D. and Guacci, V. (2000) Pds5p is an essential chromosomal protein required for both sister chromatid cohesion and condensation in Saccharomyces cerevisiae. *J Cell Biol*, **151**, 613-626.

Hartwell, L.H., Culotti, J., Pringle, J.R. and Reid, B.J. (1974) Genetic control of the cell division cycle in yeast. *Science*, **183**, 46-51.

Hartwell, L.H., Culotti, J. and Reid, B. (1970) Genetic control of the cell-division cycle in yeast. I. Detection of mutants. *Proc Natl Acad Sci U S A*, **66**, 352-359.

Hartwell, L.H. and Smith, D. (1985) Altered fidelity of mitotic chromosome transmission in cell cycle mutants of S. cerevisiae. *Genetics*, **110**, 381-395.

Hartwell, L.H., Szankasi, P., Roberts, C.J., Murray, A.W. and Friend, S.H. (1997) Integrating genetic approaches into the discovery of anticancer drugs. *Science*, **278**, 1064-1068.

Hartwell, L.H. and Weinert, T.A. (1989) Checkpoints: controls that ensure the order of cell cycle events. *Science*, **246**, 629-634.

Hauf, S., Roitinger, E., Koch, B., Dittrich, C.M., Mechtler, K. and Peters, J.M. (2005) Dissociation of cohesin from chromosome arms and loss of arm cohesion during early mitosis depends on phosphorylation of SA2. *PLoS Biol*, **3**, e69.

Hazbun, T.R., Malmstrom, L., Anderson, S., Graczyk, B.J., Fox, B., Riffle, M., Sundin, B.A., Aranda, J.D., McDonald, W.H., Chiu, C.H., Snydsman, B.E., Bradley, P., Muller, E.G., Fields, S., Baker, D., Yates, J.R., 3rd and Davis, T.N. (2003) Assigning function to yeast proteins by integration of technologies. *Mol Cell*, **12**, 1353-1365.

He, X., Asthana, S. and Sorger, P.K. (2000) Transient sister chromatid separation and elastic deformation of chromosomes during mitosis in budding yeast. *Cell*, **101**, 763-775.

He, X., Rines, D.R., Espelin, C.W. and Sorger, P.K. (2001) Molecular analysis of kinetochore-microtubule attachment in budding yeast. *Cell*, **106**, 195-206.

Heald, R. (2000) Motor function in the mitotic spindle. *Cell*, **102**, 399-402.

Hegemann, J.H., Klein, S., Heck, S., Guldener, U., Niedenthal, R.K. and Fleig, U. (1999) A fast method to diagnose chromosome and plasmid loss in Saccharomyces cerevisiae strains. *Yeast*, **15**, 1009-1019.

Hegemann, J.H., Shero, J.H., Cottarel, G., Philippsen, P. and Hieter, P. (1988) Mutational analysis of centromere DNA from chromosome VI of Saccharomyces cerevisiae. *Mol Cell Biol*, **8**, 2523-2535.

Hergovich, A., Schmitz, D. and Hemmings, B.A. (2006) The human tumour suppressor LATS1 is activated by human MOB1 at the membrane. *Biochem Biophys Res Commun*, **345**, 50-58.

Herskowitz, I. (1988a) The Hawthorne deletion twenty-five years later. *Genetics*, **120**, 857-861.

Herskowitz, I. (1988b) Life cycle of the budding yeast Saccharomyces cerevisiae. *Microbiol Rev*, **52**, 536-553.

Hieter, P., Mann, C., Snyder, M. and Davis, R.W. (1985) Mitotic stability of yeast chromosomes: a colony color assay that measures nondisjunction and chromosome loss. *Cell*, **40**, 381-392.

Ho, Y., Gruhler, A., Heilbut, A., Bader, G.D., Moore, L., Adams, S.L., Millar, A., Taylor, P., Bennett, K., Boutilier, K., Yang, L., Wolting, C., Donaldson, I., Schandorff, S., Shewnarane, J., Vo, M., Taggart, J., Goudreault, M., Muskat, B., Alfarano, C., Dewar, D., Lin, Z., Michalickova, K., Willems, A.R., Sassi, H., Nielsen, P.A., Rasmussen, K.J., Andersen, J.R., Johansen, L.E., Hansen, L.H., Jespersen, H., Podtelejnikov, A., Nielsen, E., Crawford, J., Poulsen, V., Sorensen, B.D., Matthiesen, J., Hendrickson, R.C., Gleeson, F., Pawson, T., Moran, M.F., Durocher, D., Mann, M., Hogue, C.W., Figeys, D. and Tyers, M. (2002) Systematic identification of protein complexes in Saccharomyces cerevisiae by mass spectrometry. *Nature*, **415**, 180-183.

Hoeijmakers, J.H. (2001) Genome maintenance mechanisms for preventing cancer. *Nature*, **411**, 366-374.

Houben, A. and Schubert, I. (2003) DNA and proteins of plant centromeres. *Curr Opin Plant Biol*, **6**, 554-560.

Howell, B.J., McEwen, B.F., Canman, J.C., Hoffman, D.B., Farrar, E.M., Rieder, C.L. and Salmon, E.D. (2001) Cytoplasmic dynein/dynactin drives kinetochore protein transport to the spindle poles and has a role in mitotic spindle checkpoint inactivation. *J Cell Biol*, **155**, 1159-1172.

Hoyt, M.A. and Geiser, J.R. (1996) Genetic analysis of the mitotic spindle. *Annu Rev Genet*, **30**, 7-33.

Hoyt, M.A., Stearns, T. and Botstein, D. (1990) Chromosome instability mutants of Saccharomyces cerevisiae that are defective in microtubule-mediated processes. *Mol Cell Biol*, **10**, 223-234.

Hoyt, M.A., Totis, L. and Roberts, B.T. (1991) S. cerevisiae genes required for cell cycle arrest in response to loss of microtubule function. *Cell*, **66**, 507-517.

Hryciw, T., Tang, M., Fontanie, T. and Xiao, W. (2002) MMS1 protects against replication-dependent DNA damage in Saccharomyces cerevisiae. *Mol Genet Genomics*, **266**, 848-857.

Huang, D. and Koshland, D. (2003) Chromosome integrity in Saccharomyces cerevisiae: the interplay of DNA replication initiation factors, elongation factors, and origins. *Genes Dev*, **17**, 1741-1754.

Huang, J., Hsu, J.M. and Laurent, B.C. (2004) The RSC nucleosome-remodeling complex is required for Cohesin's association with chromosome arms. *Mol Cell*, **13**, 739-750.

Huang, J. and Laurent, B.C. (2004) A Role for the RSC chromatin remodeler in regulating cohesion of sister chromatid arms. *Cell Cycle*, **3**, 973-975.

Huang, M.E., Rio, A.G., Nicolas, A. and Kolodner, R.D. (2003) A genomewide screen in Saccharomyces cerevisiae for genes that suppress the accumulation of mutations. *Proc Natl Acad Sci U S A*, **100**, 11529-11534.

Huang, T.T. and D'Andrea, A.D. (2006) Regulation of DNA repair by ubiquitylation. *Nat Rev Mol Cell Biol*, **7**, 323-334.

Hughes, T.R., Roberts, C.J., Dai, H., Jones, A.R., Meyer, M.R., Slade, D., Burchard, J., Dow, S., Ward, T.R., Kidd, M.J., Friend, S.H. and Marton, M.J. (2000) Widespread aneuploidy revealed by DNA microarray expression profiling. *Nat Genet*, **25**, 333-337.

Huxley, C., Green, E.D. and Dunham, I. (1990) Rapid assessment of S. cerevisiae mating type by PCR. *Trends Genet*, **6**, 236.

Iwanaga, Y., Kasai, T., Kibler, K. and Jeang, K.T. (2002) Characterization of regions in hsMAD1 needed for binding hsMAD2. A polymorphic change in an hsMAD1 leucine zipper affects MAD1-MAD2 interaction and spindle checkpoint function. *J Biol Chem*, **277**, 31005-31013.

Izumi, M., Yatagai, F. and Hanaoka, F. (2001) Cell cycle-dependent proteolysis and phosphorylation of human Mcm10. *J Biol Chem*, **276**, 48526-48531.

Jallepalli, P.V. and Lengauer, C. (2001) Chromosome segregation and cancer: cutting through the mystery. *Nat Rev Cancer*, **1**, 109-117.

Janke, C., Ortiz, J., Lechner, J., Shevchenko, A., Magiera, M.M., Schramm, C. and Schiebel, E. (2001) The budding yeast proteins Spc24p and Spc25p interact with Ndc80p and Nuf2p at the kinetochore and are important for kinetochore clustering and checkpoint control. *Embo J*, **20**, 777-791.

Jin, D.Y., Spencer, F. and Jeang, K.T. (1998) Human T cell leukemia virus type 1 oncoprotein Tax targets the human mitotic checkpoint protein MAD1. *Cell*, **93**, 81-91.

Jin, Q.W., Fuchs, J. and Loidl, J. (2000) Centromere clustering is a major determinant of yeast interphase nuclear organization. *J Cell Sci*, **113 (Pt 11)**, 1903-1912.

Jorgensen, P., Nishikawa, J.L., Breitkreutz, B.J. and Tyers, M. (2002) Systematic identification of pathways that couple cell growth and division in yeast. *Science*, **297**, 395-400.

Kaelin, W.G., Jr. (2005) The concept of synthetic lethality in the context of anticancer therapy. *Nat Rev Cancer*, **5**, 689-698.

Kalitsis, P., Earle, E., Fowler, K.J. and Choo, K.H. (2000) Bub3 gene disruption in mice reveals essential mitotic spindle checkpoint function during early embryogenesis. *Genes Dev*, **14**, 2277-2282.

Kanellis, P., Agyei, R. and Durocher, D. (2003) Elg1 forms an alternative PCNA-interacting RFC complex required to maintain genome stability. *Curr Biol*, **13**, 1583-1595.

Kang, J., Cheeseman, I.M., Kallstrom, G., Velmurugan, S., Barnes, G. and Chan, C.S. (2001) Functional cooperation of Dam1, Ipl1, and the inner centromere protein (INCENP)-related protein Sli15 during chromosome segregation. *J Cell Biol*, **155**, 763-774.

Kaplan, K.B., Burds, A.A., Swedlow, J.R., Bekir, S.S., Sorger, P.K. and Nathke, I.S. (2001) A role for the Adenomatous Polyposis Coli protein in chromosome segregation. *Nat Cell Biol*, **3**, 429-432.

Kapoor, T.M., Lampson, M.A., Hergert, P., Cameron, L., Cimini, D., Salmon, E.D., McEwen, B.F. and Khodjakov, A. (2006) Chromosomes can congress to the metaphase plate before biorientation. *Science*, **311**, 388-391.

Karess, R. (2005) Rod-Zw10-Zwilch: a key player in the spindle checkpoint. *Trends Cell Biol.*

Kaur, M., DeScipio, C., McCallum, J., Yaeger, D., Devoto, M., Jackson, L.G., Spinner, N.B. and Krantz, I.D. (2005) Precocious sister chromatid separation (PSCS) in Cornelia de Lange syndrome. *Am J Med Genet A*, **138**, 27-31.

Kelley, R. and Ideker, T. (2005) Systematic interpretation of genetic interactions using protein networks. *Nat Biotechnol*, **23**, 561-566.

Keogh, M.C., Kim, J.A., Downey, M., Fillingham, J., Chowdhury, D., Harrison, J.C., Onishi, M., Datta, N., Galicia, S., Emili, A., Lieberman, J., Shen, X., Buratowski, S., Haber, J.E., Durocher, D., Greenblatt, J.F. and Krogan, N.J. (2006) A phosphatase complex that dephosphorylates gammaH2AX regulates DNA damage checkpoint recovery. *Nature*, **439**, 497-501.

Kim, H.S., Park, K.H., Kim, S.A., Wen, J., Park, S.W., Park, B., Gham, C.W., Hyung, W.J., Noh, S.H., Kim, H.K. and Song, S.Y. (2005) Frequent mutations of human Mad2, but not Bub1, in gastric cancers cause defective mitotic spindle checkpoint. *Mutat Res.*

King, J.M. and Nicklas, R.B. (2000) Tension on chromosomes increases the number of kinetochore microtubules but only within limits. *J Cell Sci*, **113 Pt 21**, 3815-3823.

Kitagawa, K. and Hieter, P. (2001) Evolutionary conservation between budding yeast and human kinetochores. *Nat Rev Mol Cell Biol*, **2**, 678-687.

Kitagawa, R. and Rose, A.M. (1999) Components of the spindle-assembly checkpoint are essential in Caenorhabditis elegans. *Nat Cell Biol*, **1**, 514-521.

Kitajima, T.S., Sakuno, T., Ishiguro, K., Iemura, S., Natsume, T., Kawashima, S.A. and Watanabe, Y. (2006) Shugoshin collaborates with protein phosphatase 2A to protect cohesin. *Nature*, **441**, 46-52.

Klein, F., Mahr, P., Galova, M., Buonomo, S.B., Michaelis, C., Nairz, K. and Nasmyth, K. (1999) A central role for cohesins in sister chromatid cohesion, formation of axial elements, and recombination during yeast meiosis. *Cell*, **98**, 91-103.

Koepp, D.M., Kile, A.C., Swaminathan, S. and Rodriguez-Rivera, V. (2006) The F-box protein Dia2 regulates DNA replication. *Mol Biol Cell*, **17**, 1540-1548.

Kops, G.J., Foltz, D.R. and Cleveland, D.W. (2004) Lethality to human cancer cells through massive chromosome loss by inhibition of the mitotic checkpoint. *Proc Natl Acad Sci U S A*, **101**, 8699-8704.

Koshland, D. and Hieter, P. (1987) Visual assay for chromosome ploidy. *Methods Enzymol*, **155**, 351-372.

Kouprina, N., Pashina, O.B., Nikolaishwili, N.T., Tsouladze, A.M. and Larionov, V.L. (1988) Genetic control of chromosome stability in the yeast Saccharomyces cerevisiae. *Yeast*, **4**, 257-269.

Krantz, I.D., McCallum, J., DeScipio, C., Kaur, M., Gillis, L.A., Yaeger, D., Jukofsky, L., Wasserman, N., Bottani, A., Morris, C.A., Nowaczyk, M.J., Toriello, H., Bamshad, M.J., Carey, J.C., Rappaport, E., Kawauchi, S., Lander, A.D., Calof, A.L., Li, H.H., Devoto, M. and Jackson, L.G. (2004) Cornelia de Lange syndrome is caused by mutations in NIPBL, the human homolog of Drosophila melanogaster Nipped-B. *Nat Genet*, **36**, 631-635.

Krogan, N.J., Cagney, G., Yu, H., Zhong, G., Guo, X., Ignatchenko, A., Li, J., Pu, S., Datta, N., Tikuisis, A.P., Punna, T., Peregrin-Alvarez, J.M., Shales, M., Zhang, X., Davey, M., Robinson, M.D., Paccanaro, A., Bray, J.E., Sheung, A., Beattie, B., Richards, D.P., Canadien, V., Lalev, A., Mena, F., Wong, P., Starostine, A., Canete, M.M., Vlasblom, J., Wu, S., Orsi, C., Collins, S.R., Chandran, S., Haw, R., Rilstone, J.J., Gandi, K., Thompson, N.J., Musso, G., St Onge, P., Ghanny, S., Lam, M.H., Butland, G., Altaf-Ul, A.M., Kanaya, S., Shilatifard, A., O'Shea, E., Weissman, J.S., Ingles, C.J., Hughes, T.R., Parkinson, J., Gerstein, M., Wodak, S.J., Emili, A. and Greenblatt, J.F. (2006) Global landscape of protein complexes in the yeast Saccharomyces cerevisiae. *Nature*, **440**, 637-643.

Lachner, M., O'Carroll, D., Rea, S., Mechtler, K. and Jenuwein, T. (2001) Methylation of histone H3 lysine 9 creates a binding site for HP1 proteins. *Nature*, **410**, 116-120.

Lai, Z.C., Wei, X., Shimizu, T., Ramos, E., Rohrbaugh, M., Nikolaidis, N., Ho, L.L. and Li, Y. (2005) Control of cell proliferation and apoptosis by mob as tumor suppressor, mats. *Cell*, **120**, 675-685.

Lan, W., Zhang, X., Kline-Smith, S.L., Rosasco, S.E., Barrett-Wilt, G.A., Shabanowitz, J., Hunt, D.F., Walczak, C.E. and Stukenberg, P.T. (2004) Aurora B phosphorylates centromeric MCAK and regulates its localization and microtubule depolymerization activity. *Curr Biol*, **14**, 273-286.

Laplaza, J.M., Bostick, M., Scholes, D.T., Curcio, M.J. and Callis, J. (2004) Saccharomyces cerevisiae ubiquitin-like protein Rub1 conjugates to cullin proteins Rtt101 and Cul3 in vivo. *Biochem J*, **377**, 459-467.

Larionov, V.L., Karpova, T.S., Kouprina, N.Y. and Jouravleva, G.A. (1985) A mutant of Saccharomyces cerevisiae with impaired maintenance of centromeric plasmids. *Curr Genet*, **10**, 15-20.

Larionov, V.L., Karpova, T.S., Zhouravleva, G.A., Pashina, O.B., Nikolaishvili, N.T. and Kouprina, N.Y. (1987) The stability of chromosomes in yeast. *Curr Genet*, **11**, 435-443.

Leach, F.S., Nicolaides, N.C., Papadopoulos, N., Liu, B., Jen, J., Parsons, R., Peltomaki, P., Sistonen, P., Aaltonen, L.A., Nystrom-Lahti, M. and et al. (1993) Mutations of

a mutS homolog in hereditary nonpolyposis colorectal cancer. *Cell*, **75**, 1215-1225.

Lee, H., Yi, E.C., Wen, B., Reily, T.P., Pohl, L., Nelson, S., Aebersold, R. and Goodlett, D.R. (2004) Optimization of reversed-phase microcapillary liquid chromatography for quantitative proteomics. *J Chromatogr B Analyt Technol Biomed Life Sci*, **803**, 101-110.

Lehnertz, B., Ueda, Y., Derijck, A.A., Braunschweig, U., Perez-Burgos, L., Kubicek, S., Chen, T., Li, E., Jenuwein, T. and Peters, A.H. (2003) Suv39h-mediated histone H3 lysine 9 methylation directs DNA methylation to major satellite repeats at pericentric heterochromatin. *Curr Biol*, **13**, 1192-1200.

Lemoine, F.J., Degtyareva, N.P., Lobachev, K. and Petes, T.D. (2005) Chromosomal translocations in yeast induced by low levels of DNA polymerase a model for chromosome fragile sites. *Cell*, **120**, 587-598.

Lengauer, C., Kinzler, K.W. and Vogelstein, B. (1997) Genetic instability in colorectal cancers. *Nature*, **386**, 623-627.

Lengauer, C., Kinzler, K.W. and Vogelstein, B. (1998) Genetic instabilities in human cancers. *Nature*, **396**, 643-649.

Levitt, N.C. and Hickson, I.D. (2002) Caretaker tumour suppressor genes that defend genome integrity. *Trends Mol Med*, **8**, 179-186.

Lew, D.J. and Burke, D.J. (2003) The spindle assembly and spindle position checkpoints. *Annu Rev Genet*, **37**, 251-282.

Li, R. and Murray, A.W. (1991) Feedback control of mitosis in budding yeast. *Cell*, **66**, 519-531.

Li, Y. and Benezra, R. (1996) Identification of a human mitotic checkpoint gene: hsMAD2. *Science*, **274**, 246-248.

Liras, P., McCusker, J., Mascioli, S. and Haber, J. (1978) Characterization of a mutation in yeast causing nonrandom chromosome loss during mitosis. *Genetics*, **88**, 651-671.

Lisby, M., Barlow, J.H., Burgess, R.C. and Rothstein, R. (2004) Choreography of the DNA damage response: spatiotemporal relationships among checkpoint and repair proteins. *Cell*, **118**, 699-713.

Lisby, M., Mortensen, U.H. and Rothstein, R. (2003) Colocalization of multiple DNA double-strand breaks at a single Rad52 repair centre. *Nat Cell Biol*, **5**, 572-577.

Lisby, M., Rothstein, R. and Mortensen, U.H. (2001) Rad52 forms DNA repair and recombination centers during S phase. *Proc Natl Acad Sci U S A*, **98**, 8276-8282.

Liu, S.C., Sauter, E.R., Clapper, M.L., Feldman, R.S., Levin, L., Chen, S.Y., Yen, T.J., Ross, E., Engstrom, P.F. and Klein-Szanto, A.J. (1998) Markers of cell proliferation in normal epithelia and dysplastic leukoplakias of the oral cavity. *Cancer Epidemiol Biomarkers Prev*, **7**, 597-603.

Loeb, L.A. (2001) A mutator phenotype in cancer. *Cancer Res*, **61**, 3230-3239.

Loeillet, S., Palancade, B., Cartron, M., Thierry, A., Richard, G.F., Dujon, B., Doye, V. and Nicolas, A. (2005) Genetic network interactions among replication, repair and nuclear pore deficiencies in yeast. *DNA Repair (Amst)*, **4**, 459-468.

Longtine, M.S., McKenzie, A., 3rd, Demarini, D.J., Shah, N.G., Wach, A., Brachat, A., Philippsen, P. and Pringle, J.R. (1998) Additional modules for versatile and economical PCR-based gene deletion and modification in Saccharomyces cerevisiae. *Yeast*, **14**, 953-961.

Losada, A., Hirano, M. and Hirano, T. (1998) Identification of Xenopus SMC protein complexes required for sister chromatid cohesion. *Genes Dev*, **12**, 1986-1997.

Luke, B., Versini, G., Jaquenoud, M., Zaidi, I.W., Kurz, T., Pintard, L., Pasero, P. and Peter, M. (2006) The cullin Rtt101p promotes replication fork progression through damaged DNA and natural pause sites. *Curr Biol*, **16**, 786-792.

Lum, P.Y., Armour, C.D., Stepaniants, S.B., Cavet, G., Wolf, M.K., Butler, J.S., Hinshaw, J.C., Garnier, P., Prestwich, G.D., Leonardson, A., Garrett-Engele, P., Rush, C.M., Bard, M., Schimmack, G., Phillips, J.W., Roberts, C.J. and Shoemaker, D.D. (2004) Discovering modes of action for therapeutic compounds using a genome-wide screen of yeast heterozygotes. *Cell*, **116**, 121-137.

Luo, X., Tang, Z., Rizo, J. and Yu, H. (2002) The Mad2 spindle checkpoint protein undergoes similar major conformational changes upon binding to either Mad1 or Cdc20. *Mol Cell*, **9**, 59-71.

Maddox, P.S., Bloom, K.S. and Salmon, E.D. (2000) The polarity and dynamics of microtubule assembly in the budding yeast Saccharomyces cerevisiae. *Nat Cell Biol*, **2**, 36-41.

Maine, G.T., Sinha, P. and Tye, B.K. (1984) Mutants of S. cerevisiae defective in the maintenance of minichromosomes. *Genetics*, **106**, 365-385.

Manchester, K.L. (1995) Theodor Boveri and the origin of malignant tumours. *Trends Cell Biol*, **5**, 384-387.

Manke, I.A., Lowery, D.M., Nguyen, A. and Yaffe, M.B. (2003) BRCT repeats as phosphopeptide-binding modules involved in protein targeting. *Science*, **302**, 636-639.

Mao, Y., Abrieu, A. and Cleveland, D.W. (2003) Activating and silencing the mitotic checkpoint through CENP-E-dependent activation/inactivation of BubR1. *Cell*, **114**, 87-98.

Marston, A.L., Tham, W.H., Shah, H. and Amon, A. (2004) A genome-wide screen identifies genes required for centromeric cohesion. *Science*, **303**, 1367-1370.

Matsuda, N., Azuma, K., Saijo, M., Iemura, S., Hioki, Y., Natsume, T., Chiba, T. and Tanaka, K. (2005) DDB2, the xeroderma pigmentosum group E gene product, is directly ubiquitylated by Cullin 4A-based ubiquitin ligase complex. *DNA Repair (Amst)*, **4**, 537-545.

Mayer, M.L., Gygi, S.P., Aebersold, R. and Hieter, P. (2001) Identification of RFC(Ctf18p, Ctf8p, Dcc1p): an alternative RFC complex required for sister chromatid cohesion in S. cerevisiae. *Mol Cell*, **7**, 959-970.

Mayer, M.L., Pot, I., Chang, M., Xu, H., Aneliunas, V., Kwok, T., Newitt, R., Aebersold, R., Boone, C., Brown, G.W. and Hieter, P. (2004) Identification of Protein Complexes Required for Efficient Sister Chromatid Cohesion. *Mol Biol Cell*.

McAinsh, A.D., Tytell, J.D. and Sorger, P.K. (2003) Structure, function, and regulation of budding yeast kinetochores. *Annu Rev Cell Dev Biol*, **19**, 519-539.

Measday, V., Baetz, K., Guzzo, J., Yuen, K., Kwok, T., Sheikh, B., Ding, H., Ueta, R., Hoac, T., Cheng, B., Pot, I., Tong, A., Yamaguchi-Iwai, Y., Boone, C., Hieter, P. and Andrews, B. (2005) Systematic yeast synthetic lethal and synthetic dosage lethal screens identify genes required for chromosome segregation. *Proc Natl Acad Sci U S A*, **102**, 13956-13961.

Measday, V., Hailey, D.W., Pot, I., Givan, S.A., Hyland, K.M., Cagney, G., Fields, S., Davis, T.N. and Hieter, P. (2002) Ctf3p, the Mis6 budding yeast homolog, interacts with Mcm22p and Mcm16p at the yeast outer kinetochore. *Genes Dev*, **16**, 101-113.

Measday, V. and Hieter, P. (2002) Synthetic dosage lethality. *Methods Enzymol*, **350**, 316-326.

Meeks-Wagner, D., Wood, J.S., Garvik, B. and Hartwell, L.H. (1986) Isolation of two genes that affect mitotic chromosome transmission in S. cerevisiae. *Cell*, **44**, 53-63.

Megee, P.C., Mistrot, C., Guacci, V. and Koshland, D. (1999) The centromeric sister chromatid cohesion site directs Mcd1p binding to adjacent sequences. *Mol Cell*, **4**, 445-450.

Michaelis, C., Ciosk, R. and Nasmyth, K. (1997) Cohesins: chromosomal proteins that prevent premature separation of sister chromatids. *Cell*, **91**, 35-45.

Michel, J.J., McCarville, J.F. and Xiong, Y. (2003) A role for Saccharomyces cerevisiae Cul8 ubiquitin ligase in proper anaphase progression. *J Biol Chem*, **278**, 22828-22837.

Michel, L., Diaz-Rodriguez, E., Narayan, G., Hernando, E., Murty, V.V. and Benezra, R. (2004) Complete loss of the tumor suppressor MAD2 causes premature cyclin B degradation and mitotic failure in human somatic cells. *Proc Natl Acad Sci U S A*, **101**, 4459-4464.

Michel, L.S., Liberal, V., Chatterjee, A., Kirchwegger, R., Pasche, B., Gerald, W., Dobles, M., Sorger, P.K., Murty, V.V. and Benezra, R. (2001) MAD2 haplo-insufficiency causes premature anaphase and chromosome instability in mammalian cells. *Nature*, **409**, 355-359.

Miller, K.M., Ferreira, M.G. and Cooper, J.P. (2005) Taz1, Rap1 and Rif1 act both interdependently and independently to maintain telomeres. *Embo J*, **24**, 3128-3135.

Miller, K.M., Rog, O. and Cooper, J.P. (2006) Semi-conservative DNA replication through telomeres requires Taz1. *Nature*, **440**, 824-828.

Mohaghegh, P. and Hickson, I.D. (2001) DNA helicase deficiencies associated with cancer predisposition and premature ageing disorders. *Hum Mol Genet*, **10**, 741-746.

Mullen, J.R., Nallaseth, F.S., Lan, Y.Q., Slagle, C.E. and Brill, S.J. (2005) Yeast Rmi1/Nce4 controls genome stability as a subunit of the Sgs1-Top3 complex. *Mol Cell Biol*, **25**, 4476-4487.

Musio, A., Montagna, C., Zambroni, D., Indino, E., Barbieri, O., Citti, L., Villa, A., Ried, T. and Vezzoni, P. (2003) Inhibition of BUB1 results in genomic instability and

anchorage-independent growth of normal human fibroblasts. *Cancer Res*, **63**, 2855-2863.

Musio, A., Selicorni, A., Focarelli, M.L., Gervasini, C., Milani, D., Russo, S., Vezzoni, P. and Larizza, L. (2006) X-linked Cornelia de Lange syndrome owing to SMC1L1 mutations. *Nat Genet*, **38**, 528-530.

Myung, K., Chen, C. and Kolodner, R.D. (2001a) Multiple pathways cooperate in the suppression of genome instability in Saccharomyces cerevisiae. *Nature*, **411**, 1073-1076.

Myung, K., Datta, A. and Kolodner, R.D. (2001b) Suppression of spontaneous chromosomal rearrangements by S phase checkpoint functions in Saccharomyces cerevisiae. *Cell*, **104**, 397-408.

Nasmyth, K. (2002) Segregating sister genomes: the molecular biology of chromosome separation. *Science*, **297**, 559-565.

Neshat, M.S., Mellinghoff, I.K., Tran, C., Stiles, B., Thomas, G., Petersen, R., Frost, P., Gibbons, J.J., Wu, H. and Sawyers, C.L. (2001) Enhanced sensitivity of PTEN-deficient tumors to inhibition of FRAP/mTOR. *Proc Natl Acad Sci U S A*, **98**, 10314-10319.

Newman, J.R., Wolf, E. and Kim, P.S. (2000) A computationally directed screen identifying interacting coiled coils from Saccharomyces cerevisiae. *Proc Natl Acad Sci U S A*, **97**, 13203-13208.

Ngo, V.N., Davis, R.E., Lamy, L., Yu, X., Zhao, H., Lenz, G., Lam, L.T., Dave, S., Yang, L., Powell, J. and Staudt, L.M. (2006) A loss-of-function RNA interference screen for molecular targets in cancer. *Nature*, **441**, 106-110.

Niedernhofer, L.J., Lalai, A.S. and Hoeijmakers, J.H. (2005) Fanconi anemia (cross)linked to DNA repair. *Cell*, **123**, 1191-1198.

Nonaka, N., Kitajima, T., Yokobayashi, S., Xiao, G., Yamamoto, M., Grewal, S.I. and Watanabe, Y. (2002) Recruitment of cohesin to heterochromatic regions by Swi6/HP1 in fission yeast. *Nat Cell Biol*, **4**, 89-93.

Ohshima, K., Haraoka, S., Yoshioka, S., Hamasaki, M., Fujiki, T., Suzumiya, J., Kawasaki, C., Kanda, M. and Kikuchi, M. (2000) Mutation analysis of mitotic checkpoint genes (hBUB1 and hBUBR1) and microsatellite instability in adult T-cell leukemia/lymphoma. *Cancer Lett*, **158**, 141-150.

Ohya, Y., Sese, J., Yukawa, M., Sano, F., Nakatani, Y., Saito, T.L., Saka, A., Fukuda, T., Ishihara, S., Oka, S., Suzuki, G., Watanabe, M., Hirata, A., Ohtani, M., Sawai, H., Fraysse, N., Latge, J.P., Francois, J.M., Aebi, M., Tanaka, S., Muramatsu, S., Araki, H., Sonoike, K., Nogami, S. and Morishita, S. (2005) High-dimensional and large-scale phenotyping of yeast mutants. *Proc Natl Acad Sci U S A*, **102**, 19015-19020.

Ooi, S.L., Pan, X., Peyser, B.D., Ye, P., Meluh, P.B., Yuan, D.S., Irizarry, R.A., Bader, J.S., Spencer, F.A. and Boeke, J.D. (2006) Global synthetic-lethality analysis and yeast functional profiling. *Trends Genet*, **22**, 56-63.

Ota, T., Suto, S., Katayama, H., Han, Z.B., Suzuki, F., Maeda, M., Tanino, M., Terada, Y. and Tatsuka, M. (2002) Increased mitotic phosphorylation of histone H3

attributable to AIM-1/Aurora-B overexpression contributes to chromosome number instability. *Cancer Res*, **62**, 5168-5177.

O'Toole, E.T., Winey, M. and McIntosh, J.R. (1999) High-voltage electron tomography of spindle pole bodies and early mitotic spindles in the yeast Saccharomyces cerevisiae. *Mol Biol Cell*, **10**, 2017-2031.

Ouspenski, II, Elledge, S.J. and Brinkley, B.R. (1999) New yeast genes important for chromosome integrity and segregation identified by dosage effects on genome stability. *Nucleic Acids Res*, **27**, 3001-3008.

Pan, X., Ye, P., Yuan, D.S., Wang, X., Bader, J.S. and Boeke, J.D. (2006) A DNA integrity network in the yeast Saccharomyces cerevisiae. *Cell*, **124**, 1069-1081.

Papadopoulos, N., Nicolaides, N.C., Wei, Y.F., Ruben, S.M., Carter, K.C., Rosen, C.A., Haseltine, W.A., Fleischmann, R.D., Fraser, C.M., Adams, M.D. and et al. (1994) Mutation of a mutL homolog in hereditary colon cancer. *Science*, **263**, 1625-1629.

Parsons, A.B., Brost, R.L., Ding, H., Li, Z., Zhang, C., Sheikh, B., Brown, G.W., Kane, P.M., Hughes, T.R. and Boone, C. (2004) Integration of chemical-genetic and genetic interaction data links bioactive compounds to cellular target pathways. *Nat Biotechnol*, **22**, 62-69.

Parsons, D.W., Wang, T.L., Samuels, Y., Bardelli, A., Cummins, J.M., DeLong, L., Silliman, N., Ptak, J., Szabo, S., Willson, J.K., Markowitz, S., Kinzler, K.W., Vogelstein, B., Lengauer, C. and Velculescu, V.E. (2005) Colorectal cancer: mutations in a signalling pathway. *Nature*, **436**, 792.

Pavri, R., Zhu, B., Li, G., Trojer, P., Mandal, S., Shilatifard, A. and Reinberg, D. (2006) Histone H2B Monoubiquitination Functions Cooperatively with FACT to Regulate Elongation by RNA Polymerase II. *Cell*, **125**, 703-717.

Paweletz, N. (2001) Walther Flemming: pioneer of mitosis research. *Nat Rev Mol Cell Biol*, **2**, 72-75.

Pei, L. and Melmed, S. (1997) Isolation and characterization of a pituitary tumor-transforming gene (PTTG). *Mol Endocrinol*, **11**, 433-441.

Petronczki, M., Chwalla, B., Siomos, M.F., Yokobayashi, S., Helmhart, W., Deutschbauer, A.M., Davis, R.W., Watanabe, Y. and Nasmyth, K. (2004) Sister-chromatid cohesion mediated by the alternative RF-CCtf18/Dcc1/Ctf8, the helicase Chl1 and the polymerase-alpha-associated protein Ctf4 is essential for chromatid disjunction during meiosis II. *J Cell Sci*, **117**, 3547-3559.

Pidoux, A.L. and Allshire, R.C. (2004) Kinetochore and heterochromatin domains of the fission yeast centromere. *Chromosome Res*, **12**, 521-534.

Pidoux, A.L. and Allshire, R.C. (2005) The role of heterochromatin in centromere function. *Philos Trans R Soc Lond B Biol Sci*, **360**, 569-579.

Pinsky, B.A. and Biggins, S. (2005) The spindle checkpoint: tension versus attachment. *Trends Cell Biol*, **15**, 486-493.

Pintard, L., Willems, A. and Peter, M. (2004) Cullin-based ubiquitin ligases: Cul3-BTB complexes join the family. *Embo J*, **23**, 1681-1687.

Pot, I., Measday, V., Snydsman, B., Cagney, G., Fields, S., Davis, T.N., Muller, E.G. and Hieter, P. (2003) Chl4p and iml3p are two new members of the budding yeast outer kinetochore. *Mol Biol Cell*, **14**, 460-476.

Prakash, L. and Prakash, S. (1977) Isolation and characterization of MMS-sensitive mutants of Saccharomyces cerevisiae. *Genetics*, **86**, 33-55.

Rajagopalan, H., Jallepalli, P.V., Rago, C., Velculescu, V.E., Kinzler, K.W., Vogelstein, B. and Lengauer, C. (2004) Inactivation of hCDC4 can cause chromosomal instability. *Nature*, **428**, 77-81.

Rajagopalan, H. and Lengauer, C. (2004a) Aneuploidy and cancer. *Nature*, **432**, 338-341.

Rajagopalan, H. and Lengauer, C. (2004b) hCDC4 and genetic instability in cancer. *Cell Cycle*, **3**, 693-694.

Rajagopalan, H., Nowak, M.A., Vogelstein, B. and Lengauer, C. (2003) The significance of unstable chromosomes in colorectal cancer. *Nat Rev Cancer*, **3**, 695-701.

Riedel, C.G., Katis, V.L., Katou, Y., Mori, S., Itoh, T., Helmhart, W., Galova, M., Petronczki, M., Gregan, J., Cetin, B., Mudrak, I., Ogris, E., Mechtler, K., Pelletier, L., Buchholz, F., Shirahige, K. and Nasmyth, K. (2006) Protein phosphatase 2A protects centromeric sister chromatid cohesion during meiosis I. *Nature*, **441**, 53-61.

Rieder, C.L., Cole, R.W., Khodjakov, A. and Sluder, G. (1995) The checkpoint delaying anaphase in response to chromosome monoorientation is mediated by an inhibitory signal produced by unattached kinetochores. *J Cell Biol*, **130**, 941-948.

Rieder, C.L. and Salmon, E.D. (1994) Motile kinetochores and polar ejection forces dictate chromosome position on the vertebrate mitotic spindle. *J Cell Biol*, **124**, 223-233.

Roberts, T.M., Kobor, M.S., Bastin-Shanower, S.A., Ii, M., Horte, S.A., Gin, J.W., Emili, A., Rine, J., Brill, S.J. and Brown, G.W. (2006) Slx4 regulates DNA damage checkpoint-dependent phosphorylation of the BRCT domain protein Rtt107/Esc4. *Mol Biol Cell*, **17**, 539-548.

Rollins, R.A., Korom, M., Aulner, N., Martens, A. and Dorsett, D. (2004) Drosophila nipped-B protein supports sister chromatid cohesion and opposes the stromalin/Scc3 cohesion factor to facilitate long-range activation of the cut gene. *Mol Cell Biol*, **24**, 3100-3111.

Rouse, J. (2004) Esc4p, a new target of Medp (ATR), promotes resumption of DNA synthesis after DNA damage. *Embo J*, **23**, 2914.

Ru, H.Y., Chen, R.L., Lu, W.C. and Chen, J.H. (2002) hBUB1 defects in leukemia and lymphoma cells. *Oncogene*, **21**, 4673-4679.

Rubin, G.M., Yandell, M.D., Wortman, J.R., Gabor Miklos, G.L., Nelson, C.R., Hariharan, I.K., Fortini, M.E., Li, P.W., Apweiler, R., Fleischmann, W., Cherry, J.M., Henikoff, S., Skupski, M.P., Misra, S., Ashburner, M., Birney, E., Boguski, M.S., Brody, T., Brokstein, P., Celniker, S.E., Chervitz, S.A., Coates, D., Cravchik, A., Gabrielian, A., Galle, R.F., Gelbart, W.M., George, R.A., Goldstein, L.S., Gong, F., Guan, P., Harris, N.L., Hay, B.A., Hoskins, R.A., Li, J., Li, Z., Hynes, R.O., Jones, S.J., Kuehl, P.M., Lemaitre, B., Littleton, J.T., Morrison, D.K., Mungall, C., O'Farrell, P.H., Pickeral, O.K., Shue, C., Vosshall, L.B., Zhang, J., Zhao, Q., Zheng, X.H. and Lewis, S. (2000) Comparative genomics of the eukaryotes. *Science*, **287**, 2204-2215.

Rutherford, J.C. and Bird, A.J. (2004) Metal-responsive transcription factors that regulate iron, zinc, and copper homeostasis in eukaryotic cells. *Eukaryot Cell*, **3**, 1-13.

S, L.H. (2000) CHL1 is a nuclear protein with an essential ATP binding site that exhibits a size-dependent effect on chromosome segregation. *Nucleic Acids Res*, **28**, 3056-3064.

Saeki, A., Tamura, S., Ito, N., Kiso, S., Matsuda, Y., Yabuuchi, I., Kawata, S. and Matsuzawa, Y. (2002) Frequent impairment of the spindle assembly checkpoint in hepatocellular carcinoma. *Cancer*, **94**, 2047-2054.

Sager, J.A. and Lengauer, C. (2003) New paradigms for cancer drug discovery. *Cancer Biol Ther*, **2**, 452-455.

Sarafan-Vasseur, N., Lamy, A., Bourguignon, J., Pessot, F.L., Hieter, P., Sesboue, R., Bastard, C., Frebourg, T. and Flaman, J.M. (2002) Overexpression of B-type cyclins alters chromosomal segregation. *Oncogene*, **21**, 2051-2057.

Saunders, W.S., Shuster, M., Huang, X., Gharaibeh, B., Enyenihi, A.H., Petersen, I. and Gollin, S.M. (2000) Chromosomal instability and cytoskeletal defects in oral cancer cells. *Proc Natl Acad Sci U S A*, **97**, 303-308.

Savitsky, K., Bar-Shira, A., Gilad, S., Rotman, G., Ziv, Y., Vanagaite, L., Tagle, D.A., Smith, S., Uziel, T., Sfez, S. and et al. (1995) A single ataxia telangiectasia gene with a product similar to PI-3 kinase. *Science*, **268**, 1749-1753.

Scholes, D.T., Banerjee, M., Bowen, B. and Curcio, M.J. (2001) Multiple regulators of Ty1 transposition in Saccharomyces cerevisiae have conserved roles in genome maintenance. *Genetics*, **159**, 1449-1465.

Schule, B., Oviedo, A., Johnston, K., Pai, S. and Francke, U. (2005) Inactivating mutations in ESCO2 cause SC phocomelia and Roberts syndrome: no phenotype-genotype correlation. *Am J Hum Genet*, **77**, 1117-1128.

Schultz, J., Marshall-Carlson, L. and Carlson, M. (1990) The N-terminal TPR region is the functional domain of SSN6, a nuclear phosphoprotein of Saccharomyces cerevisiae. *Mol Cell Biol*, **10**, 4744-4756.

Sharp, J.A. and Kaufman, P.D. (2003) Chromatin proteins are determinants of centromere function. *Curr Top Microbiol Immunol*, **274**, 23-52.

Shelby, R.D., Hahn, K.M. and Sullivan, K.F. (1996) Dynamic elastic behavior of alpha-satellite DNA domains visualized in situ in living human cells. *J Cell Biol*, **135**, 545-557.

Shero, J.H., Koval, M., Spencer, F., Palmer, R.E., Hieter, P. and Koshland, D. (1991) Analysis of chromosome segregation in Saccharomyces cerevisiae. *Methods Enzymol*, **194**, 749-773.

Shichiri, M., Yoshinaga, K., Hisatomi, H., Sugihara, K. and Hirata, Y. (2002) Genetic and epigenetic inactivation of mitotic checkpoint genes hBUB1 and hBUBR1 and their relationship to survival. *Cancer Res*, **62**, 13-17.

Shigeishi, H., Mizuta, K., Higashikawa, K., Yoneda, S., Ono, S. and Kamata, N. (2005) Correlation of CENP-F gene expression with tumor-proliferating activity in human salivary gland tumors. *Oral Oncol.*

Shih, I.M., Zhou, W., Goodman, S.N., Lengauer, C., Kinzler, K.W. and Vogelstein, B. (2001) Evidence that genetic instability occurs at an early stage of colorectal tumorigenesis. *Cancer Res*, **61**, 818-822.

Shima, N., Hartford, S.A., Duffy, T., Wilson, L.A., Schimenti, K.J. and Schimenti, J.C. (2003) Phenotype-based identification of mouse chromosome instability mutants. *Genetics*, **163**, 1031-1040.

Shoemaker, D.D., Lashkari, D.A., Morris, D., Mittmann, M. and Davis, R.W. (1996) Quantitative phenotypic analysis of yeast deletion mutants using a highly parallel molecular bar-coding strategy. *Nat Genet*, **14**, 450-456.

Shor, E., Weinstein, J. and Rothstein, R. (2005) A genetic screen for top3 suppressors in Saccharomyces cerevisiae identifies SHU1, SHU2, PSY3 and CSM2: four genes involved in error-free DNA repair. *Genetics*, **169**, 1275-1289.

Sieber, O.M., Heinimann, K. and Tomlinson, I.P. (2003) Genomic instability--the engine of tumorigenesis? *Nat Rev Cancer*, **3**, 701-708.

Simon, J.A., Szankasi, P., Nguyen, D.K., Ludlow, C., Dunstan, H.M., Roberts, C.J., Jensen, E.L., Hartwell, L.H. and Friend, S.H. (2000) Differential toxicities of anticancer agents among DNA repair and checkpoint mutants of Saccharomyces cerevisiae. *Cancer Res*, **60**, 328-333.

Sjoblom, T., Jones, S., Wood, L.D., Parsons, D.W., Lin, J., Barber, T., Mandelker, D., Leary, R.J., Ptak, J., Silliman, N., Szabo, S., Buckhaults, P., Farrell, C., Meeh, P., Markowitz, S.D., Willis, J., Dawson, D., Willson, J.K., Gazdar, A.F., Hartigan, J., Wu, L., Liu, C., Parmigiani, G., Park, B.H., Bachman, K.E., Papadopoulos, N., Vogelstein, B., Kinzler, K.W. and Velculescu, V.E. (2006) The Consensus Coding Sequences of Human Breast and Colorectal Cancers. *Science*.

Skibbens, R.V. (2004) Chl1p, a DNA helicase-like protein in budding yeast, functions in sister-chromatid cohesion. *Genetics*, **166**, 33-42.

Skibbens, R.V., Corson, L.B., Koshland, D. and Hieter, P. (1999) Ctf7p is essential for sister chromatid cohesion and links mitotic chromosome structure to the DNA replication machinery. *Genes Dev*, **13**, 307-319.

Smith, R.L. and Johnson, A.D. (2000) Turning genes off by Ssn6-Tup1: a conserved system of transcriptional repression in eukaryotes. *Trends Biochem Sci*, **25**, 325-330.

Smith, S., Hwang, J.Y., Banerjee, S., Majeed, A., Gupta, A. and Myung, K. (2004) Mutator genes for suppression of gross chromosomal rearrangements identified by a genome-wide screening in Saccharomyces cerevisiae. *Proc Natl Acad Sci U S A*, **101**, 9039-9044.

Sopko, R., Huang, D., Preston, N., Chua, G., Papp, B., Kafadar, K., Snyder, M., Oliver, S.G., Cyert, M., Hughes, T.R., Boone, C. and Andrews, B. (2006) Mapping pathways and phenotypes by systematic gene overexpression. *Mol Cell*, **21**, 319-330.

Sorrentino, R., Libertini, S., Pallante, P.L., Troncone, G., Palombini, L., Bavetsias, V., Spalletti-Cernia, D., Laccetti, P., Linardopoulos, S., Chieffi, P., Fusco, A. and Portella, G. (2005) Aurora B overexpression associates with the thyroid

carcinoma undifferentiated phenotype and is required for thyroid carcinoma cell proliferation. *J Clin Endocrinol Metab*, **90**, 928-935.

Spencer, F., Gerring, S.L., Connelly, C. and Hieter, P. (1990) Mitotic chromosome transmission fidelity mutants in Saccharomyces cerevisiae. *Genetics*, **124**, 237-249.

Stark, C., Breitkreutz, B.J., Reguly, T., Boucher, L., Breitkreutz, A. and Tyers, M. (2006) BioGRID: a general repository for interaction datasets. *Nucleic Acids Res*, **34**, D535-539.

Stern, B.M. and Murray, A.W. (2001) Lack of tension at kinetochores activates the spindle checkpoint in budding yeast. *Curr Biol*, **11**, 1462-1467.

Stewart, G.S., Maser, R.S., Stankovic, T., Bressan, D.A., Kaplan, M.I., Jaspers, N.G., Raams, A., Byrd, P.J., Petrini, J.H. and Taylor, A.M. (1999) The DNA double-strand break repair gene hMRE11 is mutated in individuals with an ataxia-telangiectasia-like disorder. *Cell*, **99**, 577-587.

Stoler, S., Keith, K.C., Curnick, K.E. and Fitzgerald-Hayes, M. (1995) A mutation in CSE4, an essential gene encoding a novel chromatin-associated protein in yeast, causes chromosome nondisjunction and cell cycle arrest at mitosis. *Genes Dev*, **9**, 573-586.

Storchova, Z., Breneman, A., Cande, J., Dunn, J., Burbank, K., O'Toole, E. and Pellman, D. (2006) Genome-wide genetic analysis of polyploidy in yeast. *Nature*, **443**, 541-547.

Storchova, Z. and Pellman, D. (2004) From polyploidy to aneuploidy, genome instability and cancer. *Nat Rev Mol Cell Biol*, **5**, 45-54.

Straight, A.F., Belmont, A.S., Robinett, C.C. and Murray, A.W. (1996) GFP tagging of budding yeast chromosomes reveals that protein-protein interactions can mediate sister chromatid cohesion. *Curr Biol*, **6**, 1599-1608.

Strand, M., Prolla, T.A., Liskay, R.M. and Petes, T.D. (1993) Destabilization of tracts of simple repetitive DNA in yeast by mutations affecting DNA mismatch repair. *Nature*, **365**, 274-276.

Strathern, J., Hicks, J. and Herskowitz, I. (1981) Control of cell type in yeast by the mating type locus. The alpha 1-alpha 2 hypothesis. *J Mol Biol*, **147**, 357-372.

Strohmaier, H., Spruck, C.H., Kaiser, P., Won, K.A., Sangfelt, O. and Reed, S.I. (2001) Human F-box protein hCdc4 targets cyclin E for proteolysis and is mutated in a breast cancer cell line. *Nature*, **413**, 316-322.

Strom, L., Lindroos, H.B., Shirahige, K. and Sjogren, C. (2004) Postreplicative recruitment of cohesin to double-strand breaks is required for DNA repair. *Mol Cell*, **16**, 1003-1015.

Sudakin, V., Chan, G.K. and Yen, T.J. (2001) Checkpoint inhibition of the APC/C in HeLa cells is mediated by a complex of BUBR1, BUB3, CDC20, and MAD2. *J Cell Biol*, **154**, 925-936.

Takahashi, T., Haruki, N., Nomoto, S., Masuda, A., Saji, S. and Osada, H. (1999) Identification of frequent impairment of the mitotic checkpoint and molecular analysis of the mitotic checkpoint genes, hsMAD2 and p55CDC, in human lung cancers. *Oncogene*, **18**, 4295-4300.

Takayama, Y., Kamimura, Y., Okawa, M., Muramatsu, S., Sugino, A. and Araki, H. (2003) GINS, a novel multiprotein complex required for chromosomal DNA replication in budding yeast. *Genes Dev*, **17**, 1153-1165.

Tanaka, T., Fuchs, J., Loidl, J. and Nasmyth, K. (2000) Cohesin ensures bipolar attachment of microtubules to sister centromeres and resists their precocious separation. *Nat Cell Biol*, **2**, 492-499.

Tanaka, T.U. (2002) Bi-orienting chromosomes on the mitotic spindle. *Curr Opin Cell Biol*, **14**, 365-371.

Tao, W. (2005) The mitotic checkpoint in cancer therapy. *Cell Cycle*, **4**, 1495-1499.

Tatsuka, M., Katayama, H., Ota, T., Tanaka, T., Odashima, S., Suzuki, F. and Terada, Y. (1998) Multinuclearity and increased ploidy caused by overexpression of the aurora- and Ipl1-like midbody-associated protein mitotic kinase in human cancer cells. *Cancer Res*, **58**, 4811-4816.

Thiagalingam, S., Laken, S., Willson, J.K., Markowitz, S.D., Kinzler, K.W., Vogelstein, B. and Lengauer, C. (2001) Mechanisms underlying losses of heterozygosity in human colorectal cancers. *Proc Natl Acad Sci U S A*, **98**, 2698-2702.

Tomonaga, T., Matsushita, K., Ishibashi, M., Nezu, M., Shimada, H., Ochiai, T., Yoda, K. and Nomura, F. (2005) Centromere protein H is up-regulated in primary human colorectal cancer and its overexpression induces aneuploidy. *Cancer Res*, **65**, 4683-4689.

Tomonaga, T., Matsushita, K., Yamaguchi, S., Oohashi, T., Shimada, H., Ochiai, T., Yoda, K. and Nomura, F. (2003) Overexpression and mistargeting of centromere protein-A in human primary colorectal cancer. *Cancer Res*, **63**, 3511-3516.

Tong, A.H., Evangelista, M., Parsons, A.B., Xu, H., Bader, G.D., Page, N., Robinson, M., Raghibizadeh, S., Hogue, C.W., Bussey, H., Andrews, B., Tyers, M. and Boone, C. (2001a) Systematic genetic analysis with ordered arrays of yeast deletion mutants. *Science*, **294**, 2364-2368.

Tong, A.H., Lesage, G., Bader, G.D., Ding, H., Xu, H., Xin, X., Young, J., Berriz, G.F., Brost, R.L., Chang, M., Chen, Y., Cheng, X., Chua, G., Friesen, H., Goldberg, D.S., Haynes, J., Humphries, C., He, G., Hussein, S., Ke, L., Krogan, N., Li, Z., Levinson, J.N., Lu, H., Menard, P., Munyana, C., Parsons, A.B., Ryan, O., Tonikian, R., Roberts, T., Sdicu, A.M., Shapiro, J., Sheikh, B., Suter, B., Wong, S.L., Zhang, L.V., Zhu, H., Burd, C.G., Munro, S., Sander, C., Rine, J., Greenblatt, J., Peter, M., Bretscher, A., Bell, G., Roth, F.P., Brown, G.W., Andrews, B., Bussey, H. and Boone, C. (2004) Global mapping of the yeast genetic interaction network. *Science*, **303**, 808-813.

Tong, A.H.Y., Evangelista, M., Parsons, A.B., Xu, H., Bader, G.D., Page, N., Robinson, M., Raghibizadeh, S., Hogue, C.W.V., Bussey, H., Andrews, B., Tyers, M. and Boone, C. (2001b) Systematic Genetic Analysis with Ordered Arrays of Yeast Deletion Mutants. *Science*, **294**, 2364-2368.

Tonkin, E.T., Wang, T.J., Lisgo, S., Bamshad, M.J. and Strachan, T. (2004) NIPBL, encoding a homolog of fungal Scc2-type sister chromatid cohesion proteins and fly Nipped-B, is mutated in Cornelia de Lange syndrome. *Nat Genet*, **36**, 636-641.

Torrance, C.J., Agrawal, V., Vogelstein, B. and Kinzler, K.W. (2001) Use of isogenic human cancer cells for high-throughput screening and drug discovery. *Nat Biotechnol*, **19**, 940-945.

Toth, A., Ciosk, R., Uhlmann, F., Galova, M., Schleiffer, A. and Nasmyth, K. (1999) Yeast cohesin complex requires a conserved protein, Eco1p(Ctf7), to establish cohesion between sister chromatids during DNA replication. *Genes Dev*, **13**, 320-333.

Toth, A., Rabitsch, K.P., Galova, M., Schleiffer, A., Buonomo, S.B. and Nasmyth, K. (2000) Functional genomics identifies monopolin: a kinetochore protein required for segregation of homologs during meiosis i. *Cell*, **103**, 1155-1168.

Tutt, A., Gabriel, A., Bertwistle, D., Connor, F., Paterson, H., Peacock, J., Ross, G. and Ashworth, A. (1999) Absence of Brca2 causes genome instability by chromosome breakage and loss associated with centrosome amplification. *Curr Biol*, **9**, 1107-1110.

Uetz, P., Giot, L., Cagney, G., Mansfield, T.A., Judson, R.S., Knight, J.R., Lockshon, D., Narayan, V., Srinivasan, M., Pochart, P., Qureshi-Emili, A., Li, Y., Godwin, B., Conover, D., Kalbfleisch, T., Vijayadamodar, G., Yang, M., Johnston, M., Fields, S. and Rothberg, J.M. (2000) A comprehensive analysis of protein-protein interactions in Saccharomyces cerevisiae. *Nature*, **403**, 623-627.

Uhlmann, F., Lottspeich, F. and Nasmyth, K. (1999) Sister-chromatid separation at anaphase onset is promoted by cleavage of the cohesin subunit Scc1. *Nature*, **400**, 37-42.

Uhlmann, F., Wernic, D., Poupart, M.A., Koonin, E.V. and Nasmyth, K. (2000) Cleavage of cohesin by the CD clan protease separin triggers anaphase in yeast. *Cell*, **103**, 375-386.

Unal, E., Arbel-Eden, A., Sattler, U., Shroff, R., Lichten, M., Haber, J.E. and Koshland, D. (2004) DNA damage response pathway uses histone modification to assemble a double-strand break-specific cohesin domain. *Mol Cell*, **16**, 991-1002.

van Haaften, G., Plasterk, R.H. and Tijsterman, M. (2004) Genomic instability and cancer: scanning the Caenorhabditis elegans genome for tumor suppressors. *Oncogene*, **23**, 8366-8375.

Van Hooser, A.A., Ouspenski, II, Gregson, H.C., Starr, D.A., Yen, T.J., Goldberg, M.L., Yokomori, K., Earnshaw, W.C., Sullivan, K.F. and Brinkley, B.R. (2001) Specification of kinetochore-forming chromatin by the histone H3 variant CENP-A. *J Cell Sci*, **114**, 3529-3542.

Varley, J.M., McGown, G., Thorncroft, M., Santibanez-Koref, M.F., Kelsey, A.M., Tricker, K.J., Evans, D.G. and Birch, J.M. (1997) Germ-line mutations of TP53 in Li-Fraumeni families: an extended study of 39 families. *Cancer Res*, **57**, 3245-3252.

Varon, R., Vissinga, C., Platzer, M., Cerosaletti, K.M., Chrzanowska, K.H., Saar, K., Beckmann, G., Seemanova, E., Cooper, P.R., Nowak, N.J., Stumm, M., Weemaes, C.M., Gatti, R.A., Wilson, R.K., Digweed, M., Rosenthal, A., Sperling, K., Concannon, P. and Reis, A. (1998) Nibrin, a novel DNA double-strand break repair protein, is mutated in Nijmegen breakage syndrome. *Cell*, **93**, 467-476.

Vega, H., Waisfisz, Q., Gordillo, M., Sakai, N., Yanagihara, I., Yamada, M., van Gosliga, D., Kayserili, H., Xu, C., Ozono, K., Jabs, E.W., Inui, K. and Joenje, H. (2005) Roberts syndrome is caused by mutations in ESCO2, a human homolog of yeast ECO1 that is essential for the establishment of sister chromatid cohesion. *Nat Genet*, **37**, 468-470.

Vogelstein, B. and Kinzler, K.W. (2004) Cancer genes and the pathways they control. *Nat Med*, **10**, 789-799.

Volpe, T.A., Kidner, C., Hall, I.M., Teng, G., Grewal, S.I. and Martienssen, R.A. (2002) Regulation of heterochromatic silencing and histone H3 lysine-9 methylation by RNAi. *Science*, **297**, 1833-1837.

Wang, G., Ma, A., Chow, C.M., Horsley, D., Brown, N.R., Cowell, I.G. and Singh, P.B. (2000a) Conservation of heterochromatin protein 1 function. *Mol Cell Biol*, **20**, 6970-6983.

Wang, R.H., Yu, H. and Deng, C.X. (2004a) A requirement for breast-cancer-associated gene 1 (BRCA1) in the spindle checkpoint. *Proc Natl Acad Sci U S A*, **101**, 17108-17113.

Wang, T.L., Rago, C., Silliman, N., Ptak, J., Markowitz, S., Willson, J.K., Parmigiani, G., Kinzler, K.W., Vogelstein, B. and Velculescu, V.E. (2002a) Prevalence of somatic alterations in the colorectal cancer cell genome. *Proc Natl Acad Sci U S A*, **99**, 3076-3080.

Wang, X., Jin, D.Y., Ng, R.W., Feng, H., Wong, Y.C., Cheung, A.L. and Tsao, S.W. (2002b) Significance of MAD2 expression to mitotic checkpoint control in ovarian cancer cells. *Cancer Res*, **62**, 1662-1668.

Wang, X., Jin, D.Y., Wong, Y.C., Cheung, A.L., Chun, A.C., Lo, A.K., Liu, Y. and Tsao, S.W. (2000b) Correlation of defective mitotic checkpoint with aberrantly reduced expression of MAD2 protein in nasopharyngeal carcinoma cells. *Carcinogenesis*, **21**, 2293-2297.

Wang, Z., Cummins, J.M., Shen, D., Cahill, D.P., Jallepalli, P.V., Wang, T.L., Parsons, D.W., Traverso, G., Awad, M., Silliman, N., Ptak, J., Szabo, S., Willson, J.K., Markowitz, S.D., Goldberg, M.L., Karess, R., Kinzler, K.W., Vogelstein, B., Velculescu, V.E. and Lengauer, C. (2004b) Three classes of genes mutated in colorectal cancers with chromosomal instability. *Cancer Res*, **64**, 2998-3001.

Warren, C.D., Brady, D.M., Johnston, R.C., Hanna, J.S., Hardwick, K.G. and Spencer, F.A. (2002) Distinct chromosome segregation roles for spindle checkpoint proteins. *Mol Biol Cell*, **13**, 3029-3041.

Warren, C.D., Eckley, D.M., Lee, M.S., Hanna, J.S., Hughes, A., Peyser, B., Jie, C., Irizarry, R. and Spencer, F.A. (2004a) S-Phase Checkpoint Genes Safeguard High Fidelity Sister Chromatid Cohesion. *Mol Biol Cell.*

Warren, C.D., Eckley, D.M., Lee, M.S., Hanna, J.S., Hughes, A., Peyser, B., Jie, C., Irizarry, R. and Spencer, F.A. (2004b) S-phase checkpoint genes safeguard high-fidelity sister chromatid cohesion. *Mol Biol Cell*, **15**, 1724-1735.

Wassmann, K., Liberal, V. and Benezra, R. (2003) Mad2 phosphorylation regulates its association with Mad1 and the APC/C. *Embo J*, **22**, 797-806.

Weaver, B.A. and Cleveland, D.W. (2005) Decoding the links between mitosis, cancer, and chemotherapy: The mitotic checkpoint, adaptation, and cell death. *Cancer Cell*, **8**, 7-12.

Weaver, Z., Montagna, C., Xu, X., Howard, T., Gadina, M., Brodie, S.G., Deng, C.X. and Ried, T. (2002) Mammary tumors in mice conditionally mutant for Brca1 exhibit gross genomic instability and centrosome amplification yet display a recurring distribution of genomic imbalances that is similar to human breast cancer. *Oncogene*, **21**, 5097-5107.

Weber, S.A., Gerton, J.L., Polancic, J.E., DeRisi, J.L., Koshland, D. and Megee, P.C. (2004) The kinetochore is an enhancer of pericentric cohesin binding. *PLoS Biol*, **2**, E260.

Weiss, E. and Winey, M. (1996) The Saccharomyces cerevisiae spindle pole body duplication gene MPS1 is part of a mitotic checkpoint. *J Cell Biol*, **132**, 111-123.

Wigge, P.A. and Kilmartin, J.V. (2001) The Ndc80p complex from Saccharomyces cerevisiae contains conserved centromere components and has a function in chromosome segregation. *J Cell Biol*, **152**, 349-360.

Willingham, A.T., Deveraux, Q.L., Hampton, G.M. and Aza-Blanc, P. (2004) RNAi and HTS: exploring cancer by systematic loss-of-function. *Oncogene*, **23**, 8392-8400.

Winey, M. and Huneycutt, B.J. (2002) Centrosomes and checkpoints: the MPS1 family of kinases. *Oncogene*, **21**, 6161-6169.

Winey, M. and O'Toole, E.T. (2001) The spindle cycle in budding yeast. *Nat Cell Biol*, **3**, E23-27.

Winzeler, E.A., Shoemaker, D.D., Astromoff, A., Liang, H., Anderson, K., Andre, B., Bangham, R., Benito, R., Boeke, J.D., Bussey, H., Chu, A.M., Connelly, C., Davis, K., Dietrich, F., Dow, S.W., El Bakkoury, M., Foury, F., Friend, S.H., Gentalen, E., Giaever, G., Hegemann, J.H., Jones, T., Laub, M., Liao, H., Davis, R.W. and et al. (1999) Functional characterization of the S. cerevisiae genome by gene deletion and parallel analysis. *Science*, **285**, 901-906.

Wittmann, T., Hyman, A. and Desai, A. (2001) The spindle: a dynamic assembly of microtubules and motors. *Nat Cell Biol*, **3**, E28-34.

Wojcik, E., Basto, R., Serr, M., Scaerou, F., Karess, R. and Hays, T. (2001) Kinetochore dynein: its dynamics and role in the transport of the Rough deal checkpoint protein. *Nat Cell Biol*, **3**, 1001-1007.

Yanagida, M. (2005) Basic mechanism of eukaryotic chromosome segregation. *Philos Trans R Soc Lond B Biol Sci*, **360**, 609-621.

Yang, X., Yu, K., Hao, Y., Li, D.M., Stewart, R., Insogna, K.L. and Xu, T. (2004) LATS1 tumour suppressor affects cytokinesis by inhibiting LIMK1. *Nat Cell Biol*, **6**, 609-617.

Yang, Z., Guo, J., Chen, Q., Ding, C., Du, J. and Zhu, X. (2005) Silencing mitosin induces misaligned chromosomes, premature chromosome decondensation before anaphase onset, and mitotic cell death. *Mol Cell Biol*, **25**, 4062-4074.

Yang, Z.Y., Guo, J., Li, N., Qian, M., Wang, S.N. and Zhu, X.L. (2003) Mitosin/CENP-F is a conserved kinetochore protein subjected to cytoplasmic dynein-mediated poleward transport. *Cell Res*, **13**, 275-283.

Yates, J.R., 3rd, Eng, J.K., McCormack, A.L. and Schieltz, D. (1995) Method to correlate tandem mass spectra of modified peptides to amino acid sequences in the protein database. *Anal Chem*, **67**, 1426-1436.

Yu, H. (2002) Regulation of APC-Cdc20 by the spindle checkpoint. *Curr Opin Cell Biol*, **14**, 706-714.

Yu, L., L, P.C., Mnaimneh, S., Hughes, T.R. and Brown, G.W. (2006) A Survey of Essential Gene Function in the Yeast Cell Division Cycle. *Mol Biol Cell*.

Yuen, K.W., Montpetit, B. and Hieter, P. (2005) The kinetochore and cancer: what's the connection? *Curr Opin Cell Biol*, **17**, 576-582.

Zhang, X., Horwitz, G.A., Heaney, A.P., Nakashima, M., Prezant, T.R., Bronstein, M.D. and Melmed, S. (1999) Pituitary tumor transforming gene (PTTG) expression in pituitary adenomas. *J Clin Endocrinol Metab*, **84**, 761-767.

Zhou, H., Kuang, J., Zhong, L., Kuo, W.L., Gray, J.W., Sahin, A., Brinkley, B.R. and Sen, S. (1998) Tumour amplified kinase STK15/BTAK induces centrosome amplification, aneuploidy and transformation. *Nat Genet*, **20**, 189-193.

Zhu, B., Zheng, Y., Pham, A.D., Mandal, S.S., Erdjument-Bromage, H., Tempst, P. and Reinberg, D. (2005) Monoubiquitination of human histone H2B: the factors involved and their roles in HOX gene regulation. *Mol Cell*, **20**, 601-611.

Zou, H., McGarry, T.J., Bernal, T. and Kirschner, M.W. (1999) Identification of a vertebrate sister-chromatid separation inhibitor involved in transformation and tumorigenesis. *Science*, **285**, 418-422.

APPENDICES

Appendix 1 High confidence yeast CIN genes identified by the 3 marker loss screens

A total of 130 high confidence *yko*Δ mutants (including 115 mutants with phenotypes in >1 screen, and 15 mutants with phenotype in only 1 screen but individually verified in independent transformants) are shown. Numerical scales are used to indicate phenotype severity. In all cases, "0" indicates a phenotype indistinguishable from wild-type. A score $\geq$1 in the *ctf* column indicates severity of the sectoring phenotype as determined by visual inspection (3>2>1). The numbers in the bimater column indicate an estimated fold-increase in frequency of mated product formation compared to wild-type diploid, ranging from 2- to 5-fold. The numbers in the a-like faker column indicate a calculated fold-increase in frequency of mated products above the wild-type parental *MAT*α, ranging from 2- to 80-fold. In each assay, phenotypes ranging from prominent to subtle were noted. Subtle phenotypes that were reproducible are included. These may represent mutants that are subject to partial compensation from redundant pathways, and their contribution to genome stability may be enhanced under other growth conditions.

Failure in mutant verification by tag sequencing is indicated as "wrong" (incorrect strain(s) present), "contam" (correct strain present but a contaminating strain was also evident), or "nd" (not determined because the sequence obtained was unreadable, or that deletion collection contained no yeast to validate).

The GO annotations provided are from SGD (www.yeastgenome.org/gene_list.shtml) as of January 24, 2005. Because some phenotypes may be derived from disruption of overlapping genes, the presence of these is noted as well (data from Saccharomyces Genome Deletion Project website as of December 3, 2004, www-sequence.stanford.edu/group/yeast_deletion_project/deletions3.html). Also, a small number of phenotype adjustments made after the screens were completed is noted, and mutants that were reconfirmed in independent transformants are also indicated.

Index	ORF name	Gene Name	CTF	BiM	ALF	GO Biological Process	GO Molecular Funciton	GO Cellular Component	Description on SGD	Overlapping ORF	Overlapping Gene Name	Overlapping yeast CIN genes ?	Adjustment Notes	Reconfirmation with new transformants
1	YHR191C	CTF8	3	6	18	mitotic sister chromatid cohesion	molecular_function unknown	DNA replication factor C complex	Subunit of a complex with Ctf18p that shares some subunits with Replication Factor C and is required for sister chromatid cohesion	#N/A	#N/A		bimater data in independent test (K Yuen, T Kwok, data not shown). Missed in high throughput screen.	a-like faker phentoype reconfirmed in independent test (K Yuen, T Kwok, data not shown).
2	YLR079W	SIC1	3	6	31	G1/S transition of mitotic cell cycle*	protein binding*	cytoplasm*	P40 inhibitor of Cdc28p-Clb5p protein kinase complex	#N/A	#N/A		bimater data in independent test (K Yuen, T Kwok, data not shown). Contaminating strain also in homo dip well in high throughput screen.	ctf and a-like faker phentoype reconfirmed in independent test (K Yuen, T Kwok, data not shown).
3	YPR135W	CTF4	3	5	27	DNA repair*	DNA binding	nucleus*	Chromatin-associated protein, required for sister chromatid cohesion; interacts with DNA polymerase alpha (Pol1p) and may link DNA synthesis to sister chromatid cohesion	#N/A	#N/A			
4	YCL016C	DCC1	3	5	18	mitotic sister chromatid cohesion	molecular_function unknown	DNA replication factor C complex	Subunit of a complex with Ctf8p and Ctf18p that shares some components with Replication Factor C, required for sister chromatid cohesion	#N/A	#N/A		ctf data from independent test (K Yuen, T Kwok, data not shown). Missed in high throughput screen.	
5	YER016W	BIM1	3	5	16	microtubule nucleation*	structural constituent of cytoskeleton	spindle pole body*	Microtubule-binding protein that together with Kar9p makes up the cortical microtubule capture site and delays the exit from mitosis when the spindle is oriented abnormally	#N/A	#N/A			
6	YMR048W	CSM3	3	5	12	meiotic chromosome segregation*	molecular_function unknown	nucleus	Protein required for accurate chromosome segregation during meiosis	#N/A	#N/A			
7	YNL273W	TOF1	3	5	10	DNA replication checkpoint*	molecular_function unknown	nuclear chromosome	Protein that interacts with topoisomerase I	#N/A	#N/A			
8	YBR107C	IML3	3	5	9	chromosome segregation	molecular_function unknown	outer kinetochore of condensed nuclear chromosome	Protein with a role in kinetochore function, localizes to the outer kinetochore in a Ctf19p-dependent manner, interacts with Chl4p and Ctf19p	#N/A	#N/A			
9	YPL008W	CHL1	3	5	7	chromosome segregation*	DNA helicase activity	nucleus	Required for mitotic chromosome segregation, needed for wild-type levels of meiotic . recombination and spore viability; kinetochore protein in the DEAH box family	#N/A	#N/A			
10	YDR318W	MCM21	3	5	3	chromosome segregation	protein binding	condensed nuclear chromosome kinetochore*	Protein involved in minichromosome maintenance; component of the COMA complex that bridges kinetochore subunits that are in contact with centromeric DNA and the subunits bound to microtubules	#N/A	#N/A			
11	YDR014W	RAD61	3	4	5	response to radiation	molecular_function unknown	nucleus	Protein of unknown function; mutation confers radiation sensitivity	#N/A	#N/A			

12	YPR046W	MCM16	3	4	4	chromosome segregation	protein binding	condensed nuclear chromosome kinetochore	Protein involved in kinetochore-microtubule mediated chromosome segregation; binds to centromere DNA	#N/A	#N/A			
13	YJR135C	MCM22	3	4	4	chromosome segregation	protein binding	condensed nuclear chromosome kinetochore	Protein involved in minichromosome maintenance; component of the kinetochore; binds to centromeric DNA in a Ctf19p-dependent manner	#N/A	#N/A			
14	YLR288C	MEC3	3	3	11	chromatin silencing at telomere*	DNA binding	nucleus	Involved in checkpoint control and DNA repair; forms a clamp with Rad17p and Ddc1p that is loaded onto partial duplex DNA; DNA damage checkpoint protein	#N/A	#N/A			
15	YPL194W	DDC1	3	3	11	meiosis*	molecular_function unknown	condensed nuclear chromosome	DNA damage checkpoint protein, part of a PCNA-like complex required for DNA damage response, required for pachytene checkpoint to inhibit cell cycle in response to unrepaired recombination intermediates; potential Cdc28p substrate	#N/A	#N/A		ctf data from independent test (K Yuen, T Kwok, data not shown). Missed in high throughput screen.	
16	YDR254W	CHL4	3	3	3	chromosome segregation	DNA binding	outer kinetochore of condensed nuclear chromosome	Protein necessary for stability of ARS-CEN plasmids; suggested to be required for kinetochore function; chromosome segregation protein	#N/A	#N/A		a-like faker data from C Warren et al, Mol Biol Cell 15:1724 (2004). Missed in high throughput screen.	
17	YMR095C	SNO1	3	2	2	pyridoxine metabolism*	molecular_function unknown	cytoplasm	Protein of unconfirmed function, involved in pyridoxine metabolism; expression is induced during stationary phase; forms a putative glutamine amidotransferase complex with Snz1p, with Sno1p serving as the glutaminase	#N/A	#N/A			
18	YOR026W	BUB3	2	5	24	mitotic spindle checkpoint	molecular_function unknown	condensed nuclear chromosome kinetochore	Kinetochore checkpoint WD40 repeat protein that localizes to kinetochores during prophase and metaphase, delays anaphase in the presence of unattached kinetochores; forms complexes with Mad1p-Bub1p and with Cdc20p, binds Mad2p and Mad3p	#N/A	#N/A			
19	YML032C	RAD52	2	5	22	telomerase-independent telomere maintenance*	recombinase activity*	nucleus*	Protein that stimulates strand exchange by facilitating Rad51p binding to single-stranded DNA; anneals complementary single-stranded DNA; involved in the repair of double-strand breaks in DNA during vegetative growth and meiosis	#N/A	#N/A			
20	YMR179W	SPT21	2	5	11	regulation of transcription from Pol II promoter	molecular_function unknown	nucleus	Protein required for normal transcription at several loci including HTA2-HTB2 and HHF2-HHT2, but not required at the other histone loci; functionally related to Spt10p	#N/A	#N/A		bimater data in independent test ((K Yuen, T Kwok, data not shown). Missed in high throughput screen.	ctf and a-like faker phentoype reconfirmed in independent test (K Yuen, T Kwok, data not shown).
21	YPR164W	MMS1	2	5	2	DNA repair*	molecular_function unknown	cellular_component unknown	sensitive to methyl methanesulfonate (MMS), diepoxybutane, and mitomycin C; sensitive to diepoxybutane and mitomycin C	#N/A	#N/A		ctf data in independent test (K Yuen, T Kwok, data not shown). Missed in high throughput screen.	bimater and a-like faker phentoype reconfirmed in independent test (K Yuen, T Kwok, data not shown).

22	YBL058W	SHP1	2	4	2	sporulation (sensu Fungi)*	molecular_function unknown	cytoplasm*	UBX (ubiquitin regulatory X) domain-containing protein that regulates Glc7p phosphatase activity and interacts with Cdc48p; interacts with ubiquitylated proteins in vivo and is required for degradation of a ubiquitylated model substrate	#N/A	#N/A			
23	YPL055C	LGE1	2	2	8	meiosis*	molecular_function unknown	nucleus	Protein of unknown function; null mutant forms abnormally large cells	#N/A	#N/A		bimater data in independent test ((K Yuen, T Kwok, data not shown). Missed in high throughput screen.	ctf and a-like faker phentoype reconfirmed in independent test (K Yuen, T Kwok, data not shown).
24	YKL113C	RAD27	1	4	63	DNA repair*	5'-flap endonuclease activity	nucleus	5' to 3' exonuclease, 5' flap endonuclease, required for Okazaki fragment processing and maturation as well as for long-patch base-excision repair; member of the S. pombe RAD2/FEN1 family	#N/A	#N/A			
25	YPL024W	NCE4	1	4	56	biological_process unknown	molecular_function unknown	cytoplasm*	Protein of unknown function; GFP tagged protein localizes to the cytoplasm and nucleus	#N/A	#N/A			
26	YNL250W	RAD50	1	4	36	double-strand break repair via nonhomologous end-joining*	protein binding*	nucleus*	Subunit of MRX complex, with Mre11p and Xrs2p, involved in processing double-strand DNA breaks in vegetative cells, initiation of meiotic DSBs, telomere maintenance, and nonhomologous end joining	#N/A	#N/A		ctf data in independent test (K Yuen, T Kwok, data not shown). Missed in high throughput screen.	bimater and a-like faker phentoype reconfirmed in independent test (K Yuen, T Kwok, data not shown).
27	YGL163C	RAD54	1	4	23	chromatin remodeling*	DNA-dependent ATPase activity*	nucleus	DNA-dependent ATPase, stimulates strand exchange by modifying the topology of double-stranded DNA; involved in the recombinational repair of double-strand breaks in DNA during vegetative growth and meiosis; member of the SWI/SNF family	#N/A	#N/A		ctf data in independent test (K Yuen, T Kwok, data not shown). Missed in high throughput screen.	bimater and a-like faker phentoype reconfirmed in independent test (K Yuen, T Kwok, data not shown).
28	YOR144C	ELG1	1	4	12	DNA replication*	molecular_function unknown	cytoplasm*	Protein required for S phase progression and telomere homeostasis, forms an alternative replication factor C complex important for DNA replication and genome integrity; mutants are sensitive to DNA damage	#N/A	#N/A			
29	YCL061C	MRC1	1	4	11	chromatin silencing at telomere*	molecular_function unknown	nucleus*	S-phase checkpoint protein found at replication forks, required for DNA replication; also required for Rad53p activation during DNA replication stress, where it forms a replication-pausing complex with Tof1p and is phosphorylated by Mec1p; protein involve	#N/A	#N/A		YCL060C in the deletion collection	
30	YBR098W	MMS4	1	4	9	DNA repair*	endonuclease activity*	nucleus	endonuclease	YBR099C	#N/A	Yes	available as YBR100W and YBR098W in the 3 deletion collections	
31	YLR235C	Dubious	1	3	45	#N/A	#N/A	#N/A	#N/A	YLR234W	TOP3	Yes		
32	YLR320W	MMS22	1	3	28	double-strand break repair	molecular_function unknown	cellular_component unknown	Protein involved in resistance to ionizing radiation; acts with Mms1p in a repair pathway that may be involved in resolving replication intermediates or preventing the damage caused by blocked replication forks	#N/A	#N/A			
33	YBR073W	RDH54	1	3	15	meiotic recombination*	DNA-dependent ATPase activity*	nucleus	genetic interaction with DMC1; Putative helicase similar to RAD54	#N/A	#N/A		ctf and bimater data from independent tests (K Yuen, T Kwok, data not shown). Missed in high throughput screens.	a-like faker phenotype reconfirmed in independent test (K Yuen, T Kwok, data not shown).

34	YHR064C	SSZ1	1	2	3	protein biosynthesis	unfolded protein binding	cytoplasm	DnaK homolog, interacts with Zuo1p (DnaJ homolog) to form a ribosome-associated complex (RAC) that is bound to the ribosome via the Zuo1p subunit; Hsp70 Protein	#N/A	#N/A			
35	YLR381W	CTF3	3	4	0	chromosome segregation	protein binding	condensed nuclear chromosome kinetochore	Outer kinetochore protein that forms a complex with Mcm16p and Mcm22p; may bind the kinetochore to spindle microtubules	#N/A	#N/A			ctf and bimater phentoype reconfirmed in independent test (K Yuen, T Kwok, data not shown).
36	YEL061C	CIN8	3	4	0	mitotic sister chromatid segregation*	microtubule motor activity	mitochondrion*	Kinesin motor protein involved in mitotic spindle assembly and chromosome segregation	#N/A	#N/A		ctf data from independent test (K Yuen, T Kwok, data not shown). Missed in high throughput screen.	bimater phenotype reconfirmed in independent test (K Yuen, T Kwok, data not shown).
37	YGR184C	UBR1	3	3	0	protein monoubiquitination*	ubiquitin-protein ligase activity	proteasome complex (sensu Eukaryota)	Ubiquitin-protein ligase (E3) that interacts with Rad6p/Ubc2p to ubiquitinate substrates of the N-end rule pathway; binds to the Rpn2p, Rpt1p, and Rpt6p proteins of the 19S particle of the 26S proteasome	#N/A	#N/A			ctf and bimater phentoype reconfirmed in independent test (K Yuen, T Kwok, data not shown).
38	YGL003C	CDH1	3	3	0	ubiquitin-dependent protein catabolism*	enzyme activator activity	cytoplasm*	CDC20 homolog 1; protein required for Clb2 and Ase1 degradation	#N/A	#N/A			ctf phentoype reconfirmed in independent test (K Yuen, T Kwok, data not shown).
39	YIL009C-A	EST3	3	2	0	telomerase-dependent telomere maintenance	telomerase activity	nucleus*	Component of the telomerase holoenzyme, involved in telomere replication	#N/A	#N/A			
40	YGL086W	MAD1	2	5	0	mitotic spindle checkpoint*	molecular_function unknown	nucleus*	Coiled-coil protein involved in the spindle-assembly checkpoint; phosphorylated by Mps1p upon checkpoint activation which leads to inhibition of the activity of the anaphase promoting complex; forms a complex with Mad2p	#N/A	#N/A			ctf and bimater phentoype reconfirmed in independent test (K Yuen, T Kwok, data not shown).
41	YJL030W	MAD2	2	3	0	mitotic spindle checkpoint	molecular_function unknown	nuclear pore*	Component of the spindle-assembly checkpoint complex, which delays the onset of anaphase in cells with defects in mitotic spindle assembly; forms a complex with Mad1p	#N/A	#N/A		ctf phenotype from Warren et al Mol Biol Cell 13:3029 (2002). Wrong strain in MATa well in high throughput screen.	
42	YKL053W	Dubious	1	3	0	#N/A	#N/A	#N/A	#N/A	YKL052C	ASK1			
43	YDR378C	LSM6	1	2	0	nuclear mRNA splicing, via spliceosome	pre-mRNA splicing factor activity	small nuclear ribonucleoprotein complex	Component of small nuclear ribonucleoprotein complexes involved in RNA processing, splicing, and decay	#N/A	#N/A			
44	YER116C	SLX8	1	5	wrong	DNA recombination	DNA binding	nucleus	Protein containing a RING finger domain that forms a complex with Hex3p; mutant phenotypes and genetic interactions suggest a possible role in resolving recombination intermediates during DNA replication or repair	#N/A	#N/A			
45	YMR078C	CTF18	3	0	29	mitotic sister chromatid cohesion	molecular_function unknown	mitochondrion*	Subunit of a complex with Ctf8p that shares some subunits with Replication Factor C and is required for sister chromatid cohesion; may have overlapping functions with Rad24p in the DNA damage replication checkpoint	#N/A	#N/A		ctf phenotype from traditional screen in Spencer et al, Genetics 124:237 (1990). Wrong strain in MATa well in high throughput screen.	

46	YOR080W	DIA2	2	0	60	invasive growth (sensu Saccharomyces)	molecular_function unknown	cellular_component unknown	Protein of unknown function, involved in invasive and pseudohyphal growth	#N/A	#N/A		ctf data from independent test (F Spencer data not shown). Wrong strain in MATalpha well in high throughput screen.	
47	YAL040C	CLN3	2	0	3	G1/S transition of mitotic cell cycle*	cyclin-dependent protein kinase regulator activity	nucleus	role in cell cycle START; involved in G(sub)1 size control; G(sub)1 cyclin	#N/A	#N/A			ctf and a-like faker phentoype reconfirmed in independent test (K Yuen, T Kwok, data not shown).
48	YOR300W	Dubious	2	0	3	#N/A	#N/A	#N/A	#N/A	YOR299W	BUD7			
49	YML010WA	Dubious	2	0	2	#N/A	#N/A	#N/A	#N/A	YML010C-B	#N/A	Yes	systematic name is YML009W-B; YML010W (SPT5) is another overlapping ORF	
50	YHR167W	THP2	1	0	15	mRNA-nucleus export*	nucleic acid binding	THO complex	affects transcription elongation	#N/A	#N/A			
51	YKR082W	NUP133	1	0	14	mRNA-nucleus export*	structural molecule activity	nuclear pore	Subunit of the Nup84p subcomplex of the nuclear pore complex (NPC), localizes to both sides of the NPC, required to establish a normal nucleocytoplasmic concentration gradient of the GTPase Gsp1p	#N/A	#N/A			
52	YGR064W	Dubious	1	0	5	#N/A	#N/A	#N/A	#N/A	YGR063C	SPT4	Yes		
53	YDR290W	Dubious	1	0	4	#N/A	#N/A	#N/A	#N/A	YDR289C	RTT103	Yes		
54	YML010C-B	Dubious	1	0	3	#N/A	#N/A	#N/A	#N/A	YML010W-A	#N/A	Yes	Systematic name is YML009C-A; YML010W (SPT5) is another overlapping ORF	
55	YLR418C	CDC73	1	0	2	RNA elongation from Pol II promoter	Pol II transcription elongation factor activity	transcription elongation factor complex*	Substituent of the Paf1 complex together with RNA polymerase II, Paf1p, Hpr1p, Ctr9, Leo1, Rtf1 and Ccr4p, distinct from Srb-containing Pol II complexes; required for the expression of certain genes and modification of some histones	#N/A	#N/A			
56	YGR188C	BUB1	3	wrong	16	protein amino acid phosphorylation*	protein binding*	nucleus*	Protein kinase that forms a complex with Mad1p and Bub3p that is crucial in the checkpoint mechanism required to prevent cell cycle progression into anaphase in the presence of spindle damage, associates with centromere DNA via Skp1p	#N/A	#N/A		ctf phenotype from Warren et al Mol Biol Cell 13:3029 (2002). Wrong strain in MATa well in high throughput screen.	
57	YPL017C	Uncharacterized	3	wrong	11	biological_process unknown	S-adenosylmethionine-dependent methyltransferase activity	cytoplasm	#N/A	YPL018W	CTF19	Yes		
58	YPR141C	KAR3	3	nd	40	meiosis*	microtubule motor activity*	spindle pole body*	Minus-end-directed microtubule motor that functions in mitosis and meiosis, localizes to the spindle pole body and localization is dependent on functional Cik1p, required for nuclear fusion during mating; potential Cdc28p substrate	#N/A	#N/A			ctf phentoype reconfirmed in independent test (K Yuen, T Kwok, data not shown).

59	YGL240W	DOC1	3	nd	3	ubiquitin-dependent protein catabolism*	enzyme regulator activity	mitochondrion*	Processivity factor required for the ubiquitination activity of the anaphase promoting complex (APC), mediates the activity of the APC by contributing to substrate recognition; involved in cyclin proteolysis	#N/A	#N/A			
60	YPL018W	CTF19	3	contam	8	chromosome segregation*	protein binding	nucleus*	Outer kinetochore protein, required for accurate mitotic chromosome segregation; forms a complex with Mcm21p and Okp1p that binds to centromeres via the CBF3 complex	YPL017C	0	Yes		
61	YKL057C	NUP120	2	wrong	3	mRNA-nucleus export*	structural molecule activity	nuclear pore	Subunit of the Nup84p subcomplex of the nuclear pore complex (NPC), required for even distribution of NPCs around the nuclear envelope, involved in establishment of a normal nucleocytoplasmic concentration gradient of the GTPase Gsp1p	#N/A	#N/A			
62	YNL140C	Dubious	2	wrong	3	#N/A	#N/A	#N/A	#N/A	YNL139C	RLR1			
63	YGL058W	RAD6	1	nd	25	ubiquitin-dependent protein catabolism*	ubiquitin conjugating enzyme activity	cytoplasm*	Ubiquitin-conjugating enzyme (E2), involved in postreplication repair (with Rad18p), sporulation, telomere silencing, and uniquitin-mediated N-end rule protein degradation (with Ubr1p)	#N/A	#N/A			ctf and a-like faker phentoype reconfirmed in independent test (K Yuen, T Kwok, data not shown).
64	YDR369C	XRS2	0	5	48	double-strand break repair via nonhomologous end-joining*	protein binding*	nucleus*	classified as an early recombination function, required for DNA repair but dispensable for mitotic recombination (xrs2 is hyper-Rec during vegatative growth), required for double strand breaks, meiotic recombination and spore viability; DNA repair protein	#N/A	#N/A			
65	YLR234W	TOP3	0	5	42	meiotic recombination*	DNA topoisomerase type I activity	nucleus	DNA Topoisomerase III	YLR235C	#N/A	Yes		
66	YLR374C	Dubious	0	5	18	#N/A	#N/A	#N/A	#N/A	YLR375W	STP3			
67	YDR004W	RAD57	0	5	15	telomerase-independent telomere maintenance*	protein binding	nucleus	Protein that stimulates strand exchange by stabilizing the binding of Rad51p to single-stranded DNA; involved in the recombinational repair of double-strand breaks in DNA during vegetative growth and meiosis; forms heterodimer with Rad55p	#N/A	#N/A			
68	YHR031C	RRM3	0	5	14	DNA replication	DNA helicase activity*	nuclear telomeric heterochromatin	DNA helicase involved in rDNA replication and Ty1 transposition; structurally and functionally related to Pif1p	#N/A	#N/A			
69	YBR099C	Dubious	0	5	12	#N/A	#N/A	#N/A	#N/A	YBR098W	MMS4	Yes		
70	YDL162C	Dubious	0	5	10	#N/A	#N/A	#N/A	#N/A	YDL161W	ENT1			
71	YOR025W	HST3	0	5	9	chromatin silencing at telomere*	DNA binding	nucleus	Member of the Sir2 family of NAD(+)-dependent protein deacetylases; involved along with Hst4p in telomeric silencing, cell cycle progression, radiation resistance, genomic stability and short-chain fatty acid metabolism	#N/A	#N/A			
72	YJL007C	Dubious	0	5	2	#N/A	#N/A	#N/A	#N/A	YJLWDELTA10	#N/A			

73	YDR363W	ESC2	0	4	43	chromatin silencing at silent mating-type cassette	molecular_function unknown	nucleus	Protein involved in mating-type locus silencing, interacts with Sir2p; probably functions to recruit or stabilize Sir proteins	#N/A	#N/A			bimater and a-like faker phentoype reconfirmed in independent test (K Yuen, T Kwok, data not shown).
74	YDR532C	Uncharacterized	0	4	30	biological_process unknown	molecular_function unknown	spindle pole body	#N/A	#N/A	#N/A			
75	YHR154W	RTT107	0	4	23	negative regulation of DNA transposition	molecular_function unknown	nucleus	Regulator of Ty1 Transposition; Establishes Silent Chromatin; involved in silencing	#N/A	#N/A			bimater and a-like faker phentoype reconfirmed in independent test (K Yuen, T Kwok, data not shown).
76	YDR076W	RAD55	0	4	18	meiotic DNA recombinase assembly*	protein binding	nucleus	Protein that stimulates strand exchange by stabilizing the binding of Rad51p to single-stranded DNA; involved in the recombinational repair of double-strand breaks in DNA during vegetative growth and meiosis; forms heterodimer with Rad57p	#N/A	#N/A			
77	YOR024W	Dubious	0	4	14	#N/A	#N/A	#N/A	#N/A	#N/A	#N/A			
78	YMR190C	SGS1	0	4	14	mitotic sister chromatid segregation*	ATP-dependent DNA helicase activity	nucleolus	Nucleolar DNA helicase of the RecQ family, involved in maintenance of genome integrity; has similarity to human BLM and WRN helicases implicated in Bloom and Werner syndromes	#N/A	#N/A			
79	YOL054W	PSH1	0	4	11	RNA elongation from Pol II promoter	molecular_function unknown	nucleus	Nuclear protein, putative RNA polymerase II elongation factor; isolated as Pob3p/Spt16p-binding protein	#N/A	#N/A			
80	YDR386W	MUS81	0	4	9	DNA repair*	endonuclease activity	nucleus	Helix-hairpin-helix protein, involved in DNA repair and replication fork stability; functions as an endonuclease in complex with Mms4p; interacts with Rad54p	#N/A	#N/A			
81	YLR373C	VID22	0	4	8	vacuolar protein catabolism	molecular_function unknown	integral to plasma membrane	Vacuole import and degradation	#N/A	#N/A			
82	YML028W	TSA1	0	4	8	response to oxidative stress*	thioredoxin peroxidase activity	cytoplasm	Thioredoxin-peroxidase (TPx), reduces H2O2 and alkyl hydroperoxides with the use of hydrogens provided by thioredoxin, thioredoxin reductase, and NADPH; provides protection against oxidation systems that generate reactive oxygen and sulfur species	#N/A	#N/A			
83	YBR009C	HHF1	0	4	6	chromatin assembly or disassembly	DNA binding	nuclear nucleosome	One of two identical histone H4 proteins (see also HHF2); core histone required for chromatin assembly and chromosome function; contributes to telomeric silencing; N-terminal domain involved in maintaining genomic integrity	#N/A	#N/A			
84	YER173W	RAD24	0	4	6	meiotic recombination*	DNA clamp loader activity	nucleus*	Checkpoint protein, involved in the activation of the DNA damage and meiotic pachytene checkpoints; subunit of a clamp loader that loads Rad17p-Mec3p-Ddc1p onto DNA; homolog of human and S. pombe Rad17 protein	#N/A	#N/A			

85	YCR065W	HCM1	0	4	2	transcription initiation from Pol II promoter*	specific RNA polymerase II transcription factor activity	nucleus	Forkhead transcription factor involved in cell cycle specific transcription of SPC110, encoding a spindle pole body (SPB) calmodulin binding protein; dosage-dependent suppressor of calmodulin mutants with specific defects in SPB assembly	#N/A	#N/A			
86	YDL059C	RAD59	0	4	2	telomerase-independent telomere maintenance*	protein binding*	nucleus	Protein involved in the repair of double-strand breaks in DNA during vegetative growth via recombination and single-strand annealing; anneals complementary single-stranded DNA; homologous to Rad52p	#N/A	#N/A			
87	YLR058C	SHM2	0	4	2	one-carbon compound metabolism	glycine hydroxymethyltransferase activity	cytoplasm	serine hydroxymethyltransferase	#N/A	#N/A		a-like faker data from independent test (K Yuen, T Kwok, data not shown). Missed in high throughput screen.	bimater phenotype reconfirmed in independent test (K Yuen, T Kwok, data not shown).
88	YJR043C	POL32	0	3	26	nucleotide-excision repair*	delta DNA polymerase activity	nucleus*	Third subunit of DNA polymerase delta, involved in chromosomal DNA replication; required for error-prone DNA synthesis in the presence of DNA damage and processivity; interacts with Pol31p, PCNA (Pol30p), and Pol1p	#N/A	#N/A		bimater data from independent test (K Yuen, T Kwok, data not shown). Missed in high throughput screen.	a-like faker phenotype reconfirmed in independent test (K Yuen, T Kwok, C Warren, O Chan, data not shown).
89	YDR217C	RAD9	0	3	10	DNA repair*	protein binding	nucleus	DNA damage-dependent checkpoint protein, required for cell-cycle arrest in G1/S, intra-S, and G2/M; transmits checkpoint signal by activating Rad53p and Chk1p; hyperphosphorylated by Mec1p and Tel1p; potential Cdc28p substrate	#N/A	#N/A			
90	YOR368W	RAD17	0	3	10	meiotic recombination*	double-stranded DNA binding	nucleus	Checkpoint protein, involved in the activation of the DNA damage and meiotic pachytene checkpoints; with Mec3p and Ddc1p, forms a clamp that is loaded onto partial duplex DNA; homolog of human and S. pombe Rad1 and U. maydis Rec1 proteins	#N/A	#N/A			
91	YNL072W	RNH201	0	3	6	DNA replication	ribonuclease H activity	nucleus	Ribonuclease H2 catalytic subunit, removes RNA primers during Okazaki fragment synthesis; cooperates with Rad27p nuclease	#N/A	#N/A			
92	YLR154C	RNH203	0	3	5	DNA replication	ribonuclease H activity	cytoplasm*	Ribonuclease H2 subunit, required for RNase H2 activity	#N/A	#N/A			
93	YPR120C	CLB5	0	3	4	G1/S transition of mitotic cell cycle*	cyclin-dependent protein kinase regulator activity	nucleus	B-type cyclin with a role in DNA replication during S phase; has an additional functional role in formation of mitotic spindles along with Clb3p and Clb4p	#N/A	#N/A			
94	YDR279W	RNH202	0	3	4	DNA replication	ribonuclease H activity	nucleus	Ribonuclease H2 subunit, required for RNase H2 activity	#N/A	#N/A			
95	YAL011W	SWC3	0	3	3	chromatin remodeling*	molecular_function unknown	nucleus*	Protein of unknown function, component of the Swr1p complex that incorporates Htz1p into chromatin; required for formation of nuclear-associated array of smooth endoplasmic reticulum known as karmellae	#N/A	#N/A			
96	YML095C	RAD10	0	3	2	removal of nonhomologous ends*	single-stranded DNA specific endodeoxyribonuclease activity	nucleotide excision repair factor 1 complex	Single-stranded DNA endonuclease (with Rad1p), cleaves single-stranded DNA during nucleotide excision repair and double-strand break repair; subunit of Nucleotide Excision Repair Factor 1 (NEF1); homolog of human XPF protein	YML096W	0			

97	YDL117W	CYK3	0	3	2	cytokinesis	molecular_function unknown	cytoplasm*	SH3-domain protein located in the mother-bud neck and the cytokinetic actin ring; mutant phenotype and genetic interactions suggest a role in cytokinesis	#N/A	#N/A			
98	YER161C	SPT2	0	2	22	negative regulation of transcription from Pol II promoter	DNA binding	nucleus	Protein involved in negative regulation of transcription, exhibits regulated interactions with both histones and SWI-SNF components, has similarity to mammalian HMG1 proteins	#N/A	#N/A			
99	YLL002W	RTT109	0	2	18	negative regulation of DNA transposition	molecular_function unknown	nucleus	Regulator of Ty1 Transposition; Regulation of mitochondrial network; Killed in Mutagen, sensitive to diepoxybutane and/or mitomycin C; diepoxybutane and mitomycin C resistance	#N/A	#N/A			
100	YLR032W	RAD5	0	2	5	DNA repair	ATPase activity	nuclear chromatin	Single-stranded DNA-dependent ATPase, involved in postreplication repair; contains RING finger domain	#N/A	#N/A			
101	YJR063W	RPA12	0	2	5	transcription from Pol I promoter	DNA-directed RNA polymerase activity	DNA-directed RNA polymerase I complex	RNA polymerase I subunit A12.2; contains two zinc binding domains, and the N terminal domain is responsible for anchoring to the RNA pol I complex	#N/A	#N/A			
102	YGR078C	PAC10	0	2	3	tubulin folding	tubulin binding	cytoplasm*	Part of the heteromeric co-chaperone GimC/prefoldin complex, which promotes efficient protein folding	#N/A	#N/A			
103	YDL156W	Uncharacterized	0	2	2	biological_process unknown	molecular_function unknown	cytoplasm*	#N/A	#N/A	#N/A			
104	YLR193C	Uncharacterized	0	2	2	biological_process unknown	molecular_function unknown	mitochondrion	#N/A	#N/A	#N/A			
105	YCR066W	RAD18	wrong	5	19	DNA repair	ubiquitin conjugating enzyme activity*	nuclear chromatin	Protein involved in postreplication repair; binds single-stranded DNA and has single-stranded DNA dependent ATPase activity; forms heterodimer with Rad6p; contains RING-finger motif	#N/A	#N/A			
106	YBR026C	ETR1	wrong	5	5	aerobic respiration*	enoyl-[acyl-carrier protein] reductase activity	mitochondrion	2-enoyl thioester reductase, member of the medium chain dehydrogenase/reductase family; localized to in mitochondria, where it has a probable role in fatty acid synthesis	#N/A	#N/A			
107	YOL072W	THP1	wrong	4	19	bud site selection*	protein binding	nuclear pore*	Nuclear pore-associated protein, forms a complex with Sac3p that is involved in transcription and in mRNA export from the nucleus; contains a PAM domain implicated in protein-protein binding	#N/A	#N/A			
108	YER095W	RAD51	wrong	4	7	telomerase-independent telomere maintenance*	recombinase activity	nuclear chromosome*	Strand exchange protein, forms a helical filament with DNA that searches for homology; involved in the recombinational repair of double-strand breaks in DNA during vegetative growth and meiosis; homolog of Dmc1p and bacterial RecA protein	#N/A	#N/A			
109	YGR270W	YTA7	wrong	4	6	protein catabolism	ATPase activity	nucleus	Protein of unknown function, member of CDC48/PAS1/SEC18 family of ATPases, potentially phosphorylated by Cdc28p	#N/A	#N/A			

110	YJL115W	ASF1	wrong	3	22	DNA damage response, signal transduction resulting in induction of apoptosis	histone binding	chromatin assembly complex	anti-silencing protein that causes depression of silent loci when overexpressed; involved in silencing	#N/A	#N/A			
111	YJL092W	HPR5	wrong	3	12	DNA repair*	DNA helicase activity	nucleus	DNA helicase and DNA-dependent ATPase involved in DNA repair, required for proper timing of commitment to meiotic recombination and the transition from Meiosis I to Meiosis II; potential Cdc28p substrate	#N/A	#N/A			
112	YKR087C	OMA1	wrong	2	30	misfolded or incompletely synthesized protein catabolism	metalloendopeptidase activity	mitochondrion*	Metalloendopeptidase of the mitochondrial inner membrane, involved in turnover of membrane-embedded proteins; member of a family of predicted membrane-bound metallopeptidases in prokaryotes and higher eukaryotes	#N/A	#N/A			
113	YOR073W	SGO1	wrong	2	19	mitotic sister chromatid segregation*	molecular_function unknown	nucleus*	Protein that protects centromeric Rec8p at meiosis I; required for accurate chromosomal segregation at meiosis II and for mitotic chromosome stability; evolutionarily conserved; component of the spindle checkpoint	#N/A	#N/A			
114	YPR032W	SRO7	wrong	2	3	exocytosis*	molecular_function unknown	cytosol*	Suppressor of rho3; yeast homolog of the Drosphila tumor suppressor, lethal giant larvae	#N/A	#N/A			
115	YPR067W	ISA2	contam	3	3	iron ion transport	molecular_function unknown	mitochondrial intermembrane space	Protein required for maturation of mitochondrial and cytosolic Fe/S proteins, localizes to the mitochondrial intermembrane space, overexpression of ISA2 suppresses grx5 mutations	#N/A	#N/A			
116	YFR046C	CNN1	2	0	0	meiosis*	molecular_function unknown	nucleus	Kinetochore protein that co-purifies with Nnf1p	#N/A	#N/A			ctf phentoype reconfirmed in independent test (K Yuen, T Kwok, data not shown).
117	YDR200C	VPS64	3	0	0	protein-vacuolar targeting*	molecular_function unknown	cytoplasm*	Cytoplasmic protein required for cytoplasm to vacuole targeting of proteins; forms a complex with Far3p, Far7p, Far10p, and Far11p that is involved in pheromone-induced cell cycle arrest; also localized to the endoplasmic reticulum membrane	YDR199W	#N/A			ctf phentoype reconfirmed in independent test (K Yuen, T Kwok, data not shown).
118	YLR273C	PIG1	3	0	0	regulation of glycogen biosynthesis	protein phosphatase regulator activity	protein phosphatase type 1 complex	Putative type 1 phosphatase regulatory subunit; interacts with Gsy2p; Protein similar to Gac1p, a putative type 1 protein phosphatase targeting subunit	#N/A	#N/A			ctf phentoype reconfirmed in independent test (K Yuen, T Kwok, data not shown).
119	YGL060W	YBP2	0	4	0	biological_process unknown	molecular_function unknown	cytoplasm	Protein with a role in resistance to oxidative stress; has similarity to Ybp1p, which is involved in regulation of the transcription factor Yap1p via oxidation of specific cysteine residues	#N/A	#N/A			bimater phenotype reconfirmed in independent test (K Yuen, T Kwok, data not shown).
120	YBR113W	Dubious	0	0	56	#N/A	#N/A	#N/A	#N/A	YBR112C	CYC8	Yes		a-like faker phenotype reconfirmed in independent test (K Yuen, T Kwok, C Warren, O Chan, data not shown).

121	YGR061C	ADE6	0	0	16	purine nucleotide biosynthesis	phosphoribosylformylglycinamidine synthase activity	cytoplasm	Formylglycinamidine-ribonucleotide (FGAM)-synthetase, catalyzes a step in the 'de novo' purine nucleotide biosynthetic pathway	#N/A	#N/A		a-like faker data from independent test (C Warren, K Yuen, data not shown). Wrong strain in MATalpha well in high throughput screen.	
122	YDL074C	BRE1	0	0	11	chromatin silencing at telomere*	ubiquitin-protein ligase activity	nucleus	E3 ubiquitin ligase for Rad6p, required for the ubiquitination of histone H2B, recruitment of Rad6p to promoter chromatin and subsequent methylation of histone H3 (on L4 and L79), contains RING finger domain	#N/A	#N/A			a-like faker phenotype reconfirmed in independent test (K Yuen, T Kwok, C Warren, O Chan, data not shown).
123	YML062C	MFT1	0	0	5	mRNA-nucleus export*	nucleic acid binding	THO complex	Protein involved in mitochondrial import of fusion proteins; mitochondrial targeting protein	#N/A	#N/A			a-like faker phenotype reconfirmed in independent test (C Warren, O Chan, data not shown).
124	YBR112C	CYC8	0	nd	80	chromatin remodeling*	transcription coactivator activity*	nucleus	General transcriptional co-repressor, acts together with Tup1p; also acts as part of a transcriptional co-activator complex that recruits the SWI/SNF and SAGA complexes to promoters	YBR113W	#N/A	Yes		a-like faker phenotype reconfirmed in independent test (K Yuen, T Kwok, C Warren, O Chan, data not shown).
125	YAR015W	ADE1	wrong	0	31	purine nucleotide biosynthesis*	phosphoribosylaminoimidazolesuccinocarboxamide synthase activity	cytoplasm*	N-succinyl-5-aminoimidazole-4-carboxamide ribotide (SAICAR) synthetase, required for 'de novo' purine nucleotide biosynthesis; red pigment accumulates in mutant cells deprived of adenine	#N/A	#N/A			a-like faker phenotype reconfirmed in independent test (C Warren, K Yuen, data not shown).
126	YMR224C	MRE11	wrong	contam	30	DNA repair*	protein binding*	nucleus*	Subunit of a complex with Rad50p and Xrs2p (RMX complex) that functions in repair of DNA double-strand breaks and in telomere stability, exhibits nuclease activity that appears to be required for RMX function; widely conserved	#N/A	#N/A			a-like faker phenotype reconfirmed in independent test (C Warren, K Yuen, data not shown).
127	YHR134W	WSS1	0	wrong	28	protein sumoylation	molecular_function unknown	cellular_component unknown	weak suppressor of smt3	#N/A	#N/A			a-like faker phenotype reconfirmed in independent test (C Warren, K Yuen, data not shown).
128	YDL101C	DUN1	0	wrong	10	protein amino acid phosphorylation*	protein kinase activity	nucleus	Cell-cycle checkpoint serine-threonine kinase required for DNA damage-induced transcription of certain target genes, phosphorylation of Rad55p and Sml1p, and transient G2/M arrest after DNA damage; also regulates postreplicative DNA repair	#N/A	#N/A			a-like faker phenotype reconfirmed in independent test (K Yuen, T Kwok, C Warren, O Chan, data not shown).
129	YMR066W	SOV1	0	wrong	8	biological_process unknown	molecular_function unknown	mitochondrion	Synthesis Of Var; (putative) involved in respiration	#N/A	#N/A		a-like faker data from independent test (C Warren, K Yuen, data not shown). Contaminating strain also in MATalpha well in high throughput screen.	
130	YMR120C	ADE17	0	nd	2	purine nucleotide biosynthesis*	IMP cyclohydrolase activity*	cytosol	Enzyme of 'de novo' purine biosynthesis containing both 5-aminoimidazole-4-carboxamide ribonucleotide transformylase and inosine monophosphate cyclohydrolase activities, isozyme of Ade16p; ade16 ade17 mutants require adenine and histidine	#N/A	#N/A			a-like faker phenotype reconfirmed in independent test (C Warren, K Yuen, data not shown).

Appendix 2 Lower confidence yeast CIN genes identified by the 3 marker loss screens

163 *yko*Δ mutants were identified in only one screen. Retesting of these in new transformants suggests a higher error rate for these than for mutants identified in >1 screen. Extrapolation of the error rate obtained from a sampled subset suggests that there are 43% true positives among CTF- and ALF-only mutants, and 75% true positives in BiM-only mutants. Data are shown as in Appendix 1.

Index	ORF name	Gene Name	CTF	BiM	ALF	GO Biological Process	GO Molecular Funciton	GO Cellular Component	Description on SGD	Overlapping ORF	Overlapping Gene Name	Overlapping yeast CIN genes?	Adjustment Notes
131	YLL028W	TPO1	3	0	0	polyamine transport	spermine transporter activity*	plasma membrane*	Proton-motive-force-dependent multidrug transporter of the major facilitator superfamily; able to transport eight different compounds, including polyamines, quinidine, cycloheximide, and nystatin; involved in excess spermidine detoxification	#N/A	#N/A		ctf phenotype not confirmed in new transformants in YPH strain background
132	YOL070C	Uncharacterized	3	0	0	biological_process unknown	molecular_function unknown	cytoplasm*	#N/A	#N/A	#N/A		ctf phenotype not confirmed in new transformants in YPH strain background
133	YBL031W	SHE1	2	0	0	biological_process unknown	molecular_function unknown	microtubule cytoskeleton	Cytoskeletal protein of unknown function; overexpression causes growth arrest	#N/A	#N/A		ctf phenotype not confirmed in new transformants in YPH strain background
134	YDR289C	RTT103	2	0	0	negative regulation of DNA transposition	molecular_function unknown	cellular_component unknown	Regulator of Ty1 Transposition; regulator of Ty1 Transposition	YDR290W	#N/A	Yes	ctf phenotype not confirmed in new transformants in YPH strain background
135	YKL074C	MUD2	2	0	0	U2-type nuclear mRNA branch site recognition	pre-mRNA splicing factor activity*	commitment complex	Protein involved in early pre-mRNA splicing; component of the pre-mRNA-U1 snRNP complex, the commitment complex; interacts with Msl5p/BBP splicing factor and Sub2p; similar to metazoan splicing factor U2AF65	#N/A	#N/A		
136	YLR006C	SSK1	2	0	0	osmosensory signaling pathway via two-component system*	enzyme activator activity*	cytoplasm	Cytoplasmic response regulator, part of a two-component signal transducer that mediates osmosensing via a phosphorelay mechanism; dephosphorylated form is degraded by the ubiquitin-proteasome system; potential Cdc28p substrate	#N/A	#N/A		
137	YOR308C	SNU66	2	0	0	nuclear mRNA splicing, via spliceosome	pre-mRNA splicing factor activity	small nuclear ribonucleoprotein complex	66kD U4/U6.U5 snRNP associated protein	#N/A	#N/A		
138	YDR431W	Dubious	1	0	0	#N/A	#N/A	#N/A	#N/A	YDR430C	CYM1		
139	YGL066W	SGF73	1	0	0	histone acetylation	molecular_function unknown	SAGA complex	SaGa associated Factor 73kDa; Probable 73KkDa Subunit of SAGA histone acetyltransferase complex	#N/A	#N/A		
140	YGL071W	RCS1	1	0	0	positive regulation of transcription from Pol II promoter*	transcription factor activity	cytoplasm*	Transcription factor that binds the consensus site PyPuCACCCPu, involved in iron homeostasis and cell size regulation; activates the expression of target genes in response to low-iron conditions	#N/A	#N/A		
141	YGR063C	SPT4	1	0	0	regulation of transcription, DNA-dependent*	Pol II transcription elongation factor activity	nucleus*	Protein that forms a complex with Spt5p and mediates both activation and inhibition of transcription elongation, and plays a role in pre-mRNA processing; in addition, Spt4p is involved in kinetochore function and gene silencing	YGR064W	#N/A	Yes	
142	YGR118W	RPS23A	1	0	0	protein biosynthesis*	structural constituent of ribosome	cytosolic small ribosomal subunit (sensu Eukaryota)	Ribosomal protein 28 (rp28) of the small (40S) ribosomal subunit, required for translational accuracy; nearly identical to Rps23Bp and similar to E. coli S12 and rat S23 ribosomal proteins; deletion of both RPS23A and RPS23B is lethal	#N/A	#N/A		
143	YJR008W	Uncharacterized	1	0	0	biological_process unknown	molecular_function unknown	cytoplasm*	#N/A	#N/A	#N/A		
144	YJR074W	MOG1	1	0	0	protein-nucleus import	RAN protein binding	nucleus	Conserved nuclear protein that interacts with GTP-Gsp1p, which is a Ran homolog of the Ras GTPase family, and stimulates nucleotide release, involved in nuclear protein import, nucleotide release is inhibited by Yrb1p	#N/A	#N/A		
145	YNL206C	RTT106	1	0	0	negative regulation of DNA transposition	molecular_function unknown	nucleus	Regulator of Ty1 Transposition - same phenotype as RTT101 - RTT105, disruption causes increase in Ty1 transposition. Isolated from the same screen as the other named RTT genes.	#N/A	#N/A		
146	YPL047W	SGF11	1	0	0	transcription initiation from Pol II promoter	molecular_function unknown	nucleus*	11kDa subunit of the SAGA histone acetyltransferase complex involved in regulation of transcription of a subset of SAGA-regulated genes	#N/A	#N/A		

147	YPL061W	ALD6	1	0	0	acetate biosynthesis	aldehyde dehydrogenase activity	cytoplasm*	Cytosolic aldehyde dehydrogenase that is activated by Mg2+ and utilizes NADP+ as the preferred coenzyme	#N/A	#N/A		
148	YPL179W	PPQ1	1	0	0	protein amino acid dephosphorylation*	protein serine/threonine phosphatase activity	cytoplasm	Putative protein serine/threonine phosphatase; null mutation enhances efficiency of translational suppressors	#N/A	#N/A		
149	YJL006C	CTK2	3	wrong	contam	protein amino acid phosphorylation*	cyclin-dependent protein kinase regulator activity	nucleus	Beta subunit of C-terminal domain kinase I (CTDK-I), which phosphorylates the C-terminal repeated domain of the RNA polymerase II large subunit (Rpo21p) to affect both transcription and pre-mRNA 3' end processing; has similarity to cyclins	#N/A	#N/A		
150	YMR198W	CIK1	3	wrong	0	meiosis*	microtubule motor activity	spindle pole body*	CIK1 is important for proper organiziation of microtubule arrays and establishment of a spindle; is essential for karyogamy; and expression is regulated by KAR4 and mating; spindle pole body associated protein	#N/A	#N/A		
151	YIL084C	SDS3	2	contam	contam	chromatin silencing*	protein binding	histone deacetylase complex	Functions are similar to those of SIN3 and RPD3; (putative) transcriptional regulator	#N/A	#N/A		
152	YNL309W	STB1	2	0	nd	G1/S transition of mitotic cell cycle	transcriptional activator activity	cytoplasm*	Protein with a role in regulation of MBF-specific transcription at Start, phosphorylated by Cln-Cdc28p kinases in vitro; unphosphorylated form binds Swi6p and binding is required for Stb1p function; expression is cell-cycle regulated	#N/A	#N/A		
153	YCR081W	SRB8	1	contam	wrong	negative regulation of transcription from Pol II promoter	RNA polymerase II transcription mediator activity	transcription factor complex	RNA polymerase II mediator complex subunit	#N/A	#N/A		
154	YHR133C	NSG1	0	5	0	biological_process unknown	molecular_function unknown	cellular_component unknown	Protein of unknown function, potential homolog of mammalian Insig 1; green fluorescent protein (GFP)-fusion protein localizes to the nuclear periphery	#N/A	#N/A		bimater phenotype not confirmed in new transformants
155	YBR231C	SWC5	0	4	0	chromatin remodeling	molecular_function unknown	nucleus*	Protein of unknown function, component of the Swr1p complex that incorporates Htz1p into chromatin	#N/A	#N/A		
156	YJL179W	PFD1	0	4	0	protein folding*	unfolded protein binding	prefoldin complex	Subunit of heterohexameric prefoldin, which binds cytosolic chaperonin and transfers target proteins to it; involved in the biogenesis of actin and of alpha- and gamma-tubulin	#N/A	#N/A		
157	YDR176W	NGG1	0	3	0	histone acetylation*	transcription cofactor activity	SAGA complex*	Involved in glucose repression of GAL4p-regulated transcription; transcription factor; genetic and mutant analyses suggest that Ngg1p (Ada3p) is part of two transcriptional adaptor/HAT (histone acetyltransferase complexes, the 0.8 MD ADA complex and the 1	#N/A	#N/A		
158	YDR334W	SWR1	0	3	0	chromatin remodeling	helicase activity	nucleus*	Swi2/Snf2-related ATPase, component of the SWR1 complex; required for the incorporation of Htz1p into chromatin	#N/A	#N/A		
159	YER007W	PAC2	0	3	0	post-chaperonin tubulin folding pathway*	alpha-tubulin binding	cellular_component unknown	Microtubule effector required for tubulin heterodimer formation, binds alpha-tubulin, required for normal microtubule function, null mutant exhibits cold-sensitive microtubules and sensitivity to benomyl	#N/A	#N/A		
160	YLR085C	ARP6	0	3	0	protein-vacuolar targeting*	molecular_function unknown	cytoplasm*	Actin-related protein, involved in the carboxypeptidase Y pathway	#N/A	#N/A		
161	YOR349W	CIN1	0	3	0	post-chaperonin tubulin folding pathway*	beta-tubulin binding	cellular_component unknown	Tubulin folding factor D involved in beta-tubulin (Tub2p) folding; isolated as mutant with increased chromosome loss and sensitivity to benomyl	#N/A	#N/A		
162	YPL241C	CIN2	0	3	0	microtubule-based process	molecular_function unknown	cellular_component unknown	Tubulin folding factor C (putative) involved in beta-tubulin (Tub2p) folding; isolated as mutant with increased chromosome loss and sensitivity to benomyl	#N/A	#N/A		
163	YNL291C	MID1	0	2	0	calcium ion transport	calcium channel activity	endoplasmic reticulum*	N-glycosylated integral plasma membrane protein	#N/A	#N/A		
164	YGR058W	Uncharacterized	0	2	0	biological_process unknown	molecular_function unknown	cytoplasm*	#N/A	#N/A	#N/A		

165	YIR002C	MPH1	0	2	0	DNA repair	RNA helicase activity*	nucleus	Member of the DEAH family of helicases, functions in an error-free DNA damage bypass pathway that involves homologous recombination, mutations confer a mutator phenotype	#N/A	#N/A		
166	YPL125W	KAP120	0	2	0	protein-nucleus import	structural constituent of nuclear pore	cytoplasm*	Karyopherin with a role in the assembly or export of 60S ribosomal subunits	#N/A	#N/A		
167	YLR242C	ARV1	0	2	0	sterol transport*	molecular_function unknown	endoplasmic reticulum*	Protein with similarity to Nup120p and C.elegans R05H5.5 protein	#N/A	#N/A		
168	YML124C	TUB3	0	2	0	mitotic sister chromatid segregation*	structural constituent of cytoskeleton	spindle pole body*	Alpha-tubulin; associates with beta-tubulin (Tub2p) to form tubulin dimer, which polymerizes to form microtubules; expressed at lower level than Tub1p	#N/A	#N/A		
169	YGR014W	MSB2	0	2	0	establishment of cell polarity (sensu Fungi)*	osmosensor activity	integral to plasma membrane*	Protein that functions as an osmosensor in parallel to the Sho1p-mediated pathway, multicopy suppressor of a temperature-sensitive mutation in CDC24, potential Cdc28p substrate	#N/A	#N/A		
170	YGL151W	NUT1	0	2	0	regulation of transcription from Pol II promoter	molecular_function unknown	nucleus	Component of the RNA polymerase II mediator complex, which is required for transcriptional activation and also has a role in basal transcription	#N/A	#N/A		
171	YML102W	CAC2	0	2	0	DNA repair*	molecular_function unknown	chromatin assembly complex*	Component of the chromatin assembly complex (with Rlf2p and Msi1p) that assembles newly synthesized histones onto recently replicated DNA, required for building functional kinetochores, conserved from yeast to humans	YML102C-A	#N/A		
172	YOL012C	HTZ1	wrong	3	0	regulation of transcription from Pol II promoter*	chromatin binding	nuclear chromatin*	Histone variant H2AZ, exchanged for histone H2A in nucleosomes by the SWR1 complex; involved in transcriptional regulation through prevention of the spread of silent heterochromatin	#N/A	#N/A		
173	YDR359C	VID21	wrong	2	contam	chromatin modification	molecular_function unknown	histone acetyltransferase complex	Component of the NuA4 histone acetyltransferase complex	YDR360W	#N/A		
174	YGR285C	ZUO1	0	4	wrong	protein folding	unfolded protein binding	cytoplasm*	Cytosolic ribosome-associated chaperone, contains a DnaJ domain; together with Ssz1p, acts as a chaperone for nascent polypeptide chains	#N/A	#N/A		
175	YDL116W	NUP84	0	4	contam	mRNA-nucleus export*	structural molecule activity	nuclear pore	Subunit of the nuclear pore complex (NPC), forms a subcomplex with Nup85p, Nup120p, Nup145p-C, Sec13p, and Seh1p that plays a role in nuclear mRNA export and NPC biogenesis	#N/A	#N/A		
176	YMR311C	GLC8	0	3	wrong	glycogen biosynthesis	enzyme activator activity	cytoplasm*	Regulatory subunit of protein phosphatase 1 (Glc7p), involved in glycogen metabolism and chromosome segregation; proposed to regulate Glc7p activity via conformational alteration; ortholog of the mammalian protein phosphatase inhibitor 2	#N/A	#N/A		
177	YOL064C	MET22	0	3	wrong	sulfate assimilation*	3'(2'),5'-bisphosphate nucleotidase activity	cytoplasm	Bisphosphate-3'-nucleotidase, involved in salt tolerance and methionine biogenesis; dephosphorylates 3'-phosphoadenosine-5'-phosphate and 3'-phosphoadenosine-5'-phosphosulfate, intermediates of the sulfate assimilation pathway	#N/A	#N/A		
178	YML094W	GIM5	0	2	wrong	tubulin folding	tubulin binding	cytoplasm*	Prefoldin subunit 5; putative homolog of subunit 5 of bovine prefoldin, a chaperone comprised of six subunits; bovine prefoldin subunit 5 homolog (putative)	YML095C-A	#N/A		
179	YNR068C	Uncharacterized	0	0	27	biological_process unknown	molecular_function unknown	cellular_component unknown	#N/A	#N/A	#N/A		alf phenotype not confirmed in new transformants
180	YIR019C	MUC1	0	0	23	pseudohyphal growth*	molecular_function unknown	plasma membrane	GPI-anchored cell surface glycoprotein required for diploid pseudohyphal formation and haploid invasive growth, transcriptionally regulated by the MAPK pathway (via Ste12p and Tec1p) and the cAMP pathway (via Flo8p)	#N/A	#N/A		alf phenotype not confirmed in new transformants
181	YFL016C	MDJ1	0	0	19	protein folding*	unfolded protein binding*	mitochondrial inner membrane	Protein involved in folding of mitochondrially synthesized proteins in the mitochondrial matrix; localizes to the mitochondrial inner membrane; member of the DnaJ family of molecular chaperones	#N/A	#N/A		
182	YDL204W	RTN2	0	0	16	biological_process unknown	molecular_function unknown	endoplasmic reticulum	reticulon gene member of the RTNLA (reticulon-like A) subfamily	#N/A	#N/A		alf phenotype not confirmed in new transformants
183	YIR004W	DJP1	0	0	13	peroxisome matrix protein import	chaperone binding	cytosol	Cytosolic J-domain-containing protein, required for peroxisomal protein import and involved in peroxisome assembly, homologous to E. coli DnaJ	#N/A	#N/A		

184	YGL234W	ADE5,7	0	0	12	purine nucleotide biosynthesis*	phosphoribosylamine-glycine ligase activity*	cytoplasm	Bifunctional enzyme of the 'de novo' purine nucleotide biosynthetic pathway, contains aminoimidazole ribotide synthetase and glycinamide ribotide synthetase activities	#N/A	#N/A		
185	YMR300C	ADE4	0	0	8	purine nucleotide biosynthesis*	amidophosphoribosyltransferase activity	cytoplasm	Phosphoribosylpyrophosphate amidotransferase (PRPPAT; amidophosphoribosyltransferase), catalyzes first step of the 'de novo' purine nucleotide biosynthetic pathway	#N/A	#N/A		
186	YAR002W	NUP60	0	0	6	nucleocytoplasmic transport*	structural constituent of nuclear pore	nuclear pore	Subunit of the nuclear pore complex (NPC), functions to anchor Nup2p to the NPC in a dynamic process that is controlled by the nucleoplasmic concentration of Gsp1p-GTP; potential Cdc28p substrate	#N/A	#N/A		
187	YDL025C	Uncharacterized	0	0	7	biological_process unknown	protein kinase activity	cellular_component unknown	#N/A	#N/A	#N/A		
188	YHR076W	PTC7	0	0	7	biological_process unknown	protein phosphatase type 2C activity	mitochondrion	Mitochondrially localized type 2C protein phosphatase; expression induced by growth on ethanol and by sustained osmotic stress; possible role in carbon source utilization in low oxygen enviroments	#N/A	#N/A		
189	YJR144W	MGM101	0	0	6	DNA repair*	DNA binding	mitochondrial chromosome	Involved in mitochondrial genome maintenance; (putative) nucleic acid interactor	#N/A	#N/A		
190	YHR001W-A	QCR10	0	0	6	aerobic respiration*	ubiquinol-cytochrome-c reductase activity	mitochondrion*	8.5 kDa subunit of the ubiquinol-cytochrome c oxidoreductase complex	#N/A	#N/A		
191	YDR408C	ADE8	0	0	6	purine nucleotide biosynthesis*	phosphoribosylglycinamide formyltransferase activity	cytoplasm*	Phosphoribosyl-glycinamide transformylase, catalyzes a step in the 'de novo' purine nucleotide biosynthetic pathway	#N/A	#N/A		
192	YIL052C	RPL34B	0	0	5	protein biosynthesis	structural constituent of ribosome	cytosolic large ribosomal subunit (sensu Eukaryota)	Protein component of the large (60S) ribosomal subunit, nearly identical to Rpl34Ap and has similarity to rat L34 ribosomal protein	#N/A	#N/A		
193	YNL086W	Uncharacterized	0	0	4	biological_process unknown	molecular_function unknown	endosome	#N/A	#N/A	#N/A		
194	YBR156C	SLI15	0	0	4	protein amino acid phosphorylation*	protein kinase activator activity	spindle microtubule*	Mitotic spindle protein involved in chromosome segregation.	#N/A	#N/A		
195	YNR045W	PET494	0	0	4	protein biosynthesis	translation regulator activity	mitochondrial inner membrane	Specific translational activator for the COX3 mRNA that acts together with Pet54p and Pet122p; located in the mitochondrial inner membrane	#N/A	#N/A		
196	YLR255C	Dubious	0	0	4	#N/A	#N/A	#N/A	#N/A	#N/A	#N/A		
197	YBR277C	Dubious	0	0	4	#N/A	#N/A	#N/A	#N/A	YBR278W	DPB3		
198	YNL066W	SUN4	0	0	4	mitochondrion organization and biogenesis	glucosidase activity	cell wall (sensu Fungi)*	Protein involved in the aging process; related to glucanases	#N/A	#N/A		
199	YNR049C	MSO1	0	0	4	sporulation (sensu Fungi)*	molecular_function unknown	microsome	Probable component of the secretory vesicle docking complex, acts at a late step in secretion; shows genetic and physical interactions with Sec1p and is enriched in microsomal membrane fractions; required for sporulation	#N/A	#N/A		
200	YDR440W	DOT1	0	0	3	chromatin silencing at telomere*	protein-lysine N-methyltransferase activity	nucleus	Nucleosomal histone H3-Lys79 methylase, associates with transcriptionally active genes, functions in gene silencing at telomeres, most likely by directly modulating chromatin structure and Sir protein localization	#N/A	#N/A		
201	YHR092C	HXT4	0	0	3	hexose transport	glucose transporter activity*	plasma membrane	High-affinity glucose transporter of the major facilitator superfamily, expression is induced by low levels of glucose and repressed by high levels of glucose	#N/A	#N/A		

202	YKR024C	DBP7	0	0	3	35S primary transcript processing*	ATP-dependent RNA helicase activity	nucleolus	Putative ATP-dependent RNA helicase of the DEAD-box family involved in ribosomal biogenesis	#N/A	#N/A		
203	YDR363W-A	SEM1	0	0	3	regulation of cell cycle*	molecular_function unknown	nucleus*	Component of the lid subcomplex of the regulatory subunit of the 26S proteasome; ortholog of human DSS1	#N/A	#N/A		
204	YLL005C	SPO75	0	0	3	sporulation (sensu Fungi)	molecular_function unknown	cellular_component unknown	Meiosis-specific protein of unknown function, required for spore wall formation during sporulation; dispensible for both nuclear divisions during meiosis	#N/A	#N/A		
205	YML099C	ARG81	0	0	3	arginine metabolism*	transcription cofactor activity	nucleus	Zinc-finger transcription factor of the Zn(2)-Cys(6) binuclear cluster domain type, involved in the regulation of arginine-responsive genes; acts with Arg80p and Arg82p	YML100W-A	0		
206	YMR008C	PLB1	0	0	3	glycerophospholipid metabolism	lysophospholipase activity	cell wall (sensu Fungi)	Responsible for the production of the deacylation products of phosphatidylcholine and phosphatidylethanolamine but not phosphatidylinositol; Phospholipase B (lypophospholipase)	#N/A	#N/A		
207	YLL049W	Uncharacterized	0	0	3	biological_process unknown	molecular_function unknown	cellular_component unknown	#N/A	#N/A	#N/A		
208	YPL213W	LEA1	0	0	3	nuclear mRNA splicing, via spliceosome	pre-mRNA splicing factor activity	cytoplasm*	Component of U2 snRNP; disruption causes reduced U2 snRNP levels; physically interacts with Msl1p; putative homolog of human U2A' snRNP protein	#N/A	#N/A		
209	YDR191W	HST4	0	0	3	chromatin silencing at telomere*	DNA binding	cytoplasm*	Member of the Sir2 family of NAD(+)-dependent protein deacetylases; involved along with Hst3p in silencing at telomeres, cell cycle progression, radiation resistance, genomic stability and short-chain fatty acid metabolism	#N/A	#N/A		
210	YML009c	MRPL39	0	0	3	protein biosynthesis	structural constituent of ribosome	mitochondrial large ribosomal subunit	Mitochondrial ribosomal protein of the large subunit	#N/A	#N/A		
211	YAL008W	FUN14	0	0	3	biological_process unknown	molecular_function unknown	mitochondrion	Protein of unknown function	#N/A	#N/A		
212	YJR032W	CPR7	0	0	3	response to stress	unfolded protein binding*	cytosol	Peptidyl-prolyl cis-trans isomerase (cyclophilin), catalyzes the cis-trans isomerization of peptide bonds N-terminal to proline residues; binds to Hsp82p and contributes to chaperone activity	#N/A	#N/A		
213	YGR148C	RPL24B	0	0	3	protein biosynthesis	structural constituent of ribosome*	cytosolic large ribosomal subunit (sensu Eukaryota)	Ribosomal protein L30 of the large (60S) ribosomal subunit, nearly identical to Rpl24Ap and has similarity to rat L24 ribosomal protein; not essential for translation but may be required for normal translation rate	#N/A	#N/A		
214	YHR093W	Dubious	0	0	3	#N/A	#N/A	#N/A	Dubious open reading frame, unlikely to encode a protein; not conserved in closely related Saccharomyces species; multicopy suppressor of glucose transport defects, likely due to the presence of an HXT4 regulatory element in the region	#N/A	#N/A		
215	YLR370C	ARC18	0	0	3	actin filament organization	structural constituent of cytoskeleton	Arp2/3 protein complex	Subunit of the ARP2/3 complex, which is required for the motility and integrity of cortical actin patches	#N/A	#N/A		
216	YLR425W	TUS1	0	0	3	cell wall organization and biogenesis*	Rho guanyl-nucleotide exchange factor activity	cellular_component unknown	Guanine nucleotide exchange factor (GEF) that functions to modulate Rhop1 activity as part of the cell integrity signaling pathway; multicopy suppressor of tor2 mutation and ypk1 ypk2 double mutation; potential Cdc28p substrate	#N/A	#N/A		
217	YGR102C	Uncharacterized	0	0	3	biological_process unknown	molecular_function unknown	mitochondrion	#N/A	#N/A	#N/A		
218	YGR219W	Dubious	0	0	3	#N/A	#N/A	#N/A	#N/A	YGR220C	MRPL9		
219	YKR097W	PCK1	0	0	2	gluconeogenesis	phosphoenolpyruvate carboxykinase (ATP) activity	cytosol	Phosphoenolpyruvate carboxykinase, key enzyme in gluconeogenesis, catalyzes early reaction in carbohydrate biosynthesis, glucose represses transcription and accelerates mRNA degradation, regulated by Mcm1p and Cat8p, located in the cytosol	#N/A	#N/A		
220	YGL117W	Uncharacterized	0	0	2	biological_process unknown	molecular_function unknown	cellular_component unknown	#N/A	#N/A	#N/A		

221	YGR027C	RPS25A	0	0	2	protein biosynthesis	structural constituent of ribosome	cytosolic small ribosomal subunit (sensu Eukaryota)	Protein component of the small (40S) ribosomal subunit; nearly identical to Rps25Bp and has similarity to rat S25 ribosomal protein	#N/A	#N/A		
222	YGR141W	VPS62	0	0	2	protein-vacuolar targeting	molecular_function unknown	cellular_component unknown	Vacuolar protein sorting (VPS) protein required for cytoplasm to vacuole targeting of proteins	#N/A	#N/A		
223	YIL137C	RBF108	0	0	2	biological_process unknown	molecular_function unknown	cytoplasm	Hypothetical ORF	#N/A	#N/A		
224	YLR443W	ECM7	0	0	2	cell wall organization and biogenesis	molecular_function unknown	integral to membrane	Non-essential protein of unknown function	YLR444C	#N/A		
225	YMR106C	YKU80	0	0	2	chromatin assembly or disassembly*	RNA binding*	nuclear chromatin*	Forms heterodimer with Yku70p known as Ku, binds chromosome ends and is involved in maintaining normal telomere length and structure, in addition to participating in the formation of silent chromatin at telomere-proximal genes	#N/A	#N/A		
226	YNR048W	Uncharacterized	0	0	2	biological_process unknown	transcription regulator activity	cellular_component unknown	#N/A	#N/A	#N/A		
227	YNL257C	SIP3	0	0	2	transcription initiation from Pol II promoter	transcription cofactor activity	nucleus	Protein that activates transcription through interaction with DNA-bound Snf1p, C-terminal region has a putative leucine zipper motif; potential Cdc28p substrate	#N/A	#N/A		
228	YDR231C	COX20	0	0	2	aerobic respiration*	unfolded protein binding	mitochondrial inner membrane	Mitochondrial inner membrane protein, required for proteolytic processing of Cox2p and its assembly into cytochrome c oxidase	YDR230W	#N/A		
229	YCR095C	Uncharacterized	0	0	2	biological_process unknown	molecular_function unknown	cytoplasm	#N/A	#N/A	#N/A		
230	YDL096C	Dubious	0	0	2	#N/A	#N/A	#N/A	#N/A	YDL095W	PMT1		
231	YDL155W	CLB3	0	0	2	G2/M transition of mitotic cell cycle*	cyclin-dependent protein kinase regulator activity	cytoplasm*	Involved in mitotic induction and perhaps in DNA replication and spindle assembly; G(sub)2-specific B-type cyclin	#N/A	#N/A		
232	YGR153W	Uncharacterized	0	0	2	biological_process unknown	molecular_function unknown	cellular_component unknown	#N/A	#N/A	#N/A		
233	YHL006C	SHU1	0	0	2	biological_process unknown	molecular_function unknown	cellular_component unknown	Protein involved in recombination	#N/A	#N/A		
234	YGR171C	MSM1	0	0	2	methionyl-tRNA aminoacylation	methionine-tRNA ligase activity	mitochondrion	Mitochondrial methionyl-tRNA synthetase (MetRS), functions as a monomer in mitochondrial protein synthesis; functions similarly to cytoplasmic MetRS although the cytoplasmic form contains a zinc-binding domain not found in Msm1p	#N/A	#N/A		
235	YHR204W	MNL1	0	0	2	ER-associated protein catabolism	carbohydrate binding	endoplasmic reticulum	Alpha mannosidase-like protein of the endoplasmic reticulum required for degradation of glycoproteins but not for processing of N-linked oligosaccharides	#N/A	#N/A		
236	YFR013W	IOC3	0	0	2	chromatin remodeling	protein binding	ISW1 complex	Member of a complex (Isw1a) with Isw1p that has nucleosome-stimulated ATPase activity and represses transcription initiation by specific positioning of a promoter proximal dinucleosome; has homology to Esc8p, which is involved in silencing	#N/A	#N/A		
237	YHR087W	Uncharacterized	0	0	2	biological_process unknown	molecular_function unknown	cytoplasm*	#N/A	#N/A	#N/A		
238	YJR053W	BFA1	0	0	2	conjugation with cellular fusion*	GTPase activator activity	spindle pole body	Component of the GTPase-activating Bfa1p-Bub2p complex involved in multiple cell cycle checkpoint pathways that control exit from mitosis	#N/A	#N/A		
239	YML090W	Dubious	0	0	2	#N/A	#N/A	#N/A	#N/A	YML089C	#N/A		

240	YOR058C	ASE1	0	0	2	mitotic spindle organization and biogenesis in nucleus*	microtubule binding	spindle microtubule*	Member of a family of microtubule-associated proteins (MAPs) that function at the mitotic spindle midzone; required for spindle elongation; undergoes cell cycle-regulated degradation by anaphase promoting complex; potential Cdc28p substrate	#N/A	#N/A		
241	YDR156W	RPA14	0	0	2	transcription from Pol I promoter	DNA-directed RNA polymerase activity	DNA-directed RNA polymerase I complex	RNA polymerase I subunit A14	YDR157W	#N/A		
242	YGR071C	Uncharacterized	0	0	2	biological_process unknown	molecular_function unknown	nucleus	#N/A	#N/A	#N/A		
243	YNL089C	Dubious	0	0	2	#N/A	#N/A	#N/A	#N/A	YNL090W	RHO2		
244	YOR066W	Uncharacterized	0	0	2	biological_process unknown	molecular_function unknown	cellular_component unknown	#N/A	#N/A	#N/A		
245	YDL082W	RPL13A	0	0	2	protein biosynthesis	structural constituent of ribosome	cytosolic large ribosomal subunit (sensu Eukaryota)	Protein component of the large (60S) ribosomal subunit, nearly identical to Rpl13Bp; not essential for viability; has similarity to rat L13 ribosomal protein	#N/A	#N/A		
246	YDR171W	HSP42	0	0	2	response to stress*	unfolded protein binding	cytoplasm*	Small cytosolic stress-induced chaperone that forms barrel-shaped oligomers and suppresses the aggregation of non-native proteins; oligomer dissociation is not required for function; involved in cytoskeleton reorganization after heat shock	#N/A	#N/A		
247	YCR067C	SED4	0	0	2	ER to Golgi transport	molecular_function unknown	endoplasmic reticulum	Sed4p is an integral ER membrane protein, which, along along with its close homolog, Sec12p, is involved in vesicle formation at the ER; Intracellular transport protein	#N/A	#N/A		
248	YER156C	Uncharacterized	0	0	2	biological_process unknown	molecular_function unknown	cytoplasm*	#N/A	#N/A	#N/A		
249	YHR066W	SSF1	0	0	2	ribosomal large subunit assembly and maintenance*	rRNA binding	nucleolus	putative involvement in mating; homologous to Ssf2p	#N/A	#N/A		
250	YKL217W	JEN1	0	0	2	lactate transport	lactate transporter activity	mitochondrion*	Lactate transporter, required for uptake of lactate and pyruvate; expression is derepressed by transcriptional activator Cat8p under nonfermentative growth conditions, and repressed in the presence of glucose, fructose, and mannose	#N/A	#N/A		
251	YJL047C	RTT101	wrong	wrong	15	ubiquitin-dependent protein catabolism*	protein binding*	cytoplasm*	Cullin family member; subunit of a complex containing ubiquitin ligase activity; binds HRT1 and is modified by the ubiquitin like protein, RUB1; Regulator of Ty1 Transposition; Regulator of Ty1 Transposition	#N/A	#N/A		
252	YKL055C	OAR1	wrong	wrong	6	aerobic respiration*	3-oxoacyl-[acyl-carrier protein] reductase activity	mitochondrion	Mitochondrial 3-oxoacyl-[acyl-carrier-protein] reductase, may comprise a type II mitochondrial fatty acid synthase along with Mct1p	#N/A	#N/A		
253	YNR042W	Dubious	wrong	wrong	2	#N/A	#N/A	#N/A	#N/A	YNR041C	COQ2		
254	YJL075C	Dubious	wrong	nd	9	#N/A	#N/A	#N/A	Dubious open reading frame, unlikely to encode a protein; not conserved in closely related Saccharomyces species; 85% of ORF overlaps the verified gene NET1	YJL076W	NET1		
255	YJR060W	CBF1	wrong	contam	6	chromatin assembly or disassembly*	DNA binding*	nucleus*	Helix-loop-helix protein that binds the motif CACRTG (R=A or G), which is present at several sites including MET gene promoters and centromere DNA element I (CDEI); required for nucleosome positioning at this motif; targets Isw1p to DNA	#N/A	#N/A		
256	YOR014W	RTS1	wrong	0	19	protein biosynthesis*	protein phosphatase type 2A activity	cytoplasm*	B-type regulatory subunit of protein phosphatase 2A (PP2A)	#N/A	#N/A		

257	YNL133C	FYV6	wrong	0	18	double-strand break repair via nonhomologous end-joining	molecular_function unknown	nucleus	Protein of unknown function, required for survival upon exposure to K1 killer toxin; proposed to regulate double-strand break repair via non-homologous end-joining	#N/A	#N/A		
258	YIL018W	RPL2B	wrong	0	17	protein biosynthesis	structural constituent of ribosome	cytosolic large ribosomal subunit (sensu Eukaryota)	Protein component of the large (60S) ribosomal subunit, identical to Rpl2Ap and has similarity to E. coli L2 and rat L8 ribosomal proteins; expression is upregulated at low temperatures	#N/A	#N/A		
259	YJL127C	SPT10	wrong	0	13	chromatin remodeling*	histone acetyltransferase activity	nucleus	Putative histone acetylase, required for transcriptional regulation at core promoters, functions at or near the TATA box	#N/A	#N/A		
260	YLR304C	ACO1	wrong	0	10	tricarboxylic acid cycle*	aconitate hydratase activity	cytosol*	Mitochondrial aconitase, required for the tricarboxylic acid (TCA) cycle; mutation leads to glutamate auxotrophy	#N/A	#N/A		
261	YDR417C	Dubious	wrong	0	7	#N/A	#N/A	#N/A	#N/A	YDR418W	RPL12B		
262	YHR194W	MDM31	wrong	0	6	mitochondrion organization and biogenesis	molecular_function unknown	nucleus	Mitochondrial Distribution and Morphology	#N/A	#N/A		
263	YPR047W	MSF1	wrong	0	5	protein biosynthesis	phenylalanine tRNA ligase activity	mitochondrion	Mitochondrial phenylalanyl-tRNA synthetase alpha subunit, active as a monomer, unlike the cytoplasmic subunit which is active as a dimer complexed to a beta subunit dimer; similar to the alpha subunit of E. coli phenylalanyl-tRNA synthetase	#N/A	#N/A		
264	YDR226W	ADK1	wrong	0	5	cell proliferation	adenylate kinase activity	cytoplasm*	adenylate kinase	#N/A	#N/A		
265	YJL124C	LSM1	wrong	0	5	rRNA processing*	RNA cap binding	cytoplasmic mRNA processing body*	Component of small nuclear ribonucleoprotein complexes involved in mRNA decapping and decay	#N/A	#N/A		
266	YFL013W-A	Dubious	wrong	0	4	#N/A	#N/A	#N/A	#N/A	YFL013C	IES1		
267	YKR091W	SRL3	wrong	0	4	nucleobase, nucleoside, nucleotide and nucleic acid metabolism	molecular_function unknown	cytoplasm	Cytoplasmic protein that, when overexpressed, suppresses the lethality of a rad53 null mutation; potential Cdc28p substrate	#N/A	#N/A		
268	YKL006W	RPL14A	wrong	0	4	protein biosynthesis	structural constituent of ribosome*	cytosolic large ribosomal subunit (sensu Eukaryota)	N-terminally acetylated protein component of the large (60S) ribosomal subunit, nearly identical to Rpl14Bp and has similarity to rat L14 ribosomal protein; rpl14a csh5 double null mutant exhibits synthetic slow growth	#N/A	#N/A		
269	YJL102W	MEF2	wrong	0	2	translational elongation	translation elongation factor activity	mitochondrion	mitochondrial elongation factor G-like protein	#N/A	#N/A		
270	YPR042C	PUF2	wrong	0	2	mRNA catabolism, deadenylylation-dependent decay	mRNA binding	cytoplasm	mRNA binding protein	#N/A	#N/A		
271	YKR093W	PTR2	wrong	0	2	peptide transport	peptide transporter activity	plasma membrane	Functions in transport of small peptides into the cell; Peptide transporter	#N/A	#N/A		
272	YJR154W	Uncharacterized	wrong	0	2	biological_process unknown	molecular_function unknown	cytoplasm	#N/A	#N/A	#N/A		

273	YKR092C	SRP40	wrong	0	2	nucleocytoplasmic transport	unfolded protein binding	nucleolus	Suppressor of mutant AC40 subunit of RNA polymerase I and III; nucleolar protein that is immunologically and structurally related to rat Nopp140, a nonribosomal protein of the nucleolus and coiled bodies.	#N/A	#N/A		
274	YJR047C	ANB1	wrong	0	2	translational initiation	translation initiation factor activity	ribosome	Translation initiation factor eIF-5A, promotes formation of the first peptide bond; similar to and functionally redundant with Hyp2p; undergoes an essential hypusination modification; expressed under anaerobic conditions	#N/A	#N/A		
275	YAL016W	TPD3	nd	nd	75	protein biosynthesis*	protein phosphatase type 2A activity	cytoplasm*	protein phosphatase 2A regulatory subunit A	#N/A	#N/A		
276	YAL019W	FUN30	nd	0	3	chromosome organization and biogenesis (sensu Eukaryota)	molecular_function unknown	nucleus*	Protein whose overexpression affects chromosome stability, potential Cdc28p substrate; homolog of Snf2p	#N/A	#N/A		
277	YDR159W	SAC3	contam	wrong	5	mRNA-nucleus export*	protein binding	nuclear pore	Nuclear pore-associated protein, forms a complex with Thp1p that is involved in transcription and in mRNA export from the nucleus	#N/A	#N/A		
278	YKL221W	MCH2	contam	0	2	transport	transporter activity*	membrane	Protein with similarity to mammalian monocarboxylate permeases, which are involved in transport of monocarboxylic acids across the plasma membrane; mutant is not deficient in monocarboxylate transport	#N/A	#N/A		
279	YIL125W	KGD1	contam	0	2	tricarboxylic acid cycle*	oxoglutarate dehydrogenase (succinyl-transferring) activity	mitochondrial matrix*	Component of the mitochondrial alpha-ketoglutarate dehydrogenase complex, which catalyzes a key step in the tricarboxylic acid (TCA) cycle, the oxidative decarboxylation of alpha-ketoglutarate to form succinyl-CoA	#N/A	#N/A		
280	YOR241W	MET7	0	wrong	13	one-carbon compound metabolism	tetrahydrofolylpolyglutamate synthase activity	cytoplasm*	Folylpolyglutamate synthetase, catalyzes extension of the glutamate chains of the folate coenzymes, required for methionine synthesis and for maintenance of mitochondrial DNA, present in both the cytoplasm and mitochondria	#N/A	#N/A		
281	YGR180C	RNR4	0	wrong	9	DNA replication	ribonucleoside-diphosphate reductase activity	cytoplasm*	Ribonucleotide-diphosphate reductase (RNR), small subunit; the RNR complex catalyzes the rate-limiting step in dNTP synthesis and is regulated by DNA replication and DNA damage checkpoint pathways via localization of the small subunits	#N/A	#N/A		
282	YER070W	RNR1	0	wrong	8	DNA replication	ribonucleoside-diphosphate reductase activity	cytoplasm	Ribonucleotide-diphosphate reductase (RNR), large subunit; the RNR complex catalyzes the rate-limiting step in dNTP synthesis and is regulated by DNA replication and DNA damage checkpoint pathways via localization of the small subunits	#N/A	#N/A		
283	YPL059W	GRX5	0	wrong	7	response to osmotic stress*	thiol-disulfide exchange intermediate activity	mitochondrial matrix	Hydroperoxide and superoxide-radical responsive glutathione-dependent oxidoreductase; mitochondrial matrix protein involved in the synthesis/assembly of iron-sulfur centers; monothiol glutaredoxin subfamily member along with Grx3p and Grx4p	#N/A	#N/A		
284	YDR350C	TCM10	0	wrong	6	protein complex assembly	molecular_function unknown	mitochondrial inner membrane	Mitochondrial inner membrane protein required for assembly of the F0 sector of mitochondrial F1F0 ATP synthase, which is a large, evolutionarily conserved enzyme complex required for ATP synthesis	#N/A	#N/A		
285	YNL315C	ATP11	0	wrong	5	protein complex assembly	unfolded protein binding	mitochondrial matrix	Molecular chaperone, required for the assembly of alpha and beta subunits into the F1 sector of mitochondrial F1F0 ATP synthase	#N/A	#N/A		
286	YPL027W	SMA1	0	wrong	3	spore wall assembly (sensu Fungi)	molecular_function unknown	cellular_component unknown	Spore Membrane Assembly	#N/A	#N/A		
287	YEL013W	VAC8	0	wrong	3	protein-vacuolar targeting*	protein binding	vacuole (sensu Fungi)	Phosphorylated vacuolar membrane protein that interacts with Atg13p, required for the cytoplasm-to-vacuole targeting (Cvt) pathway; interacts with Nvj1p to form nucleus-vacuole junctions	#N/A	#N/A		
288	YNL047C	SLM2	0	wrong	2	actin cytoskeleton organization and biogenesis	phosphoinositide binding	plasma membrane	Phosphoinositide PI4,5P(2) binding protein, forms a complex with Slm1p; acts downstream of Mss4p in a pathway regulating actin cytoskeleton organization in response to stress; phosphorylated by the Tor2p-containing complex TORC2	#N/A	#N/A		
289	YDR194C	MSS116	0	wrong	2	RNA splicing	RNA helicase activity	mitochondrial matrix	Mitochondrial RNA helicase of the DEAD box family, necessary for splicing of several mitochondrial introns	#N/A	#N/A		

290	YNL213C	Uncharacterized	0	nd	13	mitochondrion organization and biogenesis	molecular_function unknown	mitochondrion	#N/A	#N/A	#N/A		
291	YOR128C	ADE2	0	nd	6	purine nucleotide biosynthesis*	phosphoribosylaminoimidazole carboxylase activity	cytoplasm	Phosphoribosylaminoimidazole carboxylase, catalyzes a step in the 'de novo' purine nucleotide biosynthetic pathway; red pigment accumulates in mutant cells deprived of adenine	#N/A	#N/A		
292	YEL003W	GIM4	0	contam	19	tubulin folding	tubulin binding	cytoplasm*	Prefoldin subunit 2; putative homolog of subunit 2 of bovine prefoldin, a chaperone comprised of six subunits; bovine prefoldin subunit 2 homolog (putative)	#N/A	#N/A		
293	YPL022W	RAD1	0	contam	5	removal of nonhomologous ends*	single-stranded DNA specific endodeoxyribonuclease activity	nucleotide excision repair factor 1 complex	Single-stranded DNA endonuclease (with Rad10p), cleaves single-stranded DNA during nucleotide excision repair and double-strand break repair; subunit of Nucleotide Excision Repair Factor 1 (NEF1); homolog of human ERCC1 protein	#N/A	#N/A		

Appendix 3 Gene ontology (GO) cellular component annotation enrichment among non-essential yeast CIN genes

Over-representation of GO cellular components in the 293 yeast CIN gene list and the high confident 130 subset, compared to all yeast genes, was determined using GO TermFinder as of August 23, 2006 (db.yeastgenome.org/cgi-bin/GO/goTermFinder.pl) (Harris et al., 2004).

GO_ID	GO_term (Cellular component)	Frequency	Genome Frequency	Probability	Genes
All 293 CIN genes					
5634	nucleus	144 out of 293 genes, 49.1%	1984 out of 7286 annotated genes, 27.2%	1.37E-15	SIC1 CTF4 CSM3 TOF1 IML3 CHL1 MCM21 RAD61 MCM16 MCM22 MEC3 DDC1 CHL4 BUB3 RAD52 SPT21 SHP1 LGE1 RAD27 RMI1 RAD50 RAD54 ELG1 MRC1 MMS4 MMS22 RDH54 CTF3 CIN8 CDH1 EST3 MAD1 MAD2 LSM6 CLN3 THP2 NUP133 CDC73 BUB1 DOC1 CTF19 NUP120 RAD6 XRS2 TOP3 RAD57 RRM3 HST3 ESC2 RTT107 RAD55 SGS1 PSH1 MUS81 HHF1 RAD24 HCM1 RAD59 POL32 RAD9 RAD17 RNH201 RNH203 CLB5 RNH202 SWC3 RAD10 SPT2 RTT109 RAD5 RPA12 YDL156W RAD18 THP1 RAD51 YTA7 ASF1 HPR5 SGO1 CNN1 BRE1 MFT1 CYC8 ADE1 MRE11 DUN1 MUD2 SNU66 SGF73 AFT1 SPT4 YJR008W MOG1 RTT106 SGF11 CTK2 SDS3 STB1 SRB8 SWC5 NGG1 SWR1 ARP6 YGR058W MPH1 KAP120 TUB3 NUT1 CAC2 HTZ1 VID21 NUP84 GLC8 NUP60 ADE8 DOT1 DBP7 SEM1 ARG81 LEA1 HST4 YKU80 SIP3 CLB3 SHU1 IOC3 YHR087W ASE1 RPA14 YGR071C YER156C SSF1 RTT101 CBF1 RTS1 FYV6 SPT10 MDM31 SRP40 TPD3 FUN30 SAC3 RNR4 RAD1
5694	chromosome	37 out of 293 genes, 12.6%	214 out of 7286 annotated genes, 2.9%	1.59E-13	CTF8 CTF4 DCC1 BIM1 TOF1 IML3 MCM21 MCM16 MCM22 DDC1 CHL4 BUB3 RAD52 ELG1 MRC1 CTF3 CIN8 MAD2 CTF18 BUB1 CTF19 RRM3 HHF1 RAD24 POL32 RAD5 RAD18 RAD51 SGO1 CNN1 SPT4 CAC2 HTZ1 MGM101 YKU80 CBF1 RTS1
44427	chromosomal part	31 out of 293 genes, 10.5%	184 out of 7286 annotated genes, 2.5%	3.21E-11	CTF8 DCC1 BIM1 IML3 MCM21 MCM16 MCM22 CHL4 BUB3 ELG1 MRC1 CTF3 CIN8 MAD2 CTF18 BUB1 CTF19 RRM3 HHF1 RAD24 POL32 RAD5 RAD18 SGO1 CNN1 SPT4 CAC2 HTZ1 YKU80 CBF1 RTS1
775	chromosome, pericentric region	18 out of 293 genes, 6.1%	61 out of 7286 annotated genes, 0.8%	1.06E-10	BIM1 IML3 MCM21 MCM16 MCM22 CHL4 BUB3 CTF3 CIN8 MAD2 BUB1 CTF19 SGO1 CNN1 SPT4 CAC2 CBF1 RTS1
776	kinetochore	16 out of 293 genes, 5.4%	54 out of 7286 annotated genes, 0.7%	1.11E-09	BIM1 IML3 MCM21 MCM16 MCM22 CHL4 BUB3 CTF3 CIN8 MAD2 BUB1 CTF19 SGO1 CNN1 SPT4 CBF1
228	nuclear chromosome	26 out of 293 genes, 8.8%	175 out of 7286 annotated genes, 2.4%	1.70E-08	CTF4 TOF1 IML3 MCM21 MCM16 MCM22 DDC1 CHL4 BUB3 RAD52 MRC1 CTF3 CIN8 MAD2 BUB1 CTF19 RRM3 HHF1 POL32 RAD5 RAD18 RAD51 SPT4 HTZ1 YKU80 RTS1
43226	organelle	204 out of 293 genes, 69.6%	3937 out of 7286 annotated genes, 54.0%	3.64E-08	CTF8 SIC1 CTF4 DCC1 BIM1 CSM3 TOF1 IML3 CHL1 MCM21 RAD61 MCM16 MCM22 MEC3 DDC1 CHL4 BUB3 RAD52 SPT21 SHP1 LGE1 RAD27 RMI1 RAD50 RAD54 ELG1 MRC1 MMS4 MMS22 RDH54 CTF3 CIN8 CDH1 EST3 MAD1 MAD2 LSM6 CTF18 CLN3 THP2 NUP133 CDC73 BUB1 KAR3 DOC1 CTF19 NUP120 RAD6 XRS2 TOP3 RAD57 RRM3 HST3 ESC2 YDR532C RTT107 RAD55 SGS1 PSH1 MUS81 HHF1 RAD24 HCM1 RAD59 POL32 RAD9 RAD17 RNH201 RNH203 CLB5 RNH202 SWC3 RAD10 SPT2 RTT109 RAD5 RPA12 YDL156W UPS1 RAD18 ETR1 THP1 RAD51 YTA7 ASF1 HPR5 OMA1 SGO1 ISA2 CNN1 VPS64 BRE1 MFT1 CYC8 ADE1 MRE11 DUN1 SOV1 TPO1 SHE1 MUD2 SNU66 SGF73 AFT1 SPT4 RPS23A YJR008W MOG1 RTT106 SGF11 ALD6 CTK2 CIK1 SDS3 STB1 SRB8 SWC5 NGG1 SWR1 ARP6 MID1 YGR058W MPH1 KAP120 ARV1 TUB3 NUT1 CAC2 HTZ1 VID21 ZUO1 NUP84 GLC8 MDJ1 RTN2 NUP60 PTC7 MGM101 QCR10 ADE8 RPL34B YNL086W SLI15 PET494 SUN4 DOT1 DBP7 SEM1 ARG81 LEA1 HST4 MRPL39 FUN14 RPL24B ARC18 YGR102C RPS25A YKU80 SIP3 COX20 CLB3 SHU1 MSM1 MNL1 IOC3 YHR087W BFA1 ASE1 RPA14 YGR071C RPL13A HSP42 SED4 YER156C SSF1 JEN1 RTT101 OAR1 CBF1 RTS1 FYV6 RPL2B SPT10 ACO1 MDM31 MSF1 ADK1 RPL14A MEF2 SRP40 ANB1 TPD3 FUN30 SAC3 KGD1 MET7 RNR4 GRX5 TCM10 ATP11 VAC8 MSS116 YNL213C RAD1
43229	intracellular organelle	204 out of 293 genes, 69.6%	3937 out of 7286 annotated genes, 54.0%	3.64E-08	CTF8 SIC1 CTF4 DCC1 BIM1 CSM3 TOF1 IML3 CHL1 MCM21 RAD61 MCM16 MCM22 MEC3 DDC1 CHL4 BUB3 RAD52 SPT21 SHP1 LGE1 RAD27 RMI1 RAD50 RAD54 ELG1 MRC1 MMS4 MMS22 RDH54 CTF3 CIN8 CDH1 EST3 MAD1 MAD2 LSM6 CTF18 CLN3 THP2 NUP133 CDC73 BUB1 KAR3 DOC1 CTF19 NUP120 RAD6 XRS2 TOP3 RAD57 RRM3 HST3 ESC2 YDR532C RTT107 RAD55 SGS1 PSH1 MUS81 HHF1 RAD24 HCM1 RAD59 POL32 RAD9 RAD17 RNH201 RNH203 CLB5 RNH202 SWC3 RAD10 SPT2 RTT109 RAD5 RPA12 YDL156W UPS1 RAD18 ETR1 THP1 RAD51 YTA7 ASF1 HPR5 OMA1 SGO1 ISA2 CNN1 VPS64 BRE1 MFT1 CYC8 ADE1 MRE11 DUN1 SOV1 TPO1 SHE1 MUD2 SNU66 SGF73 AFT1 SPT4 RPS23A YJR008W MOG1 RTT106 SGF11 ALD6 CTK2 CIK1 SDS3 STB1 SRB8 SWC5 NGG1 SWR1 ARP6 MID1 YGR058W MPH1 KAP120 ARV1 TUB3 NUT1 CAC2 HTZ1 VID21 ZUO1 NUP84 GLC8 MDJ1 RTN2 NUP60 PTC7 MGM101 QCR10 ADE8 RPL34B YNL086W SLI15 PET494 SUN4 DOT1 DBP7 SEM1 ARG81 LEA1 HST4 MRPL39 FUN14 RPL24B ARC18 YGR102C RPS25A YKU80 SIP3 COX20 CLB3 SHU1 MSM1 MNL1 IOC3 YHR087W BFA1 ASE1 RPA14 YGR071C RPL13A HSP42 SED4 YER156C SSF1 JEN1 RTT101 OAR1 CBF1 RTS1 FYV6 RPL2B SPT10 ACO1 MDM31 MSF1 ADK1 RPL14A MEF2 SRP40 ANB1 TPD3 FUN30 SAC3 KGD1 MET7 RNR4 GRX5 TCM10 ATP11 VAC8 MSS116 YNL213C RAD1

44424	intracellular part	239 out of 293 genes, 81.5%	4995 out of 7286 annotated genes, 68.5%	3.55E-07	CTF8 SIC1 CTF4 DCC1 BIM1 CSM3 TOF1 IML3 CHL1 MCM21 RAD61 MCM16 MCM22 MEC3 DDC1 CHL4 SNO1 BUB3 RAD52 SPT21 SHP1 LGE1 RAD27 RMI1 RAD50 RAD54 ELG1 MRC1 MMS4 MMS22 RDH54 SSZ1 CTF3 CIN8 UBR1 CDH1 EST3 MAD1 MAD2 LSM6 CTF18 DIA2 CLN3 THP2 NUP133 CDC73 BUB1 IRC15 KAR3 DOC1 CTF19 NUP120 RAD6 XRS2 TOP3 RAD57 RRM3 HST3 ESC2 YDR532C RTT107 RAD55 SGS1 PSH1 MUS81 TSA1 HHF1 RAD24 HCM1 RAD59 SHM2 POL32 RAD9 RAD17 RNH201 RNH203 CLB5 RNH202 SWC3 RAD10 CYK3 SPT2 RTT109 RAD5 RPA12 PAC10 YDL156W UPS1 RAD18 ETR1 THP1 RAD51 YTA7 ASF1 HPR5 OMA1 SGO1 SRO7 ISA2 CNN1 VPS64 PIG1 YBP2 ADE6 BRE1 MFT1 CYC8 ADE1 MRE11 DUN1 SOV1 ADE17 TPO1 YOL070C SHE1 MUD2 SSK1 SNU66 SGF73 AFT1 SPT4 RPS23A YJR008W MOG1 RTT106 SGF11 ALD6 PPQ1 CTK2 CIK1 SDS3 STB1 SRB8 SWC5 PFD1 NGG1 SWR1 ARP6 MID1 YGR058W MPH1 KAP120 ARV1 TUB3 NUT1 CAC2 HTZ1 VID21 ZUO1 NUP84 GLC8 MET22 GIM5 MDJ1 RTN2 DJP1 ADE5,7 ADE4 NUP60 PTC7 MGM101 QCR10 ADE8 RPL34B YNL086W SLI15 PET494 SUN4 DOT1 DBP7 SEM1 ARG81 LEA1 HST4 MRPL39 FUN14 CPR7 RPL24B ARC18 YGR102C PCK1 RPS25A TMA108 YKU80 SIP3 COX20 OCA4 CLB3 SHU1 MSM1 MNL1 IOC3 YHR087W BFA1 ASE1 RPA14 YGR071C RPL13A HSP42 SED4 YER156C SSF1 JEN1 RTT101 OAR1 CBF1 RTS1 FYV6 RPL2B SPT10 ACO1 MDM31 MSF1 ADK1 LSM1 SRL3 RPL14A MEF2 PUF2 YJR154W SRP40 ANB1 T
5622	intracellular	239 out of 293 genes, 81.5%	5032 out of 7286 annotated genes, 69.0%	8.79E-07	CTF8 SIC1 CTF4 DCC1 BIM1 CSM3 TOF1 IML3 CHL1 MCM21 RAD61 MCM16 MCM22 MEC3 DDC1 CHL4 SNO1 BUB3 RAD52 SPT21 SHP1 LGE1 RAD27 RMI1 RAD50 RAD54 ELG1 MRC1 MMS4 MMS22 RDH54 SSZ1 CTF3 CIN8 UBR1 CDH1 EST3 MAD1 MAD2 LSM6 CTF18 DIA2 CLN3 THP2 NUP133 CDC73 BUB1 IRC15 KAR3 DOC1 CTF19 NUP120 RAD6 XRS2 TOP3 RAD57 RRM3 HST3 ESC2 YDR532C RTT107 RAD55 SGS1 PSH1 MUS81 TSA1 HHF1 RAD24 HCM1 RAD59 SHM2 POL32 RAD9 RAD17 RNH201 RNH203 CLB5 RNH202 SWC3 RAD10 CYK3 SPT2 RTT109 RAD5 RPA12 PAC10 YDL156W UPS1 RAD18 ETR1 THP1 RAD51 YTA7 ASF1 HPR5 OMA1 SGO1 SRO7 ISA2 CNN1 VPS64 PIG1 YBP2 ADE6 BRE1 MFT1 CYC8 ADE1 MRE11 DUN1 SOV1 ADE17 TPO1 YOL070C SHE1 MUD2 SSK1 SNU66 SGF73 AFT1 SPT4 RPS23A YJR008W MOG1 RTT106 SGF11 ALD6 PPQ1 CTK2 CIK1 SDS3 STB1 SRB8 SWC5 PFD1 NGG1 SWR1 ARP6 MID1 YGR058W MPH1 KAP120 ARV1 TUB3 NUT1 CAC2 HTZ1 VID21 ZUO1 NUP84 GLC8 MET22 GIM5 MDJ1 RTN2 DJP1 ADE5,7 ADE4 NUP60 PTC7 MGM101 QCR10 ADE8 RPL34B YNL086W SLI15 PET494 SUN4 DOT1 DBP7 SEM1 ARG81 LEA1 HST4 MRPL39 FUN14 CPR7 RPL24B ARC18 YGR102C PCK1 RPS25A TMA108 YKU80 SIP3 COX20 OCA4 CLB3 SHU1 MSM1 MNL1 IOC3 YHR087W BFA1 ASE1 RPA14 YGR071C RPL13A HSP42 SED4 YER156C SSF1 JEN1 RTT101 OAR1 CBF1 RTS1 FYV6 RPL2B SPT10 ACO1 MDM31 MSF1 ADK1 LSM1 SRL3 RPL14A MEF2 PUF2 YJR154W SRP40 ANB1 T
779	condensed chromosome, pericentric region	12 out of 293 genes, 4.0%	50 out of 7286 annotated genes, 0.6%	1.22E-06	IML3 MCM21 MCM16 MCM22 CHL4 BUB3 CTF3 CIN8 MAD2 BUB1 CTF19 RTS1
780	condensed nuclear chromosome, pericentric region	12 out of 293 genes, 4.0%	50 out of 7286 annotated genes, 0.6%	1.22E-06	IML3 MCM21 MCM16 MCM22 CHL4 BUB3 CTF3 CIN8 MAD2 BUB1 CTF19 RTS1
43231	intracellular membrane-bound organelle	185 out of 293 genes, 63.1%	3614 out of 7286 annotated genes, 49.6%	2.11E-06	SIC1 CTF4 CSM3 TOF1 IML3 CHL1 MCM21 RAD61 MCM16 MCM22 MEC3 DDC1 CHL4 BUB3 RAD52 SPT21 SHP1 LGE1 RAD27 RMI1 RAD50 RAD54 ELG1 MRC1 MMS4 MMS22 RDH54 CTF3 CIN8 CDH1 EST3 MAD1 MAD2 LSM6 CTF18 CLN3 THP2 NUP133 CDC73 BUB1 DOC1 CTF19 NUP120 RAD6 XRS2 TOP3 RAD57 RRM3 HST3 ESC2 RTT107 RAD55 SGS1 PSH1 MUS81 HHF1 RAD24 HCM1 RAD59 POL32 RAD9 RAD17 RNH201 RNH203 CLB5 RNH202 SWC3 RAD10 SPT2 RTT109 RAD5 RPA12 YDL156W UPS1 RAD18 ETR1 THP1 RAD51 YTA7 ASF1 HPR5 OMA1 SGO1 ISA2 CNN1 VPS64 BRE1 MFT1 CYC8 ADE1 MRE11 DUN1 SOV1 TPO1 MUD2 SNU66 SGF73 AFT1 SPT4 YJR008W MOG1 RTT106 SGF11 ALD6 CTK2 SDS3 STB1 SRB8 SWC5 NGG1 SWR1 ARP6 MID1 YGR058W MPH1 KAP120 ARV1 TUB3 NUT1 CAC2 HTZ1 VID21 ZUO1 NUP84 GLC8 MDJ1 RTN2 NUP60 PTC7 MGM101 QCR10 ADE8 YNL086W PET494 SUN4 DOT1 DBP7 SEM1 ARG81 LEA1 HST4 MRPL39 FUN14 YGR102C YKU80 SIP3 COX20 CLB3 SHU1 MSM1 MNL1 IOC3 YHR087W ASE1 RPA14 YGR071C SED4 YER156C SSF1 JEN1 RTT101 OAR1 CBF1 RTS1 FYV6 SPT10 ACO1 MDM31 MSF1 ADK1 MEF2 SRP40 TPD3 FUN30 SAC3 KGD1 MET7 RNR4 GRX5 TCM10 ATP11 VAC8 MSS116 YNL213C RAD1
43227	membrane-bound organelle	185 out of 293 genes, 63.1%	3614 out of 7286 annotated genes, 49.6%	2.11E-06	SIC1 CTF4 CSM3 TOF1 IML3 CHL1 MCM21 RAD61 MCM16 MCM22 MEC3 DDC1 CHL4 BUB3 RAD52 SPT21 SHP1 LGE1 RAD27 RMI1 RAD50 RAD54 ELG1 MRC1 MMS4 MMS22 RDH54 CTF3 CIN8 CDH1 EST3 MAD1 MAD2 LSM6 CTF18 CLN3 THP2 NUP133 CDC73 BUB1 DOC1 CTF19 NUP120 RAD6 XRS2 TOP3 RAD57 RRM3 HST3 ESC2 RTT107 RAD55 SGS1 PSH1 MUS81 HHF1 RAD24 HCM1 RAD59 POL32 RAD9 RAD17 RNH201 RNH203 CLB5 RNH202 SWC3 RAD10 SPT2 RTT109 RAD5 RPA12 YDL156W UPS1 RAD18 ETR1 THP1 RAD51 YTA7 ASF1 HPR5 OMA1 SGO1 ISA2 CNN1 VPS64 BRE1 MFT1 CYC8 ADE1 MRE11 DUN1 SOV1 TPO1 MUD2 SNU66 SGF73 AFT1 SPT4 YJR008W MOG1 RTT106 SGF11 ALD6 CTK2 SDS3 STB1 SRB8 SWC5 NGG1 SWR1 ARP6 MID1 YGR058W MPH1 KAP120 ARV1 TUB3 NUT1 CAC2 HTZ1 VID21 ZUO1 NUP84 GLC8 MDJ1 RTN2 NUP60 PTC7 MGM101 QCR10 ADE8 YNL086W PET494 SUN4 DOT1 DBP7 SEM1 ARG81 LEA1 HST4 MRPL39 FUN14 YGR102C YKU80 SIP3 COX20 CLB3 SHU1 MSM1 MNL1 IOC3 YHR087W ASE1 RPA14 YGR071C SED4 YER156C SSF1 JEN1 RTT101 OAR1 CBF1 RTS1 FYV6 SPT10 ACO1 MDM31 MSF1 ADK1 MEF2 SRP40 TPD3 FUN30 SAC3 KGD1 MET7 RNR4 GRX5 TCM10 ATP11 VAC8 MSS116 YNL213C RAD1
44454	nuclear chromosome part	20 out of 293 genes, 6.8%	146 out of 7286 annotated genes, 2.0%	2.70E-06	IML3 MCM21 MCM16 MCM22 CHL4 BUB3 CTF3 CIN8 MAD2 BUB1 CTF19 RRM3 HHF1 POL32 RAD5 RAD18 SPT4 HTZ1 YKU80 RTS1
778	condensed nuclear chromosome kinetochore	11 out of 293 genes, 3.7%	45 out of 7286 annotated genes, 0.6%	2.87E-06	IML3 MCM21 MCM16 MCM22 CHL4 BUB3 CTF3 CIN8 MAD2 BUB1 CTF19

777	condensed chromosome kinetochore	11 out of 293 genes, 3.7%	45 out of 7286 annotated genes, 0.6%	2.87E-06	IML3 MCM21 MCM16 MCM22 CHL4 BUB3 CTF3 CIN8 MAD2 BUB1 CTF19
794	condensed nuclear chromosome	14 out of 293 genes, 4.7%	76 out of 7286 annotated genes, 1.0%	3.45E-06	IML3 MCM21 MCM16 MCM22 DDC1 CHL4 BUB3 CTF3 CIN8 MAD2 BUB1 CTF19 RAD51 RTS1
793	condensed chromosome	14 out of 293 genes, 4.7%	84 out of 7286 annotated genes, 1.1%	1.05E-05	IML3 MCM21 MCM16 MCM22 DDC1 CHL4 BUB3 CTF3 CIN8 MAD2 BUB1 CTF19 RAD51 RTS1
43228	non-membrane-bound organelle	65 out of 293 genes, 22.1%	951 out of 7286 annotated genes, 13.0%	1.17E-05	CTF8 CTF4 DCC1 BIM1 TOF1 IML3 MCM21 MCM16 MCM22 DDC1 CHL4 BUB3 RAD52 ELG1 MRC1 CTF3 CIN8 MAD2 LSM6 CTF18 BUB1 KAR3 CTF19 RRM3 YDR532C SGS1 HHF1 RAD24 POL32 RAD5 RPA12 RAD18 RAD51 SGO1 CNN1 SHE1 SPT4 RPS23A CIK1 TUB3 CAC2 HTZ1 ZUO1 MGM101 RPL34B SLI15 DBP7 MRPL39 RPL24B ARC18 RPS25A YKU80 BFA1 ASE1 RPA14 RPL13A HSP42 SSF1 CBF1 RTS1 RPL2B RPL14A SRP40 ANB1 TPD3
43232	intracellular non-membrane-bound organelle	65 out of 293 genes, 22.1%	951 out of 7286 annotated genes, 13.0%	1.17E-05	CTF8 CTF4 DCC1 BIM1 TOF1 IML3 MCM21 MCM16 MCM22 DDC1 CHL4 BUB3 RAD52 ELG1 MRC1 CTF3 CIN8 MAD2 LSM6 CTF18 BUB1 KAR3 CTF19 RRM3 YDR532C SGS1 HHF1 RAD24 POL32 RAD5 RPA12 RAD18 RAD51 SGO1 CNN1 SHE1 SPT4 RPS23A CIK1 TUB3 CAC2 HTZ1 ZUO1 MGM101 RPL34B SLI15 DBP7 MRPL39 RPL24B ARC18 RPS25A YKU80 BFA1 ASE1 RPA14 RPL13A HSP42 SSF1 CBF1 RTS1 RPL2B RPL14A SRP40 ANB1 TPD3
44428	nuclear part	71 out of 293 genes, 24.2%	1076 out of 7286 annotated genes, 14.7%	1.36E-05	CTF4 TOF1 IML3 MCM21 MCM16 MCM22 DDC1 CHL4 BUB3 RAD52 RAD50 MRC1 CTF3 CIN8 CDH1 EST3 MAD1 MAD2 LSM6 THP2 NUP133 CDC73 BUB1 DOC1 CTF19 NUP120 XRS2 RRM3 SGS1 HHF1 POL32 SWC3 RAD10 RAD5 RPA12 RAD18 THP1 RAD51 ASF1 MFT1 MRE11 MUD2 SNU66 SGF73 SPT4 SGF11 SDS3 STB1 SRB8 SWC5 NGG1 SWR1 ARP6 KAP120 TUB3 CAC2 HTZ1 VID21 NUP84 NUP60 DBP7 LEA1 YKU80 IOC3 ASE1 RPA14 SSF1 RTS1 SRP40 SAC3 RAD1
44464	cell part	249 out of 293 genes, 84.9%	5456 out of 7286 annotated genes, 74.8%	1.86E-05	CTF8 SIC1 CTF4 DCC1 BIM1 CSM3 TOF1 IML3 CHL1 MCM21 RAD61 MCM16 MCM22 MEC3 DDC1 CHL4 SNO1 BUB3 RAD52 SPT21 SHP1 LGE1 RAD27 RMI1 RAD50 RAD54 ELG1 MRC1 MMS4 MMS22 RDH54 SSZ1 CTF3 CIN8 UBR1 CDH1 EST3 MAD1 MAD2 LSM6 CTF18 DIA2 CLN3 THP2 NUP133 CDC73 BUB1 IRC15 KAR3 DOC1 CTF19 NUP120 RAD6 XRS2 TOP3 RAD57 RRM3 HST3 ESC2 YDR532C RTT107 RAD55 SGS1 PSH1 MUS81 VID22 TSA1 HHF1 RAD24 HCM1 RAD59 SHM2 POL32 RAD9 RAD17 RNH201 RNH203 CLB5 RNH202 SWC3 RAD10 CYK3 SPT2 RTT109 RAD5 RPA12 PAC10 YDL156W UPS1 RAD18 ETR1 THP1 RAD51 YTA7 ASF1 HPR5 OMA1 SGO1 SRO7 ISA2 CNN1 VPS64 PIG1 YBP2 ADE6 BRE1 MFT1 CYC8 ADE1 MRE11 DUN1 SOV1 ADE17 TPO1 YOL070C SHE1 MUD2 SSK1 SNU66 SGF73 AFT1 SPT4 RPS23A YJR008W MOG1 RTT106 SGF11 ALD6 PPQ1 CTK2 CIK1 SDS3 STB1 SRB8 SWC5 PFD1 NGG1 SWR1 ARP6 MID1 YGR058W MPH1 KAP120 ARV1 TUB3 MSB2 NUT1 CAC2 HTZ1 VID21 ZUO1 NUP84 GLC8 MET22 GIM5 MUC1 MDJ1 RTN2 DJP1 ADE5,7 ADE4 NUP60 PTC7 MGM101 QCR10 ADE8 RPL34B YNL086W SLI15 PET494 SUN4 MSO1 DOT1 HXT4 DBP7 SEM1 ARG81 PLB1 LEA1 HST4 MRPL39 FUN14 CPR7 RPL24B ARC18 YGR102C PCK1 RPS25A TMA108 ECM7 YKU80 YNR048W SIP3 COX20 OCA4 CLB3 SHU1 MSM1 MNL1 IOC3 YHR087W BFA1 ASE1 RPA14 YGR071C RPL13A HSP42 SED4 YER156C SSF1 JEN1 RTT101 OAR1 CBF1 RTS1 FYV6 RPL2B SPT10 ACO1 MDM31 MSF1 A
5623	cell	249 out of 293 genes, 84.9%	5457 out of 7286 annotated genes, 74.8%	1.90E-05	CTF8 SIC1 CTF4 DCC1 BIM1 CSM3 TOF1 IML3 CHL1 MCM21 RAD61 MCM16 MCM22 MEC3 DDC1 CHL4 SNO1 BUB3 RAD52 SPT21 SHP1 LGE1 RAD27 RMI1 RAD50 RAD54 ELG1 MRC1 MMS4 MMS22 RDH54 SSZ1 CTF3 CIN8 UBR1 CDH1 EST3 MAD1 MAD2 LSM6 CTF18 DIA2 CLN3 THP2 NUP133 CDC73 BUB1 IRC15 KAR3 DOC1 CTF19 NUP120 RAD6 XRS2 TOP3 RAD57 RRM3 HST3 ESC2 YDR532C RTT107 RAD55 SGS1 PSH1 MUS81 VID22 TSA1 HHF1 RAD24 HCM1 RAD59 SHM2 POL32 RAD9 RAD17 RNH201 RNH203 CLB5 RNH202 SWC3 RAD10 CYK3 SPT2 RTT109 RAD5 RPA12 PAC10 YDL156W UPS1 RAD18 ETR1 THP1 RAD51 YTA7 ASF1 HPR5 OMA1 SGO1 SRO7 ISA2 CNN1 VPS64 PIG1 YBP2 ADE6 BRE1 MFT1 CYC8 ADE1 MRE11 DUN1 SOV1 ADE17 TPO1 YOL070C SHE1 MUD2 SSK1 SNU66 SGF73 AFT1 SPT4 RPS23A YJR008W MOG1 RTT106 SGF11 ALD6 PPQ1 CTK2 CIK1 SDS3 STB1 SRB8 SWC5 PFD1 NGG1 SWR1 ARP6 MID1 YGR058W MPH1 KAP120 ARV1 TUB3 MSB2 NUT1 CAC2 HTZ1 VID21 ZUO1 NUP84 GLC8 MET22 GIM5 MUC1 MDJ1 RTN2 DJP1 ADE5,7 ADE4 NUP60 PTC7 MGM101 QCR10 ADE8 RPL34B YNL086W SLI15 PET494 SUN4 MSO1 DOT1 HXT4 DBP7 SEM1 ARG81 PLB1 LEA1 HST4 MRPL39 FUN14 CPR7 RPL24B ARC18 YGR102C PCK1 RPS25A TMA108 ECM7 YKU80 YNR048W SIP3 COX20 OCA4 CLB3 SHU1 MSM1 MNL1 IOC3 YHR087W BFA1 ASE1 RPA14 YGR071C RPL13A HSP42 SED4 YER156C SSF1 JEN1 RTT101 OAR1 CBF1 RTS1 FYV6 RPL2B SPT10 ACO1 MDM31 MSF1 A
15630	microtubule cytoskeleton	15 out of 293 genes, 5.1%	102 out of 7286 annotated genes, 1.3%	2.17E-05	BIM1 MCM21 CIN8 KAR3 CTF19 YDR532C SGO1 SHE1 CIK1 TUB3 SLI15 BFA1 ASE1 RTS1 TPD3
5663	DNA replication factor C complex	5 out of 293 genes, 1.7%	10 out of 7286 annotated genes, 0.1%	6.10E-05	CTF8 DCC1 ELG1 CTF18 RAD24
16272	prefoldin complex	4 out of 293 genes, 1.3%	6 out of 7286 annotated genes, 0.0%	0.00011	PAC10 PFD1 GIM5 GIM4
43234	protein complex	86 out of 293 genes, 29.3%	1480 out of 7286 annotated genes, 20.3%	0.00014	CTF8 DCC1 MCM21 RMI1 RAD50 ELG1 CIN8 UBR1 CDH1 EST3 MAD1 MAD2 LSM6 CTF18 DIA2 THP2 NUP133 CDC73 DOC1 CTF19 NUP120 RAD6 XRS2 TOP3 SGS1 HHF1 RAD24 POL32 SWC3 RAD10 RPA12 PAC10 THP1 ASF1 PIG1 MFT1 MRE11 MUD2 SNU66 SGF73 SPT4 RPS23A SGF11 CIK1 SDS3 STB1 SRB8 SWC5 PFD1 NGG1 SWR1 ARP6 KAP120 TUB3 CAC2 HTZ1 VID21 ZUO1 NUP84 GIM5 NUP60 QCR10 RPL34B SEM1 LEA1 MRPL39 RPL24B ARC18 RPS25A IOC3 RPA14 RPL13A HSP42 RTS1 RPL2B LSM1 RPL14A ANB1 TPD3 SAC3 KGD1 RNR4 RNR1 SLM2 GIM4 RAD1

5819	spindle	12 out of 293 genes, 4.0%	83 out of 7286 annotated genes, 1.1%	0.00016	BIM1 CIN8 KAR3 YDR532C SGO1 CIK1 TUB3 SLI15 BFA1 ASE1 RTS1 TPD3
31422	RecQ helicase-Topo III complex	3 out of 293 genes, 1.0%	3 out of 7286 annotated genes, 0.0%	0.00026	RMI1 TOP3 SGS1
46930	pore complex	9 out of 293 genes, 3.0%	51 out of 7286 annotated genes, 0.6%	0.00026	MAD1 MAD2 NUP133 NUP120 THP1 KAP120 NUP84 NUP60 SAC3
5643	nuclear pore	9 out of 293 genes, 3.0%	51 out of 7286 annotated genes, 0.6%	0.00026	MAD1 MAD2 NUP133 NUP120 THP1 KAP120 NUP84 NUP60 SAC3
30870	Mre11 complex	3 out of 293 genes, 1.0%	3 out of 7286 annotated genes, 0.0%	0.00026	RAD50 XRS2 MRE11
5874	microtubule	7 out of 293 genes, 2.3%	34 out of 7286 annotated genes, 0.4%	0.00051	BIM1 CIN8 KAR3 CIK1 TUB3 SLI15 ASE1
31965	nuclear membrane	9 out of 293 genes, 3.0%	57 out of 7286 annotated genes, 0.7%	0.00058	MAD1 MAD2 NUP133 NUP120 THP1 KAP120 NUP84 NUP60 SAC3
44453	nuclear membrane part	9 out of 293 genes, 3.0%	57 out of 7286 annotated genes, 0.7%	0.00058	MAD1 MAD2 NUP133 NUP120 THP1 KAP120 NUP84 NUP60 SAC3
44422	organelle part	116 out of 293 genes, 39.5%	2227 out of 7286 annotated genes, 30.5%	0.00063	CTF8 CTF4 DCC1 BIM1 TOF1 IML3 MCM21 MCM16 MCM22 DDC1 CHL4 BUB3 RAD52 RAD50 ELG1 MRC1 CTF3 CIN8 CDH1 EST3 MAD1 MAD2 LSM6 CTF18 THP2 NUP133 CDC73 BUB1 KAR3 DOC1 CTF19 NUP120 XRS2 RRM3 YDR532C SGS1 HHF1 RAD24 POL32 SWC3 RAD10 RAD5 RPA12 UPS1 RAD18 THP1 RAD51 ASF1 OMA1 SGO1 ISA2 CNN1 VPS64 MFT1 MRE11 TPO1 MUD2 SNU66 SGF73 SPT4 RPS23A SGF11 CIK1 SDS3 STB1 SRB8 SWC5 NGG1 SWR1 ARP6 KAP120 TUB3 CAC2 HTZ1 VID21 NUP84 MDJ1 NUP60 MGM101 QCR10 RPL34B SLI15 PET494 SUN4 DBP7 LEA1 MRPL39 FUN14 RPL24B ARC18 RPS25A YKU80 COX20 IOC3 BFA1 ASE1 RPA14 RPL13A SED4 SSF1 CBF1 RTS1 RPL2B ACO1 MDM31 ADK1 RPL14A SRP40 TPD3 SAC3 KGD1 GRX5 TCM10 ATP11 MSS116 RAD1
44446	intracellular organelle part	116 out of 293 genes, 39.5%	2227 out of 7286 annotated genes, 30.5%	0.00063	CTF8 CTF4 DCC1 BIM1 TOF1 IML3 MCM21 MCM16 MCM22 DDC1 CHL4 BUB3 RAD52 RAD50 ELG1 MRC1 CTF3 CIN8 CDH1 EST3 MAD1 MAD2 LSM6 CTF18 THP2 NUP133 CDC73 BUB1 KAR3 DOC1 CTF19 NUP120 XRS2 RRM3 YDR532C SGS1 HHF1 RAD24 POL32 SWC3 RAD10 RAD5 RPA12 UPS1 RAD18 THP1 RAD51 ASF1 OMA1 SGO1 ISA2 CNN1 VPS64 MFT1 MRE11 TPO1 MUD2 SNU66 SGF73 SPT4 RPS23A SGF11 CIK1 SDS3 STB1 SRB8 SWC5 NGG1 SWR1 ARP6 KAP120 TUB3 CAC2 HTZ1 VID21 NUP84 MDJ1 NUP60 MGM101 QCR10 RPL34B SLI15 PET494 SUN4 DBP7 LEA1 MRPL39 FUN14 RPL24B ARC18 RPS25A YKU80 COX20 IOC3 BFA1 ASE1 RPA14 RPL13A SED4 SSF1 CBF1 RTS1 RPL2B ACO1 MDM31 ADK1 RPL14A SRP40 TPD3 SAC3 KGD1 GRX5 TCM10 ATP11 MSS116 RAD1
5815	microtubule organizing center	9 out of 293 genes, 3.0%	60 out of 7286 annotated genes, 0.8%	0.00083	BIM1 KAR3 YDR532C SGO1 CIK1 TUB3 BFA1 RTS1 TPD3
5816	spindle pole body	9 out of 293 genes, 3.0%	60 out of 7286 annotated genes, 0.8%	0.00083	BIM1 KAR3 YDR532C SGO1 CIK1 TUB3 BFA1 RTS1 TPD3
5657	replication fork	7 out of 293 genes, 2.3%	39 out of 7286 annotated genes, 0.5%	0.00114	CTF8 DCC1 ELG1 MRC1 CTF18 RAD24 POL32
5678	chromatin assembly complex	3 out of 293 genes, 1.0%	5 out of 7286 annotated genes, 0.0%	0.00115	ASF1 CAC2 HTZ1
922	spindle pole	9 out of 293 genes, 3.0%	65 out of 7286 annotated genes, 0.8%	0.00144	BIM1 KAR3 YDR532C SGO1 CIK1 TUB3 BFA1 RTS1 TPD3
812	SWR1 complex	4 out of 293 genes, 1.3%	13 out of 7286 annotated genes, 0.1%	0.00202	SWC3 SWC5 SWR1 ARP6
940	outer kinetochore of condensed chromosome	2 out of 293 genes, 0.6%	2 out of 7286 annotated genes, 0.0%	0.00305	IML3 CHL4

942	outer kinetochore of condensed nuclear chromosome	2 out of 293 genes, 0.6%	2 out of 7286 annotated genes, 0.0%	0.00305	IML3 CHL4
5856	cytoskeleton	17 out of 293 genes, 5.8%	204 out of 7286 annotated genes, 2.7%	0.00415	BIM1 MCM21 CIN8 KAR3 CTF19 YDR532C SGO1 SHE1 CIK1 TUB3 SLI15 ARC18 BFA1 ASE1 HSP42 RTS1 TPD3
790	nuclear chromatin	6 out of 293 genes, 2.0%	38 out of 7286 annotated genes, 0.5%	0.00473	RRM3 HHF1 RAD5 RAD18 HTZ1 YKU80
785	chromatin	6 out of 293 genes, 2.0%	40 out of 7286 annotated genes, 0.5%	0.00602	RRM3 HHF1 RAD5 RAD18 HTZ1 YKU80
110	nucleotide-excision repair factor 1 complex	2 out of 293 genes, 0.6%	3 out of 7286 annotated genes, 0.0%	0.00669	RAD10 RAD1
16585	chromatin remodeling complex	8 out of 293 genes, 2.7%	73 out of 7286 annotated genes, 1.0%	0.01017	SWC3 ASF1 SWC5 SWR1 ARP6 CAC2 HTZ1 IOC3
5876	spindle microtubule	4 out of 293 genes, 1.3%	21 out of 7286 annotated genes, 0.2%	0.01075	CIN8 TUB3 SLI15 ASE1
44430	cytoskeletal part	15 out of 293 genes, 5.1%	190 out of 7286 annotated genes, 2.6%	0.0109	BIM1 MCM21 CIN8 KAR3 CTF19 YDR532C SGO1 CIK1 TUB3 SLI15 ARC18 BFA1 ASE1 RTS1 TPD3
817	COMA complex	2 out of 293 genes, 0.6%	4 out of 7286 annotated genes, 0.0%	0.01159	MCM21 CTF19
5971	ribonucleoside-diphosphate reductase complex	2 out of 293 genes, 0.6%	4 out of 7286 annotated genes, 0.0%	0.01159	RNR4 RNR1
347	THO complex	2 out of 293 genes, 0.6%	4 out of 7286 annotated genes, 0.0%	0.01159	THP2 MFT1
5881	cytoplasmic microtubule	3 out of 293 genes, 1.0%	13 out of 7286 annotated genes, 0.1%	0.01606	BIM1 CIK1 TUB3
5635	nuclear envelope	9 out of 293 genes, 3.0%	101 out of 7286 annotated genes, 1.3%	0.02239	MAD1 MAD2 NUP133 NUP120 THP1 KAP120 NUP84 NUP60 SAC3
5880	nuclear microtubule	2 out of 293 genes, 0.6%	6 out of 7286 annotated genes, 0.0%	0.02476	TUB3 ASE1
5871	kinesin complex	2 out of 293 genes, 0.6%	6 out of 7286 annotated genes, 0.0%	0.02476	CIN8 CIK1
159	protein phosphatase type 2A complex	2 out of 293 genes, 0.6%	6 out of 7286 annotated genes, 0.0%	0.02476	RTS1 TPD3

8287	protein serine/threonine phosphatase complex	3 out of 293 genes, 1.0%	17 out of 7286 annotated genes, 0.2%	0.032	PIG1 RTS1 TPD3
346	transcription export complex	2 out of 293 genes, 0.6%	7 out of 7286 annotated genes, 0.0%	0.03284	THP2 MFT1
5720	nuclear heterochromatin	2 out of 293 genes, 0.6%	7 out of 7286 annotated genes, 0.0%	0.03284	RRM3 YKU80
5724	nuclear telomeric heterochromatin	2 out of 293 genes, 0.6%	7 out of 7286 annotated genes, 0.0%	0.03284	RRM3 YKU80
792	heterochromatin	2 out of 293 genes, 0.6%	7 out of 7286 annotated genes, 0.0%	0.03284	RRM3 YKU80
31933	telomeric heterochromatin	2 out of 293 genes, 0.6%	7 out of 7286 annotated genes, 0.0%	0.03284	RRM3 YKU80
124	SAGA complex	3 out of 293 genes, 1.0%	19 out of 7286 annotated genes, 0.2%	0.04217	SGF73 SGF11 NGG1
5875	microtubule associated complex	4 out of 293 genes, 1.3%	34 out of 7286 annotated genes, 0.4%	0.04968	MCM21 CIN8 CTF19 CIK1
784	nuclear chromosome, telomeric region	3 out of 293 genes, 1.0%	23 out of 7286 annotated genes, 0.3%	0.06673	RRM3 SPT4 YKU80
9295	nucleoid	3 out of 293 genes, 1.0%	23 out of 7286 annotated genes, 0.3%	0.06673	MGM101 ACO1 KGD1
42645	mitochondrial nucleoid	3 out of 293 genes, 1.0%	23 out of 7286 annotated genes, 0.3%	0.06673	MGM101 ACO1 KGD1
123	histone acetyltransferase complex	4 out of 293 genes, 1.3%	40 out of 7286 annotated genes, 0.5%	0.07946	SGF73 SGF11 NGG1 VID21
44445	cytosolic part	12 out of 293 genes, 4.0%	193 out of 7286 annotated genes, 2.6%	0.09261	PAC10 RPS23A PFD1 GIM5 RPL34B RPL24B RPS25A RPL13A HSP42 RPL2B RPL14A GIM4
31970	organelle envelope lumen	3 out of 293 genes, 1.0%	27 out of 7286 annotated genes, 0.3%	0.09639	UPS1 ISA2 ADK1
5758	mitochondrial intermembrane space	3 out of 293 genes, 1.0%	27 out of 7286 annotated genes, 0.3%	0.09639	UPS1 ISA2 ADK1
781	chromosome, telomeric region	3 out of 293 genes, 1.0%	27 out of 7286 annotated genes, 0.3%	0.09639	RRM3 SPT4 YKU80
High confidence CIN genes (subset of 130)					

5634	nucleus	86 out of 130 genes, 66.1%	1984 out of 7286 annotated genes, 27.2%	2.70E-20	SIC1 CTF4 CSM3 TOF1 IML3 CHL1 MCM21 RAD61 MCM16 MCM22 MEC3 DDC1 CHL4 BUB3 RAD52 SPT21 SHP1 LGE1 RAD27 RMI1 RAD50 RAD54 ELG1 MRC1 MMS4 MMS22 RDH54 CTF3 CIN8 CDH1 EST3 MAD1 MAD2 LSM6 CLN3 THP2 NUP133 CDC73 BUB1 DOC1 CTF19 NUP120 RAD6 XRS2 TOP3 RAD57 RRM3 HST3 ESC2 RTT107 RAD55 SGS1 PSH1 MUS81 HHF1 RAD24 HCM1 RAD59 POL32 RAD9 RAD17 RNH201 RNH203 CLB5 RNH202 SWC3 RAD10 SPT2 RTT109 RAD5 RPA12 YDL156W RAD18 THP1 RAD51 YTA7 ASF1 HPR5 SGO1 CNN1 BRE1 MFT1 CYC8 ADE1 MRE11 DUN1
5694	chromosome	30 out of 130 genes, 23.0%	214 out of 7286 annotated genes, 2.9%	1.60E-18	CTF8 CTF4 DCC1 BIM1 TOF1 IML3 MCM21 MCM16 MCM22 DDC1 CHL4 BUB3 RAD52 ELG1 MRC1 CTF3 CIN8 MAD2 CTF18 BUB1 CTF19 RRM3 HHF1 RAD24 POL32 RAD5 RAD18 RAD51 SGO1 CNN1
44427	chromosomal part	25 out of 130 genes, 19.2%	184 out of 7286 annotated genes, 2.5%	3.35E-15	CTF8 DCC1 BIM1 IML3 MCM21 MCM16 MCM22 CHL4 BUB3 ELG1 MRC1 CTF3 CIN8 MAD2 CTF18 BUB1 CTF19 RRM3 HHF1 RAD24 POL32 RAD5 RAD18 SGO1 CNN1
228	nuclear chromosome	22 out of 130 genes, 16.9%	175 out of 7286 annotated genes, 2.4%	8.36E-13	CTF4 TOF1 IML3 MCM21 MCM16 MCM22 DDC1 CHL4 BUB3 RAD52 MRC1 CTF3 CIN8 MAD2 BUB1 CTF19 RRM3 HHF1 POL32 RAD5 RAD18 RAD51
776	kinetochore	14 out of 130 genes, 10.7%	54 out of 7286 annotated genes, 0.7%	1.47E-12	BIM1 IML3 MCM21 MCM16 MCM22 CHL4 BUB3 CTF3 CIN8 MAD2 BUB1 CTF19 SGO1 CNN1
775	chromosome, pericentric region	14 out of 130 genes, 10.7%	61 out of 7286 annotated genes, 0.8%	7.32E-12	BIM1 IML3 MCM21 MCM16 MCM22 CHL4 BUB3 CTF3 CIN8 MAD2 BUB1 CTF19 SGO1 CNN1
777	condensed chromosome kinetochore	11 out of 130 genes, 8.4%	45 out of 7286 annotated genes, 0.6%	7.38E-10	IML3 MCM21 MCM16 MCM22 CHL4 BUB3 CTF3 CIN8 MAD2 BUB1 CTF19
778	condensed nuclear chromosome kinetochore	11 out of 130 genes, 8.4%	45 out of 7286 annotated genes, 0.6%	7.38E-10	IML3 MCM21 MCM16 MCM22 CHL4 BUB3 CTF3 CIN8 MAD2 BUB1 CTF19
794	condensed nuclear chromosome	13 out of 130 genes, 10%	76 out of 7286 annotated genes, 1.0%	1.45E-09	IML3 MCM21 MCM16 MCM22 DDC1 CHL4 BUB3 CTF3 CIN8 MAD2 BUB1 CTF19 RAD51
779	condensed chromosome, pericentric region	11 out of 130 genes, 8.4%	50 out of 7286 annotated genes, 0.6%	2.18E-09	IML3 MCM21 MCM16 MCM22 CHL4 BUB3 CTF3 CIN8 MAD2 BUB1 CTF19
780	condensed nuclear chromosome, pericentric region	11 out of 130 genes, 8.4%	50 out of 7286 annotated genes, 0.6%	2.18E-09	IML3 MCM21 MCM16 MCM22 CHL4 BUB3 CTF3 CIN8 MAD2 BUB1 CTF19
793	condensed chromosome	13 out of 130 genes, 10%	84 out of 7286 annotated genes, 1.1%	4.74E-09	IML3 MCM21 MCM16 MCM22 DDC1 CHL4 BUB3 CTF3 CIN8 MAD2 BUB1 CTF19 RAD51
44454	nuclear chromosome part	16 out of 130 genes, 12.3%	146 out of 7286 annotated genes, 2.0%	9.45E-09	IML3 MCM21 MCM16 MCM22 CHL4 BUB3 CTF3 CIN8 MAD2 BUB1 CTF19 RRM3 HHF1 POL32 RAD5 RAD18
43227	membrane-bound organelle	93 out of 130 genes, 71.5%	3614 out of 7286 annotated genes, 49.6%	3.06E-07	SIC1 CTF4 CSM3 TOF1 IML3 CHL1 MCM21 RAD61 MCM16 MCM22 MEC3 DDC1 CHL4 BUB3 RAD52 SPT21 SHP1 LGE1 RAD27 RMI1 RAD50 RAD54 ELG1 MRC1 MMS4 MMS22 RDH54 CTF3 CIN8 CDH1 EST3 MAD1 MAD2 LSM6 CTF18 CLN3 THP2 NUP133 CDC73 BUB1 DOC1 CTF19 NUP120 RAD6 XRS2 TOP3 RAD57 RRM3 HST3 ESC2 RTT107 RAD55 SGS1 PSH1 MUS81 HHF1 RAD24 HCM1 RAD59 POL32 RAD9 RAD17 RNH201 RNH203 CLB5 RNH202 SWC3 RAD10 SPT2 RTT109 RAD5 RPA12 YDL156W UPS1 RAD18 ETR1 THP1 RAD51 YTA7 ASF1 HPR5 OMA1 SGO1 ISA2 CNN1 VPS64 BRE1 MFT1 CYC8 ADE1 MRE11 DUN1 SOV1

43231	intracellular membrane-bound organelle	93 out of 130 genes, 71.5%	3614 out of 7286 annotated genes, 49.6%	3.06E-07	SIC1 CTF4 CSM3 TOF1 IML3 CHL1 MCM21 RAD61 MCM16 MCM22 MEC3 DDC1 CHL4 BUB3 RAD52 SPT21 SHP1 LGE1 RAD27 RMI1 RAD50 RAD54 ELG1 MRC1 MMS4 MMS22 RDH54 CTF3 CIN8 CDH1 EST3 MAD1 MAD2 LSM6 CTF18 CLN3 THP2 NUP133 CDC73 BUB1 DOC1 CTF19 NUP120 RAD6 XRS2 TOP3 RAD57 RRM3 HST3 ESC2 RTT107 RAD55 SGS1 PSH1 MUS81 HHF1 RAD24 HCM1 RAD59 POL32 RAD9 RAD17 RNH201 RNH203 CLB5 RNH202 SWC3 RAD10 SPT2 RTT109 RAD5 RPA12 YDL156W UPS1 RAD18 ETR1 THP1 RAD51 YTA7 ASF1 HPR5 OMA1 SGO1 ISA2 CNN1 VPS64 BRE1 MFT1 CYC8 ADE1 MRE11 DUN1 SOV1
43226	organelle	98 out of 130 genes, 75.3%	3937 out of 7286 annotated genes, 54.0%	4.14E-07	CTF8 SIC1 CTF4 DCC1 BIM1 CSM3 TOF1 IML3 CHL1 MCM21 RAD61 MCM16 MCM22 MEC3 DDC1 CHL4 BUB3 RAD52 SPT21 SHP1 LGE1 RAD27 RMI1 RAD50 RAD54 ELG1 MRC1 MMS4 MMS22 RDH54 CTF3 CIN8 CDH1 EST3 MAD1 MAD2 LSM6 CTF18 CLN3 THP2 NUP133 CDC73 BUB1 KAR3 DOC1 CTF19 NUP120 RAD6 XRS2 TOP3 RAD57 RRM3 HST3 ESC2 YDR532C RTT107 RAD55 SGS1 PSH1 MUS81 HHF1 RAD24 HCM1 RAD59 POL32 RAD9 RAD17 RNH201 RNH203 CLB5 RNH202 SWC3 RAD10 SPT2 RTT109 RAD5 RPA12 YDL156W UPS1 RAD18 ETR1 THP1 RAD51 YTA7 ASF1 HPR5 OMA1 SGO1 ISA2 CNN1 VPS64 BRE1 MFT1 CYC8 ADE1 MRE11 DUN1 SOV1
43229	intracellular organelle	98 out of 130 genes, 75.3%	3937 out of 7286 annotated genes, 54.0%	4.14E-07	CTF8 SIC1 CTF4 DCC1 BIM1 CSM3 TOF1 IML3 CHL1 MCM21 RAD61 MCM16 MCM22 MEC3 DDC1 CHL4 BUB3 RAD52 SPT21 SHP1 LGE1 RAD27 RMI1 RAD50 RAD54 ELG1 MRC1 MMS4 MMS22 RDH54 CTF3 CIN8 CDH1 EST3 MAD1 MAD2 LSM6 CTF18 CLN3 THP2 NUP133 CDC73 BUB1 KAR3 DOC1 CTF19 NUP120 RAD6 XRS2 TOP3 RAD57 RRM3 HST3 ESC2 YDR532C RTT107 RAD55 SGS1 PSH1 MUS81 HHF1 RAD24 HCM1 RAD59 POL32 RAD9 RAD17 RNH201 RNH203 CLB5 RNH202 SWC3 RAD10 SPT2 RTT109 RAD5 RPA12 YDL156W UPS1 RAD18 ETR1 THP1 RAD51 YTA7 ASF1 HPR5 OMA1 SGO1 ISA2 CNN1 VPS64 BRE1 MFT1 CYC8 ADE1 MRE11 DUN1 SOV1
44428	nuclear part	41 out of 130 genes, 31.5%	1076 out of 7286 annotated genes, 14.7%	1.06E-06	CTF4 TOF1 IML3 MCM21 MCM16 MCM22 DDC1 CHL4 BUB3 RAD52 RAD50 MRC1 CTF3 CIN8 CDH1 EST3 MAD1 MAD2 LSM6 THP2 NUP133 CDC73 BUB1 DOC1 CTF19 NUP120 XRS2 RRM3 SGS1 HHF1 POL32 SWC3 RAD10 RAD5 RPA12 RAD18 THP1 RAD51 ASF1 MFT1 MRE11
5663	DNA replication factor C complex	5 out of 130 genes, 3.8%	10 out of 7286 annotated genes, 0.1%	1.20E-06	CTF8 DCC1 ELG1 CTF18 RAD24
44424	intracellular part	112 out of 130 genes, 86.1%	4995 out of 7286 annotated genes, 68.5%	3.01E-06	CTF8 SIC1 CTF4 DCC1 BIM1 CSM3 TOF1 IML3 CHL1 MCM21 RAD61 MCM16 MCM22 MEC3 DDC1 CHL4 SNO1 BUB3 RAD52 SPT21 SHP1 LGE1 RAD27 RMI1 RAD50 RAD54 ELG1 MRC1 MMS4 MMS22 RDH54 SSZ1 CTF3 CIN8 UBR1 CDH1 EST3 MAD1 MAD2 LSM6 CTF18 DIA2 CLN3 THP2 NUP133 CDC73 BUB1 IRC15 KAR3 DOC1 CTF19 NUP120 RAD6 XRS2 TOP3 RAD57 RRM3 HST3 ESC2 YDR532C RTT107 RAD55 SGS1 PSH1 MUS81 TSA1 HHF1 RAD24 HCM1 RAD59 SHM2 POL32 RAD9 RAD17 RNH201 RNH203 CLB5 RNH202 SWC3 RAD10 CYK3 SPT2 RTT109 RAD5 RPA12 PAC10 YDL156W UPS1 RAD18 ETR1 THP1 RAD51 YTA7 ASF1 HPR5 OMA1 SGO1 SRO7 ISA2 CNN1 VPS64 PIG1 YBP2 ADE6 BRE1 MFT1 CYC8 ADE1 MRE11 DUN1 SOV1 ADE17
5622	intracellular	112 out of 130 genes, 86.1%	5032 out of 7286 annotated genes, 69.0%	5.20E-06	CTF8 SIC1 CTF4 DCC1 BIM1 CSM3 TOF1 IML3 CHL1 MCM21 RAD61 MCM16 MCM22 MEC3 DDC1 CHL4 SNO1 BUB3 RAD52 SPT21 SHP1 LGE1 RAD27 RMI1 RAD50 RAD54 ELG1 MRC1 MMS4 MMS22 RDH54 SSZ1 CTF3 CIN8 UBR1 CDH1 EST3 MAD1 MAD2 LSM6 CTF18 DIA2 CLN3 THP2 NUP133 CDC73 BUB1 IRC15 KAR3 DOC1 CTF19 NUP120 RAD6 XRS2 TOP3 RAD57 RRM3 HST3 ESC2 YDR532C RTT107 RAD55 SGS1 PSH1 MUS81 TSA1 HHF1 RAD24 HCM1 RAD59 SHM2 POL32 RAD9 RAD17 RNH201 RNH203 CLB5 RNH202 SWC3 RAD10 CYK3 SPT2 RTT109 RAD5 RPA12 PAC10 YDL156W UPS1 RAD18 ETR1 THP1 RAD51 YTA7 ASF1 HPR5 OMA1 SGO1 SRO7 ISA2 CNN1 VPS64 PIG1 YBP2 ADE6 BRE1 MFT1 CYC8 ADE1 MRE11 DUN1 SOV1 ADE17
5657	replication fork	7 out of 130 genes, 5.3%	39 out of 7286 annotated genes, 0.5%	7.48E-06	CTF8 DCC1 ELG1 MRC1 CTF18 RAD24 POL32
43232	intracellular non-membrane-bound organelle	35 out of 130 genes, 26.9%	951 out of 7286 annotated genes, 13.0%	1.87E-05	CTF8 CTF4 DCC1 BIM1 TOF1 IML3 MCM21 MCM16 MCM22 DDC1 CHL4 BUB3 RAD52 ELG1 MRC1 CTF3 CIN8 MAD2 LSM6 CTF18 BUB1 KAR3 CTF19 RRM3 YDR532C SGS1 HHF1 RAD24 POL32 RAD5 RPA12 RAD18 RAD51 SGO1 CNN1
43228	non-membrane-bound organelle	35 out of 130 genes, 26.9%	951 out of 7286 annotated genes, 13.0%	1.87E-05	CTF8 CTF4 DCC1 BIM1 TOF1 IML3 MCM21 MCM16 MCM22 DDC1 CHL4 BUB3 RAD52 ELG1 MRC1 CTF3 CIN8 MAD2 LSM6 CTF18 BUB1 KAR3 CTF19 RRM3 YDR532C SGS1 HHF1 RAD24 POL32 RAD5 RPA12 RAD18 RAD51 SGO1 CNN1
30870	Mre11 complex	3 out of 130 genes, 2.3%	3 out of 7286 annotated genes, 0.0%	2.40E-05	RAD50 XRS2 MRE11
31422	RecQ helicase-Topo III complex	3 out of 130 genes, 2.3%	3 out of 7286 annotated genes, 0.0%	2.40E-05	RMI1 TOP3 SGS1
44464	cell part	113 out of 130 genes, 86.9%	5456 out of 7286 annotated genes, 74.8%	0.00056	CTF8 SIC1 CTF4 DCC1 BIM1 CSM3 TOF1 IML3 CHL1 MCM21 RAD61 MCM16 MCM22 MEC3 DDC1 CHL4 SNO1 BUB3 RAD52 SPT21 SHP1 LGE1 RAD27 RMI1 RAD50 RAD54 ELG1 MRC1 MMS4 MMS22 RDH54 SSZ1 CTF3 CIN8 UBR1 CDH1 EST3 MAD1 MAD2 LSM6 CTF18 DIA2 CLN3 THP2 NUP133 CDC73 BUB1 IRC15 KAR3 DOC1 CTF19 NUP120 RAD6 XRS2 TOP3 RAD57 RRM3 HST3 ESC2 YDR532C RTT107 RAD55 SGS1 PSH1 MUS81 VID22 TSA1 HHF1 RAD24 HCM1 RAD59 SHM2 POL32 RAD9 RAD17 RNH201 RNH203 CLB5 RNH202 SWC3 RAD10 CYK3 SPT2 RTT109 RAD5 RPA12 PAC10 YDL156W UPS1 RAD18 ETR1 THP1 RAD51 YTA7 ASF1 HPR5 OMA1 SGO1 SRO7 ISA2 CNN1 VPS64 PIG1 YBP2 ADE6 BRE1 MFT1 CYC8 ADE1 MRE11 DUN1 SOV1 ADE17

5623	cell	113 out of 130 genes, 86.9%	5457 out of 7286 annotated genes, 74.8%	0.00057	CTF8 SIC1 CTF4 DCC1 BIM1 CSM3 TOF1 IML3 CHL1 MCM21 RAD61 MCM16 MCM22 MEC3 DDC1 CHL4 SNO1 BUB3 RAD52 SPT21 SHP1 LGE1 RAD27 RMI1 RAD50 RAD54 ELG1 MRC1 MMS4 MMS22 RDH54 SSZ1 CTF3 CIN8 UBR1 CDH1 EST3 MAD1 MAD2 LSM6 CTF18 DIA2 CLN3 THP2 NUP133 CDC73 BUB1 IRC15 KAR3 DOC1 CTF19 NUP120 RAD6 XRS2 TOP3 RAD57 RRM3 HST3 ESC2 YDR532C RTT107 RAD55 SGS1 PSH1 MUS81 VID22 TSA1 HHF1 RAD24 HCM1 RAD59 SHM2 POL32 RAD9 RAD17 RNH201 RNH203 CLB5 RNH202 SWC3 RAD10 CYK3 SPT2 RTT109 RAD5 RPA12 PAC10 YDL156W UPS1 RAD18 ETR1 THP1 RAD51 YTA7 ASF1 HPR5 OMA1 SGO1 SRO7 ISA2 CNN1 VPS64 PIG1 YBP2 ADE6 BRE1 MFT1 CYC8 ADE1 MRE11 DUN1 SOV1 ADE17
942	outer kinetochore of condensed nuclear chromosome	2 out of 130 genes, 1.5%	2 out of 7286 annotated genes, 0.0%	0.00061	IML3 CHL4
940	outer kinetochore of condensed chromosome	2 out of 130 genes, 1.5%	2 out of 7286 annotated genes, 0.0%	0.00061	IML3 CHL4
46930	pore complex	5 out of 130 genes, 3.8%	51 out of 7286 annotated genes, 0.6%	0.00233	MAD1 MAD2 NUP133 NUP120 THP1
5643	nuclear pore	5 out of 130 genes, 3.8%	51 out of 7286 annotated genes, 0.6%	0.00233	MAD1 MAD2 NUP133 NUP120 THP1
347	THO complex	2 out of 130 genes, 1.5%	4 out of 7286 annotated genes, 0.0%	0.00241	THP2 MFT1
817	COMA complex	2 out of 130 genes, 1.5%	4 out of 7286 annotated genes, 0.0%	0.00241	MCM21 CTF19
15630	microtubule cytoskeleton	7 out of 130 genes, 5.3%	102 out of 7286 annotated genes, 1.3%	0.00249	BIM1 MCM21 CIN8 KAR3 CTF19 YDR532C SGO1
44422	organelle part	55 out of 130 genes, 42.3%	2227 out of 7286 annotated genes, 30.5%	0.00304	CTF8 CTF4 DCC1 BIM1 TOF1 IML3 MCM21 MCM16 MCM22 DDC1 CHL4 BUB3 RAD52 RAD50 ELG1 MRC1 CTF3 CIN8 CDH1 EST3 MAD1 MAD2 LSM6 CTF18 THP2 NUP133 CDC73 BUB1 KAR3 DOC1 CTF19 NUP120 XRS2 RRM3 YDR532C SGS1 HHF1 RAD24 POL32 SWC3 RAD10 RAD5 RPA12 UPS1 RAD18 THP1 RAD51 ASF1 OMA1 SGO1 ISA2 CNN1 VPS64 MFT1 MRE11
44446	intracellular organelle part	55 out of 130 genes, 42.3%	2227 out of 7286 annotated genes, 30.5%	0.00304	CTF8 CTF4 DCC1 BIM1 TOF1 IML3 MCM21 MCM16 MCM22 DDC1 CHL4 BUB3 RAD52 RAD50 ELG1 MRC1 CTF3 CIN8 CDH1 EST3 MAD1 MAD2 LSM6 CTF18 THP2 NUP133 CDC73 BUB1 KAR3 DOC1 CTF19 NUP120 XRS2 RRM3 YDR532C SGS1 HHF1 RAD24 POL32 SWC3 RAD10 RAD5 RPA12 UPS1 RAD18 THP1 RAD51 ASF1 OMA1 SGO1 ISA2 CNN1 VPS64 MFT1 MRE11
44453	nuclear membrane part	5 out of 130 genes, 3.8%	57 out of 7286 annotated genes, 0.7%	0.00374	MAD1 MAD2 NUP133 NUP120 THP1
31965	nuclear membrane	5 out of 130 genes, 3.8%	57 out of 7286 annotated genes, 0.7%	0.00374	MAD1 MAD2 NUP133 NUP120 THP1
790	nuclear chromatin	4 out of 130 genes, 3.0%	38 out of 7286 annotated genes, 0.5%	0.00499	RRM3 HHF1 RAD5 RAD18
785	chromatin	4 out of 130 genes, 3.0%	40 out of 7286 annotated genes, 0.5%	0.00596	RRM3 HHF1 RAD5 RAD18
346	transcription export complex	2 out of 130 genes, 1.5%	7 out of 7286 annotated genes, 0.0%	0.00713	THP2 MFT1
43234	protein complex	37 out of 130 genes, 28.4%	1480 out of 7286 annotated genes, 20.3%	0.01652	CTF8 DCC1 MCM21 RMI1 RAD50 ELG1 CIN8 UBR1 CDH1 EST3 MAD1 MAD2 LSM6 CTF18 DIA2 THP2 NUP133 CDC73 DOC1 CTF19 NUP120 RAD6 XRS2 TOP3 SGS1 HHF1 RAD24 POL32 SWC3 RAD10 RPA12 PAC10 THP1 ASF1 PIG1 MFT1 MRE11

5819	spindle	5 out of 130 genes, 3.8%	83 out of 7286 annotated genes, 1.1%	0.01703	BIM1 CIN8 KAR3 YDR532C SGO1
5815	microtubule organizing center	4 out of 130 genes, 3.0%	60 out of 7286 annotated genes, 0.8%	0.02306	BIM1 KAR3 YDR532C SGO1
5816	spindle pole body	4 out of 130 genes, 3.0%	60 out of 7286 annotated genes, 0.8%	0.02306	BIM1 KAR3 YDR532C SGO1
5874	microtubule	3 out of 130 genes, 2.3%	34 out of 7286 annotated genes, 0.4%	0.02344	BIM1 CIN8 KAR3
5875	microtubule associated complex	3 out of 130 genes, 2.3%	34 out of 7286 annotated genes, 0.4%	0.02344	MCM21 CIN8 CTF19
151	ubiquitin ligase complex	3 out of 130 genes, 2.3%	36 out of 7286 annotated genes, 0.4%	0.02713	CDH1 DIA2 DOC1
922	spindle pole	4 out of 130 genes, 3.0%	65 out of 7286 annotated genes, 0.8%	0.02971	BIM1 KAR3 YDR532C SGO1
5680	anaphase-promoting complex	2 out of 130 genes, 1.5%	16 out of 7286 annotated genes, 0.2%	0.03359	CDH1 DOC1
5635	nuclear envelope	5 out of 130 genes, 3.8%	101 out of 7286 annotated genes, 1.3%	0.03544	MAD1 MAD2 NUP133 NUP120 THP1
44430	cytoskeletal part	7 out of 130 genes, 5.3%	190 out of 7286 annotated genes, 2.6%	0.05469	BIM1 MCM21 CIN8 KAR3 CTF19 YDR532C SGO1
152	nuclear ubiquitin ligase complex	2 out of 130 genes, 1.5%	23 out of 7286 annotated genes, 0.3%	0.0641	CDH1 DOC1
5856	cytoskeleton	7 out of 130 genes, 5.3%	204 out of 7286 annotated genes, 2.7%	0.07376	BIM1 MCM21 CIN8 KAR3 CTF19 YDR532C SGO1
31970	organelle envelope lumen	2 out of 130 genes, 1.5%	27 out of 7286 annotated genes, 0.3%	0.08443	UPS1 ISA2
5758	mitochondrial intermembrane space	2 out of 130 genes, 1.5%	27 out of 7286 annotated genes, 0.3%	0.08443	UPS1 ISA2

Appendix 4 Gene ontology (GO) biological process annotation enrichment among non-essential yeast CIN genes

Over-representation of GO biological processes in the 293 yeast CIN gene set and the high confident 130 subset, compared to the entire yeast genome, was determined using GO TermFinder as of August 23, 2006 (db.yeastgenome.org/cgi-bin/GO/goTermFinder.pl) (Harris et al., 2004). Only GO biological processes with an e-value <1E-10 are shown.

GO_ID	GO_term (Biological Process)	Frequency	Genome Frequency	Probability	Genes
All 293 CIN genes					
6259	DNA metabolism	81 out of 293 genes, 27.6%	565 out of 7286 annotated genes, 7.7%	2.92E-24	CTF4 TOF1 MEC3 RAD52 MMS1 LGE1 RAD27 RAD50 RAD54 ELG1 MRC1 MMS4 MMS22 RDH54 DIA2 THP2 NUP133 CDC73 NUP120 RAD6 XRS2 TOP3 RAD57 RRM3 HST3 ESC2 RTT107 RAD55 SGS1 MUS81 HHF1 RAD24 RAD59 POL32 RAD9 RAD17 RNH201 RNH203 CLB5 RNH202 SWC3 RAD10 SPT2 RTT109 RAD5 RAD18 THP1 RAD51 HPR5 BRE1 MFT1 CYC8 MRE11 RTT103 SGF73 SPT4 RTT106 SGF11 SDS3 SWC5 NGG1 SWR1 ARP6 MPH1 CAC2 HTZ1 VID21 NUP84 MGM101 DOT1 HST4 YKU80 SHU1 IOC3 RTT101 CBF1 FYV6 SPT10 RNR4 RNR1 RAD1
7001	chromosome organization and biogenesis (sensu Eukaryota)	70 out of 293 genes, 23.8%	454 out of 7286 annotated genes, 6.2%	1.55E-22	CTF8 DCC1 MEC3 RAD52 SPT21 SHP1 LGE1 RAD27 RAD50 RAD54 ELG1 MRC1 CDH1 EST3 SLX8 THP2 CDC73 RAD6 XRS2 TOP3 RAD57 HST3 ESC2 YDR532C SGS1 HHF1 HCM1 RAD59 POL32 SWC3 SPT2 RAD5 RAD51 YTA7 BRE1 MFT1 CYC8 MRE11 DUN1 SGF73 SPT4 RPS23A SGF11 SDS3 SRB8 SWC5 PFD1 NGG1 SWR1 ARP6 ARV1 CAC2 HTZ1 VID21 NUP60 RPL34B SLI15 DOT1 SEM1 LEA1 HST4 YKU80 IOC3 RPA14 CBF1 FYV6 SPT10 FUN30 MET7 RNR1
51276	chromosome organization and biogenesis	70 out of 293 genes, 23.8%	465 out of 7286 annotated genes, 6.3%	5.82E-22	CTF8 DCC1 MEC3 RAD52 SPT21 SHP1 LGE1 RAD27 RAD50 RAD54 ELG1 MRC1 CDH1 EST3 SLX8 THP2 CDC73 RAD6 XRS2 TOP3 RAD57 HST3 ESC2 YDR532C SGS1 HHF1 HCM1 RAD59 POL32 SWC3 SPT2 RAD5 RAD51 YTA7 BRE1 MFT1 CYC8 MRE11 DUN1 SGF73 SPT4 RPS23A SGF11 SDS3 SRB8 SWC5 PFD1 NGG1 SWR1 ARP6 ARV1 CAC2 HTZ1 VID21 NUP60 RPL34B SLI15 DOT1 SEM1 LEA1 HST4 YKU80 IOC3 RPA14 CBF1 FYV6 SPT10 FUN30 MET7 RNR1
6974	response to DNA damage stimulus	45 out of 293 genes, 15.3%	208 out of 7286 annotated genes, 2.8%	6.90E-20	CTF8 CTF4 DCC1 MEC3 RAD52 MMS1 RAD27 RMI1 RAD50 RAD54 MMS4 YLR235C MMS22 RDH54 SLX8 RAD6 XRS2 RAD57 YBR099C RTT107 RAD55 SGS1 MUS81 RAD24 RAD59 POL32 RAD9 RAD17 RAD10 RTT109 RAD5 RAD18 RAD51 ASF1 HPR5 MRE11 DUN1 MPH1 CAC2 NUP84 MGM101 YKU80 SHU1 FYV6 RAD1
9719	response to endogenous stimulus	45 out of 293 genes, 15.3%	214 out of 7286 annotated genes, 2.9%	2.02E-19	CTF8 CTF4 DCC1 MEC3 RAD52 MMS1 RAD27 RMI1 RAD50 RAD54 MMS4 YLR235C MMS22 RDH54 SLX8 RAD6 XRS2 RAD57 YBR099C RTT107 RAD55 SGS1 MUS81 RAD24 RAD59 POL32 RAD9 RAD17 RAD10 RTT109 RAD5 RAD18 RAD51 ASF1 HPR5 MRE11 DUN1 MPH1 CAC2 NUP84 MGM101 YKU80 SHU1 FYV6 RAD1
279	M phase	45 out of 293 genes, 15.3%	245 out of 7286 annotated genes, 3.3%	3.08E-17	CTF8 CTF4 DCC1 BIM1 CSM3 TOF1 IML3 CHL1 DDC1 BUB3 RAD52 LGE1 RAD50 MMS4 RDH54 CIN8 CDH1 MAD1 MAD2 CTF18 BUB1 KAR3 DOC1 XRS2 TOP3 RAD57 RAD55 SGS1 MUS81 RAD24 RAD17 RAD10 RAD51 SGO1 MRE11 CIK1 TUB3 DOT1 BFA1 ASE1 RTT101 RTS1 TPD3 SAC3 RAD1
723	telomere maintenance	46 out of 293 genes, 15.6%	268 out of 7286 annotated genes, 3.6%	1.62E-16	CTF8 DCC1 RAD52 SPT21 SHP1 RAD27 RAD50 RAD54 ELG1 MRC1 CDH1 EST3 SLX8 THP2 CDC73 RAD6 XRS2 TOP3 RAD57 YDR532C SGS1 HCM1 RAD59 POL32 RAD5 RAD51 YTA7 BRE1 MFT1 CYC8 MRE11 DUN1 RPS23A SRB8 PFD1 ARV1 NUP60 RPL34B SLI15 SEM1 LEA1 YKU80 RPA14 FYV6 MET7 RNR1
7049	cell cycle	57 out of 293 genes, 19.4%	411 out of 7286 annotated genes, 5.6%	2.92E-16	CTF8 SIC1 CTF4 DCC1 BIM1 CSM3 TOF1 IML3 CHL1 MEC3 DDC1 BUB3 RAD52 LGE1 RAD50 MRC1 MMS4 RDH54 CIN8 CDH1 MAD1 MAD2 CTF18 CLN3 BUB1 KAR3 DOC1 XRS2 TOP3 RAD57 RAD55 SGS1 MUS81 RAD24 HCM1 RAD9 RAD17 CLB5 RAD10 RAD51 SGO1 VPS64 MRE11 DUN1 CIK1 STB1 TUB3 DOT1 SEM1 CLB3 BFA1 ASE1 RTT101 RTS1 TPD3 SAC3 RAD1
7059	chromosome segregation	30 out of 293 genes, 10.2%	111 out of 7286 annotated genes, 1.5%	5.09E-16	CTF8 CTF4 DCC1 BIM1 CSM3 TOF1 IML3 CHL1 MCM21 MCM16 MCM22 CHL4 RDH54 CTF3 CIN8 CDH1 CTF18 KAR3 DOC1 CTF19 SGS1 SGO1 CNN1 SPT4 CIK1 TUB3 GLC8 SLI15 CBF1 RTS1
6996	organelle organization and biogenesis	98 out of 293 genes, 33.4%	1111 out of 7286 annotated genes, 15.2%	8.34E-15	CTF8 DCC1 BIM1 MEC3 RAD52 SPT21 SHP1 LGE1 RAD27 RAD50 RAD54 ELG1 MRC1 CIN8 CDH1 EST3 SLX8 CLN3 THP2 NUP133 CDC73 KAR3 DOC1 NUP120 RAD6 XRS2 TOP3 RAD57 RRM3 HST3 ESC2 YDR532C SGS1 HHF1 HCM1 RAD59 POL32 CLB5 SWC3 SPT2 RAD5 RAD51 YTA7 BRE1 MFT1 CYC8 MRE11 DUN1 SGF73 SPT4 RPS23A SGF11 CIK1 SDS3 SRB8 SWC5 PFD1 NGG1 SWR1 ARP6 CIN2 ARV1 TUB3 CAC2 HTZ1 VID21 NUP84 DJP1 NUP60 MGM101 RPL34B SLI15 SUN4 DOT1 DBP7 SEM1 LEA1 HST4 ARC18 YKU80 IOC3 ASE1 RPA14 HSP42 SSF1 CBF1 FYV6 SPT10 ACO1 MDM31 TPD3 FUN30 SAC3 MET7 RNR1 VAC8 SLM2 YNL213C
6281	DNA repair	32 out of 293 genes, 10.9%	160 out of 7286 annotated genes, 2.1%	1.80E-13	CTF4 RAD52 MMS1 RAD27 RAD50 RAD54 MMS4 MMS22 RDH54 RAD6 XRS2 RAD57 RTT107 RAD55 MUS81 RAD24 RAD59 POL32 RAD9 RAD10 RAD5 RAD18 RAD51 HPR5 MRE11 MPH1 CAC2 MGM101 YKU80 SHU1 FYV6 RAD1
6302	double-strand break repair	19 out of 293 genes, 6.4%	50 out of 7286 annotated genes, 0.6%	4.39E-13	RAD52 RAD27 RAD50 RAD54 MMS22 RDH54 XRS2 RAD57 RTT107 RAD55 RAD59 RAD10 RAD5 RAD51 HPR5 MRE11 YKU80 FYV6 RAD1
6950	response to stress	52 out of 293 genes, 17.7%	440 out of 7286 annotated genes, 6.0%	3.29E-12	CTF8 CTF4 DCC1 MEC3 RAD52 MMS1 RAD27 RMI1 RAD50 RAD54 MMS4 YLR235C MMS22 RDH54 SLX8 RAD6 XRS2 RAD57 YBR099C RTT107 RAD55 SGS1 MUS81 TSA1 RAD24 RAD59 POL32 RAD9 RAD17 RAD10 RTT109 RAD5 RAD18 RAD51 ASF1 HPR5 MRE11 DUN1 SSK1 MPH1 MSB2 CAC2 NUP84 MET22 MGM101 CPR7 YKU80 SHU1 HSP42 FYV6 GRX5 RAD1
51244	regulation of cellular physiological process	64 out of 293 genes, 21.8%	625 out of 7286 annotated genes, 8.5%	3.42E-12	SIC1 BIM1 CSM3 TOF1 MEC3 DDC1 BUB3 SPT21 MMS1 ELG1 MRC1 SSZ1 CDH1 MAD1 MAD2 CLN3 BUB1 DOC1 TOP3 HST3 ESC2 RTT107 TSA1 RAD24 HCM1 RAD9 RAD17 CLB5 SPT2 RTT109 ASF1 SGO1 VPS64 PIG1 BRE1 CYC8 DUN1 RTT103 AFT1 SPT4 RPS23A RTT106 SGF11 PPQ1 CTK2 SDS3 SRB8 NUT1 CAC2 HTZ1 ZUO1 DOT1 SEM1 ARG81 HST4 YKU80 CLB3 BFA1 RTT101 SPT10 LSM1 PUF2 TPD3 SLM2
50794	regulation of cellular process	64 out of 293 genes, 21.8%	626 out of 7286 annotated genes, 8.5%	3.67E-12	SIC1 BIM1 CSM3 TOF1 MEC3 DDC1 BUB3 SPT21 MMS1 ELG1 MRC1 SSZ1 CDH1 MAD1 MAD2 CLN3 BUB1 DOC1 TOP3 HST3 ESC2 RTT107 TSA1 RAD24 HCM1 RAD9 RAD17 CLB5 SPT2 RTT109 ASF1 SGO1 VPS64 PIG1 BRE1 CYC8 DUN1 RTT103 AFT1 SPT4 RPS23A RTT106 SGF11 PPQ1 CTK2 SDS3 SRB8 NUT1 CAC2 HTZ1 ZUO1 DOT1 SEM1 ARG81 HST4 YKU80 CLB3 BFA1 RTT101 SPT10 LSM1 PUF2 TPD3 SLM2
50791	regulation of physiological process	64 out of 293 genes, 21.8%	643 out of 7286 annotated genes, 8.8%	1.15E-11	SIC1 BIM1 CSM3 TOF1 MEC3 DDC1 BUB3 SPT21 MMS1 ELG1 MRC1 SSZ1 CDH1 MAD1 MAD2 CLN3 BUB1 DOC1 TOP3 HST3 ESC2 RTT107 TSA1 RAD24 HCM1 RAD9 RAD17 CLB5 SPT2 RTT109 ASF1 SGO1 VPS64 PIG1 BRE1 CYC8 DUN1 RTT103 AFT1 SPT4 RPS23A RTT106 SGF11 PPQ1 CTK2 SDS3 SRB8 NUT1 CAC2 HTZ1 ZUO1 DOT1 SEM1 ARG81 HST4 YKU80 CLB3 BFA1 RTT101 SPT10 LSM1 PUF2 TPD3 SLM2
50789	regulation of biological process	64 out of 293 genes, 21.8%	656 out of 7286 annotated genes, 9.0%	2.67E-11	SIC1 BIM1 CSM3 TOF1 MEC3 DDC1 BUB3 SPT21 MMS1 ELG1 MRC1 SSZ1 CDH1 MAD1 MAD2 CLN3 BUB1 DOC1 TOP3 HST3 ESC2 RTT107 TSA1 RAD24 HCM1 RAD9 RAD17 CLB5 SPT2 RTT109 ASF1 SGO1 VPS64 PIG1 BRE1 CYC8 DUN1 RTT103 AFT1 SPT4 RPS23A RTT106 SGF11 PPQ1 CTK2 SDS3 SRB8 NUT1 CAC2 HTZ1 ZUO1 DOT1 SEM1 ARG81 HST4 YKU80 CLB3 BFA1 RTT101 SPT10 LSM1 PUF2 TPD3 SLM2
819	sister chromatid segregation	18 out of 293 genes, 6.1%	57 out of 7286 annotated genes, 0.7%	3.63E-11	CTF8 CTF4 DCC1 BIM1 CSM3 TOF1 IML3 CHL1 RDH54 CIN8 CDH1 CTF18 KAR3 DOC1 SGS1 SGO1 CIK1 TUB3

7067	mitosis	25 out of 293 genes, 8.5%	122 out of 7286 annotated genes, 1.6%	5.46E-11	CTF8 CTF4 DCC1 BIM1 CSM3 TOF1 CHL1 BUB3 CIN8 CDH1 MAD1 MAD2 CTF18 BUB1 KAR3 DOC1 SGS1 SGO1 CIK1 TUB3 BFA1 ASE1 RTT101 TPD3 SAC3
75	cell cycle checkpoint	17 out of 293 genes, 5.8%	51 out of 7286 annotated genes, 0.6%	5.67E-11	BIM1 CSM3 TOF1 MEC3 DDC1 BUB3 MRC1 MAD1 MAD2 BUB1 RAD24 RAD9 RAD17 SGO1 DUN1 BFA1 TPD3
87	M phase of mitotic cell cycle	25 out of 293 genes, 8.5%	123 out of 7286 annotated genes, 1.6%	6.47E-11	CTF8 CTF4 DCC1 BIM1 CSM3 TOF1 CHL1 BUB3 CIN8 CDH1 MAD1 MAD2 CTF18 BUB1 KAR3 DOC1 SGS1 SGO1 CIK1 TUB3 BFA1 ASE1 RTT101 TPD3 SAC3
6139	nucleobase, nucleoside, nucleotide and nucleic acid metabolism	110 out of 293 genes, 37.5%	1530 out of 7286 annotated genes, 20.9%	7.04E-11	CTF4 TOF1 MEC3 RAD52 SPT21 MMS1 LGE1 RAD27 RAD50 RAD54 ELG1 MRC1 MMS4 MMS22 RDH54 LSM6 DIA2 THP2 NUP133 CDC73 NUP120 RAD6 XRS2 TOP3 RAD57 RRM3 HST3 ESC2 RTT107 RAD55 SGS1 PSH1 MUS81 HHF1 RAD24 HCM1 RAD59 POL32 RAD9 RAD17 RNH201 RNH203 CLB5 RNH202 SWC3 RAD10 SPT2 RTT109 RAD5 RPA12 RAD18 THP1 RAD51 HPR5 ADE6 BRE1 MFT1 CYC8 ADE1 MRE11 ADE17 RTT103 MUD2 SNU66 SGF73 AFT1 SPT4 RTT106 SGF11 CTK2 SDS3 SRB8 SWC5 NGG1 SWR1 ARP6 MPH1 NUT1 CAC2 HTZ1 VID21 NUP84 ADE5,7 ADE4 MGM101 ADE8 DOT1 DBP7 LEA1 HST4 YKU80 SIP3 SHU1 MSM1 IOC3 YHR087W RPA14 RTT101 CBF1 FYV6 SPT10 ADK1 LSM1 SRL3 PUF2 RNR4 RNR1 MSS116 ADE2 RAD1
High confidence CIN genes (subset of 130)					
6974	response to DNA damage stimulus	37 out of 130 genes, 28.4%	208 out of 7286 annotated genes, 2.8%	2.12E-26	CTF8 CTF4 DCC1 MEC3 RAD52 MMS1 RAD27 RMI1 RAD50 RAD54 MMS4 YLR235C MMS22 RDH54 SLX8 RAD6 XRS2 RAD57 YBR099C RTT107 RAD55 SGS1 MUS81 RAD24 RAD59 POL32 RAD9 RAD17 RAD10 RTT109 RAD5 RAD18 RAD51 ASF1 HPR5 MRE11 DUN1
9719	response to endogenous stimulus	37 out of 130 genes, 28.4%	214 out of 7286 annotated genes, 2.9%	5.63E-26	CTF8 CTF4 DCC1 MEC3 RAD52 MMS1 RAD27 RMI1 RAD50 RAD54 MMS4 YLR235C MMS22 RDH54 SLX8 RAD6 XRS2 RAD57 YBR099C RTT107 RAD55 SGS1 MUS81 RAD24 RAD59 POL32 RAD9 RAD17 RAD10 RTT109 RAD5 RAD18 RAD51 ASF1 HPR5 MRE11 DUN1
6259	DNA metabolism	53 out of 130 genes, 40.7%	585 out of 7286 annotated genes, 7.7%	3.31E-25	CTF4 TOF1 MEC3 RAD52 MMS1 LGE1 RAD27 RAD50 RAD54 ELG1 MRC1 MMS4 MMS22 RDH54 DIA2 THP2 NUP133 CDC73 NUP120 RAD6 XRS2 TOP3 RAD57 RRM3 HST3 ESC2 RTT107 RAD55 SGS1 MUS81 HHF1 RAD24 RAD59 POL32 RAD9 RAD17 RNH201 RNH203 CLB5 RNH202 SWC3 RAD10 SPT2 RTT109 RAD5 RAD18 THP1 RAD51 HPR5 BRE1 MFT1 CYC8 MRE11
7049	cell cycle	44 out of 130 genes, 33.8%	411 out of 7286 annotated genes, 5.6%	8.81E-23	CTF8 SIC1 CTF4 DCC1 BIM1 CSM3 TOF1 IML3 CHL1 MEC3 DDC1 BUB3 RAD52 LGE1 RAD50 MRC1 MMS4 RDH54 CIN8 CDH1 MAD1 MAD2 CTF18 CLN3 BUB1 KAR3 DOC1 XRS2 TOP3 RAD57 RAD55 SGS1 MUS81 RAD24 HCM1 RAD9 RAD17 CLB5 RAD10 RAD51 SGO1 VPS64 MRE11 DUN1
279	M phase	35 out of 130 genes, 26.9%	245 out of 7286 annotated genes, 3.3%	7.02E-22	CTF8 CTF4 DCC1 BIM1 CSM3 TOF1 IML3 CHL1 DDC1 BUB3 RAD52 LGE1 RAD50 MMS4 RDH54 CIN8 CDH1 MAD1 MAD2 CTF18 BUB1 KAR3 DOC1 XRS2 TOP3 RAD57 RAD55 SGS1 MUS81 RAD24 RAD17 RAD10 RAD51 SGO1 MRE11
7059	chromosome segregation	23 out of 130 genes, 17.6%	111 out of 7286 annotated genes, 1.5%	6.79E-18	CTF8 CTF4 DCC1 BIM1 CSM3 TOF1 IML3 CHL1 MCM21 MCM16 MCM22 CHL4 RDH54 CTF3 CIN8 CDH1 CTF18 KAR3 DOC1 CTF19 SGS1 SGO1 CNN1
723	telomere maintenance	32 out of 130 genes, 24.6%	268 out of 7286 annotated genes, 3.6%	9.41E-18	CTF8 DCC1 RAD52 SPT21 SHP1 RAD27 RAD50 RAD54 ELG1 MRC1 CDH1 EST3 SLX8 THP2 CDC73 RAD6 XRS2 TOP3 RAD57 YDR532C SGS1 HCM1 RAD59 POL32 RAD5 RAD51 YTA7 BRE1 MFT1 CYC8 MRE11 DUN1
7001	chromosome organization and biogenesis (sensu Eukaryota)	39 out of 130 genes, 30%	454 out of 7286 annotated genes, 6.2%	7.69E-17	CTF8 DCC1 MEC3 RAD52 SPT21 SHP1 LGE1 RAD27 RAD50 RAD54 ELG1 MRC1 CDH1 EST3 SLX8 THP2 CDC73 RAD6 XRS2 TOP3 RAD57 HST3 ESC2 YDR532C SGS1 HHF1 HCM1 RAD59 POL32 SWC3 SPT2 RAD5 RAD51 YTA7 BRE1 MFT1 CYC8 MRE11 DUN1
6281	DNA repair	25 out of 130 genes, 19.2%	160 out of 7286 annotated genes, 2.1%	1.43E-16	CTF4 RAD52 MMS1 RAD27 RAD50 RAD54 MMS4 MMS22 RDH54 RAD6 XRS2 RAD57 RTT107 RAD55 MUS81 RAD24 RAD59 POL32 RAD9 RAD10 RAD5 RAD18 RAD51 HPR5 MRE11
51276	chromosome organization and biogenesis	39 out of 130 genes, 30%	465 out of 7286 annotated genes, 6.3%	1.69E-16	CTF8 DCC1 MEC3 RAD52 SPT21 SHP1 LGE1 RAD27 RAD50 RAD54 ELG1 MRC1 CDH1 EST3 SLX8 THP2 CDC73 RAD6 XRS2 TOP3 RAD57 HST3 ESC2 YDR532C SGS1 HHF1 HCM1 RAD59 POL32 SWC3 SPT2 RAD5 RAD51 YTA7 BRE1 MFT1 CYC8 MRE11 DUN1
6950	response to stress	38 out of 130 genes, 29.2%	440 out of 7286 annotated genes, 6.0%	1.8E-16	CTF8 CTF4 DCC1 MEC3 RAD52 MMS1 RAD27 RMI1 RAD50 RAD54 MMS4 YLR235C MMS22 RDH54 SLX8 RAD6 XRS2 RAD57 YBR099C RTT107 RAD55 SGS1 MUS81 TSA1 RAD24 RAD59 POL32 RAD9 RAD17 RAD10 RTT109 RAD5 RAD18 RAD51 ASF1 HPR5 MRE11 DUN1
6302	double-strand break repair	16 out of 130 genes, 12.3%	50 out of 7286 annotated genes, 0.6%	1.4E-15	RAD52 RAD27 RAD50 RAD54 MMS22 RDH54 XRS2 RAD57 RTT107 RAD55 RAD59 RAD10 RAD5 RAD51 HPR5 MRE11
819	sister chromatid segregation	16 out of 130 genes, 12.3%	57 out of 7286 annotated genes, 0.7%	1.03E-14	CTF8 CTF4 DCC1 BIM1 CSM3 TOF1 IML3 CHL1 RDH54 CIN8 CDH1 CTF18 KAR3 DOC1 SGS1 SGO1
6310	DNA recombination	25 out of 130 genes, 19.2%	194 out of 7286 annotated genes, 2.6%	1.09E-14	RAD52 MMS1 RAD50 RAD54 ELG1 MMS4 RDH54 THP2 CDC73 XRS2 TOP3 RAD57 RTT107 RAD55 SGS1 MUS81 RAD24 RAD59 RAD17 RAD10 RTT109 THP1 RAD51 MFT1 MRE11
50896	response to stimulus	41 out of 130 genes, 31.5%	604 out of 7286 annotated genes, 8.2%	2.99E-14	CTF8 CTF4 DCC1 RAD61 MEC3 RAD52 MMS1 RAD27 RMI1 RAD50 RAD54 MMS4 YLR235C MMS22 RDH54 SLX8 RAD6 XRS2 RAD57 YBR099C RTT107 RAD55 SGS1 MUS81 TSA1 RAD24 RAD59 POL32 RAD9 RAD17 RAD10 RTT109 RAD5 RAD18 RAD51 ASF1 HPR5 VPS64 MRE11 WSS1 DUN1
75	cell cycle checkpoint	15 out of 130 genes, 11.5%	51 out of 7286 annotated genes, 0.6%	3.76E-14	BIM1 CSM3 TOF1 MEC3 DDC1 BUB3 MRC1 MAD1 MAD2 BUB1 RAD24 RAD9 RAD17 SGO1 DUN1

51321	meiotic cell cycle	21 out of 130 genes, 16.1%	140 out of 7286 annotated genes, 1.9%	1.05E-13	CSM3 IML3 DDC1 RAD52 LGE1 RAD50 MMS4 RDH54 KAR3 XRS2 TOP3 RAD57 RAD55 SGS1 MUS81 RAD24 RAD17 RAD10 RAD51 SGO1 MRE11
51327	M phase of meiotic cell cycle	21 out of 130 genes, 16.1%	140 out of 7286 annotated genes, 1.9%	1.05E-13	CSM3 IML3 DDC1 RAD52 LGE1 RAD50 MMS4 RDH54 KAR3 XRS2 TOP3 RAD57 RAD55 SGS1 MUS81 RAD24 RAD17 RAD10 RAD51 SGO1 MRE11
7126	meiosis	21 out of 130 genes, 16.1%	140 out of 7286 annotated genes, 1.9%	1.05E-13	CSM3 IML3 DDC1 RAD52 LGE1 RAD50 MMS4 RDH54 KAR3 XRS2 TOP3 RAD57 RAD55 SGS1 MUS81 RAD24 RAD17 RAD10 RAD51 SGO1 MRE11
74	regulation of progression through cell cycle	21 out of 130 genes, 16.1%	145 out of 7286 annotated genes, 1.9%	2.05E-13	SIC1 BIM1 CSM3 TOF1 MEC3 DDC1 BUB3 MRC1 CDH1 MAD1 MAD2 CLN3 BUB1 DOC1 RAD24 RAD9 RAD17 CLB5 SGO1 VPS64 DUN1
51726	regulation of cell cycle	21 out of 130 genes, 16.1%	145 out of 7286 annotated genes, 1.9%	2.05E-13	SIC1 BIM1 CSM3 TOF1 MEC3 DDC1 BUB3 MRC1 CDH1 MAD1 MAD2 CLN3 BUB1 DOC1 RAD24 RAD9 RAD17 CLB5 SGO1 VPS64 DUN1
7131	meiotic recombination	14 out of 130 genes, 10.7%	47 out of 7286 annotated genes, 0.6%	2.34E-13	RAD52 RAD50 MMS4 RDH54 XRS2 TOP3 RAD57 RAD55 MUS81 RAD24 RAD17 RAD10 RAD51 MRE11
43283	biopolymer metabolism	67 out of 130 genes, 51.5%	1644 out of 7286 annotated genes, 22.5%	5.86E-13	CTF4 TOF1 MEC3 RAD52 MMS1 SHP1 LGE1 RAD27 RAD50 RAD54 ELG1 MRC1 MMS4 MMS22 RDH54 UBR1 CDH1 LSM6 SLX8 DIA2 THP2 NUP133 CDC73 BUB1 DOC1 NUP120 RAD6 XRS2 TOP3 RAD57 RRM3 HST3 ESC2 RTT107 RAD55 SGS1 MUS81 VID22 HHF1 RAD24 RAD59 POL32 RAD9 RAD17 RNH201 RNH203 CLB5 RNH202 SWC3 RAD10 SPT2 RTT109 RAD5 UPS1 RAD18 THP1 RAD51 YTA7 HPR5 OMA1 PIG1 BRE1 MFT1 CYC8 MRE11 WSS1 DUN1
724	double-strand break repair via homologous recombination	10 out of 130 genes, 7.6%	18 out of 7286 annotated genes, 0.2%	1.72E-12	RAD52 RAD50 RAD54 RDH54 XRS2 RAD57 RAD55 RAD59 RAD51 MRE11
70	mitotic sister chromatid segregation	14 out of 130 genes, 10.7%	55 out of 7286 annotated genes, 0.7%	1.88E-12	CTF8 CTF4 DCC1 BIM1 CSM3 TOF1 CHL1 CIN8 CDH1 CTF18 KAR3 DOC1 SGS1 SGO1
725	recombinational repair	10 out of 130 genes, 7.6%	19 out of 7286 annotated genes, 0.2%	2.91E-12	RAD52 RAD50 RAD54 RDH54 XRS2 RAD57 RAD55 RAD59 RAD51 MRE11
7067	mitosis	18 out of 130 genes, 13.8%	122 out of 7286 annotated genes, 1.6%	9.17E-12	CTF8 CTF4 DCC1 BIM1 CSM3 TOF1 CHL1 BUB3 CIN8 CDH1 MAD1 MAD2 CTF18 BUB1 KAR3 DOC1 SGS1 SGO1
87	M phase of mitotic cell cycle	18 out of 130 genes, 13.8%	123 out of 7286 annotated genes, 1.6%	1.04E-11	CTF8 CTF4 DCC1 BIM1 CSM3 TOF1 CHL1 BUB3 CIN8 CDH1 MAD1 MAD2 CTF18 BUB1 KAR3 DOC1 SGS1 SGO1
7127	meiosis I	14 out of 130 genes, 10.7%	65 out of 7286 annotated genes, 0.8%	1.68E-11	RAD52 RAD50 MMS4 RDH54 XRS2 TOP3 RAD57 RAD55 MUS81 RAD24 RAD17 RAD10 RAD51 MRE11
45003	double-strand break repair via synthesis-dependent strand annealing	8 out of 130 genes, 6.1%	11 out of 7286 annotated genes, 0.1%	3.72E-11	RAD52 RAD50 RAD54 RDH54 RAD57 RAD55 RAD51 MRE11
6139	nucleobase, nucleoside, nucleotide and nucleic acid metabolism	61 out of 130 genes, 46.9%	1530 out of 7286 annotated genes, 20.9%	4.1E-11	CTF4 TOF1 MEC3 RAD52 SPT21 MMS1 LGE1 RAD27 RAD50 RAD54 ELG1 MRC1 MMS4 MMS22 RDH54 LSM6 DIA2 THP2 NUP133 CDC73 NUP120 RAD6 XRS2 TOP3 RAD57 RRM3 HST3 ESC2 RTT107 RAD55 SGS1 PSH1 MUS81 HHF1 RAD24 HCM1 RAD59 POL32 RAD9 RAD17 RNH201 RNH203 CLB5 RNH202 SWC3 RAD10 SPT2 RTT109 RAD5 RPA12 RAD18 THP1 RAD51 HPR5 ADE6 BRE1 MFT1 CYC8 ADE1 MRE11 ADE17
51244	regulation of cellular physiological process	37 out of 130 genes, 28.4%	625 out of 7286 annotated genes, 8.5%	4.3E-11	SIC1 BIM1 CSM3 TOF1 MEC3 DDC1 BUB3 SPT21 MMS1 ELG1 MRC1 SSZ1 CDH1 MAD1 MAD2 CLN3 BUB1 DOC1 TOP3 HST3 ESC2 RTT107 TSA1 RAD24 HCM1 RAD9 RAD17 CLB5 SPT2 RTT109 ASF1 SGO1 VPS64 PIG1 BRE1 CYC8 DUN1
50794	regulation of cellular process	37 out of 130 genes, 28.4%	626 out of 7286 annotated genes, 8.5%	4.5E-11	SIC1 BIM1 CSM3 TOF1 MEC3 DDC1 BUB3 SPT21 MMS1 ELG1 MRC1 SSZ1 CDH1 MAD1 MAD2 CLN3 BUB1 DOC1 TOP3 HST3 ESC2 RTT107 TSA1 RAD24 HCM1 RAD9 RAD17 CLB5 SPT2 RTT109 ASF1 SGO1 VPS64 PIG1 BRE1 CYC8 DUN1
6312	mitotic recombination	10 out of 130 genes, 7.6%	27 out of 7286 annotated genes, 0.3%	8.68E-11	RAD52 RAD50 RAD54 RDH54 RAD57 RAD55 SGS1 RAD59 RAD10 RAD51
7064	mitotic sister chromatid cohesion	9 out of 130 genes, 6.9%	19 out of 7286 annotated genes, 0.2%	9.24E-11	CTF8 CTF4 DCC1 BIM1 CSM3 TOF1 CHL1 CTF18 KAR3

50791	regulation of physiological process	37 out of 130 genes, 28.4%	643 out of 7286 annotated genes, 8.6%	9.65E-11	SIC1 BIM1 CSM3 TOF1 MEC3 DDC1 BUB3 SPT21 MMS1 ELG1 MRC1 SSZ1 CDH1 MAD1 MAD2 CLN3 BUB1 DOC1 TOP3 HST3 ESC2 RTT107 TSA1 RAD24 HCM1 RAD9 RAD17 CLB5 SPT2 RTT109 ASF1 SGO1 VPS64 PIG1 BRE1 CYC8 DUN1

Appendix 5 Homologues of budding yeast CIN genes in human, mouse, worm, fly, and fission yeast

Protein sequences of yeast CIN genes were used as queries in a BLASTp alignment search against protein sequence downloads for *H. sapiens* (RefSeq protein database, as of June 2004), *M. musculus* (RefSeq protein database June 2004), *C. elegans* (Wormbase June 2004), *D. melanogaster* (FlyBase release 3.2.0), and *S. pombe* (Sanger Institute, pompep June 2004). The top BLASTp hit for each yeast query gene is listed.

Yeast ORF	Gene Name	Organism	Protein ID	Annotation	BLAST Score	E Value	Identity	Positive
YAL008W	FUN14	HUMAN	NP_006660.1	leukocyte immunoglobulin-like receptor, subfami...	29	2.4	20/51	27/51
		MOUSE	***** No hits found *****					
		FLY	FBgn0001217	Hsc70-2: Heat shock protein cognate 2	28	3.2	13/35	23/35
		WORM	CE31790	status:Confirmed TR:Q8MQ73 protein_id:AAM98030.1	27	6.2	26/90	40/90
		POMBE	SPAC29A4.17c	conserved eukaryotic protein	33	0.018	19/68	34/68
YAL011W	SWC3	HUMAN	NP_068566.2	a disintegrin and metalloproteinase domain 30 p...	32	1	17/54	26/54
		MOUSE	NP_035377.1	retinoblastoma binding protein 6 [Mus musculus]	37	0.036	31/141	56/141
		FLY	FBgn0031294	ia2	38	0.015	26/77	36/77
		WORM	CE09975	status:Partially_confirmed TR:O76719 protein_id...	35	0.11	26/105	48/105
		POMBE	SPAC23C4.02	WD repeat protein	34	0.049	24/78	35/78
YAL016W	TPD3	HUMAN	NP_859050.1	beta isoform of regulatory subunit A, protein p...	471	e-133	266/605	387/605
		MOUSE	NP_058587.1	alpha isoform of regulatory subunit A, protein ...	467	e-132	263/597	377/597
		FLY	FBgn0053297	CG33297	452	e-127	273/598	369/598
		WORM	CE30997	locus:paa-1 Protein phosphatase 2A status:Confir...	423	e-118	240/597	368/597
		POMBE	SPAP8A3.09c	protein phosphotase regulatory subunit	501	e-142	269/598	397/598
YAL019W	FUN30	HUMAN	NP_064544.1	hypothetical protein DKFZp762K2015 [Homo sapiens]	435	e-121	241/556	352/556
		MOUSE	XP_132597.2	SWI/SNF-related, matrix-associated actin-depend...	434	e-121	242/556	350/556
		FLY	FBgn0032157	CG5899	362	e-100	209/545	326/545
		WORM	CE34059	helicase status:Partially_confirmed TN:CAA88960...	417	e-116	229/544	339/544
		POMBE	SPCC1235.05c	DEAD/DEAH box helicase	581	e-166	306/576	410/576
YAL040C	CLN3	HUMAN	NP_477097.1	cyclin E2 isoform 1; G1/S-specific cyclin E2 [H...	35	0.15	32/142	66/142
		MOUSE	XP_132481.3	similar to G2/mitotic-specific cyclin B1 [Mus m...	36	0.073	33/148	63/148
		FLY	FBgn0000405	CycB: Cyclin B	44	2.00E-04	33/137	66/137
		WORM	CE23835	locus:cyb-2.2 cyclin status:Confirmed TR:Q9BLB5...	50	4.00E-06	50/208	86/208
		POMBE	SPBC19F5.01c	cyclin	72	3.00E-13	44/148	72/148
YAR002W	NUP60	HUMAN	NP_055023.1	dentin sialophosphoprotein preproprotein; denti...	60	3.00E-09	91/436	183/436
		MOUSE	NP_034210.1	dentin sialophosphoprotein [Mus musculus]	49	1.00E-05	86/470	181/470
		FLY	FBgn0036203	CG6004	69	5.00E-12	113/532	196/532
		WORM	CE08376	locus:dao-5 status:Confirmed TR:Q9XVS4 protein_...	52	1.00E-06	58/267	103/267
		POMBE	SPCC285.13c	hypothetical protein	79	2.00E-15	106/437	172/437
YAR015W	ADE1	HUMAN	NP_006443.1	phosphoribosylaminoimidazole carboxylase; phosp...	55	6.00E-08	60/257	104/257
		MOUSE	NP_080215.1	phosphoribosylaminoimidazole carboxylase [Mus m...	52	6.00E-07	58/257	104/257
		FLY	FBgn0032437	CG17024	53	2.00E-07	54/250	105/250
		WORM	CE03863	saicar synthetaseVair carboxlyase status:Confir...	46	3.00E-05	62/266	108/266
		POMBE	SPBC409.10	phosphoribosylamidoimidazole-succinocarboxamid...	359	e-100	180/308	233/308
YBL031W	SHE1	HUMAN	NP_116259.1	chromosome 6 open reading frame 111; SR rich pr...	33	0.37	40/185	76/185
		MOUSE	NP_941033.1	mKIAA1064 protein [Mus musculus]	34	0.14	30/117	52/117
		FLY	FBgn0010575	sbb: scribbler	36	0.035	25/89	39/89
		WORM	CE15943	status:Partially_confirmed TR:O45438 protein_id:...	34	0.11	27/105	46/105
		POMBE	SPAC29B12.01	SNF2 family	37	0.005	23/85	39/85
YBL058W	SHP1	HUMAN	NP_057227.2	p47 protein isoform a [Homo sapiens]	142	6.00E-34	90/298	152/298
		MOUSE	NP_938085.1	p47 protein; NSFL1 (p97) cofactor (p47) homolog...	133	2.00E-31	88/300	152/300
		FLY	FBgn0033179	p47	114	1.00E-25	111/439	184/439
		WORM	CE27555	status:Partially_confirmed TR:Q9N2W5 protein_i...	85	8.00E-17	71/229	108/229
		POMBE	SPAC343.09	UBX domain	153	3.00E-38	124/399	180/399
YBR009C	HHF1	HUMAN	NP_003539.1	histone 2, H4; H4 histone, family 2; histone IV...	150	2.00E-37	74/82	79/82
		MOUSE	NP_783587.1	histone 1, H4i [Mus musculus]	150	2.00E-37	74/82	79/82
		FLY	FBgn0013981	His4r: Histone H4 replacement	150	2.00E-37	74/82	79/82
		WORM	CE03252	locus:his-14 histone H4 status:Predicted TR:O026...	147	7.00E-37	73/82	78/82
		POMBE	SPBC8D2.03c	histone H4	149	6.00E-38	74/82	79/82
YBR026C	ETR1	HUMAN	NP_057095.1	nuclear receptor-binding factor 1; homolog of y...	185	5.00E-47	120/332	177/332
		MOUSE	NP_079573.1	nuclear receptor-binding factor 1 [Mus musculus]	182	3.00E-46	123/335	177/335
		FLY	FBgn0033883	CG16935	175	3.00E-44	107/327	181/327
		WORM	CE16575	Zinc-binding dehydrogenases status:Partially_con...	169	2.00E-42	105/292	167/292
		POMBE	SPAC26F1.04c	zinc binding dehydrogenase (predicted)	173	4.00E-44	109/327	178/327
YBR073W	RDH54	HUMAN	NP_036547.1	RAD54 homolog B isoform 1; RAD54, S. cerevisiae...	431	e-121	296/818	417/818
		MOUSE	NP_033041.2	RAD54 like [Mus musculus]	369	e-102	232/591	340/591
		FLY	FBgn0002989	okr: okra	376	e-104	222/584	332/584
		WORM	CE25143	locus:rad-54 SNF2 and others N-terminal domain s...	389	e-108	236/606	348/606
		POMBE	SPAC15A10.03c	DEAD/DEAH box helicase	384	e-107	223/581	328/581
YBR098W	MMS4	HUMAN	NP_004450.3	fetal Alzheimer antigen isoform 2; bromodomain ...	41	0.003	84/376	137/376
		MOUSE	NP_958757.1	Similar to hypothetical protein from BCRA2 regi...	37	0.053	42/153	61/153
		FLY	FBgn0037836	CG14692	43	5.00E-04	81/384	150/384
		WORM	CE35814	status:Partially_confirmed TN:AAQ91890 protein_id...	38	0.015	115/589	225/589
		POMBE	SPAC4A8.16c	translation initiation factor	37	0.006	39/175	77/175
YBR099C	YBR099C	HUMAN	NP_006092.1	kinetochore associated 2; highly expressed in c...	29	0.91	16/52	24/52
		MOUSE	NP_780377.1	PTK7 protein tyrosine kinase 7 [Mus musculus]	27	2.3	14/43	21/43
		FLY	***** No hits found *****					
		WORM	CE08243	status:Predicted TR:O16531 protein_id:AAB66028.1	29	0.5	18/58	28/58
		POMBE	SPBC1709.07	3-keto sterol reductase (predicted)	27	0.97	15/39	21/39
YBR107C	IML3	HUMAN	NP_001384.1	extracellular matrix protein 2 [Homo sapiens]	30	2	22/85	38/85
		MOUSE	NP_033114.2	RNA polymerase 1-4; RNA polymerase 1-4 (194 kDa...	28	6.4	14/54	29/54
		FLY	FBgn0051108	CG31108	31	0.53	34/142	60/142
		WORM	CE21945	locus:str-154 7TM chemoreceptor, str family s...	32	0.36	15/71	33/71
		POMBE	SPCC364.02c	involved in response to stress (PMID 11751918...	26	5.3	21/67	32/67
YBR112C	CYC8	HUMAN	NP_066963.1	ubiquitously transcribed tetratricopeptide repe...	176	1.00E-43	134/402	207/402
		MOUSE	NP_033509.1	ubiquitously transcribed tetratricopeptide repe...	177	2.00E-44	134/405	207/405
		FLY	FBgn0032207	CG5640	145	8.00E-35	97/288	151/288
		WORM	CE01878	glucose repression mediator protein status:Parti...	114	2.00E-25	100/362	162/362
		POMBE	SPBC23E6.09	TPR repeat protein	452	e-128	235/450	300/450
YBR113W	YBR113W	HUMAN	***** No hits found *****					
		MOUSE	***** No hits found *****					
		FLY	***** No hits found *****					
		WORM	***** No hits found *****					
		POMBE	***** No hits found *****					
YBR156C	SLI15	HUMAN	NP_066554.2	neurofilament, heavy polypeptide 200kDa; Neurof...	45	2.00E-04	79/383	138/383
		MOUSE	XP_357100.1	similar to dentin sialophosphoprotein prepropro...	41	0.002	98/424	166/424
		FLY	FBgn0037836	CG14692	53	7.00E-07	76/356	138/356
		WORM	CE34251	locus:unc-89 status:Partially_confirmed TR:Q7Z1...	53	4.00E-07	109/524	181/524
		POMBE	SPBC336.15	localization centromere	57	1.00E-08	33/84	50/84
YBR231C	SWC5	HUMAN	NP_006315.1	craniofacial development protein 1; phosphoprot...	62	5.00E-10	44/149	71/149
		MOUSE	NP_035931.1	craniofacial development protein 1 [Mus musculus]	71	7.00E-13	58/220	97/220

		FLY	FBgn0033046	CG14470	31	0.73	23/67	33/67
		WORM	CE27158	Yeast YB81 protein like status:Confirmed TR:P90...	40	0.001	19/54	31/54
		POMBE	SPCC576.13	chromatin remodeling complex	55	8.00E-09	23/53	37/53
YBR277C	YBR277C	HUMAN	XP_047325.4	Tho2 [Homo sapiens]	28	1.7	29/104	48/104
		MOUSE	NP_666750.1	olfactory receptor 373; GA_x6K02T2NUPS-231686-2...	30	0.4	21/73	37/73
		FLY	FBgn0032690	CG10333	27	4	23/80	31/80
		WORM	CE16484	status:Predicted TR:O45844 protein_id:CAB03439.1	31	0.15	25/88	39/88
		POMBE	SPCC417.05c	Chs Four Homologue (pers. comm. Henar Montero...	25	2.4	28-Nov	13/27
YCL016C	DCC1	HUMAN	NP_076999.1	hypothetical protein MGC5528 [Homo sapiens]	65	8.00E-11	91/376	148/376
		MOUSE	NP_898912.1	RIKEN cDNA 2600005O03 [Mus musculus]	40	0.002	21/60	30/60
		FLY	FBgn0034495	CG11788	56	4.00E-08	86/381	159/381
		WORM	CE34336	status:Partially_confirmed TR:O44992 protein_id:...	39	0.004	31/139	60/139
		POMBE	SPAC31A2.15c	replication factor C complex (predicted)	44	3.00E-05	27/84	44/84
YCL061C	MRC1	HUMAN	NP_060041.1	hypothetical protein LOC55580 [Homo sapiens]	44	9.00E-04	81/482	180/482
		MOUSE	XP_125851.4	similar to Early endosome antigen 1 (Endosome-a...	37	0.088	24/93	45/93
		FLY	FBgn0052580	CG32580	43	9.00E-04	67/285	112/285
		WORM	CE22326	reverse transcriptase status:Predicted TR:Q9N4...	42	0.002	38/176	65/176
		POMBE	SPCC737.08	midasin (predicted)	38	0.008	33/142	63/142
YCR065W	HCM1	HUMAN	NP_075555.1	forkhead box L2; Blepharophimosis, epicanthus i...	99	1.00E-20	48/93	61/93
		MOUSE	NP_032266.1	forkhead box J1; HNF-3/forkhead homolog 4 [Mus ...	99	9.00E-21	48/88	58/88
		FLY	FBgn0039937	CG11152	99	5.00E-21	45/89	61/89
		WORM	CE08367	locus:fkh-10 nuclear factor 5 like status:Predic...	105	8.00E-23	50/127	74/127
		POMBE	SPBC4C3.12	fork head domain	107	5.00E-24	50/88	64/88
YCR066W	RAD18	HUMAN	NP_064550.2	postreplication repair protein hRAD18p; RAD18, ...	95	1.00E-19	105/498	199/498
		MOUSE	NP_067360.1	RAD18 homolog; post-replication repair protein ...	89	8.00E-18	86/369	149/369
		FLY	FBgn0052369	CG32369	47	2.00E-05	17/39	25/39
		WORM	CE00312	Zinc finger, C3HC4 type (RING finger) status:Par...	52	6.00E-07	18/38	23/38
		POMBE	SPBC1734.06	zinc finger protein	148	2.00E-36	110/401	171/401
YCR067C	SED4	HUMAN	XP_379905.1	similar to intestinal membrane mucin MUC17 [Hom...	60	1.00E-08	130/662	226/662
		MOUSE	NP_034210.1	dentin sialophosphoprotein [Mus musculus]	61	4.00E-09	78/318	135/318
		FLY	FBgn0051901	CG31901	73	8.00E-13	92/406	159/406
		WORM	CE19949	status:Partially_confirmed TR:Q9N5K0 protein_id...	63	7.00E-10	94/430	162/430
		POMBE	SPBC215.13	glycoprotein (predicted)	82	5.00E-16	94/362	158/362
YCR081W	SRB8	HUMAN	NP_005111.1	trinucleotide repeat containing 11 (THR-associa...	47	1.00E-04	66/300	114/300
		MOUSE	NP_067496.1	trinucleotide repeat containing 11 (THR-associa...	37	0.089	40/186	69/186
		FLY	FBgn0001324	kto: kohtalo	38	0.049	48/224	91/224
		WORM	CE08724	locus:sym-1 Drosophila chaoptin protein like sta...	36	0.16	31/108	52/108
		POMBE	SPAC688.08	RNA polymerase II holoenzyme component (PMID 1...	70	3.00E-12	126/585	217/585
YCR095C	YCR095C	HUMAN	NP_919226.1	similar to C630007C17Rik protein [Homo sapiens]	33	0.24	30/121	55/121
		MOUSE	XP_354617.1	similar to myosin heavy chain 2b [Mus musculus]	31	1	20/78	38/78
		FLY	FBgn0031251	CG4213	32	0.55	23/104	51/104
		WORM	CE21711	status:Partially_confirmed TR:Q8MNX1 protein_id:...	30	2.4	30/114	50/114
		POMBE	SPBC17A3.03c	phosphoprotein phosphatase activity (predicted)	42	9.00E-05	47/250	91/250
YDL025C	YDL025C	HUMAN	NP_001265.1	CHK1 checkpoint homolog; CHK1 (checkpoint, S.po...	122	6.00E-28	85/300	140/300
		MOUSE	NP_031717.2	checkpoint kinase 1 homolog; rad27 homolog (S.p...	116	5.00E-26	83/300	138/300
		FLY	FBgn0011598	grp: grapes	107	2.00E-23	77/270	133/270
		WORM	CE20636	protein kinase status:Partially_confirmed TR:Q9UA...	110	2.00E-24	74/228	115/228
		POMBE	SPCC1020.10	serine/threonine protein kinase (predicted)	302	7.00E-83	170/360	217/360
YDL059C	RAD59	HUMAN	NP_002870.2	RAD52 homolog isoform alpha; recombination prot...	57	8.00E-09	40/105	55/105
		MOUSE	NP_035366.1	RAD52 homolog; RAD52 homolog, (S. cerevisiae) [...	58	4.00E-09	41/105	55/105
		FLY	FBgn0014141	cher: cheerio	31	0.66	31/109	45/109
		WORM	CE17155	status:Partially_confirmed TR:O44985 protein_id:...	30	0.76	Dec-41	20/37
		POMBE	SPBC119.14	DNA binding	57	2.00E-09	45/146	64/146
YDL074C	BRE1	HUMAN	NP_062538.5	ring finger protein 20; homolog of S. cerevisia...	116	5.00E-26	111/523	216/523
		MOUSE	NP_892044.1	ring finger protein 20 [Mus musculus]	119	8.00E-27	106/524	222/524
		FLY	FBgn0035637	CG10542	122	7.00E-28	128/587	255/587
		WORM	CE00283	locus:tag-84 status:Partially_confirmed SW:YNC4_...	89	6.00E-18	116/566	231/566
		POMBE	SPCC970.10c	zinc finger protein	161	3.00E-40	143/563	246/563
YDL082W	RPL13A	HUMAN	NP_000968.2	ribosomal protein L13; 60S ribosomal protein L1...	159	2.00E-39	90/194	124/194
		MOUSE	XP_207093.2	similar to 60S RIBOSOMAL PROTEIN L13 [Mus muscu...	160	3.00E-40	90/190	122/190
		FLY	FBgn0011272	RpL13: Ribosomal protein L13	140	6.00E-34	86/191	115/191
		WORM	CE08526	locus:rpl-13 ribosomal protein L13 status:Confi...	155	9.00E-39	91/193	118/193
		POMBE	SPAC664.05	60S ribosomal protein L13	161	6.00E-41	90/192	121/192
YDL096C	YDL096C	HUMAN	XP_379904.1	similar to mucin 11 [Homo sapiens]	27	2	16/56	27/56
		MOUSE	XP_355038.1	similar to hypothetical protein [Mus musculus]	25	8.8	23-Nov	16/22
		FLY	FBgn0004892	sob: sister of odd and bowl	28	0.7	18/61	27/61
		WORM	CE22016	status:Predicted TR:Q966B6 protein_id:AAK72311.1	28	1.1	15/42	19/42
		POMBE	SPAPB24D3.09	ABC transporter family	31	0.027	18/52	27/52
YDL101C	DUN1	HUMAN	NP_009125.1	protein kinase CHK2 isoform a; checkpoint-like ...	212	6.00E-55	141/439	202/439
		MOUSE	NP_057890.1	CHK2 checkpoint homolog; protein kinase Chk2; C...	220	2.00E-57	126/331	173/331
		FLY	FBgn0019686	lok: loki	197	1.00E-50	146/478	230/478
		WORM	CE25046	locus:cmk-1 ser/thr protein kinase status:Confi...	188	5.00E-48	107/285	163/285
		POMBE	SPCC18B5.11c	serine/threonine protein kinase	187	3.00E-48	136/464	212/464
YDL116W	NUP84	HUMAN	NP_065134.1	nuclear pore complex protein [Homo sapiens]	84	5.00E-16	128/614	256/614
		MOUSE	NP_598771.1	nucleoporin 107 [Mus musculus]	82	1.00E-15	127/615	251/615
		FLY	FBgn0027868	Nup170	96	7.00E-20	137/577	240/577
		WORM	CE18113	similar to PES-10 status:Partially_confirmed TR:...	33	0.5	42/195	77/195
		POMBE	SPBC428.01c	nucleoporin (PMID 11309419)	165	2.00E-41	173/714	318/714
YDL117W	CYK3	HUMAN	NP_597677.2	delangin isoform A; Nipped-B-like [Homo sapiens]	43	9.00E-04	55/265	97/265
		MOUSE	NP_950177.1	FCH and double SH3 domains 2; cDNA sequence BC0...	41	0.003	42/130	57/130
		FLY	FBgn0050147	Hil: Hillarin	44	5.00E-04	40/167	68/167
		WORM	CE21930	status:Partially_confirmed TR:Q9TXZ0 protein_id...	47	3.00E-05	48/156	70/156
		POMBE	SPAC9G1.06c	src (SH3) homology domain	174	4.00E-44	130/508	225/508
YDL155W	CLB3	HUMAN	NP_004692.1	cyclin B2 [Homo sapiens]	203	2.00E-52	105/262	171/262
		MOUSE	NP_031656.1	cyclin B2 [Mus musculus]	201	5.00E-52	106/270	173/270
		FLY	FBgn0015625	CycB3	150	2.00E-36	81/228	131/228
		WORM	CE27776	locus:cyb-3 status:Confirmed TR:Q95ZP8 protein_...	135	3.00E-32	80/254	141/254
		POMBE	SPBC582.03	cyclin	251	2.00E-67	122/266	183/266
YDL156W	YDL156W	HUMAN	NP_079184.1	hypothetical protein FLJ12973 [Homo sapiens]	94	3.00E-19	117/527	203/527
		MOUSE	NP_082395.2	damage specific DNA binding protein 2 [Mus musc...	50	4.00E-06	49/216	93/216
		FLY	FBgn0051033		47	2.00E-05	48/196	79/196
		WORM	CE11860	locus:rba-1 retinablastoma-binding protein RBAP...	44	2.00E-04	31/117	57/117
		POMBE	SPBC1A4.07c	WD repeat protein	47	4.00E-06	33/103	50/103

YDL162C	YDL162C	HUMAN	NP_115763.2	protein kinase, lysine deficient 4; putative pr...	32	0.066	16/40	23/40
		MOUSE	NP_694538.1	early B-cell factor 4; Olf-1/EBF-like-4/132 tra...	29	0.64	24/75	29/75
		FLY	FBgn0033258	CG8712	28	0.78	22/76	32/76
		WORM	CE31297	status:Partially_confirmed TR:Q8MQE5 protein_id...	33	0.037	24/87	41/87
		POMBE	SPCC645.06c	localization cell division site (pers. comm. ...	30	0.099	13/38	18/38
YDL204W	RTN2	HUMAN	NP_005610.1	reticulon 2 isoform A; NSP-like protein 1; Neur...	56	5.00E-08	43/169	84/169
		MOUSE	NP_038676.1	reticulon 2; NSP-like 1 [Mus musculus]	56	4.00E-08	44/177	85/177
		FLY	FBgn0053113	Rtnl1	56	4.00E-08	47/179	82/179
		WORM	CE35914	status:Confirmed TN:CAE48546 protein_id:CAE48546.1	47	2.00E-05	42/190	81/190
		POMBE	SPBC1711.05	chaperone activity (predicted)	40	5.00E-04	38/182	79/182
YDR004W	RAD57	HUMAN	NP_598193.2	RAD51-like 1 isoform 3; RecA-like protein; reco...	93	5.00E-19	75/237	118/237
		MOUSE	NP_033040.2	RAD51-like 1 [Mus musculus]	89	4.00E-18	73/238	115/238
		FLY	FBgn0003480	spn-B: spindle B	83	3.00E-16	57/174	91/174
		WORM	CE25285	locus:rad-51 status:Confirmed TN:CAE47473 prot...	81	1.00E-15	54/178	87/178
		POMBE	SPAC20H4.07	RecA family	135	8.00E-33	109/297	155/297
YDR014W	RAD61	HUMAN	NP_067002.1	hypothetical protein LOC57821 [Homo sapiens]	40	0.004	43/208	87/208
		MOUSE	XP_127654.4	similar to mKIAA0261 protein [Mus musculus]	35	0.14	18/54	30/54
		FLY	FBgn0030940	CG15040	39	0.012	46/239	97/239
		WORM	CE18346	status:Partially_confirmed TR:O45198 protein_id...	41	0.002	32/163	70/163
		POMBE	SPAC1F3.06c	involved in sporulation (required)	47	6.00E-06	114/596	230/596
YDR076W	RAD55	HUMAN	NP_002869.2	RAD51-like 3 isoform 1; recombination repair pr...	48	1.00E-05	44/174	77/174
		MOUSE	NP_033040.2	RAD51-like 1 [Mus musculus]	47	3.00E-05	43/144	67/144
		FLY	FBgn0011700	Rad51: Rad51-like	38	0.012	37/126	56/126
		WORM	CE06677	status:Partially_confirmed TR:Q23388 protein_id...	37	0.022	36/122	55/122
		POMBE	SPAC3C7.03c	RecA family	43	6.00E-05	19/59	35/59
YDR156W	RPA14	HUMAN	NP_060496.2	phosphofurin acidic cluster sorting protein 1; ...	28	1.9	17/47	28/47
		MOUSE	XP_283545.2	phosphofurin acidic cluster sorting protein 1 [...	28	1.6	17/47	28/47
		FLY	FBgn0000630	f: forked	32	0.08	19/55	28/55
		WORM	CE00573	status:Confirmed TR:Q21196 protein_id:CAA82659.1	27	3	28-Dec	14/27
		POMBE	SPCC1259.01c	40S ribosomal protein...	29	0.18	16/49	26/49
YDR159W	SAC3	HUMAN	NP_003897.2	minichromosome maintenance protein 3 associated...	117	4.00E-26	109/431	188/431
		MOUSE	NP_062307.1	minichromosome maintenance protein 3 associated...	122	2.00E-27	101/386	170/386
		FLY	FBgn0028974	xmas-2	112	1.00E-24	86/318	132/318
		WORM	CE04432	status:Partially_confirmed TR:Q19643 protein_id...	92	2.00E-18	83/334	141/334
		POMBE	SPCC576.05	SAC3/GANp family	233	1.00E-61	167/559	273/559
YDR171W	HSP42	HUMAN	NP_060959.1	ash1 (absent, small, or homeotic)-like [Homo sa...	31	1.6	28/101	38/101
		MOUSE	NP_076087.1	ARID class DNA binding protein; developmentally...	32	0.81	20/60	27/60
		FLY	FBgn0051151	CG31151	31	1.3	Nov-48	23/44
		WORM	CE05891	locus:pqn-39 status:Partially_confirmed TR:Q2057...	30	1.9	18/58	28/58
		POMBE	SPBC3E7.02c	heat shock protein	54	3.00E-08	34/112	62/112
YDR176W	NGG1	HUMAN	NP_006345.1	transcriptional adaptor 3-like isoform a [Homo ...	41	0.003	27/95	47/95
		MOUSE	NP_666273.1	Rho GTPase activating protein 24 [Mus musculus]	41	0.002	51/230	97/230
		FLY	FBgn0052955	CG32955	42	0.002	44/172	78/172
		WORM	CE24463	status:Partially_confirmed TR:Q95XW8 protein_i...	40	0.005	51/220	92/220
		POMBE	SPBC28F2.10c	kinesin-associated protein (EMBL AF351206)	134	3.00E-32	134/528	229/528
YDR191W	HST4	HUMAN	NP_036370.2	sirtuin 1; sir2-like 1; sirtuin type 1; SIR2alp...	59	4.00E-09	70/269	113/269
		MOUSE	NP_062786.1	sirtuin 1 ((silent mating type information regu...	59	6.00E-09	70/269	113/269
		FLY	FBgn0024291	Sir2	66	3.00E-11	71/271	111/271
		WORM	CE06302	locus:sir-2.1 Yeast regulatory protein SIR2 like...	58	8.00E-09	65/269	104/269
		POMBE	SPAC1783.04c	Sir2p family	214	2.00E-56	119/284	169/284
YDR194C	MSS116	HUMAN	NP_006764.3	DEAD (Asp-Glu-Ala-Asp) box polypeptide 18; Myc-...	206	3.00E-53	152/478	253/478
		MOUSE	NP_080136.2	DEAD (Asp-Glu-Ala-Asp) box polypeptide 18 [Mus ...	214	1.00E-55	156/479	259/479
		FLY	FBgn0025140	pit: pitchoune	197	2.00E-50	137/428	233/428
		WORM	CE26853	helicase status:Confirmed TR:O61815 protein_id:A...	183	2.00E-46	138/434	231/434
		POMBE	SPBC691.04	DEAD/DEAH box helicase	222	1.00E-58	139/395	223/395
YDR200C	VPS64	HUMAN	NP_055596.2	Rb1-inducible coiled coil protein 1 [Homo sapiens]	43	6.00E-04	31/142	66/142
		MOUSE	XP_127132.3	similar to mKIAA0284 protein [Mus musculus]	42	8.00E-04	22/57	34/57
		FLY	FBgn0046704	Liprin-alpha	46	5.00E-05	29/77	45/77
		WORM	CE33676	status:Predicted TR:Q8ITW1 protein_id:AAN73857.2	55	8.00E-08	42/137	66/137
		POMBE	SPBC3H7.13	FHA domain (phosphopeptide binding)	76	1.00E-14	55/137	76/137
YDR217C	RAD9	HUMAN	NP_055023.1	dentin sialophosphoprotein preproprotein; denti...	57	1.00E-07	89/587	211/587
		MOUSE	XP_129509.3	RIKEN cDNA 4933409L06 [Mus musculus]	47	1.00E-04	89/454	179/454
		FLY	FBgn0036203	CG6004	64	4.00E-10	135/789	274/789
		WORM	CE26070	status:Partially_confirmed TR:Q9N435 protein_id...	53	1.00E-06	142/831	320/831
		POMBE	SPBC342.05	BRCT domain	57	1.00E-08	41/139	60/139
YDR226W	ADK1	HUMAN	NP_001616.1	adenylate kinase 2 isoform a; adenylate kinase,...	261	3.00E-70	126/217	160/217
		MOUSE	NP_058591.2	adenylate kinase 2 [Mus musculus]	263	8.00E-71	127/217	160/217
		FLY	FBgn0022708	Adk2: Adenylate kinase-2	257	4.00E-69	126/209	163/209
		WORM	CE29198	Adenylate kinase status:Confirmed SW:P34346 prot...	242	1.00E-64	116/212	153/212
		POMBE	SPAC4G9.03	adenylate kinase (PMID 8496185)	311	3.00E-86	150/215	174/215
YDR231C	COX20	HUMAN	NP_001266.1	chromogranin A; parathyroid secretory protein 1...	28	3.3	18/54	30/54
		MOUSE	NP_079558.1	myocyte enhancer factor 2C [Mus musculus]	30	0.96	15/46	21/46
		FLY	FBgn0002354	l(3)87Df: lethal (3) 87Df	33	0.08	16/55	26/55
		WORM	CE31668	status:Partially_confirmed TR:Q9N4C3 protein_i...	31	0.46	14/44	23/44
		POMBE	SPAC20G8.03	MFS myo-inositol transporter	27	1.8	16/59	29/59
YDR254W	CHL4	HUMAN	NP_060516.2	angiogenic factor VG5Q; vasculogenesis gene on ...	31	2.1	22/64	32/64
		MOUSE	XP_109575.3	similar to membralin splice variant 2 [Mus musc...	32	0.8	18/62	29/62
		FLY	FBgn0038153	CG14376	31	1.6	19/55	24/55
		WORM	CE02109	diphthine synthase status:Partially_confirmed TR...	31	1.4	24/76	35/76
		POMBE	SPBP22H7.09c	involved in chromosome segregation (predicted)	49	1.00E-06	69/380	156/380
YDR279W	RNH202	HUMAN	NP_001291.3	core promoter element binding protein; B-cell d...	32	0.66	21/67	32/67
		MOUSE	XP_357986.1	similar to mucin 16 [Mus musculus]	28	6.2	42/189	63/189
		FLY	FBgn0029656	CG10793	30	2.6	25/87	41/87
		WORM	CE04713	locus:sur-5 acetyl-coenzyme A synthetase status:...	32	0.35	18/53	27/53
		POMBE	SPCC550.09	pex24 family	28	1.3	18/66	30/66
YDR289C	RTT103	HUMAN	NP_067038.1	chromosome 20 open reading frame 77 [Homo sapiens]	77	3.00E-14	61/256	114/256
		MOUSE	NP_081710.1	RIKEN cDNA 2610304G08 [Mus musculus]	76	3.00E-14	61/256	114/256
		FLY	FBgn0032688	CG15160	58	8.00E-09	50/207	93/207
		WORM	CE00040	status:Partially_confirmed SW:YKK4_CAEEL protein...	44	1.00E-04	48/242	105/242
		POMBE	SPBC337.03	conserved eukaryotic protein	94	4.00E-20	65/251	122/251
YDR290W	SWS1	HUMAN	XP_372507.1	similar to Olfactory receptor 11H4 [Homo sapiens]	32	0.065	23/84	41/84
		MOUSE	NP_081847.2	purinergic receptor P2Y12 [Mus musculus]	32	0.072	17/61	30/61
		FLY	FBgn0031676	CG14040	30	0.18	20/71	35/71

		WORM	CE30684	7 transmembrane receptor (rhodopsin family) stat...	29	0.49	22/79	32/79
		POMBE	SPBC21D10.09c	zinc finger protein	27	0.52	13/34	19/34
YDR318W	MCM21	HUMAN	NP_006256.1	RAD21 homolog; protein involved in DNA double-s...	37	0.029	30/119	51/119
		MOUSE	NP_033035.2	RAD21 homolog [Mus musculus]	34	0.16	30/119	50/119
		FLY	FBgn0037800	CG3996	39	0.005	32/123	64/123
		WORM	CE35814	status:Partially_confirmed TN:AAQ91890 protein_id...	31	0.83	42/224	85/224
		POMBE	SPAC25B8.14	involved in genome stability (required)	36	0.007	24/89	49/89
YDR334W	SWR1	HUMAN	NP_006653.1	Snf2-related CBP activator protein [Homo sapiens]	433	e-121	202/317	251/317
		MOUSE	XP_355376.1	RIKEN cDNA 4632409L19 [Mus musculus]	291	2.00E-78	150/322	205/322
		FLY	FBgn0020306	dom: domino	429	e-120	206/382	281/382
		WORM	CE34109	status:Partially_confirmed TR:Q9BHL1 protein_...	408	e-113	193/319	240/319
		POMBE	SPAC11E3.01c	SNF2 family	836	0	444/796	555/796
YDR350C	TCM10	HUMAN	NP_064592.1	chromosome 9 open reading frame 102 [Homo sapiens]	31	2.3	24/71	35/71
		MOUSE	NP_666231.1	RIKEN cDNA 9130404D14 [Mus musculus]	31	1.9	35/153	69/153
		FLY	FBgn0038037	Cyp9f2	31	2.3	18/46	24/46
		WORM	CE20177	status:Predicted TR:O18164 protein_id:CAA21727.1	32	0.69	30/131	58/131
		POMBE	SPBC646.02	complexed with Cdc5p (PMID 11884590)	31	0.4	24/81	40/81
YDR359C	VID21	HUMAN	NP_056224.1	E1A binding protein p400; p400 SWI2/SNF2-relate...	46	1.00E-04	26/66	38/66
		MOUSE	NP_083613.1	Domino [Mus musculus]	45	2.00E-04	24/66	39/66
		FLY	FBgn0020306	dom: domino	45	2.00E-04	24/69	38/69
		WORM	CE34109	status:Partially_confirmed TR:Q9BHL1 protein_...	52	1.00E-06	31/80	45/80
		POMBE	SPCC1795.08c	Myb family	96	2.00E-20	68/202	105/202
YDR363W	ESC2	HUMAN	NP_055023.1	dentin sialophosphoprotein preproprotein; denti...	38	0.013	34/134	51/134
		MOUSE	NP_034210.1	dentin sialophosphoprotein [Mus musculus]	38	0.014	33/134	50/134
		FLY	FBgn0052793	CG32793	33	0.33	29/122	47/122
		WORM	CE23874	status:Partially_confirmed TR:Q9U3A8 protein_id...	36	0.034	37/148	61/148
		POMBE	SPBC1711.05	chaperone activity (predicted)	35	0.015	34/188	61/188
YDR363W-A	SEM1	HUMAN		***** No hits found *****				
		MOUSE		***** No hits found *****				
		FLY		***** No hits found *****				
		WORM	CE04133	status:Partially_confirmed TR:P91122 protein_id...	27	1.4	19/62	28/62
		POMBE		***** No hits found *****				
YDR369C	XRS2	HUMAN	NP_060041.1	hypothetical protein LOC55580 [Homo sapiens]	41	0.003	98/499	188/499
		MOUSE	NP_796353.1	Rho GTPase-activating protein; GAB-associated C...	40	0.008	26/96	44/96
		FLY	FBgn0037836	CG14692	45	1.00E-04	118/559	204/559
		WORM	CE09105	status:Predicted TR:P91192 protein_id:AAB42226.1	41	0.003	61/276	114/276
		POMBE	SPAC140.02	GAR family	40	0.002	41/217	91/217
YDR378C	LSM6	HUMAN	NP_009011.1	Sm protein F [Homo sapiens]	56	5.00E-09	31/73	41/73
		MOUSE	XP_134104.1	RIKEN cDNA 2410088K19 [Mus musculus]	55	7.00E-09	31/72	40/72
		FLY	FBgn0034564	CG9344	51	2.00E-07	27/73	40/73
		WORM	CE22886	locus:lsm-6 U6 small nuclear RNA-associated S...	54	2.00E-08	31/69	38/69
		POMBE	SPAC2F3.17c	small nuclear ribonucleoprotein (snRNP)	54	5.00E-09	29/73	41/73
YDR386W	MUS81	HUMAN	NP_079404.2	MUS81 endonuclease homolog [Homo sapiens]	92	1.00E-18	91/317	151/317
		MOUSE	NP_082153.2	MUS81 endonuclease [Mus musculus]	93	6.00E-19	79/279	129/279
		FLY	FBgn0040347	mus81	112	5.00E-25	89/296	151/296
		WORM	CE08680	status:Partially_confirmed TR:P91153 protein_i...	76	6.00E-14	69/289	124/289
		POMBE	SPCC4G3.05c	endodeoxyribonuclease RUS activity (PMID 117...	183	7.00E-47	161/602	270/602
YDR408C	ADE8	HUMAN	NP_000810.1	phosphoribosylglycinamide formyltransferase, ph...	84	7.00E-17	65/197	103/197
		MOUSE	NP_034386.1	phosphoribosylglycinamide formyltransferase [Mu...	87	5.00E-18	64/197	102/197
		FLY	FBgn0000053	ade3: adenosine 3	92	2.00E-19	67/202	104/202
		WORM	CE28304	GARSVAIRSVGART status:Partially_confirmed TR:Q...	82	2.00E-16	63/213	108/213
		POMBE	SPCC569.08c	glycinamide ribonucleotide transformylase...	160	1.00E-40	87/211	138/211
YDR417C	YDR417C	HUMAN	NP_037521.1	NPC1 (Niemann-Pick disease, type C1, gene)-like...	27	2.4	20/94	35/94
		MOUSE	NP_997603.1	widely-interspaced zinc finger motifs isoform 1...	30	0.42	18/54	25/54
		FLY	FBgn0030702	CG9056	27	2	21/66	28/66
		WORM	CE18434	status:Partially_confirmed TR:O62502 protein_id:...	28	0.79	21/59	27/59
		POMBE	SPCC1235.06	involved in meiosis (predicted)	28	0.41	20/71	32/71
YDR431W	YDR431W	HUMAN		***** No hits found *****				
		MOUSE	NP_001001500.	RIKEN cDNA 9830163H01 gene [Mus musculus]	28	1.4	29-Sep	17/28
		FLY		***** No hits found *****				
		WORM	CE31997	locus:str-38 7TM receptor status:Partially_confi...	25	9.4	18-Aug	18-Nov
		POMBE	SPAC17G8.04c	protein farnesyltransferase (beta subunit) (...	26	0.76	28-Nov	15/27
YDR440W	DOT1	HUMAN	NP_115871.1	DOT1-like, histone H3 methyltransferase; histon...	111	1.00E-24	84/297	139/297
		MOUSE	NP_955354.1	histone H3 methyltransferase DOT1; histone meth...	112	5.00E-25	84/297	140/297
		FLY	FBgn0037444	CG10272	85	1.00E-16	70/285	124/285
		WORM	CE06555	status:Predicted TR:Q23200 protein_id:CAA93538.1	88	1.00E-17	59/201	100/201
		POMBE	SPBC16D10.05	a-1,3-glucan synthase	30	0.84	22/89	42/89
YDR532C	YDR532C	HUMAN	NP_002883.2	retinoblastoma-binding protein 1 isoform I; ret...	50	3.00E-06	61/273	111/273
		MOUSE	NP_064322.1	polyamine modulated factor 1 binding protein 1;...	53	4.00E-07	59/275	124/275
		FLY	FBgn0024242	Dys: dystrophin	39	0.004	61/314	128/314
		WORM	CE33068	status:Partially_confirmed TR:Q8MQ60 protein_...	54	2.00E-07	73/299	135/299
		POMBE	SPAC1486.04c	coiled-coil (PMID 10660053)	48	2.00E-06	67/362	151/362
YEL003W	GIM4	HUMAN	NP_036526.2	prefoldin 2 [Homo sapiens]	78	2.00E-15	39/100	61/100
		MOUSE	NP_035200.2	prefoldin 2 [Mus musculus]	77	2.00E-15	39/100	61/100
		FLY	FBgn0010741	l(3)01239	66	5.00E-12	38/101	55/101
		WORM	CE23815	status:Confirmed SW:Q9N5M2 protein_id:AAF39891.1	51	1.00E-07	23/99	52/99
		POMBE	SPAC227.10	prefoldin (subunit 2) (predicted)	95	3.00E-21	45/104	69/104
YEL013W	VAC8	HUMAN	NP_775104.1	armadillo repeat containing 3 [Homo sapiens]	107	3.00E-23	107/390	182/390
		MOUSE	XP_130012.3	RIKEN cDNA 4921513G22 [Mus musculus]	100	2.00E-21	103/403	180/403
		FLY	FBgn0000117	arm: armadillo	66	5.00E-11	104/430	176/430
		WORM	CE20745	locus:ima-3 importin alpha, nuclear transport f...	62	8.00E-10	82/358	151/358
		POMBE	SPBC354.14c	armadillo repeat protein	631	0	325/510	406/510
YEL061C	CIN8	HUMAN	NP_004514.2	kinesin family member 11; Eg5; thyroid receptor...	254	2.00E-67	195/688	352/688
		MOUSE	NP_034745.1	kinesin family member 11; kinesin 11; kinesin-l...	259	8.00E-69	192/673	346/673
		FLY	FBgn0004378	Klp61F: Kinesin-like protein at 61F	232	9.00E-61	191/650	327/650
		WORM	CE09600	locus:bmk-1 kinesin-like protein status:Confirm...	240	3.00E-63	190/667	322/667
		POMBE	SPAC25G10.07	kinesin-like protein	268	3.00E-72	202/671	346/671
YER007W	PAC2	HUMAN	NP_003184.1	beta-tubulin cofactor E [Homo sapiens]	139	5.00E-33	143/538	248/538
		MOUSE	NP_848027.1	tubulin-specific chaperone e; progressive motor...	137	1.00E-32	137/535	253/535
		FLY	FBgn0033055	CG7861	96	5.00E-20	92/360	162/360
		WORM	CE18021	status:Partially_confirmed TR:Q20068 protein_id:...	98	8.00E-21	112/452	199/452
		POMBE	SPAC22H10.10	LRR domain	99	1.00E-21	97/377	178/377
YER016W	BIM1	HUMAN	NP_036457.1	microtubule-associated protein, RP/EB family, m...	123	2.00E-28	83/259	126/259

	MOUSE	NP_031922.1	microtubule-associated protein, RP/EB family, m...	125	4.00E-29	84/259	128/259
	FLY	FBgn0027066	Eb1	125	4.00E-29	84/279	132/279
	WORM	CE26217	status:Partially_confirmed TR:Q9GRZ1 protein_id...	103	2.00E-22	82/299	126/299
	POMBE	SPAC18G6.15	EB1 domain	145	7.00E-36	95/294	139/294
YER070W	RNR1	HUMAN	NP_001024.1	ribonucleoside-diphosphate reductase M1 chain; ...	1081	0	512/765	638/765
		MOUSE	NP_033129.2	ribonucleotide reductase M1 [Mus musculus]	1080	0	508/765	636/765
		FLY	FBgn0011703	RnrL: Ribonucleoside diphosphate reductase large subunit	1050	0	491/760	622/760
		WORM	CE00331	locus:rnr-1 Ribonucleoside-disphosphate reductas...	1065	0	517/774	626/774
		POMBE	SPAC1F7.05	ribonucleoside reductase	1177	0	557/758	662/758
YER095W	RAD51	HUMAN	NP_002866.2	RAD51 homolog protein isoform 1; RAD51, S.cerev...	434	e-122	210/316	254/316
		MOUSE	NP_035364.1	RAD51 homolog [Mus musculus]	432	e-121	209/316	253/316
		FLY	FBgn0011700	Rad51: Rad51-like	365	e-101	178/315	234/315
		WORM	CE25285	locus:rad-51 status:Confirmed TN:CAE47473 prot...	349	1.00E-96	163/321	237/321
		POMBE	SPAC644.14c	RecA family	476	e-135	232/325	276/325
YER116C	SLX8	HUMAN	NP_055683.3	ring finger protein 10 [Homo sapiens]	55	7.00E-08	25/77	41/77
		MOUSE	NP_057907.1	ring finger protein 10; RIE2 protein [Mus muscu...	55	6.00E-08	25/77	41/77
		FLY	FBgn0052581	CG32581	55	5.00E-08	46/162	74/162
		WORM	CE21607	Zinc finger, C3HC4 type (RING finger) status:Pa...	54	1.00E-07	28/89	41/89
		POMBE	SPBC3D6.11c	zinc finger protein	55	7.00E-09	53/206	86/206
YER156C	YER156C	HUMAN	NP_067653.1	MYG1 protein [Homo sapiens]	255	3.00E-68	140/341	206/341
		MOUSE	NP_068359.1	melanocyte prolifeating gene 1; melanocyte prol...	259	1.00E-69	140/341	209/341
		FLY	FBgn0037652	CG11980	209	2.00E-54	131/334	192/334
		WORM	CE18880	Yeast hypothetical protein YEY6 like status:Conf...	254	4.00E-68	137/334	207/334
		POMBE	SPAC694.04c	metal dependent hydrolase (predicted)	306	2.00E-84	156/324	221/324
YER161C	SPT2	HUMAN	NP_056467.2	chromosome 10 open reading frame 12 [Homo sapiens]	37	0.025	51/184	72/184
		MOUSE	NP_653108.2	RIKEN cDNA 1110039B18 [Mus musculus]	35	0.081	23/88	42/88
		FLY	FBgn0050069	CG30069	38	0.007	24/81	36/81
		WORM	CE15316	status:Partially_confirmed TR:P91570 protein_id:...	37	0.017	31/120	50/120
		POMBE	SPCC126.04c	hypothetical protein	32	0.15	21/61	30/61
YER173W	RAD24	HUMAN	NP_002864.1	RAD17 homolog isoform 1; Rad17-like protein; ce...	86	8.00E-17	84/304	139/304
		MOUSE	NP_035363.1	RAD17 homolog [Mus musculus]	80	3.00E-15	74/273	131/273
		FLY	FBgn0025808	Rad17	79	1.00E-14	90/379	154/379
		WORM	CE17738	locus:hpr-17 status:Confirmed TR:O62196 protein...	49	1.00E-05	66/295	121/295
		POMBE	SPAC14C4.13	involved in DNA damage checkpoint (PMID 8019...	77	9.00E-15	72/286	137/286
YFL013W-A	YFL013W-A	HUMAN	NP_665683.1	glutathione S-transferase A1; GST, class alpha,...	31	1	14/50	26/50
		MOUSE	NP_032705.1	nuclear receptor coactivator 3 [Mus musculus]	28	4.2	22/86	38/86
		FLY	FBgn0017448	CG2187	29	2.3	Nov-46	24/42
		WORM	CE23761	locus:ndx-5 status:Partially_confirmed TR:O6225...	31	0.7	14/32	20/32
		POMBE	***** No hits found *****					
YFL016C	MDJ1	HUMAN	NP_005138.2	DnaJ (Hsp40) homolog, subfamily A, member 3; tu...	134	2.00E-31	117/413	170/413
		MOUSE	NP_076135.2	DnaJ (Hsp40) homolog, subfamily A, member 3 [Mu...	137	2.00E-32	117/413	173/413
		FLY	FBgn0002174	l(2)tid: lethal (2) tumorous imaginal discs	137	1.00E-32	117/404	171/404
		WORM	CE27991	locus:dnj-10 status:Partially_confirmed TR:Q95Q...	140	1.00E-33	111/426	179/426
		POMBE	SPCC4G3.14	DNAJ domain protein	221	1.00E-58	153/526	235/526
YFR013W	IOC3	HUMAN	NP_115784.1	bromodomain adjacent to zinc finger domain, 1B;...	37	0.055	20/64	35/64
		MOUSE	NP_892044.1	ring finger protein 20 [Mus musculus]	36	0.08	33/124	60/124
		FLY	FBgn0032414	CG17211	32	1.1	21/71	34/71
		WORM	CE34251	locus:unc-89 status:Partially_confirmed TR:Q7Z1...	35	0.11	17/43	25/43
		POMBE	SPCC18B5.08c	isoleucine-tRNA ligase (predicted)	32	0.31	25/103	43/103
YFR046C	CNN1	HUMAN	NP_003557.1	early endosome antigen 1, 162kD; early endosome...	35	0.062	36/139	65/139
		MOUSE	NP_683727.1	FYVE and coiled-coil domain containing 1; mater...	34	0.15	32/128	58/128
		FLY	FBgn0039250	CG11120	36	0.038	43/179	76/179
		WORM	CE33394	locus:duo-1 Ubiquitin carboxyl-terminal hydrolas...	40	0.002	43/162	74/162
		POMBE	SPAC29E6.03c	involved in intracellular protein ...	32	0.16	41/204	79/204
YGL003C	CDH1	HUMAN	NP_057347.2	Fzr1 protein; fizzy-related protein; CDC20-like...	337	1.00E-92	199/519	287/519
		MOUSE	NP_062731.1	Fzr1 protein; fizzy-related protein; frizzy-rel...	337	1.00E-92	201/519	285/519
		FLY	FBgn0003200	rap: retina aberrant in pattern	340	1.00E-93	205/522	286/522
		WORM	CE01695	locus:fzr-1 CDC20 protein status:Partially_conf...	326	2.00E-89	156/326	218/326
		POMBE	SPAC144.13c	Cdk inhibitor	375	e-105	211/516	297/516
YGL058W	RAD6	HUMAN	NP_003327.2	ubiquitin-conjugating enzyme E2A isoform 1; ubi...	229	7.00E-61	104/149	128/149
		MOUSE	NP_062642.1	ubiquitin-conjugating enzyme E2A, RAD6 homolog;...	229	6.00E-61	104/149	128/149
		FLY	FBgn0004436	UbcD6: Ubiquitin conjugating enzyme	227	3.00E-60	103/149	129/149
		WORM	CE27822	locus:ubc-1 ubiquitin conjugating-protein status...	224	1.00E-59	100/149	128/149
		POMBE	SPAC18B11.07c	ubiquitin conjugating enzyme	251	3.00E-68	116/150	136/150
YGL060W	YBP2	HUMAN	XP_376786.1	similar to Ceruloplasmin precursor (Ferroxidase...	33	0.63	20/54	27/54
		MOUSE	NP_033050.1	retinoic acid receptor, alpha; RAR alpha 1 [Mus...	32	0.91	28/94	46/94
		FLY	FBgn0036461	CG10006	34	0.22	37/167	72/167
		WORM	CE31818	status:Confirmed SW:YNH4_CAEEL protein_id:CAD455...	32	1.3	42/182	72/182
		POMBE	SPCC162.08c	coiled-coil (predicted)	39	0.002	43/164	73/164
YGL066W	SGF73	HUMAN	XP_379911.1	similar to KIAA1218 protein [Homo sapiens]	55	2.00E-07	28/55	37/55
		MOUSE	XP_354666.1	similar to Hypothetical protein KIAA1218 [Mus m...	57	3.00E-08	43/132	61/132
		FLY	FBgn0000114	aret: arrest	35	0.18	27/98	42/98
		WORM	CE30940	status:Partially_confirmed TR:Q8MQ82 protein_i...	33	0.58	14/40	23/40
		POMBE	SPCC126.04c	hypothetical protein	97	8.00E-21	69/230	98/230
YGL071W	RCS1	HUMAN	NP_775322.1	nuclear factor of activated T-cells 5 isoform a...	40	0.004	55/227	87/227
		MOUSE	NP_666101.1	RIKEN cDNA E130014J05 gene [Mus musculus]	33	0.45	34/153	58/153
		FLY	FBgn0011236	ken: ken and barbie	37	0.037	35/115	51/115
		WORM	CE24328	locus:tbx-37 status:Predicted SW:TX37_CAEEL pr...	39	0.011	47/195	77/195
		POMBE	SPCC1235.01	glycoprotein (predicted)	33	0.093	50/235	89/235
YGL086W	MAD1	HUMAN	NP_003541.1	MAD1-like 1; MAD1 (mitotic arrest deficient, ye...	70	6.00E-12	67/293	131/293
		MOUSE	XP_354615.1	myosin, heavy polypeptide 1, skeletal muscle, a...	63	6.00E-10	56/241	112/241
		FLY	FBgn0005634	zip: zipper	64	3.00E-10	69/271	127/271
		WORM	CE21159	status:Partially_confirmed TR:Q22276 protein_i...	66	5.00E-11	69/279	131/279
		POMBE	SPBC3D6.04c	coiled-coil (predicted)	80	9.00E-16	79/329	133/329
YGL117W	YGL117W	HUMAN	NP_659455.2	hypothetical protein FLJ25416 [Homo sapiens]	30	1.3	26/99	40/99
		MOUSE	NP_598922.1	fucosyltransferase 10; putative fucosyltransfer...	32	0.5	49/189	80/189
		FLY	FBgn0052432	CG32432	29	2.3	17/69	30/69
		WORM	CE32528	status:Predicted TR:Q9NF26 protein_id:CAB60346.2	31	0.53	15/50	28/50
		POMBE	SPAC1093.01	PPR domains	29	0.53	26/134	56/134
YGL151W	NUT1	HUMAN	NP_004478.1	golgi autoantigen, golgin subfamily b, macrogol...	33	1.6	19/54	29/54
		MOUSE	NP_032542.1	leucine rich repeat protein 1, neuronal [Mus mu...	34	0.45	53/208	90/208
		FLY	FBgn0038058	CG5608	32	1.6	42/209	90/209
		WORM	CE28808	locus:sop-3 status:Confirmed TR:Q9N4G4 protei...	33	1.1	40/167	66/167

		POMBE	SPAP8A3.05	translation release factor (predicted)	31	1	42/193	82/193
YGL163C	RAD54	HUMAN	NP_003570.1	RAD54-like protein; RAD54 homolog [Homo sapiens]	575	e-164	301/616	401/616
		MOUSE	NP_033041.2	RAD54 like [Mus musculus]	572	e-163	301/616	398/616
		FLY	FBgn0002989	okr: okra	523	e-148	285/601	374/601
		WORM	CE25143	locus:rad-54 SNF2 and others N-terminal domain s...	551	e-157	303/657	393/657
		POMBE	SPAC15A10.03c	DEAD/DEAH box helicase	821	0	451/846	552/846
YGL234W	ADE5,7	HUMAN	NP_000810.1	phosphoribosylglycinamide formyltransferase, ph...	677	0	359/796	517/796
		MOUSE	NP_034386.1	phosphoribosylglycinamide formyltransferase [Mu...	688	0	366/795	510/795
		FLY	FBgn0000053	ade3: adenosine 3	525	e-149	300/765	457/765
		WORM	CE28304	GARSVAIRSVGART status:Partially_confirmed TR:Q...	518	e-147	318/811	473/811
		POMBE	SPBC405.01	phosphoribosylamine-glycine l...	875	0	450/796	569/796
YGL240W	DOC1	HUMAN	NP_055700.1	anaphase promoting complex subunit 10; anaphase...	101	5.00E-22	50/138	80/138
		MOUSE	NP_081180.1	anaphase-promoting complex subunit 10 [Mus musc...	103	1.00E-22	50/138	81/138
		FLY	FBgn0034231	CG11419	92	2.00E-19	47/140	80/140
		WORM	CE05640	locus:apc-10 Yeast hypothetical protein like st...	55	3.00E-08	33/121	55/121
		POMBE	SPBC1A4.01	anaphase-promoting complex (APC) (P...	107	2.00E-24	54/144	81/144
YGR014W	MSB2	HUMAN	NP_055023.1	dentin sialophosphoprotein preproprotein; denti...	34	0.82	53/301	92/301
		MOUSE	NP_997126.2	mucin 19; sublingual apomucin [Mus musculus]	38	0.048	54/297	88/297
		FLY	FBgn0051901	CG31901	44	8.00E-04	54/295	89/295
		WORM	CE25697	locus:lov-1 polycistic kidney disease protein 1 ...	40	0.008	56/294	88/294
		POMBE	SPAPB1E7.04c	glycosyl hydrolase family 18	50	1.00E-06	63/337	102/337
YGR027C	RPS25A	HUMAN	XP_376420.1	similar to 40S ribosomal protein S25 [Homo sapi...	75	6.00E-15	35/74	53/74
		MOUSE	XP_145089.2	similar to 40S ribosomal protein S25 [Mus muscu...	76	3.00E-15	35/74	53/74
		FLY	FBgn0010413	RpS25: Ribosomal protein S25	73	2.00E-14	33/77	54/77
		WORM	CE04691	locus:rps-25 ribosomal protein status:Confirmed ...	69	3.00E-13	30/74	51/74
		POMBE	SPBC3D6.15	40S ribosomal protein S25	100	5.00E-23	47/76	62/76
YGR058W	YGR058W	HUMAN	NP_037364.1	programmed cell death 6; apoptosis-linked gene ...	75	6.00E-14	45/166	81/166
		MOUSE	NP_035181.1	programmed cell death 6 [Mus musculus]	75	4.00E-14	45/166	81/166
		FLY	FBgn0033529	CG17765	70	1.00E-12	47/162	76/162
		WORM	CE12418	calcium binding protein status:Predicted TR:Q95Y...	62	5.00E-10	39/142	71/142
		POMBE	SPCC11E10.06c	RNA polymerase II (elongator subunit) (predicte...	33	0.066	23/74	35/74
YGR061C	ADE6	HUMAN	NP_036525.1	phosphoribosylformylglycinamidine synthase; FGA...	617	e-176	438/1295	642/1295
		MOUSE	XP_111232.3	similar to KIAA0361 [Mus musculus]	633	0	451/1319	652/1319
		FLY	FBgn0000052	ade2: adenosine 2	586	e-167	423/1311	641/1311
		WORM	CE17651	Phosphoribosylformylglycinamidine synthase statu...	551	e-157	422/1314	654/1314
		POMBE	SPAC6F12.10c	phosphoribosylformylglycinamidine synth...	1325	0	694/1279	877/1279
YGR063C	SPT4	HUMAN	NP_003159.1	suppressor of Ty 4 homolog 1 [Homo sapiens]	88	1.00E-18	43/99	58/99
		MOUSE	NP_033322.1	suppressor of Ty 4 homolog [Mus musculus]	88	1.00E-18	43/99	58/99
		FLY	FBgn0028683	spt4	75	5.00E-15	37/102	57/102
		WORM	CE19891	locus:spt-4 status:Confirmed TR:Q9TZ93 protein_i...	79	5.00E-16	35/97	53/97
		POMBE	SPBC21C3.16c	transcriptional regulator	80	4.00E-17	44/100	60/100
YGR064W	YGR064W	HUMAN	XP_372663.2	similar to Ribosomal protein S6 kinase I (S6K) ...	28	1.4	18/71	30/71
		MOUSE	NP_808352.1	hypothetical protein LOC232337 [Mus musculus]	26	5.9	14/48	21/48
		FLY	FBgn0035086	CG12851	28	0.85	19-Oct	13/18
		WORM	CE20631	locus:srh-78 7TM chemoreceptor, srh family status:...	29	0.59	15/43	22/43
		POMBE	SPAC4F10.12	sequence orphan	26	1.5	21/65	27/65
YGR071C	YGR071C	HUMAN	XP_376023.1	zinc finger, BED domain containing 4 [Homo sapi...	47	5.00E-05	49/226	91/226
		MOUSE	NP_852077.1	hypothetical protein LOC223773 [Mus musculus]	42	0.002	38/145	58/145
		FLY	FBgn0029808	CG4064	32	2	29/104	48/104
		WORM	CE19173	status:Partially_confirmed TR:Q9XWZ9 protein_id...	34	0.27	15/48	28/48
		POMBE	SPBC16H5.13	WD repeat protein	37	0.011	91/425	161/425
YGR078C	PAC10	HUMAN	NP_003363.1	von Hippel-Lindau binding protein 1; VHL bindin...	127	4.00E-30	77/185	111/185
		MOUSE	NP_035822.1	von Hippel-Lindau binding protein 1 [Mus musculus]	112	1.00E-25	68/157	95/157
		FLY	FBgn0037893	CG6719	113	8.00E-26	67/179	102/179
		WORM	CE13349	locus:vbp-1 Human VHL binding protein like statu...	103	7.00E-23	64/186	103/186
		POMBE	SPAC3H8.07c	prefoldin (subunit 3)	127	7.00E-31	77/181	109/181
YGR102C	YGR102C	HUMAN	XP_038291.5	hypothetical protein FLJ13456 [Homo sapiens]	33	0.11	31/114	51/114
		MOUSE	NP_076365.2	elongation protein 4 homolog [Mus musculus]	30	0.79	Dec-42	25/38
		FLY	FBgn0039863	CG1815	33	0.085	31/135	57/135
		WORM	CE16099	Thiolases status:Partially_confirmed TR:O45552 p...	31	0.29	24/99	45/99
		POMBE	SPBC691.02c	Rad50p interacting protein (predicted)	30	0.14	18/47	24/47
YGR118W	RPS23A	HUMAN	NP_001016.1	ribosomal protein S23; 40S ribosomal protein S2...	231	1.00E-61	111/142	128/142
		MOUSE	NP_077137.1	ribosomal protein S23 [Mus musculus]	231	8.00E-62	111/142	128/142
		FLY	FBgn0033912	RpS23	227	2.00E-60	109/142	128/142
		WORM	CE05747	locus:rps-23 ribosomal protein S23 status:Confir...	225	5.00E-60	105/142	126/142
		POMBE	SPAC23C11.02c	40S ribosomal protein S23	250	4.00E-68	121/142	134/142
YGR141W	VPS62	HUMAN	NP_003461.1	ubiquitin specific protease 7 (herpes virus-ass...	31	2.1	25/83	36/83
		MOUSE	NP_808358.1	hypothetical protein E330007A02 [Mus musculus]	31	1.4	17/53	22/53
		FLY	FBgn0052415	CG32415	51	2.00E-06	27/89	44/89
		WORM	CE27777	locus:nlp-33 status:Confirmed TR:Q95ZN4 protein_...	30	2.5	13/32	15/32
		POMBE	SPCC663.03	ABC transporter family	31	0.38	23/75	35/75
YGR148C	RPL24B	HUMAN	NP_000977.1	ribosomal protein L24; 60S ribosomal protein L2...	120	4.00E-28	59/101	75/101
		MOUSE	NP_077180.1	ribosomal protein L24 [Mus musculus]	120	3.00E-28	59/101	75/101
		FLY	FBgn0032518	RpL24	107	3.00E-24	51/101	70/101
		WORM	CE09047	locus:rpl-24.1 60S ribosomal protein L24 status...	77	3.00E-15	44/104	63/104
		POMBE	SPAC6G9.09c	60S ribosomal protein L24	150	7.00E-38	72/101	88/101
YGR153W	YGR153W	HUMAN	XP_371175.1	zinc finger protein 229 [Homo sapiens]	32	0.33	17/42	22/42
		MOUSE	NP_081209.1	RIKEN cDNA 1810015M01 [Mus musculus]	30	1.1	20/62	27/62
		FLY	FBgn0036994	CG5199	27	8.3	Oct-44	19/40
		WORM	CE14560	locus:app-1 aminopeptidase status:Partially_conf...	30	1.1	16/59	27/59
		POMBE	SPCC1450.12	involved in intracellular protein transport (pred...	27	1.5	Dec-37	18/33
YGR171C	MSM1	HUMAN	NP_612404.1	mitochondrial methionyl-tRNA synthetase [Homo s...	305	4.00E-83	196/544	272/544
		MOUSE	NP_780648.1	mitochondrial methionyl-tRNA synthetase [Mus mu...	295	4.00E-80	195/542	269/542
		FLY	FBgn0051322		276	2.00E-74	180/547	263/547
		WORM	CE34219	status:Confirmed TR:Q8WQA1 protein_id:CAD21672.2	246	2.00E-65	150/423	222/423
		POMBE	SPAC27E2.06c	methionine-tRNA ligase (predicted)	345	7.00E-96	211/545	294/545
YGR180C	RNR4	HUMAN	NP_001025.1	ribonucleotide reductase M2 polypeptide [Homo s...	317	8.00E-87	154/321	221/321
		MOUSE	NP_033130.1	ribonucleotide reductase M2 [Mus musculus]	321	4.00E-88	157/321	222/321
		FLY	FBgn0011704	RnrS: Ribonucleoside diphosphate reductase small subunit	306	1.00E-83	150/307	211/307
		WORM	CE00874	locus:mr-2 Ribonuclease-diphosphate reductase ...	294	4.00E-80	145/330	220/330
		POMBE	SPBC25D12.04	ribonucleotide reductase	356	2.00E-99	176/332	238/332
YGR184C	UBR1	HUMAN	NP_056070.1	ubiquitin ligase E3 alpha-II; likely ortholog o...	124	9.00E-28	193/940	372/940
		MOUSE	XP_358323.1	ubiquitin ligase E3 alpha-II [Mus musculus]	96	3.00E-19	138/626	255/626

		FLY	FBgn0030809	CG9086	97	1.00E-19	192/949	371/949
		WORM	CE08535	status:Partially_confirmed TR:P91133 protein_id...	84	7.00E-16	201/979	378/979
		POMBE	SPBC19C7.02	ubiquitin-protein ligase (E3)	223	1.00E-58	288/1346	527/1346
YGR188C	BUB1	HUMAN	NP_004327.1	BUB1 budding uninhibited by benzimidazoles 1 ho...	169	1.00E-41	115/371	190/371
		MOUSE	NP_033902.1	budding uninhibited by benzimidazoles 1 homolog...	159	8.00E-39	114/390	192/390
		FLY	FBgn0025458	Bub1	146	7.00E-35	139/595	252/595
		WORM	CE06251	locus:bub-1 Eukaryotic protein kinase domain sta...	112	9.00E-25	87/324	147/324
		POMBE	SPCC1322.12c	serine/threonine protein kinase	291	3.00E-79	288/1090	477/1090
YGR219W	YGR219W	HUMAN	NP_000733.1	cholinergic receptor, nicotinic, alpha polypept...	30	0.42	20/58	27/58
		MOUSE	XP_357051.1	similar to sperm protein SSP3111; similar to te...	27	1.8	15/71	33/71
		FLY	FBgn0027836	Dgp-1	26	4.5	Dec-56	25/52
		WORM	CE18610	status:Predicted TR:Q9XV83 protein_id:CAB04142.1	28	0.65	19/78	34/78
		POMBE	SPBC947.06c	transporter	25	2.2	Sep-40	21/36
YGR270W	YTA7	HUMAN	NP_054828.2	two AAA domain containing protein; PRO2000 prot...	468	e-131	333/1023	523/1023
		MOUSE	NP_081711.1	ATPase family, AAA domain containing 2 [Mus mus...	464	e-130	329/1015	522/1015
		FLY	FBgn0024923	TER94	224	3.00E-58	122/273	172/273
		WORM	CE20665	TAT-binding homolog like status:Partially_confi...	382	e-106	242/601	346/601
		POMBE	SPAC31G5.19	TAT-binding protein homolog	680	0	401/1000	600/1000
YGR285C	ZUO1	HUMAN	XP_379909.1	similar to M-phase phosphoprotein 11 [Homo sapi...	190	1.00E-48	108/267	161/267
		MOUSE	NP_033609.1	DnaJ (Hsp40) homolog, subfamily C, member 2; zu...	189	3.00E-48	111/295	169/295
		FLY	FBgn0037051	CG10565	166	2.00E-41	95/267	150/267
		WORM	CE10050	locus:dnj-11 DNA-binding protein status:Confirm...	159	2.00E-39	88/232	144/232
		POMBE	SPBC1778.01c	zuotin-like protein	279	6.00E-76	159/438	226/438
YHL006C	SHU1	HUMAN	NP_113626.1	nudix -type motif 12; nucleoside diphosphate li...	30	0.8	18/65	29/65
		MOUSE	NP_080773.1	nudix (nucleoside diphosphate linked moiety X)-...	29	0.9	21/74	32/74
		FLY	FBgn0052191	CG32191	26	7	14/41	21/41
		WORM	CE21229	status:Confirmed TR:Q9XTB4 protein_id:CAA22133.1	33	0.039	22/68	35/68
		POMBE	SPCC1827.05c	rrm RNA recognition motif	27	0.81	19/70	36/70
YHR001W-A	QCR10	HUMAN	***** No hits found *****					
		MOUSE	NP_079620.1	eukaryotic translation initiation factor 3, sub...	25	8.8	15/37	21/37
		FLY	FBgn0040345	CG3708	28	0.69	29-Nov	18/28
		WORM	CE09973	status:Confirmed TR:O76722 protein_id:AAC26928.1	28	0.64	13/36	22/36
		POMBE	SPBP4H10.08	ubiquinol-cytochrome-c reductase complex sub...	39	1.00E-04	18/48	26/48
YHR031C	RRM3	HUMAN	XP_371352.1	formin 2 [Homo sapiens]	33	0.95	33/121	53/121
		MOUSE	NP_766041.1	PIF1 homolog; DNA helicase-like protein; PIF1 h...	218	1.00E-56	130/318	198/318
		FLY	FBgn0031540	CG3238	207	2.00E-53	142/380	204/380
		WORM	CE30311	locus:pif-1 status:Confirmed TR:Q9BL90 protein_...	238	8.00E-63	166/498	244/498
		POMBE	SPBC887.14c	DNA helicase (5'-3') (PMID 12058079)	391	e-109	238/587	355/587
YHR064C	SSZ1	HUMAN	NP_006588.1	heat shock 70kDa protein 8 isoform 1; heat shoc...	216	3.00E-56	155/536	258/536
		MOUSE	NP_112442.2	heat shock protein 8; heat shock protein cognat...	216	2.00E-56	155/536	258/536
		FLY	FBgn0001230	Hsp68: Heat shock protein 68	226	2.00E-59	152/544	267/544
		WORM	CE08110	locus:hsp-70 heat shock protein 70 status:Partia...	218	6.00E-57	153/542	261/542
		POMBE	SPAC57A7.12	heat shock protein 70 family	363	e-101	207/532	313/532
YHR066W	SSF1	HUMAN	NP_064615.3	peter pan homolog; second-step splicing factor ...	172	6.00E-43	120/367	185/367
		MOUSE	NP_663585.1	peter pan homolog; second-step splicing factor ...	171	6.00E-43	118/367	189/367
		FLY	FBgn0010770	ppan: peter pan	149	2.00E-36	111/369	181/369
		WORM	CE18041	locus:lpd-6 status:Partially_confirmed TR:O44991...	135	4.00E-32	94/324	158/324
		POMBE	SPAC1B9.03c	RNA-binding protein	237	3.00E-63	139/372	211/372
YHR076W	PTC7	HUMAN	NP_644812.1	T-cell activation protein phosphatase 2C [Homo ...	118	6.00E-27	91/255	129/255
		MOUSE	NP_796216.2	T-cell activation protein phosphatase 2C [Mus m...	119	3.00E-27	91/255	129/255
		FLY	FBgn0029949	CG15035	110	2.00E-24	91/270	132/270
		WORM	CE16565	Protein phosphatase 2C (2 domains) status:Parti...	104	6.00E-23	100/316	154/316
		POMBE	SPAC1556.03	serine/threonine protein phosphatase (SMART) ...	104	2.00E-23	88/266	127/266
YHR087W	YHR087W	HUMAN	NP_001076.1	alpha-1-antichymotrypsin, precursor; alpha-1-an...	28	1.6	31-Oct	24/30
		MOUSE	NP_080574.4	intraflagellar transport 172 protein; wimple; s...	27	3	13/33	20/33
		FLY	FBgn0034240	MESR4: Misexpression suppressor of ras 4	29	0.41	20/67	32/67
		WORM	CE31148	status:Partially_confirmed TR:Q9BIB1 protein_id...	29	0.37	22/58	28/58
		POMBE	SPBC21C3.19	conserved fungal protein	58	3.00E-10	32/86	55/86
YHR092C	HXT4	HUMAN	NP_055395.2	solute carrier family 2, (facilitated glucose t...	139	4.00E-33	110/430	183/430
		MOUSE	NP_035531.2	solute carrier family 2 (facilitated glucose tr...	139	5.00E-33	127/478	191/478
		FLY	FBgn0025593	Glut1: Glucose transporter 1	132	5.00E-31	129/478	198/478
		WORM	CE33672	glucose transport protein status:Confirmed TR:Q2...	129	3.00E-30	107/354	159/354
		POMBE	SPCC1235.13	meiotic expression upregulated	361	e-100	185/491	263/491
YHR093W	AHT1	HUMAN	XP_373792.1	hypothetical protein XP_378775 [Homo sapiens]	27	5.9	14/40	18/40
		MOUSE	***** No hits found *****					
		FLY	***** No hits found *****					
		WORM	***** No hits found *****					
		POMBE	SPAC27D7.14c	TPR repeat protein	25	7.4	Nov-38	17/34
YHR133C	NSG1	HUMAN	NP_938150.1	insulin induced gene 1 isoform 2; INSIG-1 membr...	39	0.003	24/95	46/95
		MOUSE	NP_705746.1	insulin induced gene 1; INSIG-1 membrane protei...	40	0.001	31/134	62/134
		FLY	FBgn0004876	cdi: center divider	30	1.2	19/53	26/53
		WORM	CE06467	locus:srg-41 status:Partially_confirmed TR:Q2256...	30	1.3	28/89	45/89
		POMBE	SPBC15D4.07c	involved in autophagy (predicted)	28	1	1-Jan	19/31
YHR134W	WSS1	HUMAN	NP_004949.1	FK506 binding protein 12-rapamycin associated p...	29	3.9	22/74	34/74
		MOUSE	NP_064393.1	FK506 binding protein 12-rapamycin associated p...	29	3.3	22/74	34/74
		FLY	FBgn0033237	CG14766	30	1.4	16/46	26/46
		WORM	CE34061	Zinc finger, C3HC4 type (RING finger) status:Part...	30	1.2	25/98	50/98
		POMBE	SPCC1442.07c	ubiquitin family protein	58	1.00E-09	41/144	67/144
YHR154W	RTT107	HUMAN	NP_005145.2	ubiquitin specific protease 8 [Homo sapiens]	40	0.012	76/339	137/339
		MOUSE	NP_080666.1	UBX domain containing 2 [Mus musculus]	42	0.002	44/170	70/170
		FLY	FBgn0052133	CG32133	43	9.00E-04	30/111	55/111
		WORM	CE36292	titin status:Partially_confirmed TN:AAM29672 pr...	44	4.00E-04	86/458	160/458
		POMBE	SPBC582.05c	BRCT domain	96	2.00E-20	193/970	346/970
YHR167W	THP2	HUMAN	NP_663777.1	TNF receptor-associated factor 3 isoform 1; CD4...	37	0.018	28/141	68/141
		MOUSE	NP_032172.3	Golgi autoantigen, golgin subfamily a, 3 [Mus m...	41	8.00E-04	60/247	99/247
		FLY	FBgn0013756	Mtor: Megator	30	1	41/209	84/209
		WORM	CE09349	locus:unc-54 myosin heavy chain status:Partially...	38	0.006	42/211	93/211
		POMBE	SPBC9B6.10	chaperone activity	29	0.53	38/194	79/194
YHR191C	CTF8	HUMAN	NP_003283.1	translocated promoter region (to activated MET ...	30	0.35	32/116	51/116
		MOUSE	NP_694783.1	retinoic acid, EGF, and NGF upregulated; REN; r...	30	0.31	23/81	34/81
		FLY	FBgn0050324	CG30324	27	2.4	24/81	37/81
		WORM	CE06492	status:Partially_confirmed TR:Q22664 protein_id:...	30	0.25	15/52	32/52
		POMBE	SPAC12B10.13	conserved eukaryotic protein	31	0.058	17/44	24/44

YHR194W	MDM31	HUMAN	NP_002083.1	G-rich RNA sequence binding factor 1 [Homo sapi...	30	6.2	20/40	25/40
		MOUSE	NP_034695.1	inhibin beta-C; activin [Mus musculus]	30	3.1	20/71	41/71
		FLY	FBgn0033882	CG13343	31	2.2	15/30	19/30
		WORM	CE33837	status:Partially_confirmed TR:O45204 protein_id:...	38	0.016	54/231	97/231
		POMBE	SPAC3H1.04c	conserved fungal protein	373	e-104	200/497	295/497
YHR204W	MNL1	HUMAN	XP_376201.1	ER degradation enhancer, mannosidase alpha-like...	344	1.00E-94	201/495	293/495
		MOUSE	NP_619618.1	ER degradation enhancer, mannosidase alpha-like...	344	1.00E-94	202/495	294/495
		FLY	FBgn0032480	CG5682	283	2.00E-76	176/475	258/475
		WORM	CE33766	alpha-mannosidase status:Partially_confirmed TR...	311	1.00E-84	182/494	282/494
		POMBE	SPAC23A1.04c	glycosyl hydrolase family 47	344	2.00E-95	189/475	280/475
YIL009C-A	EST3	HUMAN	NP_150647.1	alpha-1A-adrenergic receptor isoform 4; adrener...	30	1.2	17/53	27/53
		MOUSE	NP_080255.2	microtubule associated serine/threonine kinase-...	36	0.014	21/84	39/84
		FLY	FBgn0023513	CG14803	32	0.25	17/57	32/57
		WORM	CE01698	status:Partially_confirmed SW:YS21_CAEEL protei...	31	0.37	18/53	28/53
		POMBE	SPAC6G10.12c	transcrption factor	28	0.51	21/72	28/72
YIL018W	RPL2B	HUMAN	NP_150644.1	ribosomal protein L8; 60S ribosomal protein L8 ...	368	e-102	173/254	207/254
		MOUSE	NP_036183.1	ribosomal protein L8 [Mus musculus]	368	e-102	173/254	207/254
		FLY	FBgn0024939	RpL8: Ribosomal protein L8	363	e-101	168/250	203/250
		WORM	CE18478	locus:rpl-2 Ribosomal Proteins L2 status:Confirm...	343	4.00E-95	159/250	193/250
		POMBE	SPAC1F7.13c	...	365	e-102	174/254	207/254
YIL052C	RPL34B	HUMAN	NP_296374.1	ribosomal protein L34; 60S ribosomal protein L3...	98	1.00E-21	49/96	64/96
		MOUSE	XP_357642.1	similar to 60S ribosomal protein L34 [Mus muscu...	98	9.00E-22	49/96	64/96
		FLY	FBgn0037686	CG9354	108	6.00E-25	54/94	67/94
		WORM	CE26911	locus:rpl-34 status:Confirmed TR:Q95X53 protein...	97	2.00E-21	50/94	61/94
		POMBE	SPAC23A1.08c	60S ribosomal protein L34	122	9.00E-30	59/94	71/94
YIL084C	SDS3	HUMAN	NP_680476.1	ubiquitin associated protein 2 isoform 3; AD-01...	36	0.032	32/129	53/129
		MOUSE	NP_848737.2	RIKEN cDNA 2400003N08 [Mus musculus]	33	0.23	20/108	46/108
		FLY	FBgn0031124	CG1379	34	0.13	24/95	47/95
		WORM	CE35838	status:Partially_confirmed TN:CAA99795 protein_i...	32	0.42	19/78	39/78
		POMBE	SPBC19C2.10	src (SH3) homology domain	30	0.54	19/50	26/50
YIL125W	KGD1	HUMAN	NP_002532.1	oxoglutarate (alpha-ketoglutarate) dehydrogenas...	831	0	456/984	621/984
		MOUSE	NP_035086.1	oxoglutarate dehydrogenase (lipoamide); alpha-k...	834	0	460/989	626/989
		FLY	FBgn0036682		858	0	474/1015	655/1015
		WORM	CE28486	2-oxoglutarate dehydrogenase status:Partially_c...	840	0	448/990	643/990
		POMBE	SPBC3H7.03c	2-oxoglutarate dehydrogenase (lipoamide) (e1 comp...	1226	0	602/1013	755/1013
YIL137C	YIL137C	HUMAN	NP_005566.1	leucyl/cystinyl aminopeptidase; insulin-regulat...	174	3.00E-43	180/687	304/687
		MOUSE	NP_032968.1	puromycin-sensitive aminopeptidase [Mus musculus]	170	3.00E-42	151/587	263/587
		FLY	FBgn0035226	Psa: Puromycin sensitive aminopeptidase	168	1.00E-41	150/589	260/589
		WORM	CE10790	locus:pam-1 status:Partially_confirmed TR:Q20627...	172	7.00E-43	161/680	285/680
		POMBE	SPBC1921.05	aminopeptidase	180	7.00E-46	160/584	270/584
YIR002C	MPH1	HUMAN	XP_048128.5	KIAA1596 [Homo sapiens]	222	1.00E-57	155/511	255/511
		MOUSE	XP_126996.3	RIKEN cDNA C730036B14 gene [Mus musculus]	251	2.00E-66	187/616	297/616
		FLY	FBgn0038889	CG7922	214	3.00E-55	170/612	279/612
		WORM	CE26887	RNA helicase status:Partially_confirmed TR:Q95QN...	62	1.00E-09	51/194	86/194
		POMBE	SPAC9.05	DEAD/DEAH box helicase	366	e-102	260/745	363/745
YIR004W	DJP1	HUMAN	NP_061854.1	DnaJ (Hsp40) homolog, subfamily C, member 10; J...	89	5.00E-18	46/91	62/91
		MOUSE	NP_077143.1	ER-resident protein ERdj5 [Mus musculus]	89	7.00E-18	46/91	61/91
		FLY	FBgn0038145	CG8863	84	2.00E-16	45/97	61/97
		WORM	CE16015	locus:dnj-12 DnaJ, prokaryotic heat shock prote...	83	3.00E-16	46/99	64/99
		POMBE	SPAC4H3.01	DNAJ domain protein	226	4.00E-60	141/429	231/429
YIR019C	MUC1	HUMAN	NP_060700.2	nucleoporin 133kDa [Homo sapiens]	32	3.2	34/139	52/139
		MOUSE	NP_035824.1	voltage-dependent anion channel 1 [Mus musculus]	33	1.2	35/148	49/148
		FLY	***** No hits found *****					
		WORM	CE21470	status:Predicted TR:Q9TYL3 protein_id:AAD12833.1	37	0.09	38/292	61/292
		POMBE	SPBC1289.15	glucoprotein (predicted)	102	4.00E-22	57/157	79/157
YJL006C	CTK2	HUMAN	NP_003849.2	cyclin K [Homo sapiens]	67	2.00E-11	49/178	86/178
		MOUSE	NP_033962.1	cyclin K [Mus musculus]	65	7.00E-11	48/178	85/178
		FLY	FBgn0025674	CycK: Cyclin K	53	3.00E-07	40/166	76/166
		WORM	CE10334	G1VS-specfic cyclin C like status:Predicted TR:...	45	4.00E-05	45/196	85/196
		POMBE	SPBC530.13	cyclin	90	3.00E-19	80/281	127/281
YJL007C	YJL007C	HUMAN	NP_851999.1	oxidation resistance 1 [Homo sapiens]	31	0.18	18/57	29/57
		MOUSE	NP_598664.2	spondin 2, extracellular matrix protein [Mus mu...	30	0.21	18/66	34/66
		FLY	FBgn0035807	CG7492	30	0.32	20/66	31/66
		WORM	CE25507	status:Partially_confirmed TR:Q9U210 protein_...	29	0.38	20/64	29/64
		POMBE	SPAC139.06	histone acetyltransferase (type B) (cat...	27	0.46	17/54	24/54
YJL030W	MAD2	HUMAN	NP_002349.1	MAD2-like 1; MAD2 (mitotic arrest deficient, ye...	154	5.00E-38	85/197	122/197
		MOUSE	NP_062372.2	MAD2 (mitotic arrest deficient, homolog)-like 1...	155	1.00E-38	84/194	120/194
		FLY	FBgn0035640	CG17498	136	8.00E-33	70/196	122/196
		WORM	CE26559	locus:mdf-2 status:Confirmed TR:Q9NGT3 prote...	142	1.00E-34	78/194	116/194
		POMBE	SPBC20F10.06	horma domain protein	191	7.00E-50	94/194	137/194
YJL047C	RTT101	HUMAN	NP_003582.2	cullin 2 [Homo sapiens]	50	9.00E-06	71/316	134/316
		MOUSE	NP_036172.1	cullin 1 [Mus musculus]	45	2.00E-04	72/318	127/318
		FLY	FBgn0015509	lin19: lin-19-like	49	9.00E-06	72/308	126/308
		WORM	CE36545	locus:cul-4 status:Partially_confirmed SW:Q1739...	49	8.00E-06	67/290	125/290
		POMBE	SPAC17G6.12	cullin 1	54	8.00E-08	54/231	107/231
YJL075C	APQ13	HUMAN	***** No hits found *****					
		MOUSE	NP_031911.1	solute carrier family 26 (sulfate transporter),...	26	6.3	14/30	18/30
		FLY	FBgn0039624	CG11833	25	10	25-Sep	16/24
		WORM	CE29360	status:Predicted TR:Q23135 protein_id:AAL02529.1	27	2.3	29-Dec	15/28
		POMBE	SPAC1834.05	glycosyl transferase family 22	25	4.4	13-Jul	13-Oct
YJL092W	HPR5	HUMAN	XP_047357.4	KIAA0342 gene product [Homo sapiens]	39	0.029	37/130	56/130
		MOUSE	NP_031954.1	MAP/microtubule affinity-regulating kinase 2; E...	36	0.16	30/126	52/126
		FLY	FBgn0051368	CG31368	36	0.15	21/55	35/55
		WORM	CE15746	locus:lmn-1 Intermediate filament proteins (2 doma...	35	0.22	35/150	64/150
		POMBE	SPAC4H3.05	DNA helicase	218	3.00E-57	161/493	256/493
YJL102W	MEF2	HUMAN	NP_115756.2	mitochondrial elongation factor G2 isoform 1; e...	380	e-105	269/813	400/813
		MOUSE	NP_796240.2	RIKEN cDNA A930009M04 gene [Mus musculus]	381	e-106	266/810	399/810
		FLY	FBgn0051159	CG31159	274	2.00E-73	234/786	359/786
		WORM	CE19822	Elongation factor Tu family (contains ATPVGTP ...	291	1.00E-78	241/801	374/801
		POMBE	SPBC660.10	involved in translational elongation (factor g)	380	e-106	269/788	410/788
YJL115W	ASF1	HUMAN	NP_054753.1	ASF1 anti-silencing function 1 homolog A; anti-...	197	9.00E-51	91/158	119/158
		MOUSE	NP_079817.1	ASF1 anti-silencing function 1 homolog A [Mus m...	199	2.00E-51	92/158	120/158
		FLY	FBgn0029094	asf1: anti-silencing factor 1	198	2.00E-51	91/154	116/154

		WORM	CE36095	anti-silencing protein status:Confirmed TN:CAA99...	167	4.00E-42	79/156	109/156
		POMBE	SPCC663.05c	chaperone activity	218	9.00E-58	109/173	135/173
YJL124C	LSM1	HUMAN	NP_055277.1	Lsm1 protein [Homo sapiens]	96	2.00E-20	53/117	80/117
		MOUSE	XP_357867.1	similar to Lsm1 protein [Mus musculus]	86	1.00E-17	48/109	74/109
		FLY	FBgn0034600	CG4279	96	1.00E-20	54/128	82/128
		WORM	CE05848	locus:lsm-1 Yeast J0714 like status:Partially_co...	74	5.00E-14	35/72	50/72
		POMBE	SPBC3D6.08c	small nuclear ribonucleoprotein (snRNP)	120	1.00E-28	58/133	92/133
YJL127C	SPT10	HUMAN	NP_060146.1	hypothetical protein FLJ20125 [Homo sapiens]	39	0.009	27/141	60/141
		MOUSE	NP_080526.1	RIKEN cDNA 4930429M06Rik [Mus musculus]	39	0.013	27/141	60/141
		FLY	FBgn0030940	CG15040	45	1.00E-04	50/255	93/255
		WORM	CE35745	locus:ifg-1 status:Partially_confirmed TN:CAE474...	39	0.008	45/205	86/205
		POMBE	SPAC21E11.04	L-azetidine-2-carboxylic acid acetyltransfer...	98	4.00E-21	46/117	72/117
YJL179W	PFD1	HUMAN	NP_002613.2	prefoldin 1; prefoldin subunit 1 [Homo sapiens]	37	0.002	17/57	34/57
		MOUSE	NP_080303.1	prefoldin 1 [Mus musculus]	39	6.00E-04	18/57	34/57
		FLY	FBgn0033661	CG13185	28	1.2	14/60	32/60
		WORM	CE33192	status:Partially_confirmed TR:Q86NB8 protein_id...	29	0.49	16/51	26/51
		POMBE	SPAC26H5.02c	AAA family ATPase	27	0.52	14/37	22/37
YJR008W	YJR008W	HUMAN	NP_057039.1	C21orf19-like protein; HCV NS5A-transactivated ...	193	1.00E-49	126/337	187/337
		MOUSE	NP_598532.1	RIKEN cDNA 0610016J10 [Mus musculus]	194	5.00E-50	127/337	187/337
		FLY	FBgn0038110	CG8031	205	3.00E-53	132/334	178/334
		WORM	CE30736	status:Confirmed SW:YC4P_CAEEL protein_id:AAM29...	190	1.00E-48	119/335	180/335
		POMBE	SPAC4H3.04c	conserved eukaryotic protein	218	1.00E-57	128/331	187/331
YJR032W	CPR7	HUMAN	NP_005029.1	peptidylprolyl isomerase D; cyclophilin 40; cyc...	165	4.00E-41	126/390	182/390
		MOUSE	NP_080628.1	peptidylprolyl isomerase D [Mus musculus]	179	2.00E-45	128/391	190/391
		FLY	FBgn0039581	Moca-cyp	140	1.00E-33	86/192	106/192
		WORM	CE03745	locus:cyp-9 cyclophilin related protein status:C...	155	4.00E-38	93/195	114/195
		POMBE	SPAC1B3.03c	cyclophilin	191	1.00E-49	137/390	192/390
YJR043C	POL32	HUMAN	NP_003971.1	microtubule-associated protein 7 [Homo sapiens]	39	0.004	23/88	48/88
		MOUSE	NP_598708.2	nuclear mitotic apparatus protein 1 [Mus musculus]	41	0.001	29/110	54/110
		FLY	FBgn0052662	CG32662	41	0.001	28/96	47/96
		WORM	CE29598	status:Partially_confirmed TR:Q21730 protein_id...	45	7.00E-05	60/285	105/285
		POMBE	SPBC31E1.05	RNA export mediator	42	9.00E-05	38/159	72/159
YJR047C	ANB1	HUMAN	NP_001961.1	eukaryotic translation initiation factor 5A; el...	210	4.00E-55	94/144	124/144
		MOUSE	NP_853613.1	eukaryotic translation initiation factor 5A [Mu...	210	3.00E-55	94/144	124/144
		FLY	FBgn0034967	eIF-5A	201	2.00E-52	93/152	121/152
		WORM	CE02249	locus:iff-2 initiation factor 5A status:Confirme...	188	8.00E-49	96/157	121/157
		POMBE	SPAC26H5.10c	translation initiation factor	241	3.00E-65	112/157	137/157
YJR053W	BFA1	HUMAN	XP_379932.1	similar to KIAA1549 protein [Homo sapiens]	30	3.6	19/55	26/55
		MOUSE	NP_859418.1	mucin 6, gastric; gastric mucin-like protein [M...	32	0.8	19/59	26/59
		FLY	FBgn0029772	CG15783	33	0.44	21/55	28/55
		WORM	CE02127	status:Predicted TR:Q17863 protein_id:CAA90539.1	35	0.076	55/285	105/285
		POMBE	SPAC222.10c	two-component GAP for GTPase spg1 (PMID 97423...	59	1.00E-09	51/209	88/209
YJR060W	CBF1	HUMAN	NP_006512.2	transcription factor binding to IGHM enhancer 3...	51	1.00E-06	31/93	52/93
		MOUSE	NP_766060.1	transcription factor E3 [Mus musculus]	51	1.00E-06	31/93	52/93
		FLY	FBgn0023094	cyc: cycle	44	1.00E-04	22/62	39/62
		WORM	CE33716	status:Confirmed TR:Q86MJ1 protein_id:AAO91678.1	49	5.00E-06	32/91	49/91
		POMBE	SPAC3F10.12c	DNA binding (predicted)	85	1.00E-17	43/106	68/106
YJR063W	RPA12	HUMAN	NP_740753.1	zinc ribbon domain containing, 1; transcription...	75	1.00E-14	44/119	60/119
		MOUSE	NP_075651.1	nuclear RNA polymerase I small specific subunit...	71	1.00E-13	40/114	57/114
		FLY	FBgn0038903	Rpl12	80	3.00E-16	43/117	61/117
		WORM	CE08185	DNA-directed RNA polymerase I like status:Parti...	60	2.00E-10	36/112	55/112
		POMBE	SPCC1259.03	DNA-directed RNA polymerase activity (PMID 1...	145	2.00E-36	69/125	90/125
YJR074W	MOG1	HUMAN	NP_057576.2	RAN guanine nucleotide release factor; homolog ...	66	2.00E-11	50/171	81/171
		MOUSE	NP_067304.1	RAN guanine nucleotide release factor [Mus musc...	68	4.00E-12	46/168	77/168
		FLY	FBgn0033046	CG14470	30	1.3	20/92	38/92
		WORM	CE24361	status:Partially_confirmed TR:Q9N3T0 protein_i...	32	0.17	26/91	42/91
		POMBE	SPCC1840.01c	GTPase (PMID 11290708)	83	2.00E-17	57/199	97/199
YJR135C	MCM22	HUMAN	NP_663777.1	TNF receptor-associated factor 3 isoform 1; CD4...	34	0.1	35/137	64/137
		MOUSE	NP_035812.2	utrophin [Mus musculus]	33	0.11	33/121	52/121
		FLY	FBgn0039680	CG1911	32	0.39	37/174	74/174
		WORM	CE31066	endosomal protein P162 like status:Confirmed TR:...	32	0.2	25/106	47/106
		POMBE	SPBC409.21	localization signal recognition particle (pre...	30	0.21	34/150	72/150
YJR144W	MGM101	HUMAN	NP_006411.1	ADP-ribosylation factor guanine nucleotide-exch...	30	1.7	16/65	29/65
		MOUSE	NP_034712.1	inter-alpha trypsin inhibitor, heavy chain 2 [M...	34	0.1	38/158	56/158
		FLY	FBgn0053207	pxb	34	0.095	18/41	25/41
		WORM	CE06138	locus:fmo-12 flavin-containing monoxygenase stat...	30	0.92	19/62	29/62
		POMBE	SPBC30D10.08	mitochondrial nucleoid protein	241	9.00E-65	113/193	146/193
YJR154W	YJR154W	HUMAN	XP_376821.1	similar to transcription elongation factor B po...	30	2.5	18/49	26/49
		MOUSE	NP_066302.1	ATP-binding cassette, sub-family B, member 11; ...	32	0.56	21/58	27/58
		FLY	FBgn0037819	CG14688	35	0.079	31/127	48/127
		WORM	CE24085	status:Partially_confirmed TR:Q9NAM7 protein_i...	35	0.069	24/93	39/93
		POMBE	SPBC21C3.20c	C2 domain	27	5	18/64	27/64
YKL006W	RPL14A	HUMAN	XP_056681.4	similar to ribosomal protein L14; 60S ribosomal...	83	7.00E-17	47/125	62/125
		MOUSE	NP_080250.1	ribosomal protein L14 [Mus musculus]	82	1.00E-16	48/125	62/125
		FLY	FBgn0017579	RpL14: Ribosomal protein L14	67	4.00E-12	37/115	54/115
		WORM	CE19677	locus:rpl-14 status:Confirmed TR:Q9XVE9 protein...	85	9.00E-18	50/125	65/125
		POMBE	SPAC1805.13	60S ribosomal protein L14	103	8.00E-24	57/126	74/126
YKL053W	YKL053W	HUMAN	NP_055560.1	family with sequence similarity 38, member A [H...	28	1.4	16/55	29/55
		MOUSE	XP_134537.3	RIKEN cDNA 2310061F22 [Mus musculus]	30	0.25	16/55	30/55
		FLY	***** No hits found *****					
		WORM	***** No hits found *****					
		POMBE	SPAC18G6.05c	HEAT repeat	23	7.9	25-Oct	15/24
YKL055C	OAR1	HUMAN	NP_056325.2	DKFZP566O084 protein [Homo sapiens]	73	2.00E-13	68/263	111/263
		MOUSE	NP_663403.1	similar to human DKFZp566O084 protein [Mus musc...	73	2.00E-13	67/265	113/265
		FLY	FBgn0029648	CG3603	73	2.00E-13	66/267	111/267
		WORM	CE19130	locus:dhs-11 AlcoholVother dehydrogenases, sh...	79	2.00E-15	71/267	117/267
		POMBE	SPAC3G9.02	3-oxoacyl-[acyl carrier protein] reductase activit...	84	3.00E-17	70/228	106/228
YKL057C	NUP120	HUMAN	NP_055269.1	sestrin 1; p53 regulated PA26 nuclear protein [...	32	1.8	25/85	40/85
		MOUSE	NP_033510.1	tetratricopeptide repeat protein [Mus musculus]	33	0.92	37/157	73/157
		FLY	FBgn0034058	CG8315	34	0.38	22/66	34/66
		WORM	CE33429	status:Partially_confirmed TR:O17122 protein_id:A...	37	0.067	37/162	64/162
		POMBE	SPBC3B9.16c	nucleoporin	44	1.00E-04	74/368	145/368
YKL074C	MUD2	HUMAN	NP_009210.1	U2 small nuclear ribonucleoprotein auxiliary fa...	34	0.29	14/42	25/42

		MOUSE	XP_124040.2	similar to U2AF65 protein [Mus musculus]	36	0.065	14/42	26/42
		FLY	FBgn0005411	U2af50: U2 small nuclear riboprotein auxiliary factor 50	38	0.016	23/86	41/86
		WORM	CE30403	locus:uaf-1 status:Confirmed TR:Q8MXS2 protein...	33	0.26	13/42	24/42
		POMBE	SPBC146.07	U2AF large subunit (U2AF-59)	44	7.00E-05	16/44	29/44
YKL113C	RAD27	HUMAN	NP_004102.1	flap structure-specific endonuclease 1; maturat...	405	e-113	207/352	258/352
		MOUSE	NP_032025.2	flap structure specific endonuclease 1 [Mus mus...	405	e-113	208/352	260/352
		FLY	FBgn0025832	Fen1: Flap endonuclease 1	389	e-108	198/383	265/383
		WORM	CE22109	locus:crn-1 endonuclease status:Confirmed TR:Q9...	378	e-105	195/369	254/369
		POMBE	SPAC3G6.06c	FEN-1 endonuclease	433	e-122	213/359	272/359
YKL217W	JEN1	HUMAN	NP_689991.1	hypothetical protein MGC33302 [Homo sapiens]	45	2.00E-04	45/171	72/171
		MOUSE	NP_795976.1	integral membrane transport protein UST1R [Mus ...	40	0.003	78/384	150/384
		FLY	FBgn0032879	CG9317	48	1.00E-05	82/396	142/396
		WORM	CE10512	status:Partially_confirmed TR:O44130 protein_id...	41	0.002	36/141	60/141
		POMBE	SPAPB1E7.08c	membrane transporter	40	7.00E-04	107/521	195/521
YKL221W	MCH2	HUMAN	NP_061063.2	solute carrier family 16, member 10; T-type ami...	69	7.00E-12	81/385	140/385
		MOUSE	NP_033223.1	solute carrier family 16, member 2; monocarboxy...	66	4.00E-11	83/406	149/406
		FLY	FBgn0035173	CG13907	53	3.00E-07	46/222	83/222
		WORM	CE32237	status:Predicted TR:Q966D6 protein_id:AAK68412.2	53	3.00E-07	34/136	54/136
		POMBE	SPCC18.02	MFS amine transporter	38	0.002	22/108	50/108
YKR024C	DBP7	HUMAN	NP_073616.6	DEAD (Asp-Glu-Ala-Asp) box polypeptide 31 isofo...	290	3.00E-78	198/598	312/598
		MOUSE	XP_355323.1	similar to DEAD (Asp-Glu-Ala-Asp) box polypepti...	291	1.00E-78	203/627	323/627
		FLY	FBgn0027602	CG8611	264	2.00E-70	188/578	290/578
		WORM	CE26853	helicase status:Confirmed TR:O61815 protein_id:A...	170	3.00E-42	128/415	209/415
		POMBE	SPBC21H7.04	DEAD/DEAH box helicase	447	e-126	293/767	427/767
YKR082W	NUP133	HUMAN	NP_060041.1	hypothetical protein LOC55580 [Homo sapiens]	37	0.065	29/125	62/125
		MOUSE	XP_135197.2	expressed sequence AI462446 [Mus musculus]	33	0.79	29/108	45/108
		FLY	FBgn0052580	CG32580	36	0.15	24/63	33/63
		WORM	CE25227	status:Partially_confirmed TR:Q9N569 protein_i...	33	0.63	32/135	63/135
		POMBE	SPAC1805.04	nucleoporin (PMID 11564755)	157	1.00E-38	227/1094	458/1094
YKR087C	OMA1	HUMAN	NP_660286.1	metalloprotease related protein 1 [Homo sapiens]	124	6.00E-29	80/300	145/300
		MOUSE	NP_080185.1	RIKEN cDNA 2010001O09 [Mus musculus]	124	7.00E-29	82/296	145/296
		FLY	FBgn0036153	CG7573	31	0.77	14/41	24/41
		WORM	CE34628	status:Partially_confirmed TR:P91220 protein_id:...	28	5.7	Nov-39	20/35
		POMBE	SPAP14E8.04	metallo peptidase	216	2.00E-57	122/308	179/308
YKR091W	SRL3	HUMAN	NP_570899.1	angiomotin like 1; junction-enriched and associ...	32	0.13	17/62	28/62
		MOUSE	NP_075825.2	bromodomain containing 3; bromodomain-containin...	32	0.14	33/144	55/144
		FLY	FBgn0037804	CG11870	35	0.02	30/97	48/97
		WORM	CE29914	status:Partially_confirmed TR:Q22860 protein...	34	0.031	25/82	42/82
		POMBE	SPBC13E7.03c	SAM domain (sterile alpha motif)	28	0.37	17/50	22/50
YKR092C	SRP40	HUMAN	NP_004732.1	nucleolar and coiled-body phosphoprotein 1; nuc...	69	8.00E-12	39/94	57/94
		MOUSE	***** No hits found *****					
		FLY	FBgn0037137	Nopp140	62	4.00E-10	33/77	44/77
		WORM	CE08376	locus:dao-5 status:Confirmed TR:Q9XVS4 protein_...	54	1.00E-07	30/81	42/81
		POMBE	SPBC1711.05	chaperone activity (predicted)	53	6.00E-08	33/71	42/71
YKR093W	PTR2	HUMAN	NP_663623.1	solute carrier family 15, member 4; peptide-his...	134	1.00E-31	126/530	215/530
		MOUSE	NP_598656.1	solute carrier family 15, member 4; peptide-his...	131	1.00E-30	124/516	210/516
		FLY	FBgn0037730	CG9444	113	3.00E-25	112/463	196/463
		WORM	CE11268	locus:opt-3 oligopeptide transporter status:Conf...	99	6.00E-21	90/377	156/377
		POMBE	SPBC13A2.04c	PTR family peptide transporter	478	e-136	241/495	315/495
YKR097W	PCK1	HUMAN	NP_061313.1	transporter 2, ATP-binding cassette, sub-family...	33	0.52	27/105	46/105
		MOUSE	XP_146397.1	similar to hypothetical protein [Mus musculus]	33	0.58	44/166	62/166
		FLY	FBgn0053300	CG33300	30	4.6	24/94	40/94
		WORM	CE33321	locus:asp-2 status:Confirmed TR:Q86NE0 protein_...	33	0.47	27/98	43/98
		POMBE	SPBC359.05	transporter activity	31	0.35	27/88	41/88
YLL002W	RTT109	HUMAN	NP_036580.2	signal transducer and activator of transcriptio...	30	4.4	19/69	33/69
		MOUSE	NP_780397.2	RIKEN cDNA 2900024D24 [Mus musculus]	30	3.7	19/55	26/55
		FLY	FBgn0032269	CG7363	30	3.4	57/267	100/267
		WORM	CE09053	status:Predicted TR:O16193 protein_id:AAG24023.1	30	1.8	15/36	20/36
		POMBE	SPBC342.06c	involved in DNA repair (predicted)	76	7.00E-15	69/258	110/258
YLL005C	SPO75	HUMAN	XP_041116.3	chromosome 14 open reading frame 171 [Homo sapi...	42	0.001	39/164	64/164
		MOUSE	NP_659043.1	cDNA sequence BC014795; hypothetical protein MG...	39	0.011	34/176	73/176
		FLY	FBgn0033259	CG11210	41	0.003	53/322	113/322
		WORM	CE33084	locus:srh-102 G-protein coupled receptor, srh f...	42	0.001	37/136	60/136
		POMBE	SPAC24H6.13	DUF221	160	5.00E-40	107/396	187/396
YLL028W	TPO1	HUMAN	NP_872344.2	hypothetical protein MGC29671 [Homo sapiens]	35	0.15	33/162	63/162
		MOUSE	XP_126365.1	RIKEN cDNA 9830002I17 [Mus musculus]	35	0.097	33/162	64/162
		FLY	FBgn0028468	rtet: tetracycline resistance	39	0.006	40/140	56/140
		WORM	CE34241	status:Predicted TR:Q7Z118 protein_id:AAP68960.1	35	0.078	28/154	57/154
		POMBE	SPBC530.15c	unknown specificity	332	1.00E-91	174/470	258/470
YLL049W	YLL049W	HUMAN	NP_062826.2	methyltransferase like 3; putative methyltransf...	32	0.23	16/41	25/41
		MOUSE	NP_034394.1	nuclear receptor subfamily 6, group A, member 1...	30	0.75	23/82	40/82
		FLY	FBgn0025582	Int6: Int6 homologue	29	1.6	22/93	40/93
		WORM	CE01471	locus:zyg-11 Leucine Rich Repeat (2 copies) sta...	36	0.009	27/90	45/90
		POMBE	SPAC343.13	glutamyl-tRNA amidotransferase (predicted)	29	0.38	14/54	26/54
YLR006C	SSK1	HUMAN	NP_005044.1	UV excision repair protein RAD23 homolog A; RAD...	37	0.064	54/234	90/234
		MOUSE	NP_033036.2	RAD23a homolog [Mus musculus]	35	0.21	52/223	88/223
		FLY	FBgn0037836	CG14692	35	0.11	25/70	37/70
		WORM	CE20072	status:Partially_confirmed TR:Q9XUP9 protein_id:...	33	0.63	38/170	70/170
		POMBE	SPBC887.10	mitotic catastrophe suppressor	177	4.00E-45	90/167	118/167
YLR032W	RAD5	HUMAN	NP_620636.1	SWI/SNF-related matrix-associated actin-depende...	263	6.00E-70	179/562	289/562
		MOUSE	NP_033236.1	SWI/SNF related, matrix associated, actin depen...	250	4.00E-66	172/568	287/568
		FLY	FBgn0002542	lds: lodestar	216	5.00E-56	182/674	301/674
		WORM	CE11083	helicase status:Partially_confirmed TR:O17550 p...	119	9.00E-27	101/372	156/372
		POMBE	SPAC13G6.01c	zinc finger protein	490	e-139	346/1034	524/1034
YLR058C	SHM2	HUMAN	NP_004160.3	serine hydroxymethyltransferase 1 (soluble) iso...	520	e-148	250/465	339/465
		MOUSE	NP_082506.1	serine hydroxymethyl transferase 2 (mitochondri...	512	e-145	245/454	335/454
		FLY	FBgn0029823	CG3011	504	e-143	244/463	335/463
		WORM	CE29661	locus:mel-32 status:Confirmed SW:P50432 prote...	520	e-148	256/454	332/454
		POMBE	SPAC24C9.12c	serine hydroxymethyltransferase (predicted)	619	e-178	302/463	364/463
YLR079W	SIC1	HUMAN	XP_032278.5	signal-induced proliferation-associated 1 like ...	37	0.02	26/106	43/106
		MOUSE	NP_035031.1	cytoplasmic nuclear factor of activated T-cells...	39	0.003	30/84	42/84
		FLY	FBgn0003277	RpII215: RNA polymerase II 215kD subunit	36	0.021	24/76	36/76
		WORM	CE03712	status:Partially_confirmed TR:Q22715 protein_id:...	38	0.006	45/196	68/196

		POMBE	SPBC23G7.08c	GTPase activating protein	32	0.091	24/96	38/96
YLR085C	ARP6	HUMAN	NP_071941.1	ARP6 actin-related protein 6 homolog; actin-rel...	176	2.00E-44	127/436	209/436
		MOUSE	NP_080190.1	actin-related protein 6 [Mus musculus]	177	1.00E-44	127/436	213/436
		FLY	FBgn0011741	Actr13E: Actin-related protein 13E	172	3.00E-43	116/430	203/430
		WORM	CE30856	actin status:Confirmed SW:Q09443 protein_id:CAA...	146	2.00E-35	102/396	184/396
		POMBE	SPCC550.12	actin-like protein	218	9.00E-58	139/439	218/439
YLR154C	RNH203	HUMAN	NP_004614.2	tetratricopeptide repeat domain 4 [Homo sapiens]	27	3.5	30-Nov	17/29
		MOUSE	***** No hits found *****					
		FLY	FBgn0053125	CG33125	26	4.5	21-Oct	21-Dec
		WORM	CE20200	status:Partially_confirmed TR:Q9XXS3 protein_id...	25	5.4	17-Nov	17-Dec
		POMBE	SPBC14F5.12c	centromere binding protein	25	1.6	14/35	20/35
YLR193C	YLR193C	HUMAN	XP_371496.1	similar to Px19-like protein (25 kDa protein of...	102	2.00E-22	56/170	87/170
		MOUSE	NP_079872.4	PX19 homolog [Mus musculus]	100	4.00E-22	55/170	87/170
		FLY	FBgn0033413	CG8806	89	9.00E-19	55/158	84/158
		WORM	CE02936	Yeast hypothetical protein L8167.12 like status:...	63	6.00E-11	33/108	59/108
		POMBE	SPAP8A3.10	conserved eukaryotic protein	123	1.00E-29	64/151	93/151
YLR234W	TOP3	HUMAN	NP_004609.1	topoisomerase (DNA) III alpha; topo III-alpha [...	442	e-124	264/632	368/632
		MOUSE	NP_033436.1	topoisomerase (DNA) III alpha; topoisomerase 3 ...	439	e-123	261/632	370/632
		FLY	FBgn0040268	Top3alpha: Topoisomerase 3alpha	384	e-107	237/639	343/639
		WORM	CE28138	locus:top-3 DNA topoisomerase III status:Confi...	421	e-118	254/631	356/631
		POMBE	SPBC16G5.12c	DNA topoisomerase III	524	e-149	289/654	399/654
YLR235C	YLR235C	HUMAN	NP_079003.1	hypothetical protein FLJ23259 [Homo sapiens]	29	0.77	17/45	25/45
		MOUSE	XP_134826.2	similar to mPLZF(B)=promyelocytic leukemia zinc...	28	1.9	17/58	31/58
		FLY	FBgn0038830	CG17272	27	2.3	17/52	27/52
		WORM	CE06558	status:Partially_confirmed TR:Q23220 protein_id:...	26	6.1	15/49	24/49
		POMBE	SPAC3F10.09	1-(5-phosphoribosyl)-5-[(5-phosphoribosylamino)me...	26	1.4	19-Oct	14/18
YLR242C	ARV1	HUMAN	NP_073623.1	likely ortholog of yeast ARV1 [Homo sapiens]	55	6.00E-08	25/61	35/61
		MOUSE	NP_081131.1	ARV1 homolog; ARV1 homolog (yeast) [Mus musculus]	57	2.00E-08	26/61	34/61
		FLY	FBgn0052442	CG32442	44	1.00E-04	18/62	31/62
		WORM	CE02292	status:Partially_confirmed TR:Q21765 protein_id:...	53	2.00E-07	25/61	31/61
		POMBE	SPAPB1A10.15	involved in sterol metabolism (predicted)	83	4.00E-17	63/265	108/265
YLR255C	YLR255C	HUMAN	XP_029101.7	KIAA0947 protein [Homo sapiens]	28	1.6	15/44	23/44
		MOUSE	NP_666832.1	olfactory receptor 308; olfactory receptor MOR1...	26	5.2	13/28	18/28
		FLY	FBgn0036987	CG5274	25	6.4	Nov-39	18/35
		WORM	***** No hits found *****					
		POMBE	SPBC3F6.05	GTPase activating protein	25	2.4	Dec-39	19/35
YLR273C	PIG1	HUMAN	NP_005389.1	protein phosphatase 1, regulatory (inhibitor) s...	52	2.00E-06	41/135	65/135
		MOUSE	NP_058550.1	protein phosphatase 1, regulatory (inhibitor) s...	53	5.00E-07	41/135	64/135
		FLY	FBgn0036428	CG9238	41	0.002	32/110	49/110
		WORM	CE35731	status:Partially_confirmed TN:AAM69103 protein...	49	1.00E-05	33/123	55/123
		POMBE	SPAC26F1.09	TBC domain protein	32	0.19	30/105	43/105
YLR288C	MEC3	HUMAN	NP_057427.2	centromere protein F (350/400kD); mitosin; cent...	32	0.75	28/138	61/138
		MOUSE	NP_080957.2	DVL-binding protein DAPLE [Mus musculus]	31	1.4	30/146	62/146
		FLY	FBgn0030388	CG11245	31	1.3	23/67	32/67
		WORM	CE19401	status:Partially_confirmed TR:O76597 protein_i...	36	0.046	29/107	51/107
		POMBE	SPCC737.08	midasin (predicted)	30	0.87	21/82	36/82
YLR304C	ACO1	HUMAN	NP_001089.1	aconitase 2 precursor; aconitate hydratase; cit...	999	0	491/761	587/761
		MOUSE	NP_542364.1	aconitase 2, mitochondrial [Mus musculus]	1006	0	494/761	588/761
		FLY	FBgn0010100	Acon: Aconitase	1003	0	493/749	573/749
		WORM	CE25005	locus:aco-2 Aconitate hydratase status:Confirm...	1010	0	493/748	588/748
		POMBE	SPAC24C9.06c	aconitate hydratase (predicted)	1048	0	505/745	595/745
YLR320W	MMS22	HUMAN	NP_115583.1	hypothetical protein FLJ21742 [Homo sapiens]	37	0.14	40/182	75/182
		MOUSE	NP_033098.1	Rho-associated coiled-coil forming kinase 2; Rh...	35	0.35	28/135	64/135
		FLY	FBgn0032408	CG6712	38	0.05	38/164	71/164
		WORM	CE32277	status:Partially_confirmed TR:Q9GUM5 protein_id...	35	0.21	34/168	63/168
		POMBE	SPAC16A10.07c	involved in telomere maintenance	39	0.004	37/154	70/154
YLR370C	ARC18	HUMAN	NP_005710.1	actin related protein 2/3 complex subunit 3; AR...	166	8.00E-42	82/178	120/178
		MOUSE	NP_062798.1	actin related protein 2/3 complex, subunit 3; a...	167	4.00E-42	83/178	119/178
		FLY	FBgn0038369	Arpc3A	145	9.00E-36	77/171	109/171
		WORM	CE20206	locus:arx-5 status:Partially_confirmed SW:Q9XWV...	138	1.00E-33	79/180	108/180
		POMBE	SPBC1778.08c	ARP2/3 actin-organizing complex	191	3.00E-50	96/179	133/179
YLR373C	VID22	HUMAN	XP_290667.3	KIAA0350 protein [Homo sapiens]	31	4.6	39/174	74/174
		MOUSE	NP_659210.1	myosin, heavy polypeptide 2, skeletal muscle, a...	30	5.1	33/135	58/135
		FLY	FBgn0051169	CG31169	33	0.56	40/165	62/165
		WORM	CE03705	locus:sec-5 status:Partially_confirmed SW:SEC5_C...	33	0.63	24/99	50/99
		POMBE	SPCC417.07c	gamma tubulin complex (associated with) (PMI...	32	0.36	33/165	65/165
YLR374C	YLR374C	HUMAN	XP_372887.1	similar to minus agglutinin [Homo sapiens]	27	3.5	14/46	21/46
		MOUSE	NP_071877.2	sirtuin 2 (silent mating type information regul...	26	5.3	1-Dec	13/30
		FLY	FBgn0004177	mts: microtubule star	27	2.9	18/55	26/55
		WORM	CE01700	status:Confirmed SW:YS22_CAEEL protein_id:CAA87...	28	0.9	15/55	25/55
		POMBE	SPCC613.04c	UCS-domain protein (PMID 1085282)	27	0.78	18-Sep	18-Nov
YLR381W	CTF3	HUMAN	NP_852607.2	synleurin [Homo sapiens]	33	0.96	41/186	78/186
		MOUSE	XP_137955.2	apolipoprotein B [Mus musculus]	31	2.4	33/135	56/135
		FLY	FBgn0038693	CG5237	33	0.44	25/77	34/77
		WORM	CE15042	status:Predicted TR:O17516 protein_id:AAB63927.1	33	0.66	24/93	44/93
		POMBE	SPAC1687.20c	localization centromere	48	5.00E-06	96/478	184/478
YLR418C	CDC73	HUMAN	NP_078805.3	parafibromin; chromosome 1 open reading frame 2...	68	1.00E-11	34/106	58/106
		MOUSE	NP_666103.1	cDNA sequence BC027756; cDNA sequence, BC027756...	68	8.00E-12	34/106	58/106
		FLY	FBgn0037657	CG11990	69	3.00E-12	31/102	59/102
		WORM	CE29790	status:Partially_confirmed TR:Q9N5U5 protein_id...	70	2.00E-12	30/91	46/91
		POMBE	SPBC17G9.02c	involved in RNA elongation from Pol II promoter ...	157	3.00E-39	100/330	152/330
YLR425W	TUS1	HUMAN	NP_062541.2	intersectin 2 isoform 3; SH3 domain protein 1B;...	57	9.00E-08	55/211	97/211
		MOUSE	NP_035495.2	SH3 domain protein 1B; intersectin 2; Eh domain...	57	8.00E-08	53/211	98/211
		FLY	FBgn0051146	CG31146	35	0.29	42/188	73/188
		WORM	CE34221	status:Partially_confirmed TR:Q7YTU1 protein...	37	0.065	52/245	95/245
		POMBE	SPCC645.06c	localization cell division site (pers. comm. ...	150	1.00E-36	250/1182	448/1182
YLR443W	ECM7	HUMAN	NP_008954.1	Rap guanine nucleotide exchange factor (GEF) 4;...	31	2	17/53	28/53
		MOUSE	NP_067450.1	disintegrin metalloprotease (decysin); decysin ...	35	0.07	19/58	32/58
		FLY	FBgn0036930	fat2	30	2.7	32/134	57/134
		WORM	CE23602	SET domain status:Partially_confirmed TR:Q18690 ...	36	0.043	29/103	45/103
		POMBE	SPAC22H12.05c	fasciclin domain protein (3)	31	0.28	15/63	34/63
YML009C	MRPL39	HUMAN	NP_004882.1	mitochondrial ribosomal protein L33 isoform a; ...	37	0.003	18/47	29/47
		MOUSE	NP_080072.1	mitochondrial ribosomal protein L33 [Mus musculus]	34	0.019	17/47	28/47

		FLY	FBgn0038551	CG7357	25	5.9	16/41	23/41
		WORM	CE32865	locus:twk-11 status:Partially_confirmed TR:Q8I7...	25	7.2	13/35	20/35
		POMBE	SPBC4F6.08c	mitochondrial ribosomal protein subunit YmL...	39	9.00E-05	19/49	28/49
YML009C-A	YML009C-A	HUMAN	NP_689418.1	taste receptor, type 1, member 2; G protein-cou...	29	0.69	13/33	17/33
		MOUSE	NP_032901.2	phospholipase D1; choline phosphatase 1 [Mus mu...	28	1.4	27-Nov	17/26
		FLY	FBgn0039244	CG11069	27	1.6	22-Sep	14/21
		WORM	CE21939	chemoreceptor status:Predicted TR:Q9UAU9 prote...	25	9.2	15/48	22/48
		POMBE	SPAC1639.01c	GNS1/SUR4 family protein	25	1.9	13/47	23/47
YML009W-B	YML009W-B	HUMAN	NP_115971.2	ubiquitin specific protease 32 [Homo sapiens]	27	7.6	18/61	30/61
		MOUSE	NP_659175.1	type I transmembrane receptor (seizure-related ...	27	3.8	14/31	19/31
		FLY	FBgn0031965	CG7093	28	2.1	25/79	33/79
		WORM	CE20298	status:Partially_confirmed TR:Q9U255 protein_...	29	1.1	14/46	23/46
		POMBE	SPBC19C7.06	proline-tRNA ligase (predicted)	27	1.2	17/80	35/80
YML028W	TSA1	HUMAN	NP_005800.3	peroxiredoxin 2 isoform a; thioredoxin-dependen...	263	7.00E-71	129/193	149/193
		MOUSE	NP_035693.2	peroxiredoxin 2; thioredoxin peroxidase 1; Prx ...	254	2.00E-68	125/193	147/193
		FLY	FBgn0040309	Jafrac1: thioredoxin peroxidase 1	234	2.00E-62	115/192	143/192
		WORM	CE32361	locus:tag-56 status:Confirmed TR:Q8IG31 protein...	252	9.00E-68	126/190	149/190
		POMBE	SPCC576.03c	thioredoxin peroxidase	250	7.00E-68	125/191	151/191
YML032C	RAD52	HUMAN	NP_002870.2	RAD52 homolog isoform alpha; recombination prot...	164	2.00E-40	94/220	128/220
		MOUSE	NP_035366.1	RAD52 homolog; RAD52 homolog, (S. cerevisiae) [...	167	2.00E-41	91/200	124/200
		FLY	FBgn0051916	CG31916	34	0.15	25/96	44/96
		WORM	CE11558	status:Partially_confirmed TR:Q94248 protein_id...	32	0.67	36/174	68/174
		POMBE	SPAC30D11.10	involved in DNA repair (PMID 8290356)	193	3.00E-50	123/367	192/367
YML062C	MFT1	HUMAN	NP_005955.1	myosin, heavy polypeptide 10, non-muscle; myosi...	40	0.004	54/262	112/262
		MOUSE	XP_111038.2	RIKEN cDNA 4933407G07 [Mus musculus]	41	0.001	40/157	71/157
		FLY	FBgn0002741	Mhc: Myosin heavy chain	41	0.001	56/256	104/256
		WORM	CE31066	endosomal protein P162 like status:Confirmed TR:...	40	0.001	50/227	91/227
		POMBE	SPAC1093.06c	dynein heavy chain (PMID 1085550...	40	4.00E-04	24/82	44/82
YML090W	YML090W	HUMAN	NP_059509.1	ubiquilin 3 [Homo sapiens]	27	3.5	17/68	32/68
		MOUSE	NP_038872.1	Zinc finger protein 68 [Mus musculus]	27	3.9	1-Nov	19/31
		FLY	FBgn0032256	RluA-2	25	8.2	23-Oct	23-Nov
		WORM	CE05172	locus:rhr-2 erythrocyte plasma membrane glycopro...	28	1.5	Dec-43	23/39
		POMBE	SPBC25B2.03	glutaredoxin (inferred from context)	24	6.4	Oct-38	16/34
YML094W	GIM5	HUMAN	NP_002615.2	prefoldin 5 isoform alpha; myc modulator-1; c-m...	107	3.00E-24	51/124	88/124
		MOUSE	NP_064415.1	prefoldin 5; EIG-1; c-myc binding protein MM-1 ...	107	2.00E-24	51/124	88/124
		FLY	FBgn0038976	CG7048	102	9.00E-23	51/141	95/141
		WORM	CE00827	status:Confirmed SW:Q21993 protein_id:AAK29855.1	75	1.00E-14	42/124	70/124
		POMBE	SPBC215.02	prefoldin (subunit 5)	103	8.00E-24	54/140	90/140
YML095C	RAD10	HUMAN	NP_001974.1	excision repair cross-complementing 1 isofrom 2...	70	1.00E-12	39/129	74/129
		MOUSE	NP_031974.1	excision repair cross-complementing rodent repa...	72	3.00E-13	39/139	75/139
		FLY	FBgn0028434	Ercc1	62	2.00E-10	46/143	73/143
		WORM	CE30750	DNA excision repair protein status:Confirmed TR:...	43	1.00E-04	27/120	57/120
		POMBE	SPBC4F6.15c	endonuclease complex subunit (predicted)	79	4.00E-16	43/117	72/117
YML099C	ARG81	HUMAN	NP_056382.1	slit and trk like 5 [Homo sapiens]	35	0.18	27/96	44/96
		MOUSE	NP_083549.1	SLIT and NTRK-like family, member 5; slit and t...	35	0.26	27/96	44/96
		FLY	FBgn0003149	Prm: Paramyosin	33	0.71	25/86	41/86
		WORM	CE30351	locus:cor-1 Coronin (beta transducin) status:P...	36	0.095	36/122	50/122
		POMBE	SPBC15D4.02	zinc finger protein	53	2.00E-07	22/42	26/42
YML102W	CAC2	HUMAN	NP_005432.1	chromatin assembly factor 1 subunit B; M-phase ...	266	2.00E-71	158/459	243/459
		MOUSE	NP_082359.1	chromatin assembly factor 1 subunit B [Mus musc...	261	8.00E-70	159/480	244/480
		FLY	FBgn0033526	Caf1-105	230	1.00E-60	144/447	239/447
		WORM	CE29917	status:Partially_confirmed TR:Q95XL9 protein_...	150	1.00E-36	117/418	196/418
		POMBE	SPAC26H5.03	WD repeat protein	171	1.00E-43	94/221	132/221
YML124C	TUB3	HUMAN	NP_116093.1	tubulin alpha 6 [Homo sapiens]	628	e-180	297/440	350/440
		MOUSE	NP_033474.1	tubulin, alpha 6; tubulin alpha 6 [Mus musculus]	629	e-180	298/440	350/440
		FLY	FBgn0003884	alphaTub84B: alpha-Tubulin at 84B	630	0	299/440	349/440
		WORM	CE18680	locus:tba-4 tubulin alpha-2 chain status:Partia...	625	e-179	296/440	348/440
		POMBE	SPBC16A3.15c	tubulin (alpha 1)	629	0	304/447	347/447
YMR008C	PLB1	HUMAN	XP_172929.5	similar to phospholipase A2, group IVB (cytosol...	52	1.00E-06	63/273	99/273
		MOUSE	XP_195168.3	similar to phospholipase A2, group IVB (cytosol...	49	1.00E-05	57/265	94/265
		FLY	FBgn0039251	CG17462	31	2	16/34	19/34
		WORM	CE17619	status:Partially_confirmed TR:Q93410 protein_id:...	30	2.9	24/91	36/91
		POMBE	SPBC1348.10c	lysophospholipase (predicted)	395	e-110	221/579	336/579
YMR048W	CSM3	HUMAN	NP_060328.1	timeless-interacting protein; tipin [Homo sapiens]	55	8.00E-08	35/122	61/122
		MOUSE	NP_079648.1	timeless-interacting protein [Mus musculus]	54	1.00E-07	35/119	61/119
		FLY	FBgn0032698	CG10336	47	2.00E-05	32/131	59/131
		WORM	CE20718	status:Partially_confirmed TR:Q9TXI0 protein_id:...	51	6.00E-07	39/152	73/152
		POMBE	SPBC30D10.04	conserved eukaryotic protein	49	8.00E-07	19/63	39/63
YMR066W	SOV1	HUMAN	NP_003696.2	solute carrier family 25 (mitochondrial carrier...	33	0.92	21/69	33/69
		MOUSE	NP_766024.1	solute carrier family 25 (mitochondrial carrier...	33	0.78	22/69	33/69
		FLY	FBgn0030979	CG14190	33	0.73	19/66	28/66
		WORM	CE31980	status:Partially_confirmed TR:Q8I4G7 protein_id:...	32	1.1	26/107	43/107
		POMBE	SPAC27D7.02c	conserved eukaryotic protein	32	0.28	33/128	50/128
YMR078C	CTF18	HUMAN	NP_071375.1	CTF18, chromosome transmission fidelity factor ...	150	3.00E-36	171/732	296/732
		MOUSE	NP_663384.1	CTF18, chromosome transmission fidelity factor ...	151	2.00E-36	169/705	295/705
		FLY	FBgn0015376	cutlet: cutlet	138	1.00E-32	155/709	272/709
		WORM	CE06149	Yeast Chl2p like status:Confirmed TR:Q21350 prot...	135	7.00E-32	119/462	205/462
		POMBE	SPBC902.02c	AAA family ATPase (predicted)	231	3.00E-61	182/672	320/672
YMR095C	SNO1	HUMAN	NP_002709.2	alpha isoform of regulatory subunit B", protei...	29	2.2	17/57	28/57
		MOUSE	NP_034120.1	cytoplasmic linker 2; cytoplasmic linker protei...	29	1.9	14/34	20/34
		FLY	FBgn0036448	CG9311	30	1	19/101	35/101
		WORM	CE23636	locus:pes-7 ras GTPase-activating protein like s...	28	2.6	25/92	42/92
		POMBE	SPAC222.08c	imidazoleglycerol phosphate synthase activity (pr...	105	4.00E-24	82/227	114/227
YMR106C	YKU80	HUMAN	NP_001460.1	thyroid autoantigen 70kDa (Ku antigen); thyroid...	41	0.003	37/138	60/138
		MOUSE	NP_034377.1	thyroid autoantigen; thyroid autoantigen 70 kDa...	44	4.00E-04	44/149	66/149
		FLY	FBgn0041627	Ku80	45	2.00E-04	64/269	107/269
		WORM	CE00660	locus:cku-80 status:Partially_confirmed TR:Q2182...	40	0.003	52/241	97/241
		POMBE	SPBC543.03c	Ku domain protein	82	2.00E-16	102/508	193/508
YMR120C	ADE17	HUMAN	NP_004035.2	5-aminoimidazole-4-carboxamide ribonucleotide f...	702	0	356/588	443/588
		MOUSE	NP_080471.1	5-aminoimidazole-4-carboxamide ribonucleotide f...	691	0	354/591	440/591
		FLY	FBgn0039241	CG11089	699	0	356/589	434/589
		WORM	CE31457	status:Confirmed TR:Q95QQ4 protein_id:AAL27234.2	653	0	333/596	416/596
		POMBE	SPCPB16A4.03	IMP cyclohydrolase	824	0	406/585	485/585

YMR179W	SPT21	HUMAN	XP_370738.1	helicase with SNF2 domain 1 [Homo sapiens]	33	1	30/132	66/132
		MOUSE	XP_129477.3	RIKEN cDNA 1600013L13 [Mus musculus]	38	0.026	60/276	104/276
		FLY	FBgn0003137	Ppn: Papilin	35	0.21	39/174	71/174
		WORM	CE16169	Zinc finger, C3HC4 type (RING finger) status:Pa...	36	0.081	53/228	92/228
		POMBE	SPAPB1E7.04c	glycosyl hydrolase family 18	40	8.00E-04	58/232	93/232
YMR190C	SGS1	HUMAN	NP_000048.1	Bloom syndrome protein [Homo sapiens]	412	e-115	222/560	336/560
		MOUSE	NP_031576.2	Bloom syndrome protein homolog [Mus musculus]	411	e-114	224/572	336/572
		FLY	FBgn0002906	mus309: mutagen-sensitive 309	441	e-123	235/561	346/561
		WORM	CE31724	locus:him-6 helicase status:Confirmed SW:O18017...	363	e-100	202/545	311/545
		POMBE	SPAC2G11.12	RecQ type DNA helicase	501	e-142	283/669	402/669
YMR198W	CIK1	HUMAN	NP_002069.2	golgi autoantigen, golgin subfamily a, 4; golgi...	54	4.00E-07	112/563	219/563
		MOUSE	NP_776123.2	centromere protein E; kinesin 10; kinesin famil...	51	2.00E-06	64/254	103/254
		FLY	FBgn0002741	Mhc: Myosin heavy chain	52	1.00E-06	62/259	102/259
		WORM	CE09167	status:Partially_confirmed TR:O17763 protein_id...	54	2.00E-07	56/229	109/229
		POMBE	SPCC162.08c	coiled-coil (predicted)	46	1.00E-05	60/296	125/296
YMR224C	MRE11	HUMAN	NP_005582.1	meiotic recombination 11 homolog A isoform 1; d...	388	e-108	222/543	320/543
		MOUSE	NP_061206.1	meiotic recombination 11 homolog A [Mus musculus]	397	e-110	224/541	314/541
		FLY	FBgn0020270	mre11: meiotic recombination 11	304	1.00E-82	191/500	275/500
		WORM	CE06573	locus:mre-11 Human MRE11 protein like status:Par...	276	2.00E-74	177/494	258/494
		POMBE	SPAC13C5.07	exonuclease	456	e-129	253/601	362/601
YMR300C	ADE4	HUMAN	NP_002694.3	phosphoribosyl pyrophosphate amidotransferase p...	234	8.00E-62	162/472	243/472
		MOUSE	NP_742158.1	phosphoribosyl pyrophosphate amidotransferase [...	228	5.00E-60	160/472	242/472
		FLY	FBgn0041194	Prat2: Phosphoribosylamidotransferase 2	224	1.00E-58	153/478	246/478
		WORM	CE01074	Amidophosphoribosyltransferase status:Partially_...	215	5.00E-56	156/493	254/493
		POMBE	SPAC4D7.08c	amidophosphoribosyltransferase (PM...	590	e-169	301/526	375/526
YMR311C	GLC8	HUMAN	NP_006232.1	protein phosphatase 1, regulatory (inhibitor) s...	40	0.002	37/119	52/119
		MOUSE	NP_080076.1	protein phosphatase 1, regulatory (inhibitor) s...	46	2.00E-05	40/149	65/149
		FLY	FBgn0035797	CG14837	36	0.015	34/156	59/156
		WORM	CE28515	status:Partially_confirmed TR:Q9N537 protein_i...	35	0.029	34/137	57/137
		POMBE	SPBC16E9.02c	CUE domain protein	35	0.01	37/193	73/193
YNL047C	LIT1	HUMAN	NP_149033.2	microfilament and actin filament cross-linker p...	42	0.002	25/95	50/95
		MOUSE	NP_035312.2	pleckstrin homology, Sec7 and coiled-coil domai...	41	0.003	48/199	88/199
		FLY	FBgn0035498	CG14991	39	0.009	31/99	44/99
		WORM	CE17405	inositol-1,4,5-triphosphate 5-phosphatase status...	35	0.15	20/67	34/67
		POMBE	SPAC637.13c	hypothetical protein	99	2.00E-21	97/491	195/491
YNL066W	SUN4	HUMAN	XP_375633.1	solute carrier family 8 member 2 [Homo sapiens]	33	0.38	18/37	22/37
		MOUSE	NP_031555.1	brevican [Mus musculus]	29	6.1	20/69	28/69
		FLY	FBgn0035779	CG8562	30	2.5	24/111	43/111
		WORM	***** No hits found *****					
		POMBE	SPAC1002.13c	beta-glucosidase (predicted)	280	3.00E-76	137/258	166/258
YNL072W	RNH201	HUMAN	NP_006388.2	ribonuclease HI, large subunit [Homo sapiens]	181	7.00E-46	108/268	158/268
		MOUSE	XP_356211.1	similar to 2400006P09Rik protein [Mus musculus]	186	1.00E-47	108/255	156/255
		FLY	FBgn0031252	CG13690	167	9.00E-42	110/279	149/279
		WORM	CE28960	locus:rnh-2 status:Confirmed SW:RNHL_CAEEL prote...	179	1.00E-45	108/269	155/269
		POMBE	SPAC4G9.02	ribonuclease H	207	1.00E-54	122/286	170/286
YNL086W	YNL086W	HUMAN	XP_041964.5	KIAA0523 protein [Homo sapiens]	28	1.2	15/48	24/48
		MOUSE	NP_690855.1	PLU1; putative DNA/chromatin binding motif 1 [M...	31	0.16	23/75	38/75
		FLY	FBgn0040232	cmet: CENP-meta	31	0.14	21/59	31/59
		WORM	CE06755	peptidase status:Partially_confirmed TR:Q17592 p...	30	0.17	Dec-37	21/33
		POMBE	SPAC3A11.05c	meiosis specific protein	27	0.34	22/98	38/98
YNL089C	YNL089C	HUMAN	XP_378883.1	hypothetical protein XP_378883 [Homo sapiens]	27	5.8	16/46	24/46
		MOUSE	NP_997442.1	olfactory receptor 776; GA_x6K02T2PULF-10947193...	28	2.2	22/68	33/68
		FLY	FBgn0052046	CG32046	32	0.14	22/71	37/71
		WORM	CE12064	status:Predicted TR:O17238 protein_id:AAB71006.1	27	4.1	23-Oct	16/22
		POMBE	SPAC1F8.06	glycoprotein (predicted)	26	2	25/97	48/97
YNL133C	FYV6	HUMAN	NP_004809.2	DEAD (Asp-Glu-Ala-Asp) box polypeptide 23; U5 s...	33	0.13	28/85	40/85
		MOUSE	XP_128190.2	DEAD (Asp-Glu-Ala-Asp) box polypeptide 23 [Mus ...	33	0.11	28/85	40/85
		FLY	FBgn0052662	CG32662	33	0.059	29/126	61/126
		WORM	CE04898	status:Partially_confirmed TR:Q9GYK8 protein_id...	35	0.014	22/74	36/74
		POMBE	SPAC12G12.07	sequence orphan	35	0.004	21/82	43/82
YNL140C	YNL140C	HUMAN	NP_060481.2	hypothetical protein FLJ10154 [Homo sapiens]	30	0.74	20/69	35/69
		MOUSE	NP_789819.1	RIKEN cDNA 9430010O03 [Mus musculus]	30	0.64	20/69	35/69
		FLY	FBgn0033929	Tfb1	28	2.9	22/105	44/105
		WORM	CE17280	status:Partially_confirmed TR:Q9UAY5 protein_id:...	32	0.18	27/97	39/97
		POMBE	SPAC2F7.09c	NTP binding (predicted)	26	2.7	19/50	24/50
YNL206C	RTT106	HUMAN	NP_003137.1	structure specific recognition protein 1; recom...	55	1.00E-07	37/143	65/143
		MOUSE	NP_892035.1	structure specific recognition protein 1 [Mus m...	52	6.00E-07	34/142	63/142
		FLY	FBgn0010278	Ssrp: Structure specific recognition protein	45	1.00E-04	32/140	66/140
		WORM	CE08542	locus:hmg-3 single-strand recognition protein s...	50	3.00E-06	37/145	69/145
		POMBE	SPAC6G9.03c	hypothetical protein	88	2.00E-18	83/358	156/358
YNL213C	YNL213C	HUMAN	NP_057729.1	mesenchymal stem cell protein DSC92; neurite ou...	40	0.001	21/54	33/54
		MOUSE	NP_113552.2	neugrin; neurite outgrowth associated protein [...	37	0.008	20/54	32/54
		FLY	FBgn0028494	CG6424	32	0.25	26/113	48/113
		WORM	CE20601	status:Partially_confirmed TR:Q9XTI8 protein_id:...	35	0.026	29/102	51/102
		POMBE	SPAC6B12.06c	conserved fungal protein	72	4.00E-14	39/107	62/107
YNL250W	RAD50	HUMAN	NP_005723.2	RAD50 homolog isoform 1 [Homo sapiens]	515	e-146	357/1334	658/1334
		MOUSE	NP_033038.1	RAD50 homolog [Mus musculus]	512	e-145	366/1339	657/1339
		FLY	FBgn0034728	rad50	464	e-130	361/1367	670/1367
		WORM	CE21149	locus:rad-50 DNA repair protein RAD50 like statu...	367	e-101	332/1330	605/1330
		POMBE	SPAC1556.01c	involved in DNA repair	647	0	427/1336	710/1336
YNL257C	SIP3	HUMAN	NP_003878.1	development- and differentiation-enhancing fact...	35	0.34	30/117	50/117
		MOUSE	NP_722483.2	centaurin, beta 1 [Mus musculus]	35	0.22	72/372	130/372
		FLY	FBgn0039056	cenB1A: centaurin beta 1A	36	0.16	91/430	161/430
		WORM	CE32715	status:Confirmed TR:Q8MPT3 protein_id:AAN65296.1	39	0.021	83/431	169/431
		POMBE	SPAC19A8.02	pleckstrin homology domain	125	4.00E-29	182/893	326/893
YNL273W	TOF1	HUMAN	NP_003911.1	timeless homolog [Homo sapiens]	54	6.00E-07	74/315	134/315
		MOUSE	NP_035719.1	timeless homolog [Mus musculus]	53	1.00E-06	75/312	133/312
		FLY	FBgn0038118	timeout: timeout	36	0.12	60/307	131/307
		WORM	CE30612	status:Partially_confirmed TR:Q8MNV1 protein_id:...	35	0.31	65/272	112/272
		POMBE	SPBC216.06c	involved in mating-type switching (PMID 65873...	236	1.00E-62	223/958	412/958
YNL291C	MID1	HUMAN	NP_061937.3	sidekick 2; Drosophila sidekick-like; chicken s...	31	2.6	17/44	22/44
		MOUSE	NP_766388.2	sidekick 2 [Mus musculus]	31	2.2	17/44	22/44
		FLY	FBgn0032330	Samuel: Samuel	33	0.41	21/70	30/70

		WORM	CE33299	status:Partially_confirmed TR:Q86S82 protein_id...	32	0.8	15/54	26/54
		POMBE	SPAC1F5.08c	involved in calcium ion transport (PMID 1...	163	6.00E-41	106/336	166/336
YNL309W	STB1	HUMAN	XP_379904.1	similar to mucin 11 [Homo sapiens]	45	7.00E-05	80/363	127/363
		MOUSE	NP_536705.1	mucin 4 [Mus musculus]	52	5.00E-07	69/326	115/326
		FLY	FBgn0035500	CG14998	47	2.00E-05	79/376	141/376
		WORM	CE32567	locus:mel-11 status:Partially_confirmed TR:Q8I0...	49	4.00E-06	75/329	125/329
		POMBE	SPAC4H3.11c	hypothetical protein	37	0.006	28/141	55/141
YNL315C	ATP11	HUMAN	NP_073582.1	ATP synthase mitochondrial F1 complex assembly ...	69	4.00E-12	49/164	80/164
		MOUSE	NP_851383.1	ATP synthase mitochondrial F1 complex assembly ...	64	9.00E-11	48/163	78/163
		FLY	FBgn0022344	CG10340	78	7.00E-15	77/280	121/280
		WORM	CE23943	neurofilament triplet M protein status:Partiall...	37	0.012	28/101	49/101
		POMBE	SPAC3A12.12	F1 ATPase chaperone (PMID 12206899)	142	6.00E-35	93/263	141/263
YNR042W	YNR042W	HUMAN	XP_379877.1	similar to Nuclear envelope pore membrane prote...	31	0.32	22/55	29/55
		MOUSE	XP_357389.1	similar to hypothetical protein FLJ32000 [Mus m...	28	1.4	16/51	23/51
		FLY	FBgn0051308	CG31308	29	0.96	13/36	17/36
		WORM	CE27767	locus:eat-20 EGF-like domain (3 domains) statu...	28	1.5	14/46	23/46
		POMBE	SPCC962.02c	survivin	27	1.2	23-Dec	15/22
YNR045W	PET494	HUMAN	NP_001090.2	prostatic acid phosphatase precursor [Homo sapi...	34	0.2	32/100	51/100
		MOUSE	XP_359111.1	similar to RNP particle component [Mus musculus]	34	0.23	23/129	58/129
		FLY	FBgn0034258	eIF3-S8	30	2.3	18/56	31/56
		WORM	CE06368	locus:hcp-2 status:Partially_confirmed TR:Q22257...	37	0.022	39/165	74/165
		POMBE	SPBC8D2.11	hypothetical protein	30	0.69	21/85	41/85
YNR048W	YNR048W	HUMAN	NP_060717.1	hypothetical protein FLJ10856 [Homo sapiens]	192	4.00E-49	128/371	181/371
		MOUSE	NP_598479.1	RIKEN cDNA 2010200I23 [Mus musculus]	190	1.00E-48	126/372	178/372
		FLY	FBgn0030752	CG9947	181	6.00E-46	120/351	178/351
		WORM	CE07425	status:Confirmed TR:Q21844 protein_id:AAC48073.1	176	2.00E-44	120/353	172/353
		POMBE	SPBC1773.11c	CDC50 domain protein	320	3.00E-88	159/367	235/367
YNR049C	MSO1	HUMAN	XP_052597.6	ubiquitin specific protease 53 [Homo sapiens]	31	0.53	23/73	33/73
		MOUSE	NP_081815.3	RIKEN cDNA 6330415M09 [Mus musculus]	30	1	20/56	28/56
		FLY	FBgn0031291	CG4124	30	0.93	17/68	34/68
		WORM	CE29966	dehydrogenase status:Partially_confirmed TR:Q20...	34	0.057	22/71	38/71
		POMBE	SPAC6G9.05	Nudix family hydrolase	28	0.85	21/72	29/72
YNR068C	YNR068C	HUMAN	XP_062871.5	similar to Centromeric protein E (CENP-E protei...	32	0.46	16/62	35/62
		MOUSE	NP_032342.1	Hus1 homolog [Mus musculus]	28	4.4	13/41	24/41
		FLY	FBgn0051237	Rpb4	29	2.4	15/58	26/58
		WORM	CE03490	status:Partially_confirmed TR:Q21588 protein_id:CA...	28	3.6	14/36	22/36
		POMBE	SPAC1142.03c	AT hook protein (inferred from c...	30	0.25	24/86	40/86
YOL012C	HTZ1	HUMAN	NP_958844.1	H2A histone family, member V isoform 3; purine-...	145	1.00E-35	74/102	86/102
		MOUSE	NP_058030.1	H2A histone family, member Z; histone H2A.Z [Mu...	145	9.00E-36	74/102	86/102
		FLY	FBgn0001197	His2Av: Histone H2A variant	144	1.00E-35	72/97	84/97
		WORM	CE07426	histone H2A variant status:Confirmed TR:Q27511 p...	139	5.00E-34	70/100	84/100
		POMBE	SPBC11B10.10(	histone H2A variant	150	4.00E-38	74/98	86/98
YOL054W	PSH1	HUMAN	NP_005073.1	tripartite motif-containing 25; Zinc finger pro...	55	1.00E-07	31/70	37/70
		MOUSE	XP_126545.2	similar to estrogen-responsive finger protein [...	52	5.00E-07	26/64	32/64
		FLY	FBgn0039150	CG13605	54	2.00E-07	21/52	30/52
		WORM	CE05942	locus:nhl-1 Zinc finger, C3HC4 type (RING finger...	50	3.00E-06	22/54	30/54
		POMBE	SPCC548.05c	zinc finger protein	71	3.00E-13	46/157	68/157
YOL064C	MET22	HUMAN	NP_005527.1	inositol(myo)-1(or 4)-monophosphatase 1 [Homo s...	46	5.00E-05	54/205	81/205
		MOUSE	NP_444491.1	inositol (myo)-1(or 4)-monophosphatase 2 [Mus m...	45	9.00E-05	57/216	80/216
		FLY	FBgn0037063	CG9391	58	9.00E-09	75/315	114/315
		WORM	CE29761	myo-inositol-1-monophosphatase status:Confirmed ...	34	0.094	22/63	32/63
		POMBE	SPCC1753.04	3'(2'),5'-bisphosphate nucleotidase	246	4.00E-66	149/341	205/341
YOL070C	YOL070C	HUMAN	XP_379905.1	similar to intestinal membrane mucin MUC17 [Hom...	39	0.007	72/330	108/330
		MOUSE	NP_848770.1	ankyrin 2, brain [Mus musculus]	39	0.006	46/208	85/208
		FLY	FBgn0027356	Amph: Amphiphysin	40	0.004	44/182	78/182
		WORM	CE35572	MYB-related protein like status:Partially_confir...	34	0.14	46/187	80/187
		POMBE	SPAC17C9.03	translation initiation factor	45	3.00E-05	63/263	101/263
YOL072W	THP1	HUMAN	NP_060856.1	hypothetical protein FLJ11305 [Homo sapiens]	52	7.00E-07	44/176	81/176
		MOUSE	NP_848823.1	RIKEN cDNA A730042J05 gene [Mus musculus]	57	3.00E-08	47/176	83/176
		FLY	FBgn0036184	CG7351	46	5.00E-05	46/176	73/176
		WORM	CE29189	status:Partially_confirmed SW:YPIA_CAEEL protei...	52	8.00E-07	61/251	104/251
		POMBE	SPBC1105.07c	THO complex (predicted)	47	6.00E-06	85/394	153/394
YOR014W	RTS1	HUMAN	NP_006236.1	delta isoform of regulatory subunit B56, protei...	521	e-148	261/478	338/478
		MOUSE	NP_033384.2	delta isoform of regulatory subunit B56, protei...	517	e-147	261/478	336/478
		FLY	FBgn0042693	PP2A-B'	502	e-142	245/475	329/475
		WORM	CE20505	status:Confirmed TR:Q9U3Q1 protein_id:CAA98423.1	495	e-140	242/455	321/455
		POMBE	SPCC188.02	protein phosphatase regulatory subunit (PMID 1...	521	e-148	259/493	347/493
YOR024W	YOR024W	HUMAN	NP_689641.2	FERM and PDZ domain containing 2 [Homo sapiens]	28	0.91	14/52	26/52
		MOUSE	XP_126554.5	RIKEN cDNA 9630002H22 [Mus musculus]	28	1.4	19/57	25/57
		FLY	***** No hits found *****					
		WORM	CE00112	locus:elo-4 Yeast hypothetical YCR34W status:Par...	26	4.2	18/52	27/52
		POMBE	SPAC2E1P3.05(	conserved fungal protein	28	0.29	16/73	28/73
YOR025W	HST3	HUMAN	NP_036370.2	sirtuin 1; sir2-like 1; sirtuin type 1; SIR2alp...	115	5.00E-26	96/303	136/303
		MOUSE	NP_062786.1	sirtuin 1 ((silent mating type information regu...	115	7.00E-26	96/303	136/303
		FLY	FBgn0024291	Sir2	115	6.00E-26	100/337	156/337
		WORM	CE06302	locus:sir-2.1 Yeast regulatory protein SIR2 like...	100	2.00E-21	88/332	150/332
		POMBE	SPAC1783.04c	Sir2p family	173	5.00E-44	115/307	173/307
YOR026W	BUB3	HUMAN	NP_004716.1	BUB3 budding uninhibited by benzimidazoles 3 ho...	109	2.00E-24	85/287	142/287
		MOUSE	NP_033904.2	budding uninhibited by benzimidazoles 3 homolog...	109	2.00E-24	85/287	142/287
		FLY	FBgn0025457	Bub3	103	1.00E-22	81/285	138/285
		WORM	CE19233	WD domain, G-beta repeat (2 domains) status:Con...	113	1.00E-25	88/300	146/300
		POMBE	SPAC23H3.08c	WD repeat protein	104	1.00E-23	85/289	139/289
YOR058C	ASE1	HUMAN	NP_003283.1	translocated promoter region (to activated MET ...	39	0.022	37/194	79/194
		MOUSE	NP_660132.1	protein regulator of cytokinesis 1 [Mus musculus]	46	9.00E-05	65/331	123/331
		FLY	FBgn0030241	feo: fascetto	49	2.00E-05	64/307	122/307
		WORM	CE17314	locus:xnp-1 helicase status:Confirmed SW:Q9U7E0 ...	39	0.015	47/244	98/244
		POMBE	SPAPB1A10.09	microtubule-associated protein (predicted)	81	7.00E-16	103/489	200/489
YOR066W	YOR066W	HUMAN	NP_056969.2	pre-mRNA cleavage complex II protein Pcf11; PCF...	35	0.21	28/143	54/143
		MOUSE	NP_032782.1	occludin [Mus musculus]	35	0.14	42/159	65/159
		FLY	FBgn0036340	SRm160	35	0.17	32/129	55/129
		WORM	CE22858	status:Partially_confirmed TR:Q9N4I3 protein_i...	36	0.05	31/127	56/127
		POMBE	SPBC215.13	glycoprotein (predicted)	38	0.003	73/411	136/411
YOR073W	SGO1	HUMAN	NP_056109.1	tripartite motif-containing 37; MUL protein; RI...	37	0.03	25/74	35/74

		MOUSE	NP_032900.2	phospholipase C, beta 3 [Mus musculus]	35	0.13	25/112	56/112
		FLY	FBgn0037344	CG2926	36	0.053	30/110	48/110
		WORM	CE23322	status:Partially_confirmed SW:Y8CB_CAEEL prot...	42	0.001	26/85	44/85
		POMBE	SPBP35G2.03c	shugoshin	43	1.00E-04	29/98	54/98
YOR080W	DIA2	HUMAN	NP_006810.1	stress-induced-phosphoprotein 1 (Hsp70/Hsp90-or...	44	4.00E-04	41/174	67/174
		MOUSE	NP_058017.1	stress-induced phosphoprotein 1; stress-inducib...	45	2.00E-04	42/174	67/174
		FLY	FBgn0024352	Hop: Hsp70/Hsp90 organizing protein homolog	42	0.001	42/173	68/173
		WORM	CE12646	status:Confirmed TR:O16259 protein_id:AAG24172.1	45	2.00E-04	40/172	68/172
		POMBE	SPCC338.16	F-box protein	42	2.00E-04	76/317	127/317
YOR128C	ADE2	HUMAN	NP_006443.1	phosphoribosylaminoimidazole carboxylase; phosp...	35	0.11	36/145	58/145
		MOUSE	XP_138610.2	similar to 3-phosphoglycerate dehydrogenase [Mu...	34	0.27	22/72	35/72
		FLY	FBgn0020513	ade5	36	0.051	42/145	61/145
		WORM	CE09072	locus:pyc-1 pyruvate carboxylase status:Confirme...	37	0.026	38/162	71/162
		POMBE	SPCC1322.13	phosphoribosylaminoimidazole carboxylase	580	e-166	308/568	399/568
YOR144C	ELG1	HUMAN	NP_079133.3	hypothetical protein FLJ12735 [Homo sapiens]	48	2.00E-05	33/119	56/119
		MOUSE	XP_111221.4	similar to hypothetical protein FLJ12735 [Mus m...	45	2.00E-04	31/119	55/119
		FLY	FBgn0036574	CG16838	50	7.00E-06	58/264	102/264
		WORM	CE19136	status:Partially_confirmed TR:Q9XX13 protein_i...	39	0.01	56/231	101/231
		POMBE	SPBC947.11c	replication factor C complex (predicted) (ISS)	86	2.00E-17	55/210	106/210
YOR241W	MET7	HUMAN	NP_004948.2	folylpolyglutamate synthase; folylpolyglutamate...	69	1.00E-11	36/79	50/79
		MOUSE	NP_034366.1	folylpolyglutamyl synthetase [Mus musculus]	305	5.00E-83	193/468	270/468
		FLY	FBgn0030407	CG2543	230	1.00E-60	146/394	211/394
		WORM	CE29283	status:Partially_confirmed TR:Q95QJ2 protein_id...	248	4.00E-66	161/451	237/451
		POMBE	SPBC1709.17	folylpolyglutamate synthase (predicted)	370	e-103	212/494	289/494
YOR300W	YOR300W	HUMAN	NP_003419.1	zinc finger protein 84 (HPF2) [Homo sapiens]	26	5.9	Nov-38	19/34
		MOUSE	XP_207093.2	similar to 60S RIBOSOMAL PROTEIN L13 [Mus muscu...	27	2.4	29/94	42/94
		FLY	FBgn0051163	CG31163	32	0.083	22/71	31/71
		WORM	CE24404	locus:haf-7 status:Partially_confirmed TR:Q9U2...	28	0.65	22/77	38/77
		POMBE	SPAC637.12c	MYST-family HAT (pers. comm. S. Forsburg)	27	0.45	13/24	14/24
YOR308C	SNU66	HUMAN	NP_005137.1	squamous cell carcinoma antigen recognized by T...	55	2.00E-07	128/642	233/642
		MOUSE	NP_058578.2	squamous cell carcinoma antigen recognized by T...	50	5.00E-06	20/37	28/37
		FLY	FBgn0032388	CG6686	43	4.00E-04	123/649	232/649
		WORM	CE27372	status:Partially_confirmed TR:O01524 protein_id...	42	8.00E-04	16/32	22/32
		POMBE	SPAC167.03c	involved in mRNA splicing	92	1.00E-19	142/639	252/639
YOR349W	CIN1	HUMAN	NP_002261.2	transportin 1; karyopherin (importin) beta 2; i...	37	0.096	27/82	41/82
		MOUSE	NP_848831.1	transportin 1; karyopherin (importin) beta 2 [M...	37	0.081	27/82	41/82
		FLY	FBgn0027509	CG7261	45	3.00E-04	40/178	78/178
		WORM	CE09437	status:Partially_confirmed TR:Q19493 protein_id:...	36	0.085	42/187	78/187
		POMBE	SPBC11C11.04(	tubulin specific chaperone (cofactor D)	39	0.003	49/192	82/192
YOR368W	RAD17	HUMAN	NP_003494.1	CDC7 cell division cycle 7; Cell division cycle...	30	3.9	20/64	31/64
		MOUSE	NP_033993.1	cell division cycle 7; cell division cycle 7-li...	32	0.51	27/89	40/89
		FLY	FBgn0026375	RhoGAPp190	32	0.81	25/111	44/111
		WORM	CE24884	status:Partially_confirmed TR:Q9N6F2 protein_id:...	31	0.93	35/136	56/136
		POMBE	SPAC1952.07	involved in DNA repair (PMID 7254221)	63	8.00E-11	65/280	122/280
YPL008W	CHL1	HUMAN	NP_085911.1	DEAD/H (Asp-Glu-Ala-Asp/His) box polypeptide 11...	401	e-112	295/937	445/937
		MOUSE	XP_128714.3	RIKEN cDNA 4732462I11 gene [Mus musculus]	395	e-110	290/954	444/954
		FLY	FBgn0026876	CG11403	340	2.00E-93	276/936	436/936
		WORM	CE03493	CHL1 protein status:Partially_confirmed TR:Q214...	322	5.00E-88	257/927	420/927
		POMBE	SPAC3G6.11	DEAD/DEAH box helicase (predicted)	449	e-127	294/884	462/884
YPL017C	YPL017C	HUMAN	NP_000099.1	dihydrolipoamide dehydrogenase precursor; E3 co...	250	1.00E-66	155/486	246/486
		MOUSE	NP_031887.2	dihydrolipoamide dehydrogenase [Mus musculus]	244	7.00E-65	152/484	245/484
		FLY	FBgn0036762	CG7430	248	7.00E-66	154/465	238/465
		WORM	CE31971	dihydrolipoamide dehydrogenase status:Confirmed T...	255	4.00E-68	158/465	248/465
		POMBE	SPAC1002.09c	dihydrolipoamide dehydrogenase (predicte...	276	4.00E-75	165/470	253/470
YPL018W	CTF19	HUMAN	NP_671695.1	A-kinase anchor protein 9 isoform 4; yotiao; A-...	33	0.24	18/64	39/64
		MOUSE	NP_033775.1	activation-induced cytidine deaminase; activati...	33	0.21	27/106	48/106
		FLY	FBgn0039490	CG5882	32	0.43	25/76	35/76
		WORM	CE18439	zinc finger protein status:Predicted TR:O61872 pro...	31	1.1	25/78	38/78
		POMBE	SPBC1685.04	sequence orphan	30	0.49	16/46	32/46
YPL022W	RAD1	HUMAN	NP_005227.1	excision repair cross-complementing rodent repa...	395	e-109	299/1014	494/1014
		MOUSE	NP_056584.1	excision repair cross-complementing rodent repa...	379	e-105	294/1003	474/1003
		FLY	FBgn0002707	mei-9: meiotic 9	347	2.00E-95	270/976	461/976
		WORM	CE24855	DNA repair protein RAD16 like status:Partially_...	207	2.00E-53	234/1010	428/1010
		POMBE	SPCC970.01	ss DNA endonuclease	456	e-129	333/1020	507/1020
YPL024W	NCE4	HUMAN	NP_079221.1	chromosome 9 open reading frame 76 [Homo sapiens]	28	7.3	16/38	19/38
		MOUSE	XP_354745.1	similar to mitogen regulated protein 4 precurso...	30	1.6	13/48	29/48
		FLY	FBgn0040232	cmet: CENP-meta	31	0.68	14/41	24/41
		WORM	CE16168	casein kinase status:Partially_confirmed TR:O18...	34	0.054	19/62	30/62
		POMBE	SPAC26A3.03c	hypothetical protein	39	6.00E-04	41/191	80/191
YPL027W	SMA1	HUMAN	NP_079050.2	hypothetical protein FLJ21924 [Homo sapiens]	33	0.23	29/107	46/107
		MOUSE	NP_035859.1	excision repair cross-complementing rodent repa...	29	2.2	15/53	30/53
		FLY	FBgn0036448	CG9311	28	3.5	15/56	28/56
		WORM	CE05160	locus:dnj-2 DNAJ protein like status:Partially_c...	28	3	18/54	28/54
		POMBE	SPAPB1E7.11c	sequence orphan	27	2.4	18/77	34/77
YPL047W	SGF11	HUMAN	XP_375456.1	hypothetical protein DKFZp761G2113 [Homo sapiens]	39	5.00E-04	18/41	24/41
		MOUSE	XP_126779.3	similar to CG13379-PA [Mus musculus]	39	4.00E-04	18/41	24/41
		FLY	FBgn0036804	CG13379	33	0.021	18/54	28/54
		WORM	CE00238	Zinc-finger motif C2H2 type status:Partially_con...	28	0.86	15/68	33/68
		POMBE	SPBC1734.06	zinc finger protein	28	0.26	Oct-36	17/32
YPL055C	LGE1	HUMAN	XP_029353.3	KIAA1509 [Homo sapiens]	30	2.3	17/45	25/45
		MOUSE	NP_766331.1	RIKEN cDNA A430081P20 [Mus musculus]	30	1.5	20/57	24/57
		FLY	FBgn0052705	CG32705	32	0.49	20/73	34/73
		WORM	CE35283	locus:pqn-31 status:Partially_confirmed TN:AAQ...	34	0.086	22/100	44/100
		POMBE	SPAC1D4.14	THO complex (predicted)	32	0.15	20/94	40/94
YPL059W	GRX5	HUMAN	NP_057501.2	chromosome 14 open reading frame 87 [Homo sapiens]	109	6.00E-25	48/90	69/90
		MOUSE	NP_082695.1	RIKEN cDNA 2900070E19 [Mus musculus]	109	5.00E-25	48/90	69/90
		FLY	FBgn0030584	CG14407	96	7.00E-21	38/93	68/93
		WORM	CE22220	status:Confirmed TR:Q9XTU9 protein_id:CAB11547.1	107	2.00E-24	54/98	67/98
		POMBE	SPAPB2B4.02	PICOT domain	126	1.00E-30	62/109	78/109
YPL061W	ALD6	HUMAN	NP_000681.2	mitochondrial aldehyde dehydrogenase 2 precurso...	444	e-125	226/475	314/475
		MOUSE	NP_033786.1	aldehyde dehydrogenase 2, mitochondrial [Mus mu...	442	e-124	226/475	312/475
		FLY	FBgn0032114	CG3752	429	e-120	226/480	313/480
		WORM	CE23852	locus:alh-2 aldehyde dehydrogenase status:Predi...	463	e-130	232/475	330/475

		POMBE	SPAC9E9.09c	aldehyde dehydrogenase (predicted)	475	e-135	240/490	328/490
YPL125W	KAP120	HUMAN	NP_057422.3	Ran binding protein 11 [Homo sapiens]	275	1.00E-73	253/1034	454/1034
		MOUSE	NP_083941.2	importin 11 [Mus musculus]	280	4.00E-75	258/1042	459/1042
		FLY	FBgn0053139	Ranbp11	168	2.00E-41	231/1093	428/1093
		WORM	CE27001	locus:imb-5 importin beta, nuclear transport fa...	41	0.004	29/120	54/120
		POMBE	SPCC1322.06	karyopherin	282	2.00E-76	252/1021	448/1021
YPL179W	PPQ1	HUMAN	NP_002699.1	protein phosphatase 1, catalytic subunit, alpha...	367	e-102	174/299	218/299
		MOUSE	NP_114074.1	protein phosphatase 1, catalytic subunit, alpha...	366	e-101	173/299	218/299
		FLY	FBgn0004103	Pp1-87B: Protein phosphatase 1 at 87B	367	e-101	172/294	215/294
		WORM	CE20735	locus:gsp-1 serine\threonine protein phosphata...	369	e-102	175/299	220/299
		POMBE	SPAC57A7.08	serine/threonine protein phosphatase	373	e-104	180/348	236/348
YPL194W	DDC1	HUMAN	NP_787061.1	transcription factor ELYS [Homo sapiens]	35	0.21	41/214	81/214
		MOUSE	NP_062632.2	soc-2 (suppressor of clear) homolog; Ras-bindin...	33	0.51	23/81	37/81
		FLY	FBgn0032223	GATAd	35	0.16	35/172	72/172
		WORM	CE25769	status:Predicted TR:Q9N5Y9 protein_id:AAF60370.2	39	0.006	48/242	97/242
		POMBE	SPAC29E6.03c	involved in intracellular protein ...	34	0.047	48/243	95/243
YPL213W	LEA1	HUMAN	NP_003081.1	u2 small nuclear ribonucleoprotein polypeptide ...	59	4.00E-09	59/220	98/220
		MOUSE	NP_067311.3	U2 small nuclear ribonucleoprotein polypeptide ...	58	6.00E-09	58/220	98/220
		FLY	FBgn0033210	U2A	64	7.00E-11	59/251	115/251
		WORM	CE20974	status:Confirmed SW:RU2A_CAEEL protein_id:AAK31...	71	5.00E-13	49/186	93/186
		POMBE	SPBC1861.08c	U2 snRNP complex	81	1.00E-16	59/196	94/196
YPL241C	CIN2	HUMAN	NP_115786.1	golgi-associated microtubule-binding protein HO...	34	0.12	29/117	50/117
		MOUSE	NP_083799.2	DEP domain containing 1 [Mus musculus]	35	0.06	23/70	33/70
		FLY	FBgn0029873	CG3918	36	0.025	34/136	60/136
		WORM	CE36222	locus:exc-4 chloride channel status:Confirmed...	31	0.7	25/102	41/102
		POMBE	SPBC146.03c	condensin subunit	35	0.01	34/87	42/87
YPR032W	SRO7	HUMAN	XP_045911.6	tomosyn-like [Homo sapiens]	78	4.00E-14	122/543	211/543
		MOUSE	NP_766028.1	RIKEN cDNA A830015P08 [Mus musculus]	75	2.00E-13	120/543	210/543
		FLY	FBgn0030412	tomosyn	60	5.00E-09	58/240	102/240
		WORM	CE36463	locus:vab-10 status:Partially_confirmed	35	0.15	36/150	66/150
		POMBE	SPAC1F3.03	WD repeat protein	237	7.00E-63	218/905	394/905
YPR042C	PUF2	HUMAN	NP_055491.1	pumilio homolog 1 [Homo sapiens]	51	5.00E-06	53/228	97/228
		MOUSE	NP_109647.1	pumilio 1 [Mus musculus]	54	7.00E-07	54/229	99/229
		FLY	FBgn0003165	pum: pumilio	53	1.00E-06	35/144	66/144
		WORM	CE31253	locus:puf-9 pumilo repeats status:Partially_con...	57	6.00E-08	69/308	126/308
		POMBE	SPBC56F2.08c	RNA-binding protein	249	1.00E-66	174/546	274/546
YPR046W	MCM16	HUMAN	NP_976221.1	high density lipoprotein binding protein; vigil...	39	0.003	34/167	75/167
		MOUSE	NP_898837.1	Cdc42 binding protein kinase beta [Mus musculus]	41	4.00E-04	38/156	72/156
		FLY	FBgn0000246	c(3)G: crossover suppressor on 3 of Gowan	34	0.038	27/117	51/117
		WORM	CE03434	status:Partially_confirmed TR:Q21022 protein_id:...	34	0.043	33/163	77/163
		POMBE	SPAC1556.01c	involved in DNA repair	33	0.027	40/162	73/162
YPR047W	MSF1	HUMAN	NP_006558.1	phenylalanine-tRNA synthetase [Homo sapiens]	303	2.00E-82	164/454	247/454
		MOUSE	NP_077236.1	phenylalanine-tRNA synthetase 1 (mitochondrial)...	311	7.00E-85	174/454	250/454
		FLY	FBgn0020766	Aats-phe: Phenylalanyl-tRNA synthetase	310	1.00E-84	177/460	258/460
		WORM	CE26224	status:Confirmed TR:Q9U1Z3 protein_id:CAC14396.3	273	2.00E-73	170/475	252/475
		POMBE	SPCC736.03c	phenylalanyl-tRNA synthetase	353	3.00E-98	186/442	280/442
YPR067W	ISA2	HUMAN	NP_919255.1	HESB like domain containing 1 [Homo sapiens]	45	2.00E-05	31/110	45/110
		MOUSE	XP_203592.1	RIKEN cDNA 0710001C05 [Mus musculus]	45	2.00E-05	31/110	45/110
		FLY	FBgn0039205	CG13623	40	0.001	21/51	28/51
		WORM	CE35683	status:Partially_confirmed TN:CAA22453 protein....	42	1.00E-04	25/113	48/113
		POMBE	SPBC3B9.17	iron-sulfur protein (predicted) (PMID 11941510...	40	2.00E-04	44/181	70/181
YPR120C	CLB5	HUMAN	NP_114172.1	cyclin B1; G2/mitotic-specific cyclin B1 [Homo ...	158	6.00E-39	81/226	137/226
		MOUSE	NP_031656.1	cyclin B2 [Mus musculus]	160	2.00E-39	90/264	154/264
		FLY	FBgn0000405	CycB: Cyclin B	132	5.00E-31	81/283	149/283
		WORM	CE28122	locus:cyb-2.1 cyclin B status:Partially_confir...	117	8.00E-27	73/187	105/187
		POMBE	SPBC582.03	cyclin	206	4.00E-54	104/225	145/225
YPR135W	CTF4	HUMAN	NP_009017.1	WD repeat and HMG-box DNA binding protein 1; AN...	92	1.00E-18	151/720	263/720
		MOUSE	NP_766186.2	RIKEN cDNA D630024B06 [Mus musculus]	67	7.00E-11	146/703	244/703
		FLY	FBgn0033972	CG12797	37	0.04	24/97	45/97
		WORM	CE02005	status:Partially_confirmed SW:YRG5_CAEEL protein...	34	0.38	23/94	41/94
		POMBE	SPAPB1E7.02c	WD repeat protein	207	5.00E-54	222/925	380/925
YPR141C	KAR3	HUMAN	XP_371813.1	kinesin family member C1 [Homo sapiens]	261	2.00E-69	161/388	215/388
		MOUSE	NP_058041.1	kinesin family member C1 [Mus musculus]	259	4.00E-69	160/385	214/385
		FLY	FBgn0002924	ncd: non-claret disjunctional	249	4.00E-66	149/374	216/374
		WORM	CE01083	locus:klp-3 kinesin like protein status:Partial...	215	7.00E-56	135/352	194/352
		POMBE	SPAC664.10	kinesin-like protein	370	e-103	227/545	310/545
YPR164W	MMS1	HUMAN	NP_998783.1	suppression of tumorigenicity 5 isoform 1 [Homo...	32	2.6	22/89	39/89
		MOUSE	NP_035438.1	nuclear receptor co-repressor 1; retinoid X rec...	33	1.3	25/107	50/107
		FLY	FBgn0038279	CG3837	33	0.91	55/235	100/235
		WORM	CE33214	status:Partially_confirmed TR:Q86S59 protein_id...	35	0.35	24/87	40/87
		POMBE	SPAC17H9.06c	serine-rich protein	34	0.12	45/187	78/187

Appendix 6 A subset of yeast CIN genes identify human homologues that are mutated in cancer or are associated with other human diseases

Human proteins from RefSeq with BLASTp alignments to 293 yeast CIN protein queries (e-value $<10^{-10}$, July 2004) were searched against OMIM (www.ncbi.nlm.nih.gov/omim) and cancer census (Futreal et al., 2004) protein datasets for disease association. Top hit alignments (Rank of hit = 1) (including ones shown in Table II.3 already) and non-top alignments (rank of hit >1 and e-value $<10^{-10}$) are shown.

Top Hits mutated in cancer

Yeast ORF	Yeast Gene	Human Hit	Huam Protein Hit Description	NP#	E-value	Rank of hit	Disease Description, OMIM#	MIM#	Reference
YMR120C	ADE17	ATIC	5-aminoimidazole-4-carboxamide ribonucleotide formyltransferase/IMP cyclohydrolase; AICARFT/IMPCHASE	NP_004035.2	0	1	Anaplastic large cell lymphoma		Cancer census
YGL163C	RAD54	RAD54L	RAD54-like protein	NP_003570.1	1E-164	1	Non-Hodgkin lymphoma; Breast cancer, invasive intraductal; Colon adenocarcinoma	603615	OMIM
YAL016W	TPD3	PPP2AR1B	beta isoform of regulatory subunit A, protein phosphatase 2 isoform b	NP_859050.1	1E-133	1	Lung cancer, 211980	603113	OMIM
YER095W	RAD51	RAD51	RAD51 homolog protein isoform 1; RecA-like protein	NP_002866.2	1E-122	1	susceptibility to Breast cancer, 114480	179617	OMIM
YBR073W	RDH54	RAD54B	RAD54 homolog B isoform 1	NP_036547.1	1E-121	1	Non-Hodgkin lymphoma; Colon adenocarcinoma	604289	OMIM
YMR190C	SGS1	BLM	Bloom syndrome protein	NP_000048.1	1E-115	1	Bloom syndrome, 210900	604610	OMIM, Cancer census
YPL022W	RAD1	ERCC4	excision repair cross-complementing rodent repair deficiency, complementation group 4	NP_005227.1	1E-109	1	Xeroderma pigmentosum, group F, 278760	133520	OMIM, Cancer census
YMR224C	MRE11	MRE11A	meiotic recombination 11 homolog A isoform 1	NP_005582.1	1E-108	1	Ataxia-telangiectasia-like disorder, 604391	600814	OMIM
YDL101C	DUN1	CHK2	checkpoint-like protein CHK2	NP_009125.1	6E-55	1	Li-Fraumeni syndrome, 151623; Osteosarcoma, somatic, 259500; susceptibility to Breast cancer, 114480; Prostate cancer, familial, 176807; susceptibility to colorectal cancer	604373	OMIM
YGR188C	BUB1	BUB1	BUB1 budding uninhibited by benzimidazoles 1 homolog	NP_004327.1	1E-41	1	Colorectal cancer with chromosomal instability	602452	OMIM
YGL086W	MAD1	MAD1	MAD1 (mitotic arrest deficient, yeast, homolog)-like 1	NP_003541.1	5E-12	1	Lymphoma, somatic; Prostate cancer, somatic, 176807	602686	OMIM
YLR418C	CDC73	HRPT2	parafibromin	NP_078805.3	9E-12	1	Hyperparathyroidism-jaw tumor syndrome, 145001; Hyperparathyroidism, familial primary, 145000; Parathyroid adenoma with cystic changes, 145001	607393	OMIM

Non-top Hits mutated in cancer (top hit is also mutated in cancer)

Yeast ORF	Yeast Gene	Human Hit	Huam Protein Hit Description	NP#	E-value	Rank of hit	Disease Description, OMIM#	MIM#	Reference
YGL163C	RAD54	RAD54B	RAD54 homolog B isoform 1; RAD54, S. cerevisiae, homolog of, B	NP_036547.1	1E-124	2	Non-Hodgkin lymphoma; Colon adenocarcinoma	604289	OMIM
YBR073W	RDH54	RAD54L	RAD54-like protein; RAD54 homolog	NP_003570.1	1E-102	2	Non-Hodgkin lymphoma; Breast cancer, invasive intraductal; Colon adenocarcinoma	603615	OMIM
YGL163C	RAD54	ERCC6	excision repair cross-complementing rodent repair deficiency, complementation group 6; Rad26 (yeast) homolog	NP_000115.1	1E-65	3	Cockayne syndrome-2, type B; Cerebrooculofacioskeletal syndrome, 214150; De Sanctis-Cacchione syndrome, 278800	133540	OMIM
YBR073W	RDH54	ERCC6	excision repair cross-complementing rodent repair deficiency, complementation group 6; Rad26 (yeast) homolog	NP_000115.1	8E-61	3	Cockayne syndrome-2, type B; Cerebrooculofacioskeletal syndrome, 214150; De Sanctis-Cacchione syndrome, 278800	133540	OMIM
YMR190C	SGS1	WRN	Werner syndrome protein; Werner Syndrome helicase	NP_000544.1	2E-67	5	Werner syndrome, 277700	604611	OMIM, Cancer census
YMR190C	SGS1	RECQL4	RecQ protein-like 4; RecQ protein 4	NP_004251.1	2E-45	6	Rothmund-Thomson syndrome, 268400	603780	OMIM, Cancer census
YMR190C	SGS1	DDX6	DEAD (Asp-Glu-Ala-Asp) box polypeptide 6	NP_004388	2.00E-12	7	B-cell Non-Hodkin Lymphoma		Cancer census
YER095W	RAD51	RAD51L1	RAD51-like 1 isoform 1; RecA-like protein; recombination repair protein; DNA repair protein RAD51 homolog 2; RAD51 homolog B	NP_002868.1	8E-22	6	Lipoma, Uterine leiomyoma		Cancer census
YDL101C	DUN1	AKT2	v-akt murine thymoma viral oncogene homolog 2; Murine thymoma viral (v-akt) homolog-2; rac protein kinase beta	NP_001617.1	2E-24	137	Ovarian tumor, Pancreatic tumor		Cancer census
YDL101C	DUN1	CDK6	cyclin-dependent kinase 6	NP_001250.1	2E-22	156	acute lymphocytic leukemia		Cancer census
YDL101C	DUN1	STK11	serine/threonine protein kinase 11	NP_000446.1	8E-22	175	Peutz-Jeghers syndrome, 175200; Melanoma, malignant sporadic; Pancreatic cancer, sporadic	602216	OMIM, Cancer census
YDL101C	DUN1	PRKCA	protein kinase C, alpha; Protein kinase C, alpha polypeptide	NP_002728.1	9E-21	192	Pituitary tumor, invasive	176960	OMIM
YDL101C	DUN1	PIM1	pim-1 oncogene; Oncogene PIM1	NP_002639.1	8E-19	231	Non-Hodgkin lymphoma		Cancer census

YDL101C	DUN1	CDK4	cyclin-dependent kinase 4; cell division kinase 4; melanoma cutaneous malignant, 3	NP_000066.1	2E-18	239	Melanoma	123829	OMIM, Cancer census
YDL101C	DUN1	ABL1	v-abl Abelson murine leukemia viral oncogene homolog 1 isoform b; Abelson murine leukemia viral (v-abl) oncogene homolog 1; proto-oncogene tyrosine-protein kinase ABL1	NP_009297.1	4E-15	321	Leukemia, Philadelphia chromosome-positive, resistant to Imatinib	189980	OMIM
YDL101C	DUN1	ABL1	v-abl Abelson murine leukemia viral oncogene homolog 1 isoform a; Abelson murine leukemia viral (v-abl) oncogene homolog 1; proto-oncogene tyrosine-protein kinase ABL1	NP_005148.1	4E-15	320	Chronic myeloid leukemia, Acute lymphocytic leukemia		Cancer census
YDL101C	DUN1	BRAF	v-raf murine sarcoma viral oncogene homolog B1; Murine sarcoma viral (v-raf) oncogene homolog B1	NP_004324.2	2E-13	349	Melanoma, melignant, somatic; Colorectal cancer, somatic; Adenocarcinoma of lung, somatic, 211980; Nonsmall cell lung cancer, somatic	164757	OMIM, Cancer census
YDL101C	DUN1	ABL2	v-abl Abelson murine leukemia viral oncogene homolog 2 isoform a; Abelson murine leukemia viral (v-abl) oncogene homolog 2; Abelson-related gene	NP_005149.2	1E-11	393	Acute myelogenous leukemia		Cancer census
YDL101C	DUN1	LCK	lymphocyte-specific protein tyrosine kinase; oncogene LCK; membrane associated protein tyrosine kinase	NP_005347.2	4E-11	407	T-cell acute lymphoblastic leukemia		Cancer census
Non-top Hits mutated in cancer									
Yeast ORF	**Yeast Gene**	**Human Hit**	**Huam Protein Hit Description**	**NP#**	**E-value**	**Rank of hit**	**Disease Description, OMIM#**	**MIM#**	**Reference**
YAL019W	FUN30	ERCC6	excision repair cross-complementing rodent repair deficiency, complementation group 6; Rad26 (yeast) homolog	NP_000115.1	1E-59	19	Cockayne syndrome-2, type B; Cerebrooculofacioskeletal syndrome, 214150; De Sanctis-Cacchione syndrome, 278800	133540	OMIM
YAL019W	FUN30	RAD54B	RAD54 homolog B isoform 1; RAD54, S. cerevisiae, homolog of, B	NP_036547.1	2E-53	21	Non-Hodgkin lymphoma; Colon adenocarcinoma	604289	OMIM
YAL019W	FUN30	RAD54L	RAD54-like protein; RAD54 homolog	NP_003570.1	5E-46	24	Non-Hodgkin lymphoma; Breast cancer, invasive intraductal; Colon adenocarcinoma	603615	OMIM
YPL008W	CHL1	BRIP1	BRCA1 interacting protein C-terminal helicase 1	NP_114432.1	9E-56	4	Breast cancer, early-onset, 114480	605882	OMIM
YPL008W	CHL1	ERCC2	excision repair cross-complementing rodent repair deficiency, complementation group 2 protein; malignancy-associated protein	NP_000391.1	1E-24	8	Xeroderma pigmentosum, group D, 278730; Trichothiodystrophy, 601675; Cerebrooculofacioskeletal syndrome, 214150	126340	OMIM, Cancer census
YDR194C	MSS116	DDX10	DEAD (Asp-Glu-Ala-Asp) box polypeptide 10	NP_004389.2	2E-45	2	Acute myelogenous leukemia		Cancer census
YDR194C	MSS116	EIF4A2	eukaryotic translation initiation factor 4A, isoform 2	NP_001958.1	7E-37	19	Non-Hodgkin lymphoma		Cancer census
YDR334W	SWR1	ERCC6	excision repair cross-complementing rodent repair deficiency, complementation group 6; Rad26 (yeast) homolog	NP_000115.1	1E-44	19	Cockayne syndrome-2, type B; Cerebrooculofacioskeletal syndrome, 214150; De Sanctis-Cacchione syndrome, 278800	133540	OMIM
YDR334W	SWR1	RAD54B	RAD54 homolog B isoform 1; RAD54, S. cerevisiae, homolog of, B	NP_036547.1	4E-33	24	Non-Hodgkin lymphoma; Colon adenocarcinoma	604289	OMIM
YDR334W	SWR1	RAD54L	RAD54-like protein; RAD54 homolog	NP_003570.1	2E-27	26	Non-Hodgkin lymphoma; Breast cancer, invasive intraductal; Colon adenocarcinoma	603615	OMIM
YKR024C	DBP7	DDX10	DEAD (Asp-Glu-Ala-Asp) box polypeptide 10	NP_004389.2	7E-41	4	Acute myelogenous leukemia		Cancer census
YKR024C	DBP7	EIF4A2	eukaryotic translation initiation factor 4A, isoform 2	NP_001958.1	1E-20	32	Non-Hodgkin lymphoma		Cancer census
YBR009C	HHF1	HIST1H4I	histone 1, H4i (H4FM)	NP_003486	1.00E-37	10	Non-Hodgkin lymphoma		Cancer census
YNL250W	RAD50	MYH11	smooth muscle myosin heavy chain 11 isoform SM1	NP_002465.1	4E-25	11	Acute myelogenous leukemia		Cancer census
YNL250W	RAD50	MYH9	myosin, heavy polypeptide 9, non-muscle	NP_002464.1	2E-20	26	Anaplastic large cell lymphoma		Cancer census
YNL250W	RAD50	TRIP11	thyroid hormone receptor interactor 11; thyroid receptor interacting protein 11	NP_004230.1	1E-19	30	Acute myelogenous leukemia		Cancer census
YNL250W	RAD50	TPR	translocated promoter region (to activated MET oncogene); Tumor potentiating region (translocated promoter region)	NP_003283.1	8E-19	33	Papillary thyroid tumor		Cancer census
YNL250W	RAD50	ELKS	Rab6-interacting protein 2 isoform alpha	NP_055879.1	1E-18	34	Papillary thyroid tumor		Cancer census
YNL250W	RAD50	CEP1	centrosomal protein 1; centriole associated protein; centriolin	NP_008949.3	7E-16	47	Non-Hodgkin lymphoma		Cancer census
YNL250W	RAD50	NUMA1	nuclear mitotic apparatus protein 1	NP_006176.1	6E-12	85	Leukemia, acute promyelocytic, NUMA/RARA type	164009	OMIM, Cancer census
YNL250W	RAD50	GOLGA5	Golgi autoantigen, golgin subfamily a, 5; golgin-84; ret-fused gene 5	NP_005104.2	2E-11	95	Thyroid carcinoma, papillary, 188550	606918	OMIM, Cancer census

YDR004W	RAD57	RAD51L1	RAD51-like 1 isoform 1	NP_002868.1	4E-19	3	Lipoma, uterine leiomyoma		Cancer census
YDR004W	RAD57	XRCC3	X-ray repair cross complementing protein 3; X-ray-repair, complementing defective, repair in Chinese hamster; DNA repair protein XRCC3	NP_005423.1	2E-17	4	susceptibility to Melanoma, cutaneous malignant; susceptibility to Breast cancer	600675	OMIM
YDR004W	RAD57	RAD51	RAD51 homolog protein isoform 1; RAD51, S.cerevisiae, homolog of, A; recombination protein A; RecA, E. coli, homolog of; RecA-like protein; DNA repair protein RAD51 homolog 1	NP_002866.2	7E-15	7	susceptibility to Breast cancer, 114480	179617	OMIM
YKL113C	RAD27	ERCC5	xeroderma pigmentosum complementation group G	NP_000114.1	7E-14	6	Xeroderma pigmentosum, group G, 278780; Cerebrooculofacioskeletal syndrome, 214150	133530	OMIM, Cancer census
YCR065W	HCM1	FOXO1A	forkhead box O1A	NP_002006.2	3E-13	49	Rhabdomyosarcoma, alveolar, 268220	136533	OMIM, Cancer census
YCR065W	HCM1	FOXO3A	forkhead box O3A; forkhead (Drosophila) homolog (rhabdomyosarcoma) like 1; forkhead, Drosophila, homolog of, in rhabdomyosarcoma-like 1	NP_001446.1	1E-12	52	Acute leukemia		Cancer census
YCR065W	HCM1	MLLT7	myeloid/lymphoid or mixed-lineage leukemia (trithorax homolog, Drosophila); translocated to, 7; myeloid/lymphoid or mixed-lineage leukemia (trithorax (Drosophila) homolog); translocated to, 7	NP_005929.1	2E-12	53	Acute leukemia		Cancer census
YPR120C	CLB5	CCND1	G1/S-specific cyclin D1	NP_444284.1	3E-15	11	Parathyroid adenomatosis 1; Centrocytic lymphoma; Multiple myeloma, 254500; modification of von Hippel-Lindau disease, 193300; susceptibility to Colorectal cancer	168461	OMIM
YPR120C	CLB5	CCND2	cyclin D2	NP_001750	6.00E-11	13	non Hodgkin lymphoma, chronic lymphatic leukemia		Cancer census
YLR032W	RAD5	RAD54L	RAD54-like protein	NP_003570.1	2E-13	30	Non-Hodgkin lymphoma; Breast cancer, invasive intraductal; Colon adenocarcinoma	603615	OMIM
YLR032W	RAD5	RAD54B	RAD54 homolog B isoform 1; RAD54, S. cerevisiae, homolog of, B	NP_036547.1	4E-13	32	Non-Hodgkin lymphoma; Colon adenocarcinoma	604289	OMIM
YLR032W	RAD5	ERCC6	excision repair cross-complementing rodent repair deficiency, complementation group 6; Rad26 (yeast) homolog	NP_000115.1	5E-12	33	Cockayne syndrome-2, type B; Cerebrooculofacioskeletal syndrome, 214150; De Sanctis-Cacchione syndrome, 278800	133540	OMIM
YDL025C	YDL025C	PIM1	pim-1 oncogene	NP_002639.1	3E-17	29	Non-Hodgkin lymphoma		Cancer census
YDL025C	YDL025C	AKT2	v-akt murine thymoma viral oncogene homolog 2; Murine thymoma viral (v-akt) homolog-2; rac protein kinase beta	NP_001617.1	6E-17	39	Ovarian tumor, Pancreatic tumor		Cancer census
YDL025C	YDL025C	CHEK2	protein kinase CHK2 isoform a; checkpoint-like protein CHK2; serine/threonine-protein kinase CHK2	NP_009125.1	1E-15	68	Li-Fraumeni syndrome, 151623; Osteosarcoma, somatic, 259500; {Breast cancer, susceptibility to}, 114480; Prostate cancer, familial, 176807; {Breast and colorectal cancer, susceptibility to}	604373	OMIM
YDL025C	YDL025C	STK11	serine/threonine protein kinase 11	NP_000446.1	9E-15	105	Peutz-Jeghers syndrome, 175200; Melanoma, malignant sporadic; Pancreatic cancer, sporadic	602216	OMIM, Cancer census
YDL025C	YDL025C	CDK4	cyclin-dependent kinase 4; cell division kinase 4; melanoma cutaneous malignant, 3	NP_000066.1	7E-12	212	Melanoma	123829	OMIM, Cancer census
YDL155W	CLB3	CCND1	G1/S-specific cyclin D1	NP_444284.1	3E-13	12	Parathyroid adenomatosis 1; Centrocytic lymphoma; Multiple myeloma, 254500; modification of von Hippel-Lindau disease, 193300; susceptibility to Colorectal cancer	168461	OMIM
YEL013W	VAC8	CTNNB1	catenin (cadherin-associated protein), beta 1	NP_001895.1	2E-11	6	Colorectal cancer; Hepatoblastoma; Pilomatricoma, 132600; Ovarian carcinoma, endometrioid type; Hepatocellular carcinoma, 114550	116806	OMIM, Cancer census
YDL074C	BRE1	MYH9	myosin, heavy polypeptide 9, non-muscle	NP_002464.1	3E-14	6	Anaplastic large cell lymphoma		Cancer census
YDL074C	BRE1	TRIP11	thyroid hormone receptor interactor 11; thyroid receptor interacting protein 11	NP_004230.1	7E-14	8	Acute myelogenous leukemia		Cancer census
YDL074C	BRE1	MYH11	smooth muscle myosin heavy chain 11 isoform SM1	NP_002465.1	3E-12	13	Acute myelogenous leukemia		Cancer census

Top Hit associated with other diseases

Yeast ORF	Yeast Gene		Huam Protein Hit Description	NP#	E-value	Rank of hit	Disease Description, OMIM#	MIM#	Reference
YPL061W	ALD6		mitochondrial aldehyde dehydrogenase 2 precursor	NP_000681.2	1E-126	1	Alcohol intolerance, acute; Fetal alcohol syndrome	100650	OMIM
YPL017C	YPL017C		dihydrolipoamide dehydrogenase precursor; E3 component of pyruvate dehydrogenase	NP_000099.1	1E-66	1	Lipoamide dehydrogenase deficiency	246900	OMIM
YER007W	PAC2		beta-tubulin cofactor E	NP_003184.1	5E-33	1	Kenny-Caffey syndrome-1, 244460; Hypoparathyroidism-retardation-dysmorphism syndrome, 241410	604934	OMIM
YCR065W	HCM1		forkhead box L2; Blepharophimosis, epicanthus inversus, and ptosis 1; blepharophimosis, epicanthus inversus and ptosis; forkhead transcription factor FOXL2	NP_075555.1	1E-20	1	Blepharophimosis, epicanthus inversus, and ptosis, type 1, 110100; Blepharophimosis, epicanthus inversus, and ptosis, type 2, 110100	605597	OMIM

Non Top Hit associated with other diseases

Yeast ORF	Yeast Gene		Huam Protein Hit Description	NP#	E-value	Rank of hit	Disease Description, OMIM#	MIM#	Reference
YPL061W	ALD6		aldehyde dehydrogenase 5A1 precursor isoform 2; mitochondrial succinate semialdehyde dehydrogenase; NAD(+)-dependent succinic semialdehyde dehydrogenase	NP_001071.1	1E-69	12	Succinic semialdehyde dehydrogenase deficiency	271980	OMIM
YPL061W	ALD6		aldehyde dehydrogenase 5A1 precursor isoform 1; mitochondrial succinate semialdehyde dehydrogenase; NAD(+)-dependent succinic semialdehyde dehydrogenase	NP_733936.1	6E-67	14	Succinic semialdehyde dehydrogenase deficiency	271980	OMIM
YPL061W	ALD6		aldehyde dehydrogenase 6A1 precursor; mitochondrial acylating methylmalonate-semialdehyde dehydrogenase	NP_005580.1	1E-51	16	Methylmalonate semialdehyde dehydrogenase deficiency	603178	OMIM
YPL061W	ALD6		aldehyde dehydrogenase 4A1 precursor; mitochondrial delta-1-pyrroline 5-carboxylate dehydrogenase; P5C dehydrogenase	NP_733844.1	1E-29	18	Hyperprolinemia, type II, 239510	606811	OMIM
YPL061W	ALD6		aldehyde dehydrogenase 4A1 precursor; mitochondrial delta-1-pyrroline 5-carboxylate dehydrogenase; P5C dehydrogenase	NP_003739.2	1E-29	19	Hyperprolinemia, type II, 239510	606811	OMIM
YPL061W	ALD6		aldehyde dehydrogenase 3A2; aldehyde dehydrogenase 10; fatty aldehyde dehydrogenase	NP_000373.1	2E-25	23	Sjogren-Larsson syndrome	270200	OMIM
YGR270W	YTA7		valosin-containing protein; yeast Cdc48p homolog; transitional endoplasmic reticulum ATPase	NP_009057.1	3E-58	3	Inclusion body myopathy with early-onset Paget disease and frontotemporal dementia, 605382	601023	OMIM
YGR270W	YTA7		peroxisomal biogenesis factor 6; Peroxisomal biogenesis factor 6 (peroxisomal AAA-type ATPase 1); peroxisome biogenesis factor 6	NP_000278.2	3E-41	13	Peroxisomal biogenesis disorder, complementation group 4; Peroxisomal biogenesis disorder, complementation group 6	601498	OMIM
YGR270W	YTA7		spastin isoform 2	NP_955468.1	2E-40	14	Spastic paraplegia-4, 182601	604277	OMIM
YGR270W	YTA7		spastin isoform 1	NP_055761.2	2E-40	15	Spastic paraplegia-4, 182601	604277	OMIM
YGR270W	YTA7		peroxisome biogenesis factor 1	NP_000457.1	4E-38	19	Zellweger syndrome-1, 214100; Adrenoleukodystrophy, neonatal, 202370; Refsum disease, infantile, 266510	602136	OMIM
YGR270W	YTA7		paraplegin isoform 1; cell matrix adhesion regulator; cell adhesion regulator	NP_003110.1	3E-31	30	Spastic paraplegia-7	602783	OMIM
YGR270W	YTA7		paraplegin isoform 2; cell matrix adhesion regulator; cell adhesion regulator	NP_955399.1	1E-11	34	Spastic paraplegia-7	602783	OMIM
YDL101C	DUN1		phosphorylase kinase, gamma 2 (testis); Phosphorylase kinase, gamma 2 (testis/liver)	NP_000285.1	9E-42	34	Glycogenosis, hepatic, autosomal	172471	OMIM
YDL101C	DUN1		ribosomal protein S6 kinase, 90kDa, polypeptide 3; ribosomal protein S6 kinase, 90kD, polypeptide 3	NP_004577.1	7E-39	40	Coffin-Lowry syndrome, 303600; Mental retardation, X-linked nonspecific, type 19	300075	OMIM
YDL101C	DUN1		skeletal myosin light chain kinase	NP_149109.1	2E-27	112	Cardiomyopathy, hypertrophic, midventricular, digenic, 192600	606566	OMIM
YDL101C	DUN1		p21-activated kinase 3; bPAK; p21-activated kinase-3; hPAK3; CDKN1A	NP_002569.1	2E-25	126	Mental retardation, X-linked 30	300142	OMIM
YDL101C	DUN1		titin isoform novex-2; connectin; CMH9, included; cardiomyopathy, dilated 1G (autosomal dominant)	NP_597681.1	2E-25	130	Cardiomyopathy, familial hypertrophic, 9; Cardiomyopathy, dilated, 1G, 604145, Tibial muscular dystrophy, tardive, 600334	188840	OMIM

YDL101C	DUN1		titin isoform novex-1; connectin; CMH9, included; cardiomyopathy, dilated 1G (autosomal dominant)	NP_597676.1	2E-25	129	Cardiomyopathy, familial hypertrophic, 9; Cardiomyopathy, dilated, 1G, 604145, Tibial muscular dystrophy, tardive, 600334	188840	OMIM
YDL101C	DUN1		titin isoform N2-B; connectin; CMH9, included; cardiomyopathy, dilated 1G (autosomal dominant)	NP_003310.2	2E-25	127	Cardiomyopathy, familial hypertrophic, 9; Cardiomyopathy, dilated, 1G, 604145, Tibial muscular dystrophy, tardive, 600334	188840	OMIM
YDL101C	DUN1		titin isoform N2-A; connectin; CMH9, included; cardiomyopathy, dilated 1G (autosomal dominant)	NP_596869.1	2E-25	128	Cardiomyopathy, familial hypertrophic, 9; Cardiomyopathy, dilated, 1G, 604145, Tibial muscular dystrophy, tardive, 600334	188840	OMIM
YDL101C	DUN1		protein kinase C, gamma; Protein kinase C, gamma polypeptide	NP_002730.1	4E-18	249	Spinocerebellar ataxia 14, 605361	176980	OMIM
YDL101C	DUN1		rhodopsin kinase; G protein-coupled receptor kinase 1b	NP_002920.1	2E-17	257	Oguchi disease-2, 258100	180381	OMIM
YDL101C	DUN1		myosin IIIA	NP_059129.2	2E-16	284	Deafness, autosomal recessive 30, 607101	606808	OMIM
YDL101C	DUN1		interleukin-1 receptor-associated kinase 4; interleukin-1 receptor associated kinase 4	NP_057207.1	2E-12	371	IRAK4 deficiency, 607676	606883	OMIM
YDL101C	DUN1		myotonic dystrophy protein kinase; dystrophia myotonica 1	NP_004400.3	3E-12	373	Myotonic dystrophy, 160900	605377	OMIM
YDL101C	DUN1		zeta-chain (TCR) associated protein kinase 70kDa; Zeta-chain associated protein kinase, 70kD (syk-related tyrosine kinase); syk-related tyrosine kinase; zeta-chain (TCR) associated protein kinase (70 kD)	NP_001070.2	1E-11	387	Selective T-cell defect	176947	OMIM
YDL101C	DUN1		c-mer proto-oncogene tyrosine kinase	NP_006334.1	3E-11	404	Retinitis pigmentosa, MERTK-related, 268000	604705	OMIM
YPR141C	KAR3		kinesin family member 21A; NY-REN-62 antigen	NP_060111.2	1E-36	17	Fibrosis of extraocular muscles, congenital, 1, 135700	608283	OMIM
YPR141C	KAR3		kinesin family member 1B isoform b; kinesin superfamily protein KIF1B; Charcot-Marie-Tooth neuropathy 2A (hereditary motor sensory neuropathy II)	NP_055889.2	3E-35	23	Charcot-Marie-Tooth disease, type 2A, 118210	605995	OMIM
YPR141C	KAR3		kinesin family member 1B isoform alpha; kinesin superfamily protein KIF1B; Charcot-Marie-Tooth neuropathy 2A (hereditary motor sensory neuropathy II)	NP_904325.2	3E-35	24	Charcot-Marie-Tooth disease, type 2A, 118210	605995	OMIM
YPR141C	KAR3		kinesin family member 5A; spastic paraplegia 10 (autosomal dominant)	NP_004975.1	6E-35	26	Spastic paraplegia 10, 604187	602821	OMIM
YEL061C	CIN8		kinesin family member 21A; NY-REN-62 antigen	NP_060111.2	1E-35	16	Fibrosis of extraocular muscles, congenital, 1, 135700	608283	OMIM
YEL061C	CIN8		kinesin family member 1B isoform b; kinesin superfamily protein KIF1B; Charcot-Marie-Tooth neuropathy 2A (hereditary motor sensory neuropathy II)	NP_055889.2	3E-35	17	Charcot-Marie-Tooth disease, type 2A, 118210	605995	OMIM
YEL061C	CIN8		kinesin family member 1B isoform alpha; kinesin superfamily protein KIF1B; Charcot-Marie-Tooth neuropathy 2A (hereditary motor sensory neuropathy II)	NP_904325.2	3E-35	18	Charcot-Marie-Tooth disease, type 2A, 118210	605995	OMIM
YEL061C	CIN8		kinesin family member 5A; spastic paraplegia 10 (autosomal dominant)	NP_004975.1	4E-33	23	Spastic paraplegia 10, 604187	602821	OMIM
YHR092C	HXT4		solute carrier family 2 (facilitated glucose transporter), member 1	NP_006507.1	1E-31	3	Glucose transport defect, blood-brain barrier, 606777	138140	OMIM
YHR092C	HXT4		solute carrier family 2 (facilitated glucose transporter), member 2	NP_000331.1	4E-31	6	{Diabetes mellitus, noninsulin-dependent}; Fanconi-Bickel syndrome, 227810	138160	OMIM
YHR092C	HXT4		solute carrier family 2 (facilitated glucose transporter), member 4	NP_001033.1	2E-30	7	{Diabetes mellitus, noninsulin-dependent}	138190	OMIM
YBR073W	RDH54		transcriptional regulator ATRX isoform 1; RAD54 (Saccharomyces cerevisiae); DNA dependent ATPase and helicase; Zinc finger helicase; X-linked nuclear protein; helicase 2, X-linked	NP_000480.2	2E-31	23	Alpha-thalassemia/mental retardation syndrome, 301040; Juberg-Marsidi syndrome, 309590; Sutherland-Haan syndrome, 309470; Smith-Fineman-Myers syndrome, 309580; Alpha-thalassemia myelodysplasia syndrome, somatic, 300448; Sutherland-Haan syndrome-like, 300465	300032	OMIM

YBR073W	RDH54		transcriptional regulator ATRX isoform 3; RAD54 (Saccharomyces cerevisiae); DNA dependent ATPase and helicase; Zinc finger helicase; X-linked nuclear protein; helicase 2, X-linked	NP_612115.1	2E-31	25	Alpha-thalassemia/mental retardation syndrome, 301040; Juberg-Marsidi syndrome, 309590; Sutherland-Haan syndrome, 309470; Smith-Fineman-Myers syndrome, 309580; Alpha-thalassemia myelodysplasia syndrome, somatic, 300448; Sutherland-Haan syndrome-like, 300465	300032	OMIM
YBR073W	RDH54		transcriptional regulator ATRX isoform 2; RAD54 (Saccharomyces cerevisiae); DNA dependent ATPase and helicase; Zinc finger helicase; X-linked nuclear protein; helicase 2, X-linked	NP_612114.1	2E-31	24	Alpha-thalassemia/mental retardation syndrome, 301040; Juberg-Marsidi syndrome, 309590; Sutherland-Haan syndrome, 309470; Smith-Fineman-Myers syndrome, 309580; Alpha-thalassemia myelodysplasia syndrome, somatic, 300448; Sutherland-Haan syndrome-like, 300465	300032	OMIM
YBR073W	RDH54		SWI/SNF-related matrix-associated actin-dependent regulator of chromatin a-like 1; HepA-related protein; SMARCA-like protein 1	NP_054859.2	1E-16	35	Schimke immunoosseous dysplasia, 242900	606622	OMIM
YNL250W	RAD50		myosin heavy chain 6; myosin heavy chain, cardiac muscle alpha isoform	NP_002462.1	2E-25	9	Cardiomyopathy, familial hypertrophic, 192600	160710	OMIM
YNL250W	RAD50		desmoplakin; desmoplakin (DPI, DPII)	NP_004406.1	6E-25	12	Keratosis palmoplantaris striata II; Dilated cardiomyopathy with woolly hair and keratoderma, 605676; Arrhythmogenic right ventricular dysplasia 8, 607450; Skin fragility-woolly hair syndrome, 607655	125647	OMIM
YNL250W	RAD50		myosin, heavy polypeptide 7, cardiac muscle, beta	NP_000248.1	6E-25	13	Cardiomyopathy, familial hypertrophic, 1, 192600; ?Central core disease, one form; Cardiomyopathy, dilated, 115200; Myopathy, myosin storage, 608358	160760	OMIM
YNL250W	RAD50		myosin, heavy polypeptide 2, skeletal muscle, adult	NP_060004.2	5E-22	22	Inclusion body myopathy-3, 605637	160740	OMIM
YNL250W	RAD50		myosin, heavy polypeptide 9, non-muscle	NP_002464.1	2E-20	26	May-Hegglin anomaly, 155100; Fechtner syndrome, 153640; Sebastian syndrome, 605249; Deafness, autosomal dominant 17, 603622; Epstein syndrome, 153650	160775	OMIM
YNL250W	RAD50		plectin 1, intermediate filament binding protein 500kDa isoform 11; plectin 1, intermediate filament binding protein, 500kD	NP_958786.1	4E-12	79	Muscular dystrophy with epidermolysis bullosa simplex, 226670; Epidermolysis bullosa simplex, Ogna type, 131950	601282	OMIM
YNL250W	RAD50		plectin 1, intermediate filament binding protein 500kDa isoform 8; plectin 1, intermediate filament binding protein, 500kD	NP_958784.1	4E-12	81	Muscular dystrophy with epidermolysis bullosa simplex, 226670; Epidermolysis bullosa simplex, Ogna type, 131950	601282	OMIM
YNL250W	RAD50		plectin 1, intermediate filament binding protein 500kDa isoform 6; plectin 1, intermediate filament binding protein, 500kD	NP_958782.1	4E-12	82	Muscular dystrophy with epidermolysis bullosa simplex, 226670; Epidermolysis bullosa simplex, Ogna type, 131950	601282	OMIM
YNL250W	RAD50		plectin 1, intermediate filament binding protein 500kDa isoform 10; plectin 1, intermediate filament binding protein, 500kD	NP_958785.1	4E-12	77	Muscular dystrophy with epidermolysis bullosa simplex, 226670; Epidermolysis bullosa simplex, Ogna type, 131950	601282	OMIM
YNL250W	RAD50		plectin 1, intermediate filament binding protein 500kDa isoform 2; plectin 1, intermediate filament binding protein, 500kD	NP_958780.1	4E-12	83	Muscular dystrophy with epidermolysis bullosa simplex, 226670; Epidermolysis bullosa simplex, Ogna type, 131950	601282	OMIM
YNL250W	RAD50		plectin 1, intermediate filament binding protein 500kDa isoform 8; plectin 1, intermediate filament binding protein, 500kD	NP_958783.1	4E-12	78	Muscular dystrophy with epidermolysis bullosa simplex, 226670; Epidermolysis bullosa simplex, Ogna type, 131950	601282	OMIM
YNL250W	RAD50		plectin 1, intermediate filament binding protein 500kDa isoform 3; plectin 1, intermediate filament binding protein, 500kD	NP_958781.1	4E-12	80	Muscular dystrophy with epidermolysis bullosa simplex, 226670; Epidermolysis bullosa simplex, Ogna type, 131950	601282	OMIM
YNL250W	RAD50		plectin 1, intermediate filament binding protein 500kDa isoform 1; plectin 1, intermediate filament binding protein, 500kD	NP_000436.1	8E-12	87	Muscular dystrophy with epidermolysis bullosa simplex, 226670; Epidermolysis bullosa simplex, Ogna type, 131950	601282	OMIM
YGL163C	RAD54		transcriptional regulator ATRX isoform 1; RAD54 (Saccharomyces cerevisiae); DNA dependent ATPase and helicase; Zinc finger helicase; X-linked nuclear protein; helicase 2, X-linked	NP_000480.2	3E-32	24	Alpha-thalassemia/mental retardation syndrome, 301040; Juberg-Marsidi syndrome, 309590; Sutherland-Haan syndrome, 309470; Smith-Fineman-Myers syndrome, 309580; Alpha-thalassemia myelodysplasia syndrome, somatic, 300448; Sutherland-Haan syndrome-like, 300465	300032	OMIM

YGL163C	RAD54		transcriptional regulator ATRX isoform 3; RAD54 (Saccharomyces cerevisiae); DNA dependent ATPase and helicase; Zinc finger helicase; X-linked nuclear protein; helicase 2, X-linked	NP_612115.1	3E-32	26	Alpha-thalassemia/mental retardation syndrome, 301040; Juberg-Marsidi syndrome, 309590; Sutherland-Haan syndrome, 309470; Smith-Fineman-Myers syndrome, 309580; Alpha-thalassemia myelodysplasia syndrome, somatic, 300448; Sutherland-Haan syndrome-like, 300465	300032	OMIM
YGL163C	RAD54		transcriptional regulator ATRX isoform 2; RAD54 (Saccharomyces cerevisiae); DNA dependent ATPase and helicase; Zinc finger helicase; X-linked nuclear protein; helicase 2, X-linked	NP_612114.1	3E-32	25	Alpha-thalassemia/mental retardation syndrome, 301040; Juberg-Marsidi syndrome, 309590; Sutherland-Haan syndrome, 309470; Smith-Fineman-Myers syndrome, 309580; Alpha-thalassemia myelodysplasia syndrome, somatic, 300448; Sutherland-Haan syndrome-like, 300465	300032	OMIM
YDR226W	ADK1		adenylate kinase 1	NP_000467.1	2E-23	7	Hemolytic anemia due to adenylate kinase deficiency	103000	OMIM
YLR032W	RAD5		transcriptional regulator ATRX isoform 1; RAD54 (Saccharomyces cerevisiae); DNA dependent ATPase and helicase; Zinc finger helicase; X-linked nuclear protein; helicase 2, X-linked	NP_000480.2	2E-22	5	Alpha-thalassemia/mental retardation syndrome, 301040; Juberg-Marsidi syndrome, 309590; Sutherland-Haan syndrome, 309470; Smith-Fineman-Myers syndrome, 309580; Alpha-thalassemia myelodysplasia syndrome, somatic, 300448; Sutherland-Haan syndrome-like, 300465	300032	OMIM
YLR032W	RAD5		transcriptional regulator ATRX isoform 3; RAD54 (Saccharomyces cerevisiae); DNA dependent ATPase and helicase; Zinc finger helicase; X-linked nuclear protein; helicase 2, X-linked	NP_612115.1	2E-22	7	Alpha-thalassemia/mental retardation syndrome, 301040; Juberg-Marsidi syndrome, 309590; Sutherland-Haan syndrome, 309470; Smith-Fineman-Myers syndrome, 309580; Alpha-thalassemia myelodysplasia syndrome, somatic, 300448; Sutherland-Haan syndrome-like, 300465	300032	OMIM
YLR032W	RAD5		transcriptional regulator ATRX isoform 2; RAD54 (Saccharomyces cerevisiae); DNA dependent ATPase and helicase; Zinc finger helicase; X-linked nuclear protein; helicase 2, X-linked	NP_612114.1	2E-22	6	Alpha-thalassemia/mental retardation syndrome, 301040; Juberg-Marsidi syndrome, 309590; Sutherland-Haan syndrome, 309470; Smith-Fineman-Myers syndrome, 309580; Alpha-thalassemia myelodysplasia syndrome, somatic, 300448; Sutherland-Haan syndrome-like, 300465	300032	OMIM
YAL019W	FUN30		transcriptional regulator ATRX isoform 1; RAD54 (Saccharomyces cerevisiae); DNA dependent ATPase and helicase; Zinc finger helicase; X-linked nuclear protein; helicase 2, X-linked	NP_000480.2	9E-22	29	Alpha-thalassemia/mental retardation syndrome, 301040; Juberg-Marsidi syndrome, 309590; Sutherland-Haan syndrome, 309470; Smith-Fineman-Myers syndrome, 309580; Alpha-thalassemia myelodysplasia syndrome, somatic, 300448; Sutherland-Haan syndrome-like, 300465	300032	OMIM
YAL019W	FUN30		transcriptional regulator ATRX isoform 3; RAD54 (Saccharomyces cerevisiae); DNA dependent ATPase and helicase; Zinc finger helicase; X-linked nuclear protein; helicase 2, X-linked	NP_612115.1	9E-22	31	Alpha-thalassemia/mental retardation syndrome, 301040; Juberg-Marsidi syndrome, 309590; Sutherland-Haan syndrome, 309470; Smith-Fineman-Myers syndrome, 309580; Alpha-thalassemia myelodysplasia syndrome, somatic, 300448; Sutherland-Haan syndrome-like, 300465	300032	OMIM
YAL019W	FUN30		transcriptional regulator ATRX isoform 2; RAD54 (Saccharomyces cerevisiae); DNA dependent ATPase and helicase; Zinc finger helicase; X-linked nuclear protein; helicase 2, X-linked	NP_612114.1	9E-22	30	Alpha-thalassemia/mental retardation syndrome, 301040; Juberg-Marsidi syndrome, 309590; Sutherland-Haan syndrome, 309470; Smith-Fineman-Myers syndrome, 309580; Alpha-thalassemia myelodysplasia syndrome, somatic, 300448; Sutherland-Haan syndrome-like, 300465	300032	OMIM
YAL019W	FUN30		SWI/SNF-related matrix-associated actin-dependent regulator of chromatin a-like 1; HepA-related protein; SMARCA-like protein 1	NP_054859.2	8E-13	35	Schimke immunoosseous dysplasia, 242900	606622	OMIM

YDR334W	SWR1		transcriptional regulator ATRX isoform 1; RAD54 (Saccharomyces cerevisiae); DNA dependent ATPase and helicase; Zinc finger helicase; X-linked nuclear protein; helicase 2, X-linked	NP_000480.2	1E-19	31	Alpha-thalassemia/mental retardation syndrome, 301040; Juberg-Marsidi syndrome, 309590; Sutherland-Haan syndrome, 309470; Smith-Fineman-Myers syndrome, 309580; Alpha-thalassemia myelodysplasia syndrome, somatic, 300448; Sutherland-Haan syndrome-like, 300465	300032	OMIM
YDR334W	SWR1		transcriptional regulator ATRX isoform 3; RAD54 (Saccharomyces cerevisiae); DNA dependent ATPase and helicase; Zinc finger helicase; X-linked nuclear protein; helicase 2, X-linked	NP_612115.1	1E-19	33	Alpha-thalassemia/mental retardation syndrome, 301040; Juberg-Marsidi syndrome, 309590; Sutherland-Haan syndrome, 309470; Smith-Fineman-Myers syndrome, 309580; Alpha-thalassemia myelodysplasia syndrome, somatic, 300448; Sutherland-Haan syndrome-like, 300465	300032	OMIM
YDR334W	SWR1		transcriptional regulator ATRX isoform 2; RAD54 (Saccharomyces cerevisiae); DNA dependent ATPase and helicase; Zinc finger helicase; X-linked nuclear protein; helicase 2, X-linked	NP_612114.1	1E-19	32	Alpha-thalassemia/mental retardation syndrome, 301040; Juberg-Marsidi syndrome, 309590; Sutherland-Haan syndrome, 309470; Smith-Fineman-Myers syndrome, 309580; Alpha-thalassemia myelodysplasia syndrome, somatic, 300448; Sutherland-Haan syndrome-like, 300465	300032	OMIM
YDR334W	SWR1		SWI/SNF-related matrix-associated actin-dependent regulator of chromatin a-like 1; HepA-related protein; SMARCA-like protein 1	NP_054859.2	6E-18	35	Schimke immunoosseous dysplasia, 242900	606622	OMIM
YCR065W	HCM1		forkhead box E1; forkhead (Drosophila)-like 15; thyroid transcription factor-2; Forkhead, drosophila, homolog-like 15	NP_004464.2	1E-18	24	Bamforth-Lazarus syndrome, 241850	602617	OMIM
YCR065W	HCM1		forkhead box C2; MFH-1,mesenchyme forkhead 1; forkhead (Drosophila)-like 14; forkhead (Drosophila)-like 14 (MFH-1, mesenchyme forkhead 1); forkhead, Drosophila, homolog-like 14	NP_005242.1	4E-17	29	Lymphedema-distichiasis syndrome, 153400; Lymphedema, hereditary II, 153200; Yellow nail syndrome, 153300; Lymphedema and ptosis, 153000	602402	OMIM
YCR065W	HCM1		forkhead box E3; forkhead (Drosophila)-like 12; Forkhead, drosophila, homolog-like 12	NP_036318.1	1E-16	34	Anterior segment mesenchymal dysgenesis, 107250	601094	OMIM
YCR065W	HCM1		forkhead box C1; forkhead (Drosophila)-like 7; iridogoniodysgenesis type 1; Forkhead, drosophila, homolog-like 7; forkhead-related activator 3	NP_001444.1	2E-16	35	Iridogoniodysgenesis, 601631; Anterior segment mesenchymal dysgenesis; Rieger anomaly; Axenfeld anomaly; Iris hypoplasia and glaucoma	601090	OMIM
YCR065W	HCM1		forkhead box P3; JM2 protein; immunodeficiency, polyendocrinopathy, enteropathy, X-linked; immune dysregulation, polyendocrinopathy, enteropathy, X-linked; scurfin	NP_054728.2	1E-15	37	Immunodysregulation, polyendocrinopathy, and enteropathy, X-linked, 304790; {Diabetes mellitus, type I, susceptibility to}, 222100	300292	OMIM
YCR065W	HCM1		winged-helix nude; winged helix nude	NP_003584.2	3E-14	42	T-cell immunodeficiency, congenital alopecia, and nail dystrophy	600838	OMIM
YCR065W	HCM1		forkhead box P2 isoform III; trinucleotide repeat containing 10; forkhead/winged-helix transcription factor; speech and language disorder 1; CAG repeat protein 44	NP_683698.1	2E-13	46	Speech-language disorder-1, 602081	605317	OMIM
YCR065W	HCM1		forkhead box P2 isoform III; trinucleotide repeat containing 10; forkhead/winged-helix transcription factor; speech and language disorder 1; CAG repeat protein 44	NP_683697.1	2E-13	47	Speech-language disorder-1, 602081	605317	OMIM
YCR065W	HCM1		forkhead box P2 isoform II; trinucleotide repeat containing 10; forkhead/winged-helix transcription factor; speech and language disorder 1; CAG repeat protein 44	NP_683696.1	2E-13	45	Speech-language disorder-1, 602081	605317	OMIM
YCR065W	HCM1		forkhead box P2 isoform I; trinucleotide repeat containing 10; forkhead/winged-helix transcription factor; speech and language disorder 1; CAG repeat protein 44	NP_055306.1	2E-13	48	Speech-language disorder-1, 602081	605317	OMIM
YLR085C	ARP6		alpha 1 actin precursor; alpha skeletal muscle actin	NP_001091.1	5E-17	2	Myopathy, nemaline, 161800, 256030; Myopathy, actin	102610	OMIM

YLR085C	ARP6		actin, alpha, cardiac muscle precursor	NP_005150.1	1E-16	4	Cardiomyopathy, dilated, 115200; Cardiomyopathy, familial hypertrophic, 192600	102540	OMIM
YLR085C	ARP6		actin, gamma 1 propeptide; cytoskeletal gamma-actin; actin, cytoplasmic 2	NP_001605.1	9E-16	8	Deafness, autosomal dominant 20/26, 604717	102560	OMIM
YDL025C	YDL025C		p21-activated kinase 3; bPAK; p21-activated kinase-3; hPAK3; CDKN1A	NP_002569.1	8E-16	62	Mental retardation, X-linked 30	300142	OMIM
YDL025C	YDL025C		rhodopsin kinase; G protein-coupled receptor kinase 1b	NP_002920.1	3E-14	118	Oguchi disease-2, 258100	180381	OMIM
YDL025C	YDL025C		ribosomal protein S6 kinase, 90kDa, polypeptide 3; ribosomal protein S6 kinase, 90kD, polypeptide 3	NP_004577.1	4E-14	128	Coffin-Lowry syndrome, 303600; Mental retardation, X-linked nonspecific, type 19	300075	OMIM
YDL025C	YDL025C		skeletal myosin light chain kinase	NP_149109.1	3E-11	237	Cardiomyopathy, hypertrophic, midventricular, digenic, 192600	606566	OMIM
YDL074C	BRE1		myosin, heavy polypeptide 9, non-muscle	NP_002464.1	3E-14	6	May-Hegglin anomaly, 155100; Fechtner syndrome, 153640; Sebastian syndrome, 605249; Deafness, autosomal dominant 17, 603622; Epstein syndrome, 153650	160775	OMIM
YDL074C	BRE1		myosin, heavy polypeptide 7, cardiac muscle, beta	NP_000248.1	2E-13	12	Cardiomyopathy, familial hypertrophic, 1, 192600; ?Central core disease, one form; Cardiomyopathy, dilated, 115200; Myopathy, myosin storage, 608358	160760	OMIM
YDL074C	BRE1		myosin heavy chain 6; myosin heavy chain, cardiac muscle alpha isoform	NP_002462.1	7E-12	15	Cardiomyopathy, familial hypertrophic, 192600	160710	OMIM
YDL074C	BRE1		myosin, heavy polypeptide 2, skeletal muscle, adult	NP_060004.2	2E-11	22	Inclusion body myopathy-3, 605637	160740	OMIM
YEL013W	VAC8		junction plakoglobin; gamma-catenin	NP_002221.1	2E-14	4	Naxos disease, 601214	173325	OMIM
YEL013W	VAC8		junction plakoglobin; gamma-catenin	NP_068831.1	2E-14	3	Naxos disease, 601214	173325	OMIM
YGL003C	CDH1		peroxisomal biogenesis factor 7; peroxisome biogenesis factor 7	NP_000279.1	2E-13	6	Rhizomelic chondrodysplasia punctata, type 1, 215100; Refsum disease, 266500	601757	OMIM
YGL003C	CDH1		platelet-activating factor acetylhydrolase, isoform Ib, alpha subunit (45kD); lissencephaly 1 protein; Platelet-activating factor acetylhydrolase, isoform 1B, alpha subunit	NP_000421.1	3E-12	11	Lissencephaly-1, 607432; Subcortical laminar heterotopia	601545	OMIM
YGL003C	CDH1		guanine nucleotide-binding protein, beta-3 subunit; guanine nucleotide-binding protein G(I)/G(S)/G(T) beta subunit 3; G protein, beta-3 subunit; GTP-binding regulatory protein beta-3 chain; transducin beta chain 3	NP_002066.1	3E-12	10	{Hypertension, essential, susceptibility to}, 145500	139130	OMIM
YBR112C	CYC8		Bardet-Biedl syndrome 4	NP_149017.2	2E-12	11	Bardet-Biedl syndrome 4, 209900	600374	OMIM
YKL221W	MCH2		solute carrier family 16, member 2; X-linked PEST-containing transporter; monocarboxylate transporter 8	NP_006508.1	7E-12	2	Monocarboxylate transporter 8 deficiency	300095	OMIM